



# 7th International Symposium on Technetium and Rhenium – Science and Utilization July 4 -8, 2011, Moscow, Russia

## BOOK OF PROCEEDINGS



RUSNANO



**PUROLITE**<sup>®</sup>  
ION EXCHANGE RESINS



ROSATOM



**UNLV**  
UNIVERSITY OF NEVADA LAS VEGAS



**AMERICAN  
ELEMENTS**

PUBLISHING HOUSE GRANITSA

MOSCOW 2011

RUSSIAN ACADEMY OF SCIENCES,

IPCE RAS, MUCTR, ISTC, RFBR, RUSNANO, ROSATOM, ACADEMINVESTSERVICE, FMBC FMBA



**7th International Symposium on  
Technetium and Rhenium –  
Science and Utilization**

**July 4 -8, 2011, Moscow, Russia**

**BOOK OF PROCEEDINGS**

Edited by

K.E. German, B.F. Myasoedov, G.E. Kodina, A.Ya. Maruk, I. D. Troshkina

Publishing House GRANITSA, MOSCOW 2011

7th International Symposium on Technetium and Rhenium – Science and Utilization –

BOOK OF PROCEEDINGS - July 4 -8, 2011, Moscow, Russia (Eds. K.E. German, B.F. Myasoedov, G.E. Kodina, A.Ya. Maruk, I. D. Troshkina), Publishing Group Granica: Moscow, 2011, 461 p.

© IPCE RAS 2011  
© RUSNANO 2011  
© ISTC 2011  
© ACADEMINVESTSERVICE 2011  
© RFBR 2011  
© GRANICA 2011

Publishing House GRANITSA, 2011

UDK 546.718 : 548.736

ISBN 978-5-94691-473-4

CONTENTS :

<b>Opening ceremony:</b>	
<b>B.F. Myasoedov</b> Welcome address	13
<b>K.E. German</b> , F. Poineau. Technetium: new trends in investigation and application	15
<b>E.N. Kablov</b> , N.V. Petrushin, V.V. Sidorov. Rhenium in nickel-base superalloys for single crystal gas turbine blades	18
<b>M.Ozawa</b> . ISTR Retrospectives and Prospects - in view points of Nuclear Fuel Cycle	20
<b>Session 1. Fundamental Physics and Chemistry of Tc and Re</b>	
<b>T. Yoshimura</b> , C. Suo, S. Ishizaka, A. Ito, E. Sakuda, A. Shinohara, N. Kitamura. Spectroscopic and photophysical properties of chalcogenide-capped octahedral hexarhenium complexes with N-heteroaromatic ligands	26
<b>Y.V. Mironov</b> , S.S. Yarovoi, K.A. Brylev, V.E. Fedorov. Rhenium octahedral chalcydroxo cluster complexes	27
<b>F. Poineau</b> , A. P. Sattelberger, B. L. Scott, P. Forster, Ph. Weck, E. Johnstone, K. R. Czerwinski. Technetium halides: from molecular to extended structures	28
<b>E.N. Pryamilova</b> , O.V. Chernyshova, D.V. Drobot. Synthesis of rhenium alkoxides via anodic dissolution	30
<b>Th. Gerber</b> , K. Potgieter, P. Mayer. Rhenium coordination chemistry: old ligands die hard.	30
<b>T.Kobayashi</b> , X.Gaona, D.Fellhauer, M. Altmaier. Redox behaviour of the Tc(VII)/Tc(IV) couple in diluted NaCl solution in various reducing systems	31
<b>A.E. Miroslavov</b> , G.V. Sidorenko, A.A. Lumpov, D.N. Suglobov, M.S. Grigor'ev, V.V. Gurzhii. Technetium(I) hexacarbonyl cation and its reactivity	37
<b>G.V. Sidorenko</b> , A.E. Miroslavov, D.N. Suglobov, M.S. Grigor'ev, V.V. Gurzhii. Structural Chemistry of Technetium Carbonyl Compounds	38
<b>D.V. Drobot</b> , O.V. Chernyshova, O.S. Kriyzhovets, K.A. Smirnova, I.V. Masilin, A.V. Shevelkov, M.V. Tsodikov, A.V. Chistyakov, O.V. Petrakova, E.G. Il'in. "Soft" chemistry methods appear as an effective way for production of superdispersive (nano-sized) materials based on Re and d-elements of V-VIII groups	44
<b>C. Kremer</b> , R. Chiozzone. Structure and magnetic properties of polynuclear complexes containing Re(IV)	53
<b>A.I. Irtegov</b> , M.A. Kurykin, V.N. Khrustalev, E.E. Nikishina, D.V. Drobot. Polyfluorinated $\beta$ -diketonates of rhenium	54
<b>W.M. Kerlin</b> , T. Yordanova, F. Poineau, P.M. Forster, A.P. Sattelberger, K.R. Czerwinski. Preparation of technetium metal-metal bonded acetate dimers via hydrothermal route	55
<b>Povarova K.B.</b> Physicochemical principles of the development of rhenium-based and rhenium-containing alloys	56
<b>E.V. Johnstone</b> , F. Poineau, P.F. Weck, E. Kim, P.M. Forester, B. Scott, T. Hartmann, A.P. Sattelberger, K.R. Czerwinski. Synthesis and characterization of low-valent binary technetium chlorides	57
<b>V.E. Fedorov</b> , Yu.V. Mironov, N.G. Naumov, K.A. Brylev. Recent results in rhenium cluster chemistry	58
<b>O.S. Kriyzhovets</b> , D.V. Drobot, A.V. Shevelkov, O.V. Petrakova. Heteroligand alkoxides of rheniumcontaining O-Et and O <sup>-1</sup> Pr ligands	59
<b>A.A. Aminjonov</b> . Status and prospects of studies on the chemistry of coordination compounds of rhenium(V)	65
<b>N.G. Kabirov</b> , S.M. Safarmamadov, A.A. Aminjonov Effect of the rhenium(V) complex of 3,4-dimethyl-1,2,4-triazol-5-thiol on the diacetate cellulose light fastness	73
<b>A.V. Ermolaev</b> , A.I. Smolentsev, K.A. Brylev, V.E. Fedorov, Y.V. Mironov. Octahedral rhenium(III) chalcocyanohydroxo cluster complexes	74



<b>M.V. Sukhanov</b> , V.I. Pet'kov. Technetium and Rhenium Orthophosphates with Kosnarite-Type Structure	75
<b>A.Yu.Didyk</b> , V.S.Kulikauskas, R. Wiśniewski. Depth distribution of D-ions with 25 keV energy implanted into pure Mn, Tc* and Re foils up to high fluencies $(1\div 2)\times 10^{18}$ D <sup>+</sup> /cm <sup>2</sup> , measured by ERD method	79
<b>Z.Ch.Kadirova</b> , Kh.T. Sharipov, Sh. Juraev, N.A. Parpiev. Coordination compounds of biologically active N-containing heterocyclic ligands	85
<b>N.G. Kabirov</b> , S.M. Safarmamadov, A.A. Aminjonov . Chelation of rhenium (V) with 3-ethyl-4-methyl-1,2,4-triazol-5-thiol in 3 M HCl medium	86
<b>K.S. Mabatkadamova</b> , N.G. Kabirov, S.M. Safarmamadov, A.A. Aminjonov Complexation in the system Re (V) – 1-methyl-2-merkptoimidazolE – 8 mol/l HCl	91
<b>F. Poineau</b> , I. Denden, R. Essehli, K. German, K. Czerwinski and M. Fattahi. Speciation of Tc in sulfuric media. Effect of $\alpha$ -radiation from Arronax Cyclotron	96
<b>A. Ya. Maruk</b> , M. S. Grigor'ev, K. E. German. Synthesis, Crystal Structure and Properties of Triphenylguanidium Tetraoxidorhenate Hemihydrate	97
<b>A.M. Fedosseev</b> , M.S. Grigoriev. Synthesis and crystal structure of [AnO <sub>2</sub> (HMPA) <sub>4</sub> ](MO <sub>4</sub> ) <sub>2</sub> (An = U, Pu; M = Cl, Tc, Re)	98
K.E. German, A.Ya. Maruk, F. Poineau, P.Weck, G.A. Kirakosyan, <b>V.P. Tarasov</b> , K. Czerwinski, A. Sattelberger. Transformation of Tc(VII) in acids: TcO <sub>3</sub> (OH)(H <sub>2</sub> O) <sub>2</sub> and TcO <sub>3</sub> (H <sub>2</sub> O) <sub>3</sub> <sup>+</sup> in HClO <sub>4</sub> and polymeric species in solids and acetonitrile solutions	99
I.M. Gayfulin, <b>Yu.V. Mironov</b> , A.I. Smolentsev. New compounds based on the cluster anions [Re <sub>4</sub> Q <sub>4</sub> (CN) <sub>12</sub> ] <sup>4-</sup> (Q=S, Se, Te) and cations (1,10-phenH) <sup>+</sup> , Nd <sup>3+</sup> , Er <sup>3+</sup>	101
<b>A.A. Aminjonov</b> . Mutual substitution of ligands in complex compounds of rhenium(V)	102
<b>Fathi Habashi</b> . Rhenium and its position in the periodic table	104
<b>G.V. Kolesnikov</b> , V.N. Khrustalev, K.E. German, I.G. Tananaev, G.A. Kirakosyan, E.A. Katayev. Macrocyclic receptors for pertechnetate and perrhenate anions	105
<b>Session 2. Tc in the Nuclear Fuel Cycle and in the Environment. Analytical Chemistry of Tc and Re</b>	106
<b>M. Ozawa</b> , T. Suzuki, S. Koyama, Y. Fujii, M. Saito. How to manage technetium (nuclear rare metal) and actinides, towards future reprocessing system providing non-proliferation	107
<b>T. Boytsova</b> , V. Korolev, Y. Pokhitonov, V. Babain, M. Ozawa, T. Suzuki. Combined separation of Pd and Tc from the raffinates of the spent nuclear fuel reprocessing	112
<b>A.A. Kozar'</b> , V.F. Peretruchin, K.V. Rotmanov, V.A. Tarasov. The elaboration of technology bases for the artificial stable ruthenium preparation from technetium-99 transmutation products	113
K.E. German, <b>Ya.A. Obruchnikova</b> , D.N. Tumanova, V.F. Peretruchin, Ph. Moisy. Technetium catalytic effect and speciation in nitric acid solutions in presence of Np(V), Th(IV) and Zr(IV) and reducing nitrogen derivatives	114
D.N. Kolupaev, <b>A.B. Melentev</b> , A.N. Mashkin, V.A. Misharin, A.V. Ananyev, V.P. Shilov, K.E. German, I.G. Tananaev. Composition and catalytic properties of technetium-based sediments and interphase substances found in the uranium-plutonium separation stage of the PUREX process	121
<b>T.V. Khijniak</b> . Interaction of microorganisms and radionuclides	127
<b>S.N. Britvin</b> , Y.I. Korneyko, S.V. Krivovichev, W. Depmeier. Layered hydrazinium titanate : reductive adsorbent for irreversible immobilization of technetium	137
<b>S.V. Yudintsev</b> , E.E. Konovalov, B.S. Nikonov. Re and Tc in cermet waste forms	136
<b>M. Chotkowski</b> , A. Czerwiński. Electrochemical and spectroelectrochemical investigations of TcO <sub>4</sub> <sup>-</sup> electroreduction in acidic media	137
<b>L.V. Borisova</b> , V.V. Minin. Stabilization of rhenium (VI) compounds in solution and using them in analysis	138
A.A. Grechnikov, <b>L.V. Borisova</b> , V.A. Ryabukhin. Novel approach to the mass-	144

spectrometric determination of trace amounts of rhenium using its complexes with organic reagents	
<b>K. Leszczynska-Sejda</b> , G. Benke, K. Anyszkiewicz, A. Chmielarz, S. Cupial. Method for hexamminecobalt (III) perrhenate synthesis from perrhenic acid	148
<b>D. Golovanov</b> . Modern X-ray analytical instruments of Bruker AXS	149
<b>R.A. Aliev</b> . Preparation of <sup>95m,g</sup> Tc, <sup>96</sup> Tc by irradiation of molybden with ALPHA-particles and deuterons	150
<b>S. Alwaer</b> . Modernization method for production of Fission Mo-99 from Low-Enriched-Uranium Foil (LEU-Foil)	151
<b>A.A. Kozar'</b> , V.F. Peretruxhin. <sup>99</sup> Tc transmutation target heterogeneity for the artificial stable ruthenium purification from <sup>106</sup> Ru	160
<b>G.S. Bulatov</b> , K.N. Gedgovd, D.Yu. Lyubimov. The behavior of technetium, americium and neptunium in the spent FBR (U,Pu)N fuel after fast neutron irradiation as a function of the temperature and burn-up	162
<b>E. Pichuzhkina</b> , S. Tomilin. Compounds of Curium with Technetium	166
V.I. Volk, K.N. Dvoyeglazov, <b>V.L. Vidanov</b> , L.N. Sergeeva. Extraction-chromatographic purification of uranium extract from technetium	167
E.E. Konovalov, T.O. Mishevets, <b>S.S. Shulepov</b> , Yu.D. Boltoev. Metal-thermal Immobilization of High-active Technetium Waste into Matrices Based on Metal Glass Crystalline Composites	168
N.N. Popova, <b>G.L. Bykov</b> , I.G. Tananaev, B.G. Ershov. Application of modified wood materials for extraction of technetium(VII) from aqueous medium	169
K.E. German, <b>A.B. Melentev</b> , Ya. V. Zubavichus <sup>2</sup> , S.N. Kalmykov <sup>3</sup> , A.A. Shiryayev, I.G. Tananaev. Structure and properties of insoluble Technetium compounds formed in Technetium - Hydrazine - DTPA -nitric acid- solutions	173
<b>A.B. Melentev</b> , A.N. Mashkin, O.V. Tugarina, K.E. German, I.G. Tananaev. The behavior of the technetium - hydrazine - nitric acid - TBP system in presence of the complexing agents	174
<b>A.M. Safiulina</b> , K.E. German, E.I. Goryunov, I.B. Goryunova, E.E. Nifantiev, I.G. Tananaev, B.F. Myasoedov. Technetium(VII) extraction with hybrid phosphor-nirogenated derivative ligands	175
M.K. Abdulhatov, S.A. Bartenev, M.J. Goikhman, A.V. Griбанov, V.S. Gusel'nikov, M.P. Zykov, J.N. Novikov, J.N. Sazanov, <b>N.G. Firsin</b> . New materials for immobilization of technetium-containing waste for the purpose of their isolation from the environment	176
<b>German K.E.</b> , Peretruxhin V.F., D.N. Tumanova, A.Yu. Tsivadze. Technetium sulfides – role in chemistry and ecology	181
K.E. German, <b>T. V. Khijniak</b> , V.F., Peretruxhin . Technetium limnology as frame for its ecology and the key for underground storage	187
<b>Yu.I. Korneyko</b> , V.M. Garbuzov, B.E. Burakov. Kassiterite as a Durable Host-Phase for Technetium Immobilization	190
A.G. Maslennikov, <b>K.V. Rotmanov</b> , N.G. Kravchenko, V.M. Radchenko, M.V. Kormilitsyn, V.F. Peretruxhin. Electrochemical Investigation of Corrosion and Dissolution of Metallic Technetium and Tc-Ru Alloys in 0,5 – 6,0 M HNO <sub>3</sub>	191
<b>R.A. Aliev</b> , S.N. Kalmykov, I.G. Tananaev, I.A. Ivanov. Tc-99 determination in contaminated groundwater	192
O. Batuk, <b>S.N. Kalmykov</b> , E.V. Zakharova. Sorption of Tc-99 and Np-237 by depleted UO <sub>2</sub>	193
<b>Yu.I. Urusov</b> , K.E. German, A.V. Kopytin, A.F. Zhukov. ReO <sub>4</sub> <sup>-</sup> and TcO <sub>4</sub> <sup>-</sup> ion-selective bubble-through flow cells	194
<b>Session 3. Re Hydrometallurgy</b>	201
<b>I. D. Troshkina</b> . Rhenium in Nuclear Fuel Cycle	202

<b>Z.S. Abisheva</b> , A.N. Zagorodnyaya. Rhenium of Kazakhstan	208
<b>E.A. Ospanov</b> , E.I. Gedgagov, N.A. Ospanov, S.V. Zakharyan. Development of the technology for production of high-purity ammonium perrhenate at Balkhash copper smelter, Republic of Kazakhstan	217
E.I. Gedgagov, <b>Nekhoroshev N.E.</b> Use of ion-exchange resins for production of high-purity ammonium perrhenate when processing rhenium-containing ore and secondary raw material	218
<b>M. Mikhaylenko</b> , Purolite <sup>®</sup> ion exchange resins for recovery and purification of rhenium	222
<b>O. Bozhkov</b> , Ch. Tzvetkova, L. Borisova. Phytomining of Re - an Alternative Method for Re Production	223
V.P. Volkov, <b>N.M. Mescheryakov</b> . Sorptive Recovery of Rhenium from Circulating Solutions of Uranium in Situ Leaching Operation at Navoi GMK, Uzbekistan	230
<b>A.G. Kasikov</b> , A.M. Petrova. Rhenium(VII) solvent extraction by mixtures of tertiary amine and oxygen-containing extragents from sulphate media	232
A.N. Zagorodnyaya, <b>Z.S. Abisheva</b> , S.E. Sadykanova. Interphase Substances of Rhenium Extraction Circuit are a source for production of rhenium and radiogenic osmium	235
<b>L. Ya. Agapova</b> , Z. S. Abisheva, S. K. Kilibayeva, I. A. Sapukov. Electrodeposition of rhenium alloys in form of powders and coatings from water solutions by membrane electrolysis	241
<b>Z.S. Abisheva</b> , L.Ya. Agapova, E.I. Ponomareva, Z.T. Abdrakhmanova Application of electro dialysis method for high purity metal rhenium obtaining	247
<b>E.A. Salahova</b> , V.A. Majidzade, F.S. Novruzova, A.F. Qeybatova, P.E. Kalantarova. The electrolytic subsidence of rhenium from acid electrolytes	253
<b>A.A. Blokhin</b> , E.E. Maltseva, M.A. Pleshkov, Ju.V. Murashkin, M.A. Mikhaylenko. Sorption recovery of rhenium from acidic sulfate and mixed nitrate-sulfate solutions containing molybdenum	254
<b>Ch. Tzvetkova</b> , O. Bozhkov, L. Borisova. Rhenium Phytomining by Alfalfa (Medicago) from soils of ore dressing regions at laboratory conditions	262
<b>A.G. Kasikov</b> , A.M. Petrova, N.S. Areshina, A.A. Blokhin, E.E. Maltseva. Rhenium recovery from gas-purification wastes of THE Kola mining Company	265
A.G. Kasikov, <b>A.M. Petrova</b> . Solvent extraction of rhenium(VII) from acid solutions with high-molecular aliphatic alcohols	268
A.A. Palant, O.M. Levchuk, A.M. Levin, <b>O.V. Reshetova</b> . Production of the high purity NH <sub>4</sub> ReO <sub>4</sub> using electro dialysis method	271
<b>R.D. Allabergenov</b> , Kh.T. Sharipov, R.Kh. Sharipov, A.A. Niyazmatov. Regularities of Rhenium Salts Oxidizing Leaching	272
I.D. Troshkina, <b>A.V. Shilyaev</b> , N.V. Balanovskiy, A.M. Chekmarev, O.A. Chernyadeva. Rhenium Sorption from Uranium-Containing Solution by Nanostructured Ionites	277
<b>A. A. Abdusalomov</b> , I. D. Troshkina, A. M. Chekmarev, N. P. Ismailov. Sorption of palladium from the rhenium containing sulfuric acid solution	281
I. D. Troshkina, <b>T. G. Abdrakhmanov</b> , N. A. Smirnov, A. B. Mayboroda, K. I. Potapova, A. M. Chekmarev. Ultrafiltration Separation of Rhenium and Uranium Using Nitrogen-Containing Polyelectrolytes	285
<b>I.D. Troshkina</b> , L.A. Zemskova, A.M. Chekmarev, A.V. Plevaka, Aye Minn, A.V. Shilyaev, A.V. Voit, D. N. Tumanova. Recovery of Rhenium from Aqueous Solutions by Fibrous Materials	288
<b>A.G. Kasikov</b> , A.M. Petrova, P.B. Gromov, V.T. Kalinnikov. Rhenium recycling from heat-resistant rhenium-containing nickel-based superalloys	293
<b>A.M. Safiulina</b> , K.E. German, N.N. Popova, M.Yu. Burtsev. Installation for liquid-liquid extraction concentrating and recovery of Rhenium from aqueous sulfate solution	297

I. D. Troshkina, <b>M.V. Vazchenkov</b> , A. M. Chekmarev. Recovery of rhenium from oil shale	298
<b>Session 4. Tc and Re in Nuclear Medicine</b>	299
<b>G.E.Kodina.</b> Tc-99m and Re-188 in Russian Nuclear Medicine	300
<b>H. Braband.</b> The fac-{TcO <sub>3</sub> } <sup>+</sup> core – a challenge for high-valent technetium chemistry	301
<b>A.Ya. Maruk</b> , A.B. Bruskin, G.E. Kodina. New radiopharmaceuticals based on technetium-99m with bifunctional chelating agents	307
V.N. Korsunsky, V.N. Oshchepkov, <b>S.V. Shiryaev</b> , E.Z. Rabinovich. “Rezoskan, <sup>99m</sup> Tc” in the diagnosis of metastatic bone lesions	308
<b>V.S. Skuridin</b> , V.L. Sadkin, E.S. Stasiuk, N. V. Varlamova, A.C. Rogov, E.A. Nesterov. Obtaining Technetium-99m Labelled Nanocolloides Based on Aluminium Oxide for Medical Diagnostics	309
<b>E.A. Nesterov</b> , V.S. Skuridin, M.L. Belyanin, J.V. Nesterova, V.L. Sadkin, A.S. Rogov, I.V. Chikova. Receiving of nanosized colloids based on modified DTPA molecule labeled with technetium-99m	313
<b>N.I. Gorshkov</b> , A.Yu. Murko, Yu.I. Zolotova. O.V. Nazarova, I.I. Malakhova, V.D.Krasikov, R. Schibli. Synthesis and complex analysis of biologically active polymers (poly-N-vinylpyrrolidone) with Re(CO) <sub>3</sub> species	311
A.N. Klyopov, <b>V.V. Krylov</b> , Y.A. Kurachenko, Eu.S. Matusevich, Eu.V. Snigirev, O.P. Aleksandrova. Development of dosimetric support and planning of radionuclide therapy with radiopharmaceutical labeled <sup>188</sup> Re	317
<b>A. Hammadi.</b> Education and training in nuclear medicine, radiopharmacy, medical physics and molecular imaging: the INSTN experienced approach	318
<b>M.L. Bonardi</b> , F. Groppi, E. Lapshina, S. Manenti, L. Gini. High Specific Activity Radionuclides IN NCA FORM: Re-186g produced by Cyclotron	319
<b>M.P.Zykov</b> , A.T.Filyanin, G.E.Kodina, A.Yu.Tsivadze, V.N. Romanovsky, D.A.Tkachuk, O.A.Filyanin, S.P.Orlov, V.A.Novojilov. Optimization of parameters of the <sup>188</sup> Re obtaining process in a centrifugal extractor	320
<b>A.A. Semenova</b> , N.G. Baranov, D.V. Stepchenkov, E.V. Sulim, V.M. Petriev. <sup>188</sup> W/ <sup>188</sup> Re generator production technology for nuclear medicine	321
N.G. Baranov, D.V. Stepchenkov, N.A.Nerozin, <b>E.V. Sulim</b> , Yu.V.Minko, A.A.Semenova. Substantiation of Engineering Parameters of a Rhenium-188 Stationary Generator for Radionuclide Therapy	327
<b>A.N. Klyopov</b> , V.M. Petriev, V.G. Skvortsov, V.V. Kanygin, V.K. Shiryaeva, O.P. Aleksandrova. Mathematical models for pharmacokinetics and dosimetry in experimental radiobiological researches of bone-seeking radiopharmaceutical <sup>188</sup> Re-KOEDF	332
N.D. Betenekov, <b>E.I. Denisov</b> , L.M. Sharygin, M.N. Golubev. The generator <sup>99m</sup> Tc based on inorganic sorbent “Thermoxide-5”	337
<b>V.E. Baulin</b> , Kovalenko O.V., Usolkin A.N., Voroshilov Y.A., Yakovlev N.G., Tsivadze A.Yu. Investigation of the sorbents on the basis of the new phosphoryl-containing ligands for allocation, concentration and purification of the molybdenum from the irradiated uranium targets	338
<b>L. Fuks</b> , E. Gniazdowska, P. Kozminski. Novel technetium and rhenium complexes with the N-heterocyclic aldehyde thiosemicarbazones - potential radiopharmaceuticals	339
<b>E. Gniazdowska</b> , P. Kozminski, K. Bankowski. <sup>99m</sup> Tc-labelled vasopressin analog d(CH <sub>2</sub> ) <sub>5</sub> [D-Tyr(Et <sup>2</sup> ),Ile <sup>4</sup> ,Eda <sup>9</sup> ] a vp as a potential radiopharmaceutical for small-cell lung cancer (SCLC) imaging	343
<b>A.O. Malysheva</b> , G.E. Kodina, O.E. Klementyeva. Complexes of technetium-99m and rhenium-188 with zoledronic acid in nuclear medicine	347
V.G. Merkulov, <b>E.V. Chibisov</b> , V.V. Zukau, Yu.S. Maslennikov, G.G. Glukhov. Production of <sup>188</sup> W and extraction of <sup>188</sup> Re at IRT-T	351



D.V. Stepchenkov, <b>N.A. Nerozin</b> , Baranov N.G., Sulim E.V., Semenova A.A.	352
Technetium-99m Generator Production and Application Experience	
<b>N.B. Epstein</b> , G.M. Khomushku, L.D. Artamonova, V.G. Skvortsov. Determination of	355
ascorbic acid in kit by high-performance liquid chromatography	
<b>N. S. Al-Hokbany</b> , I. J. Al-Jammaz. Synthesis and characterization complex of the	356
{ReO} <sup>3+</sup> core with SN and N donor ligands	
N. Taratonenkova, A. Malysheva, G. Kodina, O. Klementieva. Preparation and	369
biological study of «Nanotech, <sup>99m</sup> Tc»	
Y.N. Reshetnik, Bykov A.N., Kodina G.E., Malysheva A.O. Sorption removal of	373
Na <sup>99m</sup> TcO <sub>4</sub> from extracts of extraction generator <sup>99</sup> Mo/ <sup>99m</sup> Tc	
<b>Session 5. Applications of Tc and Re in technology, including their alloys in</b>	374
<b>Modern Constructing Materials</b>	
<b>B.D. Bryskin</b> , E.D. Sayre. The fabrication development of rhenium used in high	375
temperature rockets and high temperature space power reactor	
<b>T. Leonhardt</b> , J. Ciulik. Making and Shaping of Rhenium and Rhenium Containing	379
Alloys	
<b>I.V. Mazilin</b> , D.V. Drobot. Heterometallic Rhenium, Nickel, Co-alkoxides as	380
precursors for functional materials synthesis	
A.P. Parshin, <b>R.N. Manuylov</b> , S.A. Melnikov, G.M. Voldman. Metallothermic method	386
for producing rhenium-based alloys	
F. Morito, M.I. Danylenko, A.V. Krajnikov. Rhenium effect in Mo-Re welds	387
P.P.Oleynikov, P.A.Zaytsev, <b>A.A.Ulanovskiy</b> , S.N.Nenashev, T.Ju.Goncharuk. Use of	388
Tungsten and Rhenium Alloys for Manufacturing of High-Temperature Thermocouples	
W5%Re/W20%Re	
<b>Povarova K.B</b> , Kazanskaya N.K. Modern structural materials based on the W-	394
Mo-Re system	
<b>E.D. Sayre</b> . Technetium – a Rare Metal Produced by Man for Structural and Medical	395
use	
<b>N.S. Beknazarova</b> , A.A. Aminjonov. Influence of oxochloro-thiopyrine rhenium(V)	400
complex on radiation firmness of cellulose diacetate	
I.G.Roberov, N.B.Gorina, G.S.Burkhanov. Plastic deformation of rhenium and	407
platinum-group metals	
<b>Session 6. Tc and Re nanotechnology and applications in the field of nanomaterials</b>	408
<b>Ya.V. Zubavichus</b> , A.A. Veligzhanin, A.A. Chernyshov, E.V. Guseva. Synchrotron	409
diagnostics of functional nanomaterials	
<b>A.I. Kostylev</b> , U.G. Pokrovskiy, I.D. Troshkina, N.G. Firsin, A.M. Chekmarev	411
Manufacture of nano- and ultradisperse powders of rhenium and refractory metals from	
technogenic raw materials	
N.R. Antipkin, G.A. Biljalova, <b>M.A. Bogorodskaya</b> , A.O. Bogorodsky, A.B. Sazonov,	416
A.S. Chagovets Non-stoichiometric synthesis of rhenium heptasulfide hydrosol	
<b>K.A. Smirnova</b> , D.V. Drobot, A.I. Lvovskiy, O.V. Petrakova.	422
Controlled synthesis of ultra dispersed (nano sized) Rhenium oxides (IV) and (VI):	
synthesis of precursors and properties of the materials	
<b>G.V. Sidorenko</b> , A.E. Miroslavov, D.N. Suglobov, A.A. Lumpov, A.N. Yalfimov.	426
Volatile technetium carbonyl compounds and prospects for their application	
<b>E.V. Abkhalimov</b> , B.G. Ershov. Synthesis and characterization of Ni-M (M = Pd, Pt)	427
nanoparticle pair structures	
<b>R.D. Solovov</b> , P.A. Morozov, B.G. Ershov. Pd nanoparticles in aqueous solutions:	428
synthesis and properties	
<b>V.Yu. Murzin</b> , Ya.V. Zubavichus, M.V. Chukalina, A.A. Shiryaev, K.E. German.	429
Wavelet analysis of EXAFS spectra as applied to polynuclear and cluster transition	
metal complexes	

<b>A.A. Shiryaev.</b> Nanodiamonds for biomedical and sorption applications: structure and defects	434
<b>Tananaev I.G.,</b> K.E. German. Nanotechnologies in radiochemical technology and radioecology including technetium speciation and separations	435
<b>G.S. Bulatov,</b> K.N. Gedgovd, D.Yu. Lyubimov. High temperature interaction of rhenium, molybdenum and tungsten metals with uranium mononitride	437
A.M. Fedosseev, <b>A.A. Bessonov,</b> Ph. Moisy. Thermal behavior of perrhenate complexes of Neodymium and preparation of nanodimensional rhenium cermetes	438
Ya.A. Obruchnikova, <b>A.A. Shiryaev,</b> A.M. Safiulina, A.V. Karpukhin, I.I. Kulakova, K.E. German. Technetium(VII) sorption by modified nanodiamonds from aqueous and nitric acid solutions	439
<b>K.E. German,</b> M.S. Grigoriev, A.Ya. Maruk, Ya. V. Zubavichus, V.Yu. Murzin, Ya.A. Obruchnikova, A.A. Shiryaev. Stabilization of nano-rhenium and nano-technetium in amorphous carbon matrix	440
<b>A.V. Kopytin,</b> Yu. A. Politov, E.G. Ilyin, Yu.I. Urusov, K.E.German. Ion selective electrodes based on monocrystalline $\text{KTiOPO}_4$ with nanocapillar conductivity for determination of $\text{K}^+$ -ions	445
<b>Yu.V.Plekhanov,</b> K.E.German. Quantum chemical study of subnanodimensional mixed clusters of technetium and ruthenium	450
<b>G.V. Sidorenko,</b> A.E. Miroslavov, and D.N. Suglobov. Deposition of technetium coatings by thermolysis of volatile carbonyl compounds	451
<b>Session 7. ROUND TABLE: Tc and Re as business projects Axial presentation:</b>	452
Timofei Petrov: Introduction of innovative Russian radionuclide pharmaceuticals into the local and global markets	453
Author index	455

LOCAL SCIENTIFIC COMMITTEE

B.F. Myasoedov	IPCE RAS, Moscow – <i>Chairman</i>
A.Yu. Tsivadze	IPCE RAS, Moscow - <i>Co-Chairman</i>
E.N. Kablov	VIAM, Moscow
A.I. Nikolaev	ICTREMRM KSC RAS, Apatity
G.I. Burhanov	IMET RAS, Moscow
A.M. Chekmarev	Mendeleev MUCTR, Moscow
B.G. Ershov	IPCE RAS, Moscow
I.G. Tananaev	IPCE RAS, Moscow
K.E. German	IPCE RAS, Moscow - <i>Co-Chairman, Secretary</i>
I.D. Troshkina	Mendeleev MUCTR, Moscow - <i>Co-Secretary (Re Section)</i>
V.N. Andreev	IPCE RAS, Moscow
A.A. Blokhin	SPBSPU, St.-Petersburg
A.V. Bychkov	IAEA, Vienna
D.V. Drobot	Lomonosov MITHT, Moscow
A. A. Belova	RUSNANO, Moscow
K.N. Frolov	RUSNANO, Moscow
E.I. Gedgagov	GINTSVETMET, Moscow
M.S. Grigoriev	IPCE RAS, Moscow
M.V. Kormilitsyn	NIIAR, Dimitrovgrad
A.A. Kasikov	ICTREMRM KSC RAS, Apatity
G.E. Kodina	Burnazyan FMBC FMBA, Moscow - <i>Co-Secretary</i>
D.N. Kolupaev	PA "Mayak", Ozyorsk
L.N. Kolomiets	IPCE RAS, Moscow
E.G. Kudryavtsev	ROSATOM , Moscow
V.A. Lebedev	IPCE RAS, Moscow
A.E. Miroslavov	Khlopin Radium Institute, St.-Petersburg
A.A. Palant	IMET RAS, Moscow
V. F. Peretrukhin	IPCE RAS, Moscow
K.B. Povarova	IMET RAS, Moscow
G.A. Sarychev	VNIIHT, Moscow
V.I. Volk	Bochvar VNIINM, Moscow



INTERNATIONAL ADVISORY COMMITTEE

Honorary Chairman - B.F. Myasoedov (Russia)  
Chairman – K.E. German (Russia)  
Chairman – T. Sekine (Japan)  
R. Alberto (Switzerland)  
B. Bryskin (USA)  
K. Czerwinski (USA)  
J. R. Dilworth (England)  
Y. Fujii (Japan)  
T.I.A. Gerber (South Africa)  
G.E. Kodina (Russia)  
Ph. Moisy (France)  
M. Ozawa (Japan)  
V.F. Peretrukhin (Russia)  
A. Sattelberger (USA)  
I.D. Troshkina (Russia)  
A.Yu. Tsivadze (Russia)  
F. Poineau (USA)

Contacts :

Co-Chairman

K.E. German, IPCE RAS

Phone: +7 (495)335-2004; Fax: +7 (495)333-8522;

e-mail: istr2011@mail.ru; german@ipc.rssi.ru

Co-Chairman

T.Sekine, Tohoku University

Senday, Japan

Scientific secretary

I.D. Troshkina, MUCTR (Rhenium Section)

Phone: +7(495)496-7609; Fax: +7(495)490-7523;

e-mail: tid@rctu.ru.

Scientific secretary

G.E. Kodina, FMBC FMBA (Section of Nuclear Medicine)

тел. +7(499)193-0188

e-mail: [gkodina@yandex.ru](mailto:gkodina@yandex.ru)

**Web site: [www.technetium-99.ru](http://www.technetium-99.ru)**





**ISTR2011 REGISTRATION DESK**



**Acad. B.F. Myasoedov welcome the ISTR2011 delegates.**

#### WELCOME ADDRESS

On behalf of the International Advisory Committee and the Local Organizing and Scientific Committee, we are honored and pleased to welcome you at the 7-th International Symposium on Technetium and Rhenium –Science and Utilization . The Symposium is held on the 4-8 July 2011 in the principle building of the Presidium of Russian Academy of Sciences under the auspices of the Frumkin Institute of Physical Chemistry and Electrochemistry of Russian Academy of Sciences, Interdisciplinary Council on Radiochemistry at RAS and State Corporation ROSATOM, International Sciences and Technology Center, Japan Atomic Energy Agency, University of Nevada (USA), the Mendeleev Russian Chemistry Community, the Russian Nuclear Society, the DIAMED ltd, Purolyte ltd, Bruker ltd., Academinvestservice Ltd., Farmsintez Ltd. and others. Our intention is to collect here the multidisciplinary investigator community in the field of technetium and rhenium sciences and utilization both oriented to the development of nuclear chemistry, new radiopharmaceuticals and non-radioactive sciences and industry, ecology and metallurgy for mutual coordination of the research efforts. The Symposium approaches the multidisciplinary issues related to the development of state-of-art and production of new technologies in Tc and Re, throughout the comparison of their properties, common in view of Periodic Table to validate their utilization. Moscow is the perfect location for the Symposium. This city, being the capital of Russia, has recently got new pulse for development. It is also the artistic and cultural capital of Russia well known for its hospitality. Frumkin Institute of Physical Chemistry and Electrochemistry of Russian Academy of Sciences, with its high professionalism and competence, will take care of the logistics and hospitality during the Symposium. We are happy welcoming you in Moscow!

Academician Boris F. Myasoedov  
Academician Aslan Yu. Tsivadze  
Konstantin E. German



**A.Yu.Tsivadze, B.F. Myasoedov, A.M. Chekmarev, B. Bryskin**

## TECHNETIUM: NEW TRENDS IN INVESTIGATION AND APPLICATION

K.E. German<sup>1</sup>, F. Poineau<sup>2</sup>

<sup>1</sup> Frumkin Institute of Physical Chemistry and Electrochemistry of RAS (Moscow, Russia)

<sup>2</sup> University of Nevada Las Vegas (Las Vegas, USA)

Technetium has a noble history of scientific community research efforts with different periods characterized by the principle interest sliding from broad general chemistry to nuclear medicine, ecology, transmutation etc...[1-3]. Great efforts in elaboration of Tc separation technology resulted in production of more than 1 kg of technetium in form of  $\text{KTcO}_4$  and some about 0.5 kg of technetium in metallic state [4] in IPC AN USSR (ex-IPCE RAS). This quantity was distributed in between the institutions of MINATOM and USSR Academy of Sciences in 1976 – 1982 providing extensive scientific researches. Many Tc applications having been considered at that time including battery production, standard radiosource production, ophthalmic applicators, defectoscopes etc. all these being based on the Tc metal foil produced by Oleg Balakhovsky (Fig. 1).



Fig. 1. Oleg Balakhovsky demonstrating the effect of Tc foil radiation onto the electroscope discharge.

Finally the production of Tc was organized in USSR and by the 1986 year more than 100 kg of Tc was separated from the spent nuclear fuel reprocessing solutions. The Chernobyl accident was the evident reason for the refocussing of the researches from nuclear applications to the



environmentally faced studies. The IPCE RAS was also engaged in these new research efforts that determined the investigation subjects for the 1990-2000 decade.

Surprisingly we could note that the last years are marked with the return to broadly understood general chemistry. This is evidently due to the improvement of the research investigating methods, now making possible to readdress the questions that were waiting the answer for many decades.

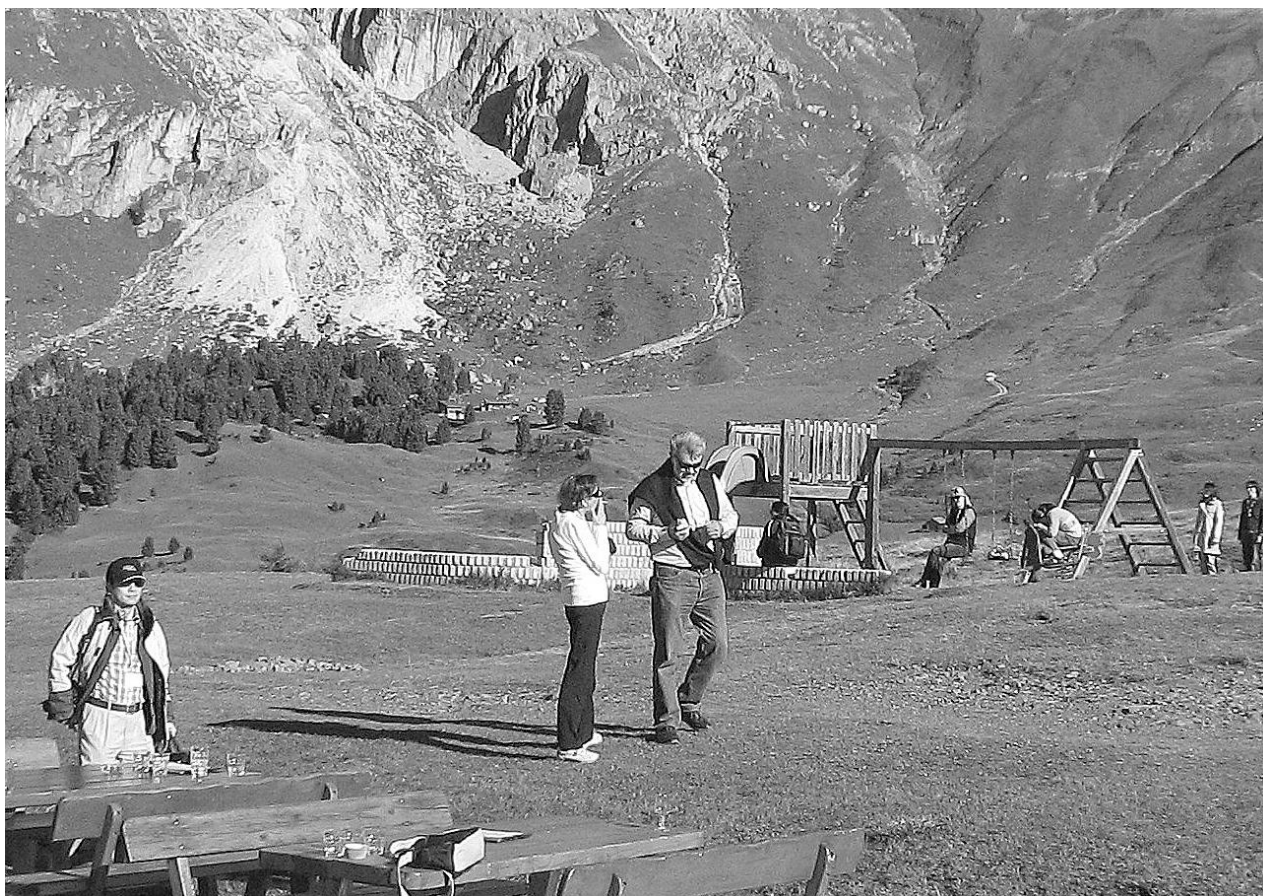
It is worth recalling the main gaps in Tc chemistry and thermodynamics having been indicated in 1999 [1]. Joseph A. Rard (Fig.2) and co-authors have summarized the most important information needed to improve the quality of the technetium thermodynamic data base for the safety assessment of nuclear waste disposal. These items included some questions of Tc metal state, numerous oxides (also mixed-valent oxides), protonation constants for the formation of undissociated pertechnetic acid,  $\text{TcO}_3(\text{OH})(\text{aq})$  or  $\text{HTcO}_4(\text{aq})$  and its genesis in acids, numerous inconsistency of solubility measurements ( $\text{TcO}_2(\text{s})$ ,  $\text{TcS}_2(\text{s})$ ,  $\text{Tc}_2\text{S}_7(\text{s})$ , etc.) and the properties of  $\text{TcF}_6(\text{s})$ .



Fig. 2. Joseph Rard (left) is perfect demonstrating [1]:  
Tc chemistry is not just a kitchen but also chemical thermodynamics (Oarai, Japan – 2005)

Some of these were tried to be answered during the last decade and reviewed in this work. Important progress was obtained in nano-disperse Tc metal structure and properties and its dependence on the carbon impurity present [2-3]. Better understanding of Tc sulfides and their solubility was due to a combination of ultramicrocentrifugative speciation and EXAFS spectroscopic structure determination [4-5]. Another improvement gained for Tc(VII) species including  $\text{TcO}^{3+}$  and pertechnic acid evolution was due to both synthetic and spectroscopic (Tc-NMR and EXAFS) studies [6-7].

It's worth mentioning that a huge part of technetium chemistry mostly of radiopharmaceutical value was systematically discussed at the TERACHEM International Symposiums serie having been conducted by Prof. U. Mazzi and his colleagues (the latter hold in Bressanone in 2010 (Fig.3).



Prof. U. Mazzi while organizing the tour to Dolomites for TERACHEM 2010 delegates

Very indicative for metal carbide and many other substance analyses are the implementations of wavelet ideas for the EXAFS results treatment that are also discussed at ISTR2011 [8]. It is also interesting to note that even some simple binary compounds of Tc are still to be discovered: synthesis, spectroscopic and structural characterization of several new technetium binary halides, including  $TcCl_2$ ,  $TcCl_3$ ,  $TcBr_3$  and  $TcBr_4$  and the formation mechanism of these new halides was presented and discussed at this Symposium [9,10]. Application of Tc was critically reconsidered, with huge interest to be paid to Tc transmutation into stable Ru-100. Anyhow some other new applications were focused with the attempts providing direct usage of Tc radioactivity.

### References.

1. *Rard, J.A., Rand, M.H., Andregg, G., Etc. Chemical Thermodynamics, Vol. 3. Chemical Thermodynamics of Technetium (M.C.A. Sandino and E. Östhols, eds.), OECD Nuclear Energy Agency, Data Bank, Issy-les-Moulineaux, France 1999, 567 p.*
2. German K.E., etc. // *Journ. Nucl. Radiochem. Sci.* (2006) V. 6, No.3, pp. 211-214.
3. Peretrukhin V.F., etc. // *J. de la Soc. de Chim. D.I. Mendeleiev* (2007) v.51, No 6, p.11-23.
4. German K., Reich T., Sergeant C., etc. Proceedings of OECD/NEA Workshop on pyrochemistry. 14-16 March 2000. Palais-des-Papes, Avignon (France).
5. M. Simonoff, K. E. German, C. Sergeant etc. *Journee Radiochimie 2000, Gif-sur-Yvette, 28-29 September, 2000, France.*
6. F.Poineau, Ph.F.Weck, K.German, etc. // *Dalton Trans.* (2010) 39 (37), pp. 8616-8619.
7. Supel J., Abram U. Hagenbach, etc. // *Inorg. Chem.* (2007) 46(14), 5591-5595.
8. V.Yu Murzin., Ya.V.Zubavichus, M.V.Chukalina, et all. *This issue.* 2011, p.172.
9. F. Poineau, E. V. Johnstone, Ph. F. Weck, E. Kim, P. M. Forster, B. L. Scott, A. P. Sattelberger, K. R. Czerwinski. // *J. Am. Chem. Soc.*, 2010, 132 (45), pp. 15864–15865.
10. F. Poineau, A. P. Sattelberger, B. L. Scott, P. Forster, Ph. Weck, E. Johnstone and K. R. Czerwinski. *This issue.* 2011, p.31 and 60.

## **RHENIUM IN NICKEL-BASE SUPERALLOYS FOR SINGLE CRYSTAL GAS TURBINE BLADES**

E.N. Kabloy, N.V. Petrushin, V.V. Sidorov

All-Russian Scientific Research Institute of Aviation Materials, Moscow, admin@viam.ru

Development of high effective materials and new technologies for their manufacture and application is the major factor of development of competitive aviation gas turbine engines. According to CIAM data in the period from 1970 to 2000 dynamics of efficiency increase of aviation engines of different generations was characterized by increase in the maximal gas temperature at the input of the turbine from 1300-1450 K (third generation) up to 1800-1950 K (fifth generation). Such growth has been attained owing to creation of new materials, basically nickel-base superalloys with high operational characteristics, perfection of cooling systems of turbine blades. In promising engines of the sixth generation the gas temperature will increase up to 2000-2200 K due to application in the turbine of single crystal blades from the rhenium and ruthenium alloyed nickel-base superalloys.

Studies carried out have shown that rhenium is one of the most effective alloying elements in nickel-base superalloys. Rhenium alloying was found to increase the incipient melting temperatures of alloys and the temperature of complete dissolution of a hardening  $\gamma'$ -Ni<sub>3</sub>Al-based phase in a nickel-based  $\gamma$  solid solution. Rhenium decreases the self-diffusion coefficient of nickel and hinders diffusion processes in nickel alloys at operating temperatures.

The rhenium concentration reaches 3-4 wt.% in second generation single crystal superalloys and 5-6% in third generation superalloys. The superalloys designed at the All-Russian Scientific Research Institute of Aviation Materials (VIAM) contain 6-12% Re. These high-rhenium superalloys with a single-crystal structure were designed with a computer.

It is shown that for stabilization of phase structure and decrease in probability of precipitation of TCP phases it is possible to alloy with ruthenium high-rhenium nickel superalloys. Joint alloying with rhenium and ruthenium has synergetic influence on characteristics of single crystal nickel superalloys. As a result their high-temperature stress rupture and temperature efficiency considerably increases. Application in engines of developed rhenium- and ruthenium –bearing nickel superalloys having stress rupture of 120-130MPa at temperature of 1100 °C for 1000 hours, will provide increase by 50-60 °C of working temperature of single crystal blades made of these alloys.

The domestic sources of rhenium are examined for provision with rhenium the production of Re bearing alloys. Scientific and industrial complex on development and series production Re bearing superalloys is arranged in VIAM.





Organizing Committee at the Opening lecture  
(acad. B.F. Myasoedov, acad. A.Yu. Tsyvadze, A. Belova (ROSNANO), S. Vorobiev (ISTC), second row: workgroup Ya. Obruchnikova, N. Kravchenko and E. Nazarov)



## ISTR RETROSPECTIVES AND PROSPECTS - IN VIEW POINTS OF NUCLEAR FUEL CYCLE

**M.Ozawa.**

Tokyo Institute of Technology, Research Laboratory for Nuclear Reactors,  
2-12-1 N-21, Ookayama, Meguro-ku, Tokyo, 152-8550, Japan

### History of Technetium Symposium

1. Tc 1993 – Topical Symposium on the Behavior and Utilization of Technetium (Sendai, Japan, March 18-20, 1993)
2. Tc 1996 – Russian-Japanese Seminar on Technetium (Moscow, Russia, July 1-5, 1996)
3. Tc 1999 – 2nd Japan - Russian Joint Seminar on Technetium (Shizuoka, Japan Nov.29 - Dec.2 1999)
4. Tc 2002 – 3rd Russian - Japanese Seminar on Technetium (Dubna, Russia, June 23 – July 1, 2002)
5. IST 2005 – International Symposium on Technetium – Science and Utilization (Oarai, Ibaraki, Japan, May 24-27, 2005) (Fig. 1).
6. IST 2008 – 6th International Symposium on Technetium and Rhenium – Science and Utilization (Port Elizabeth, South Africa, October 7-10, 2008) . The 6<sup>th</sup> delegates honored Prof.Yoshihara for his pioneering role in the Tc chemistry. (Fig.2).
7. ISTR 2011 - 7th International Symposium on Technetium and Rhenium – Science and Utilization (Moscow, Russia - July 4-8, 2011)
8. ISTR2014 -8<sup>th</sup> (USA)

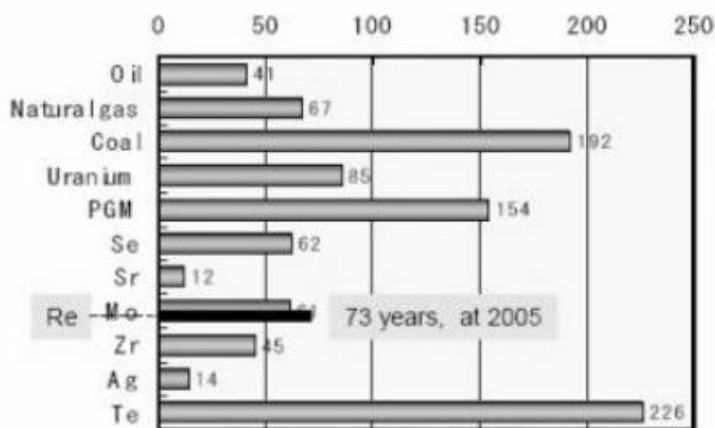


**Fig. 1. JAEA Children's Science Center, O-arai, was attacked by TSUNAMI. Re-opened on 19<sup>th</sup> April, 2011**



Fig.2. International Advisory Board of the ISTR2008

*Will Tc itself be a Rare Metals, or a substitute for Re ?*



R/P Ratio (year) at 2004 on Estimated Available Time

- Re is the rarest element in the earth and the universe, and will probably be deficient within a 100 years together with Mo.
- On the contrary, Tc is rather rich in the spent nuclear fuel.

• Natural fossil fuels (Oil, Gas) and U are limited in 40-80 years. Rare metals and coal are limited to around 200 years.

• Worldwide CO<sub>2</sub> issue (waste of Oil !) is inevitable.

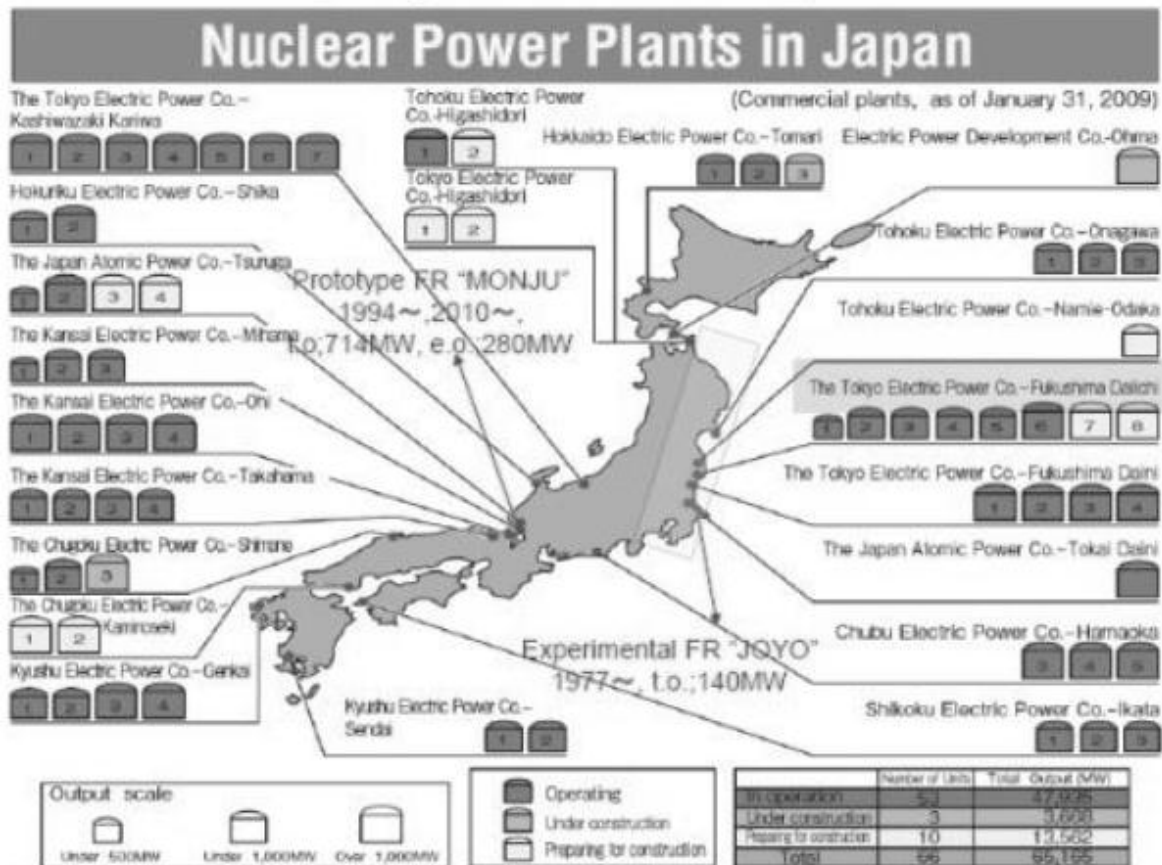
← F/W Nuclear (FBR) Renaissance  
 A/W → Fukushima NPP

• In turn, PGM seems to be rather abundant, however its resource is extremely localized. Strategy of producing countries will strongly affect the stable supply and prices.

• Rare earth resource is also world-widely localized. About 1% of national GDP will drop if ca. 20% of those supply decreased.

← F/W Urban Mine, Nuclear Ore

## Fukushima NPP crisis



## Tc released by Chernobyl

Radionuclide released during the Chernobyl Accident

Core inventory on 26 April 1986			Total release during the accident	
Nuclide	Half-life	Activity (PBq)	Percent of inventory	Activity (PBq)
<sup>133</sup> Xe	5.3 d	6500	100	6500
<sup>131</sup> I	8.0 d	3200	50 - 60	1760
<sup>134</sup> Cs	2.0 y	180	20 - 40	54
<sup>137</sup> Cs	30.0 y	280	20 - 40	85
<sup>132</sup> Te	78.0 h	2700	25 - 60	1150
<sup>89</sup> Sr	52.0 d	2300	6	115
<sup>90</sup> Sr	28.0 y	200	6	10
<sup>140</sup> Ba	12.8 d	4800	6	240
<sup>95</sup> Zr	1.4 h	5600	4	196
<sup>99</sup> Mo	67.0 h	4800	4	168
<sup>103</sup> Ru	39.6 d	4800	4	168
<sup>106</sup> Ru	1.0 y	2100	4	73
<sup>141</sup> Ce	33.0 d	5600	4	196
<sup>144</sup> Ce	285.0 d	3300	4	116
<sup>239</sup> Np	2.4 d	27000	4	95
<sup>238</sup> Pu	86.0 y	1	4	0.035
<sup>239</sup> Pu	24 400.0 y	0.85	4	0.03
<sup>240</sup> Pu	6 580.0 y	1.2	4	0.042
<sup>241</sup> Pu	13.2 y	170	4	6
<sup>242</sup> Cm	163.0 d	26	4	0.9

total **73559**                      total **10933** 15% released  
**7.3E19Bq**                              **1.09E19Bq**

from Chernobyl: Assessment of Radiological and Health Impact. Chapter 2.  
 The release, dispersion and deposition of radionuclides.  
 2002 update of Chernobyl: Ten years on  
<http://www.oecd-nea.org/rp/chernobyl/c02.html>

### γ Contamination of a returned Japanese traveler from Kiev

粒子状の放射性物質が付き者 Total 57.1nCi

<sup>131</sup> I	16 (μCi)	28 (%)
<sup>95</sup> Zr- <sup>95</sup> Nb	8	14
<sup>103</sup> Ru- <sup>103m</sup> Rh	6.5	11.4
<sup>141</sup> Ce	6.0	10.5
<sup>144</sup> Ce- <sup>144</sup> Pr	5.4	9.5
<sup>140</sup> Ba- <sup>140</sup> La	5.0	8.8
<sup>132</sup> Te- <sup>132</sup> I	2.5	4.4
<sup>239</sup> Np	2.5	4.4

<sup>137</sup> Cs- <sup>137m</sup> Ba	0.7	1.2
<sup>134</sup> Cs	0.4	0.7
<sup>99</sup> Mo- <sup>99m</sup> Tc	0.2	0.4



## Tc released by Fukushima

### Water

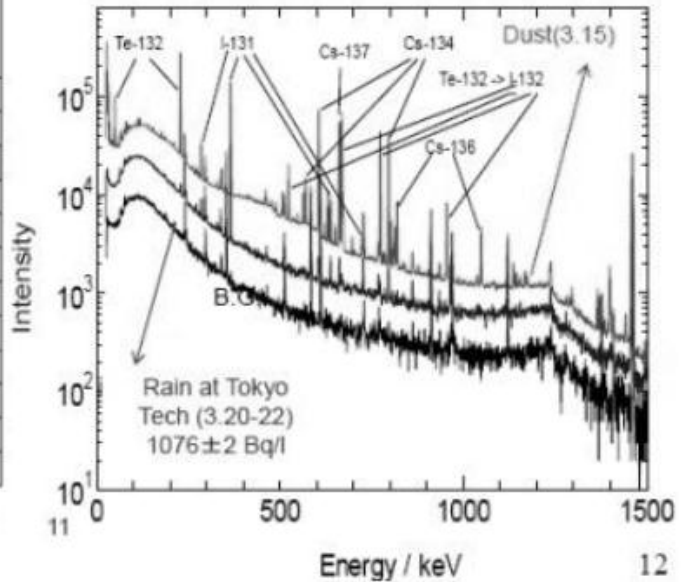
• Analysis of contaminated water at TB of Fukushima 1

Nuclides	Bq/cc		Percent of Inventory (dissolved ratio)
	Measured (by TEPCO)	Core Inventory	
Y-91			
Co-60	7.60E+02		
Tc-99m	2.50E+03	1.98E+07	0.013%
I-131	1.20E+06	9.93E+07	1.208%
Cs-134	1.80E+06	7.27E+07	2.474%
Cs-136	2.30E+04	1.01E+07	0.227%
Cs-137	1.80E+05	5.88E+07	0.306%
Ba-140	5.20E+04	2.51E+08	0.021%
La-140	9.40E+03	2.89E+08	0.003%
Ce-144	2.20E+06	4.07E+08	0.540%
合計	5.47E+06	1.21E+09	0.453%
I, Cs	3.20E+06	2.41E+08	1.329%

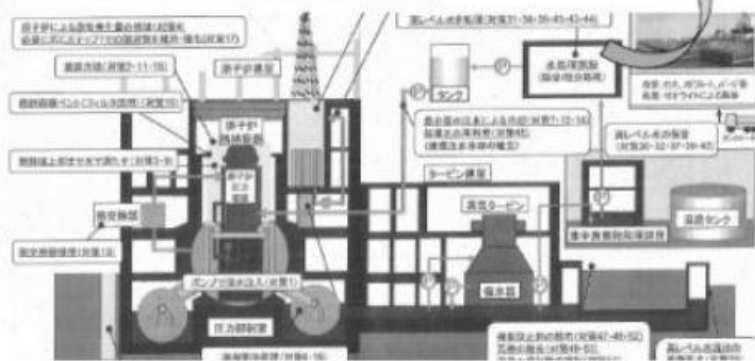
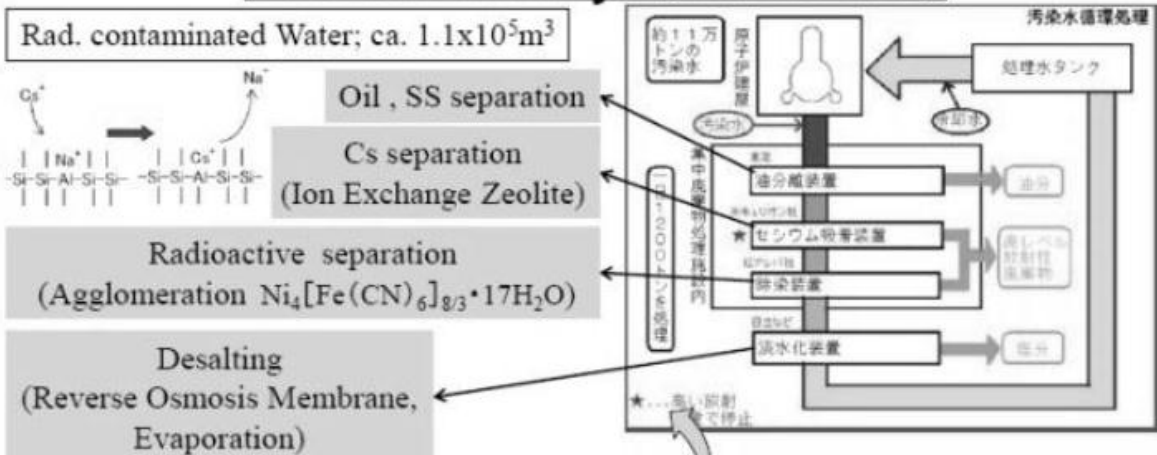
\*Tc release from Fukushima NPP 1 is estimated to be very little

### Atmosphere

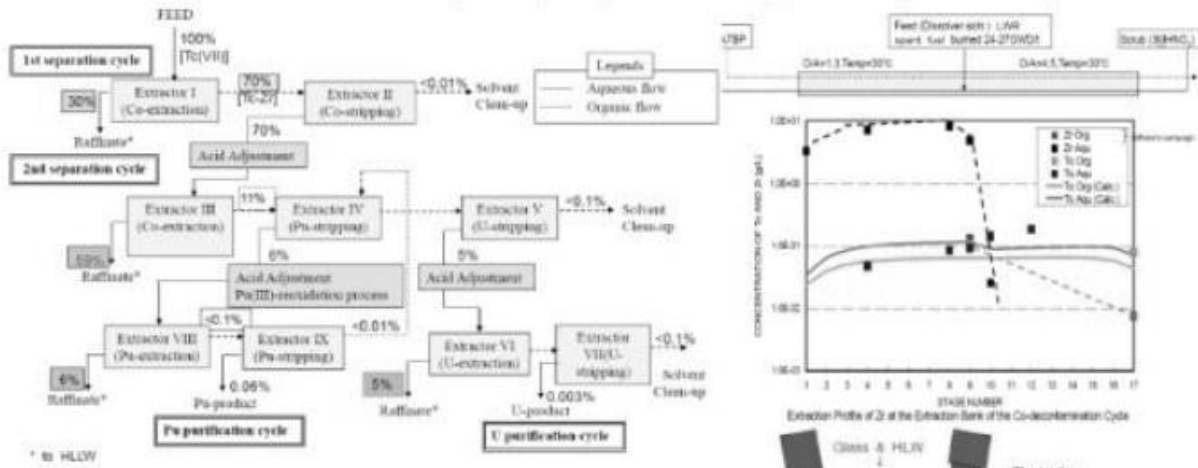
γ-Spectrum of samples at Tokyo  
\*No <sup>241</sup>Am (<sup>241</sup>Pu) and <sup>99</sup>Mo detected at Tokyo



## Decontamination of Rad. water in TB

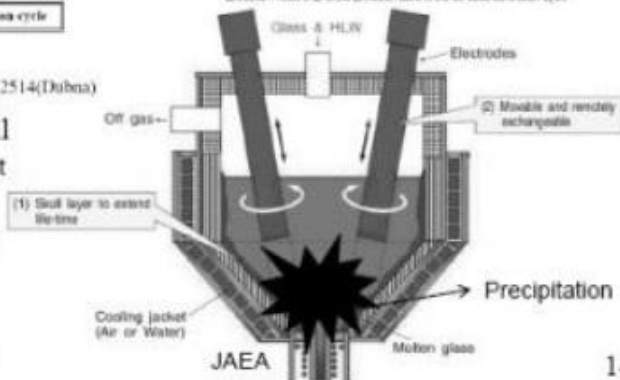


## Nuclear Fuel Cycle (Reprocessing, Vitrification)



Tc Balance at the Tokai-Reprocessing Plant, Tc2002, Paper No.2514(Dubna)

- PGM elements, especially RuO<sub>2</sub> particle will increase viscosity of melted glass, and might be precipitated at the bottom of melter. RuO<sub>2</sub> also will cause troubles by increasing of electrical conductivity of melted glass.
- Behavior of other PGM, Zr, Mo and TcO<sub>2</sub> must also investigated in this point of view.



14

## Tc prospects, beyond the catastrophe (Conclusion)

- 1 Separation (Nuclear Fuel Cycle)
  - Environmental (land, sea) contamination and remediation, Bioaccumulation
  - Reprocessing scheme, especially undissolved residue
  - Vitrification behavior; prior separation of PGM, Tc, Mo?
- 2 Utilization
  - Catalyst (Hydrogen production, Fuel-cell, etc)
  - Material (Anti-corrosive, Heat-resistant alloy), Re substitute
  - <sup>99m</sup>Tc generation (<sup>235</sup>U fission, Mo(*n, γ*), (*n, 2n*)) for medical use
  - β<sup>-</sup> source radioisotope micro battery ?, like <sup>63</sup>Ni, <sup>147</sup>Pm (Cornell Univ., etc)
- 3 Transmutation
  - "Raw element" for precious metal production

Tc Battery  
IPC-RAS

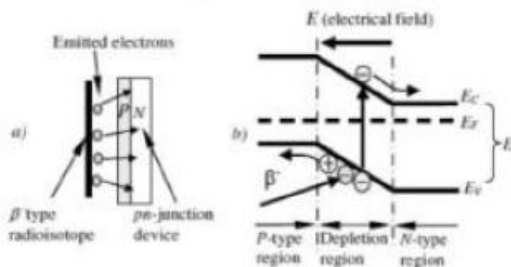


Figure 1. Betavoltaic effect a) Schematic diagram of betavoltaic battery b) Potential diagram of a betavoltaic effect



## Fundamental Research in Physics and Chemistry of Tc and Re.



**A. BELOVA (ROSNANO), S. VOROBIEV (ISTC) AND  
M. OZAWA (SESSION CHAIRMAN)**

## SPECTROSCOPIC AND PHOTOPHYSICAL PROPERTIES OF CHALCOGENIDE-CAPPED OCTAHEDRAL HEXARHENIUM COMPLEXES WITH N-HETEROAROMATIC LIGANDS

Takashi Yoshimura, Chiaki Suo, Shoji Ishizaka, Akitaka Ito, Eri Sakuda, Atsushi Shinohara, and Noboru Kitamura

Department of Chemistry, Graduate School of Science, Osaka University, Toyonaka 560-0043, Japan,  
tyoshi@chem.sci.osaka-u.ac.jp

Department of Chemical Sciences and Engineering, Graduate School of Chemical Sciences and Engineering,  
Department of Chemistry, Faculty of Science, Hokkaido University, Sapporo 060-0810, Japan

It is known that the 24 valence octahedral hexanuclear molybdenum, tungsten, and rhenium complexes with an  $M_6Q_8$  core ( $M = \text{Re}, Q = \text{S}, \text{Se}, \text{Te}; M = \text{Mo}, \text{W}, Q = \text{Cl}, \text{Br}, \text{I}$ ) show photoluminescence.

In this study, the new hexarhenium complexes with N-heteroaromatic ligands were synthesized and their photoluminescent properties were characterized.

Photoirradiation of an  $\text{CH}_3\text{CN}$  solution of  $(\text{Bu}_4\text{N})_4[\text{Re}_6\text{S}_8\text{Cl}_6]$  in the presence of 10 equiv. of pyridine (py) gave  $(\text{Bu}_4\text{N})_3[\text{Re}_6\text{S}_8\text{Cl}_5\text{py}]$ . Emission spectroscopy in deaerated  $\text{CH}_3\text{CN}$  at 296 K was conducted at 355 nm excitation.

The mono-py complex exhibited broad and structureless emission with the maximum wavelength ( $\lambda_{\text{em}}$ ) = 754 nm, the emission quantum yield ( $\Phi_{\text{em}}$ ) = 0.040, and the emission lifetime ( $\tau_{\text{em}}$ ) = 4.6  $\mu\text{s}$ .

The spectroscopic and photophysical data are similar to those of  $(\text{Bu}_4\text{N})_4[\text{Re}_6\text{S}_8\text{X}_6]$  and the previously reported py coordinate complexes  $(\text{Bu}_4\text{N})_{4-n}[\text{Re}_6\text{S}_8\text{Cl}_{6-n}(\text{py})_n]$  ( $n = 2, 3$ ). The present results indicate that the emissive state is the cluster core-centered excited triplet state.

A mono-ppy (ppy = 4-phenylpyridine) complex  $(\text{Bu}_4\text{N})_3[\text{Re}_6\text{S}_8\text{Cl}_5\text{ppy}]$  were synthesized by the similar method to prepare the mono-py complex. The complex showed emission at 739 nm ( $\Phi_{\text{em}} = 0.0089$ ) in deaerated  $\text{CH}_3\text{CN}$  and at 690 nm in the crystalline phase at 296 K with an excitation wavelength at 355 nm. The emission lifetime ( $\tau_{\text{em}}$ ) of 0.33  $\mu\text{s}$  in  $\text{CH}_3\text{CN}$  indicates that the excited-state is composed a triplet character. The transient absorption spectrum in deaerated  $\text{CH}_3\text{CN}$  showed a band at 410 nm. This spectral feature is well observed in the absorption of aromatic anion; the absorption spectrum of the  $\text{ppy}^-$  also shows the bands in these regions. These facts indicate that the excited-state of mono-ppy complex involves the  $\pi^*$  character of ppy.

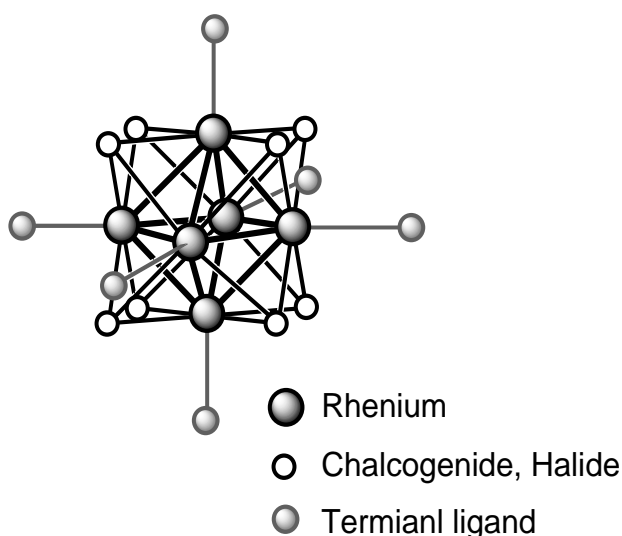


Fig.1. Octahedral Hexarhenium Complex.



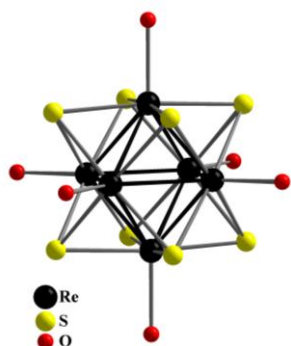
## 1.2.

**RHENIUM OCTAHEDRAL CHALCOHYDROXO CLUSTER COMPLEXES**

Y.V. Mironov, S.S. Yarovoi, K.A. Brylev, V.E. Fedorov

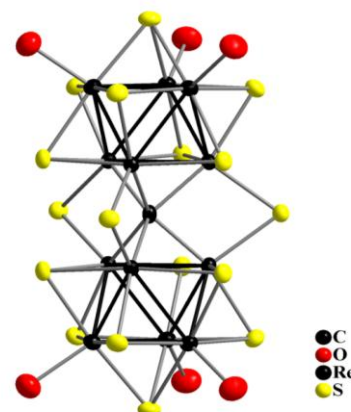
Nikolaev Institute of Inorganic Chemistry of SB RAS, Novosibirsk,  
Russian Federation, e-mail: yuri@niic.nsc.ru

In recent years considerable research has been put into the design of solids with extended polymeric structures based on rhenium cluster cyano complexes. Here we present a new group of compounds that are also able to form polymeric compounds— anionic octahedral chalc hydroxo complexes  $[\text{Re}_6\text{Q}_8(\text{OH})_6]^{4-}$  ( $\text{Q} = \text{S}$  or  $\text{Se}$ ) and bioctahedral thiohydroxo one  $[\text{Re}_{12}\text{CS}_{17}(\text{OH})_6]^{6-}$ . The  $\text{Re}_6$ -based complexes were synthesized by the reaction of  $\text{Re}_6\text{Q}_8\text{Br}_2$  with molten  $\text{KOH}$  in the air, while the  $\text{Re}_{12}$  one was obtained by the reaction of  $\text{ReS}_2$  with  $\text{KCN}$  at  $750^\circ\text{C}$  with further interaction of the obtained product with molten  $\text{KOH}$ .



$[\text{Re}_6\text{Q}_8(\text{OH})_6]^{4-}$  ( $\text{Q} = \text{S}, \text{Se}$ ) anions consist of six rhenium atoms forming an octahedron, eight chalcogen atoms ( $\text{S}$  or  $\text{Se}$ ) form a cube around the octahedron.  $\text{OH}$  terminal group coordinates each  $\text{Re}$  atom.

Cluster unit  $[\text{Re}_{12}\text{CS}_{17}(\text{OH})_6]^{6-}$  consists of two  $\text{Re}_6$  octahedra bonded by three  $\mu_2\text{-S}$  bridges and one common  $\mu_6\text{-C}$  atom. Each  $\text{Re}_6$  cluster is capped by 7  $\mu_3\text{-S}$  and additionally by  $\text{C}$  ligand; one might say that here the typical octahedral cluster core  $\{\text{Re}_6\text{Q}_8\}$  (where  $\text{Q} = \text{S}_7\text{C}$ ) is formed. Such bonding and coordination allow to recognize in this structure the trigonal  $\mu_6\text{-C}$ -centered prisms  $\{\text{Re}_6\text{C}\}$  in which the triangle faces belong to two adjacent  $\text{Re}_6$  octahedra. Six outward  $\text{Re}$  atoms (three from each  $\text{Re}_6$  cluster unit) are coordinated by  $\text{OH}$  ligands.



In this work we present the data on preparation of  $\text{OH}$ -bridged complexes based on cluster anions  $[\text{Re}_6\text{Q}_8(\text{OH})_6]^{4-}$  ( $\text{Q} = \text{S}, \text{Se}$ ) and cations of the II main group elements. The first example of chain structure with 3d transition metals, namely,  $[\text{Ni}(\text{en})_2(\text{H}_2\text{O})_2][\{\text{Ni}(\text{en})_2\}\text{Re}_6\text{S}_8(\text{OH})_6]$  has been also obtained. Also we present the data of study of the substitution reactions of  $\text{OH}$  ligands by organic and inorganic ligands.

The authors are grateful to Russian Foundation for Basic Research (grants N 11-03-00157-a and 10-03-01040-a) for financial support.



1.3.

## TECHNETIUM HALIDES: FROM MOLECULAR TO EXTENDED STRUCTURES

Frederic Poineau<sup>1\*</sup>, Alfred P. Sattelberger<sup>2</sup>, Brian L. Scott<sup>3</sup>, Paul Forster<sup>1</sup>,  
Philippe Weck<sup>1</sup>, Erik Johnstone<sup>1</sup> and Kenneth R. Czerwinski<sup>1</sup>

<sup>1</sup> Department of Chemistry, University of Nevada Las Vegas, Las Vegas, NV, 89154, USA

<sup>2</sup> Energy Sciences and Engineering Directorate, Argonne National Laboratory, Argonne, IL 60439, USA

<sup>3</sup> Materials Physics and Applications Division, Los Alamos National Laboratory, Los Alamos, NM 87545, USA

\*poineauf@unlv.nevada.edu

Binary transition metal halides exhibit a rich chemistry, and the study of their structure, bonding and physical properties permits a better understanding of the physico-chemical trends across the periodic table.

Because technetium and rhenium are members of the same group in the periodic table, the occurrence of analogous coordination compounds is expected. In the case of the halides, thirteen binary phases have been reported for rhenium, but only three were, until recently, known for technetium, i.e., TcF<sub>6</sub>, TcF<sub>5</sub>, and TcCl<sub>4</sub>.

The direct stoichiometric reactions between technetium metal and elemental bromine or chlorine as well as the reaction between the quadruple bonded dimer Tc<sub>2</sub>(OAc)<sub>4</sub>Cl<sub>2</sub> with HX<sub>g</sub> (X = Cl, Br) have, to the best of our knowledge, never been reported.

In this talk, we provide details of these reactions, which have led to the synthesis, spectroscopic and structural characterization of several new technetium binary halides, including TcCl<sub>2</sub>, TcCl<sub>3</sub>, TcBr<sub>3</sub> and TcBr<sub>4</sub>.

The structures and formation mechanism of these new halides will be presented, discussed, and compared with those of rhenium and molybdenum homologues.

Emphasis will be on TcCl<sub>2</sub> which exhibits a new solid-state structure type with metal-metal multiple bonds. Synthetic reaction using technetium binary halides as precursor will also be presented.

1.4.

## SYNTHESIS OF RHENIUM ALKOXIDES VIA ANODIC DISSOLUTION

E.N. Pryamilova, O.V. Chernyshova, D.V. Drobot

Lomonosov's Moscow State Academy of Fine Chemical Technology, Moscow, Vernadskogo avenue 86  
(e-mail: [san13greal@yandex.ru](mailto:san13greal@yandex.ru), [oxcher@mail.ru](mailto:oxcher@mail.ru))

At the first time the research of the process of rhenium anodic dissolution in absolute alcohols was carried out using the electrochemical technological complex "ECC – 1012", the measurement of potential being based on noncompensatory feed-back method. The device allows both to investigate, and to realize technological processes in optimum modes at controllable parameters.

The main application of rhenium is preparation of structural alloys with other refractory metals. These alloys possess valuable mechanical properties and stability against evaluated temperature and corrosive medium. Another application of rhenium is preparation of highly-active and selective catalysts for organic and hetero-organic synthesis. The using of rhenium alkoxides and oxoalkoxides permits to escape difficulties occurring in the traditional methods of preparation of Re-based alloys and oxide materials.

The electrochemical synthesis of rhenium alkoxides is of heightened interest, because it is flexible, less complicated in hardware design and it allows carrying out the process under maximum control via setting definite parameters. The electrochemical synthesis of alkoxides corresponds to the anodic dissolution of rhenium in the required non-aqueous alcohol in the presence of a background electrolyte. According to this method the processes of rhenium anodic dissolution in absolute alcohols ROH (R = Me, Et, i-Pr etc) with the addition of LiCl were researched and rhenium complexes  $\text{Re}_4\text{O}_4(\text{OEt})_{12}$ ,  $\text{Re}_4\text{O}_2(\text{OBu}^n)_8 \cdot 8\text{Bu}^n\text{OH}$ ,  $\text{Re}_4\text{O}_6(\text{O}^i\text{Pr})_{10}$ ,  $\text{Re}_4\text{O}_6(\text{OMe})_{12}$  etc were obtained for the first time with further investigation of their properties [1].

In order to observe the influence of electrochemical factors on the anodic dissolution the number of processes were carried out under controlled potential. The constancy of electrochemical parameters was supported by means of electrochemical complex "ECC – 1012". Besides, heteroligand complexes of common formulas  $\text{Re}_4\text{O}_x(\text{OEt})_y(\text{OPr}^i)_z$ ,  $\text{Re}_4\text{O}_x(\text{OEt})_y(\text{OCH}_2\text{CF}_3)_z$  were prepared for the first time. The possible mechanism of rhenium anodic dissolution and its further behavior in the solution was suggested.

The research was carried out under the support of the RFBR grant № 09-03-00328.

1. Drobot D.V., Shcheglov P.A. Reviews, Rhenium alkoxides // Russian Chemical Bulletin, International Edition. October 2005. v. 54, № 10, p. 2177-2188.

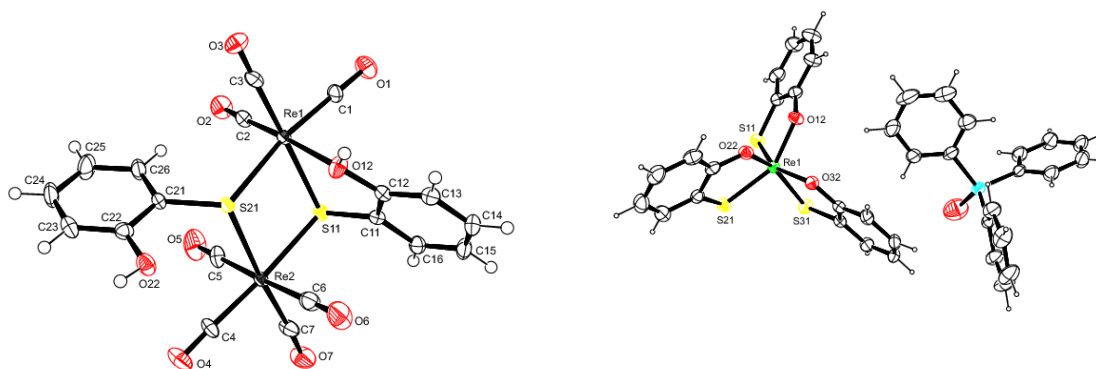
## 1.5.

**RHENIUM COORDINATION CHEMISTRY: OLD LIGANDS DIE HARD**Thomas Gerber<sup>1</sup>, Kim Potgieter<sup>1</sup>, Peter Mayer<sup>1</sup> Chemistry Department, Nelson Mandela Metropolitan University, 6000 Port Elizabeth, South Africa<sup>2</sup> Chemistry Department, Ludwig-Maximilians University, D-18377 Munich, Germany

The development of the coordination chemistry of Re and Tc has mainly focused on the +V and +I oxidation states, since they are easily accessible from the permethylates. There is currently a general notion amongst researchers in this field that there is very little scope in the further exploration of the coordination chemistry of these oxidation states, since all routes and possibilities have been exhausted, and the new focus has shifted to the states +II, +III, +IV and +VI.

We have used relatively simple and common organic molecules, like 2-aminobenzenethiol, 1,2-diaminobenzene, 2-aminophenol, imidazoles, thiazoles, and their derivatives, as possible ligands for rhenium(I) and (V). In many instances, surprisingly unexpected complexes were found, depending on the starting complexes used and the reaction conditions. For example, with the simple ligand 2-aminobenzenethiol, the unusual disulfide-bridged rhenium(I) complex **1** and rhenium(VI) complex **2** have been obtained.

Many other examples of unusual complexes with simple ligands will be presented and discussed in terms of their spectroscopic and crystallographic data.



## 1.6.

# REDOX BEHAVIOUR OF THE Tc(VII)/Tc(IV) COUPLE IN DILUTED NaCl SOLUTION IN VARIOUS REDUCING SYSTEMS

Taishi Kobayashi, Xavier Gaona, David Fellhauer<sup>1</sup>, Marcus Altmaier

Karlsruhe Institute of Technology, Institute für Nukleare Entsorgung, P. O. Box 3640, 76021 Karlsruhe, Germany

<sup>1</sup>European Commission, Joint Research Centre, Institute for Transuranium Elements, P. O. Box 2340, 76125 Karlsruhe, Germany

**Keywords:** technetium, redox behaviour,  $\text{TcO}_2 \cdot x\text{H}_2\text{O}(\text{coll,hyd})$ ,  $E_h$ -pH conditions, dilute NaCl

### Abstract:

The redox behaviour of the Tc(VII)/Tc(IV) couple over a wide range of pH conditions in 0.1 M NaCl/NaOH solution was investigated in various homogenous and heterogenous reducing systems. Stock solution of Tc(VII) was added to each reducing system, and after given periods, the Tc concentration was measured and compared to the initial Tc(VII) concentration ( $1 \cdot 10^{-5} \text{ mol/dm}^3$ ). The results can be systematized according to  $E_h$ -pH conditions in solution and a general borderline for the reduction of Tc(VII) to Tc(IV) independent of the reducing systems is obtained. The experimental borderline is slightly lower than the calculated equilibrium line between  $\text{TcO}_4^-$  and  $\text{TcO}_2(\text{s}) \cdot x\text{H}_2\text{O}(\text{s})$ . This may suggest that more soluble solid phase such as small Tc(IV) oxyhydroxide particles are formed under the given conditions. Reaction kinetics are also discussed and correlated to the measured redox potentials and the reduction borderline.

### Introduction

The migration behaviour of <sup>99</sup>Technetium in geological systems relevant to nuclear waste disposal is primarily depending on its oxidation state. In +VII oxidation state, Tc exists as the anionic  $\text{TcO}_4^-$  ion which is highly soluble and mobile in the environment, while Tc in +IV oxidation state under reducing condition is easily hydrolyzed to form sparingly soluble Tc(IV) oxyhydroxide solid phases. The redox potential of the Tc(VII)/Tc(IV) couple has been investigated in many studies by measuring the electrode potential [1-4]. Meyer et al. reduced Tc(VII) to Tc(IV) solids ( $\text{TcO}_2 \cdot 1.6\text{H}_2\text{O}$ ) electrochemically in acidic solution, and determined the standard potential of  $\text{TcO}_4^-/\text{TcO}_2 \cdot 1.6\text{H}_2\text{O}(\text{s})$  couple to be  $E^\circ = 0.747 \pm 0.004 \text{ V}$  according to  $\text{TcO}_4^- + 4\text{H}^+ + 3\text{e}^- = \text{TcO}_2 \cdot 1.6\text{H}_2\text{O}(\text{s}) + 0.4\text{H}_2\text{O}$  [4]. A comprehensive review of the thermodynamic data has been performed [5], and Tc predominant diagram ( $E_h$ -pH diagram) was proposed based on the selected thermodynamic data. On the other hand, in laboratory and natural systems, where many kinds of solution species and solids containing iron ions and minerals were used as reductants, various Tc redox behaviours have been observed [6-13]. For the reliable quantitative prediction of Tc migration behaviour, it is important to systematize Tc redox behaviour with the  $E_h$ -pH diagram from the aspect of thermodynamic data. In the current study, the redox behaviour of Tc(VII)/Tc(IV) couple was investigated in various kinds of homogeneous (anthraquinone, hydroquinone, 2-hydroxy-1,4-naphthoquinone, and  $\text{Na}_2\text{S}_2\text{O}_4$  systems) and heterogeneous (Fe(II)/Fe(III), Fe powder, Sn(II) systems) reducing systems, and compared to the thermodynamically calculated equilibrium line for  $\text{TcO}_4^-/\text{TcO}_2 \cdot x\text{H}_2\text{O}(\text{s})$  within the  $E_h$ -pH diagram. The systematization of Tc redox processes in various reducing systems offers a straightforward approach for predicting the predominant oxidation state of Tc under repository relevant conditions and is also important for the reliable prediction of Tc migration behavior in geological system.

## Experimental

Aliquots of NaTcO<sub>4</sub> stock solution was added to 0.1 mol/dm<sup>3</sup> (M) NaCl/NaOH pre-equilibrated with the following reducing agents (p.a. grade chemicals); 3 mM anthraquinone disulfonate (AQDS) (ratio of oxidized form (ox.) to reduced form (red.) = 1:3), 3 mM hydroquinone solutions, Fe(II)/Fe(III) mixed solutions and precipitates (Fe(II):Fe(III) = 1 mM:0.1 mM), 1 mM Na<sub>2</sub>S<sub>2</sub>O<sub>4</sub> solutions, Fe powder suspensions (1 mg/15 ml), 2-hydroxy-1,4-naphthoquinone (Lawsone) solutions (ox.:red. = 1:3), and 1 mM Sn(II) solutions and precipitates. The initial Tc(VII) concentration was set to 10<sup>-5</sup> M. The hydrogen ion concentration (pHc) of the sample solutions were adjusted by adding HCl (Merck) and carbonate-free NaOH (Baker), using a combination glass electrode (type ROSS, Orion) calibrated against standard buffers (pHc 2 – 12, Merck). The redox potential was measured with a combined Pt and Ag/AgCl reference electrode (Metrohm). The measured redox potentials were converted to redox potential (E<sub>h</sub>) versus the standard hydrogen electrode (S.H.E.) by the correction for the potential of the Ag/AgCl reference electrode (+208 mV for 3 M KCl junction electrolyte). The apparent electron activity (pe = -log a<sub>e-</sub>) was calculated from E<sub>h</sub> = -(RT/F) ln a<sub>e-</sub> according to the relation: pe = 16.9 E<sub>h</sub> (V) at 25 °C.

After given periods up to several months, pHc and E<sub>h</sub> values were measured and the supernatants of the solutions filtrated through 10 kD (2-3 nm) ultrafiltration membranes (Pall Life Sciences). The Tc concentration was determined by Liquid Scintillation Counting (TriCarb 2500 Tr/AB instrument, Canberra-Packard) with a detection limit of ~10<sup>-8</sup> M. The Tc oxidation state of the soluble species was investigated by solvent extraction technique, where TcO<sub>4</sub><sup>-</sup> was extracted into chloroform using 1 mM tetraphosphonylchloride (TPPC). All samples were prepared and stored in an Ar glove box under inert gas atmosphere.

## Result and Discussion

### 1. Redox behaviour of Tc(VII)/Tc(IV) in the individual reducing systems

The Tc concentrations after ultrafiltration were investigated over a wide pHc range as a function of time. In **hydroquinone solutions**, Tc concentration was constant at the initial TcO<sub>4</sub><sup>-</sup> concentration level from pHc 2.2 to 12.3 for up to 8 months (Fig. 1). The E<sub>h</sub> values are slightly higher than the equilibrium line between TcO<sub>4</sub><sup>-</sup> and TcO<sub>2</sub>·xH<sub>2</sub>O(s) calculated from the literature [5]. In

the oxidation state analysis for the samples at pHc 3.9, 8.5, and 12.3, more than 99% of total Tc in the solutions was extracted to the organic phase, indicating that dominant species is TcO<sub>4</sub><sup>-</sup> and no reduction of Tc(VII) had occurred.

In **AQDS redox buffer solutions** at pHc 5.0 and 8.1, the initial Tc concentration (10<sup>-5</sup> M) decreased rapidly to about 10<sup>-7</sup> M, suggesting that TcO<sub>4</sub><sup>-</sup> was reduced and sparingly soluble TcO<sub>2</sub>·xH<sub>2</sub>O(s) had precipitated. In contrast, at pHc 10.5, a considerably slower reduction was observed. Under alkaline condition at pHc > 11, E<sub>h</sub> values are higher than the calculated TcO<sub>4</sub><sup>-</sup> /

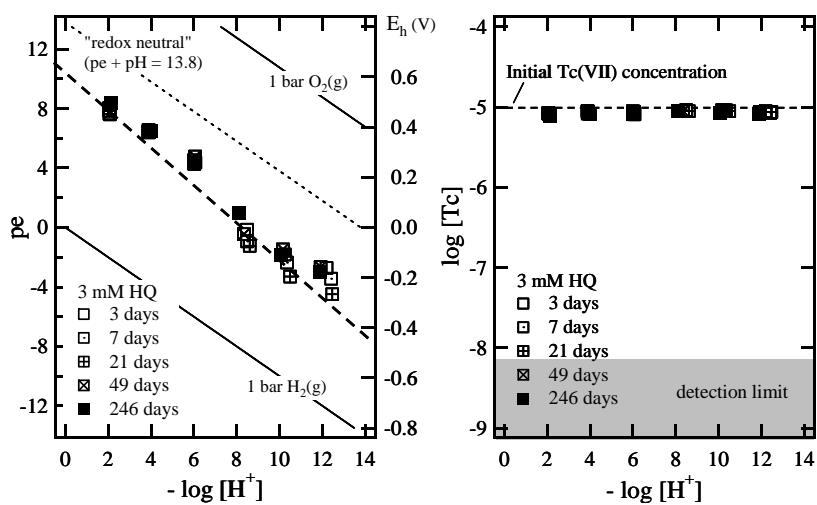


Fig. 1. E<sub>h</sub> and Tc concentrations (10 kD filtration) in 3 mM than hydroquinone (HQ) solutions as a function of pHc. The broken line represents the calculated equilibrium line between TcO<sub>4</sub><sup>-</sup> and TcO<sub>2</sub>(s)·xH<sub>2</sub>O(s) [5].

$\text{TcO}_2 \cdot x\text{H}_2\text{O}(\text{s})$  equilibrium line and the Tc concentration is constant at initial  $\text{TcO}_4^-$  concentration level, indicating that no reduction of Tc(VII) occurred within the investigated time.

In **Lawsone redox buffer solutions**, the Tc concentration decreased from the initial Tc(VII) concentration level over the entire investigated pHc range of 2 - 12. In the alkaline pH region, extremely slow reduction was observed and not reached the equilibrium state up to 85 days.

In the systems with **Sn(II)**, the white Sn(II) hydroxide precipitate was observed in the range of 5-11 before adding Tc(VII) stock solution. At higher pH the precipitates disappear and anionic Sn(II) hydrolysis species ( $\text{Sn}(\text{OH})_3^-$ ) considered dominant [14]. The Tc concentration decreases rapidly over the pHc range 2 - 11 and stable conditions are achieved within several days (Fig. 2).  $\text{pHc} > 11$ , the concentration of reduced Tc(IV) species increases with increasing pHc. The results of the oxidation state analysis by solvent extraction under these pH conditions indicate negligible contribution of remaining Tc(VII), suggesting the formation of anionic Tc(IV) hydrolysis species such as anionic  $\text{TcO}(\text{OH})_3^-$  as proposed in the literature [15,16].

In  **$\text{Na}_2\text{S}_2\text{O}_4$  solution** in the pHc range 6.9 - 10.9, the Tc concentrations in the solutions decrease and stable state conditions ( $10^{-7}$  -  $10^{-8}$  M) are achieved within a few weeks, indicating the reduction of Tc(VII) to a Tc(IV) solid. Similarly to the literature where  $\text{Na}_2\text{S}_2\text{O}_4$  was used to reduce Tc(VII) for the preparation of Tc(IV) solid phase ( $\text{TcO}_2 \cdot x\text{H}_2\text{O}$ ) [17], a black-colored Tc(IV) solid phase was immediately precipitated, however, an aging time of a few weeks is needed to reach equilibrium state. At  $\text{pHc} > 11$ , the Tc concentrations after reduction increase with an increase of pHc, suggesting the formation of anionic Tc(IV) species similar to Sn(II) system. It should be noted that at pH 6.9, the amount of Tc(VII) in the solution was more than 30 %, as under neutral pH conditions  $\text{Na}_2\text{S}_2\text{O}_4$ , which is supposed to maintain reducing conditions, is not stable over prolonged periods of a few months.

In the system of **Fe(II)/Fe(III) mixed solutions and precipitates**, at  $\text{pHc} = 2.1$  and  $\text{pe} = 11.3$ , no change in the Tc concentration was observed up to 49 days. On the other hand, at  $\text{pHc} 6.0$  ( $\text{pe} = -0.2$ ) and  $\text{pHc} 8.4$  ( $\text{pe} = -0.2$ ), Fe(II)/Fe(III) solid phase precipitates were observed before adding Tc(VII) stock solution and the Tc concentrations decreased to almost detection limit ( $10^{-8}$  M) within three days after Tc(VII) was added. The reduction of Tc(VII) with Fe(II)/Fe(III) redox buffers and suspensions of the precipitates has been reported in several studies. Cui et al. reported that the  $\text{TcO}_4^-$  concentration at  $\text{pH} < 7.5$  was constant at initial concentration level over a few days in the presence of about  $10^{-5}$  M aqueous Fe(II) [8]. Ben Said et al. showed, reduction kinetics were also depending on the Fe(II) concentration, Fe(II)/Fe(III) ratio, and initial Tc(VII) concentration [9]. The difference between Cui et al. [8], Ben Said et al. [9], and our results probably arise from the different experimental conditions such as Fe(II) concentration. Unfortunately, the redox potentials in these studies were not reported. Zachara et al. also investigated the reduction of Tc(VII) in Fe(II) systems in near neutral pH range and the redox behavior was

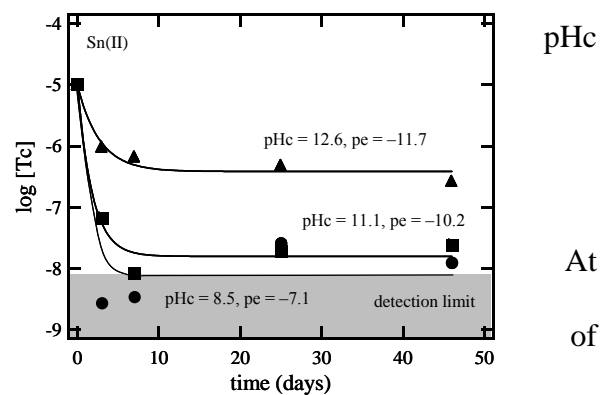


Fig. 2. Tc concentrations (10 kD filtration) in 1 mM Sn(II) solutions and precipitates as a function of time.

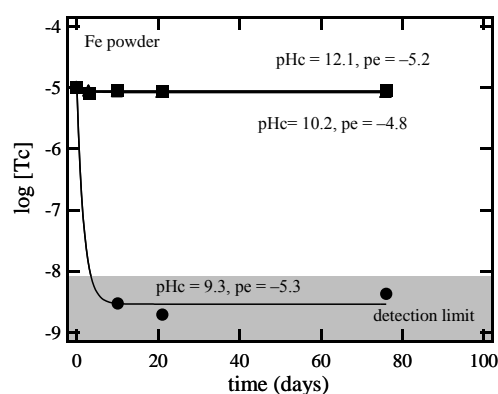


Fig. 3. Tc concentrations (10 kD filtration) in 1 mg / 15 ml Fe powder suspensions as a function of time.



supported by measured redox potentials [11]. The observed rapid reduction at pH > 6.8 generally agrees with the results in this study, although the reported  $E_h$  values were higher than those in this study.

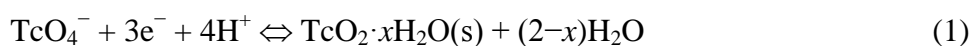
In the samples containing corroding **Fe powder** in the pHc range 6 - 10, the Tc concentration rapidly decreased to the detection limit ( $10^{-8}$  M) within three days. In contrast, no reduction was observed in all samples at pHc > 10 as shown in Fig. 3.

## 2. General trends of Tc(VII)/Tc(IV) redox behaviour and kinetic effects

The results discussed above are summarized in the  $E_h$ -pH diagram shown in Fig. 4. Samples in which no reduction was observed are plotted as filled symbols. Samples in which initial Tc(VII) was completely or partly reduced are plotted as open symbols. The bold dot line and broken line in the figure represent an experimental borderline for Tc(VII) reduction obtained in this study and the calculated equilibrium line between  $TcO_4^-$  and  $TcO_2 \cdot xH_2O(s)$  [5], respectively. The reduction of Tc(VII) to Tc(IV) occurred in both homogeneous solutions and heterogeneous suspensions with redox potentials below the experimental borderline. In the systems with redox potentials above the borderline, Tc(VII) was not reduced. It should be noted that in Fe powder systems, no reduction was observed at pHc = 10.2 and pe = -4.8 up to 49 days, on the other hand, Tc(VII) was slowly reduced at pHc = 10.5 and pe = -4.0 in

the AQDS / AH<sub>2</sub>QDS solution. In Fe powder suspension, the deviation of measured  $E_h$  values are relatively large, compared to stable  $E_h$  values in the AQDS / AH<sub>2</sub>QDS solution.

In the investigated systems, the reduction of Tc(VII) to Tc(IV) can be described with the equilibrium constant ( $K$ ), and the equilibrium line (50 % Tc(VII), 50 % Tc(IV)) is calculated from the equation (shown as broken line in Fig. 1 and 4):



$$\log K^0 = \log [TcO_4^-] - 3 pe + 4 \log [H^+] \quad (2)$$

with  $\log K^0 = 37.8 \pm 0.6$  ( $I = 0$ ) from the data selected by the Rard et al. [5]. For 0.1 M NaCl/NaOH solution, the  $K$  value was corrected using the SIT method and ion interaction coefficients of  $\epsilon(H^+, Cl^-) = 0.12 \text{ kg} \cdot \text{mol}^{-1}$  and  $\epsilon(ClO_4^-, Na^+) = 0.01 \text{ kg} \cdot \text{mol}^{-1}$  [18], which is taken as analog for  $\epsilon(TcO_4^-, Na^+)$ . Under the condition of initial Tc concentration ( $[Tc]_{init} = 10^{-5} \text{ M}$ , i.e.,  $\log [TcO_4^-] = \log ([Tc]_{init} / 2) = -5.30$ ), the calculated borderline was  $pe = -1.3 \cdot (-\log [H^+]) + 11.0$ . The results in Fig. 4 indicates that the experimental borderline for the reduction of Tc(VII) (bold dot line) is about 2 pe-units (about 100 mV) lower than the calculated line (broken line). This may suggest that the reduction with slow kinetics by reducing chemicals lead to different solid phases, or at least different particle size distribution compared to more crystalline solid phases assumed for the thermodynamic calculation. The value of  $\log K^0$  for the Tc(IV) solid phase selected by Rard et al. [5] was calculated from the standard redox potential ( $E^0$ ) of Eq. (1), which was determined from the investigation of redox potential measurement data of the  $TcO_4^-/TcO_2 \cdot xH_2O(s)$  couple [1], [4]. In the literature, the solid phases were prepared by electrochemical reduction of macroscopic amounts of  $TcO_4^-$ . Under the experimental condition of lower initial Tc concentration in this study, Tc(VII)

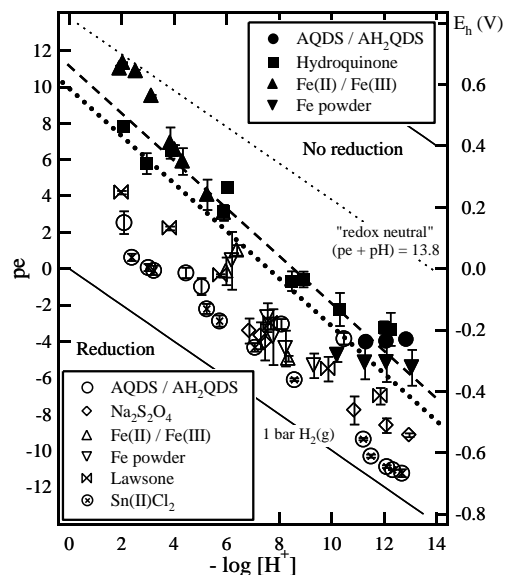


Fig. 4. Experimental plots on the reduction of Tc(VII) ( $[TcO_4^-]_{init} = 10^{-5} \text{ M}$ ). Samples reduced as open symbols, samples not reduced as filled symbols.

may be precipitated not as  $\text{TcO}_2 \cdot x\text{H}_2\text{O}(\text{s})$  but rather small colloidal particles,  $\text{TcO}_2 \cdot x\text{H}_2\text{O}(\text{coll, hyd})$ . This explanation would be similar to the Np(V) reduction processes and the role of colloidal Np(IV) phases described recently by Neck et al. [19]. In their study on the reduction of Np(V) to Np(IV), the experimental borderline was also observed to be lower than the calculated equilibrium line from the thermodynamic constant of  $\text{NpO}_2(\text{am, hyd})$  and  $\text{NpO}_2(\text{coll, hyd})$  considered as small solid phase particles was proposed. In Fig. 4, the experimental borderline was determined to be  $p_e = -1.3 \cdot \text{pH} + 9.3$ , and  $\log K$  for  $\text{TcO}_2 \cdot x\text{H}_2\text{O}(\text{coll, hyd})$  was obtained to be 33.1 at  $I = 0.1$ .

The kinetics for the reduction of Tc(VII) generally showed a significant dependence on  $E_h$  in homogeneous solutions systems (Fig. 5). The reduction rate decreased when  $E_h$  increased from strongly negative values, such as in Sn(II) system, to near the reduction borderline and in the systems such as Lawsons, the rate of reduction was extremely slow. On the other hand, a rapid decrease of the initial Tc concentration was observed in suspensions where the  $E_h$  values were lower than the borderline in Fig.4. In Fe powder suspensions at  $p_{\text{Hc}} < 10$ , the Tc concentration decreased to detection limit level ( $10^{-8}$  M) within 3 days, although the  $E_h$  values were closed to those in the Lawsons system, where slow kinetics were observed.

### Conclusions.

The redox behaviour of Tc(VII)/Tc(IV) couple was investigated in various homogeneous and heterogeneous reducing systems and systematized according to pH- $E_h$  conditions. A borderline for the reduction of Tc(VII) independent of reducing systems was shown and Tc(VII) was reduced when the redox potential values were below this borderline in both homogeneous solutions and heterogeneous suspensions. In the systems with redox potentials above the borderline, initial Tc(VII) concentration did not changed, indicating no reduction of Tc(VII). The experimental borderline was about 2 pe unit lower than the equilibrium line calculated from the standard potential of  $\text{TcO}_4^-/\text{TcO}_2(\text{s}) \cdot x\text{H}_2\text{O}(\text{s})$ , which was electrochemically prepared from macroscopic amounts of  $\text{TcO}_4^-$ . The difference may suggest that analog solid phases with significantly smaller particle size control the redox processes investigated in this study. For the confirmation of the proposed  $\text{TcO}_2 \cdot x\text{H}_2\text{O}(\text{coll, hyd})$ , further investigation including solid phase analysis is needed. The kinetics of the Tc(VII) reduction was generally correlated to the  $E_h$ -pH conditions, however in the systems of Fe powder suspension and Fe(II)/Fe(III) precipitates more rapid reduction was observed. This possibly implies the intrinsic properties of mineral surfaces and surface mediated redox processes.

**Acknowledgement:** The research leading to these results has received funding from the European Union's European Atomic Energy Community's (Euratom) Seventh Framework Programme FP7/2007-2011 under grant agreement n° 212287 (RECOSYproject). This work was partially supported by the German BMWi under the project of VESPA.

### References.

1. J. Cobble, W. Smith, G. Boyd, *J. Am. Chem. Soc.* **75**, 5777-5787 (1953).
2. G. Cartledge, W. Smith, *J. Phys. Chem.* **59**, 1111-1112 (1955).
3. B. Gorski, H. Koch, *J. Inorg. Nucl. Chem.* **31**, 3565-3571 (1969).
4. R. Meyer, W. Arnold, *Radiochim. Acta* **55**, 19-22 (1991).

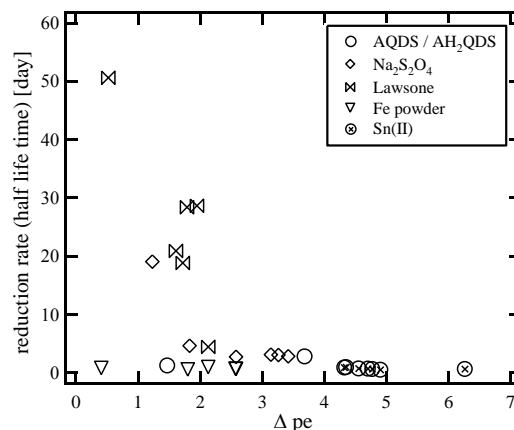


Fig. 5. Reduction rate half life time as a function of the difference of pe values between the measured value in each reducing system and experimental borderline in Fig. 4 ( $\square$  pe).



5. Rard, J., Rand, M., Anderegg, G., Wanner, H. *Chemical Thermodynamics of Technetium*, Elsevier, Amsterdam 1999.
6. E. Bondietti, C. Francis, *Science*. **203**, 1337-1340 (1979).
7. K. Lieser, Ch. Bauscher, *Radiochim. Acta*, **42**, 205-213 (1987).
8. D. Cui, T. Eriksen, *Environ. Sci. Technol.* **30**, 2259-2262 (1996).
9. K. Ben Said, M. Fattahi, C. Musikas, A. Delorme-Hiver, J. Abbe, *Radiochim. Acta*. **83**, 195-203 (1998).
10. E. Maset, S. Sidhu, A. Fisher, A. Heydon, P. Worsfold, A. Cartwright, M. Keith-Roach, *Environ. Sci. Technol.*, **40**, 5472-5477 (2006).
11. J. Zachara, S. Heald, B. Jeon, R. Kukkadapu, C. Liu, J. McKinley, A. Dohnalkova, D. Moore, *Geochim. Cosmochim. Acta*. **71**, 2137-2157 (2007).
12. I. Llorens, P. Deniard, E. Gautron, A. Olicard, M. Fattahi, S. Jobic, B. Grambow, *Radiochim. Acta*, **96**, 569-574 (2008).
13. J. Begg, I. Burke, J. Chamock, K. Morris, *Radiochim. Acta*, **96**, 631-636 (2008).
14. C. I. House, G. H. Kersall, *Electrochimica Acta*. **29**, 1459-1464 (1984).
15. T. Eriksen, P. Ndalamba, J. Bruno, M. Caceci, *Radiochim. Acta*, **58/59**, 67-70 (1992).
16. P. Warwick, S. Aldridge, N. Evans, S. Vines, *Radiochim. Acta*, **95**, 709-716 (2007).
17. N. Hess, Y. Xia, D. Rai, S. Conradson, *J. Solution Chem.* **33**, 199-226 (2004).
18. Guillaumont, R., Fanghänel, Th., Fuger, J., Grenthe, I., Neck, V., Palmer, D., Rand, M., *Update on the Chemical Thermodynamics of Uranium, Neptunium, Plutonium, Americium and Technetium*, Elsevier, Amsterdam 2003.
19. Neck, M. Altmaier, D. Fellhauer, J. Runke, Th. Fanghänel, Collaborative Project “Redox Phenomena Controlling Systems” 1<sup>st</sup> Annual Workshop Proceedings, 65-73 (2009).



Welcome to Moscow, Lenininsky prospect, 31

## 1.7. TECHNETIUM(I) HEXACARBONYL CATION AND ITS REACTIVITY

A.E. Miroslavov<sup>1</sup>, G.V. Sidorenko<sup>1</sup>, A.A. Lumpov<sup>1</sup>, D.N. Suglobov<sup>1</sup>,  
M.S. Grigor'ev<sup>2</sup>, and V.V. Gurzhii<sup>3</sup>

<sup>1</sup> Khlopin Radium Institute, Research and Production Association, Federal State Unitary Enterprise,  
2-i Murinskii pr. 28, St. Petersburg, 194021 Russia

<sup>2</sup> Frumkin Institute of Physical Chemistry and Electrochemistry RAS, Moscow, Russia

<sup>3</sup> St. Petersburg State University, St. Petersburg, Russia

Technetium(I) hexacarbonyl cation  $[\text{Tc}(\text{CO})_6]^+$  was prepared by autoclave carbonylation of  $[\text{Tc}(\text{CO})_3(\text{H}_2\text{O})_3]^+$  with CO at 100°C in the presence of strong acids with weakly coordinating anions ( $\text{HClO}_4$ ,  $\text{CF}_3\text{SO}_3\text{H}$ ,  $\text{HPF}_6$ ). With strongly coordinating acid anions (e.g.,  $\text{Cl}^-$ ), the pentacarbonyl complex with the acid anion is formed. The  $[\text{Tc}(\text{CO})_6]^+$  cation, isolated in the form of perchlorate, was characterized by single crystal X-ray diffraction (SC XRD) and by IR ( $\nu_{\text{CO}}$ , MeCN: 2095  $\text{cm}^{-1}$ ) and  $^{99}\text{Tc}$  NMR ( $\delta_{\text{Tc}}$ , MeOH: -1924 ppm) spectroscopy. The crystal structure of  $[\text{Tc}(\text{CO})_6]\text{ClO}_4$  consists of one crystallographically independent  $\text{Tc}(\text{CO})_6^+$  cation and disordered  $\text{ClO}_4^-$  anion (Fig. 1).

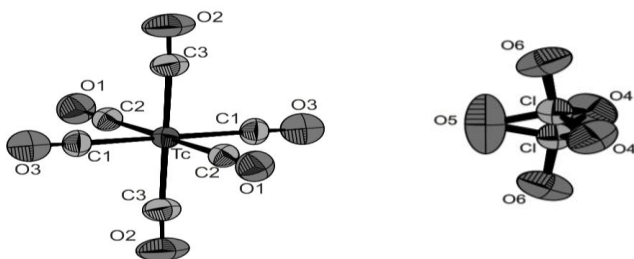


Fig. 1.  $[\text{Tc}(\text{CO})_6]^+$  cation (left) and disordered perchlorate anion (right) in the structure of  $[\text{Tc}(\text{CO})_6]\text{ClO}_4$ .

Since  $[\text{Tc}(\text{CO})_6]^+$  is an analog of MIBI, it was of interest to study its cardiotropic properties. For this purpose we examined the resistance of this complex to substitution of carbonyl groups in solution. As an incoming ligand, we tested acetonitrile (mild  $\sigma$  donor). As seen from the IR data,  $[\text{Tc}(\text{CO})_6]^+$  slowly reacts with MeCN to form  $[\text{Tc}(\text{CO})_3(\text{MeCN})_3]^+$ . As in the case of pentacarbonyl halides [1], the rate-determining step of decarbonylation is detachment of carbonyl group. The rate constant of this reaction ( $2.83 \times 10^{-7} \text{ s}^{-1}$ , 304.4 K) is more than 1.5 orders of magnitude lower than that of decarbonylation of the most stable complex among pentacarbonyl halides,  $[\text{TcI}(\text{CO})_5]$  ( $76 \times 10^{-7} \text{ s}^{-1}$ , 303.1 K, in  $\text{CCl}_4$  [1]). Thus, the  $[\text{Tc}(\text{CO})_6]^+$  cation is fairly resistant to thermal decarbonylation, despite relatively large lengths of the Tc–CO bonds. However,  $[\text{Tc}(\text{CO})_6]^+$  is instantaneously hydrolyzed in an aqueous solution in the presence of an alkali to form an unidentified yellow precipitate, which is probably a mixture of different compounds. Vacuum sublimation of this product yielded  $\text{Tc}_2(\text{CO})_{10}$  and  $\text{Tc}_3\text{H}_3(\text{CO})_{12}$ , identified by SC XRD. We suggest that in this case decarbonylation involves nucleophilic attack of  $\text{OH}^-$  anion at the carbonyl carbon atom, followed by decarboxylation of the intermediate and secondary transformations of the decarboxylation product.

We also prepared  $[\text{}^{99\text{m}}\text{Tc}(\text{CO})_6]^+$  by autoclave carbonylation of  $[\text{}^{99\text{m}}\text{Tc}(\text{CO})_3(\text{H}_2\text{O})_3]^+$  in aqueous solutions of  $\text{HPF}_6$  or  $\text{CF}_3\text{SO}_3\text{H}$  with a yield of 40 and 15%, respectively. The key point of the synthesis is complete removal of halide ions from the reaction mixture.  $[\text{}^{99\text{m}}\text{Tc}(\text{CO})_6]^+$  is stable in acidic aqueous solutions and in the presence of histidine for a day.

1. A.E. Miroslavov, G.V. Sidorenko, A.A. Lumpov, V.A. Mikhalev, D.N. Suglobov, *Radiokhimiya* **51**: 6–10 (2009).

1.8.

## STRUCTURAL CHEMISTRY OF TECHNETIUM CARBONYL COMPOUNDS

G.V. Sidorenko<sup>1</sup>, A.E. Miroslavov<sup>1</sup>, D.N. Suglovov<sup>1</sup>, M.S. Grigor'ev<sup>2</sup>, and V.V. Gurzhii<sup>3</sup>

<sup>1</sup> Khlopin Radium Institute, Research and Production Association, Federal State Unitary Enterprise,  
2-i Murinskii pr. 28, St. Petersburg, 194021 Russia

<sup>2</sup> Frumkin Institute of Physical Chemistry and Electrochemistry RAS, Moscow, Russia

<sup>3</sup> St. Petersburg State University, St. Petersburg, Russia

**Keywords:** technetium, carbonyls, structure, single crystal X-ray diffraction

### Abstract:

The results of structural studies of Tc carbonyl compounds are summarized. The stoichiometry and geometry of the mono- and polynuclear complexes are discussed in relation to the donor–acceptor properties of the ligands, taking into account the *trans* effect. Correlations between the structure and reactivity of the complexes are considered.

In this report we summarize the results of structural studies of Tc carbonyl compounds. By now, crystal structures have been determined for approximately 100 Tc carbonyl complexes, of which 17 complexes have been studied by us. Most of the data refer to octahedral Tc(I) complexes, with some Tc(III) and Tc(0) compounds also studied. Tc(III) typically forms seven-coordinate complexes with CO ligands (see, e.g., [1]), but with sterically hindered ligands five-coordinate complexes are formed [2]. Here and hereinafter, the denticity of  $\pi$ -coordinated ligands like cyclopentadienyl is counted by the number of  $\pi$ -electron pairs involved in the coordination. The known Tc(0) complexes are technetium decacarbonyl  $\text{Tc}_2(\text{CO})_{10}$  [3, 4] (Fig. 1) and some of its derivatives [5].

The composition of Tc(I) carbonyl complexes is dictated by formation of closed 18-electron valence shell around the central atom. Therefore, the known complexes have typically octahedral structure. Representatives of practically all the theoretically possible mononuclear Tc(I) carbonyl complexes have been prepared and structurally characterized (here and hereinafter: M, monodentate; B, bidentate; T, tridentate ligands):  $[\text{Tc}(\text{CO})_6]^+$ ,  $[\text{Tc}(\text{CO})_5\text{M}]$ ,  $[\text{Tc}(\text{CO})_4\text{B}]$ ,  $[\text{Tc}(\text{CO})_3\text{T}]$ ,  $[\text{Tc}(\text{CO})_3\text{BM}]$ ,  $[\text{Tc}(\text{CO})_3\text{M}_3]$ ,  $[\text{Tc}(\text{CO})_2\text{M}_4]$ ,  $[\text{Tc}(\text{CO})_2\text{BM}_2]$ ,  $[\text{Tc}(\text{CO})_2\text{TM}]$ ,  $[\text{Tc}(\text{CO})\text{TM}_2]$ . The charge of the complex species depends on whether the ligands are neutral or charged, and in this notation the charge is omitted.

The *trans* effect makes preferential mutual *cis* arrangement of carbonyl ligands. The Tc–CO bonds in *trans* position weaken each other, and therefore technetium carbonyls containing more than three carbonyl ligands, in which such bonds are inevitably present, are relatively unstable. Nevertheless, many representatives of this group, including hexacarbonyl cation [6] (Fig. 2), are sufficiently stable to be isolated and studied by single crystal X-ray diffraction. All the available structural data for technetium(I) pentacarbonyls  $[\text{Tc}(\text{CO})_5\text{M}]$  were obtained in our studies [7–9], with both neutral ( $\text{Bu}^t\text{NC}$ ,  $\text{PPh}_3$ ) and anionic (Cl, Br, I) ligands as M. Typical examples are shown in Figs. 3 and 4. As for mononuclear tetracarbonyl complexes  $[\text{Tc}(\text{CO})_4\text{B}]$ , the only available example of structurally studied complexes is the xanthate ( $\text{B} = \text{MeOCS}_2^-$ ) examined in our recent study [10] (Fig. 5). The most stable (and the most numerous) are *fac*-tricarbonyl complexes with  $\sigma$ - or  $\pi$ -donor ligands in *trans* position to each CO group  $\{[\text{Tc}(\text{CO})_3\text{T}], [\text{Tc}(\text{CO})_3\text{BM}], [\text{Tc}(\text{CO})_3\text{M}_3]\}$ . Typical examples are given in [10–14] (Fig. 6). The *fac*-tricarbonyl moiety is so stable and its steric requirements are so strong that, even with the porphyrin ligand strongly dictating the square planar geometry, a binuclear complex with tridentate coordination of the ligand to each Tc atom is formed [15]. Only ligands with pronounced  $\pi$ -acceptor properties are capable to form *mer* structures [16] or to further replace CO groups. All the di- and monocarbonyl complexes studied contain other  $\pi$ -

acceptor ligands apart from CO (most frequently phosphines, see, e.g., [17, 18]).

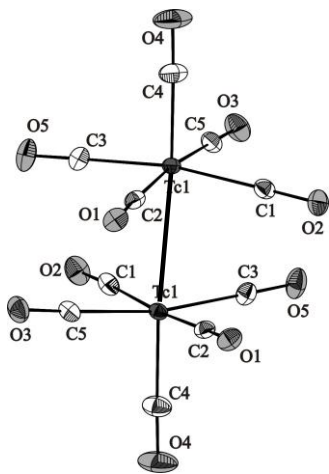


Fig. 1. Molecular structure of  $Tc_2(CO)_{10}$  [4].

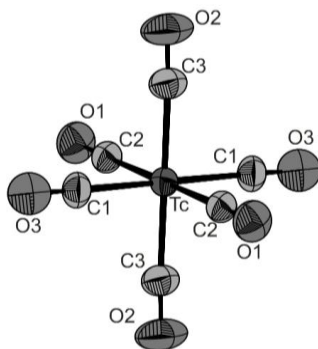


Fig. 2. Structure of the  $[Tc(CO)_6]^+$  cation [6].

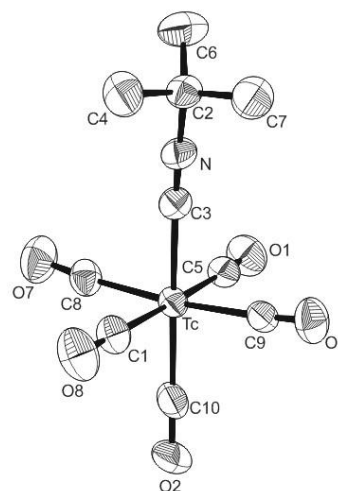


Fig. 3. Structure of the  $[Tc(CO)_5(Bu'NC)]^+$  cation [9].

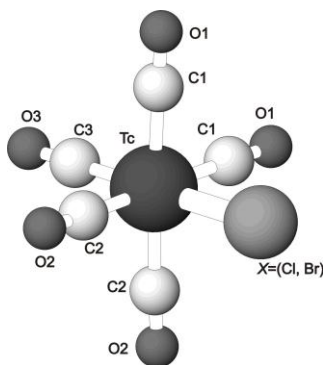


Fig. 4. Molecular structure of  $[TcX(CO)_5]$  ( $X = Cl, Br$ ) [8].

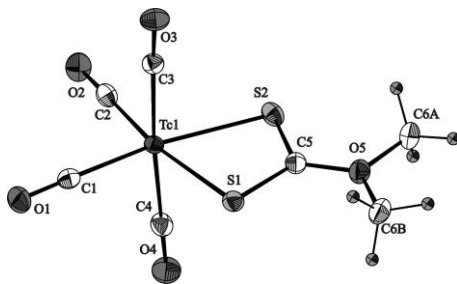


Fig. 5. Molecular structure of  $[Tc(MeOCS_2)(CO)_4]$  (the OMe group is disordered over two sites) [10].

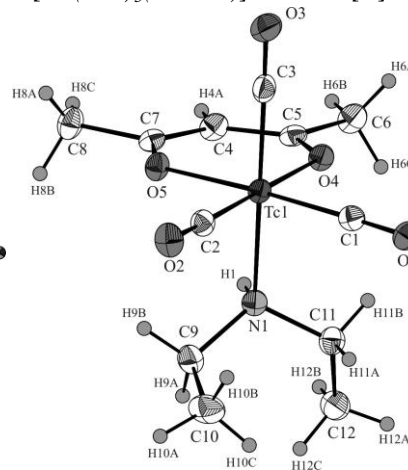


Fig. 6. Molecular structure of  $[Tc(acac)(Et_2NH)(CO)_3]$  [13].

The deficiency of ligands leads to formation of binuclear complexes. Numerous polynuclear Tc carbonyl complexes with bridging coordination of ligand donor atoms are known, in particular, a series of dimers  $[Tc(CO)_4M]_2$  and  $[Tc(CO)_3B]_2$ . Typical examples of the former complexes are tetracarbonyl halide dimers [19] (Fig. 7). However, with  $M = H$ , a triangular trimer is formed, with the Tc–Tc distance suggesting certain direct bonding [4, 20] (Fig. 8).

With bidentate ligands, the dimers are formed by bridging coordination of one of the donor atoms of the ligand. In this case, the ligand arrangement can be either *cis* or *trans* relative to the bridging core. Both examples are known; in particular, a Schiff base complex forms a centrosymmetric *trans* dimer [21], whereas a dithiocarbamate complex has a noncentrosymmetric *cis* structure [10] (Fig. 9). The *cis* dimers are formed, according to IR spectra, by tricarbonyl- $\beta$ -diketonates in solution and in the gas phase [22, 23]. Tricarbonyltechnetium acetylacetonate dimer in the crystal has a unique structure. The dimer is formed by bridging bonding with the  $\gamma$ -C atom of the acetylacetonate ligand and has the cage structure [13] (Fig. 10). Along with neutral dimers, anionic dimers with triple bridges of the composition  $[Tc(CO)_3]_2X_3^-$  are known (see, e.g., [24]). Binuclear complexes are also formed with some polydentate ligands that can span two tricarbonyltechnetium fragments. One of examples, the



porphyrin complex, has already been mentioned.

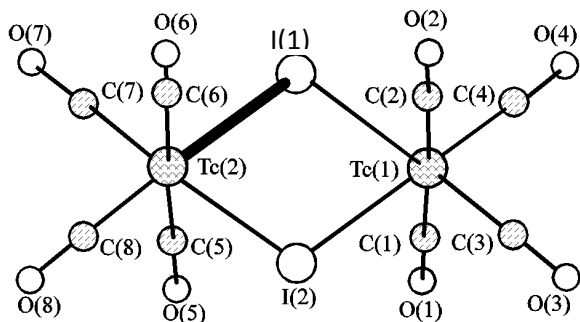


Fig. 7. Molecular structure of  $[TcI(CO)_4]_2$  [19].

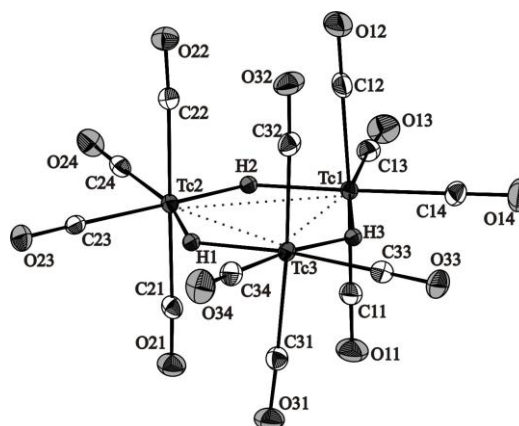


Fig. 8. Molecular structure of  $[TcH(CO)_4]_3$  [4].

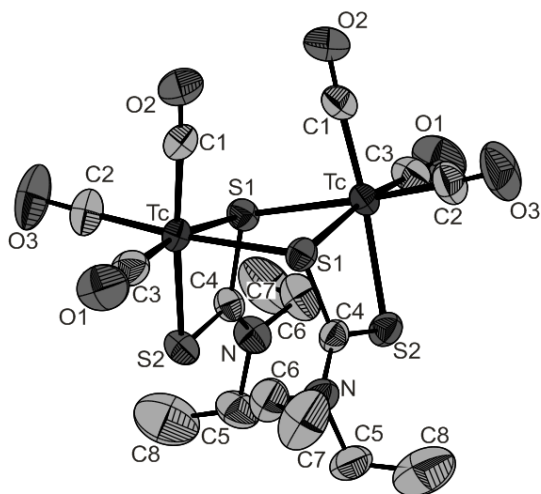


Fig. 9. Molecular structure of  $[Tc(Et_2NCS_2)(CO)_3]_2$  [10].

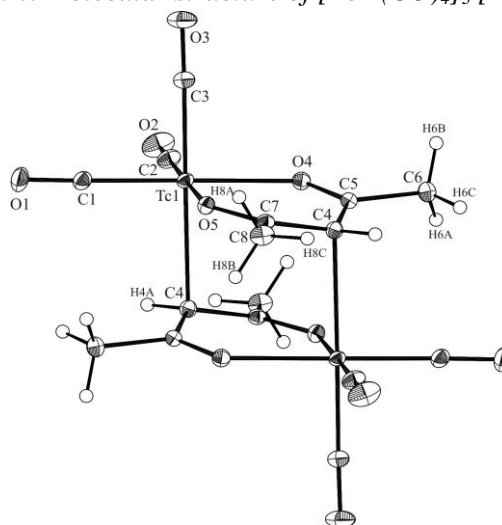


Fig. 10. Molecular structure of  $[Tc(acac)(CO)_3(Et_3NH)]$  [13].

In tricarbonyl complexes with single monodentate ligand,  $\mu_2$ -bridging is insufficient to attain coordination saturation, each monodentate ligand links three Tc atoms, and the structure as a whole is tetrameric and cubane-like. All the examined compounds of this type [25–28] (Fig. 11) have similar molecular structure but are not isostructural. They crystallize in different crystal systems and have different crystal packing. A related complex with  $CH_3O^-$  bridging ligands and  $Na^+$  in place of one of tricarbonyltechnetium groups is also known [29].

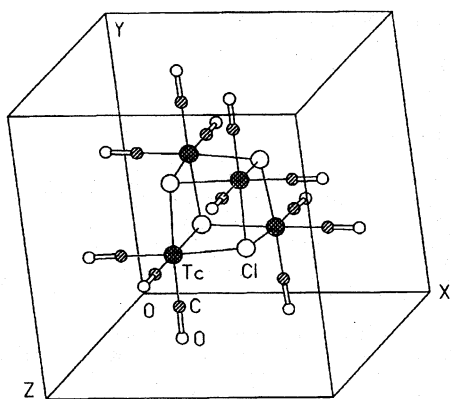


Fig. 11. Crystal structure of  $[TcCl(CO)_3]_4$  (body-centered cubic structure, only the molecule in the cell center is shown) [26].

Many transition metal carbonyls contain bridging CO ligands. Such coordination mode is not typical of Tc, but a few examples are known (see, e.g., [30]). In all these cases, CO bridging is observed in combination with direct Tc–Tc bonding.

After having discussed the compositions and topologies of Tc carbonyl complexes, let us discuss their geometries and correlations with the reactivity.

The length of Tc–CO bond in *trans* position to  $\sigma$ - and  $\pi$ -donor ligands and in *cis* position to other CO groups  $[Tc-CO]$  is, on the average, about 1.9 Å. The Tc–CO bonds in *trans* position to each other  $[Tc-CO^*]$  are

weakened by the *trans* effect and are longer by 0.05–0.1 Å. The Tc–CO bond lengths in some higher technetium carbonyls are compared in Table 1.

Table 1. Bond lengths (Å) in higher technetium carbonyls (asterisk denotes CO groups *trans* to other ligands, and dagger, CO groups *trans* to each other)

Complex	Tc–CO*	Tc–CO <sup>†</sup>	Difference
[Tc(CO) <sub>6</sub> ] <sup>+</sup> [6]	–	2.024–2.032	–
[TcCl(CO) <sub>5</sub> ] [8]	1.915	av. 2.016	0.099
[TcBr(CO) <sub>5</sub> ] [8]	1.937	av. 2.021	0.084
[TcI(CO) <sub>5</sub> ] [7]	1.938	2.015	0.077
[Tc(CO) <sub>5</sub> ] <sub>2</sub> [4]	1.946	av. 1.998	0.052
[Tc(CO) <sub>5</sub> (PPh <sub>3</sub> ) <sup>+</sup> [9]	2.005	av. 2.000	0.005
[Tc(CO) <sub>5</sub> (Bu <sup>†</sup> NC)] <sup>+</sup> [9]	1.999	av. 2.014	–0.014
[TcI(CO) <sub>4</sub> ] <sub>2</sub> [19]	av. 1.91	av. 2.00	0.09
[Tc(MeOCS <sub>2</sub> )(CO) <sub>4</sub> ] [10]	av. 1.940	av. 2.008	0.068
[TcH(CO) <sub>4</sub> ] <sub>3</sub> [4]	av. 1.943	av. 2.002	0.059

inert in CO substitution, despite the fact that the Tc–CO bonds in it are even longer than the Tc–CO<sub>*trans*</sub> bonds in [Tc(CO)<sub>5</sub>M] complexes.

Table 2. Average angle X–Tc–*cis*-CO, deg, and Wiberg indices  $\sum W(X\cdots C, X\cdots O)$

X	Angle (XRD)	Angle (QCC)	$\sum W$
Cl	89.23	86.7	0.24
Br	88.27	86.5	
I	87.8	86.5	0.36

though without pronounced trend along the halogen series, which suggests that the leaning is an intrinsic property of a molecule rather than a result of packing effects. Leaning toward the sixth ligand is also observed in Tc<sub>2</sub>(CO)<sub>10</sub>.

Higher Tc carbonyls exhibit, along with the tendency to dissociative CO replacement, also another kind of reactivity, manifested in reactions with strong nucleophiles. This kind of reactivity is considerably less studied, no quantitative data on the reaction kinetics have been obtained, and the reaction mechanism is insufficiently understood. However, in this case there is no anomaly in the behavior of the hexacarbonyl cation. This cation, being very inert in CO replacement with weak nucleophiles such as CH<sub>3</sub>CN, which probably occurs by the dissociative mechanism, appears to be highly reactive toward stronger nucleophiles such as OH<sup>–</sup> ion [4]. The reaction is believed to start with the nucleophilic attack at the carbonyl C atom. The *trans* effect primarily reduces the metal-to-ligand  $\pi$ -electron donation. As a result, the Tc–CO bond length increases and the carbonyl C atom becomes more electrophilic. [TcBr(CO)<sub>5</sub>] also reacts relatively slowly with CH<sub>3</sub>CN but is very reactive toward Et<sub>2</sub>NH. At the same time, tricarbonyl complexes with donor ligands, in which there are no weak Tc–CO bonds, appear to be considerably more resistant to nucleophilic agents. For example, the [Tc(CO)<sub>3</sub>(H<sub>2</sub>O)<sub>3</sub>]<sup>+</sup> cation in alkaline solutions undergoes only protolytic transformations and olation, with the CO groups remaining intact [32]. These data, though scarce yet, suggest that the correlation between the Tc–CO bond length and its reactivity toward nucleophiles does take place, in contrast to the correlation with the reactivity in dissociative processes.

Some interesting correlations can also be found for the Tc– $\sigma$  donor bond lengths. Let us

In [Tc(CO)<sub>5</sub>M] complexes, the difference in the lengths of these bonds decreases in the series M = Cl, Br, I and is practically leveled off in going to  $\pi$ -acceptor ligands M (PPh<sub>3</sub>, Bu<sup>†</sup>NC). If we include in this series Tc<sub>2</sub>(CO)<sub>10</sub>, considering the Tc(CO)<sub>5</sub> fragment as ligand M, it will occupy the place between I and  $\pi$ -acceptor ligands. The reactivity of Tc carbonyl complexes in dissociative carbonylation reactions does not correlate with the Tc–CO bond length and decreases in the order M = Cl, Br, I, CO [31], apparently due to the stabilization of the five-coordinate intermediate formed by CO elimination. The complex [Tc(CO)<sub>6</sub>]<sup>+</sup> is particularly

The reactivity of [Tc(CO)<sub>5</sub>M] complexes can also be influenced by the *cis* interaction OC $\cdots$ M revealed by quantum-chemical calculations, which increases in going from M = Cl to M = I (Table 2). Such interaction is also suggested by angular distortions of the [Tc(CO)<sub>5</sub>M] octahedra [M = halogen, Tc(CO)<sub>5</sub>]: The equatorial CO groups lean toward ligand M to the extent increasing in going from Cl to I, despite an increase in the ligand size. Quantum-chemical calculations also show this leaning,



compare pentacarbonyltechnetium halides with tricarbonyl halide complexes in which the remaining two sites are occupied by  $\sigma$ -donor ligands. For example, in  $[\text{TcBr}(\text{CO})_5]$  [8] the Tc–Br bond is appreciably shorter [2.6123(9) Å] than in  $[\text{TcBr}(\text{CO})_3(\text{en})]$  [12] [2.640(1) Å]. Similar result is obtained by quantum-chemical calculations of  $[\text{TcCl}(\text{CO})_5]$  (2.478 Å) and  $[\text{TcCl}_3(\text{CO})_3]^{2-}$  (2.563 Å) [8]. Elongation of the Tc–Cl bond in the latter complex is accompanied by an appreciable decrease in its Wiberg index (from 0.38 to 0.32). These results correlate with the physical and chemical properties of the complexes. In particular, pentacarbonyltechnetium halides behave as hydrophobic covalent molecules showing no pronounced tendency to electrolytic dissociation [6]. At the same time, when the coordination sphere contains only three CO groups with the other sites occupied by  $\sigma$ -donor ligands such as  $\text{H}_2\text{O}$  molecules, the complexation with halide ions is relatively weak [33]. Furthermore, Tc pentacarbonyl halides are readily volatile [34], whereas the ethylenediamine complex is much less volatile, despite practically the same molecular weight and size [34], which may be due to stronger polarity of the molecule, in particular, to higher ionicity of the Tc–Br bond.

Thus, structural studies are useful not only for identification of the newly synthesized Tc compounds, but also for better understanding of their physical and chemical properties.

## References

- [1] G. Bandoli, D.A. Clemente, U. Mazzi. *J. Chem. Soc., Dalton Trans.* 373 (1978).
- [2] N. de Vries, J.C. Dewan, A.G. Jones, A. Davison. *Inorg. Chem.* **27**: 1574 (1988).
- [3] M.F. Bailey, L.F. Dahl. *Inorg. Chem.* **4**: 1140 (1965).
- [4] G.V. Sidorenko, A.E. Miroslavov, M.S. Grigor'ev, V.V. Gurzhiy, A.A. Lumpov, V.A. Mikhalev, D.N. Suglobov. *Radiokhimiya* **53** (1): 42 (2011).
- [5] B. Kanellakopoulos, B. Nuber, K. Raptis, M.L. Ziegler. *Z. Naturforsch.* **46b**: 55 (1991).
- [6] V.V. Gurzhiy, A.E. Miroslavov, G.V. Sidorenko, A.A. Lumpov, S.V. Krivovichev, D.N. Suglobov. *Acta Crystallogr.* **E64**: m1145 (2008).
- [7] M.S. Grigor'ev, A.E. Miroslavov, G.V. Sidorenko, D.N. Suglobov. *Radiokhimiya* **39** (3): 204 (1997).
- [8] G.V. Sidorenko, V.V. Gurzhiy, A.E. Miroslavov, O.V. Sizova, S.V. Krivovichev, A.A. Lumpov, D.N. Suglobov. *Radiokhimiya* **51** (3): 207 (2009).
- [9] A.E. Miroslavov, A.A. Lumpov, G.V. Sidorenko, E.M. Levitskaya, N.I. Gorshkov, D.N. Suglobov, R. Alberto, H. Braband, V.V. Gurzhiy, S.V. Krivovichev, I.G. Tana-naev. *J. Organomet. Chem.* **693**: 4 (2008).
- [10] A.E. Miroslavov, G.V. Sidorenko, D.N. Suglobov, A.A. Lumpov, V.V. Gurzhiy, M.S. Grigor'ev, V.A. Mikhalev. *Inorg. Chem.* **50**: 1098 (2011).
- [11] D.R. van Staveren, S. Mundwiler, U. Hoffmanns, Jae Kyoung Pak, B. Spingler, N. Metzler-Nolte, R. Alberto. *Org. Biomol. Chem.* **2**: 2593 (2004).
- [12] N.A. Baturin, M.S. Grigor'ev, S.V. Kryuchkov, A.E. Miroslavov, G.V. Sidorenko, D.N. Suglobov. *Radiokhimiya* **36** (3) 202 (1994).
- [13] G.V. Sidorenko, M.S. Grigor'ev, V.V. Gurzhiy, S.V. Krivovichev, A.E. Miroslavov, D.N. Suglobov. *Radiokhimiya* **52** (2): 126 (2010).
- [14] P. Kurz, B. Spingler, T. Fox, R. Alberto. *Inorg. Chem.* **43**: 3789 (2004).
- [15] M. Tsutsui, C.P. Hsung, D. Ostfeld, T.S. Srivastava, D.L. Cullen, E.F. Meyer Jr. *J. Am. Chem. Soc.* **97**: 3952 (1975).
- [16] R. Alberto, W.A. Herrmann, P. Kiprof, F. Baumgartner. *Inorg. Chem.* **31**: 895 (1992).
- [17] R. Rossi, A. Marchi, L. Magon, A. Duatti, U. Casellato, R. Graziani. *Inorg. Chim. Acta* **160**: 23 (1989).
- [18] J.E. Joachim, C. Apostolidis, B. Kanellakopoulos, D. Meyer, B. Nuber, K. Raptis, J. Rebizant, M.L. Ziegler. *J. Organomet. Chem.* **492**: 199 (1995).
- [19] M.S. Grigor'ev, A.E. Miroslavov, G.V. Sidorenko, D.N. Suglobov. *Radiokhimiya* **39** (3): 207 (1997).
- [20] R. Alberto, R. Schibli, P.A. Schubiger, U. Abram, R. Hubener, H. Berke, T.A. Kaden. *Chem.*

- Commun.* 1291 (1996).
- [21] T. Takayama, A. Harano, T. Sekine, H. Kudo. *J. Nucl. Radiochem. Sci.* **6**: 149 (2005).
- [22] I.V. Borisova, A.E. Miroslavov, G.V. Sidorenko, D.N. Suglobov, L.L. Shcherbakova. *Radiokhimiya* **33** (4): 27 (1991).
- [23] A.E. Miroslavov, I.V. Borisova, G.V. Sidorenko, D.N. Suglobov. *Radiokhimiya* **33** (6): 14 (1991).
- [24] R. Alberto, R. Schibli, P.A. Schubiger, U. Abram, T.A. Kaden. *Polyhedron* **15**: 1079 (1996).
- [25] R. Alberto, R. Schibli, A. Egli, U. Abram, S. Abram, T.A. Kaden, P.A. Schubiger. *Polyhedron* **17**: 1133 (1998).
- [26] N.A. Baturin, M.S. Grigor'ev, S.V. Kryuchkov, A.E. Miroslavov, G.V. Sidorenko, D.N. Suglobov. *Radiokhimiya* **36** (3): 199 (1994).
- [27] M.S. Grigor'ev, A.E. Miroslavov, G.V. Sidorenko, Yu.T. Struchkov, D.N. Suglobov, A.I. Yanovskii. *Radiokhimiya* **37** (3) 193 (1995).
- [28] A.E. Miroslavov, N.I. Gorshkov, M.S. Grigor'ev, G.V. Sidorenko, D.N. Suglobov. *Radiokhimiya* **39** (1) 41 (1997).
- [29] W.A. Herrmann, R. Alberto, J.C. Bryan, A.P. Sattelberger. *Chem. Ber.* **124**: 1107 (1991).
- [30] K. Raptis, B. Kanellakopoulos, B. Nuber, M.L. Ziegler. *J. Organomet. Chem.* **405**: 323 (1991).
- [31] A.E. Miroslavov, G.V. Sidorenko, A.A. Lumpov, V.A. Mikhalev, D.N. Suglobov. *Radiokhimiya* **51** (1): 6 (2009).
- [32] N.I. Gorshkov, A.E. Miroslavov, A.A. Lumpov, D.N. Suglobov. *Radiokhimiya* **42** (3): 213 (2000).
- [33] N.I. Gorshkov, A.E. Miroslavov, A.A. Lumpov, D.N. Suglobov, V.A. Mikhalev. *Radiokhimiya* **45** (2): 116 (2003).
- [34] I.V. Borisova, A.E. Miroslavov, G.V. Sidorenko, D.N. Suglobov. *Radiokhimiya* **33** (6): 8 (1991).



G.Sidorenko, F. Poineau and A.Miroslavov at the registration desk

1.9.

## “SOFT” CHEMISTRY METHODS APPEAR AS AN EFFECTIVE WAY FOR PRODUCTION OF SUPERDISPERSIVE (NANO-SIZED) MATERIALS BASED ON Re AND D-ELEMENTS OF V-VIII GROUPS.

D.V. Drobot<sup>1</sup>, O.V. Chernyshova<sup>1</sup>, O.S. Kriyzhovets<sup>1</sup>, K.A. Smirnova<sup>1</sup>, I.V. Mazilin<sup>1</sup>, A.V. Shevelkov<sup>2</sup>, M.V. Tsodikov<sup>3</sup>, A.V. Chistyakov<sup>3</sup>, O.V. Petrakova<sup>1</sup>, E.G. Il'in<sup>4</sup>.

<sup>1</sup> Moscow State Academy of Fine Chemical Technology, Moscow, Russia, . Pr. Vernadskogo 86, 119571 Moscow, Russia e-mail [dvdrobot@mail.ru](mailto:dvdrobot@mail.ru), [oxcher@mail.ru](mailto:oxcher@mail.ru)

<sup>2</sup> Lomonosov Moscow State University, Moscow, Russia

<sup>3</sup> A.V. Topchiev Institute of Petrochemical Synthesis, Russian Academy of Science, Moscow, Russia

<sup>4</sup> N.S. Kurnakov Institute of General and Inorganic Chemistry, Russian Academy of Science, Moscow, Russia.

**Key words:** rhenium, alkoxides, synthesis, thermal decomposition, materials.

### Abstract.

The paper represents a listing of results obtained by developing the original methods of controlled synthesis of cluster and mono-, bi- and trimetallic oxo-alkoxide derivatives of rhenium and d-elements of V – VIII groups. The developed techniques of the synthesis of metal alkoxides include: 1) anodic dissolution of the metals in the alcohol media; 2) direct reaction of the rhenium (VII) oxide with alkoxide derivatives of the transition elements.

By such techniques were obtained tetranuclear rhenium cluster alkoxocomplexes:  $\text{Re}_4\text{O}_4(\text{OEt})_{12}$ ,  $\text{Re}_4\text{O}_6(\text{O}^i\text{Pr})_{10}$ ; individual rhenium alkoxocomplexes with variable ratio of oxo- and alkoxo-ligands  $\text{Re}_4\text{O}_2(\text{OMe})_{16}$ ,  $\text{Re}_4\text{O}_6(\text{OMe})_{12}$ ,  $\text{Re}_4\text{O}_{6-y}(\text{OMe})_{12+y}$ ; bimetallic rhenium, molybdenum or tungsten alkoxocomplexes  $\text{ReMoO}_2(\text{OMe})_7$ ,  $\text{Re}_{4-x}\text{Mo}_x\text{O}_{6-y}(\text{OMe})_{12+y}$ ,  $\text{Re}_{4-x}\text{W}_x\text{O}_{6-y}(\text{OMe})_{12+y}$ ; bimetallic rhenium, niobium or tantalum alkoxocomplexes  $\text{Nb}_2(\text{OMe})_8(\text{ReO}_4)_2$ ,  $\text{Ta}_2(\text{OMe})_8(\text{ReO}_4)_2$ ,  $\text{Nb}_4\text{O}_2(\text{OMe})_{14}(\text{ReO}_4)_2$ ,  $\text{Ta}_4\text{O}_2(\text{OMe})_{14}(\text{ReO}_4)_2$ ,  $\text{Nb}_4\text{O}_2(\text{OEt})_{14}(\text{ReO}_4)_2$ ,  $\text{Ta}_4\text{O}_2(\text{OEt})_{14}(\text{ReO}_4)_2$ ; trimetallic rhenium, niobium or tantalum alkoxocomplexes:  $\text{Nb}_{2-x}\text{Ta}_x(\text{OMe})_8(\text{ReO}_4)_2$ ,  $\text{Nb}_{4-x}\text{Ta}_x\text{O}_2(\text{OMe})_{14}(\text{ReO}_4)_2$ ,  $\text{Nb}_{4-x}\text{Ta}_x\text{O}_2(\text{OEt})_{14}(\text{ReO}_4)_2$ . All compounds mentioned above are characterized with X-ray single crystal study, IR – spectroscopy, DTG.

It has been shown, that thermal decomposition of alkoxide derivatives in inert or hydrogen atmosphere leads to formation nano- size powders of individual rhenium and its alloys at low temperature. Thermal decomposition in air leads to formation individual metal oxides or its solid solutions.

It has been demonstrated that the alkoxide derivatives could be promising precursors for next generation catalysts manufacturing.

This paper presents review of the results obtained at Moscow State University of the Fine Chemical Technologies and Swedish University of Agriculture Science.

The interest in rhenium alkoxides is caused by the possibility of their application as precursors for the preparation of highly reactive fine (up to to nanoscale ) powders of rhenium metal or its alloys with refractory metals at very low temperature ( below 500°C ) [1, 2]. The principal application of rhenium is the production of structural alloys with various refractory metals, in particular with W, Mo, Nb, Ta, Ni . Recently demonstrated applications of rhenium oxides, as selective catalysts in many oxidation reactions in organic synthesis and in complete oxidation of the car exhaust gases have made the alkoxide derivatives also attractive for the synthesis of rhenium-based oxide nanocomposite [1-5].

This manuscript is devoted generalization of the data on synthesis of cluster, heterometallic and heteroligand alkoxides of rhenium, discussion of their molecular structures and properties. Using these compounds as precursors is the approach to obtain functional materials. Precursors design allows realize its main advantage: obtaining compounds of a specified metals ration which is required for synthesis of a target product.

The development of the preparation methods for the Re-containing materials ( alloys with refractory metals, simple and complex oxides and so on ) implies the solution of the following problems:

Search for and development of methods for the synthesis of rhenium alkoxides and oxoalkoxide derivatives, including cluster and heterometallic ones;

Study of their physicochemical properties including the structure in the solid state and the thermal decomposition processes;

Determination of the chemical and phase compositions of the products of thermal decomposition of rhenium alkoxides and oxoalkoxide derivatives under various conditions and the search for rational applications of the materials produced in this way. Fig.1 illustrates main ideas of the investigation and Fig.2 illustrates overview of the employed methods for the Re-containing compounds synthesis. We participated in the development of the two approaches to the preparation of alkoxides, namely, reactions using rhenium ( V11) oxide and the electrochemical method.

A number of studies [6,7,8-10]. have demonstrated that the reaction of  $Re_2O_7$  with metal alkoxides (Mo, W, Nb, Ta) is an efficient way for the synthesis of heterometallic alkoxides. Thus, trimetallic rhenium-containing compounds were obtained for the first time.

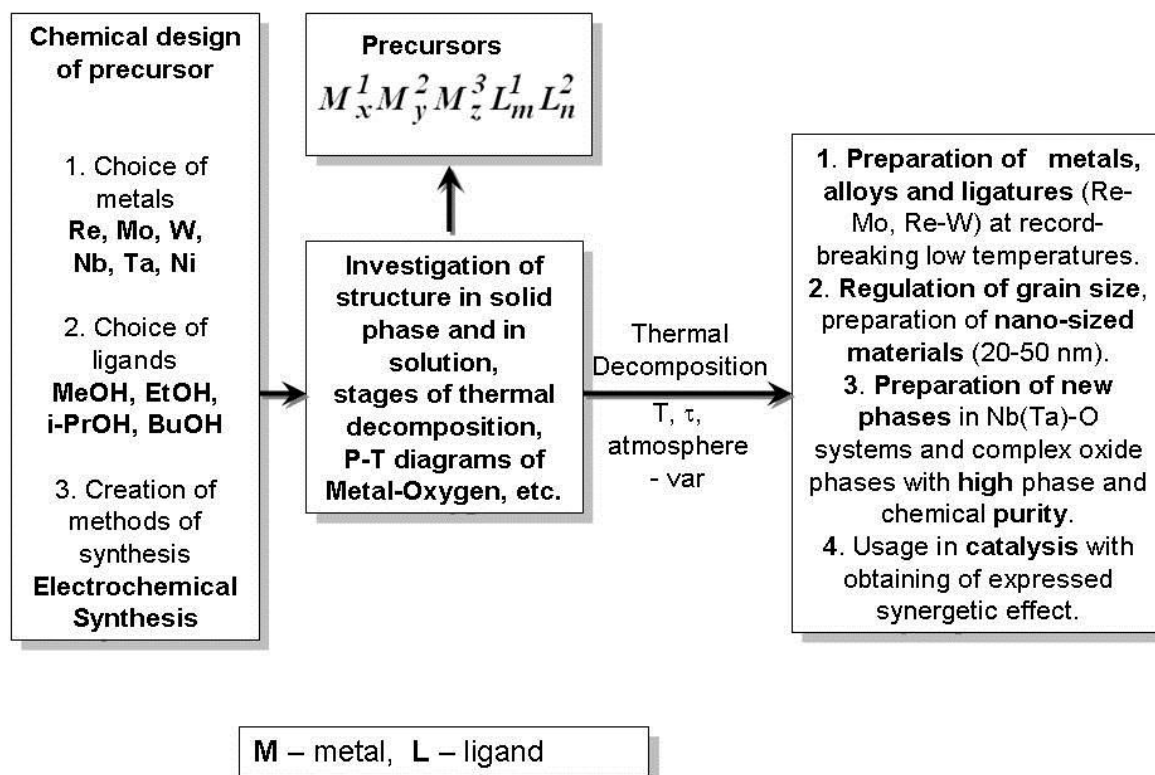


Fig.1. The procedure of preparation of Rhenim based ulro-dispersed materials

One more approach to the synthesis of rhenium alkoxides is based on electrochemistry. This method consist of anodic dissolution of metals in required alcohol. The first data on the application of this method to rhenium derivatives were published only recently [11]. This method was used to prepare the following compounds:  $Re_4O_6(OMe)_{12}$ ,  $Re_4O_2(OMe)_{16}$ ,  $Re_4O_{6-y}(OMe)_{12+y}$ ,  $Re_4O_6(OPr^i)_{10}$ ,  $ReMoO_2(OMe)_7$ ,  $Re_{4-x}Mo_xO_{6-y}(OMe)_{12+y}$ , and  $Re_{4-x}W_xO_{6-y}(OMe)_{12+y}$  [6,11-14]. In the synthesis of



rhenium alkoxides, lithium chloride is used as a conductive additive. The process is carried out in water-cooled cell equipped with a reflux condenser at an electrolyte temperature of 15–50 °C. Crystallization from the electrolyte obtained by anodic dissolution of rhenium in alcohols affords individual Re compounds. Bimetallic derivatives were prepared by the successive anodic dissolution of two metals or by dissolution of metal alkoxide.

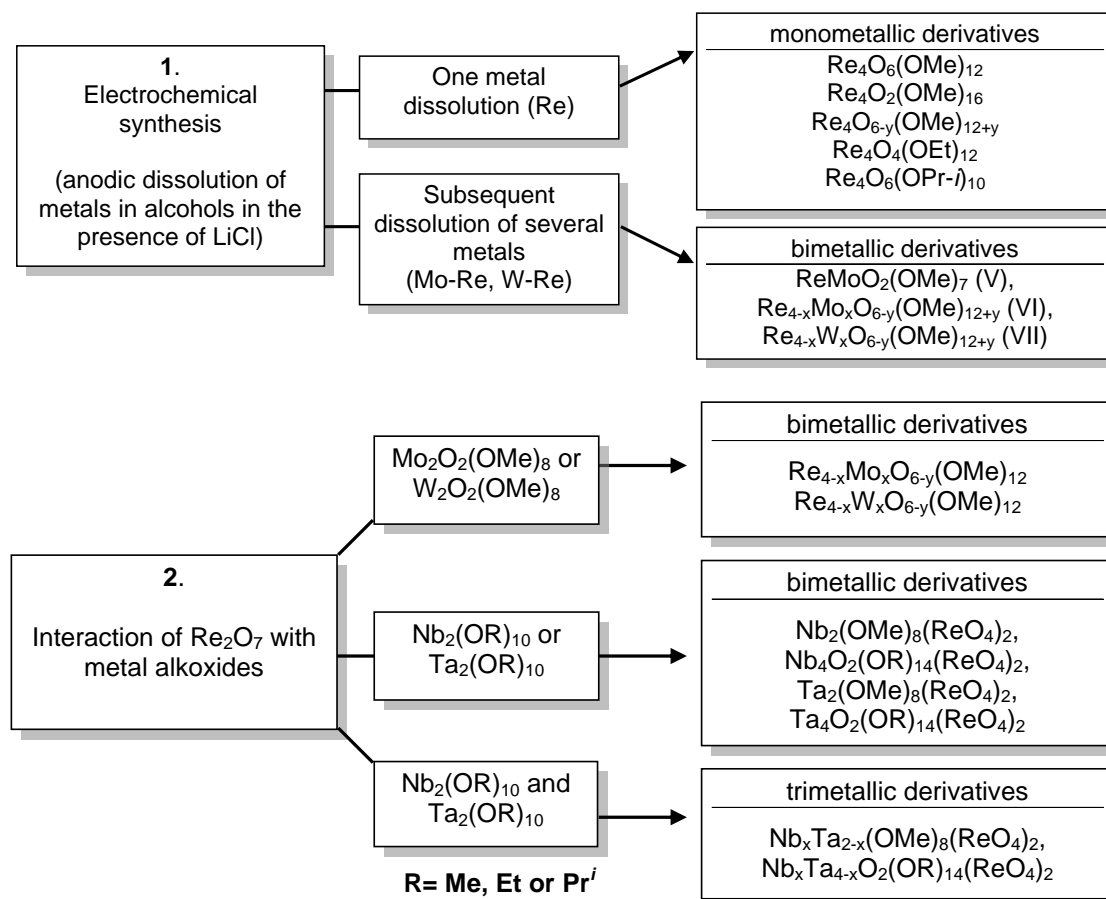


Fig.2. Synthetic approaches to rhenium-containing alkoxide derivatives

The variation of the electrochemical parameters of the process carried out in an undivided cell also allowed the researchers to obtain crystals with variable composition, namely,  $Re^V$  and  $Re^{VI}$  derivative,  $Re_4O_{6-y}(OMe)_{12+y}$ . The electrolysis in a divided cell (*i.e.*, under conditions suppressing the cathodic reduction of rhenium derivatives) gave the rhenium(VI) complex  $Re_4O_6(OMe)_{12}$ .

An important factor affecting the properties of mono- and heterometallic alkoxides is their association and condensation through the formation of bridging alkoxy or oxo ligands, respectively.

The association and condensation involving rhenium(V) derivatives results in tetranuclear species  $Re_4O_{6-y}(OMe)_{12+y}$  containing rhenium simultaneously in different oxidation states (+6 and +5). This type of process ensures the formation of compounds with isomorphous replacement of atoms having similar properties. When binuclear complexes of rhenium and other metals (for example,  $[MoO(OMe)_4]_2$ ,  $ReMoO_2(OMe)_7$ , and  $[WO(OMe)_4]_2$ ) are simultaneously present in a solution in different ratios, compounds  $Re_{4-x}Mo_xO_{6-y}(OMe)_{12+y}$  and  $Re_{4-x}W_xO_{6-y}(OMe)_{12+y}$  containing both metals are formed. The central fragment of the complexes  $Nb_{4-x}Ta_xO_2(OMe)_{14}(ReO_4)_2$  composed of four niobium/tantalum atoms is formed upon condensation of the starting binuclear niobium/tantalum derivatives due to the formation of oxo bridges.

An important aspect of practical application is that the methods developed for the synthesis of bi- and trimetallic alkoxides allow one to obtain specimens with a pre-specified ratio of metals. This opens up the way for deliberate action on the composition and properties of materials.

The structure of rhenium alkoxides is shown in Fig. 3 [4].

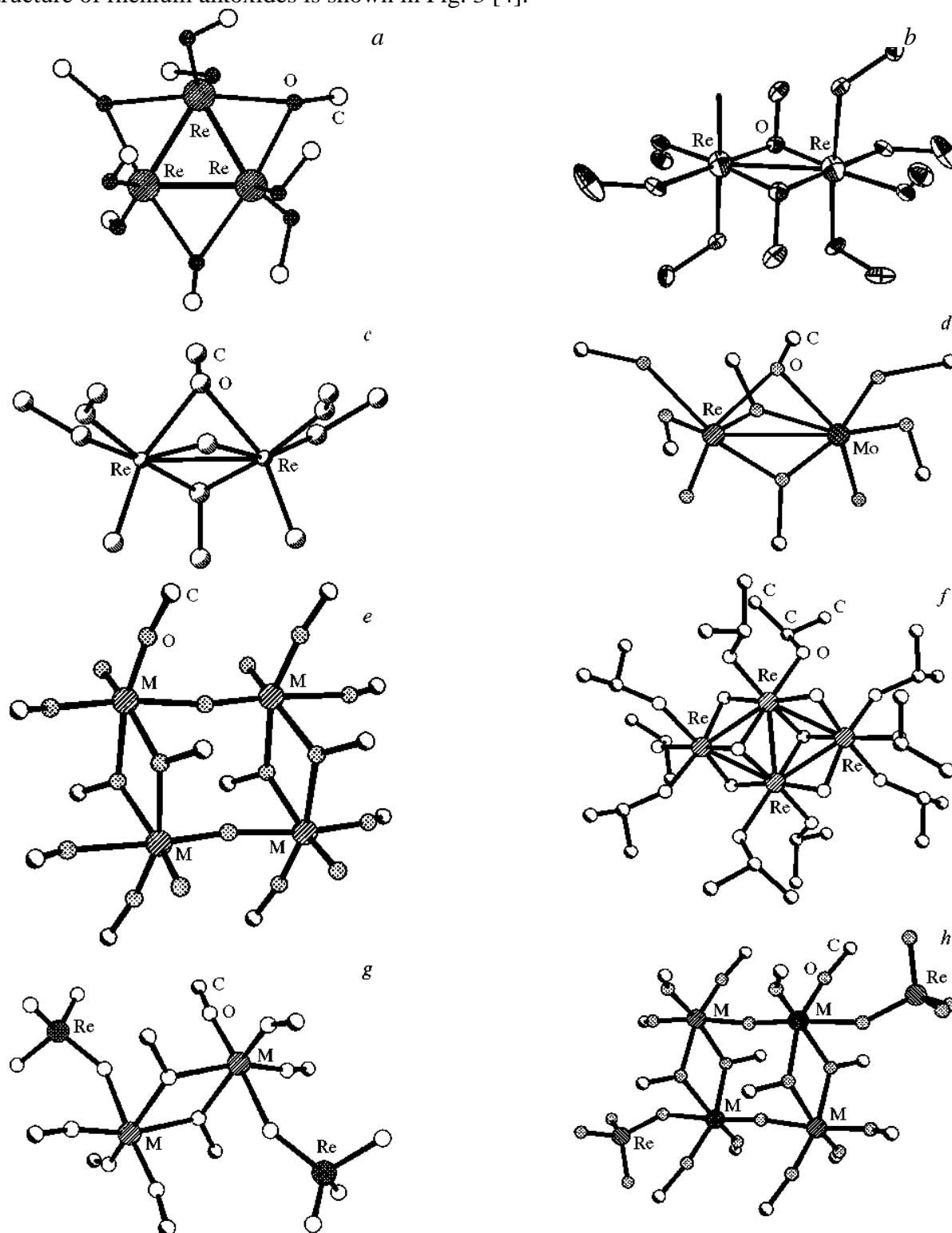


Fig.3. Structure of rhenium alkoxides:  $Re_3(OR)_9$  ( $R = Pr^i, CH_2Bu^i$ ) (a);  $Re_2(OMe)_{10}$  (b);  $Re_2O_3(OMe)_6$  (c);  $ReMoO_2(OMe)_7$  (d);  $Re_4O_6(OMe)_{12}$  ( $M = Re$ ),  $Re_{4-x}Mo_xO_6(OMe)_{12}$  ( $M = Re, Mo$ ),  $Re_{4-x}W_xO_6(OMe)_{12}$  ( $M = Re, W$ ) (e);  $Re_4O_6(OPr^i)_{10}$  (f);  $Nb_2(OMe)_8(ReO_4)_2$  ( $M = Nb$ ),  $Ta_2(OMe)_8(ReO_4)_2$  ( $M = Ta$ ),  $Nb_{2-x}Ta_x(OMe)_8(ReO_4)_2$  ( $M = Nb, Ta$ ) (g);  $Nb_4O_2(OMe)_{14}(ReO_4)_2$  ( $M = Nb$ ),  $Ta_4O_2(OMe)_{14}(ReO_4)_2$  ( $M = Ta$ ),  $Nb_{4-x}Ta_xO_2(OMe)_{14}(ReO_4)_2$  ( $M = Nb, Ta$ ) (h).



Association or condensation of metal complexes in lower oxidation states may give metal-metal bonds. The structural criterion for the formation of these bonds is that the metal-metal distance is comparable with or shorter than that in the structure of the corresponding metals [15], or shorter than twice the effective metallic radius, which is 2,76 for Re (Tabl.1) [16-19].

Table 1. Characteristics of metal-metal bonds in alkoxide compounds

Compound	r(M–M), Å	M–M bond order	Refs.
Re <sub>4</sub> O <sub>6-y</sub> (OMe) <sub>12+y</sub>	3,45; 3,65	no bond	*
Re <sub>4</sub> O <sub>4</sub> (OEt) <sub>12</sub>	2,54(2); 2,648(19); 2,65(2)	>1, ~1	*
Re <sub>4</sub> O <sub>6</sub> (OPr <sup>i</sup> ) <sub>10</sub>	2,5204(7) - 2,5501(5)	>1	*
ReMoO <sub>2</sub> (OMe) <sub>7</sub>	2,658(2)	1	*
Re <sub>2</sub> O <sub>3</sub> (OMe) <sub>6</sub>	2,559(1)	1	[16]
Re <sub>2</sub> (OMe) <sub>10</sub>	2,5319(7)	2	[17]
Re <sub>3</sub> (OPr <sup>i</sup> ) <sub>9</sub>	2,36	2	[18]
Re <sub>3</sub> (OCH <sub>2</sub> Bu <sup>t</sup> ) <sub>9</sub>	2,365(1) - 2,372(1)	2	[19]

\* Own data

The structure of ReMoO<sub>2</sub>(OMe)<sub>7</sub> [7] is composed of two distorted MO<sub>6</sub> octahedra (M = Re or Mo) with a common face and terminal oxo ligands (M—M bond). The distribution of the atoms of two metals among the crystal positions is random and partially ordered, the populations being 0.71(1) Re + 0.29(1) Mo and 0.29(1) Re + 0.73(1) Mo.

The structure of the isopropoxide complex, Re<sub>4</sub>O<sub>6</sub>(O<sup>i</sup>Pr)<sub>10</sub> (Fig.3), contains a planar rhombus of metal atoms with all five bonds of essentially the same length (2.52 – 2.55 Å [20], compare Re=Re 2.532 Å in Re<sub>2</sub>(OMe)<sub>10</sub> [21]) – rather short for the very low number of the electrons available for bonding in that structure (6 electrons for 5 bonds). The structure of Re<sub>4</sub>O<sub>4</sub>(OEt)<sub>12</sub> contains also a planar Re<sub>4</sub>-core close to a rhombus in its geometry. It belongs as well as the structure of the oxoisopropoxide derivative to the well-known M<sub>4</sub>X<sub>16</sub> core type structure type, originating from hexagonal dense packing of metal and ligand atoms, one of the most typical for metal alkoxides [22, 23]. Two additional electrons available for bonding do not lead to pronounced shortening of the Re–Re distances, on contrary, the structure of the compound Re<sub>4</sub>O<sub>4</sub>(OEt)<sub>12</sub> contains only two shorter symmetrically equivalent bonds (2,54(2) Å Re(1)–Re(2)), which is comparable with the length of a double Re=Re bond. The other two symmetrical bonds and the shorter diagonal of the rhombus have almost the same lengths and are considerably longer (2,65 Å). These values are considerably higher than even the single Re–Re bond length in Re<sub>2</sub>O<sub>3</sub>(OMe)<sub>6</sub> (2,56 Å), where the metal atoms as well as in Re<sub>4</sub>O<sub>4</sub>(OEt)<sub>12</sub> are connected by both oxo- and alkoxobridges.

The structure of Re<sub>4</sub>O<sub>6</sub>(OPr<sup>i</sup>)<sub>10</sub> [7,13] contains four ReO<sub>6</sub> octahedra connected by common edges and five Re—Re bonds with a higher order. The metal atoms are located in one plane and are connected by two μ<sub>3</sub>- and four μ<sub>2</sub>-oxo bridges.

The compound Re<sub>4</sub>O<sub>6</sub>(OPr<sup>i</sup>)<sub>10</sub> is of interest as regards the metal—metal bonds. In this structure, the Re—Re distances, equal to 2.5204(7)—2.5501(5) Å, are comparable with the length of a localized Re—Re bond with a higher order (see Table I). Since two Re atoms in this complex occur in +5 oxidation state and the other two atoms, in +6 oxidation state, there are six electrons available for

their binding to each other. Clusters similar to  $\text{Re}_4\text{O}_6(\text{OPr}^i)_{10}$  with five virtually equal metal—metal distances have been found previously [24,25], only in a system with ten electrons (Table 2).

Table 2. Metal–Metal Bonds in clusters based on  $\text{Ti}_4(\text{OMe})_{16}$  core structure

Compound	L.1, Å	L.2, Å	D, Å	Number of core cluster electrons	Ref.
$\text{Ba}_{1,14}\text{Mo}_8\text{O}_{16}$	2,616(1)	2,578(1)	2,578(1)	10	[24]
$\text{Ba}_{1,14}\text{Mo}_8\text{O}_{16}$	2,847(1)	2,546(1)	2,560(1)	8,28 (average)	[24]
$\text{W}_4(\text{OEt})_{16}$	2,936(2)	2,646(2)	2,763(1)	8	[25]
$\text{Re}_4\text{O}_4(\text{OEt})_{12}$	2,54(2)	2,648(19)	2,65(2)	8	[*]
$\text{Re}_4\text{O}_6(\text{OPr-}i)_{10}$	2,5501(5)	2,5399(5)	2,5204(7)	6	[*]
$\text{Mo}_4\text{O}_8(\text{OPr-}i)_4(\text{Py})_4$	3,472(1)	2,600(1)	3,218(1)	4	[25]

\* Own data

The structure of tetranuclear rhenium methoxy derivatives  $\text{Re}_4\text{O}_{6-y}(\text{OMe})_{12+y}$  and related bimetallic complexes is based on planar  $\text{Re}_4$  fragment. The structure of  $\text{Re}_4\text{O}_{6-y}(\text{OMe})_{12+y}$  [6,11] is characterized by the  $\text{ReO}_6$  octahedra sharing edges and faces; the rhenium atoms occupy the vertices of a nearly regular quadrangle and are bound alternately by oxo bridges and double alkoxy bridges. No metal—metal bonds are present. When  $y = 0$ , one terminal oxo ligand per rhenium atom is present, while for  $y = 4$ , the structure does not contain terminal oxo ligands. For  $0 < y < 4$ , these occur in the statistic disorder with alternative methoxy groups (*i.e.*, the crystals are built by joint packing of molecules containing different numbers of oxo and alkoxy groups).

The structure of  $\text{Re}_{4-x}\text{Mo}_x\text{O}_{6-y}(\text{OMe})_{12+y}$  [6] is similar to that of  $\text{Re}_4\text{O}_{6-y}(\text{OMe})_{12+y}$ . Some rhenium atoms are replaced by molybdenum atoms in the isomorphous manner. The distribution of the metal atoms of two sorts among the positions is random and partially ordered (from 0.83(2) Re + 0.17(1) Mo to 0.98(2) Re + 0.02(2) Mo for the crystal with  $x = 0.4$ ). The structure of the derivative  $\text{Re}_{4-x}\text{W}_x\text{O}_{6-y}(\text{OMe})_{12+y}$  is similar to that of  $\text{Re}_{4-x}\text{Mo}_x\text{O}_{6-y}(\text{OMe})_{12+y}$ .

Bi- and trimetallic derivatives of rhenium, niobium, and tantalum exist as two structures containing perrhenate groups. One is based on  $\text{M}_2(\text{OMe})_{10}$  ( $\text{M} = \text{Nb}$  or  $\text{Ta}$ ) and the other, on fragments consisting of four metal atoms. In the complex  $\text{Nb}_{4-x}\text{Ta}_x\text{O}_2(\text{OMe})_{14}(\text{ReO}_4)_2$ , [7-10] four niobium (or tantalum) atoms form a fragment resembling the structure of  $\text{Re}_4\text{O}_{6-y}(\text{OMe})_{12+y}$ . Trimetallic complexes are formed due to isomorphous replacement of niobium atoms by tantalum. The distribution of the metal atoms of two sorts among the positions is statistic, partially ordered (for the crystal with  $x = 2$ , the populations of the position connected to the  $\text{ReO}_4$  group are  $(0.70 \pm 0.05)$  Nb +  $(0.30 \pm 0.05)$  Ta; for the other position,  $(0.29 \pm 0.05)$  Nb +  $(0.71 \pm 0.05)$  Ta).

Isomorphous replacement of atoms with similar properties affords crystalline complexes with variable composition in which the ratio of the two metals can be varied over a broad range.

For example, the replacement of rhenium by molybdenum or tungsten gives rise to rhenium-based tetra-nuclear complexes  $\text{Re}_{4-x}\text{Mo}_x\text{O}_{6-y}(\text{OMe})_{12+y}$ ; ( $0 < x < 2.82$ ) and  $\text{Re}_{4-x}\text{W}_x\text{O}_{6-y}(\text{OMe})_{12+y}$  ( $0 < x < 2$ ) [6,14]. Since tetranuclear structure is not encountered for individual molybdenum or tungsten derivatives, in this case, the isomorphous replacement of rhenium by these metals is possible only in a limited range of compositions.

In the case of  $Nb_{4-x}Ta_xO_2(OMe)_{14}(ReO_4)_2$  and  $Nb_{2-x}Ta_x(OMe)_8(ReO_4)_2$ , the Nb : Ta ratio susceptible for isomorphous replacement of niobium by tantalum is boundless. The bimetallic niobium/rhenium ( $x = 0, x' = 0$ ) and tantalum/rhenium complexes ( $x = 4, x' = 2$ ) as well as trimetallic complexes with a variable composition ( $0 < x < 4, 0 < x' < 2$ ) [7-9] have been prepared. Studies of the thermal properties of rhenium alkoxides have shown that they decompose at relatively low temperatures (100—300 °C) yielding either oxide or metal phases, depending on the process conditions (Fig.4). [7,8,12].

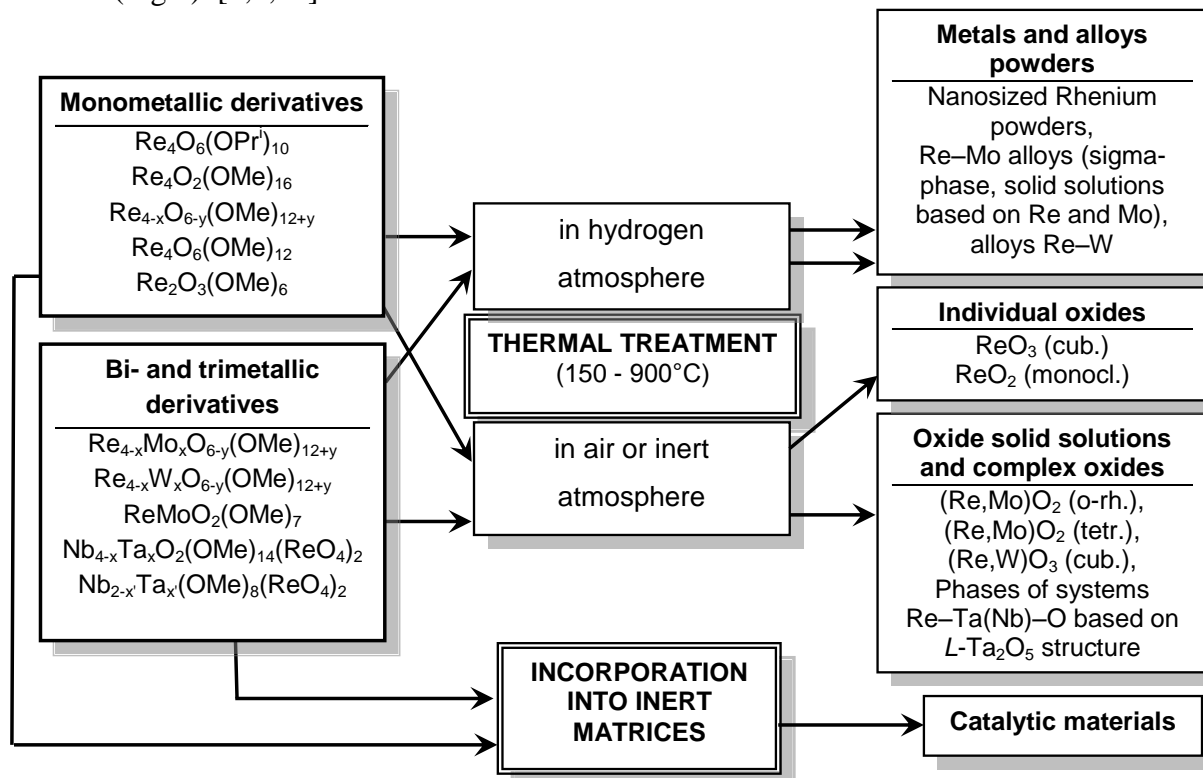


Fig.4. Alkoxides as a basis for fabrication of rhenium-containing materials

Decomposition of individual rhenium alkoxides  $Re_4O_6(OPr^i)_{10}$ ,  $Re_4O_2(OMe)_{16}$ ,  $Re_{4-x}O_{6-y}(OMe)_{12+y}$ , and  $Re_4O_6(OMe)_{12}$  in air or in an inert atmosphere affords rhenium oxides,  $ReO_3$  or monoclinic  $ReO_2$ , as highly dispersed powders with an average particle size of less than 30—50 nm.. Similar decomposition of the bimetallic derivatives  $Re_{4-x}Mo_xO_{6-y}(OMe)_{12+y}$  and  $Re_{4-x}W_xO_{6-y}(OMe)_{12+y}$  yields single-phase specimens of rhenium/molybdenum  $(Re,Mo)O_2$  or rhenium/tungsten  $(Re,W)O_3$  solid solutions. By decomposition of bi- and trimetallic rhenium, niobium, and tantalum derivatives, complex oxide phases of the  $Re-Ta(Nb)-O$  systems based on a block type structure derived from  $L-Ta_2O_5$  were prepared for the first time (Table 3).

Table 3. Structure of  $(Nb_{1-x}Ta_x)_4O_2(OMe)_{14}(ReO_4)_2$  ( $x = 0,3; 0,5; 0,7$ ) and thermal properties

№	Source complex	Product	a, Å	b, Å	c, Å	V, Å <sup>3</sup>
1*	$(Nb_{0,7}Ta_{0,3})_4O_2(OMe)_{14}(ReO_4)_2$	$(Nb_{0,7}Ta_{0,3})_2O_5$	6,18(6)	40,25(6)=11×3,659	3,922(2)	975,1(17)
2*	$(Nb_{0,5}Ta_{0,5})_4O_2(OMe)_{14}(ReO_4)_2$	$(Nb_{0,5}Ta_{0,5})_2O_5$	6,18(6)	40,31(5)=11×3,665	3,918(18)	975,9(16)
3*	$(Nb_{0,3}Ta_{0,7})_4O_2(OMe)_{14}(ReO_4)_2$	$(Nb_{0,3}Ta_{0,7})_2O_5$	6,177(10)	40,29(10)=11×3,663	3,909(3)	973(3)
4**	$L(\gamma)-Ta_2O_5$ (ICCD-JCPDS № 25-0922)		6,198(5)	40,29(3)=11×3,663	3,888(5)	970,9
5**	$L(\gamma, T)-Nb_2O_5$ (ICCD-JCPDS № 27-1313)		6,168(1)	29,312(1)=8×3,664	3,938(1)	712,0

\* Experiment    \*\* Literature data

Phase composition of the products obtained by thermal decomposition of  $(Nb_{1-x}Ta_x)_4O_2(OMe)_{14}(ReO_4)_2$  ( $x = 0,3; 0,5; 0,7$ ) in air

Decomposition of alkoxide in a hydrogen atmosphere allows one to prepare nano-sized powders of rhenium metal (from individual derivatives) or rhenium alloys (from the bimetallic complexes  $\text{Re}_{4-x}\text{Mo}_x\text{O}_{6-y}(\text{OMe})_{12+y}$ , and  $\text{Re}_{4-x}\text{W}_x\text{O}_{6-y}(\text{OMe})_{12+y}$ ).

Rhenium alkoxides proved to be promising starting materials for the development of catalysts by insertion into a zeolite matrix. In particular, mono- and bimetallic rhenium alkoxides  $\text{Re}_2\text{O}_3(\text{OMe})_6$  and  $\text{ReMoO}_2(\text{OMe})_7$  (it is cluster compound) have been used to prepare new-generation catalysts by insertion of these compounds into a NaY zeolite matrix followed by their thermal decomposition. A substantial advantage of this approach is the possibility of preserving the high-dispersed state *via* stabilization of clusters, including those containing two different metals, in the zeolite cavities. Decomposition of the alkoxides inserted in the matrix affords metal or oxide nanoclusters whose mobility is restricted inside the pores. In the case of bimetallic systems, it is possible to obtain, directly in the pores, highly dispersed particles uniform not only in their size but also in their composition, which is pre-specified by the ratio of the metals in the initial compound. A study of the catalytic properties of the materials obtained by this method showed a substantial positive synergistic effect for the product of insertion of the bimetallic complex compared with the materials based on individual rhenium and molybdenum compounds. [26] This has been confirmed when using bimetallic (Re-W, Re-Ta) alkoxoderivatives as precursors in the production of catalysts for the reactions of alcohol reductive dehydration (Fig. 5) [27].

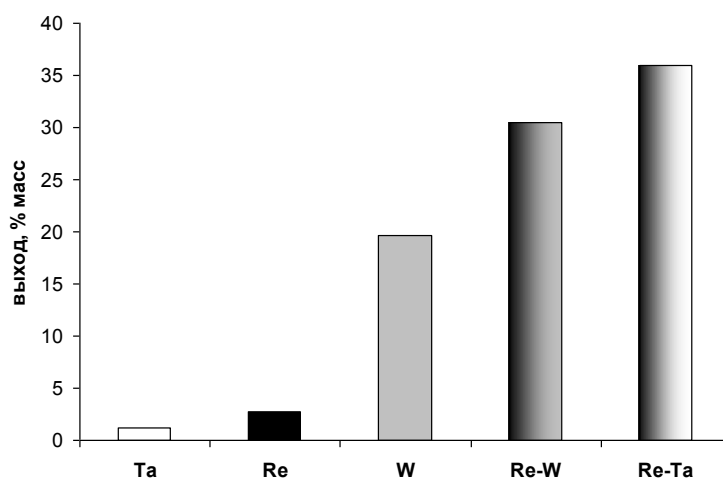


Fig.5. The relationship between alkane-olefins fractions C5 – C9 yield and composition of active components in cross coupling reaction of ethanol and glycerin.

### Conclusion.

The traditional method for alkoxide synthesis is based on ligand substitution reactions. This method was used to prepare individual rhenium alkoxides. Alternative synthetic routes include reactions of rhenium(VII) oxide with alcohols and alkoxides of other metals and anodic dissolution of metals in alcohols. These methods made it possible to synthesize both known and new monometallic rhenium alkoxides and also to synthesize for the first time bi- and trimetallic rhenium, molybdenum, tungsten, niobium, and tantalum complexes. The isomorphous replacement of metals in bi- and trimetallic derivatives opens up the way to the alkoxide derivatives with variable composition, in which the ratio of the metals can be varied over a broad range.

An important structural feature of alkoxides and oxoalkoxides is the presence of alkoxy and oxo bridges, which ensure the formation of polynuclear (in particular, heterometallic) compounds.

### Acknowledgements.

The authors show their gratitude to professors G.A. Seisenbaeva and V.G. Kessler (Department of Chemistry SLU, Uppsala, Sweden) for creative collaboration on the different steps of the work and to the RFBR (projects 06-03-32444 and 09-03-00328) for the financial support.

### References.

1. R. H. Tuffias, R. B. Kaplan, and M. A. Appel, Proc. Int. Symp: "Rhenium and Rhenium Alloys" (Orlando, Florida (USA), 1997).



2. R. W. Broomfield, D. A. Ford, H. K. Bhangu, M. C. Thomas, D. J. Frasier, P. S. Burkholder, K. Harris, G. L. Erickson, and J. B. Wahl: *Proc. Int. Symp. "Rhenium and Rhenium Alloys" (Orlando, Florida (USA), 1997)*.
3. M. A. Ryashentseva and Kh. M. Minachev: *Renii i ego soedineniya v geterogennom katalize [Rhenium and its Compounds in Heterogeneous Catalysis]* (Nauka, Moscow, 1983).
4. P. A. Shcheglov, D. V. Drobot (2005). *Russian Chemical Bulletin. International Edition.* 54, 2247.
5. A. A. Palant, I. D. Troshkina, A. M. Chekmarev : *Metallurgy of rhenium* (Nauka, Moscow, 2007).
6. G. A. Seisenbaeva, A. V. Shevelkov, J. Tegenfeldt, L. Kloo, D. V. Drobot, and V. G. Kessler (2001). *J. Chem. Soc., Dalton Trans.* 2762.
7. D. V. Drobot, P. A. Shcheglov, G. A. Seisenbaeva, and V. G. Kessler (2002). *Izv. Vuzov. Tsvetnaya metallurgiya [Higher School Bull. Nonferrous Metallurgy]*. 6, 32.
8. P. A. Shcheglov, D. V. Drobot, G. A. Seisenbaeva, S. Gohil, and V. G. Kessler (2002). *Chem. Mater.* 14, 2378.
9. P. A. Shcheglov, G. A. Seisenbaeva, S. Gohil, D. V. Drobot, and V. G. Kessler (2002). *Polyhedron.* 21, 2317.
10. Pat. RF 2227788 (*Byul. Izobret.*, 2004), 12.
11. V. G. Kessler, A. V. Shevelkov, G. V. Khvorykh, G. A. Seisenbaeva, N. Ya. Turova, and D. V. Drobot (1995). *Zh. Neorgan. Khim.* 40, 1477.
12. P. A. Shcheglov, D. V. Drobot, Yu. V. Syrov, and A. S. Maltseva (2004). *Neorgan. Materialy.* 40, 220.
13. P. A. Shcheglov, G. A. Seisenbaeva, D. V. Drobot, and V. G. Kessler (2001). *Inorg. Chem. Commun.* 4, 227.
14. G. A. Seisenbaeva, A. V. Shevelkov, V. G. Kessler, N. N. Belanishvili, and D. V. Drobot (1999). *Zh. Neorgan. Khim.* 44, 383.
15. F. A. Cotton and R. A. Walton: *Multiple Bonds Between Metal Atoms* (J. Wiley and Sons, New York—Chichester, 1982).
16. P. G. Edwards, G. Wilkinson, M. B. Hursthouse, K. M. Abdul Malik (1980). *J. Chem. Soc. Dalton Trans.* 2467.
17. J. C. Bryan, D. R. Wheeler, D. L. Clark, J. C. Huffman, A. P. Sattelberger (1991). *J. Am. Chem. Soc.* 113, 3184.
18. D. M. Hoffman, D. Lappas, D. A. Wierda (1993). *J. Am. Chem. Soc.* 115, 10538.
19. W.-W. Zhuang, B. E. Truitt, D. M. Hoffman (1997). *Inorg. Chem.* 36, 3330.
20. G.A. Seisenbaeva, A.I. Baranov, P.A. Shcheglov, V.G. Kessler (2004). *Inorg. Chim. Acta.* 357, 468.
21. J. C. Bryan, D. R. Wheeler, D. L. Clark, J. C. Huffman, A. P. Sattelberger (1991). *J. Amer. Chem. Soc.* 113, 3184.
22. D.A. Wright, D.A. Williams (1968). *Acta Crystallogr.* 24, 1107.
23. N. Ya Turova., E. P. Turevskaya., V. G. Kessler, M. I. Yanovskaya: *The Chemistry of Metal Alkoxides* (Boston, Dordrecht, London: Kluwer Academic Publishers. 2002).
24. C. C. Torardi, R. E. McCarley (1981). *J. of Solid State Chem.* 37, 393
25. M. H. Chisholm, J. C. Huffman (1981). *J. Amer. Chem. Soc.* 103, 6093
26. A. L. Kustov, V. G. Kessler, B. V. Romanovsky, G. A. Seisenbaeva, D. V. Drobot, and P. A. Shcheglov (2004). *J. Mol. Catal. A.* 216, 101.

M.V. Tsodicov, A.V. Chistyakov, F.A. Yandieva, V.Ya. Kugel, O.V. Buhtenko, T.A. Zhdanova, A.E. Gehman, I.I. Moiseev, D.V. Drobot, O.V. Petrakova. Patent 2391133 RF, MPK C1 B01J 21/04, B01J 23/30, B01J 23/36, C07C 1/20, C07C 9/16, C07C 9/00, C07C 11/00. Method of alkanolefin hydrocarbon production – № 2008139448/04, applied for 06.10.08; published 10.06.10, Bull. № 16.

1.10.

## STRUCTURE AND MAGNETIC PROPERTIES OF POLYNUCLEAR COMPLEXES CONTAINING Re(IV)

Carlos Kremer, Raúl Chiozzone

Cátedra de Química Inorgánica, Facultad de Química,  
Montevideo, Uruguay, (e-mail: ckremer@fq.edu.uy)

One of the major goals in inorganic supramolecular chemistry today is the design of polynuclear coordination arrays and the study of their magnetic properties. With the generation of well-defined architectures it is possible to understand the different factors which determine the exchange coupling between spin carriers. Most of the results found in the literature are focused on polynuclear complexes containing metal ions belonging to the first transition series. With this information the study of those systems containing 4d or 5d metal ions becomes very interesting. In this presentation we revise the structure and magnetic properties of Re(IV) mononuclear and polynuclear complexes.

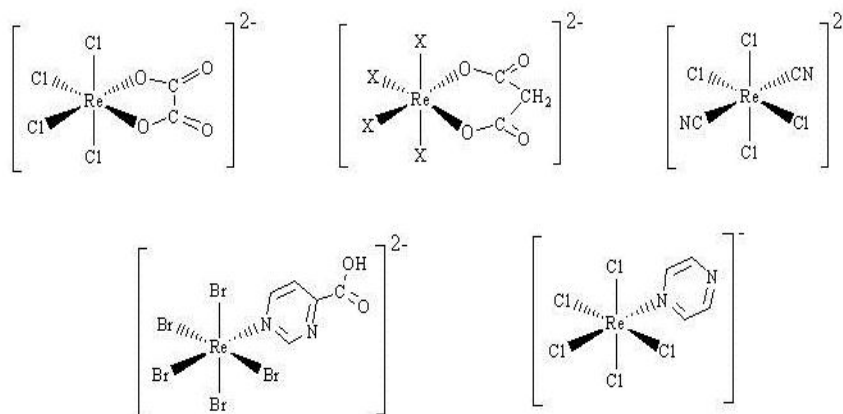


*Fig. 1. Some Re(IV) mononuclear complexes used as building blocks.*

Rhenium(IV), a  $5d^3$  ion with a  $^4A_{2g}$  electronic ground state, usually forms octahedral complexes which are reasonably stable against redox processes and inert to ligand substitution. Complexes containing dicarboxylic ligands,  $[\text{ReX}_4(\text{ox})]^{2-}$  and  $[\text{ReX}_4(\text{mal})]^{2-}$  ( $\text{X} = \text{Cl}, \text{Br}$ ; ox = oxalate; mal = malonate), N-donor ligands,  $[\text{ReCl}_5(\text{pyz})]^-$  (pyz = pyrazine),  $[\text{ReBr}_5(\text{Hpyzc})]^-$  (Hpyzc = 2-pyrazinecarboxylic acid), and  $[\text{ReCl}_4(\text{CN})_2]^{2-}$ , are some examples of mononuclear rhenium complexes that have been prepared and fully characterized. The presence of ligands which can act as donors toward a second metal ion (Fig. 1) is a common structural feature that has allowed the "complex as ligand" approach for the design of higher nuclearity compounds. Their structures range from discrete binuclear complexes (for example in  $[\text{ReCl}_4(\mu\text{-ox})\text{Mn}(\text{dmphen})_2]$ , dmphen = 2,9-dimethyl-1,10-phenanthroline) to extended chain-like compounds (for example in  $[\text{ReCl}_4(\mu\text{-mal})\text{Mn}(\text{dmphen})(\text{H}_2\text{O})_2]$ ) are presented in this work. In addition, the magneto-structural studies of these mono- and polynuclear complexes are also discussed.

1.11.

## POLYFLUORINATED $\beta$ -DIKETONATES OF RHENIUM

A.I. Irtegov<sup>1</sup>, M.A. Kurykin<sup>2</sup>, V.N. Khrustalev<sup>2</sup>, E.E. Nikishina<sup>1</sup>,  
D.V. Drobot<sup>1</sup>.

<sup>1</sup>Lomonosov's Moscow State Academy of Fine Chemical Technology, Moscow, Vernadskogo avenue 86,

<sup>2</sup>A.N.Nesmeyanov Institute of Organoelement Compounds Russian Academy of Sciences,

Moscow, Vavilov st., 28.

[irteg@mail.ru](mailto:irteg@mail.ru), [mak@ineos.ac.ru](mailto:mak@ineos.ac.ru)

Fluorinated  $\beta$ -diketonates of metals possess a number of properties useful for technology, the most valuable properties are good solubility in organic solvents and high volatility. Therefore they can be used for solving two important problems: preparation of catalysts and film coatings by CVD. In recent years rhenium has become one of the most in-demand metals for both these problems.

We have prepared the earlier described complex  $\text{ReOCl}_2(\text{OEt})_2\text{PPh}_3$  and studied its reactions with  $\beta$ -diketones HL ( $\text{CH}_3\text{COCH}_2\text{COCH}_3$ ,  $\text{CF}_3\text{COCH}_2\text{COCF}_3$ ,  $\text{C}_2\text{F}_5\text{COCH}_2\text{COC}_2\text{F}_5$ ,  $\text{C}_3\text{F}_7\text{COCH}_2\text{COC}_3\text{F}_7$ ,  $\text{C}_4\text{F}_9\text{COCH}_2\text{COC}_4\text{F}_9$ ,  $\text{C}_3\text{F}_7\text{OCF}(\text{CF}_3)\text{COCH}_2\text{COCF}(\text{CF}_3)\text{OC}_3\text{F}_7$ ). A number of new rhenium complexes  $\text{ReCl}_2\text{L}\cdot 2\text{PPh}_3$  were obtained. We have studied thermal properties and spectral characteristics of the synthesized compounds. The fluorinated rhenium complexes were shown to have high volatilities and vaporize without decomposition, this can be used in preparation of rhenium-containing films.

The details of the synthesis and physicochemical properties of the complexes will be considered in the presentation.

The work was financially supported by the Russian Foundation for Basic Research (Grant no. 09-03-00328a).

1.12.

## PREPARATION OF TECHNETIUM METAL-METAL BONDED ACETATE DIMERS VIA HYDROTHERMAL ROUTE

W.M. Kerlin<sup>1</sup>, T. Yordanova<sup>2</sup>, F. Poineau<sup>1</sup>, P.M. Forster<sup>1</sup>,  
A.P. Sattelberger<sup>3</sup>, K.R. Czerwinski<sup>1</sup>

<sup>1</sup>Department of Chemistry, Radiochemistry Program, University of Nevada Las Vegas,  
Las Vegas, NV 89154, USA

<sup>2</sup>Laboratory for Computational Molecular Design, Ecole Polytechnique Fédérale de Lausanne,  
Lausanne, ch-1015, Switzerland

<sup>3</sup>Energy Engineering and Systems Analysis Directorate, Argonne National Laboratory,  
Argonne, IL 60439, USA

Recent results of hydrothermal reactions with pertechnetate, Tc(VII), have produced various low-valent compounds such as dication hexahalotechanate (IV) and Tc-Tc dimers.

The reaction of potassium pertechnetate in acetic acid /hydrochloric acid in an atmosphere of hydrogen gas yields red hexagonal crystals of known tetraacetatodichloro ditechtnetate(III),  $Tc_2(\mu-O_2CCH_3)_4Cl_2$  and blue triacetatodiaquadichloro ditechtnetate (II)(III) hydrate.

Single crystal XRD analysis on both Tc dimers has been determined and the unit cell parameters will be presented.

Additional characterization of the  $Tc_2(\mu-O_2CCH_3)_3Cl_2(H_2O)_2 \cdot H_2O$  including UV-Vis, and FT-IR will shown. DFT calculations will be given for the  $Tc_2(\mu-O_2CCH_3)_2Cl_4$   $Tc_2(\mu-O_2CCH_3)_3Cl_2(H_2O)_2 \cdot H_2O$ , and  $Tc_2(\mu-O_2CCH_3)_4Cl_2$ .

Currently, work explores *in situ* hydrogen generation via Zn or sodium borohydride, as well as the use of alternative reducing agents, allowing for many more reactions to be carried out in conventional autoclaves.

Results of the Zn and sodium borohydride reactions will be discussed. These one step reactions of reducing Tc(VII) to low valent technetium provides high yield intermediates for potential waste forms and use in nuclear fuel cycle separations.

**Acknowledgments:** SISGR-Fundamental Chemistry of Technetium-99 Incorporated into Metal Oxide, Phosphate and Sulfide: Toward Stabilization of Low-Valent Technetium  
Contract No. 47824B Basic Energy Sciences, DOE

### References:

1. L. I. Zaitseva, A.S. Kotel'nikova and A.A. Reszvov, *Russ. J. Inorg. Chem.* 1980, **25**, 1449.
2. Cotton, A.F., C.A. Murillo, R.A. Walton.; *Multiple Bonds Between Metal Atoms*, Springer Science and Business Media, Inc.: New York, 2005, p. 257-259.
3. V. I. Spitsyn, B. Baierl, S.V. Kryuchkov, A.F. Kuzina and M. Varen, *Dokl. Akad. Nauk.* 1981, **256**, 608.



1.13.

## **PHYSICOCHEMICAL PRINCIPLES OF THE DEVELOPMENT OF RHENIUM-BASED AND RHENIUM-CONTAINING ALLOYS**

Povarova K.B.

Baikov Institute of Metallurgy and Materials Science RAS. [povarova@imet.ac.ru](mailto:povarova@imet.ac.ru)

Rhenium (Re) is a hcp transition metal belonging to Group VII of the third long period of the periodic table (atomic number 75). The melting/boiling points (3453/6173 K), density (21.04 g/cm<sup>3</sup>), and elastic modulus (479 GPa) of Re are higher than those of the most refractory metals. The maximum operating temperature, at which the weight loss by evaporation is ≤1% per 10 hours, reaches 2950 K.

Rhenium belongs to rare metals (its clark is ~10<sup>-7</sup> - 10<sup>-6</sup>%) and is difficult to manufacture (because of strong strain hardening) and expensive metal.

The unique properties of Re and some its alloys, which can be used in the environments impossible for operating of other materials, determine high interest in them. For example, in short-term and long-term strength at temperatures above 2400K, Re surpasses the best high-temperature cold-brittle tungsten alloys and, unlike them, has a plasticity reserve at temperatures down to cryogenic ones, high resistance to thermal shock and thermal cycling (290-2500K), low gas permeability, and does not form any stable interstitial phases.

The physicochemical approaches to the design of structural alloys with Re are developed.

Use of Re as an alloying element (AE) or as an alloy base is determined by two factors: the mutual solubility of Re and AE and four "rhenium effects", which have no analogs. A high solubility of Re in bcc Group VI metals (W, Mo and Cr) has allowed the development of a new class of high-temperature alloys and the alloys with special physical and chemical properties (W-Re, Mo-Re, and W-Mo-Re), in which the addition of 25-35 at. % Re simultaneously increases low-temperature ductility and strength of cold-short Group VI metals ("Re effect-1").

The ability of Re to drastically increase the strain hardening rate of W and Mo alloys ("Re effect-2") allowed the development of the alloys with  $\sigma_B$  of up to 6000 MPa for elastic members.

A substantial increase in low-temperature ductility of W and Mo alloys at 2-7 at. % Re ("Re effect-3") allowed the development of cost-effective high-temperature rhenium alloys for bulk products.

The ability of Re to increase the high-temperature strength and service life of modern nickel-base superalloys is widely used as "Re effect-4".

1.14.

## SYNTHESIS AND CHARACTERIZATION OF LOW-VALENT BINARY TECHNETIUM CHLORIDES

E.V. Johnstone, F. Poineau, P.F. Weck, E. Kim<sup>1</sup>, P.M. Forester, B. Scott<sup>2</sup>, T. Hartmann, A.P. Sattelberger<sup>3</sup>, K.R. Czerwinski

Department of Chemistry, University of Nevada Las Vegas, Las Vegas, NV 89154, USA

<sup>1</sup> Department of Physics and Astronomy, University of Nevada Las Vegas, Las Vegas, NV 89154, USA

<sup>2</sup> Materials Physics and Applications Division, Los Alamos National Laboratory,  
Los Alamos, NM 87545, USA

<sup>3</sup> Energy Engineering and Systems Analysis Directorate, Argonne National Laboratory,  
Argonne, IL 60439, USA

Binary transition metal halides (BTMH) are an area of fundamental chemistry that exhibits an array of unique chemical and physical properties. Of the Group V, VI, and VII elements, the binary technetium halides for many years were considerably lacking in comparison with only three isolated and characterized in the solid state (TcF<sub>6</sub>, TcF<sub>5</sub>, and TcCl<sub>4</sub>) [1]. More recently, the discovery of TcBr<sub>4</sub> and TcBr<sub>3</sub> has generated interest in pursuing low-valent binary technetium chlorides [2].

In this work two novel binary technetium halides TcCl<sub>2</sub> and TcCl<sub>3</sub> were synthesized in quantifiable amounts in the solid state and analyzed using various physicochemical characterization methods including single-crystal and powder X-ray diffraction (XRD), UV-Vis, X-ray absorption fine structure (XAFS), and elemental analysis, as well as density functional theory calculations (DFT).

Technetium dichloride was synthesized from the stoichiometric reaction of technetium metal and elemental chlorine at elevated temperatures as a novel compound with new structure-type consisting of an eclipsed conformation of [Tc<sub>2</sub>Cl<sub>8</sub>] units containing a Tc-Tc triple bond [3].

Technetium trichloride was prepared from the reaction of Tc<sub>2</sub>(O<sub>2</sub>CCH<sub>3</sub>)<sub>4</sub>Cl<sub>2</sub> with passing HCl (g) at elevated temperatures and characterized as a novel compound isostructural to ReCl<sub>3</sub> with a triangular Tc<sub>3</sub><sup>3+</sup> core structure containing metal-metal double bonds [4]. The low-valent technetium chlorides synthesized exhibit new and interesting chemical structures and properties, and even show potential as waste forms or use in separations for the nuclear fuel cycle.

**Acknowledgments:** SISGR-Fundamental Chemistry of Technetium-99 Incorporated into Metal Oxide, Phosphate and Sulfide: Toward Stabilization of Low-Valent Technetium Contract No. 47824B Basic Energy Sciences, DOE

### References:

- Schwochau, K. *Technetium: Chemistry and Radiopharmaceutical Applications*, Wile-VCH: Weinheim, 2000, p. 113.
- F. Poineau, E. Rodriguez, P.M. Forester, A.P. Sattelberger, A.K. Cheetham, and K.R. Czerwinski, *J. Am. Chem. Soc.* **131**, 910-911 (2009).
- F. Poineau B.L. Scott, P.F. Weck, E.V. Johnstone, P.M. Forester, E. Kim, K.R. Czerwinski, and A.P. Sattelberger, *J. Am. Chem. Soc.*, submitted
- F. Poineau, E.V. Johnstone, P.F. Weck, E. Kim, P.M. Forester, B.L. Scott, A.P. Sattelberger, and K.R. Czerwinski, *J. Am. Chem. Soc.* **132**, 15864-15865 (2010).

1.15.

**RECENT RESULTS IN RHENIUM CLUSTER CHEMISTRY**

V.E. Fedorov, Yu.V. Mironov, N.G. Naumov, K.A. Brylev

Nikolaev Institute of Inorganic Chemistry, Siberian Branch of Russian Academy of Sciences, Novosibirsk, Russia  
(e-mail: fed@niic.nsc.ru)

Metal cluster compounds are very interesting and important representatives in rhenium chemistry. Authors of this paper carry out the systematic investigation of rhenium cluster complexes during long time. The results of this study are preparation of more than two hundred of new cluster rhenium compounds of different nuclearity -  $\text{Re}_4$ ,  $\text{Re}_6$ ,  $\text{Re}_9$ ,  $\text{Re}_{12}$ , discovery of some key cluster complexes, among of them several compounds have original crystal structures and very interesting physical and chemical properties.

The systematic studies of tetrahedral  $[\text{Re}_4\text{Q}_4(\text{TeY}_2)_4\text{Y}_8]$  ( $\text{Q}=\text{S}, \text{Se}, \text{Te}$ ;  $\text{Y}=\text{Cl}, \text{Br}$ ) and octahedral  $\text{Re}_6\text{Q}_8\text{L}_6$  cluster compounds opened the possibility for synthesis of complexes with diverse compositions and structures. Study of octahedral chalcocyanide complexes  $[\text{Re}_6\text{Q}_8(\text{CN})_6]^{4-}$  ( $\text{Q}=\text{S}, \text{Se}, \text{Te}$ ) was shown that using high temperature reactions it is possible to substitute inner  $\mu_3$ -Q ligands in cluster core with formation of mixed ligand units  $\{\text{Re}_6\text{Q}_{8-x}\text{Q}'_x\}$ . Similar reactions give the equilibrium between different chemical forms  $[\text{Re}_6\text{Q}_{8-x}\text{Q}'_x(\text{CN})_6]^{4-}$  that is in common with classical reactions of stepwise ligands substitution which are typical in coordination chemistry.

Experimental conditions of reactions bringing to condensation of cluster fragments into complexes having more high nuclearity were found: for example, octahedral  $[\text{Re}_6\text{Se}_8\text{Br}_6]^{4-}$  and bioctahedral  $[\text{Re}_9\text{Se}_{11}\text{Br}_6]^{2-}$  complexes were prepared from triangle compound  $\text{Re}_3\text{Br}_9$ ; and twelvenuclear complexes with inserted carbon atom  $[\text{Re}_{12}(\mu_6\text{-C})\text{S}_{17}(\text{CN})_6]^{8-/6-}$  were synthesized in the process of further condensation of octahedral clusters. The latter is unique complex in the cluster chemistry of transition metals.

Chalcocyanide cluster complexes  $[\text{Re}_4\text{Q}_4(\text{CN})_{12}]^{4-}$ ,  $[\text{Re}_6\text{Q}_8(\text{CN})_6]^{4-}$  ( $\text{Q}=\text{S}, \text{Se}, \text{Te}$ ) and  $[\text{Re}_{12}\text{CS}_{17}(\text{CN})_6]^{6-}$  were studied broadly and carefully. Due to ambidentate nature of CN ligands these complexes are very suitable building blocks in design of coordination cyano-bridge polymers of different dimensionality with structures of chain-like, layered and framework types.

The methods for synthesis of hybrid tetrahedral and octahedral complexes coordinated organic N- and P-donor ligands were developed. Some rhenium complexes possessing bright red luminescence are synthesized; similar complexes are perspective preparation in procedure of photodynamic therapy. It was found that emission properties of cluster complexes may be regulated by modification of their electron structures via substitution of inner or external ligands in complexes.

Broad studies of chemistry of rhenium cluster complexes of different compositions, nuclearity and structures have expanded essentially a fundamental knowledge in the field of coordination chemistry of not only rhenium but also transition metals integrally. Obtained regularity can be used as fundamental base in design of new cluster compounds and materials with complex of necessary functional properties.

**Acknowledgment.** Authors thank Russian Foundation for Basic Research (grants N 09-03-92004-HHC and 10-03-01040-a ) for financial support.

1.16.

## HETEROLIGAND ALKOXIDES OF RHENIUM CONTAINING O-Et AND O-<sup>i</sup>Pr LIGANDS

O.S. Kriyzhovets<sup>‡</sup>, D.V. Drobot<sup>‡</sup>, A.V. Shevelkov\*.

<sup>‡</sup>Moscow State University of Fine Chemical Technologies named after M.V. Lomonosov, 119571, Russian Federation, Moscow, prospect Vernadskogo 86, e-mail: [vinilova.olka@bk.ru](mailto:vinilova.olka@bk.ru); [dvdrobot@mail.ru](mailto:dvdrobot@mail.ru)

\*Lomonosov Moscow State University, Chemistry Department, 119071, Russian Federation, Moscow, Leninskie Gory, e-mail: [shev@inorg.chem.msu.ru](mailto:shev@inorg.chem.msu.ru)

**Keywords:** anodic dissolution, rhenium alkoxides, heteroligand alkoxides, nanopowder, extended Huckel calculations

### Abstract:

Currently homometallic and heterometallic rhenium alkoxides are already well known to science, and because of close attention to them there are practically no gaps for researchers in studying of that rhenium alkoxides. Existing works on this subject pointed to the lack of study and novelty of chemical synthesis of heteroligand rhenium alkoxides. But the analysis of the literature data revealed an extraordinary closeness of the structures of rhenium isopropyl alkoxide and ethyl alkoxide (subsequent  $\text{Re}_4\text{O}_6(\text{OPr}^i)_{10}$  [1] and  $\text{Re}_4\text{O}_4(\text{OEt})_{12}$  [2] respectively; the metal-cluster frames of them have the same structure (similar to the initial structure of  $\text{Ti}_4(\text{OMe})_{16}$ [3]), that enables the synthesis of rhenium heteroligand complexes containing -O-Et and -O-<sup>i</sup>Pr ligands. We report quantum-chemical analysis of the ligand nature influence on the stability of rhenium alkoxides by the Extended Huckel Method, the electrochemical synthesis of heteroligand complexes with general formula  $\text{Re}_4\text{O}_n(\text{O-Et})_x(\text{O-Pr}^i)_y$  (at an initial molar ratio of EtOH: Pr<sup>i</sup>OH = 1:1; 2:1; 1:2 in the electrolyte) and the study of physical-chemical (including thermal) properties of the heteroligand complexes and products of their thermal decomposition by X-ray Phase Analysis, Element Analysis, DTG, DSC and IR-spectroscopy.

### Introduction:



The substantial difference between the saturated vapor pressure above Re oxides and other refractory metals oxides and incongruent sublimation of lower Re oxides hamper the production of specimens with a required set of properties. This determines the relevance of the research aimed at developing new methods of synthesis of rhenium-containing metallic and oxide materials. One of possible ways to monitor microstructure and composition of the materials is to deliberate the choice of the starting compounds - precursors. Properties of a selected precursor and properly chosen methods of processing allow one to control the composition and microstructure, opening the way to obtain materials with required characteristics. In many cases modern materials and designs require strict control of the composition (0.1%) and the microstructure parameters (at the nanometers sizes) [4]. An effective approach to producing functional materials based on the d-elements (individual nanopowders of metals, alloys and ligatures, simple and complex oxides, bimetallic catalysts) with a given set of properties and qualities is alkoxotechnology [5]. In this work we report the precursors (heteroligand alkoxides of rhenium) obtained by alkoxotechnology as well as the results of the investigations of the dependence of the synthesized products composition and compositions of the product their thermal destruction upon the ratio of the initial components.

### Quantum-chemical calculations:

The analysis of the previous results [1,2] shows that  $\text{Re}_4\text{O}_6(\text{OPr}^i)_{10}$  has an already regular cluster frame  $\text{Re}_4$  (metal-metal bond Re-Re= 2.52-2.55 Å), whereas  $\text{Re}_4\text{O}_4(\text{OEt})_{12}$  possesses a distorted structure of the cluster frame evidenced by the metal-metal bond length (Re-Re=2.54-2.65 Å). Due

to the closeness of their structures the possibility to produce heteroligand complexes based on one or another structure with probable substitution of a certain number of ligands clearly exists. For preliminary estimation of the possible existence of heteroligand rhenium alkoxides, the quantum-chemical calculations were performed using the Extended Huckel approach realized by the CACAO program package. To facilitate calculations, the  $-\text{CH}_3$  and  $-\text{CF}_3$  radicals were used instead of  $-\text{C}_2\text{H}_5$  and  $-\text{CH}_2\text{CF}_3$  ones (as simplified analogues). The findings can not be used as referenced data and were employed only for the comparative analysis.

Table 1. The common data for the  $\text{Re}_4$  clusters in the  $\text{Re}_4\text{O}_6(\text{OPr}^i)_{10}$  and  $\text{Re}_4\text{O}_4(\text{OEt})_{12}$

complex	oxidation level of Rhenium	Charged cluster	Number of cluster electrons	symmetry	form
$\text{Re}_4\text{O}_6(\text{OPr}^i)_{10}$	Re (V, VI)	$[\text{Re}_4]^{22+}$	e=6	$\text{D}_{2h}$	
$\text{Re}_4\text{O}_4(\text{OEt})_{12}$	Re (V)	$[\text{Re}_4]^{20+}$	e=8	$\text{C}_{2h}$	

● - Re

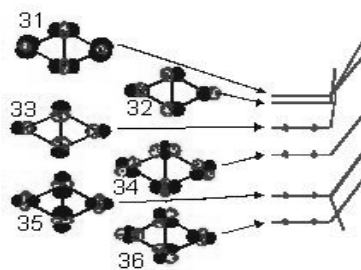


Fig.1. Diagram of the boundary surfaces of atomic d-orbitals of rhenium atoms comparatively to each other in the  $[\text{Re}_4]^{20+}$  with the 8 cluster electrons.

First of all, we compared the  $\text{Re}_4$  cluster for both structures,  $\text{Re}_4\text{O}_6(\text{OPr}^i)_{10}$  and  $\text{Re}_4\text{O}_4(\text{OEt})_{12}$  (Tab.1). This data enables an analysis of energy states for clusters  $[\text{Re}_4]^{22+}$  and  $[\text{Re}_4]^{20+}$  of complexes  $\text{Re}_4\text{O}_6(\text{OPr}^i)_{10}$  and  $\text{Re}_4\text{O}_4(\text{OEt})_{12}$  correspondingly (that comes to agreement with the number of cluster electrons in each structure). The analysis of the diagrams of molecular orbitals marked out 6 bounding molecular orbitals in each case. That is evidenced by the analysis of the boundary surfaces of the atomic d-orbitals of rhenium atoms comparatively to each other. (Fig.1). These results agree nicely with the data described earlier in the literature for the system with 8 cluster electrons ( $[\text{Re}_4]^{20+}$ ). Calculations for both  $\text{C}_{2h}$  and  $\text{D}_{2h}$  symmetries were performed with different number of cluster electrons (6 and 8). However, only insignificant differences between the energy states of two structures were observed. Thus a cluster with the cluster frame  $\text{Re}_4$  can exist with slight geometry variations meaning that compounds with variable geometry and composition can be prepared; moreover, the formation of complexes based on

isopropyl alkoxide structure and on ethyl alkoxide structure is equally probable. On the next stages of the calculations only the  $\text{C}_{2h}$  symmetry was used since this provides the way to simplify the process of adding the radicals into the cluster system. 4  $\mu_2\text{-O}$  and 2  $\mu_3\text{-O}$  ligands were used for construction of the first model and 2  $\mu_2\text{-O}$ , 2  $\mu_3\text{-O}$  and 2  $\mu_2\text{-OCH}_3$  ligands for the second model of charged clusters (for  $[\text{Re}_4\text{O}_6]^{10+}$  and  $[\text{Re}_4\text{O}_6(\text{CH}_3)_2]^{10+}$  respectively). The number of bonding cluster orbitals remains the same for such structures and equals to 6. From the energy diagrams one can see that both fragments of heteroligand complexes can be stable because of small differences between their energy states. On the third stage we estimated the influence of terminal bonds on both charged cluster structures  $[\text{Re}_4\text{O}_6]^{10+}$  and  $[\text{Re}_4\text{O}_6(\text{CH}_3)_2]^{10+}$ . We input 6 terminal bonds  $-\text{CH}_3$  to every structure (Fig.2).



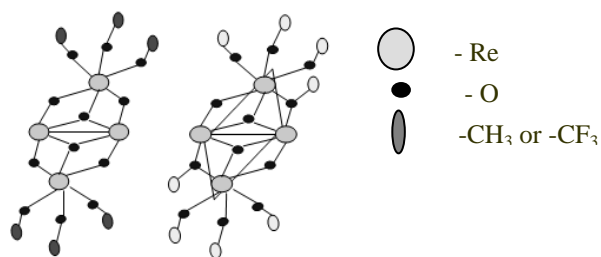


Fig.2. Cluster structures for the third stage of quantum-chemical calculations

Afterwards we changed all  $-\text{CH}_3$  ligands with the  $-\text{CF}_3$  ones. The diagrams of the energy states for these cluster structures show that the fluorine-containing radical stabilizes the complex structure only if it sits in the  $\mu_2$ - $\text{OCF}_3$  position. Substitutions of the  $-\text{OCH}_3$  ligands by the  $-\text{OCF}_3$  ligands at the terminal position does not influence apparently the order and location of 6 d-d bonding orbitals, which are responsible for the bonding in the cluster. The HOMO-LUMO separation responsible for the electrostatic interaction is increased when H is replaced with F. The fluorine contribution to the orbitals responsible for Re-Re bonds is negligible. This trend is observed for all structures of this model. Thus, the nature of the fluorine influence is based on the electrostatic factors. The fourth stage of the calculations was similar to the second one ( $[\text{Re}_4\text{O}_6]^{10+}$  and  $[\text{Re}_4\text{O}_6(\text{CH}_3)_2]^{10+}$  respectively). But, importantly, we replaced 2  $\mu_3$ -O ligands by the  $\mu_3$ -S ones. This lowers significantly the energy of bonding molecular orbitals resulting in more stable structures in comparison with initial  $[\text{Re}_4\text{O}_6]^{10+}$  and  $[\text{Re}_4\text{O}_6(\text{CH}_3)_2]^{10+}$ . This raises the question whether the synthesis of the sulfur-containing analogue with  $\mu_3$ -S ligands is realizable.

## Experimental

Table 2. The initial molar ratios and the conditions for the anodic dissolution of rhenium metal with mixtures of a) EtOH and Pr<sup>i</sup>OH and b) EtOH and  $\text{CF}_3\text{CH}_2\text{OH}$

№	n(EtOH):n(i-PrOH) in electrolyte	U, V	I, mA	t, h.
I	1:1	110-160	260-80	17
II	2:1	50-100	160-110	26,3
III	1:2	60-150	100-30	24,8
	n(EtOH):n( $\text{CF}_3\text{CH}_2\text{OH}$ ) in electrolyte	U, V	I, mA	t, h.
IV	1:1	35-70	170-130	31,7
V	2:1	50-70	195-110	32
VI	0:1	30-60	80-20	37,7

To obtain heteroligand rhenium alkoxides the anodic dissolution of rhenium with alcohol mixtures was applied. The conditions of the syntheses (I-VI) and initial molar ratios of alcohols in the electrolytes (I-VI) are given in Tab.2. The products of anodic dissolutions are very sensitive even to traces of atmospheric moisture and oxygen. Therefore, all manipulations were carried out in a dry box with nitrogen atmosphere. A glass electrochemical cell with water cooling and a condenser were the facilities for every synthesis.

To prevent the decomposition of the formed compounds a tube with a drying agent ( $\text{P}_2\text{O}_5$ ) was used. The water-free EtOH, Pr<sup>i</sup>OH and  $\text{CF}_3\text{CH}_2\text{OH}$  were used as an electrolyte, a  $2\text{ cm}^2$  platinum plate as a cathode, and rhenium bars as an anode. Alcohols were dehydrated prior using in the synthesis. Concentration of lithium chloride (used as background electrolyte) was 0,1 M to provide optimal conductivity and low chlorine contamination. Before use, LiCl was annealed (180 – 200 °C) in vacuum for an hour to dehydrate it. The electrochemical process was controlled by measuring voltage and temperature. Once the chemical reaction completed, the resulting liquid was transferred into a glass flask and subjected to solvent vacuum evaporation to yield a final powder. The rhenium content was determined gravimetrically as nitron perrhenate  $\text{C}_{20}\text{H}_{16}\text{N}_4 \cdot \text{HReO}_4$  [6], carbon and hydrogen by organic microanalysis with CHN-O-RAPID (Heraeus GmbH, Germany). X-ray diffraction patterns were obtained on a XDR 6000 powder diffractometer (Shimadzu, Japan) with Cu  $K_\alpha$ -radiation; IR-spectra in the range  $4000\text{-}400\text{ cm}^{-1}$  were recorder on an EQUINOX 55 spectrometer (BRUKER, Germany), with the sample kept between IR-transparent KRS-5 plates in

liquefied petrolatum to prevent decomposition; Thermal analysis was performed in air on a Q-1500 D derivatograph (MOM, Hungary) up to 430°C with 5°C/min heating rate.

## Results and Discussion

*Table 3. The data of element analysis on the content of Re for the first synthesis in compare with the literary data.*

complex	Re, %
[2] $\text{Re}_4\text{O}_4(\text{OEt})_{12}$	55,20
[1] $\text{Re}_4\text{O}_6(\text{OPr}^i)_{10}$	52,00
I	55,24

As one can see from the Tab.3, the results of the elemental analysis (synthesis I) on the content of Re for the heteroligand product of the reaction comes to agreement with the well-known facts. As regards the IR-spectroscopy analysis, the peaks corresponding to 909  $\text{cm}^{-1}$ , 912  $\text{cm}^{-1}$ , 910  $\text{cm}^{-1}$ , 913  $\text{cm}^{-1}$  and 911  $\text{cm}^{-1}$  for the liquid products of syntheses I,II, III, IV,V respectively are absent in the spectrum of pure EtOH and  $\text{Pr}^i\text{OH}$  alcohols and relate to the  $\nu(\text{Re}-\text{O}-\text{Re})$  [7,8]. Altogether, this is a good evidence to the fact that heteroligand complexes were obtained. From Tab.4 one can see all related

*Table 4. An appropriate frequencies for the liquid products of syntheses I-III.*

frequencies for the liquid heteroligand alkoxides of syntheses I-III. Consequently we can draw a conclusion that intensities and shapes of IR-spectra are influenced by the initial molar ratios of the individual alcohols in the electrolyte. And therefore, the ending products depend on the initial ratio of alcohols in the electrolyte. The DTA/DTG method also proved that the initial ratio of the alcohols influenced on the products of the thermal decomposition of the heteroligand alkoxides because there are certain differences in the shape of the curves presented in Fig.3, which illustrates 3 stages of the decomposition of complex I.

At 85°C an endothermic effect is present. This peak corresponds to the

No	Appropriation frequencies, $\text{cm}^{-1}$
I	$\nu \text{ O-H} = 3340$ $\nu \text{ C-O} = 1051-1162$ $\nu \text{ C-H} = 2885-2972$ $\nu \text{ Re=O} = 954$ $\nu \text{ Re-O (bridge)} = 653-909$ $\nu \text{ Re-O(R)} = 488$
II	$\nu \text{ O-H} = 3468$ $\nu \text{ C-O} = 1047-1162$ $\nu \text{ C-H} = 2902-2975$ $\nu \text{ Re=O} = 1005$ $\nu \text{ Re-O (bridge)} = 816-946$ $\nu \text{ Re-O(R)} = 477-582$
III	$\nu \text{ O-H} = 3470$ $\nu \text{ C-O} = 1093-1161$ $\nu \text{ C-H} = 2933-2978$ $\nu \text{ Re=O} = 961-1001$ $\nu \text{ Re-O (bridge)} = 913-938$ $\nu \text{ Re-O(R)} = 477$

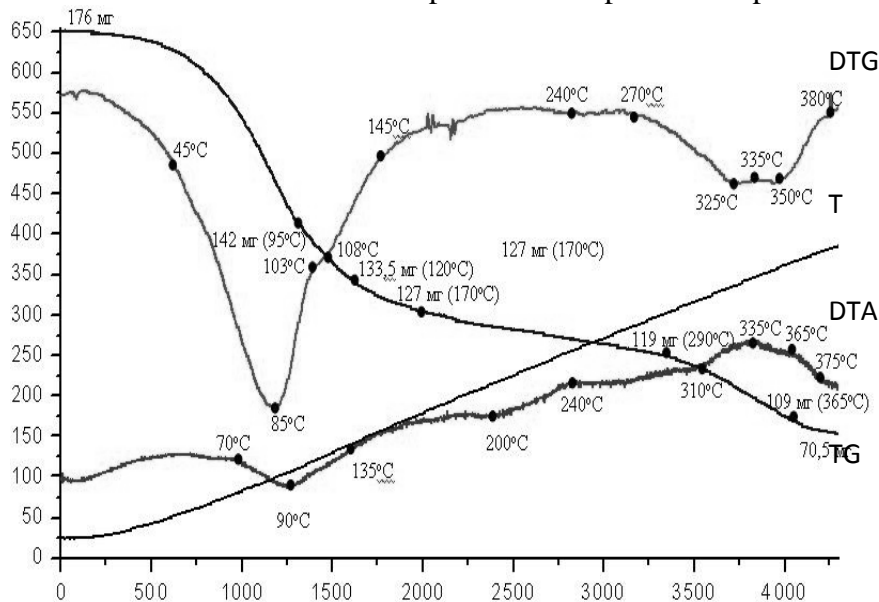


Fig.3. Thermogram of heating for the complex I

loss of 27,8% mass for the heteroligand complex I. (While the total decrease of weight was determined as 40,06% of the initial weight of complex I). For complexes II and III we donot observe the same

trend. They have regular loss in mass until 400°C (total weight loss was 24,26% and 20,30% with respect to the initial mass of complexes II and III, respectively). Also, for complexes II and III the thermal effects are less sharp as in the case of I. This can be due to the different ligands ratio in the heteroligand alkoxide structure. The thermal decompositions of  $\text{Re}_4\text{O}_n(\text{OEt})_x(\text{OPr}^i)_y$  in oxidative atmosphere under 255°C is followed by the formation of rhenium oxides nanopowder. In the case of I it is presented on Fig.4. In other cases (complexes II and III and also IV, V) one can see similar

diffraction patterns. The thermal decomposition of the fluorine-containing complexes in oxidative atmosphere under 400°C also results in formation of rhenium oxides. In inert atmosphere (Ar) we have another illustration for the decomposition of heteroligand complexes (DSC, Tab.5). Therefore, the nature of atmosphere significantly influences the decomposition ways of heteroligand alkoxides of rhenium.

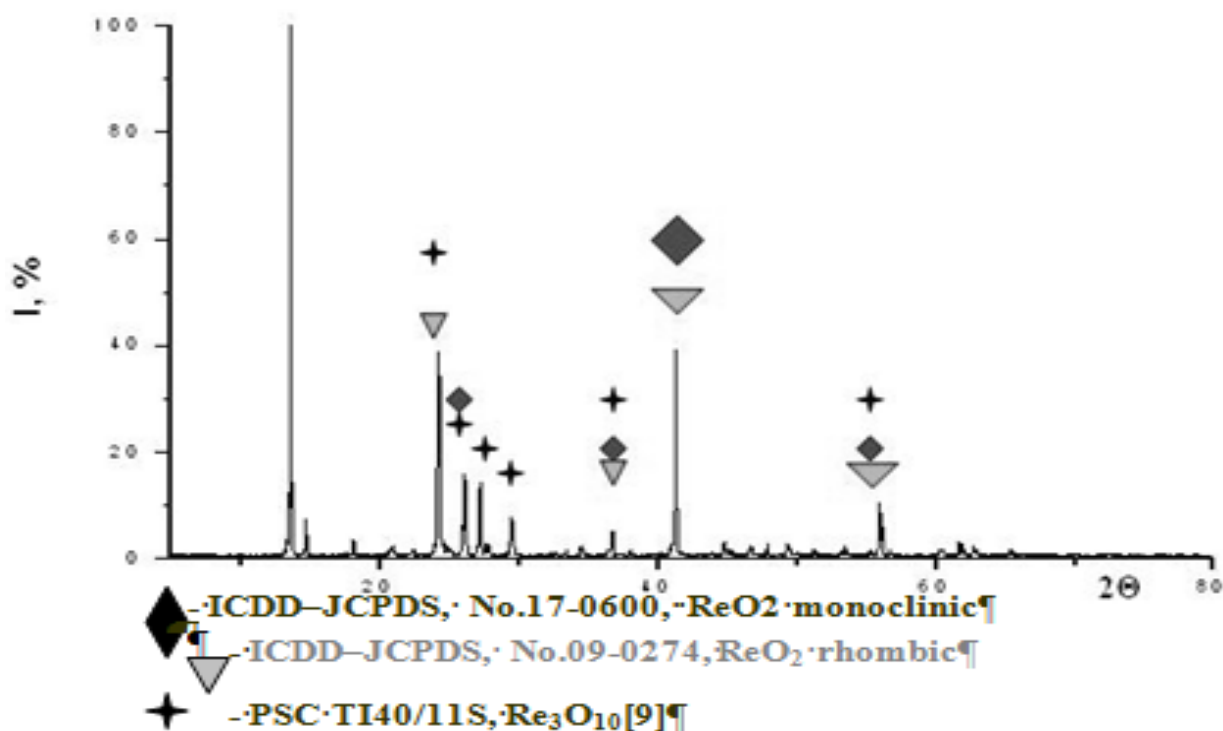


Fig.4. X-ray analysis of the decomposed product of the complex I

Table 5. DSC effects for heteroligand complex I at 500°C.

complex	DSC effect, °C	General mass loss, %
I	endothermic - 115, 412	17,45

## Conclusions.

By means of experimental and theoretical methods we revealed the fact that heteroligand complexes of rhenium with general formula  $\text{Re}_4\text{O}_n(\text{OEt})_x(\text{OPr}^i)_y$  have been obtained. The complexes are characterized by X-ray phase analysis, element analysis, DTG, DSC and IR-spectroscopy. The formation of both heteroligand alkoxides complexes based on  $\text{Re}_4\text{O}_6(\text{OPr}^i)_{10}$  structure and one based on  $\text{Re}_4\text{O}_4(\text{OEt})_{12}$  is shown to be equally probable.

In the  $\text{Re}_4\text{O}_4(\text{OEt})_{12}$  complex, part of  $-(\text{OEt})$  ligands can be substituted by  $-(\text{CH}_2\text{CF}_3)$  ones. The replacement of H atoms with F ones increases the stability of the complex only if the ligand sits in the  $\mu_2$  position.

The structure with the  $\text{Re}_4$  cluster-frame can exist, and  $\mu_3$ -O ligands in it are likely to be substituted by  $\mu_3$ -S ligands, and the S-containing complex is expected to be more stable than the O-containing one.

The thermal decomposition leads to rhenium (IV) oxides as products in different modifications (monoclinic and orthorhombic) and also produces the metastable phase  $\text{Re}_3\text{O}_{10}$  that is evidenced by XRD.

**Acknowledgements:** We thank Dr. Yuri A. Velikodniy for XRD Analyses, Elena E. Nikishina for DTA Analyses; Dr. Sergey Savilov for DSC Analyses; Valeri V. Kravchenko for IR Spectra and Vyacheslav I. Proshkin for technical support. Work was supported by RFBR (grant # 09-03-00328).

### References.

1. P.A. Sheglov. Mono-, Bi- and trimetallic oxo- alkoxoderivatives of rhenium (synthesis, properties and application), Diss. Cand. Chem. Science. MIFCT - Moscow (2002) 141p.
  2. O. A. Nikonova, K. Jansson, V. Kessler, M. Sundberg, A. I. Baranov, A. V. Shevelkov, P. A. Shcheglov, D. V. Drobot and G. A. Seisenbaeva . Electrochemical synthesis, structural characterization and decomposition of rhenium oxoethoxide,  $\text{Re}_4\text{O}_4(\text{OEt})_{12}$ . Ligand influence on the structure and bonding in the tetranuclear planar rhenium alkoxide clusters. *Inorg. Chem*, **47**: 1295-1300 (2008).
  3. P.A. Sheglov, D.V. Drobot. Alkoxoderivatives of rhenium. *Izv. AS, Ser. Chem.*, **10**: 1-12 (2005).
  4. Worden K.; New smart materials and constructions. Properties and applications. M: Technosphere, 2006, p. 224.
  5. N.A. Turova. Metal oxoalkoxides. Synthesis, properties and structures. *Russian Chemical Reviews*. **73**: 1041-1064 (2004).
  6. Hillebrad V.F., Lendel H.E., Bright G.A.; A Practical Guide to Inorganic Chemical Analysis. Chemistry. Moscow. 1966, p. 372.
  7. Nakomoto K.; Infrared spectra of inorganic and organic compounds, M. «Mir», 1966, p. 412.
  8. Smit A.; Applied Infrared Spectroscopy: Transl. from Eng, M.: Mir, 1982, p. 328.
- T. Hartmann. Preparation, characterization and physical properties of new compounds in the system  $\text{Ln}_2\text{O}_3 - \text{ReO}_2 - \frac{1}{2} \text{Re}_2\text{O}_7$  (Ln = lanthanides or yttrium). zur Erlangung des akademischen Grades eines Dr.-Ing. genehmigte Dissertation von. Vom Fachbereich Material- und Geowissenschaften der Technischen Universität Darmstadt - Darmstadt (2004) 72p.



The New Principle Building  
of the Presidium of Russian Academy  
of Sciences and the principle  
interpreter of the ISTR2011  
Yana Obruchnikova

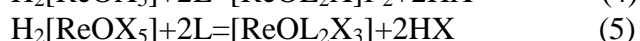
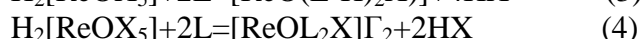
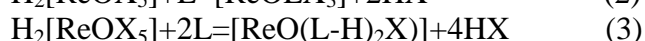
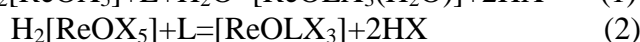
1.17.

## STATUS AND PROSPECTS OF STUDIES ON THE CHEMISTRY OF COORDINATION COMPOUNDS OF RHENIUM (V)

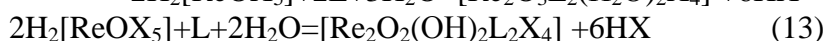
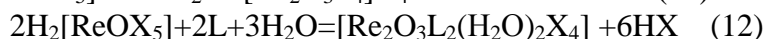
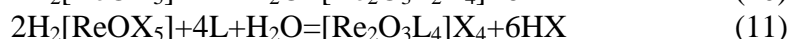
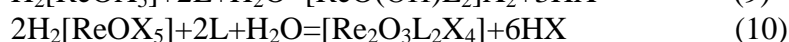
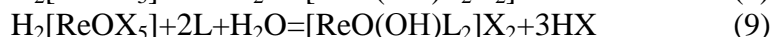
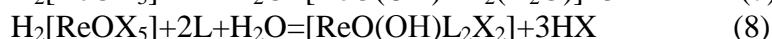
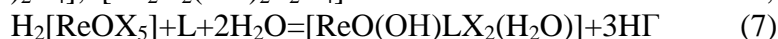
A.A. Aminjonov

Tajik National University. Dushanbe. [azimjon51@mail.ru](mailto:azimjon51@mail.ru)

As a result of the made perennial purposeful researches by us are received a series of important results on processes of a complex formation of rhenium (V) by sulphur or nitrogen of organic compound ligands. In particular we managed to synthesis and identify more than 2500 new complexes of rhenium (V). Reactions of their formation are offered. It is positioned that on composition of formed complexes affect both interrelations of initial reagents, and concentration halogen acids. It was shown that in medium HX (where X - Cl, Br or F) of 6 mol/l produced oxo complexes compositions,  $[\text{ReOLX}_3(\text{H}_2\text{O})]$ ;  $[\text{ReOLX}_3]$ ;  $[\text{ReO}(\text{L-H})_2\text{X}]$ ;  $[\text{ReOL}_2\text{X}]_2$ ;  $[\text{ReOL}_2\text{X}_3]$ ;  $[\text{ReOL}_4\text{X}]_2$  by the following general reactions;



In reactions (2) and (4) ligands are bidentat, as in reaction (3) - bidentat deprotonated. In the concentration range of 4 to 6 mol/l HX, depending on the nature of the ligand formed a monomerization or dimerization with oxygen bridges oxo hydroxyl complexes types:  $[\text{ReO}(\text{OH})\text{LX}_2(\text{H}_2\text{O})]$ ;  $[\text{ReO}(\text{OH})\text{L}_2\text{X}_2]$ ;  $[\text{ReO}(\text{OH})\text{L}_2\text{X}]_2$ ;  $[\text{Re}_2\text{O}_3\text{L}_2\text{X}_4]$ ;  $[\text{Re}_2\text{O}_3\text{L}_4\text{X}_4]$ ;  $[\text{Re}_2\text{O}_3\text{L}_2(\text{H}_2\text{O})_2\text{X}_4]$ ;  $[\text{Re}_2\text{O}_2(\text{OH})_2\text{L}_2\text{X}_4]$  in accordance with the reactions;



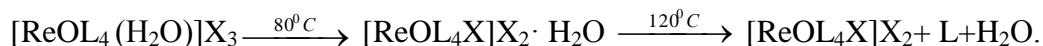
In reactions (10) and (11) ligands are bidentate. In media with concentration HX below 4 mol/l predominantly formed dimeric complexes with an oxygen bridge.

We were able to develop a universal method of synthesis of complexes of rhenium (V) in environments with low concentrations of HX whose essence lies in the fact that in order to prevent hydrolytic processes in aqueous solution of ligand added to the calculated amount of  $\text{H}_2[\text{ReOX}_5]$  in 6 mol/l HCl and 7 mol/l HBr.

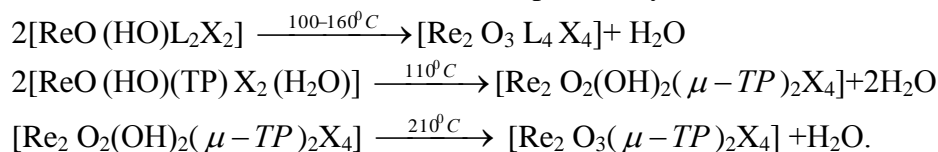
It is established that the formation of complexes of rhenium (V) with alkyl hydroxide derivatives of thiosemicarbazide in medium HX (1-7 mol/l) occurs only when the ratio Re: L  $\leq$  1:1. At high ratios Re:L is the hydrolytic cleavage of the alkyl hydroxide groups and formation of the corresponding thiosemicarbazide complexes. Revealed that the reactions at the interface by mixing a benzene solution of thiosemicarbazide with solutions alkyl hydroxide  $\text{H}_2[\text{ReOX}_5]$  in mediums HX environments, provides the highest yield and best purity of the complexes of rhenium (V) with this class of ligands.



According to X-ray studies of the synthesized complexes of rhenium (V) are crystalline and have either an orthorhombic or tetragonal. Based on the data magnetic chemicals, potentiometric and infrared spectroscopic studies confirmed the immutability of the oxidation state of rhenium in the synthesized complexes. A study of thermal decomposition process of the ligands and complexes showed a significant increase in thermal stability of the ligands in the coordination of triazoles. The inverse association was found for the rhenium complexes two substituted thiosemicarbazide rhenium (V). For complexes of rhenium (V) with 2-mercaptoimidazole and its derivatives were found following the reaction with the formation of hydrate thermo gravimetric isomers.



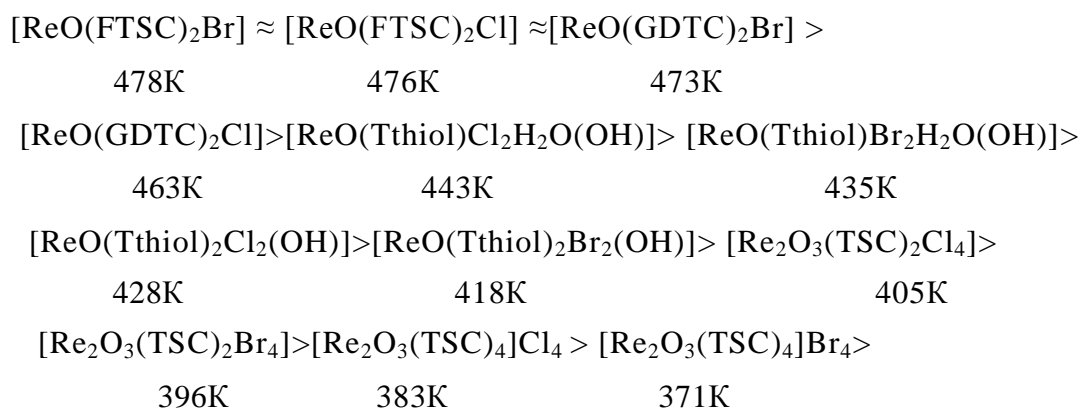
It is proved that the Slow complexes of rhenium (V) with benzo-2,1,3-thiadiazole in 50-60<sup>0</sup>C in an oven formed Re<sub>2</sub>O<sub>5</sub>. The process thermo gravimetric of monomeric hydroxo rhenium (V) proceeds with the formation of dimeric compounds by the reactions



For thiosemicarbazide methylenesemicarbazide complexes of rhenium (V) proposed the following reaction of thermolysis



Depending on the nature of the coordinated ligand onset temperature of decomposition of complexes of rhenium (V) changes in the following order:



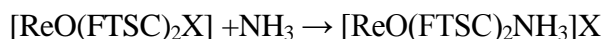
Using a flow-type reactor, kinetics of the formation of thiocyanate complexes of rhenium (V) with thiosemicarbazide. Held kinetic analysis showed that the range of degrees of conversion of 0,005 ≤ α ≤ 0,58 studied process is best described by the equation k=[1-(1-α)], and at higher values of α-diffusion equation Yandera. The results of kinetic analysis of the formation of thiocyanate complex of rhenium (V) c TSC are presented in Table I.

Table I. Kinetic parameters of the process of thermal decomposition oxohalogen- thiosemicarbazide complexes of rhenium (V)

№	The composition of compounds	Mechanism	Interval α, %	Stand. deviat.	E, kJ/mole	A
1.	[Re <sub>2</sub> O <sub>3</sub> (TSC) <sub>2</sub> Cl <sub>4</sub> ]	[1-(1-α) <sup>1/3</sup> ]	0,7÷52,3	120,91	120,1	1,65·10 <sup>13</sup>
2.	[Re <sub>2</sub> O <sub>3</sub> (TSC) <sub>2</sub> Br <sub>4</sub> ]		0,5÷58,8	1,01	118,8	1,15·10 <sup>13</sup>
3.	[Re <sub>2</sub> O <sub>3</sub> (TSC) <sub>4</sub> Cl <sub>4</sub> ]		2,7÷39,2	0,62	113,2	8,15·10 <sup>10</sup>
4.	[Re <sub>2</sub> O <sub>3</sub> (TSC) <sub>4</sub> Br <sub>4</sub> ]		3,9÷36,3	0,58	99,6	7,45·10 <sup>10</sup>

Presented in Table I show that compounds with a ratio of Re: TSC = 1:1, are more stable than the complexes of 1:2. In addition, at the same ratio of Re: TSC are more stable chloride complexes. The data on the thermal stability oxohalogen complexes of rhenium (V) with thiosemicarbazide correlate with the results of IR spectroscopic data on the magnitude of the shear bands  $\nu$  (C = S).

The kinetics of interaction with the complexes of  $\text{NH}_3^{(g)}$   $[\text{ReO}(\text{FTSC})_2\text{X}]$ , where X - F<sup>-</sup>, Cl<sup>-</sup>, Br<sup>-</sup>, I<sup>-</sup>, CH<sub>3</sub>COO<sup>-</sup>, NO<sub>3</sub><sup>-</sup> has shown that with increasing temperature generally slows down the speed of the process and reduces the number of moles of accession ammonia. In the first stage of the reaction is displaced by ammonia entering into the inner sphere complexes by the scheme:

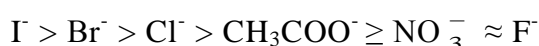


Mathematical processing of experimental data using kinetic equations, based on certain physical models, showed that the interaction of chloride, bromide and iodide complex with the  $\text{NH}_3^{(g)}$  by the equation  $k\tau = [-\ln(1-\alpha)]^{1/4}$  and fluoride, nitrate and acetate, respectively,  $k\tau = [1-(1-\alpha)]^{1/3}$  calculated rate constants are Table. 2.

Table 2. Rate constants of the interaction of complexes of general composition  $[\text{ReO}(\text{FTSC})_2\text{X}]$  with gaseous ammonia in the range 293-323K

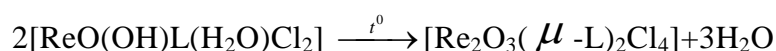
№	Composition complexes	$(k, \text{sec}^{-1}) \cdot 10^{-3}$			
		293K	303K	313K	323K
1.	$[\text{ReO}(\text{FTSC})_2\text{J}]$	28,0	10,0	5,8	3,3
2.	$[\text{ReO}(\text{FTSC})_2\text{Br}]$	11,0	7,7	2,4	1,1
3.	$[\text{ReO}(\text{FTSC})_2\text{Cl}]$	4,2	2,7	2,0	1,2
4.	$[\text{ReO}(\text{FTSC})_2\text{CH}_3\text{COO}]$	2,7	2,1	1,5	0,92
5.	$[\text{ReO}(\text{FTSC})_2\text{NO}_3]$	2,3	1,7	1,0	0,55
6	$[\text{ReO}(\text{FTSC})_2\text{F}]$	2,2	1,8	1,5	1,0

From the data of Table 2 shows that k values decrease with increasing temperature. A similar dependence of k on temperature was observed Pavlyuchenko MM and Lazerko GA in the study of the interaction of  $\text{NH}_3^{(g)}$  with the chlorides of cobalt and zinc. The rate of interaction with the complexes of  $\text{NH}_3^{(g)}$   $[\text{ReO}(\text{FTSC})_2\text{X}]$  depends on the nature atsidoligandov lability which at 293K changes in the following order:

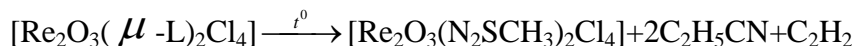


On the basis of thermo gravimetric studies show that the decomposition temperature of the onset of intense complexes of rhenium (V) depends on the nature of the alkyl radical, which is part thioamino ligands. On this basis suggest appropriate ranks.

Found that the thermal decomposition of uncoordinated sulfur compounds azole series depends on the nature of the alkyl radical and its provisions. We propose the following series of temperature changes in the beginning of intensive thermal decomposition of the ligands: 1,2,4-triazole (105 ° C) < 4-methyl-1,2,4-triazolthiol-5 (200 ° C) < (210 ° C) < 1,2,4-triazolthiol-5 (220 ° C) < 3-methyl-1,2,4-triazolthiol-5 (230 ° C). Studies conducted on the process of thermal decomposition of complexes of rhenium (V) 3-Et-4-Met-1,2,4-Thiol and 3,4-DiMet-1,2,4-Thiol, show that the majority of the synthesized compounds contain water of crystallization and the first stage of thermal decomposition of these complexes is related to their thermo dehydration. For the monomeric complexes containing water of crystallization, together with and coordinated water, the second stage of thermal decomposition removes the molecules of coordinated water with subsequent dimerization of the reaction:



The third stage of thermal decomposition is connected with partial decomposition of the molecules of 3-Et-4-Met-1,2,4-Thiol and 3,4-DiMet-1,2,4-Thiol and the formation of new compounds containing the deprotonated molecule of thiourea.

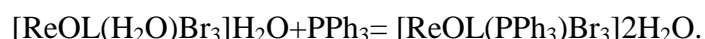


Investigation of thermal properties of complexes of rhenium (V) with Ethio and 1-Et-2MI showed that increasing the number of coordinated molecules Ethio and 1-Et-2MI leads to a slight decrease in temperature of the beginning of the process thermo dehydration, but does not affect the temperature of the end of this process and the peak temperature endo effect. This increases the temperature of the onset of decomposition of complexes. It is established that, irrespective of the nature of halide ions with the number of coordinated molecules Ethio, 1-Et-2MI increases the number of molecules of water in the complexes. It is shown that the replacement of chloride complexes demerization ions to bromide to 300 ° C to slow the process of thermolysis, while above this temperature there is an opposite effect. This means that for the chloride and bromide complexes of rhenium (V) depending on  $\Delta m = f(T)$  there is a point of intersection, which varies from the effect of halide ions on the process of thermolysis of complexes of rhenium (V). A similar point of intersection of the curve and there is  $\Delta m = f(T)$  for two- and tetra complexes, from which changes the effect of the coordinated molecules Ethio and 1-Et-2MI the process of thermolysis of complexes of rhenium (V).

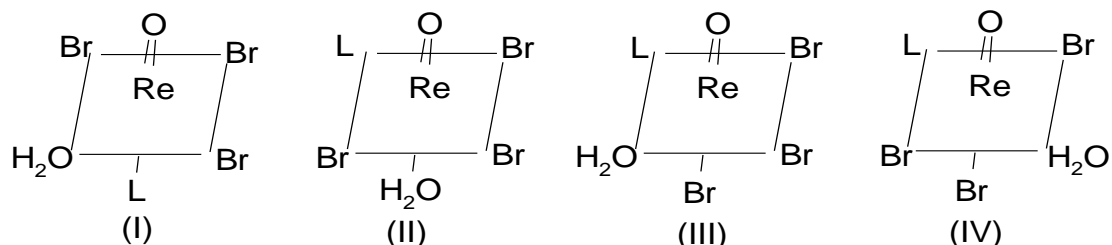
Investigated the acidic properties of some synthesized complexes and determined their basicity. Calculated acid dissociation constants of the successive test compounds.

Prior to the beginning of our research processes of mutual substitution of ligands in complexes of rhenium (V) remained virtually unstudied. We carried out studies on the substitution of coordinated ligands in the complexes of rhenium (V) other ligands, particularly thiocyanate ligand, molecules of ammonia, dimethylformamide, pyridine, acetonitrile, dimethyl sulfoxide, quinoline, triphenylphosphine.

On the basis of experimental studies on the mutual substitution of ligands in complexes of rhenium (V) made some conclusions about the spatial arrangement of the ligands in the octahedral plane. In particular, it was determined that the action of triphenylphosphine in 2-merkaptobenzimidazolny complex rhenium (V) of  $[\text{ReOL}(\text{H}_2\text{O})\text{Br}_3]\text{H}_2\text{O}$  in the medium of acetone formed complex of  $[\text{ReOL}(\text{PPh}_3)\text{Br}_3]2\text{H}_2\text{O}$  from the equation



Even with an excess of triphenylphosphine, compounds with a large number of molecules coordinated  $\text{PPh}_3$  is formed. For the original complex structure  $[\text{ReOL}(\text{H}_2\text{O})\text{Br}_3]$ , there are four possible spatial arrangement of the ligands:



If the source of the complex  $[\text{ReOL}(\text{H}_2\text{O})\text{Br}]\cdot\text{H}_2\text{O}$  would have the configuration (I) or (III), after replacement of water molecules on triphenylphosphine, due to the large trans influence of the latter was replaced by bromide ion, which is in trans position to triphenylphosphine, that is, would form a complex of  $\text{trans-}[\text{ReOL}(\text{PPh}_3)_2\text{Br}_2]^+$ . Configuration (II) is unlikely, because in the IR spectrum of the original complex  $[\text{ReOL}(\text{H}_2\text{O})\text{Br}_3]\text{H}_2\text{O}$  maintained an intense band corresponding

to stretching vibrations rhenium (Re = O) group. If in a trance - the position of the oxygen renilnoy was a water molecule, the intensity of this band would have decreased to low. Also note that the literature no data on the complexes of rhenium (V), in which triphenylphosphine would be in trans-position relative to oxygen.

In the case of configuration (IV) molecule of triphenylphosphine, replacing a water molecule, stands in the trans position to the molecule 2-merkaptobenzimidazola (L) in the equatorial plane. The second molecule of triphenylphosphine can not supplant any molecule of 2-MBI, or bromide ions in cis-position, due to steric reasons. According to the literature in the triphenylphosphine complexes of rhenium (V) forms only the trans isomers. As a result of these factors, the process stops at the formation of  $[\text{ReOL}(\text{PPh}_3)\text{Br}_3]2\text{H}_2\text{O}$ . Thus, the study of the interaction of triphenylphosphine with a complex composition  $[\text{ReOL}(\text{H}_2\text{O})\text{Br}_3]\text{H}_2\text{O}$  yielded evidence that this complex has a configuration of (IV).

Based on data for the study of processes of mutual substitution of ligands in complexes of rhenium (V) was proposed following a number of mutual substitution of the ligands:

$\text{L} \approx \text{P}(\text{Ph})_3 > \text{SCN}^- > \text{NH}_3 > \text{Cl}^-$ ,  $\text{Br}^- > \text{S} > \text{H}_2\text{O}$ , where L - tioamidnoe connection and S-DMF, DMSO, Py, Hin,  $\text{CH}_3\text{CN}$ .

Investigating the interaction of ammonia with the amide and complexes thioamides rhenium (V), set up three types of reactions. The first type includes reactions which take place only with the displacement of halide ions from the inner sphere complexes. The second type of reactions include dimerization reaction of monomeric complexes with the replacement of halide ligands. The third type of reactions are reactions that result in coordinated thiocyanate ions are converted into tioamidinovuyu group, although the molecules of ammonia thiocyanate ions from the inner sphere complexes are not displaced.

It is established that the reaction of ammonia complexes of rhenium (V) with inorganic and organic acids occur in different ways and depend on many factors, including the nature of the acid and its strength.

By using the developed electrodes reversible ligand (20) based on the sulfur-containing organic compounds and their oxidized forms, the values of step formation constants of complexes of rhenium (V) in media with different concentrations of HCl and HBr in the temperature range 273-338K. A method for determining the formation constants of complexes of rhenium (V) by the potentiometric method in environments with low concentrations of HHal. The regularities of the influence of the ionic environment, temperature and nature of the ligand on tioamidnogo stability of the complexes of rhenium (V). The regularities in the change of  $E^0$ , depending on the nature tioamidnogo connection. We propose some general guidelines on the use of reversible redox systems for the study of complex formation.

As a result of targeted research identified several aspects of the practical use of complexes of rhenium (V) with amide and tioamidnymi ligands. In particular, we show that tioamidnye compounds and complexes of rhenium (V) with greatly increased resistance to radiation and reduce the electrified polymer materials. The features of rhenium complexes more stable effect (V). In this case revealed an unusual stabilizing effect of the complexes in contrast to the uncoordinated ligands. The regularities of the influence of the number of coordinated ligands and the structure of the complexes on the radiation resistance of polymers. It is shown that some complexes of rhenium (V) increases the radiation resistance of polymers, both in terms of photo-aging, and in photo mechanics.

Study of the biological action of complexes of rhenium (V) and the ligand is shown that the coordination of ligands to rhenium (V) leads to a significant reduction in their toxicity. The effect of organic and inorganic ligands on the toxicity of the complexes of rhenium (V).

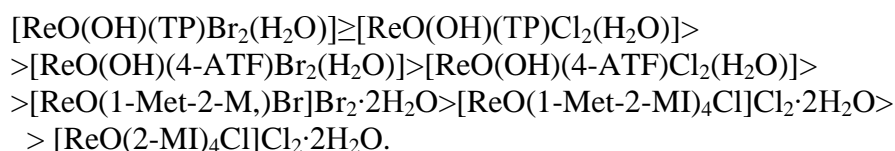
The values of  $\text{LD}_{50}$  values found for some of the ligands and complex compounds of rhenium (V) are given in Table. 3. From Table. Figure 3 shows that the complex compounds of rhenium (V) with 1-methyl-2-merkptoimidazolom, thiosemicarbazide, 4-phenylthiosemicarbazide and 1-formyl-3-thiosemicarbazide are low-toxic compounds. It should be noted that complexes with 1,2,4-triazole and 4-amino-1,2,4-triazole are practically non-toxic compounds.

Table 3. LD<sub>50</sub> values of complex compounds of rhenium (V)

№ п/п	Complex compounds rhenium (V)	Solubility in water	LD <sub>50</sub>	
			Inside - peritoneal introduction	Oral introduction
1.	L-1-methyl-2-merkptoimidazol [ReOL <sub>4</sub> Br]Br <sub>2</sub> ·2H <sub>2</sub> O	soluble	750±39	900±40
2.	[ReOL <sub>4</sub> Cl]Cl <sub>2</sub> ·2H <sub>2</sub> O	"-		850±32
3.	[ReOL <sub>2</sub> Br <sub>3</sub> ]·2H <sub>2</sub> O	"-		700
4.	[ReOL <sub>2</sub> Cl <sub>3</sub> ]·2H <sub>2</sub> O	"-		465
5.	L - 2 merkptoimidazol [ReOL <sub>4</sub> Cl]Cl <sub>2</sub> ·2H <sub>2</sub> O	"-	105±10,4	550±19,3
6.	L - thiosemicarbazide [ReOL <sub>2</sub> Cl]Cl <sub>2</sub> ·H <sub>2</sub> O	"-	140±4,61	
7.	[ReOL <sub>2</sub> Br]Br <sub>2</sub> ·H <sub>2</sub> O	"-	383±38	
8.	[Re <sub>2</sub> O <sub>3</sub> L <sub>4</sub> ]Br <sub>4</sub>	"-	433±51,3	
9.	[ReOLBr <sub>3</sub> ] L - 4-phenyl-3-thiosemicarbazide	insoluble insoluble		
10.	[ReOL <sub>2</sub> Br <sub>2</sub> ]·2H <sub>2</sub> O			320±20
11.	[ReOL <sub>2</sub> Cl <sub>3</sub> ]·2H <sub>2</sub> O L-1-formyl-3-thiosemicarbazide	"-		290±20
12.	[ReOL <sub>2</sub> NH <sub>3</sub> ]Cl	"-		183
13.	[ReOL <sub>2</sub> Cl] L - 1,2,4-triazole	"-	260±30	650±40
14.	[ReO(OH)]Cl <sub>2</sub> ·H <sub>2</sub> O	"-		>4000
15.	[ReO(OH)]Br <sub>2</sub> ·H <sub>2</sub> O L - 4-amino-1,2,4-triazole	"-		>4500
16.	[Re <sub>2</sub> O <sub>3</sub> L <sub>2</sub> Cl <sub>4</sub> (H <sub>2</sub> O) <sub>2</sub> ]	"-		~2000
17.	[Re <sub>2</sub> O <sub>3</sub> L <sub>2</sub> Br <sub>4</sub> (H <sub>2</sub> O) <sub>2</sub> ]	"-		~3000

It must be emphasized the fact a significant reduction in toxicity with thiosemicarbazide coordination of its molecules with rhenium (V). Thus, if the TSC for free intraperitoneal LD<sub>50</sub> is equal to 14 ± 2,15, ie is a toxic compound, the complex composition [ReOLBr<sub>3</sub>] is equal to the LD<sub>50</sub> 433±51,3. For thiosemicarbazide complexes observed increase in the degree of toxicity with increasing number of coordinated organic ligand molecules, and for the 1-methyl-2-merkptoimidazolnyh complexes observed an inverse relationship. In analyzing the impact of inclusion in the composition of the complexes of halide ions established that the bromide compounds are less toxic than similar chloride compounds. Based on these studies we can conclude that the introduction of formyl group of the thiosemicarbazide leads to a decrease in toxicity rhenium complex of more than two times. Due to poor solubility of 4-feniltiosemikarbazidnyh complexes, their toxicity is investigated only by the oral route of administration. These compounds were administered in the form of 1-2% water-glycerol solutions with a ratio of water: glycerol = 10:1. 1,2,4-triazole and 4-amino-1,2,4-triazole complexes when administered orally in the form of water-glycerol solutions were practically non-toxic compounds.

Total Calc. 3 change the toxicity of complexes of rhenium (V) with amide ligands and tioamidnyimi can be arranged in the following order:





Among the complexes synthesized by us were found compounds with rengenokonstrastnymi properties, seizure and antivitamin activity, dose-dependent effect antiyazvennym, radioprotective and antithyroid action, as well as the substance showing an anabolic effect.

Some complex compounds of rhenium (V) showed resistance at temperatures of curing the matrix, giving the composite materials set the necessary properties, samozatuhaemost, heat resistance, corrosion-and high dielectric properties. It was possible to show the principal possibility to achieve a monolithic matrix, reducing the time to cure, the implementation of the single-stage curing of thermosetting binders of different chemical nature, improving the number of properties and imparting new properties of composite materials. In this case elimination makrodefektnosti matrix is achieved by optimal amounts of the complex and the choice of the new regime (selected according to criteria monolithic matrix) curing the composite material using a nondestructive method of electro control. In particular, the processes of curing of thermosetting binders LBS-4, ENFB, BFOS 0.01% modified complexes of rhenium (V) compared to the known modes of accelerated respectively 7.9, 9.4; 9.6 times. In this modified polymers are homogeneous and have acquired a new quality - samozatuhaemost. By introducing a complex of rhenium (V) in the epoksiuretanovogo polymer consisting of heterogeneous oligomers, obtained the matrix of new generations capable of forming interpenetrating structures, where the defective areas of hardening due to the formation of network polymers kation different chemical nature. In this direction, developed the scientific foundations of technology for the processing of polymer composite materials with desired properties.

Interesting data on the effect of some synthesized complexes on the germination and vigor of seeds of some crops.

Perfection has no limits and therefore chemistry of coordination compounds of rhenium (V) should be developed and far and wide, attracting new more advanced methods of research, equipment, and theoretical views. In our opinion, in the short term is expedient to continue studies in the following areas of chemistry of coordination compounds of rhenium (V):

- using new classes of ligands targeted synthesis of complexes of rhenium (V);
- study of the processes of mutual substitution of ligands in complexes of rhenium (V);
- research the process of chelation of rhenium (V) in HCl solutions at constant concentration  $[H^+]$  and  $[Cl^-]$ -ion at different temperatures;

$\Delta H$ -determination of the processes of formation of complexes of rhenium (V) by the calorimetric method;

- study of the processes of interaction of donor molecules as NO and CO complexes with rhenium (V);

- determination of kinetic parameters of the interaction of ammonia with complexes of rhenium (V) depending on the nature of coordinated organic and inorganic ligands;

- investigation of the complexation of rhenium (V) using different electrical methods;

- search the complexes of rhenium (V) compounds exhibit high biological activity in order to create new and effective drugs;

- study towards obtaining new nano composites with complexes of rhenium (V) ions and other metals;

- works on the comparison of stability, physicochemical and other properties of the complexes of rhenium (V) with ions of other metals;

- developed oxidation-reduction electrode systems based on rhenium compounds in different oxidation;

- establishment of the laws on the influence of various factors on the electrified and other electrical properties, as well as on the radiation resistance of polymer and polymer composites modified complexes of rhenium (V).



I.G. Tananaev, A.A. Aminjonov, K.E. German

1.P1.

## EFFECT OF THE RHENIUM(V) COMPLEX OF 3,4-DIMETHYL-1,2,4-TRIAZOL-5-THIOL ON THE CELLULOSE DIACETATE LIGHT FASTNESS

N.G. Kabirov, S.M. Safarmamadov, A.A. Aminjonov

Tajik National University. Dushanbe. [azimjon51@mail.ru](mailto:azimjon51@mail.ru)

The effect of various concentrations of 3,4-dimethyl-1,2,4-triazol-5-thiol and the complex compound  $[\text{ReOL}_2(\text{OH})\text{Cl}_2]$  (L-3,4-dimethyl-1,2,4-triazol-5-thiol) light fastness diacetate cellulose (DAS) has been studied. As an example, the table shows the experimental data depending on the tensile strength of the DAS complex concentration and time of UV irradiation.

*Table 1. The dependence of the tensile strength of DAS on the concentration of complex composition  $[\text{ReOL}_2(\text{OH})\text{Cl}_2]$ , where L-3,4-dimethyl-1,2,4-triazol-5-thiol and UV irradiation ( $\lambda = 254\text{nm}$ ,  $I = 0,040 \text{ Kal/cm}^2\text{min}$ )*

The concentration of additives, %	Exposure time, h						
	0	2	5	10	15	20	25
0	10,6	7,2	6,0	4,7	3,0	2,6	1,1
0,01	10,2	9,6	10,2	9,4	8,3	8,0	7,6
0,05	9,5	9,3	9,9	10,8	10,0	9,3	7,0
1	9,8	10,1	9,8	9,2	6,0	5,2	4,0
3	10,1	9,2	8,4	6,8	5,1	4,6	3,0
5	10,5	9,4	8,3	5,9	4,8	4,1	2,9

The table shows that the introduction various amounts of the complex compound  $[\text{ReOL}_2(\text{OH})\text{Cl}_2]$  to the DAS has little effect on its initial tensile strength. However, there is a general tendency to the coefficient increasing of light fastness DAS at the introduction into it of various amounts of complex composition  $[\text{ReOL}_2(\text{OH})\text{Cl}_2]$ . In addition, the curve of the tensile strength of the UV irradiation time for the modified films at additives concentrations equal to 0.05% it is the maximum. It means, the tensile strength of modified film exceeds its initial tensile strength.

Studies have shown that the coordination compounds of rhenium (V) shows great light stabilizing activity against DAS compared to uncoordinated ligand.

1.P2.

## OCTAHEDRAL RHENIUM(III) CHALCOCYANOHYDROXO CLUSTER COMPLEXES

A.V. Ermolaev, A.I. Smolentsev, K.A. Brylev, V.E. Fedorov, Y.V. Mironov

Nikolaev Institute of Inorganic Chemistry, Siberian Branch of Russian Academy of Sciences, 3 Acad. Lavrentiev  
Prosp., 630090 Novosibirsk, Russia (e-mail: [erandrey@yandex.ru](mailto:erandrey@yandex.ru))

In recent years the compounds containing hexarhenium cluster anions  $[\{\text{Re}_6(\mu_3\text{-Q})_8\}\text{L}_6]^{n-}$  (Q = S, Se; L = Cl, Br, I) have been intensively investigated. The rapid development of rhenium cluster chemistry has led to the discovery of substitution reactions of L on other ligands, including organic. Polymeric compound  $\text{Re}_6\text{Q}_8\text{Br}_2$  prepared from the reaction of Re with the appropriate stoichiometry of Q and  $\text{Br}_2$  at  $800^\circ\text{C}$  in sealed quartz ampoule. Octahedral rhenium(III) cluster chalcocyanohydroxocomplexes have been prepared from the reaction of polymeric chalcobromide  $\text{Re}_6\text{Q}_8\text{Br}_2$  with molten KOH at  $220\text{-}250^\circ\text{C}$  in air.

In this work we present our data in the synthesis and structural study of compounds with  $[\text{Re}_6\text{Q}_8(\text{CN})_n(\text{OH})_{6-n}]^{4-}$  (n = 2, 4) cluster anions containing two type terminal ligands –  $\text{OH}^-$  and  $\text{CN}^-$ . Such clusters are interesting because CN - ligands can form bridging bonds through the nitrogen atom and OH - ligands can be easily replaced by both inorganic ligands and organic molecules and ions. For these complexes we have proposed a simple and convenient method based on the interaction of  $\text{K}_4[\text{Re}_6\text{Q}_8(\text{OH})_6]\cdot 8\text{H}_2\text{O}$  with KCN in aqueous solution. It has been found that when Q = S the cluster anion  $[\text{Re}_6\text{S}_8(\text{CN})_2(\text{OH})_4]^{4-}$  formed; however, if Q = Se the composition  $[\text{Re}_6\text{Se}_8(\text{CN})_4(\text{OH})_2]^{4-}$  was found.

The structure of  $[\text{Cu}(\text{NH}_3)_4]_2[\text{Re}_6\text{S}_8(\text{CN})_2(\text{OH})_4]\cdot 2\text{H}_2\text{O}$  cluster complex was determined by single-crystal X-ray diffraction. In addition, the presence of four  $\text{OH}^-$  groups in the cluster anion was confirmed by the fact that as a result of its interaction with molten 3,5-dimethylpyrazole the molecular complex  $[\text{Re}_6\text{S}_8(\text{CN})_2(3,5\text{-Me}_2\text{PzH})_4]\cdot 2\text{H}_2\text{O}$  formed.

The structure of  $[\text{Re}_6\text{Se}_8(\text{CN})_4(\text{OH})_2]^{4-}$  cluster anion was confirmed by single-crystal X-ray diffraction for complex *trans*- $[\text{Ni}(\text{NH}_3)_5]_2[\text{Re}_6\text{Se}_8(\text{CN})_4(\text{OH})_2]\cdot 6\text{H}_2\text{O}$  obtained by reaction of  $\text{Cs}_4[\text{Re}_6\text{Se}_8(\text{CN})_4(\text{OH})_2]\cdot 2\text{H}_2\text{O}$  with  $\text{NiCl}_2\cdot 6\text{H}_2\text{O}$  in an ammonia solution.

In addition, the compounds were characterized by a set of physical-chemical methods.

*This research was supported by Russian Foundation for Basic Research (Grant 11-03-00157) and by GC № 02.740.11.0628 of FFP “SSESIR 2009-2013”*

1.P3.

## TECHNETIUM AND RHENIUM ORTHOPHOSPHATES WITH KOSNARITE-TYPE STRUCTURE

M.V. Sukhanov, V.I. Pet'kov

Lobachevsky State University of Nizhni Novgorod (pr. Gagarina 23, Nizhni Novgorod, Russian Federation)

**Keywords:** technetium (IV) and rhenium (IV) orthophosphates, synthesis, crystal structure, kosnarite

### Abstract

This work represents an attempt to incorporate chemically technetium (IV) and rhenium (IV) in the cationic crystallographic positions of the kosnarite-type structure obtaining  $AM_2(PO_4)_3$  ( $A = Li, Na, K, Cs; M = Tc, Re$ ) compounds. The phosphates were prepared by the combined method using of solids  $TcO_2$  or  $K_2TcCl_6$ ,  $NH_4ReO_4$ ,  $ACl$  and phosphoric acid solution. Drying mixtures and their thermal treating in sealed glass ampoules allowed us to obtain the crystalline phosphates  $ATc_2(PO_4)_3$ ,  $ARe_2(PO_4)_3$  ( $A = Na, K$ ) with the kosnarite-type structure determined by the Rietveld refinement. Compounds were characterized using XRD, DSC, IR-spectroscopy and microprobe analysis.

### Introduction

The major problem of inorganic technetium chemistry is its fixation from commercial nuclear wastes in ceramic matrices and also a search of useful properties and possible areas of their application. NZP-ceramics with the kosnarite mineral  $KZr_2(PO_4)_3$  (sp. gr.  $R\bar{3}c$ ,  $Z = 6$ ) structure are well-known matrices for the toxic component immobilization of different waste forms including highly radioactive waste and have some useful properties e.g. catalytic [1, 2]. Up to now, our knowledge about of rhenium phosphates are limited by several works [3–5] devoted rhenium pyrophosphate  $ReP_2O_7$  and there are no literature data about solid technetium phosphates. In the current work we investigated the possibility of Tc(IV) and Re(IV) incorporation in the phosphates  $AM_2(PO_4)_3$  ( $A = Li, Na, K, Cs; M = Tc, Re$ ) with the kosnarite-type structure. This research may provide a more detailed understanding for inorganic chemistry of technetium and rhenium.

### Experimental

Under rhenium phosphate synthesis the crystalline salts  $NH_4ReO_4$ ,  $ACl$  and concentrated phosphoric acid solution were used. Technetium phosphates were made of  $TcO_2$  or  $K_2TcCl_6$  exposed to preliminary hydrolysis by concentrated ammonia solution ( $K_2TcCl_6 + 4NH_4OH \xrightarrow{\text{hydrolysis}} TcO_2 \cdot 2H_2O + 2KCl + 4NH_4Cl$ ). In the last case there was fourfold KCl excess in the dried residuum in comparison with the quantity needed for  $KTc_2(PO_4)_3$  synthesis. The synthesis scheme of  $AM_2(PO_4)_3$  phosphates is shown on the figure 1.



Powder XRD patterns were collected at room temperature with a XRD-6000 type diffractometer (Shimadzu) using CuK $\alpha$  radiation. The structures were refined with the RIETAN-97 software package. The A:M:P molar ratio and homogeneity of the single phases were determined with a Camebax microprobe. IR spectra were obtained by means of a FSM-1201 spectrophotometer in the frequency range 1400–400 cm<sup>-1</sup>. Synchronous differential thermal and gravimetric analysis was carried out on a LABSYS TG-DTG/DSC thermal analyzer (Setaram) in an argon atmosphere within 25–1200°C at a heating rate of 10°C·min<sup>-1</sup>.

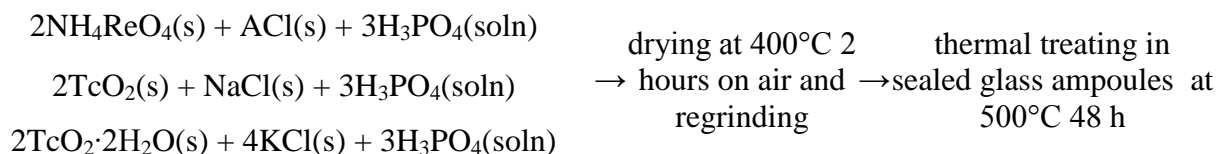


Fig. 1. Scheme of synthesis of the phosphates (s – solid, soln – solution).

## Results and Discussion

Phosphate synthesis results showed that reaction mixtures drying of short duration in the air at 400°C promoted initial reaction passing of salt decomposition and their interaction with phosphoric acid, allowed us to remove volatile compounds (H<sub>2</sub>O, HCl, NH<sub>3</sub>) and did not lead to distinct rhenium and technetium oxidation that greatly simplified the synthesis. Endothermic effects on DTA curve of reaction mixture for NaRe<sub>2</sub>(PO<sub>4</sub>)<sub>3</sub> synthesis refer to the evaporation of water, hydrochloric acid, the decomposition of ammonia perrhenate and its interaction with phosphoric acid correspondingly (Fig. 2a). The mixtures dried at 400°C according to XRD data were amorphous. Heating in the air could not be used at all synthesis stages. In the air at 500°C the thermal treatment of the mixtures dried at 400°C resulted in ReP<sub>2</sub>O<sub>7</sub> formation. Long being of these mixtures in sealed glass ampoules at 500°C allowed us to obtain crystalline products in all the systems. NaRe<sub>2</sub>(PO<sub>4</sub>)<sub>3</sub> and KRe<sub>2</sub>(PO<sub>4</sub>)<sub>3</sub> samples were phase-pure kosnarite-type phosphates. Crystalline TcO<sub>2</sub> using did not permit us to receive the pure phosphate NaTc<sub>2</sub>(PO<sub>4</sub>)<sub>3</sub>. The sample contained two phases: mostly kosnarite-type phase and 22 wt.% TcP<sub>2</sub>O<sub>7</sub>. The sample KTc<sub>2</sub>(PO<sub>4</sub>)<sub>3</sub> synthesized from the dry hydrolysis residuum of K<sub>2</sub>TcCl<sub>6</sub> was also double phase and contained KCl. After KCl excess washing with water and the product recrystallization in the sealed glass ampoules at 500°C, the pure KTc<sub>2</sub>(PO<sub>4</sub>)<sub>3</sub> sample was prepared. In ARe<sub>2</sub>(PO<sub>4</sub>)<sub>3</sub> (A = Li, Cs) systems kosnarite-type phosphate forming were not observed. DTA of NaRe<sub>2</sub>(PO<sub>4</sub>)<sub>3</sub> obtained at 500°C allowed us to reveal the area of intensive sample crystallization (exothermic effect at 738°C) and the temperature of its decomposition beginning (endothermic effect at 980°C) (Fig. 2b). The disproportionation product of NaRe<sub>2</sub>(PO<sub>4</sub>)<sub>3</sub> according to XRD were ReP<sub>2</sub>O<sub>7</sub> and metal Re (Fig. 3).

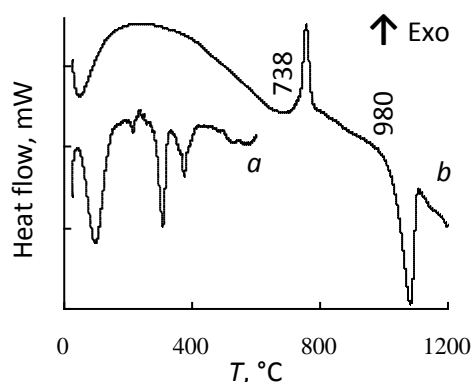


Fig. 2. DTA curves of reaction mixture for NaRe<sub>2</sub>(PO<sub>4</sub>)<sub>3</sub> synthesis (a) and NaRe<sub>2</sub>(PO<sub>4</sub>)<sub>3</sub> obtained at 500°C (b).

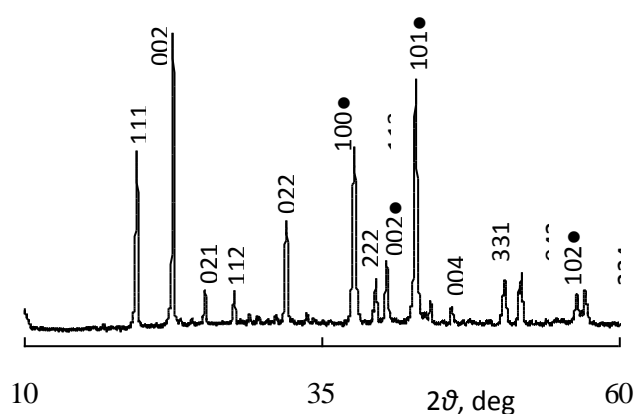


Fig. 3. XRD-pattern of disproportionation product of NaRe<sub>2</sub>(PO<sub>4</sub>)<sub>3</sub>: ReP<sub>2</sub>O<sub>7</sub> (sp. gr. P $\bar{a}$ 3) and Re (●) (sp. gr. P6<sub>3</sub>/c).

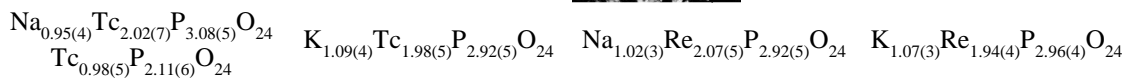
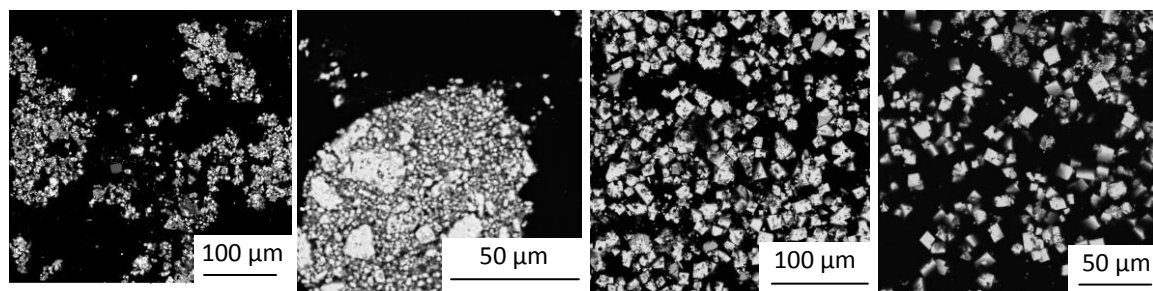


Fig. 4. Microstructure and chemical composition of the sample phosphates.

The results of the electron microprobe analysis confirmed that the monophase phosphate samples were crystalline (crystallite size  $\sim 10 \mu\text{m}$ ), homogenous and their composition corresponded to the theoretical one to within the inaccuracy of the method (Fig. 4).

The crystal structures of sodium and potassium contained phosphates were determined by the Rietveld refinement (Fig. 5). Details of X-ray diffraction experiment, unit cell parameters, and structure refinement details are presented in Table. In the three-dimensional structures  $[(\text{Tc,Re})_2(\text{PO}_4)_3]^-$  units consisting of two  $\text{ReO}_6$ - or  $\text{TcO}_6$ -octahedra and three  $\text{PO}_4$ -tetrahedra are linked to form the ribbons parallel to the  $c$  axis. These ribbons are linked together by  $\text{PO}_4$ -tetrahedra. The framework cavities are populated by  $\text{Na}^+$  and  $\text{K}^+$  ions. The calculated bond lengths between the atoms are typical of rhenium and technetium compounds:  $\text{Tc-O}$  1.959(3)–2.001(5) Å,  $\text{Re-O}$  2.000(7)–2.032(7) Å,  $\text{P-O}$  1.44(1)–1.62(1) Å,  $\text{Na-O}$  2.50(1)–2.53(1) Å,  $\text{K-O}$  2.63(1)–2.73(1) Å. The framework of  $\text{KM}_2(\text{PO}_4)_3$  phosphates with large kation  $\text{K}^+$  is considerably deformed in comparison with  $\text{Na}$ -containing phosphates (Fig. 4).  $\text{Tc}^{4+}$  and  $\text{Re}^{4+}$  ions are relatively small (0.58 and 0.63 Å correspondingly) and not able to form

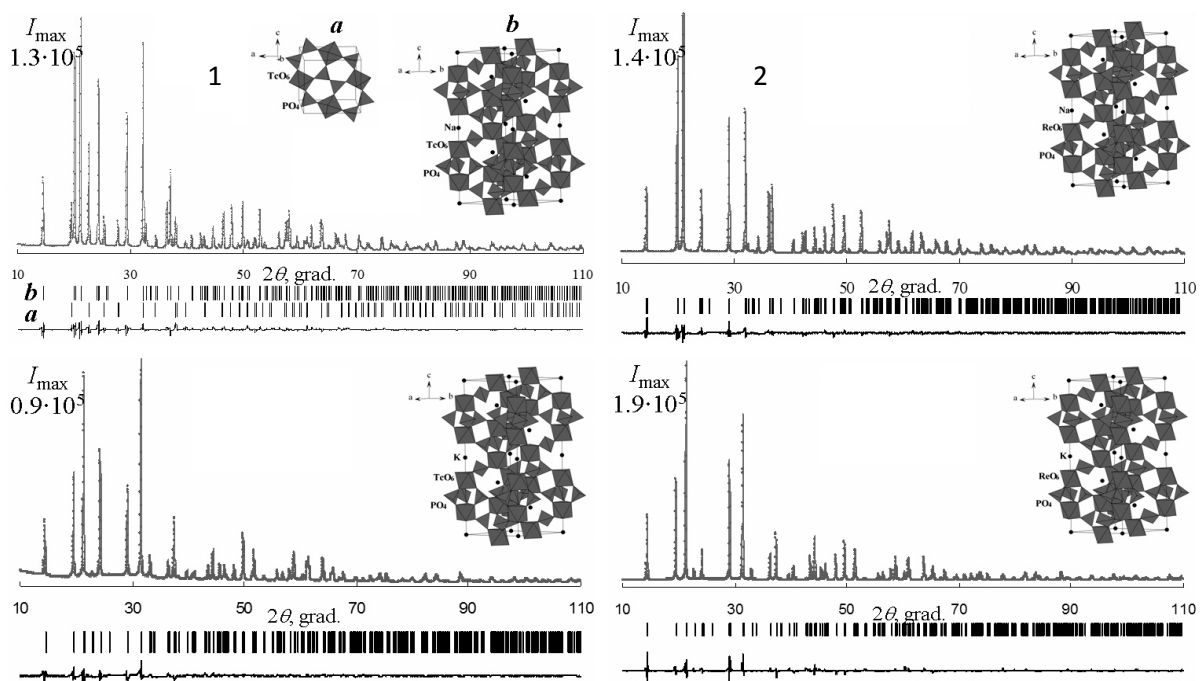


Fig. 4. Experimental (solid line) and calculated (asterisks) X-ray diffraction pattern of the synthesized samples:  $\text{NaTc}_2(\text{PO}_4)_3$  (1b),  $\text{TcP}_2\text{O}_7$  (1a),  $\text{NaRe}_2(\text{PO}_4)_3$  (2),  $\text{KTc}_2(\text{PO}_4)_3$  (3),  $\text{KRe}_2(\text{PO}_4)_3$  (4). Crystal structures and the positions of the reflections in the calculated XRD pattern are shown in the figures.

Table. Details of the X-Ray diffraction experiment and results of crystal structure refinement of technetium- and rhenium-containing phosphates

Characteristic	NaTc <sub>2</sub> (PO <sub>4</sub> ) <sub>3</sub>	TcP <sub>2</sub> O <sub>7</sub>	KTc <sub>2</sub> (PO <sub>4</sub> ) <sub>3</sub>	NaRe <sub>2</sub> (PO <sub>4</sub> ) <sub>3</sub>	KRe <sub>2</sub> (PO <sub>4</sub> ) <sub>3</sub>
Space group, Z	$R\bar{3}c$ , 6	$P\bar{a}3$ , 4	$R\bar{3}c$ , 6	$R\bar{3}c$ , 6	$R\bar{3}c$ , 6
$a$ , Å	8.4091(1)	7.8643(2)	8.2917(2)	8.4541(1)	8.3155(2)
$c$ , Å	22.2602(3)	-	23.2255(5)	22.3320(3)	23.3867(5)
$V$ , Å <sup>3</sup>	1363.18(4)	486.39(3)	1382.87(5)	1382.25(3)	1400.48(5)
$\rho_{XRD}$ , g/cm <sup>3</sup>	3.696(1)	3.726(1)	3.761(1)	4.904(1)	4.954(1)
$2\theta$ range, deg	10.00 – 110.00				
Number of reflection	301		197	195	199
Number of parameters refinement	55		34	36	34
$R_{wp}$ , %	6.92		6.45	4.33	6.57
$S$	5.13		4.02	3.73	6.14

a framework containing large Cs<sup>+</sup> ions as with Ti<sup>4+</sup> (0.61 Å). Also there are ATi<sub>2</sub>(PO<sub>4</sub>)<sub>3</sub> (A = Li, Na, K, Rb) phosphates having the kosnarite-type structure, CsTi<sub>2</sub>(PO<sub>4</sub>)<sub>3</sub> having the kosnarite-type structure cannot be synthesized.

The IR spectroscopic data of the synthesized phosphates are in agreement with the X-ray diffraction data and suggest that these compounds belong to the orthophosphate class. The IR spectra of technetium- and rhenium-containing phosphates are similar to those of double phosphate of alkali metal and zirconium or titanium. In the IR spectra, the adsorption bands observed at frequencies of 987–1226 cm<sup>-1</sup> are assigned to the  $\nu_3$  stretching vibrations of the P–O bonds in the PO<sub>4</sub>-tetrahedra, the adsorption band at a frequency of 914 cm<sup>-1</sup> is attributed to the  $\nu_1$  stretching vibrations, and the adsorption bands in the range 547–659 cm<sup>-1</sup> correspond to the  $\nu_4$  bending vibrations.

### Conclusions

Thus, the crystalline phosphates ATc<sub>2</sub>(PO<sub>4</sub>)<sub>3</sub>, ARe<sub>2</sub>(PO<sub>4</sub>)<sub>3</sub> (A = Na, K) with the kosnarite-type structure were synthesized by the combined method. Tc<sup>4+</sup> and Re<sup>4+</sup> were shown to enter octahedral framework positions in the kosnarite-type structure.

**Acknowledgments:** The work was supported by the Russian Foundation for Basic Research, project no. 11-03-00032.

### References

1. V.I. Pet'kov, M.V. Sukhanov, M.M. Ermilova, N.V. Orekhova, G.F. Tereshchenko. *Russian J. Applied Chem.* **83**(10): 1731–1741 (2010).
2. V.A. Sadykov, S.N. Pavlova, G.V. Zabolotnaya et al. *Kinet. Katal.* **42**(3): 432–441 (2001).
3. E. Banks, R. Sacks. *Mat. Res. Bull.*, **17**(8): 1053–1055 (1982).
4. K. Popa, V. Brandel, A. Cecal. *Rev. Roumaine de Chim.* **46**(5): 509–515 (2001).
5. V.V. Lisnyak, N.V. Stus, D.A. Stratiichuk, N.M. Belyavina, V.Ya. Markiv. *Phosphorus, Sulfur, and Silicon.* **183**: 2248–2255 (2008).

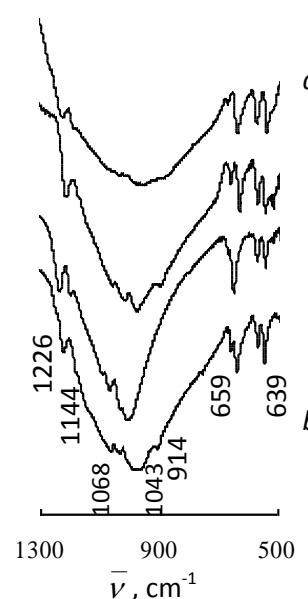


Fig. 5. IR-spectra of samples: NaTc<sub>2</sub>(PO<sub>4</sub>)<sub>3</sub> (a), KTc<sub>2</sub>(PO<sub>4</sub>)<sub>3</sub> (b), NaRe<sub>2</sub>(PO<sub>4</sub>)<sub>3</sub> (c), KRe<sub>2</sub>(PO<sub>4</sub>)<sub>3</sub> (d).

1.P4.

## DEPTH DEUTERIUM AND HYDROGEN CONCENTRATIONS IN SET OF Re-Mo FOILS MEASURED AFTER ACTION OF PULSE HIGH TEMPERATURE DEUTERIUM PLASMA

A.Yu. Didyk<sup>1</sup>, V.S. Kulikauskas<sup>2</sup>, R. Wiśniewski<sup>3</sup>, A.N. Majorov<sup>4</sup>

<sup>1</sup>Joint Institute for Nuclear Research, Flerov Laboratory of Nuclear Reactions,  
Dubna, Moscow Region, Russian Federation

<sup>2</sup>Skobeltsyn Institute of Nuclear Physics of Lomonosov Moscow State University,  
Moscow, Russian Federation

<sup>3</sup>National Centre for Nuclear Research, 05-400 Otwock/Świerk, Poland

<sup>4</sup>Lebedev Physical Institute of Russian Academy of Sciences, Moscow, Russian Federation

**Keywords:** plasma-focus set-up, high temperature plasma, elastic recoil detection, shock waves, depth concentration, diffusion parameters, rhenium-molybdenum alloy, transport of deuterium, hydrogen

### Abstract

The depth distributions of deuterium and hydrogen atom concentrations in sets of Re-Mo alloy foils after action of high temperature deuterium plasma bombardment using “Plasma Focus” set-up (PF-4) were measured using elastic recoil detection method. It is established that the implanted deuterium and existing hydrogen atoms are transferred to a large depths in the set of foils, much deeper than the projected ranges of deuterium ions from the plasma with the maximum it’s velocities of about  $10^8$  cm/s. The increasing of depth hydrogen concentrations in the set of Re-Mo foils was determined. The coloring of three first Re-Mo foil surfaces nearer to PF-4 set-up are observed too. The obtained results can be explained by large power density of pulse deuterium plasma arising of shock waves and large mechanical tension which influence on the transport and redistribution of deuterium ions and hydrogen atoms at large depths.

### 1. Introduction

In recent years, due to significant big advances in laser technology and the creation of powerful pulse lasers in the pico- ( $10^{-12}$  s) and femtosecond ( $10^{-15}$  s), second life has received a relatively new area of science - the physics of high energy density [1, 2]. This trend has evolved in the direction of studying the action of short pulses with condensed matter, *i.e.*, processes such as laser sputtering, ablation, intermixing of impurities, the creation of new phases and influence of the of powerful shock waves [3, 4]. In addition, it was formed another important area of research on effects of high-power laser pulses for developing of a laser-controlled nuclear fusion. As it is known, the accumulation of plasma components (deuterium and tritium) and the fusion fragments of thermonuclear reactions as of helium atoms in the first wall material at operating fusion reactor should be. Therefore, the study of processes of accumulation and adsorption-desorption processes of light gases and especially of tritium is essential [3, 4]. An another important problem for modern energetic complexes and engines is the storage of hydrogen in metal and alloys for accumulation of hydrogen [5-7]. Besides that it is well known that rhenium ion can adsorb up to nine hydrogen ions and create chemical composition complex as  $\text{ReH}_9^{-2}$ , *i.e.* may be such triple alkaline-rhenium hydride like  $\text{K}_2\text{ReH}_9$  (or deuteride- $\text{K}_2\text{ReH}_9$ ) can be used for hydrogen-deuterium storage. The use of installations as the "Plasma Focus" for high-power plasma streams and study its effects on materials is also very relevant in terms of modeling of such processes. The aim of this paper is to study the



propagation of shock waves in the metal foils on the effects caused by the processes of redistribution and accumulation of deuterium or hydrogen atoms under the deuterium plasma bombardment.

## 2. Research technique and results

The studies were performed using "Plasma Focus" set-up (PF-4) of Lebedev Physics Institute of RAS [3, 4, 8-13]: the energy of the capacitor battery is 3.6-4 kJ, the maximum current  $\approx 400$  kA, the plasma flow velocity up to  $10^8$  cm/s, the plasma density up to  $\approx 10^{18}$  cm<sup>-3</sup>, the plasma pulse duration of 50-100 ns, the energy flux density up to  $10^8$ - $10^{10}$  W/cm<sup>2</sup>, the neutron yield up to  $10^8$  neutrons per pulse, the time between pulses of at least 5-6 minutes. The choice of hydrogen and deuterium plasma was due to the possibilities of further measurements with the detection of elastically scattered recoil (elastic recoil detection - ERD-[14]) concentration profiles of hydrogen and deuterium atoms after plasma treatment of the targets consist on the multilayer metallic foils and combinations of other material, including non metallic foils [9-13]. A scheme of the elements of the PF-4 set-up is presented in Fig.1.

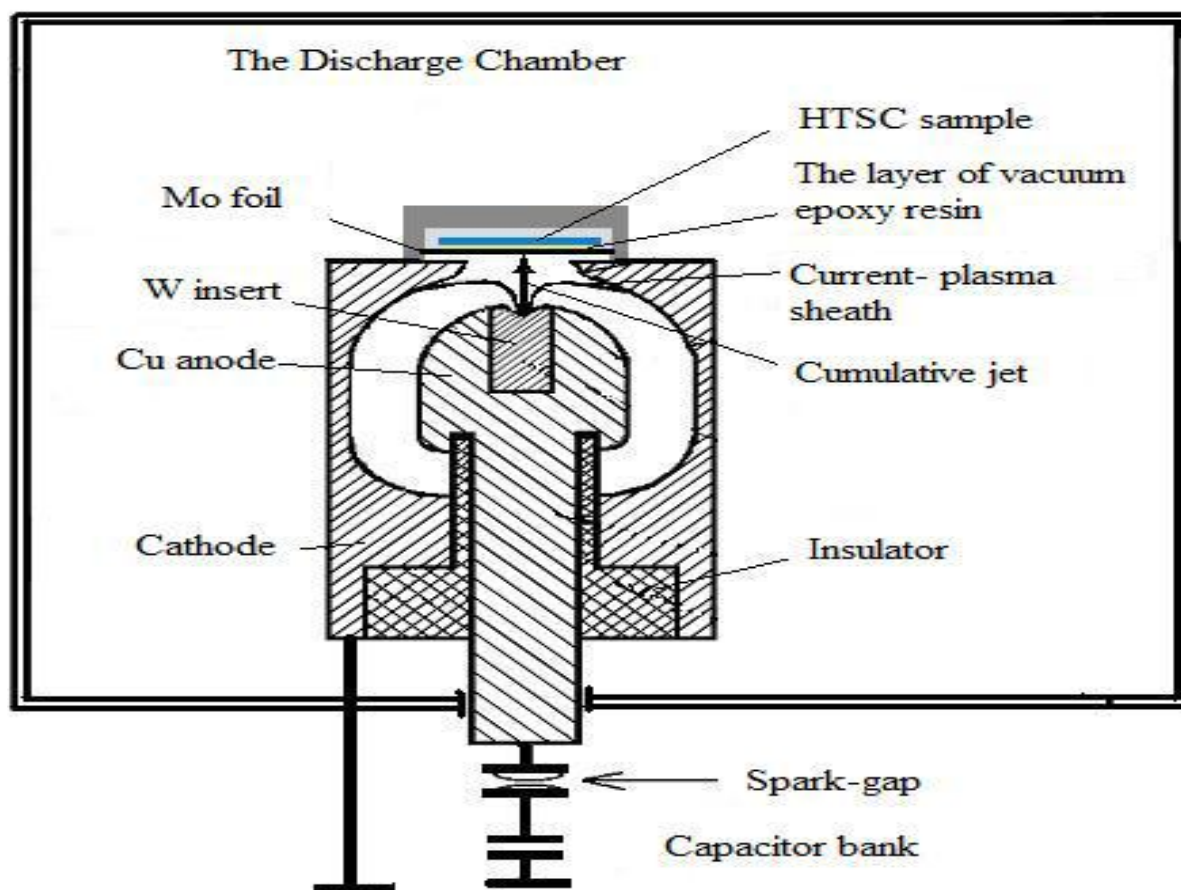


Fig.1. The scheme of the elements of the FS-4 [8] for irradiation of samples using the example of second generation high temperature superconductor (HTSC) sample (the example)[8].

It is seen from Fig.1, near the target's set of foils, which is schematically shown in Fig.2 [9-13], cumulative jet stream can be focused to a relatively small surface. The density of a pulsed plasma power on the target can be varied by changing of the distance between tungsten insert and target (Fig.1 and Fig.2). In our experiments that distance was 35 mm.



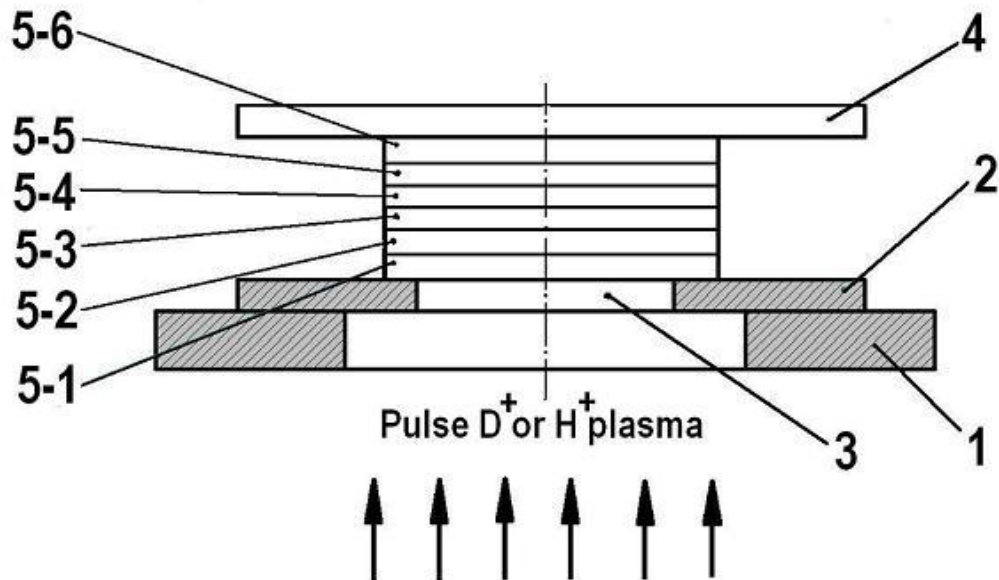


Fig.2. The scheme of PF-4 pulse high temperature plasma action on the set of foils. Here 1 –holder for the set of foils, 2 - front aperture diaphragm with round hole (10 mm or 15 mm in diameter), 3, 4 - clamping plate, and from 5-1 to 5-6 a set of six foils.

Deuterium plasma was used at our experiments to study of shock wave action on chosen materials of foils [9-13]. Set of foils consisted on six tightly pressed Re-Mo foils with chemical composition 50 at.% of Re and 50 at.% of Mo metals. Thickness of each foil was 50  $\mu\text{m}$ , i.e. whole thickness of foil set was 300  $\mu\text{m}$ . The number of plasma pulses was 15. Deuterium pressure in the PF-4 chamber was 2 Torr. The measurements of the neutron yield from fusion D-D reactions were carried out using activating neutron detectors (see, as example [14]) during bombardment by deuterium pulse plasma. The yield of neutron was measured and measured level was a little higher than background, i.e. the yield of neutrons from D-D reaction took place. Let us denote the appropriate set of foils, as  ${}^1\text{Re-Mo-1}^2$ ,  ${}^1\text{Re-Mo-2}^2$ ,  ${}^1\text{Re-Mo-3}^2 \dots {}^1\text{Re-Mo-6}^2$  (see [9 - 13]). Here top indexes correspond to nearer and further surfaces of foils to PF-4. The measurements of depth concentrations of introduced deuterium ions from plasma and initial hydrogen atoms which usually present in metals and alloys were carried out using elastic recoil detection method (ERD) [15].

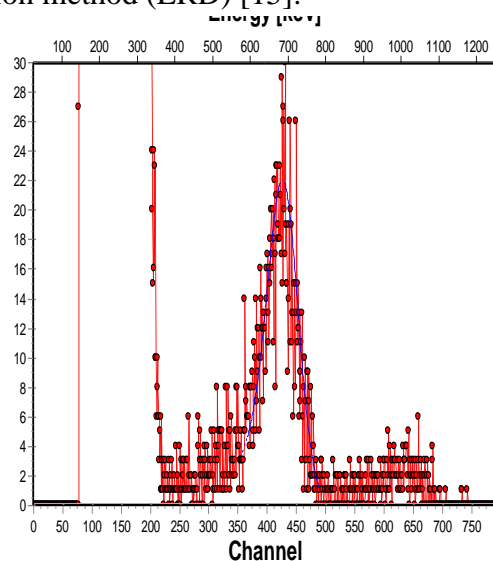


Fig.3. Spectrum of elastic recoils detection of hydrogen and deuterium from the bulk near the surface of  ${}^1\text{Re-Mo-1}$  foil.

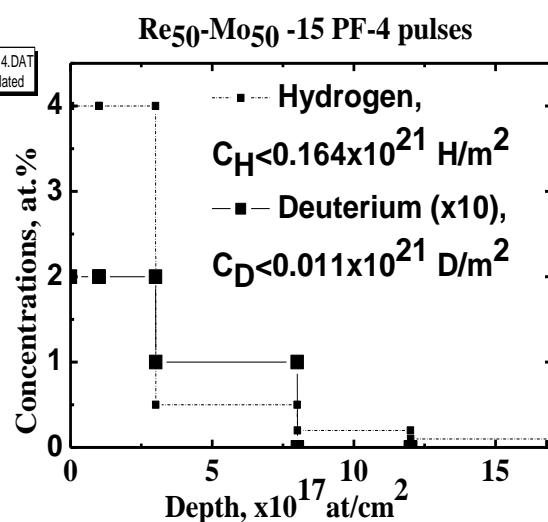


Fig.4. Depth distribution of hydrogen and deuterium atoms from the bulk near the surface of  ${}^1\text{Re-Mo-1}$  foil.

The ERD spectra for first three Re-Mo-foils together with the depth distributions of deuterium and hydrogen by pairs are presented in Figs.3- 4; Figs.5- 6 and Figs.7- 8, respectively. The ERD spectra were obtained using the analyzing beam of helium ions with energy 2.3 MeV at grazing angle of incidence on the sample of  $15^\circ$  with an electrostatic generator EG-5 in the SINP of MSU. Processing of spectra was carried out using a standard simulation program-processing SIMNRA 6.05. Note that the projected range of helium ions  $R_p = 0.90 \pm 0.36 \mu\text{m}$ , where the calculation is made using the program TRIM-2007.

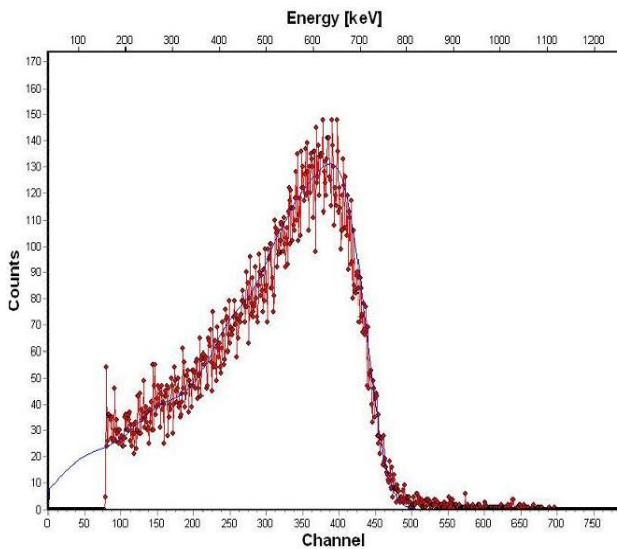


Fig.5. Spectrum of elastic recoils detection of hydrogen and deuterium from the bulk near the surface of <sup>1</sup>Re-Mo-2 foil.

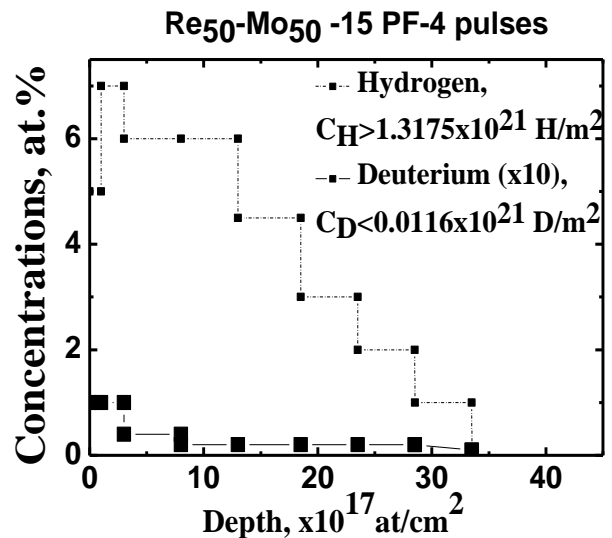


Fig.6. Depth distribution of hydrogen and deuterium atoms from the bulk near the surface of <sup>1</sup>Re-Mo-2 foil.

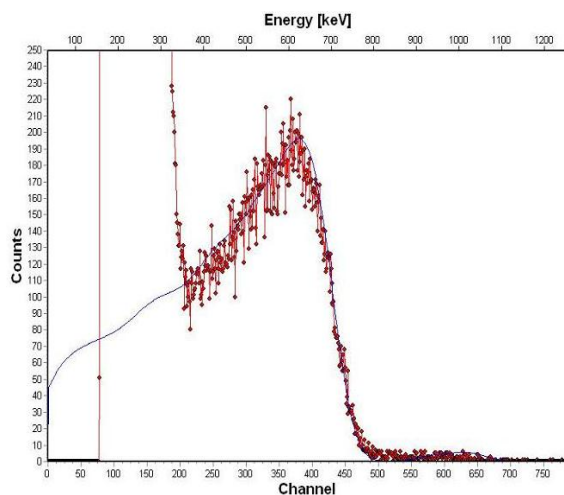


Fig.7. Spectrum of elastic recoils detection of hydrogen and deuterium from the bulk near the surface of <sup>1</sup>Re-Mo-2 foil.

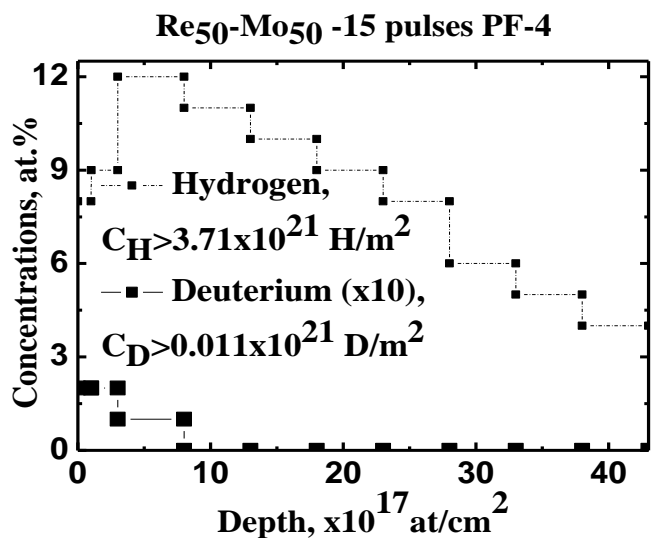


Fig.8. Depth distribution of hydrogen and deuterium atoms from the bulk near the surface of <sup>1</sup>Re-Mo-2 foil.

All three of the ERD experimental spectra are represented for more visual representation of the observed effect - deep penetration of deuterium in the set of Re-Mo-foils and also the deep changes of hydrogen concentrations too. The integral concentrations of deuterium and hydrogen in bulk Re-

Mo alloy near the nearest surface to PF-4 are presented in Figs. 4, 6 and 8. It is necessary to note that maximum depths of recoils which can be studied by ERD analysis are less than  $R_p < 1 \mu\text{m}$ . Summary of these values are, as well, presented in Table 1.

Table 1. Integral concentrations in each foils of deuterium atoms, introduced into foils from deuterium plasma of PF-4, and concentrations of hydrogen atom spreading measured by ERD analysis.

	First foil in set, <sup>1</sup> Re-Mo-1	Second foil in set, <sup>1</sup> Re-Mo-2	Third foil in set, <sup>1</sup> Re-Mo-3
Maximum concentration of hydrogen near surface of foils	4%	7%	12%
Integral concentration of deuterium, $C_D$	$<0.011 \cdot 10^{21} \text{ D/M}^2$	$<0.012 \cdot 10^{21} \text{ D/M}^2$	$>0.021 \cdot 10^{21} \text{ D/M}^2$
Integral concentration of hydrogen, $C_H$	$0.164 \cdot 10^{21} \text{ H/M}^2$	$>1.32 \cdot 10^{21} \text{ H/M}^2$	$>3.71 \cdot 10^{21} \text{ H/M}^2$

As can be seen in all the foils deuterium atoms are present (see also ERD spectra - Figs. 3, 5 and 7). More interesting fact is the presence of hydrogen with increasing of maximum concentrations and integral concentrations in the each following foil in set. It should be noted that the direct impact of deuterium plasma due to contact with the samples from the lateral surfaces of the foil set was completely excluded by the fact that all three Re-Mo foils (position 5-1, 5-2 and 5-3 in Fig. 2) was held tightly to one another between the front aperture diaphragm 2 and clamping plate 4 (see Fig. 2). In addition, at high concentration of deuterium and hydrogen atoms on the surface of the all three foils was observed a characteristic colored spot with a diameter of 10 mm, which corresponds exactly to the diameter of the entrance aperture (see also [9 - 13] and [16]).

### 3. Conclusion

The ERD studies of six Re-Mo foil set (with thickness of each foil 50  $\mu\text{m}$ ) after exposure by 15 pulse high-temperature deuterium plasma using installation PF-4 were carried out. It is established that there were transport of introduced into set of foils deuterium ions from deuterium plasma and presented in initial foils hydrogen atoms to large depths into all three measured foils. Addition concentrations of deuterium and hydrogen atoms in volumes near the surfaces of each three foils changed the metallic color of initial foil surfaces nearer to PF-4 to blue color after action of deuterium plasma (see also [9 - 13] and [16]). These three spots on three first foils have a diameter exactly equal to diameter of front aperture diaphragm (see Fig. 2, detail position 2). Surface and integral concentrations of hydrogen are increased from foil to foil very significantly (see Table 1).

The effect of ultra-deep penetration of hydrogen and deuterium can be explained by the influence of powerful shock waves [1 - 4, 8 - 13]. This explanation is confirmed by possible accelerated diffusion of impurities in the presence of external driving forces  $F$  (see [17, 18]). In this case the diffusion laws ought to be presented in the form (see [17], page 11), where for the one-dimensional case the operator  $\nabla = \frac{\partial}{\partial X}$ :

$$J = -D\nabla C + \alpha \langle V \rangle_F, \quad (1)$$

$$\frac{\partial C}{\partial t} = \nabla [D\nabla C] - \alpha \cdot \nabla \langle V \rangle_F, \quad (2)$$

where the external driving force  $F$  imparts to each atom the average additional velocity  $\langle V \rangle_F$  and  $\alpha$  is the proportionality factor. The average velocity of each atom  $\langle V \rangle_F$  can be compared to the speed of propagation of the shock wave exceeding by several times the speed of propagation of the sound in a material [1 - 4]. As is known, under intense pulse action an elastic wave begins to propagate in the material and transforms, at a certain depth  $X_0$  depending on the material and pulse power density on the surface, into a shock wave with an abrupt front – a compression-extension wave behind the shock wave front. One can also make the following estimates. The velocity of sound in metals exceeds  $V \geq 2.0 \cdot 10^3$  m/s, plasma pulse duration is of the order  $t = 50 \div 100$  nanoseconds, consequently, the maximal depth of transfer of light impurities of hydrogen and deuterium ( $X_M$ ) can exceed the value  $X_M = V \cdot t > 100 \div 200$   $\mu\text{m}$ . The estimated value of the hydrogen penetration depth is in the order-of-magnitude agreement with the experimental values in this paper and in [9 - 13].

## References

1. V.E. Fortov. Extreme states of matter on earth and in space. Fizmatlit, 2008, 264 p.
2. V.E. Fortov. Extreme states of matter. Fizmatlit, 2010, 304 p.
3. Encyclopedia of the low-temperature plasma. Series B, helper applications, databases, and V. IX -3, edited by VA Gribkov, M., ed.: JANUS-K, 2007, 591 p.
4. L.I. Ivanov, N.N. Pimenov, V.A. Gribkov. Physics and Chemistry of Materials Processing, 2009, № 1, 23 p.
5. Handbook of Hydrogen Storage, New Materials for Future Energy Storage. Edited by Michael Hirscher, Handbook of Hydrogen Storage, WILEY-VCH Verlag GmbH & Co. KGaA, 2010, 341 p.
6. Hydrogen in Metals, Volumes 1. Basic Properties. Edited by G. Alefeld and J. Volkl, Springer-Verlag, Berlin-Heidelberg-New York, 1978; Izd. M.: "Mir", 1981, 475 p.
7. Hydrogen in Metals, Volumes 2. Applied aspects. Edited by G. Alefeld and J. Volkl, Springer-Verlag, Berlin-Heidelberg-New York, 1978; Izd. M.: "Mir", 1981, 430 p.
8. L.H. Antonova, I.V. Borovitskaya, P.V. Gorshkov, et.al. Reports of the Russian Academy of Sciences, T. 428, № 4, 471-473, 2009, p.471
9. A.Yu. Didyk. Preprint P14-2011-87, Dubna, JINR, 2011, 14 p.
10. A.Yu. Didyk. Preprint P14-2011-88, Dubna, JINR, 2011, 14 p.
11. A.Yu. Didyk, L.I. Ivanov, O.N. Krokhin et.al.. Reports of the Russian Academy of Sciences, 2011 (in press).
12. A.Yu. Didyk, I.V. Borovitskaja, R. Wiśniewski et al. Surface. X-ray, Synchrotron and Neutron Techniques, 2011 (in press).
13. A.Yu. Didyk, R. Wiśniewski, L.I. Ivanov et al. Surface. X-ray, Synchrotron and Neutron Techniques, 2011 (in press).
14. I.V. Volobuev, V.A. Gribkov, S. Denus et al. Brief Communications in Physics, Moscow, 1987, № 11, p.32.
15. V.V. Zatekin, V.S. Kulikauskas, L.S. Novikov et al. Surface. X-ray, Synchrotron and Neutron Techniques, 2008, № 4, p.23.
16. F.J.A. Den Broeder, S.J. Van der Molen, M. Kremers et al. Nature 1988, No 394, 656 p.
17. B.S. Bokshtein. Diffusion in metals. M.: Metallurgiya, 1978, 248 p.
18. V.Ya. Geguzin. Diffusion zone, M.: Metallurgiya, 1976, 320 p.

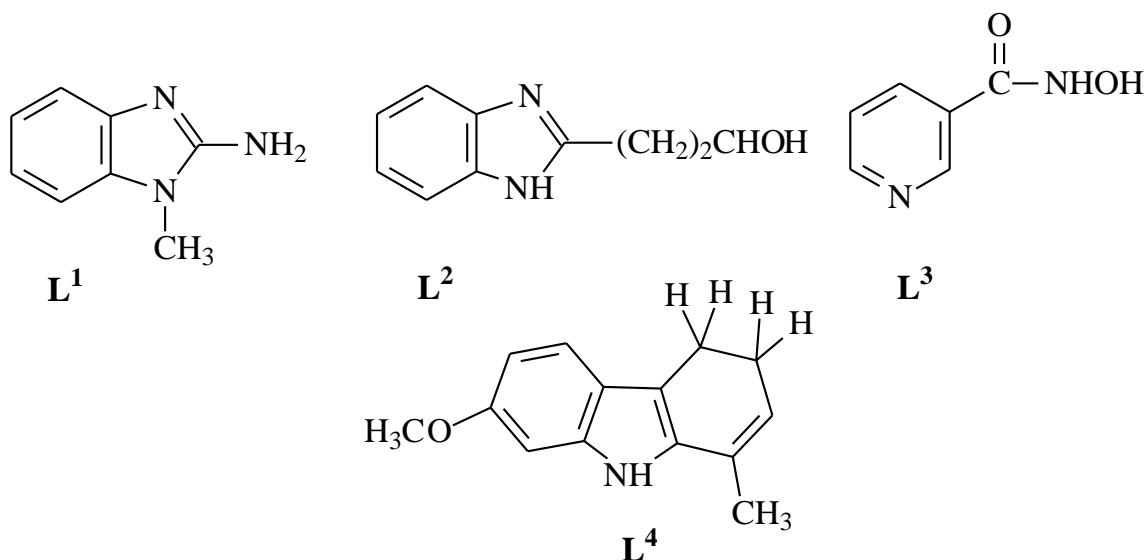
1.P5.

## COORDINATION COMPOUNDS OF BIOLOGICALLY ACTIVE N-CONTAINING HETEROCYCLIC LIGANDS

Z.Ch.Kadirova<sup>1</sup>, Kh.T. Sharipov<sup>1</sup>, Sh. Juraev<sup>1</sup>, N.A. Parpiev<sup>2</sup>

Tashkent Chemical-Technological Institute, Navoi St. 32, Tashkent, Uzbekistan  
National University of Uzbekistan named by Mirzo Ulugbek, Vuzgorodok, Chemical Faculty, Tashkent,  
Uzbekistan, [zuhra\\_kadirova@yahoo.com](mailto:zuhra_kadirova@yahoo.com)

The synthesis of rhenium coordination compounds strongly depends on reaction conditions, metal precursor and ligand nature. The rhenium compounds with some biologically active heterocyclic ligands were prepared and characterized by spectral methods and thermal analysis. The 2-amino-1-methyl-1H-benzimidazole-2 ( $L^1$ ), 3 (benzimidazole-2-yl) - propanol-1 ( $L^2$ ), N-hydroxy-3-pyridinecarboxamide ( $L^3$ ), 7-methoxy-1-methyl- 4,9-dihydro-3H -pyrido [3,4-b] indole ( $L^4$ ) ligands contained the 5- and 6-membered heterocycles are existed in stable protonated forms in acid solution.



The reaction of hexachloridorhenate (IV) with  $L^1$ - $L^4$  yields to formation hexachlororhenates (IV) consisted from the complex metaloanions and the protonated molecules of organic ligands as cations.

These salts have poor solubility in water and can exist in the concentrated acid solution that can have application in extraction of rhenium by precipitation.

The synthesized compounds showed the solid-phase dehydrohalogenation and the temperatures of thermal effects depended on structure of organic cations.

The Re(V) precursor  $\text{ReOCl}_3(\text{PPh}_3)_2$  is reduced by  $\text{PPh}_3$  in the presence of  $L^1$ , giving good yields of rhenium(III) complexes. Good solubility of complexes in organic solvents is used for rhenium extraction.

The composition and structure of complexes were established on the base of elemental and thermal analysis, IR, NMR- data.



1.P6.

## CHELATION OF RHENIUM (V) WITH 3-ETHYL-4-METHYL-1,2,4-TRIAZOL-5-THIOL IN 3 MOL/L HCL MEDIUM

N.G. Kabirov, S.M. Safarmamadov, A.A. Aminjonov

Tajik National University. Dushanbe. [azimjon51@mail.ru](mailto:azimjon51@mail.ru)

**Keywords:** rhenium(V), 3-ethyl-4-methyl-1,2,4-triazolthiole-5-thiol

### Abstract

The process of chelation of rhenium (V) with 3-ethyl-4-methyl-1,2,4-triazolthiole-5-thiol in 3 M HCl medium in the range 273-338K. The values of stepwise formation constants of all forms of complexes formed in system  $H_2[ReOCl_5]$  - 3-ethyl-4-methyl-1,2,4-triazolthiol - 3 M HCl. The values of the thermodynamic functions of complexation process are estimated.

### Introduction

Conduction researches in solutions can to a certain extent shed light on the mechanisms of formation of complex compounds. To perform these studies, one of the available methods is potentiometric titration with ligand redox electrodes based on sulfur-containing compounds and their oxidized forms. Ligand environment designed electrode systems play a special role in the formation of sulfur-containing compounds of azoles and their oxidized forms. Representative of this class of compounds are 1,2,4-triazolthiol and its derivatives, which have been used as a substrate for a redox ligand electrodes in the middle of the eighties. By potentiometric titration processes complexation of rhenium (V) with 1,2,4-triazolthiole and some of its alkylderivates were studied. The authors of [1] developed a reversible ligand electrode based on 3-ethyl-4-methyl-1,2,4-triazolthiole-5-thiol and its oxidized form. The purpose of this paper is to study the process of chelation of rhenium (V) with 3-ethyl-4-methyl-1,2,4-triazolthiole-5-thiol in 3 M HCl medium in the 273-338K temperature range.

### Experimental

To determine the stepwise formation constants of complexes of rhenium (V) with 3-ethyl-4-methyl-1,2,4-triazolthiole-5-thiol in 3 M HCl medium in the temperature range 273-338K using potentiometric method, which is described in [1] in detail. The equilibrium concentrations of 3-ethyl-4-methyl-1,2,4-triazole-5-thiol was calculated using the formula:

$$\lg[L] = \frac{E_{ucx} - E_i}{1,983 \cdot 10^{-4} \cdot T} + \lg C_L^{ucx} + \frac{1}{2} \lg \frac{V_{ucx}}{V_{\text{общ}}}$$

where  $E_{ish}$  - the equilibrium potential of the source system in the absence of rhenium (V);  $E_i$  is the equilibrium potential of the system at a given point of titration,  $C_L$  - initial analytical concentration of ligand;  $V_{ish}/V_{\text{общ}}$  - ratio of the original volume of the total, and T - the temperature of the experiment. Bjerrum formation function was determined by the formula:

$$\bar{n} = \frac{C_L - [L]}{C_{\text{Re(V)}}}$$

where  $C_L$  - the concentration of 3-ethyl-4-methyl-1,2,4-triazolthiole at each point of the titration;  $[L]$  - equilibrium concentration of 3-ethyl-4-methyl-1,2,4-triazolthiole at each point of the titration;  $C_{\text{Re(V)}}$  - the concentration of rhenium (V) at each point of the titration. All calculations were performed using «Pentium-IV» computer.

### Results and discussion

Studies have shown that during the addition of  $H_2[ReOCl_5]$  to 3-ethyl-4-methyl-1,2,4-triazole-5-thiol in 3 M HCl medium is a sequential change in color of the solution from red to purple, then to the blue and green. Adding to the green solution of 3-ethyl-4-methyl-1,2,4-triazole-5-thiol leads to the opposite change in color of the solution. This fact confirms the aliasing of complex rhenium (V) 3-ethyl-4-methyl-1,2,4-triazole-5-thiol, and indicates the reversibility of this process. In the titration system consisting of 3-ethyl-4-methyl-1,2,4-triazole-5-thiol and its oxidized form solution  $H_2[ReOCl_5]$  observed increase in the magnitude of the equilibrium potential, which indicates that participation in complexation with rhenium (V) 3-ethyl-4-methyl-1,2,4-triazole-5-thiol, but not its oxidized form. At each point of the titration, equilibrium is established within 5-10 minutes. As an example, Table 1 shows the experimental results to determine the function of education 3-ethyl-4-methyl-1,2,4-triazole-5-thiol complexes of oxorhenium (V) chloride in medium 3 mole/l HCl at 273K.

Table 1. Determining the formation function of 3-ethyl-4-methyl-1,2,4-triazole-5-thiol complexes of oxorhenium (V) chloride in 3 M HCl medium at 273K

№	$C_{Re(V)} \cdot 10^4$	$C_L \cdot 10^2$	$\Delta E, mB$	$[L] \cdot 10^4$	$\bar{n}$
	mol/l				
1	2	3	4	5	6
1.	14,1	1,321	19,55	58,67	5,22
2.	16,8	1,311	22,80	50,91	4,79
3.	19,4	1,301	24,90	46,39	4,32
4.	22,0	1,292	28,35	39,92	4,05
5.	24,6	1,282	34,00	31,28	3,94
6.	27,1	1,273	39,10	25,10	3,77
7.	29,6	1,264	40,40	23,66	3,47
8.	32,1	1,254	48,00	17,07	3,38
9.	34,5	1,246	49,35	16,06	3,15
10.	36,9	1,297	53,00	13,71	2,98
11.	39,2	1,228	60,30	10,01	2,87
12.	41,6	1,220	61,55	9,46	2,71
13.	43,8	1,211	64,30	8,39	2,57
14.	46,1	1,203	67,00	7,46	2,45
15.	50,5	1,186	73,55	5,58	2,30
16.	55,9	1,167	84,00	3,67	2,02
17.	61,1	1,148	89,70	2,78	1,83
18.	66,1	1,129	94,36	2,26	1,67
19.	71,0	1,111	103,00	1,55	1,54
20.	75,7	1,094	108,80	1,20	1,43
21.	88,03	1,077	110,75	1,10	1,33
22.	84,7	1,061	112,60	1,01	1,24
23.	97,2	1,014	119,30	0,74	1,04
1	2	3	4	5	6
24.	105,0	9,86	120,80	0,69	0,93
25.	119,3	9,33	122,15	0,63	0,78
26.	132,1	8,86	114,40	0,85	0,66
27.	149,1	8,24	104,50	1,25	0,54
28.	168,3	7,53	64,40	6,59	0,41

Potentiometric titration curves of 3-ethyl-4-methyl-1,2,4-triazole-5-thiol complexes of rhenium (V) formation at different temperatures are shown in Figure 1. It is seen that the curves of

3-ethyl-4-methyl-1,2,4-triazole-5-thiol rhenium (V) complexes formation, without changing its shape with increasing temperature, shifting toward lower values of  $-\lg[L]$ , which indicates that identity of the process of complexation in the range 273-338K. Established that during the interaction of rhenium (V) 3-ethyl-4-methyl-1,2,4-triazole-5-thiol in 3 M HCl medium in the temperature range 273-338K in series form five complete form.

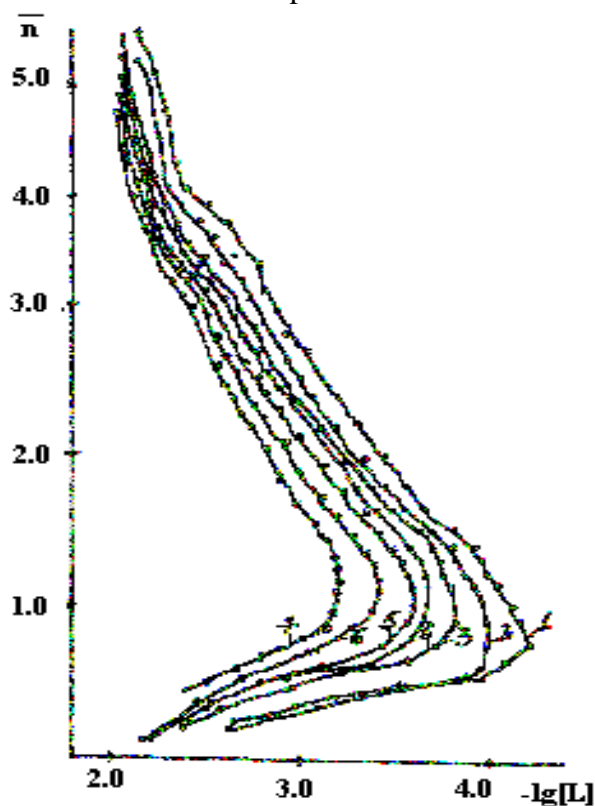


Figure 1. Curves education 3-ethyl-4-methyl-1,2,4-triazole-5-thiol complexes of rhenium (V) in medium 3 mole/l HCl at temperatures: 1-273; 2-288, 3-298, 4-308; 5-318, 6-328, 7-338K.

Determined by the method of Bjerrum formation curve, the values of  $pK_i$  3-ethyl-4-methyl-1,2,4-triazole-5-thiol complexes of rhenium (V) in 3 M HCl medium are presented in Table 2.

Table 2.  $pK_i$  values 3-ethyl-4-methyl-1,2,4-triazole-5-thiol complexes of rhenium (V) in medium 3 mole/l HCl at 273-338K

T, K	$pK_1$	$pK_2$	$pK_3$	$pK_4$	$pK_5$
273	3,61	3,82	3,12	2,69	3,00
288	3,59	3,70	2,99	2,54	2,25
298	3,01	3,63	2,89	2,41	2,16
308	2,83	3,60	2,84	2,36	2,13
318	2,80	3,40	2,75	2,18	2,10
328	2,66	3,25	2,67	2,26	2,06
338	2,50	3,10	2,58	2,21	2,03

The data presented in Table 2 show the closeness of the numerical values of the constants of step formations. All stepwise stability constants decrease with increasing temperature, indicating that the exothermicity of the complexation process. Reducing the quantities of step formation constants 3-ethyl-4-methyl-1,2,4-triazole-5-thiol complexes in the 3 M HCl medium with an increase in temperature can be explained by the fact that with the rise of temperature the competition between chloride ions and 3-ethyl-4-methyl-1,2,4-triazole-5-thiol molecules increases on the one hand, and the other the competition between water molecules and these organic ligand for a place in the coordination sphere increases also. Regardless of the chloride ions with water

molecules or competition takes place with increasing temperature, the occurrence of the molecules of 3-ethyl-4-methyl-1,2,4-triazole-5-thiol the internal sphere of the complex is difficult.

With the use of certain quantities of  $pK_i$  entities curves at different temperatures using the temperature coefficient were calculated thermodynamic functions of complexation process rhenium (V) 3-ethyl-4-methyl-1,2,4-triazole-5-thiol in medium 3 mole/l HCl, which are presented in Table 3.

Table 3. Thermodynamic functions of the educational process 3-ethyl-4-methyl-1,2,4-triazole-5-thiol complexes of rhenium (V) in 3 M HCl medium.

№	The composition of compounds	$\Delta H$ , $\kappa J/mole$	$\Delta G$ , $\kappa J/mole$	$\Delta S$ , $J/mole \cdot K$
1	$[ReOLCl_4]^-$	-21,27	-20,71	-1,88
2	$[ReOL_2Cl_3]$	-14,18	-16,49	9,26
3	$[ReOL_3Cl_2]^+$	-11,49	-13,75	7,58
4	$[ReOL_4Cl]^{2+}$	-8,51	-12,32	12,8
5	$[ReOL_5]^{3+}$	-21,99	-13,38	-28,9

The data in Table 3 show that the first phase of complex value of  $\Delta S$  is negative, and the second is positive. The value of  $\Delta G$  with the increase of the number of coordinated molecules of 3-ethyl-4-methyl-1,2,4-triazole-5-thiol, becomes less negative, which is associated with increased steric hindrance at the following occurrence of the molecules of 3-ethyl-4-methyl-1,2,4-triazole-5-thiol in the inner sphere of complexes.

The values of stability constants were used to calculate the distribution curves of all complex forms, resulting in the rhenium (V) - 3-ethyl-4-methyl-1,2,4-triazole-5-thiol - 3 M HCl in the temperature range 273 - 338K, which allowed to define the field dominance of a complex shape. As an example, Figure 2 shows the distribution curves of the 3-ethyl-4-methyl-1,2,4-triazole-5-thiol complexes of rhenium (V) in 3 M HCl medium at a temperature of 273K.

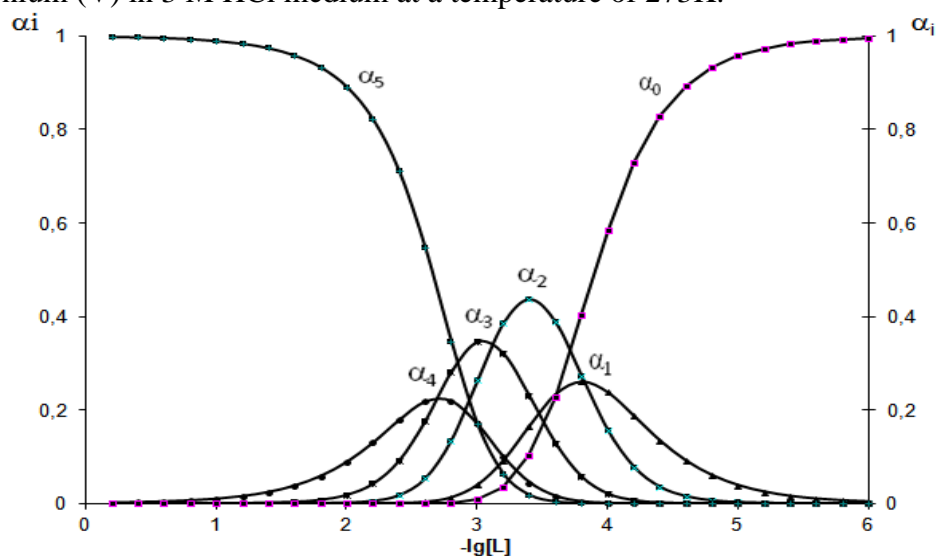


Fig.2. Distribution curves of 3-ethyl-4-methyl-1,2,4-triazole-5-thiol complexes of rhenium (V) in 3 M HCl medium at 273K.

Analysis of the distribution curves shows that with the increasing of number of coordinated molecules of the organic ligand, equilibrium value of the maximum yield of complex forms for the 3-ethyl-4-methyl-1,2,4-triazole-5-thiol complexes of rhenium (V) in 3 M HCl medium changes monotone.

## References

1. Aminjanov AA. Ligand electrodes and their use for the study of complex formation. // Interparticle interactions in solutions. Dushanbe, 1991,-C.6-17.
2. Aminjanov AA., Akhmedov K.U. Investigation of the process of complexation of rhenium (V) with 1,2,4-triazololom-3 (5) in the medium 6 mol / l HCl spectrophotometrically. // Complexation in solution. , Dushanbe, 1991, p.58-65.
3. Aminjanov AA, Kurbanov NM The study of complexation of rhenium (V) with 3-methyl-1,2,4-triazololom-5 at different temperatures. // Zhurn.neorgan.himii. -1990. -T. 35, № 3. -C. 672-678.
4. Aminjanov AA, SM Safarmamadov Complexation of rhenium (V) with 4-methyl-1 ,2,4-triazololom-5 among 6 mol / l HCl // Zhurn.neorg.himii. -1993. -T.38, № 2. -S.291-295.
5. Aminjanov AA, SM Safarmamadov The study of complex formation of rhenium (V) with 4-methyl-1,2,4-triazololom-5 medium 6 mole/l HBr. // Izv.vuzov. Chemistry and him.tehnologiya. -1993. -T.38, № 8. -P.34-38.
6. Aminjanov AA Gagieva SC The study of complexation of rhenium (V) c 3-methyl-4-phenyl-1 ,2,4-triazololom-5 among 6 mole/l HCl. // Russ. inorganic. himii.-1996, v.46. № 11.-S.1970-1976.
7. AA Aminjanov, KV Romer, GD Zegzhda, JN Kukushkin. Potentiometric study of complexation of rhenium (V) with 1-methyl-2-merkptoimidazolom / / Journal of Inorganic Chemistry. , Moscow, 1975.-v.20, № 1.-S. 115-117.



N.Kravchenko, Prof. M. Ozawa, E. Johnstone, E. Nazarov at the Award Ceremony



1.P7.

**COMPLEXATION IN THE SYSTEM Re (V) ÷ 1-METHYL-2-MERKAPTOIMIDAZOL ÷ 8 M HCL**

K.S. Mabatkadamova, N.G. Kabirov, S.M. Safarmamadov, A.A. Aminjonov

Tajik National University. (Rudaki Avenue 17., Dushanbe, Republic Tajikistan)

**Overview:**

The process of chelation of rhenium (V) with 1-methyl-2merkaptoimidazolom in 8 mol/l HCl medium was studied by potentiometric titration method. Stepwise formation constants of oxochloro-1-methyl-2-merkaptimidazole complexes with rhenium (V) and the magnitude of the thermodynamic functions of complexation process were determined.

**Keywords:** stability constant, renium (V), complexation, potentiometric titration, thermodynamic functions

In [1,2] the optimal conditions for the synthesis of complexes of rhenium (V) with 1-methyl-2-merkaptimidazole in the medium of 6 M HCl were determined. It is shown that in this environment, depending on the ratio of initial reagents, rhenium (V) forms complexes with 1-methyl-2-merkaptimidazole of compositions  $[\text{ReOL}_2\text{Cl}_3]\cdot\text{H}_2\text{O}$  and  $[\text{ReOL}_4\text{Cl}]\text{Cl}_2\cdot 2\text{H}_2\text{O}$ . The composition and structure of the synthesized complexes established by elemental analysis, IR spectroscopy and conductometric methods. The study of IR spectra of complexes obtained showed that the molecule of 1-methyl-2-merkaptimidazole in forming complexes behave as monodentate ligand coordinated to rhenium (V) through the donor atom of sulfur. In [3] Kukushkin et al published data on the synthesis of two- and tetra-complexes of oxo rhenium (V) bromide with 1-methyl-2-merkaptimidazole in the 6 M HBr medium. In [1] the study of the oxidation of 1-methyl-2-merkaptimidazole and creation on the basis of its redox electrode is also reported. Using of the system studied in the process of rhenium (V) chelation with 1-methyl-2-merkaptimidazole in the 6 M HCl medium. The author [4] studied the complexation of rhenium (V) with 1-methyl-2-merkaptimidazole in 7.4 M HCl medium in the temperature range of 273-338K. It was found that the increasing of HCl concentration from 6 to 7 M leads to an increase in the stability constants of monosubstituted complex of rhenium (V). However, for other forms of complex with increasing concentrations of HCl, a decrease values of their formation constants. In this regard, for a more detailed setting influence of the concentration of HCl in the process of chelation of rhenium (V) with 1-methyl-2-merkaptimidazole, we carried out the research of rhenium (V) complex with the organic ligand in the 8 M HCl medium.

**Experimental part**

In the potentiometric method of determining the formation constants in HCl solution with a concentration 8 M, containing a redox electrode on the basis of 1-methyl-2-merkaptimidazole and its oxidized form platinum electrode was immersed. As a reference electrode silver chloride electrode was used. After reaching a constant value of building the system was titrated with  $[\text{ReOCl}_5]$  solution 2 to 8 M HCl. In the titration of RSSR / RS, where RS-1-methyl-2-merkaptimidazole hydrochloric acid solution  $[\text{ReOCl}_5]$  the potential of the system was sets constant during 5-10 minutes.

Equilibrium concentration of 1-methyl-2-merkaptimidazole was calculated according to potentiometric titration using the equation:

$$\lg[L] = \frac{E_{ucx.} - E_i}{1,9837 \cdot 10^{-4} T} + \lg C_L^{ucx.} + \frac{1}{2} \lg \frac{V_{ucx.}}{V_{\text{объ.}}},$$

where  $E_{\text{orig}}$  - the original equilibrium potential system in the absence of rhenium (V);  $E_i$  - equilibrium potential of the system at a given point of titration;  $C_L$ -initial analytical concentration of

ligand;  $V_{\text{orig}} / V_{\text{tot}}$  - the ratio of the initial volume to the total volume;  $T$  - the temperature of the experiment in K. Having determined the equilibrium concentration of 1-methyl-2-mercaptoimidazole at each point of the titration, the formation function was calculated by the equation:

$$\bar{n} = \frac{C_L - [L]}{C_{Me}}$$

It should be noted that all the calculations to determine the equilibrium concentration of the ligand, the function of education, and thermodynamic functions of the mole fractions was performed on a specially designed computer programs for Pentium-4.

### Results and discussion

As an example, in table 1 shows the experimental data to determine the function of education 1-methyl-2-mercapto-imidazole complexes of oxo rhenium (V) chloride in the 8 M HCl medium at 273K.

The value of the constant formation of complexes with half-integer values of the complexation function was estimated by building  $n = f(-\lg [L])$  dependence for each specific temperature on the basis of the data in table 1.

Figure 1 shows the formation curves of oxochloro-1-methyl-2-merkaptoimidazole complexes with rhenium (V) in the 8 M HCl medium at different temperatures.

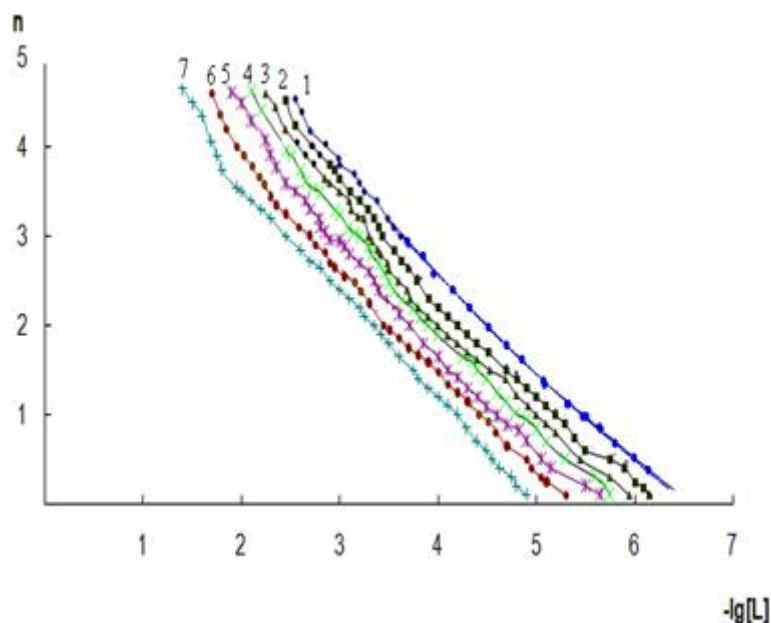


Fig. 1. Curves formation 1-methyl-2-mercapto-imidazole complexes of oxo rhenium (V) chloride in the 8 M HCl medium at 273 (1), 288 (2), 298 (3), 308 (4), 318 (5), 328 (6) and 338 K (7)

As seen from fig. 1, the curves of formation, almost without changing its shape as the temperature rises only shifted towards higher values of the equilibrium concentration of 1-methyl-2-mercaptoimidazole which indicates the identity of the process of complex formation in the temperature range 273-338K.

In the range 273-338K for the system  $H_2[ReOCl_5]$  - 1-methyl-2-mercaptoimidazole in 8 M HCl, the maximum is set equal to 4.7, which indicates the formation of five complex forms in this system. Comparison of the formation curves of 1-methyl-2-mercaptoimidazole complexes of rhenium (V) from the 8 M HCl medium with the data obtained by the author [2], in 7 M HCl shows that increasing concentrations of HCl to 1 M leads to a shift formation curve towards lower values of the equilibrium concentration of the ligand, although the shapes of the education differ little from each other.

Table 1. Determining the function of education 1-methyl-2-mercaptoimidazole complexes of oxo rhenium (V) chloride in the 8 M HCl medium at 273 K

$\Delta E, \text{ mB}$	$C_L, \text{ mol / l}$	$C_{Re}, \text{ mol / l}$	$[L], \text{ mol / l}$	$\bar{n}$
1	2	3	4	5
50.51	0.0241	0.00446	0.00281838	4.59
58.34	0.0238	0.00491	0.00199526	4.18
73.86	0.0236	0.00530	0.00102329	3.87
74.20	0.0234	0.00579	0.00100000	3.80
82.12	0.0232	0.00622	0.00070795	3.70
84.63	0.0230	0.00664	0.00063096	3.60
87.13	0.0228	0.00746	0.00056234	3.50
93.76	0.0224	0.00826	0.00041687	3.40
99.41	0.0221	0.00902	0.00032359	3.20
102.23	0.0217	0.01040	0.00028184	3.10
105.25	0.0210	0.01251	0.00023988	3.00
108.44	0.0200	0.01376	0.00019953	2.95
107.30	0.0195	0.01551	0.00020417	2.80
109.34	0.0186	0.01659	0.00015849	2.55
116.92	0.0181	0.01811	0.00012589	2.50
121.42	0.0174	0.01951	0.00010000	2.43
125.91	0.1680	0.02030	0.00007079	2.25
133.43	0.0163	0.02240	0.00005623	2.15
137.51	0.0154	0.02420	0.00004467	2.10
138.80	0.0145	0.02580	0.00003981	2.00
143.06	0.0138	0.02725	0.00003162	1.90
147.25	0.0131	0.02856	0.00002512	1.80
151.56	0.0125	0.02975	0.00001995	1.60
156.79	0.0124	0.03080	0.00001585	1.50
164.54	0.0122	0.03180	0.00001122	1.40
169.57	0.0120	0.03204	0.00000891	1.30
170.87	0.0113	0.03254	0.00000794	1.25
176.08	0.0112	0.03301	0.00000631	1.10
179.21	0.0101	0.03362	0.00000501	1.05
184.61	0.0101	0.03340	0.00000398	0.95
205.48	0.0195	0.03741	0.00000316	0.82
210.22	0.0190	0.03860	0.00000251	0.65
211.36	0.0184	0.03979	0.00000158	0.60
214.27	0.0160	0.03380	0.00000178	0.50
222.25	0.0159	0.03390	0.00000126	0.42
218.03	0.0158	0.03400	0.00000110	0.24
218.01	0.0156	0.03410	0.00000071	0.18

Formation curves of step stability constants oxochloro-1-methyl-2-mercapto-imidazole complexes of rhenium (V) in the 8 M HCl medium, determined by the method of Bjerrum, are presented in table 2.

Decrease in the values of the formation constants with increasing temperature (Table 2) indicates the exothermicity of the complexation process. However, the temperature factor affects their values differently. Since the value of K1, with increasing temperature from 273 to 338K, was 33 fold decreased, and the quantities K2 and K3 was, respectively, 10.7 and 10.9 fold decreased.

Table 2. Formation constants oxochloro-1-methyl-2-mercaptoimidazole complexes of rhenium (V) in the 8 M HCl medium at 273-338 K.

T, K	K <sub>1</sub>	K <sub>2</sub>	K <sub>3</sub>	K <sub>4</sub>	K <sub>5</sub>
273K	1.1·10 <sup>6</sup>	7.4·10 <sup>4</sup>	9.3·10 <sup>3</sup>	1.9·10 <sup>3</sup>	3.1·10 <sup>2</sup>
288K	5.6·10 <sup>5</sup>	4.4·10 <sup>4</sup>	6.4·10 <sup>3</sup>	1.3·10 <sup>3</sup>	2.6·10 <sup>2</sup>
298K	3.5·10 <sup>5</sup>	3.6·10 <sup>4</sup>	4.6·10 <sup>3</sup>	1.0·10 <sup>3</sup>	1.6·10 <sup>2</sup>
308K	2.1·10 <sup>5</sup>	2.5·10 <sup>4</sup>	3.2·10 <sup>3</sup>	7.5·10 <sup>2</sup>	1.4·10 <sup>2</sup>
318K	1.1·10 <sup>5</sup>	1.4·10 <sup>4</sup>	2.3·10 <sup>3</sup>	3.5·10 <sup>2</sup>	9·10 <sup>1</sup>
328K	9.1·10 <sup>4</sup>	9.3·10 <sup>3</sup>	1.9·10 <sup>3</sup>	1.1·10 <sup>2</sup>	6·10 <sup>1</sup>
338K	3.3·10 <sup>4</sup>	6.9·10 <sup>3</sup>	8.5·10 <sup>2</sup>	8·10 <sup>1</sup>	3·10 <sup>1</sup>

This experimental finding can be explained by the fact that the formation of mono substituted complex proceeds with a large release of heat than the two- and tri-substituted complexes, as evidenced by the reaction of  $\Delta H$  these complexes are calculated by us using the temperature coefficient. Comparison of the PK<sub>1</sub> for 1-methyl-2-mercaptoimidazole complexes of oxo rhenium (V) chloride in the 8 M HCl medium with similar values obtained in the 7 M HCl medium [2] shows that changing the acid concentration in 1 M of leads to the decrease in the value of all the stability constants of step. The author of [2], studying the complexation of rhenium (V) with 1-methyl-2-merkaptoimidazole notes that the change in concentration of HCl from 6 to 7 M leads only to an increase in the stability constant of monosubstituted complex, and the other constants are reduced. The decrease of the stability constants with increasing HCl concentration can be explained by an increase in competition for the coordination site between chloride ions and molecules of 1-methyl-2-mercaptoimidazole. Formation constants 1-methyl-2-mercaptoimidazole complexes of oxo rhenium (V) chloride curves defined by education we were used to estimate the thermodynamic characteristics of complexation process by the temperature coefficient (Fig. 2).

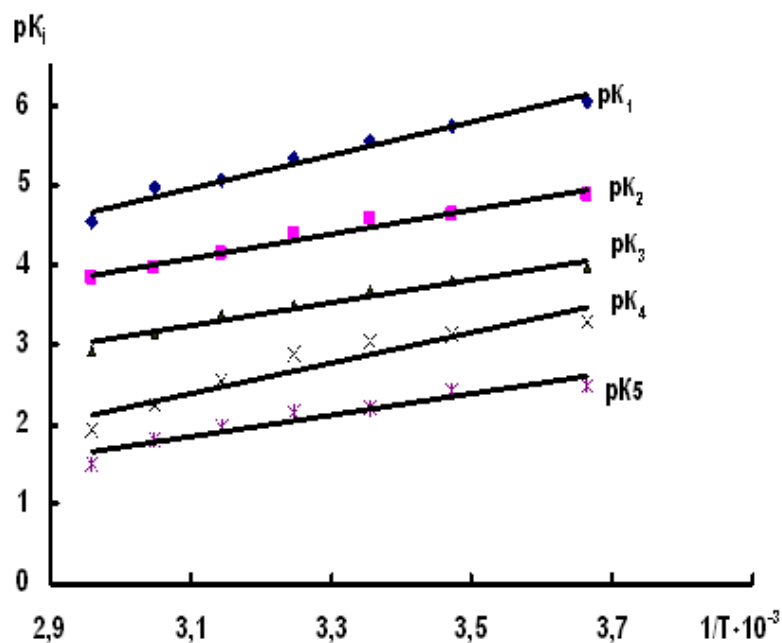


Fig. 2. The dependence of the PKI = f (1 / T) for 1-methyl-2-mercaptoimidazole complexes of oxo rhenium (V) chloride in the 8 M HCl medium.

Depending curves on the PKI 1/T in the temperature range 273-338 K, for all complex forms are linear. The table 3 shows the values of the thermodynamic functions of the formation process 1-methyl-2-mercaptoimidazole complexes of oxorhenium (V) chloride in the 8 M HCl medium. The value of  $\Delta S$  and  $\Delta H$  on the all stages of complex formation is negative. Maximum heat release system is observed during the formation of mono- and tetrasubstitued rhenium (V) complexes. The

value of  $\Delta G$  with increasing number of coordinating molecules of 1-methyl-2-mercaptoimidazole becomes less negative, due to the space obstruction of the occurrence of subsequent molecules organic ligand in the inner complex sphere.

Table 3. The values of thermodynamic functions of the educational process oxochloro-1-methyl-2-mercaptoimidazole complexes of rhenium (V) in the 8 M HCl medium.

The composition of compounds	$\Delta H$ , kJ / mol	$\Delta G$ , kJ / mol	$\Delta S$ , kJ / mol <sup>-1</sup> ·K
[ReOLCl <sub>4</sub> ] <sup>-</sup>	-39.37	-31.36	-26.89
[ReOL <sub>2</sub> Cl <sub>3</sub> ]	-28.79	-25.55	-10.84
[ReOL <sub>3</sub> Cl <sub>2</sub> ] <sup>+</sup>	-26.82	-20.74	-20.41
[ReOL <sub>4</sub> Cl] <sup>2+</sup>	-36.48	-16.45	-67.20
[ReOL <sub>5</sub> ] <sup>3+</sup>	-26.39	-12.53	-46.55

The values of formation constants were used to calculate the distribution curves of all complex forms, resulting in a system [ReOCl<sub>5</sub>] - 1-methyl-2-mercaptoimidazole in 8 M HCl. As an example, figure 2 shows the curves of the distribution of all forms of complexes formed in this system at a temperature of 273K.

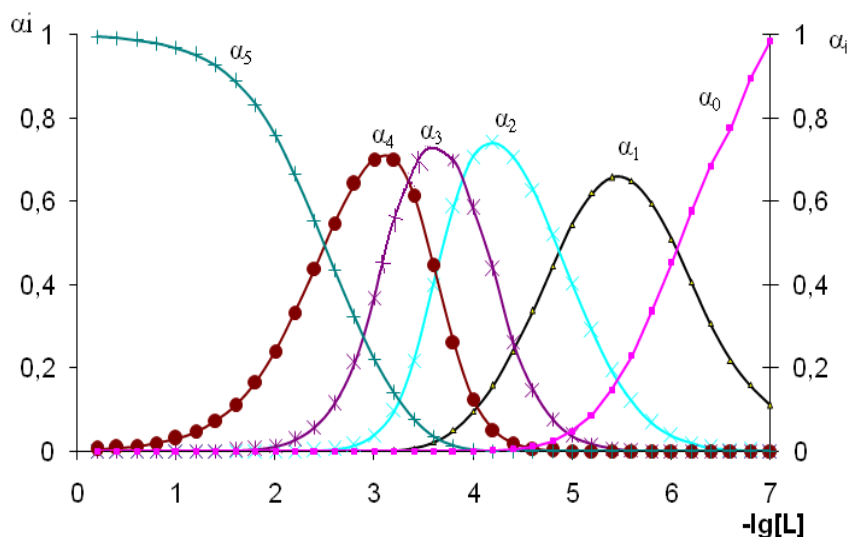


Fig. 2. The distribution curves 1-methyl-2-mercaptoimidazole complexes of oxo rhenium (V) chloride in the 8 M HCl medium at 273 K, where  $\alpha_0$ -[ReOCl<sub>5</sub>]<sup>2-</sup>,  $\alpha_1$ -[ReOLCl<sub>4</sub>]<sup>-</sup>,  $\alpha_2$ -[ReOL<sub>2</sub>Cl<sub>3</sub>],  $\alpha_3$ - [ReOL<sub>3</sub>Cl<sub>2</sub>]<sup>+</sup>,  $\alpha_4$ - [ReOL<sub>4</sub>Cl]<sup>2+</sup>  $\alpha_5$ -[ReOL<sub>5</sub>]<sup>3+</sup>.

The analysis of the distribution function of the temperature showed that with increasing temperature, the output of all forms of complex decreases. These experimental data were used to develop methods of synthesis of complex compounds of rhenium (V) with 1-methyl-2-mercaptoimidazole.

#### Reference

1. K.V. Kotegov, A.A. Aminjanov, Yu.N., Kukushkin, T.V. Zegzhda // JNCh Moscow. v.20, № 1, - p.115-117. (1975)
2. A.A. Aminjanov, Complex compounds of rhenium (V) c sulfur compounds azole series: Ph.D. in Chemistry. / AA Aminjanov.- Leningrad, 1975. -20 Sec.
3. K.V. Kotegov, T.V. Zegzhda, A.A. Aminjanov, Yu.N. Kukushkin, The study of complexation of rhenium-V oxobromide with 1-methyl-2-merkaptoimidazole // JNCh.. T.22. № 10. - S.2742-2743(1977)/
4. A.A. Aminjanov, Complex compounds of rhenium (V) with amide and tioamid ligands. Dissertation of doctor of chemical sciences, Ivanovo (1992) 42p.



## SPECIATION OF TECHNETIUM IN SULFURIC MEDIA. EFFECT OF $\alpha$ -RADIATION FROM THE ARRONAX CYCLOTRON.

F. Poineau<sup>1</sup>, I. Denden<sup>2</sup>, R. Essehli<sup>2</sup>, K. German<sup>3</sup>, K. Czerwinski<sup>1</sup> and M. Fattahi<sup>2</sup>

1- Department of Chemistry, University of Nevada Las Vegas, Las Vegas, USA

2 - Laboratory Subatech, School of Mines of Nantes, No 4 rue Alfred Kastler, Nantes, France,

(e-mail: [massoud.fattahi-vanani@subatech.in2p3.fr](mailto:massoud.fattahi-vanani@subatech.in2p3.fr))

3 - IPCE Russian Academy of Science, Moscow, Russia

The speciation of technetium in the sulfuric media has been performed under reducing conditions and the effect of  $\alpha$ -radiation from the Arronax Cyclotron has been studied. Characterization of the species has been performed by spectroscopic techniques (EXAFS, UV-Visible). It was demonstrated that heptavalent technetium is very sensitive to reduction in sulfuric media between 12 M to 18 M [H<sub>2</sub>SO<sub>4</sub>] and could be reduced to Tc(V) by MeOH. Reduction of TcO<sub>3</sub>(H<sub>2</sub>O)<sub>2</sub>OH (Tc: 10 mmol, 15 M H<sub>2</sub>SO<sub>4</sub>) by MeOH (10  $\mu$ l) is fast, the formation of a green solution was observed. New “Tc-green” species were studied by UV-vis spectroscopy (bands at 390 nm and 715 nm) and XANES\EXAFS. Similar spectra obtained between 12 M and 18 M [H<sub>2</sub>SO<sub>4</sub>]. No reaction was observed below 12 M [H<sub>2</sub>SO<sub>4</sub>].

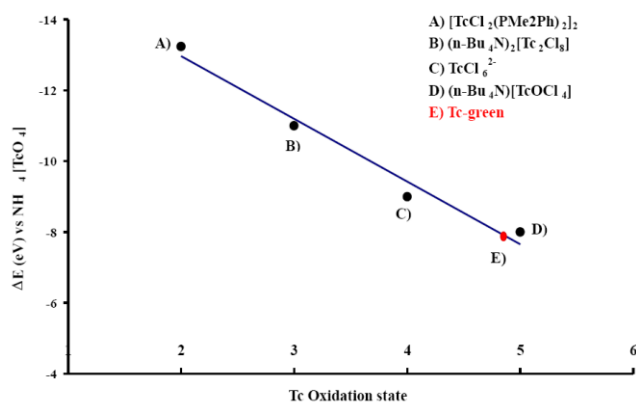


Fig.1. XANES data for known Tc compounds and new green Tc specie as a function of Tc oxidation state

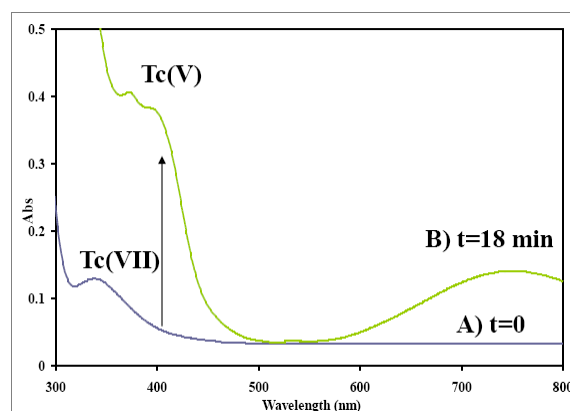


Fig.2. UV-visible spectra of TcO<sub>3</sub>(OH)(H<sub>2</sub>O)<sub>2</sub> in 18 M [H<sub>2</sub>SO<sub>4</sub>] before (A) and after 18 min of  $\alpha$ -irradiation (B)

The EXAFS spectroscopy data confirm the existence of monomeric octahedral complex (with one O atom at 1.60(2) Å: Tc=O characteristic of Tc(V), five O atoms at 2.04(2) Å : Tc-O; Tc-OH, Tc-H<sub>2</sub>O, Tc-O(S); and two S atoms at 3.23(3) Å : Tc...S indicative of two monodentate bisulfate anions) being consistent with Tc<sup>V</sup>O(HSO<sub>4</sub>)<sub>2</sub>(H<sub>2</sub>O)<sub>2</sub>(OH). It was also shown that heptavalent technetium is unstable under  $\alpha$ -radiation in 18 M H<sub>2</sub>SO<sub>4</sub> being reduced to Tc<sup>V</sup>O(HSO<sub>4</sub>)<sub>2</sub>(H<sub>2</sub>O)<sub>2</sub>(OH) by [H<sub>2</sub>SO<sub>4</sub>] radiolysis products.

Funding for this research was provided by a SISGR Grant from the U.S. Department of Energy under Contract No. 47824B. Use of the Advanced Photon Source was supported by the U. S. Department of Energy, Office of Science, Office of Basic Energy Sciences, under Contract No. DE-AC02-06CH11357.

1.P8.

## SYNTHESIS, CRYSTAL STRUCTURE AND PROPERTIES OF TRIPHENYLGUANIDIUM TETRAOXIDORHENATE HEMIHYDRATE

A. Ya. Maruk\*, M. S. Grigor'ev, K. E. German

Frumkin Institute of Physical Chemistry and Electrochemistry, Russian Academy of Sciences

Leninskii pr. 31, Moscow, 117071 Russia

\*E-mail: [amaruk@list.ru](mailto:amaruk@list.ru)

Triphenylguanidinium tetraoxidorhenate hemihydrate was synthesized ( $[(C_6H_5NH)_3C]ReO_4 \cdot 0.5H_2O$ ) and studied with X-ray diffraction. Also a number of physical properties were studied. Compound under study crystallizes in the triclinic system (space group P-1,  $Z = 4$ , at 293 K:  $a = 9.8716(17)$ ,  $b = 14.093(2)$ ,  $c = 15.439(3)$  Å,  $\alpha = 99.632(9)$ ,  $\beta = 101.802(9)$ ,  $\gamma = 95.361(10)$  deg). The compound has no isostructural analogues. In all structures containing triphenylguanidinium cation, found in the Cambridge Structural Database (CSD version 5.31, August 2010), the position of the phenyl rings corresponds to the conformation that differ from that observed in the known compounds (p.e. [1, 2]). In the ( $[(C_6H_5NH)_3C]ReO_4 \cdot 0.5H_2O$ ) structure phenyl rings in triphenylguanidinium cations occupy the position corresponding to high-symmetry ( $C_{3h}$ ) conformation that has been never before observed, and this conformation is being realized in both crystallographically independent cations.

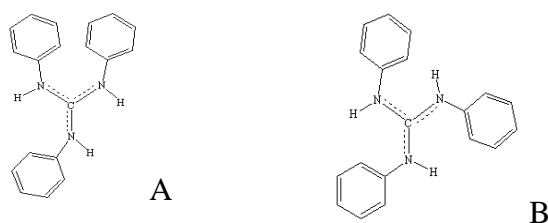


Fig. Cation conformations known from literature (A) and found in this study (B)

Perrhenate anions are in the form of weakly distorted tetrahedra and do not differ from those anions described in the literature. The system of hydrogen bonds is presented by infinite branched chains in the [110] direction, combining the two independent formula units.

The compounds under study is promising for conversion into a metal rhenium. In this connection thermal studies were carried out. The following physical properties were identified: the upper limit of thermal stability of triphenylguanidinium tetraoxidorhenate hemihydrate (393 K) and its enthalpy of dehydration ( $\Delta H_{\text{degidr}}^{(393 \text{ K})} = 10,0(3)$  kJ/mol), the melting point of anhydrous triphenylguanidinium tetraoxidorhenate (448 K), and its enthalpy of melting ( $\Delta H_m^{(448 \text{ K})} = 31,0(9)$  kJ/mol).

If the thermolysis is conducted in an atmosphere of inert gas (argon) and the sample is subjected to recrystallization annealing at a temperature above 1250 K, the solid product is *nanodimensional metal rhenium* dispersed in a matrix of amorphous carbon. Chemical analysis showed the dependence of the ratio of rhenium to carbon in the solid phase of process macrokinetic options (the rate of temperature increase, the rate of inert gas flushing, water content in the system and in the gas phase). If the thermal decomposition is carried out in an atmosphere of a reducing gas (eg. hydrogen), the solid product is almost pure metallic rhenium.

The work was supported by RFBR grant 09-03-00017-a.

1. Silva, P.S.P., Domingos, S.R., Silva, M.R. et al. // Acta Crystallogr. E.. V. 64. P. o1082 (2008).
2. Polyanskaya, T.M., Il'inchik, E.A., Volkov, V.V. et al. // Journal of Structural Chemistry. Vol. 49, No. 3, pp. 494-503, 2008

1.P9.

## SYNTHESIS AND CRYSTAL STRUCTURE OF $[\text{AnO}_2(\text{HMPA})_4](\text{MO}_4)_2$ (An = U, Pu; M = Cl, Tc, Re)

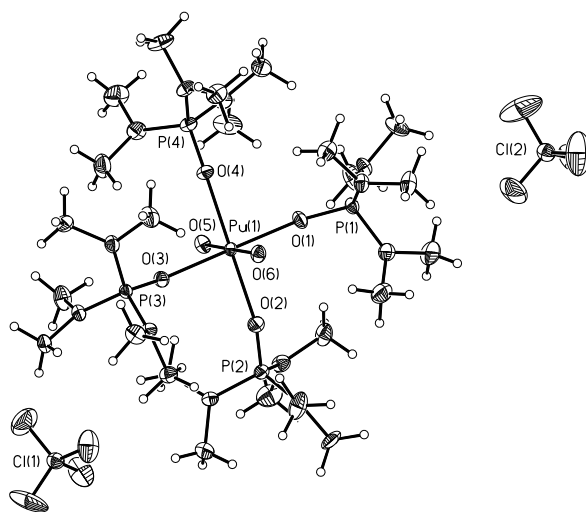
A.M. Fedosseev, M.S. Grigoriev

Institution of Russian Academy of Sciences - A.N. Frumkin Institute of Physical Chemistry and Electrochemistry of RAS (Moscow, Russia)

Synthesis was performed by using  $\text{UO}_3$  or  $\text{PuO}_3 \cdot \text{H}_2\text{O}$  as starting material, which was dissolved in stoichiometric amount of aqueous solution of corresponding acid  $\text{HMO}_4$  with concentration less than 0.1 M. Obtained solutions were dried at heating up to temperature less than  $100^\circ\text{C}$  and solid residue was dissolved in excess of hexamethylphosphortriamide (tris(dimethylamino) phosphine oxide, HMPA). Large elongated crystals were obtained during slow evaporation of reaction mixture in a flow of air.

All the compounds crystallize in an orthorhombic space group *Pbca* and are isostructural with earlier studied uranyl HMPA complexes with periodate [1], perbromate [1] and perchlorate [2] anions. Full structural data were available only for  $[\text{UO}_2(\text{HMPA})_4](\text{ClO}_4)_2$ .

Crystal data for  $[\text{PuO}_2(\text{HMPA})_4](\text{ClO}_4)_2$  (Bruker KAPPA APEX II autodiffractometer,  $\text{MoK}_\alpha$  radiation):  $a = 13.9939(4)$ ,  $b = 15.0970(4)$ ,  $c = 45.7102(13)$  Å at 100 K,  $Z = 8$ ,  $R1 = 0.0463$ .



Molecular structure of  $[\text{PuO}_2(\text{HMPA})_4](\text{ClO}_4)_2$

Interatomic distances in a series of isostructural compounds will be discussed.

### References

1. Gusev Yu. K., Lychev A.A., Mashirov L.G., Suglobov D.N. Radiokhimiya (1985) **27**, 412.
2. Nassimbeni L.R., Rodgers A.L. Cryst. Struct. Commun. (1976) **5**, 301.

1.P10.

## TRANSFORMATION OF Tc(VII) IN ACIDS: $\text{TcO}_3(\text{OH})(\text{H}_2\text{O})_2$ and $\text{TcO}_3(\text{H}_2\text{O})_3^+$ in $\text{HClO}_4$ AND POLYMERIC Tc(VII) SPECIES IN SOLIDS AND ACETONITRILE SOLUTIONS

K.E. German<sup>1</sup>, A.Ya. Maruk<sup>1</sup>, F. Poineau<sup>2</sup>, Ph. Weck<sup>2</sup>,  
G.A. Kirakosyan<sup>1</sup>, V.P. Tarasov<sup>1</sup>, K. Czerwinski<sup>2</sup>, A. Sattelberger<sup>3</sup>

<sup>1</sup> Frumkin Institute of Physical Chemistry and Electrochemistry of RAS (Moscow, Russia)

<sup>2</sup> University of Nevada Las Vegas (Las Vegas, USA)

<sup>3</sup> Energy Sciences and Engineering Directorate, Argonne National Laboratory, Argonne, IL 60439, USA

In course of our pertechnic acid investigation the common Tc(VII) – pertechnetate ionic form - was recently shown to decompose in 7-18M concentrated sulfuric acid solutions producing the octahedral  $\text{TcO}_3(\text{OH})(\text{H}_2\text{O})_2$  species [1]. It was worth studying if other acids could make any similar effect. Perchloric acid and nitric acid were chosen for this study.

The results differed considerably: in perchloric acid (Fig.1) the transformation of Tc(VII) was similar to the observed in sulfuric acid [1], while no notable changes in UV and NMR spectra were seen for Tc(VII) in nitric acid.

Some similarity of Tc(VII) speciation in sulfuric and perchloric acids was seen by EXAFS, although the Tc(VII) solutions in  $\text{HClO}_4$  were not that resistant to synchrotron radiation.

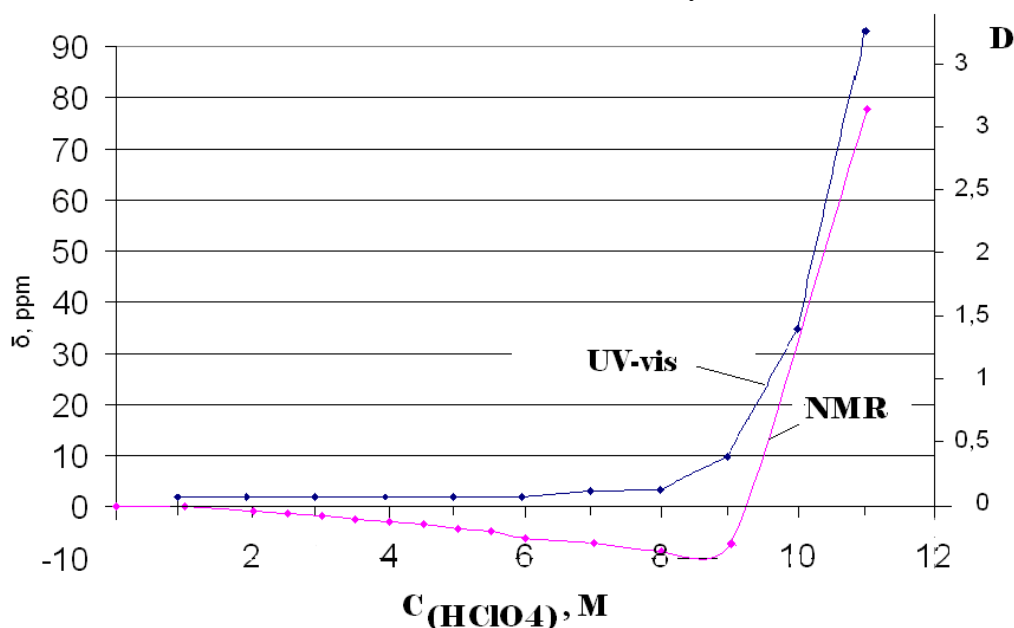


Fig. 1. NMR- $\text{Tc}^{99}$  shift ( $\delta$ , ppm), and UV-vis spectra evolution ( $D$  at 350 nm) for Tc(VII) in 1-11M  $\text{HClO}_4$

The solid  $\text{HTcO}_4$  and its solutions in  $\text{CH}_3\text{CN}$  were analyzed by  $^{99}\text{Tc}$  and  $^1\text{H}$  NMR in a field of 7.04 T.  $\text{HTcO}_4$  and its deuterated analog  $\text{DTcO}_4$  were prepared by oxidizing Tc metal in  $\text{O}_2$  at  $500^\circ\text{C}$ , dissolving  $\text{Tc}_2\text{O}_7$  in  $\text{H}_2\text{O}$  or  $\text{D}_2\text{O}$ , the solution brought to dryness with  $\text{Mg}(\text{ClO}_4)_2$ . The samples were dark red polycrystalline blocks. Elemental analysis gave the ratio  $\text{H}/\text{Tc} \approx 1$ .

The  $^1\text{H}$  NMR spectrum of a fresh  $\text{HTcO}_4$  powder at 259 K showed two splitted signals: a strong signal at 5.6 ppm with the width at half-maximum of 400 Hz and a weak signal at  $\sim 0$  ppm (relative to the external  $\text{H}_2\text{O}$  reference). Decreasing temperature to 120 K resulted in the broadening of the spectrum to 4 kHz; however, the expected fine structure of the spectrum (as the Pake doublet) was not observed. This permits a tentative conclusion that the compound under study is not a crystal hydrate and the lattice hydrogen is highly mobile. The extremely informative is the  $^{99}\text{Tc}$  NMR

spectrum of red pertechnetic acid powder (Fig.2) The spectral pattern and resonance parameters indicate that technetium has two states in the structure, none of them corresponding to the  $\text{TcO}_4^-$  ion.

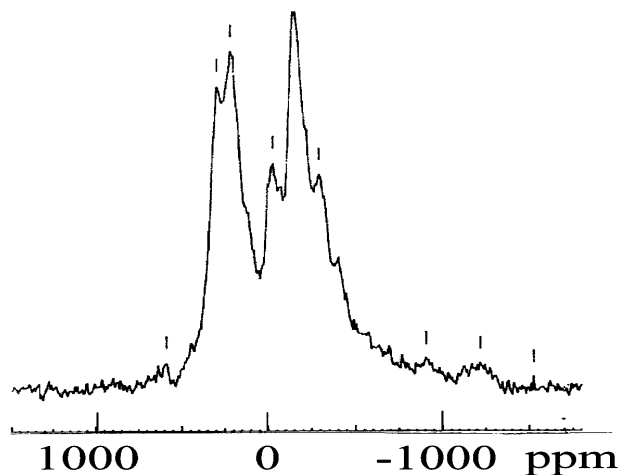


Fig.2. Solid state Tc-99 NMR spectrum of pure red  $\text{HTcO}_4$  (solid)

The spectrum of a fine powder of red pertechnetic acid (figure) showed two signals at  $\delta_1 = +213(5)$  and  $\delta_2 = -147(5)$  ppm (referenced to the external standard, a 0.1 M  $\text{KTcO}_4$  solution; reported in part in [2]); the integrated intensity ratio was  $I_1 : I_2 = 2 : 3$ . Each of the signals had a multiplet structure due to first-order quadrupole interactions: the quadrupole coupling constants were  $C_Q(1) = \sim 0.25(1)$  and  $C_Q(2) = 0.43(1)$  MHz and the asymmetry parameter of the  $^{99}\text{Tc}$  EFG tensor was  $\eta = 0$  in both cases.

1. F. Poineau, P. Weck, K. German et al. *Dalton Trans.*, 2010, 39 (37), pp. 8616.
2. G.Kirakosyan, K.German, V.Tarasov, M. Grigoriev. *3-d Russian-Japanese Seminar on Technetium, Book of Synopses*, (2002) pp. 49-51.



1.P11.

**NEW COMPOUNDS BASED ON THE CLUSTER ANIONS  $[\text{Re}_4\text{Q}_4(\text{CN})_{12}]^{4-}$   
(Q=S, Se, Te) AND CATIONS (1,10-phenH)<sup>+</sup>, Nd<sup>3+</sup>, Er<sup>3+</sup>**

I.M. Gayfulin, Yu.V. Mironov, A.I. Smolentsev

Nikolaev Institute of Inorganic Chemistry SB RAS, Novosibirsk

yuri@niic.nsc.ru

Coordination polymers of rhenium tetrahedral cluster cyanides where Q is either sulphur, selenium or tellurium, have been intensively investigated in the past decade. The strong covalent Re–C≡N–M interactions have allowed numerous polymeric coordination compounds to be obtained with transition, post-transition metals and lanthanides.

High coordination numbers inherent to the lanthanide(III) ions lead to many structural variations in resulting compounds. The type of structure depends mainly on the number of cyano groups of the cluster anion involved in interaction with lanthanide cations.

In this work we present five new compounds based on the anions  $[\text{Re}_4\text{Q}_4(\text{CN})_{12}]^{4-}$  (Q=S, Se, Te). Three of them adopt ionic structure, while two others are polymeric. Slow evaporation of acidic water solutions of  $\text{K}_4[\text{Re}_4\text{Q}_4(\text{CN})_{12}]$  (Q=S, Se, Te) and ten-fold excess of 1,10-phenanthroline results in ionic compounds of composition  $(1,10\text{-phenH})_4[\text{Re}_4\text{Q}_4(\text{CN})_{12}] \cdot n\text{H}_2\text{O}$  (Q=S, Se, n=6; Q=Te, n=8). In case these solutions were mixed with  $\text{LnCl}_3$  (Ln=Nd, Er) without acid, amorphous brown precipitate has dropped. Polymeric compounds  $[\text{Ln}(\text{OH})(\text{phen})(\text{H}_2\text{O})_2][\text{Ln}(\text{OH})(\text{phen})(\text{H}_2\text{O})_3][\text{Re}_4\text{Q}_4(\text{CN})_{12}]$  (Q=Se, Te) were crystallized by heating of this precipitates in a sealed glass ampoules in a mother solution.

In the structures of ionic compounds the 1,10-phenanthroline cations, phenH<sup>+</sup>, are packed in an infinite stacks. Shortest distances between aromatic rings are about 3,3 Å, that is a typical value for  $\pi$ - $\pi$  stacking interactions. All structural units, phenH<sup>+</sup> cations,  $[\text{Re}_4\text{Q}_4(\text{CN})_{12}]^{4-}$  anions and crystallization water molecules, are involved in the system of hydrogen bonds.

Structures of polymeric compounds consist of endless chains, in which every cluster anion  $[\text{Re}_4\text{Q}_4(\text{CN})_{12}]^{4-}$  gives three cyano groups for bonding interactions with lanthanide atoms. The full coordination environment of lanthanide atoms also includes phenanthroline molecule, water molecules and two OH<sup>-</sup> groups. These OH<sup>-</sup> groups bridge two lanthanide atoms into dimers with the distance among Ln atoms of about 3.7 Å. The polymeric chains are linked together by hydrogen bonds between coordinated water molecules and cyano groups.

All compounds have been characterized by different physico-chemical methods.

1.P12.

## MUTUAL SUBSTITUTION OF LIGANDS IN COMPLEX COMPOUNDS OF RHENIUM (V)

A.A. Aminjonov

Tajik National University, Dushanbe. [azimjon51@mail.ru](mailto:azimjon51@mail.ru)

Since the discovery of a prominent Swiss scientist Alfred Werner coordination theory has passed 118 years. During this period, scientists synthesized a huge number of complex compounds and the mechanism of their formation. Proved the prevalence of complex in nature and identified areas for their practical use. It is difficult to call the field of industry, medicine, catalysis, which are not used to coordination compounds. However, the problem of mutual substitution of coordinated ligands in the inner sphere of complex compounds remains one of the most important problems of modern coordination chemistry. It is worth recalling that in 1961, AM Butlerov was proposed the problem of mutual influence of atoms in a molecule, which was developed prominent Russian scientist VV Markovnikov. In the works Chugaeva LA and Kiltynovich SS were marked by the influence of inner-sphere ligand facts. Research conducted by other scientists showed that the Trans pattern can be extended to the chemistry of complex compounds of Pt (IV), Co (III), Rh (III) and Ir (III). Tsisinfluence of ammonia molecule on the rate of substitution of the adjacent ligands have been firmly established in 1957, Greenberg A. Kukushkin and Yu. N. They showed that the rate of substitution of chloride - ion to ammonia in tetrachloroplatinate (II) Potassium is smaller than in the salt Cossa.

Now for some metals in particular the valence state of trance set series - and tsisinfluence ligands. However, the chemistry of rhenium, which is characteristic for the valence states are 9: -3, -1 to 7 focused studies of the processes of mutual substitution of coordinated ligands was conducted. In this research we have established several types of chemical reactions in accordance with which there are processes of mutual substitution of ligands in complexes of rhenium (V).

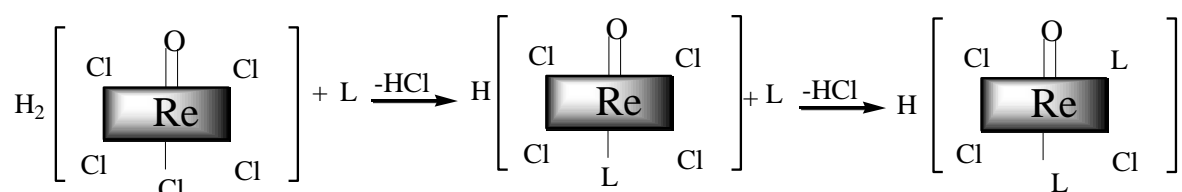
The first types of reactions are reactions that occur on heating the complexes in the absence of solvent. It is shown that when heated outer-sphere complexes of general composition  $(AmH)_2[ReOCl_5]$ , where Am - ammonia, quinoline, methylquinoline, dimetilhinolin, is replacing inner-outer-ligands. In reactions of this type of proton transfer occurs on the inner-sphere chloride ligand. Another type of solid-phase transformations of complexes of rhenium (V) is that the oxygen ligand complex as a result of the dimerization takes the place of another ligand.



The process of thermal decomposition of complexes of general composition  $[ReO(OH)(TP)(S)_2]$ , where T is Cl, Br, S-DMF, DMSO, SN<sub>3</sub>SN, Hin, Py describes the general reaction

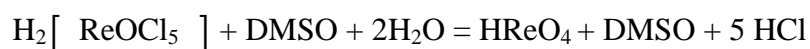


The second types of reactions are reactions that occur in the solution of the following general scheme:

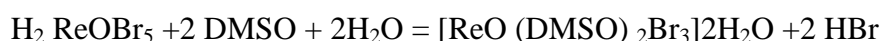


Under this scheme, we have synthesized a large number of complexes of rhenium (V) with sulfur-containing ligands azole series.

The third types established by our reactions are those reactions that are influenced by environment and rhenium (V) in the initial complex of  $H_2 ReOCl_5$  under the influence of ligands is oxidized to rhenium (VII) to form ion  $ReO_4^-$ . For example:



The reaction of HBr in the medium flows through the circuit



The fourth type of reaction are those reactions in which one replaces the other atsidoligand and labiliziruet atsidoligand being in trance - the situation to him, then the organic ligand interacts with the complex formed.

By the fifth type of reaction include the reaction of solvatokomplexes. For example:



By the sixth type of reaction are reactions occurring in the interaction of ammonia with solid complexes of rhenium (V) that is at the interface:

a) Reactions which take place only with the displacement of halide ions from the inner sphere complexes;

b) The dimerization reaction of monomeric complexes with the replacement of halide ligands;

a) Reaction, which resulted in the coordinated thiocyanate ions are converted into tioamidinovy group.

By the seventh type reactions are reactions in the environment of acetone resulting in the coordinated thiocyanate ions are converted into group's tioamidinovy

By the eighth type of reaction are the processes of interaction with the acids of rhenium complexes amminocontain (V).

By the ninth type of reaction include the reaction of the starting compounds such as  $H_2[ReOG_5]$  with two displays (double displays) complexes of rhenium (V) resulting in the formation monosubstituted complexes.

Thus, through focused research on the process of mutual substitution of ligands in complex compounds of rhenium (V) we propose the following series of mutual substitution legandov: LP (Ph) 3> SCN-> Cl-, Br-> S> H<sub>2</sub>O, where L tioamidnoe-connection, S-DMF, DMSO, Py, Xin, CH<sub>3</sub>CN.

Definition of standard redox potentials of 1,2,4-triazolthiola and some of its alkyl derivatives allowed to determine the next number in the changing values of real potentials, depending on the position and number of radicals in the molecule 1,2,4 - triazolthiol - 5 at 298K: 3-CH<sub>3</sub>-1,2,4-tthiol (209 mV) <3-Et (211.5 mV) <3-Et-4-Met (261 mV) <1,2,4-tthiol (266 mV) <3,4 - Dimet (276,9 mV) <4-Met (320,5 mV) <3Et-4Ph (323,4 mV).

Donor properties, if reducing properties triazolthiols in this series increases. This confirms the increase in Trans - activity of these compounds with a decrease in E<sub>0</sub>.

1.P13.

## **RHENIUM AND ITS POSITION IN THE PERIODIC TABLE**

Fathi Habashi

Department of Mining, Metallurgical, and Materials Engineering  
Laval University, Quebec City, Canada G1V 0A6

The discovery of rhenium by Ida Noddack *et al.* in 1925 was a result of an intensive study of the Periodic Table.

The search for the missing elements which were predicted by Dimitri Mendeleev between 1869 and 1891 was intensive especially when the prediction came true after the discovery of gallium, scandium, and germanium between 1875 and 1886.

Ida Noddack's scientific career centered around her intensive study of the Periodic Table. This resulted in two major discoveries.

The first was based on her realization that the missing element dvi-manganese should have properties similar to its neighbours in the horizontal period of the Periodic Table and not to members of the vertical group of which manganese was the only member known. In this way she was able to look for and discover the metal rhenium.

Thus Noddack introduced the concept of a horizontal similarity for the elements titanium to manganese while the vertical similarities still existed but only for Zr – Hf, Nb – Ta, and Mo – W below this horizontal group.

The second discovery was a daring hypothesis that the so-called element 93, a trans-uranium element that was supposedly formed by bombarding uranium (element 92) by neutrons, and was put under rhenium in the manganese group (in the old Periodic Table) was not correct. Instead, she suggested that the uranium atom might have split into two fragments - a phenomenon that later became known as fission.

1.P14.

## MACROCYCLIC RECEPTORS FOR PERTECHNETATE AND PERRHENATE ANIONS

G.V. Kolesnikov<sup>a</sup>, V.N. Khurstalev<sup>a</sup>, K.E. German<sup>b</sup>, I.G. Tananaev<sup>b</sup>, G.A. Kirakosyan<sup>b</sup> and E.A. Katayev<sup>c</sup>

<sup>a</sup> Nesmeyanov Institute of Organoelement Compounds, Russian Academy of Sciences Vavilov st., 28, Moscow, 119071, Russian Federation

<sup>b</sup> Frumkin Institute of Physical Chemistry and Electrochemistry Russian Academy of Sciences, Leninskiy pr. 31, 119071, Moscow, Russian Federation

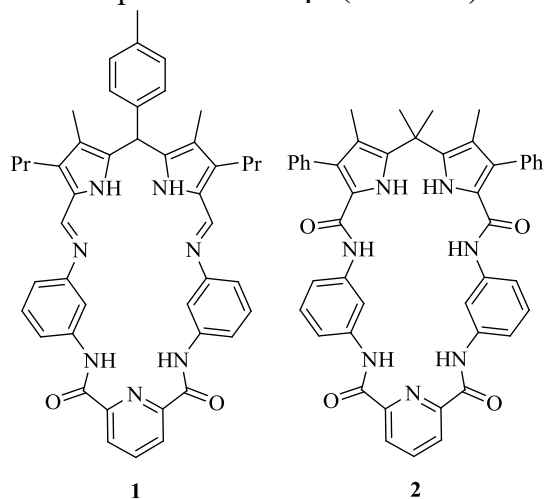
<sup>c</sup> Institut für Organische Chemie, Universität Regensburg, 93040 Regensburg, Germany, email: evgeny.katayev@chemie.uni-r.de

The design and synthesis of receptors capable of selective recognition of  $\text{MO}_4^-$  ( $\text{M} = \text{Re}$ ,  $^{99}\text{Tc}$ ) are of great interest because they can greatly benefit the development of efficient extractants, sensors and materials for these anions as well as new approaches for labeling of organic compounds without any reduction step of  $\text{Re(VII)}$  and  $\text{Tc(VII)}$ . Neutral receptors are known to be promising in the sense of high binding selectivity for target anions.

The neutral macrocyclic dipyrromethane based hosts capable of  $\text{MO}_4^-$  ( $\text{M} = \text{Re}$ ,  $^{99}\text{Tc}$ ) recognition were synthesized. When in protonated form, **1** binds perrhenate with strong H-bonds from pyrrole and imine NH's, weak – from amide NH's and benzene CH's, according to the X-ray analysis. The H-bond network of **2** is similar to that of  $[\mathbf{1H}_2]^{2+}$ , and the coordination mode of **2** with  $\text{ReO}_4^-$  was found to be equal, according to the DFT studies. The nonprotonated form of **1** binds to  $\text{ReO}_4^-$  using only pyrrole NH's, amide NH's and benzene CH's, according to the DFT studies.

Affinities of the receptors towards both  $\text{MO}_4^-$  ( $\text{M} = \text{Re}$ ,  $^{99}\text{Tc}$ ) were acquired by direct UV-vis titrations and towards  $^{99}\text{TcO}_4^-$  specifically by reverse  $^{99}\text{Tc}$  NMR titration. Binding constants were found to be one of the largest known to date ( $K_{\text{MO}_4} \approx 10^3\text{-}10^5 \text{ M}^{-1}$ ). Receptors possess selectivity towards target anions.

We gratefully acknowledge Russian Academy of Sciences program “Chemistry and Physico-Chemistry of Supramolecular Systems and Atomic Clusters”.





## **Tc in the Nuclear Fuel Cycle and in the Environment. Analytical Chemistry of Tc and Re**



The chairmen of the Second section of ISTR2011 in view of the  
Presidium of Russian Academy of Sciences

2.1.

**HOW TO MANAGE TECHNETIUM (NUCLEAR RARE METAL) AND ACTINIDES, TOWARD FUTURE REPROCESSING SYSTEM PROVIDED BY PROLIFERATION RESISTANCE**

M.Ozawa, T.Suzuki, S.Koyama, H.Sagara and M.Saito

Tokyo Institute of Technology, Research Laboratory for Nuclear Reactors, 2-12-1 N-21, Ookayama, Meguro-ku, Tokyo, 152-8550, Japan

**Keywords:** Nuclear rare metals, Cycle strategy, Separation, Transmutation and Utilization (S&T,U) , Proliferation resistance

**Abstract:**

Aiming at utilization of elements / nuclides in spent fuel (*i.e.*, nuclear rare metals (NRM) including Tc ) and minimization of long-term risks of radioactive wastes as well, a new fuel cycle concept has been progressed during the phase-I period (FY2005-2010). The strategy is based on a *Trinitarian* research as such separation, transmutation and utilization (S&T,U), especially relied upon advanced radiochemical separation technologies. A catalytic electrolytic extraction (CEE), utilizing under potential deposition (UPD) by Pd<sub>adatom</sub>/Rh<sub>adatom</sub>, is advantageous for separation and utilization (and/or stockpile) of light platinum group metals (PGM), Tc and Re. Their co-deposits have been showed highly catalytic ability for electrolytic production of hydrogen. Tertiary pyridine resin (TPR) will not only strongly adsorb PGM, Tc and Re, but also perfectly separate spent fuel into the groups of U/Pu/Np, Am, Cm and lanthanides (Ln), etc. Owing to MA (<sup>237</sup>Np, <sup>241</sup>Am) recycling into nuclear fuel, proliferation resistance of Pu would be strengthened by their neutron capture reactions to <sup>238</sup>Pu and <sup>242</sup>Pu.

The new fuel cycle strategy will conclude, some fission products like Tc, Mo, PGM, Lns and Tc must be separated and utilized as resources or alternatives. On the other hand, MA and even long-lived radioactive Lns such as Sm, Eu, etc, should be recycled and dopted to enhance proliferation resistance of Pu. Nuclear fission reaction must be utilized multidirectionally.

**Introduction (Nuclear Rare Metals, “Kopernikanische Wendung“)**

Fission reaction of <sup>235</sup>U will generate more than 40 elements and 400 nuclides in the spent fuel. Among them, 31 elements are categorized as rare metals (NRM ; Nuclear Rare Metal), and some are highly enriched in the spent fuel. Typical yields for such noticeable NRM as Pd, Ru, Rh (light PGM) and Tc, La, Nd (light Ln) will reach to more than 3kg to ca.10kg per metric ton of the reference FBR spent fuel (150GWd/t, cooled 5 years). By a close investigation, individual " exit strategy " can be individually proposed toward their utirization / recycling[1]. Namely,

- i) Use as elements; Low radio-toxicity <sup>99</sup>Tc (*e.g.*, exemption Level  $\geq 10^4$ Bq/g) shuold be used as catalyst as the same as Re, or irs alternative material.

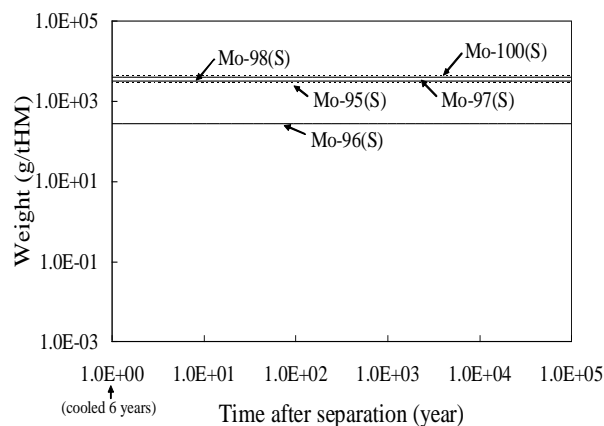
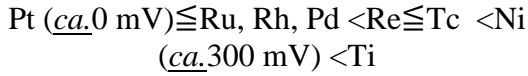


Fig.1 Isotopic abundance of FP Mo

Hydrogen overpotential ( $\eta$ ) of metals are periodically changed as their *d*-electron orbital characteristics. Although data on Tc is very limited,  $\eta_{Tc}$  in the acidic solution seem to be the following [2];



Ni electrode is currently available for commercial hydrogen production in alkali solution.  $\eta_{Tc}$  is lower than  $\eta_{Ni}$  by ca.100mV.

Ru and Rh can be used after the stockpile at least 40 years and 80 years, respectively, to be lower than their exemption; i.e., BSS level of  $^{106}Ru$  and NRPB level of  $^{102}Rh$ . Pd is approximately the same radiotoxicity as Tc ( $^{107}Pd:10^5 Bq/g$ (NRPB)).

Notably, natural isotopic abundance of Mo(%) are  $^{92}Mo:14.8$ ,  $^{94}Mo:9.25$ ,  $^{95}Mo:15.9$ ,  $^{96}Mo:16.6$ ,  $^{97}Mo:9.5$ ,  $^{98}Mo:24.1$  and  $^{100}Mo:9.63$ . Thus, higher order isotopic abundance of FBR Mo, as shown in Fig.1, will be beneficial for production of  $^{99}Mo$ . Very low radioactive Dy, La and Nd seem to be highly strategic and become important resource in the forefront industries.

ii) Use as nuclear fuel; Doping of  $^{237}Np$ ,  $^{241}Am$  and Cm to enhance proliferation resistance of Pu as discussed in section 3. Doping radioactive Lns like Pm, Sm, Eu, etc may also contribute to increase proliferation resistances of Pu.

iii) Use as radiochemicals;  $^{137}Cs$  as radiation source of  $\gamma$  alternating to  $^{60}Co$ , and  $^{90}Sr$ ,  $^{238}Pu$ ,  $^{241}Am$  and  $^{242,244}Cm$  as heat sources.

iv) Use as commerce of high expence stable Ru, during long-term stockpile of  $^{99}Tc$ , decay product  $^{99}Ru$  (stable) will gradually increased as shown in Fig.2. While stable  $^{100}Ru$  can also be obtained by transmutation of  $^{99}Tc$ , pure  $^{99}Ru$  isotope (very expensive 39,040\$/g) would be obtained without of any transmutation processing.

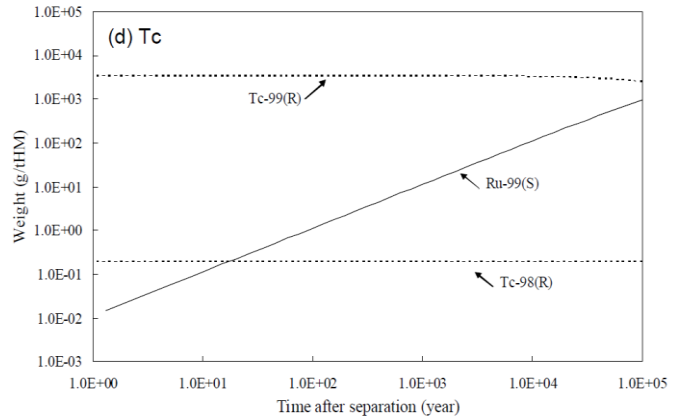


Fig.2 Isotopic abundance of FP  $^{99}Tc$

### Fuel cycle strategy and hydrometallurgical chemistry toward utilization

Toward simultaneous realization of utilization of elements / nuclides and ultimate minimization of the ecological risks, a new fuel cycle paradigm is necessary to be built. Hence, Adv.-ORIENT (Advanced Optimization by Recycling Instructive Elements) Cycle strategy is set under the following tactics [3]. 1/ Higher purity on NRM for utilization, allowing lower DF on actinides just for burning in FBR. 2/ To reduce the secondary rad. wastes; adopt soft hydrometallurgical, but non-SX separation process, with salt-free reagents. 3/ Deep separation of all

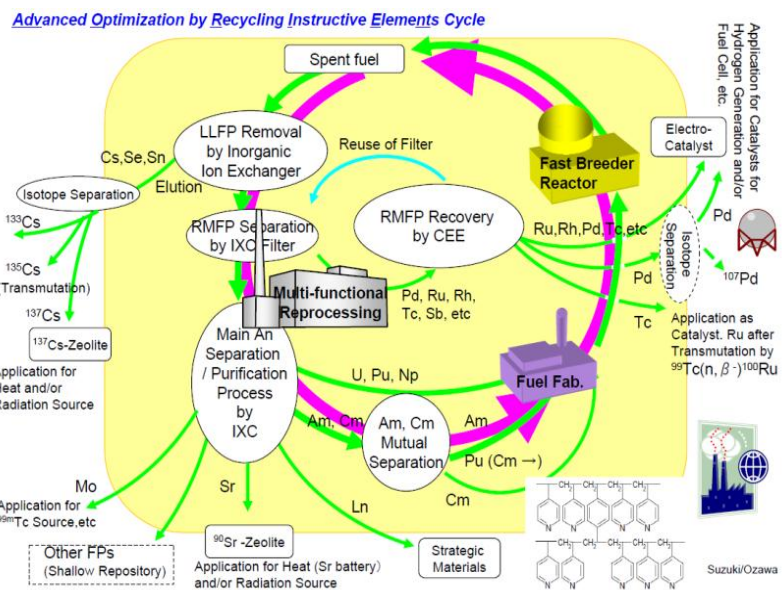


Fig.3 New fuel cycle concept based on S&T,U

actinides into 3-4 groups, U, Pu/U/Np, Am and Cm, directly from the spent fuel by IXC method. Eventually, pure Lns can be recovered. 4/ To sharpen the separability, hydrochloric acid (HCl) media is allowed in combination with nitric acid (HNO<sub>3</sub>) media. As shown the concept in Fig.3, the most significant policy change is that NRM shall be no longer wastes but main product along with actinides in the fuel cycle. In the point of back-end chemistry, precedent separation of some of NRM is preferable because some will disturb decontamination of actinides in the reprocessing and the vitrification of HLLW as well. A period to reduce the radio-toxicity below the level equivalent to 60 ton of natural uranium is one of the indexes on environmental impact of repositied 1 ton of HLLW. In adv.-ORIENT Cycle, by putting the separation factors of 99.9% for all An, 99% for <sup>137</sup>Cs, <sup>90</sup>Sr and the other NRM, and 90% for RE, such a period can be dramatically reduced to around 1×10<sup>2</sup> years.

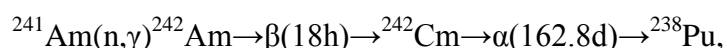
Catalytic electrolytic extraction (CEE), utilizing under potential deposition (UPD) with forming of undissolvable metal solid solution in acidic media, can effectively separate Ru, Tc and Re (Tc simulator) from either HNO<sub>3</sub> or HCl solution. Pd and Rh themselves were easy to be deposited. In dilute HCl media, such CEE occurred more distinctively than in dilute HNO<sub>3</sub> media. For instance, in the four NRM metal ions mixture solution (corresponded to FBR spent fuel composition), observed deposition yields were typically in the following order; Pd, Rh (>99%) > Re (91%) > Ru (85%) > Tc (69%). During the CEE, Pd or Rh might act as *promoter* at the surface of electrode (*i.e.*, *Pd<sub>adatom</sub>*, *Rh<sub>adatom</sub>*) and *mediator* in the bulk solution (*i.e.*, redox ion pair).

Tertiary pyridine resin (TPR), composing a nitrogen atom in six-membered ring, is characterized to simultaneously have two functions as weakly basic anion-exchanger and soft donor ligand. It will show high thermochemical and radiochemical stabilities especially in HCl media. An original idea of combinatory use of conc.HCl and conc.HNO<sub>3</sub> media was based on such facts that recognition of softer ions like Am<sup>3+</sup> and Cm<sup>3+</sup> (5-*f* elements) was clearer than Ln<sup>3+</sup> (4-*f* elements) in HCl media, and in HNO<sub>3</sub> media the distribution depended just on the difference of ionic radius independently either 4-*f* or 5-*f* elements. Extractabilities of both Am<sup>3+</sup> and Cm<sup>3+</sup> improved by enhancing complexation of protonated pyridine with anions due to the dehydration brought by co-existing methanol, and thereby increasing SF<sub>Am3+/Cm3+</sub>.

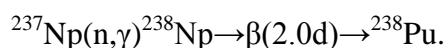
The CEE method is advantageous because NRM would be recovered in solid state at the electrode surface as metal (Ru, Rh, Pd, (Tc)) and/or oxide (Tc, Re). Recovered NRM was sphere micro deposits foamed by coagulating with nano particles in the case of Pd<sup>2+</sup> involved CEE. Those deposits were dense, and mechanically stable, with showing electrochemically high catalytic reactivity on electrolytic hydrogen production. Ru has been confirmed as a dominant element for the reactivity, while Pd played as just a "starter" nucleus and a "binder" among the involved elements during the deposition. Higher reactivity of Tc than Re will suggest exploring new application fields of it. Further, a new evaluation was initiated to evaluate the producibility on more valuable PGM (*e.g.*, Rh) by re-irradiation of FP Ru, and <sup>99m</sup>Tc by FP Mo, both separated from the spent fuel. For this purpose, parametric studies are necessary to optimize, fuel and reactor types, fabrication and irradiation conditions, etc.

### Enhancement of proliferation resistance of Pu by MA and Ln recycling

Proliferation resistance of Pu will be enhanced by increasing of even mass number of actinides of <sup>238</sup>Pu, <sup>242</sup>Pu and <sup>242</sup>Cm, etc. <sup>238</sup>Pu and <sup>242</sup>Pu, characterized specifically by high decay heat to fabricate weapon difficult, are high spontaneous fission neutron source to deteriorate the quality of the Pu toward nuclear explosion [4]. Therefore, those become "isotopic barrier" against proliferation. Such <sup>238</sup>Pu will be generated in the reactors by the following neutron capture reactions of MA,







Sagara, et al reported the irradiation results of pure  $^{241}\text{Am}$  oxide sample in the experimental fast reactor “Joyo”. Under the neutron fluence conditions ( $\times 10^{22}[\text{n}/\text{cm}^2]$ ) like core: 8.15, Ax.-ref: 2.48 and Rd.-ref: 4.18, neutron capture ratio was 65% (for generating Pu and Cm) and fission ratio was 28% at the center of core with harder neutron spectrum [5]. However, at the reflector region neutron capture reaction increased to be more than 80% with decreasing fission reaction, conversely. Relative isotopic abundance of  $^{238}\text{Pu}$  plus  $^{242}\text{Pu}$  was more than 98% in the both case, and that of  $^{242}\text{Cm}$  was more than 97%, where the transmutation ratio of Pu/Am was less than 7% and 2% for Cm/Am. Evidently, transmutation of  $^{241}\text{Am}$  was successfully achieved, and the isotopic ratios of  $^{238}\text{Pu}$  and  $^{242}\text{Pu}$  were increased. When MA doping is 2% against DU, the ratio of  $^{238}\text{Pu}$  plus  $^{242}\text{Pu}$  will be more than 10%, and that will satisfy both criteria on  $^{238}\text{Pu}$  content, e.g., 9% [6] and attractiveness factor calculated as 6% [4].

Separation of pure MA and PGM from the spent fuel was successfully demonstrated [7] utilizing previously described IXC separation scheme [8]. Irradiated MOX fuel (143.8GWd/t) at the fast experimental reactor “Joyo” was dedicated for the experiment. As experimental results, the recovery ratio of  $^{241}\text{Am}$  was more than 95 % whole through the processes, and the impurities of  $^{241}\text{Am}$  product against Ln ( $^{144}\text{Ce}+^{154}\text{Eu}$ ),  $^{243}\text{Cm}$  and  $\gamma\text{FP}$  ( $^{106}\text{Ru}+^{125}\text{Sb}+^{137}\text{Cs}$ ) were very low, less than 0.3ppm, 1 ppm and 1.8ppm, respectively. The separation degree on  $^{243}\text{Cm}$  from  $^{241}\text{Am}$  product was more than  $2.2 \times 10^3$ . Possibly, TPR chromatography method will meet well with the MA ( $^{241}\text{Am}$ ) recycling in the points of increasing proliferation resistance as well as decreasing environmental burden. Further study will focus on clarifying Np behavior, preferably controlling its behavior together with Pu. Intra-group separation of Ln and PGM (including Tc), and engineering feasibility and simplification in HCl / HNO<sub>3</sub> hybrid media is issue in the phase II.

## Conclusion

Aiming at utilization of elements / nuclides of rad.wastes, a new fuel cycle concept has been progressed. The strategy is based on a *Trinitarian research* as such separation, transmutation and utilization, especially relied upon advanced radiochemical separation technologies like ion exchange and electrochemistry by a combinatorial manner. A catalytic electrolytic extraction method, utilizing under potential deposition by Pd<sub>adatom</sub>/Rh<sub>adatom</sub>, is advantageous for separation and utilization (or stockpile) of light platinum group metals and Tc. Tertiary pyridine resin will not only strongly adsorb Tc and Re but also generate co-products of U/Pu/Np, Am, Cm and Ln, thereby sufficiently strengthen the proliferation resistant character (increase  $^{238}\text{Pu}$  content) of recycled Pu is achieved. The separation scenario of all of actinides and fission products in the spent fuel should be strategically re-developed to satisfy the various requirements.

**Condolence:** During preparing this manuscript, the most powerful, magnitude 9.0 earthquake and tsunami attacked Tohoku-Kanto pacific region on Friday March 11, 2011. These caused a great disaster on Fukushima NPPs and the situation is not settled-down yet. With the deepest sympathy with regret, and sincere gratitude for helps by foreign countries.

## References

1. M. Ozawa, Separation and Utilization of Nuclear Rare Metals and Actinides in Advanced Reprocessing System, 香山科學會議 第389回「核燃料再処理放射化学」北京・香山飯店The 389<sup>th</sup> Xiangshan Science Conference Workshop of Nuclear Fuel Reprocessing, *Proc. Radiochemical Challenges in Nuclear Fuel reprocessing*, pp.27-29, Xiangshan Hotel, Beijing, China, Dec22-24, 2010.
2. H.Kita, et al., *Denkikagaku*, 38,17(1970)(in Japanese)
3. Masaki Ozawa, Tatsuya Suzuki, Shinichi Koyama, Hiroshi Akatsuka, Hitoshi Mimura and



Yasuhiko Fujii, A New Back-end Cycle Strategy for Enhancing Separation, Transmutation and Utilization of Materials (Adv.-ORIENT Cycle), *Progress in Nuclear Energy*, 50(2008)476-482, ELSEVIER (2008).

4. Masaki Saito, Protected Plutonium Production by Transmutation of Minor Actinides for Peace and Sustainable Prosperity, *Proc. of Global 2009*, Paper 9397, Paris, France, September 6-11, 2009.

5. Hiroshi Sagara, Tetsuro Yamamoto, Shinichi Koyama, Shigetaka Maeda, Tomooki Shiba and Masaki Saito, Numerical Analysis of Irradiated Am Samples in Experimental Fast Reactor Joyo, *Actinides2009, IOP conf. Series: Materials Science and Engineering* 9(2010)012006.

6. G.Kessler, et al., *Nuclear eng. and design*, 238(2008)3429-3444.

7. Shinichi Koyama, Masaki Ozawa, Tatsuya Suzuki and Yasuhiko Fujii Development of a Multi-functional Reprocessing Process Based on Ion-Exchange Method by Using Tertiary Pyridine-Type Resin, *Journal of Nuclear Science and Technology*, Vol.43, No.6 pp.681-689 (2006).

8. Tatsuya Suzuki, Yasuhiko Fujii, Wu Yan, Hitoshi Mimura, Shinichi Koyama, Masaki Ozawa, Adsorption Behavior of VII Group Elements on Tertiary Pyridine Resin in Hydrochloric Acid Solution, *J Radioanal Nucl Chem* (2009) 282;641-644..



F. Poineau, C. Kremer, D. Suglobov, acad. B.F. Myasoedov, K.E. German at the ISTR2011 Welcome party

## 2.2.

# COMBINED SEPARATION OF Pd AND Tc FROM THE RAFFINATES OF THE SPENT NUCLEAR FUEL REPROCESSING

T. Boytsova\*, V. Korolev\*, Y. Pokhitonov\*, V. Babain\*, M. Ozawa\*\*, T. Suzuki\*\*

\* RPA «V.G. Khlopin Radium Institute», Saint-Petersburg, Russia, 28, 2<sup>nd</sup> Murinsky ave., 194021. E-mail: radium@atom.nw.ru

\*\* Tokyo Institute of Technology, Tokyo, Japan, 2-12-1 O-okayama, Meguro-ku, 152-8550. E-mail: [tasuzuki@nr.titech.ac.jp](mailto:tasuzuki@nr.titech.ac.jp)

A small amount of “reactor” Pd, Ru, Rh and Tc metals is needed for investigation of the possibility of production and use of electrodes in hydrogen energetics covered by a composite made of these “reactor” metals. One of the sources of these metals is the raffinates of the first extraction cycle of the spent nuclear fuel (SNF) reprocessing.

The purpose of this study was to investigate the Tc and Pd sorption behaviors, to search the agents for their desorption, to test the determined conditions of the metals separation with use of real SNF reprocessing solutions.

The examples of individual Pd and Tc sorption by anion exchange resin from nitric acid solutions are well-known. However, their combined separation wasn't mentioned earlier.

In this study the strongly basic anionite BII-1AII, which had been previously applied to separate a “reactor” Pd, was used as a sorbent.

Tc and Pd sorption under static and dynamic conditions were studied. It is shown that the combined sorption should be carried out at a HNO<sub>3</sub> concentration not more than 2 M. When passing through the sorbent at least 50 column volumes (c.v.) of the model solution (C<sub>HNO<sub>3</sub></sub> = 2 M; C<sub>Pd</sub> = 100 mg / l; C<sub>Tc</sub> = 100 mg / l) almost 100% of Pd and 30% of Tc were sorbed on the resin.

The conditions for 100% Pd and Tc separation from the feed solution were found.

The desorption with DTPA solution in the wide range of acidity allows to achieve both combined 100% yeild of Pd and Tc in 15 c.v. and individual desorption of these metals (Pd in 8 c.v., Tc in 15 c.v. ).

An example of the combined separation of Pd and Tc from the SNF was given in the study. Distribution of Pd and Tc by fractions of experiment solutions, factors of purification of these metals from gamma impurities and obtained dynamic exchange capacities are shown.

2.4.

## THE ELABORATION OF TECHNOLOGY BASES FOR THE ARTIFICIAL STABLE RUTHENIUM PREPARATION FROM TECHNETIUM-99 TRANSMUTATION PRODUCTS

A.A. Kozar<sup>1</sup>, V.F. Peretrukhin<sup>1</sup>, K.V. Rotmanov<sup>2</sup>, V.A. Tarasov<sup>2</sup>

<sup>1</sup> Frumkin Institute of Physical Chemistry and Electrochemistry of RAS, 31/4, Leninsky prosp., Moscow, 119071 Russia, [kozar@ipc.rssi.ru](mailto:kozar@ipc.rssi.ru)

<sup>2</sup> Federal State Unitary Enterprise State Scientific Centre – Research Institute of Atomic Reactors, Dimitrovgrad 10, 433510 Russia, [orip@niiar.ru](mailto:orip@niiar.ru)

The bases of technology have been elaborated for the artificial stable ruthenium preparation from the <sup>99</sup>Tc transmutation products. The process includes the following steps: the isolation technetium from spent fuel with additional purification of Tc from actinides, the manufacture of technetium targets, their irradiation with high flux of thermal and epithermal neutrons, the exposure of irradiated targets for the short-lived radionuclides decay, chemical separation of ruthenium from technetium and the exposure of prepared ruthenium up to the fission product <sup>106</sup>Ru decay.

The metallic targets have been prepared from technetium which contained  $\sim 5 \cdot 10^{-8}$  g actinide impurity per gram Tc. The irradiation of the targets has been carried out with thermal neutron flux  $6.8 \cdot 10^{14} - 1.14 \cdot 10^{15} \text{ cm}^{-2} \cdot \text{s}^{-1}$  (epithermal neutrons part is 0.06 – 0.1) during 73 – 425 eff. days and burn up has been achieved 19 – 70% (for 3 different groups of Tc targets).

The dissolution of irradiated targets has been carried out in KOH solution in presence of excess of KIO<sub>3</sub> at 70 – 80°C. Volatilization of RuO<sub>4</sub> from KTcO<sub>4</sub> solution and other chemical methods have been applied for the isolation of ruthenium.

Total Ru separation factor has been achieved  $10^{12}$ . The exposure of prepared artificial ruthenium during 10 years needed for the diminution of the <sup>106</sup>Ru, <sup>106</sup>Rh radioactivity of the metal up to the level required for its any application.

About 5 grams of stable ruthenium have been prepared in this work from 10 g of the technetium. This artificial ruthenium was nearly monoisotopic and contained 97.5 – 99.7% <sup>100</sup>Ru depending on <sup>99</sup>Tc burn-up. The achieved <sup>99</sup>Tc transmutation rate and targets burn-up value are records for today and may be increased by the rise of the epithermal component in the neutron flux.

## 2.5.

## TECHNETIUM CATALYTIC EFFECT AND SPECIATION IN NITRIC ACID SOLUTIONS IN PRESENCE OF Np(V), Th(IV) and Zr(IV) AND REDUCING NITROGEN DERIVATIVES

K.E. German, Ya.A. Obruchnikova, D.N. Tumanova, V.F. Peretrukhin, Ph. Moisy\*.

IPCE RAS, Moscow, Leninskii pr.31- 4, 119071 Russia

\* - CEA – Marcoule, DEN DRCP, BP17171 – 30207, Bagnols sur Ceze, France

The technetium species develop the catalytic effect being of high importance for the reprocessing of the spent nuclear fuel [1]. One would just mark that the large-scale reprocessing in the UK was delayed by 5 years in the startup stage due to the harmful Tc-effect [2]. An important item of Tc separation from the reprocessing solutions is the mutual effect of a number of redox stable (Zr) and redox sensitive elements (especially Tc, see p.e. [3-6] and Np) present in these wastes. Two technetium valence states (VII and IV) are considered to be rather stable under the conditions of spent nuclear fuel reprocessing.

In the previous report we have demonstrated the catalytic effect of Tc(VII and V) on the reduction of Np(V) to Np(IV) with hydrazine in nitric acid resulted in Np(V) disappearance and in the accumulation of Np(IV) different species, so that the free ionic form of Np(IV) accumulated in lower concentration, compared to decrease in Np(V) concentration. This fact indicated the possible Np(IV) complex formation with some of the reaction product [7-8]. The Tc(VII) participation in this reduction process was anticipated taking into account the common catalytic properties of technetium, while the interaction of An(IV) with Tc reduced species was difficult to predict and needed some additional experimental study that was demonstrated in [9-10] with simulated waste solutions with Th(IV) taken for typical example of An(IV). The existence of such species was difficult to predict based only on the accepted thermodynamic data [3], although the possibility of deep Tc reduction even to Tc(II) species in nitric acid was already demonstrated in [12], and the importance of hydrolyses and polymerization in aqueous solutions of different acids were shown in [8-11]. Anyhow such questions as the influence of the Tc valence state in the catalytic action on Np behavior remained unclear as only Tc(V) and Tc(VII) species were tested in [7-10] and the corresponding study of the Tc(IV) species is being undertaken in this report. Because of the possible interference of the Tc(V and IV) and Np(V,IV) optical spectra, the procedure of spectra analyses elaborated in the previous report was used for the optical separation of individual Tc and Np species before the kinetic treatment of the experimental data aiming the determination of the reaction orders in Np(V), Tc(IV),  $N_2H_5^+$ ,  $H^+$ .

The experimental procedures was based on the conventional spectrophotometric methods for the kinetic measurements of Np(V) and Tc(IV). For the determination of Np(V) concentrations the NIR absorption peak at 980 nm was used. The constant initial concentrations of Np(V) and  $N_2H_5NO_3$  were used in all the experiments, while  $C_0(Tc(IV))$  varied as  $(0.24 - 1.2) \cdot 10^{-3}$  mol/l. The temperature interval from 25 to 55°C was set-up in different sets. Tc(IV) concentrations were measured at the 400 nm (after the Np(IV) spectra contribution corrections), while Tc(V) was determined according to the development of the shoulder at 470-500 nm with similar corrections for Np and Tc(IV).

In the present work the Tc was initially reduced to Tc(IV) previous to addition to the test solutions. In such a case no induction period was needed for the Np(V) reduction reaction similar to the Tc(V) effect, studied before [8]. Similar to the previous report, the deconvolution analysis of the spectra was critical for the understanding of the chemical reactions in the system under consideration. While the Tc(VII) spectrum is well known and completely characterized, some misunderstanding exists for Tc(IV), Tc(III) and Tc(V) in acidic solutions. We consider the most reliable for spectroscopic standard purpose to use Tc(IV) spectrum registered after dissolution of

TcO<sub>2</sub> \*nH<sub>2</sub>O in sulfuric acid under argon atmosphere. Utilization of these spectra as a standard was fruitful in the previous work for the Tc – Np spectra deconvolution. It is important and possible because the spectroscopic parameters have been determined in separate tests.

Anyhow the Tc(IV) stock solution for the kinetic tests was each time freshly prepared by reduction of 10<sup>-2</sup> M Tc in 1.5M nitric acid with excess of hydrazine nitrate. The following dilution of the aliquots in test solution influenced only the Tc concentration.

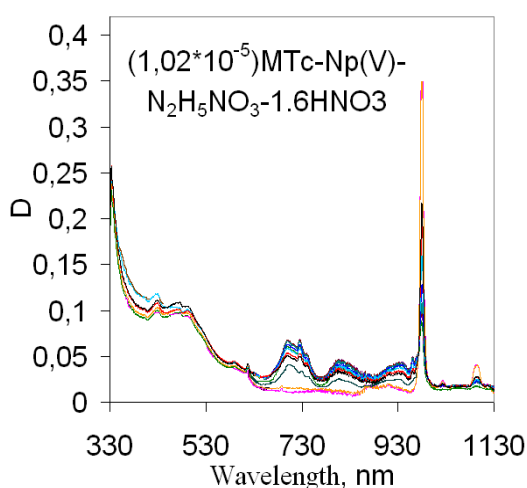


Fig.1. Typical view of Np(V) reduction with hydrazine catalyzed with Tc(IV) ([Tc(IV)]=1.02\*10<sup>-5</sup> M, [HNO<sub>3</sub>]=1,6 M).

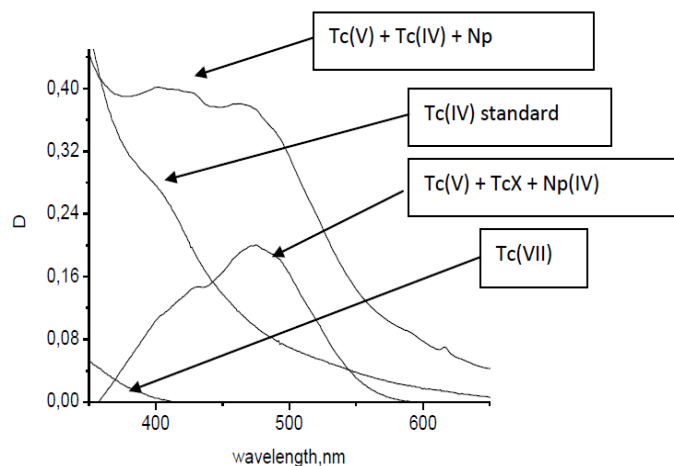


Fig.2. Deconvolution of typical mixed spectrum of Tc(IV) – Tc(V)-Np(IV) solution

The mixed Tc(IV) –Tc(V)-Np spectra could be subtracted one from another as shown at the Fig. 6-3, where the presence of at least three different Tc species can be seen from the deconvolution analyses.

At least one of the intermediate Tc species has unknown molar extinction coefficient therefore the quantification of the Tc valences was impossible in this solution system by optical spectra measurements. Anyhow we can estimate from the subtracted spectra that the initial Tc(IV) is partially oxidized in course of the catalytic process and the total reduction of Np(V) to Np(IV) is run with a mixture of Tc (IV) and Tc(V) species stabilized in the nitric acid solution in presence of hydrazine.

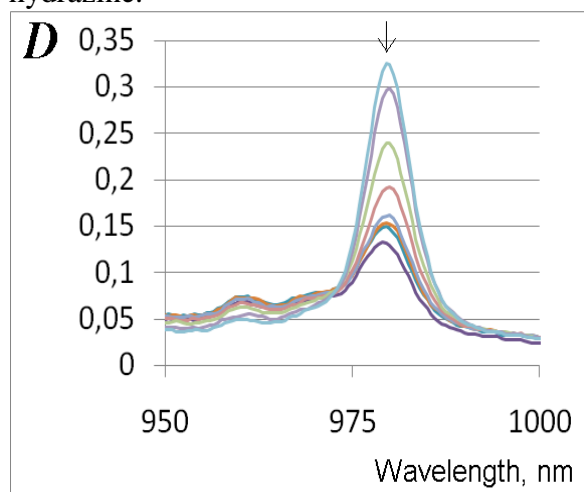


Fig. 3. The typical evolution of the Np(V) spectrum in "Np-region" (980 nm) in the course of Np reduction with hydrazinium, catalyzed by Tc(IV).

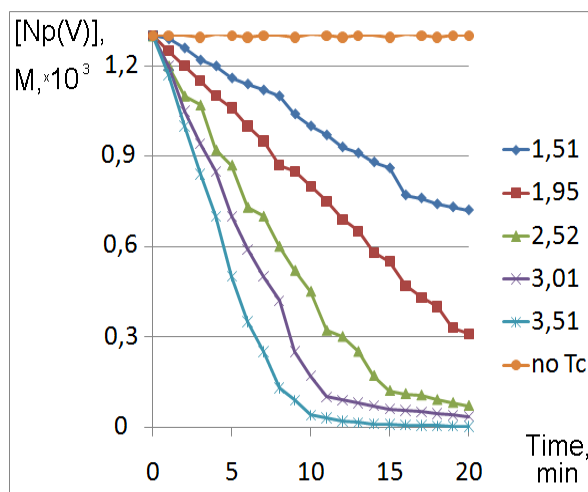


Fig. 4. Np(V) reduction with 0.052 M H<sub>2</sub>N<sub>5</sub>NO<sub>3</sub> catalyzed by Tc(IV) (0.98\*10<sup>-4</sup> M) in 1.51, 1.95, 2.52, 3.01 and 3,51 M nitric acid.

The registration of the spectra evolution in "Np-region" (980 nm) gave evidence that the change in the absorption at 980 nm is completely due to Np(V) reduction to Np(IV) (Fig. 3). In the



tests with the previously prepared Tc(IV) being added to the solution as a catalyst for Np(V) to Np(IV) reduction with  $\text{N}_2\text{H}_5^+$  in 1.5 M  $\text{HNO}_3$ , the Tc spectrum underwent just very small transformations while the peak Np(V) (Fig.3) decreased with time. When this previously synthesized Tc(IV) compound dropped into the Np(V)-hydrazinium-  $x \cdot \text{HNO}_3$  solutions with different acidities *no* induction period was observed at 36 °C (Fig. 4) as well as at other temperatures up to 55 °C.

The Np(V) to Np(IV) half-reduction time for this reaction increased from 5 to 25 min while the acidity of the solutions was decreasing from 3.51 to 1,52 M  $\text{HNO}_3$ . The kinetics was practically linear within the 0.8 conversion factor thus indicating the zero order in [Np] for this reaction in this acidity region (1.5-3.5 M).

The reaction rate constants are tabulated in the Tab.1.

Table 1.  $K_o^I$  for Np(V) reduction with hydrazine catalyzed by Tc(IV) at different  $C(\text{HNO}_3)$ .

[ $\text{HNO}_3$ ], M	$K_o^I, *10^4$ mol/l*min	lg[ $\text{HNO}_3$ ]	lg $K_o^I$
1,51	0,29	0,179	-0,538
1,95	0,49	0,290	-0,310
2,52	0,84	0,401	-0,076
3,01	1,19	0,479	0,075
3,51	1,61	0,545	0,206

Table 2. The temperature dependence of the reaction rate constant  $K_o^I$  for Np(V) reduction catalyzed with Tc(IV).

T, °C	1/T, 1/K	$K_o^I, *10^4$ mol/l*min	lg $K_o^I$
20	0,00341	0,4	-0,398
25	0,00336	0,6	-0,222
30	0,00330	0,8	-0,0969
35	0,00325	1,3	0,114
40	0,00320	1,9	0,279
45	0,00314	3,1	0,491
50	0,00310	4,4	0,643

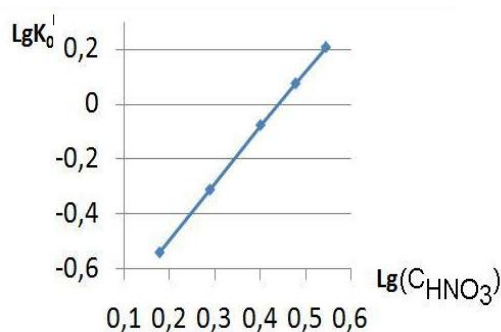


Fig. 5. Reaction order determination from  $LgK_o^I = f(Lg(C_{\text{HNO}_3}))$

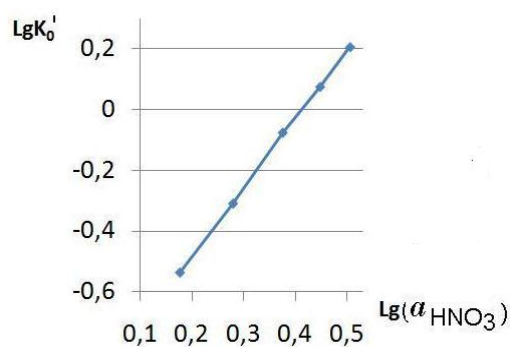


Fig. 6. Reaction rate constant  $K_o^I$  as a function of  $a_{\text{HNO}_3}$

The Np(V) reduction reaction order was determined from  $\lg K_o^I = f(\lg(C_{\text{HNO}_3}))$ , the dependence corresponds to the *second* order of the reaction kinetics (Fig. 5.). The correction of the data for the activity of  $\text{H}^+$  in nitric acid gave similar dependence for the  $K_o^I$  (Fig. 6).

The temperature dependence of the reaction rate constant was determined at the temperatures of 20 – 50 °C (Tab.2, Fig.7).

The resulting activation energy was estimated as 41,9 (3) J/M.

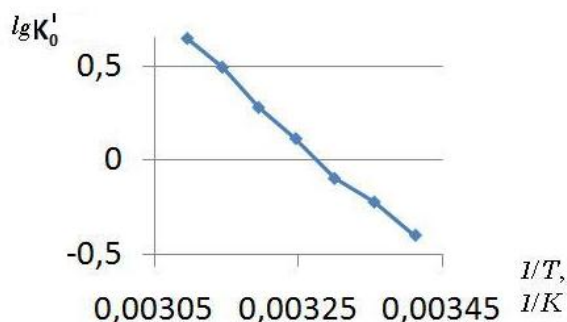


Fig. 7. Reaction rate constant  $K_o^I$  as a function of inverse temperature (for 20 – 50 °C temperature interval).

The effect of technetium(IV) ions concentration on the catalytic Np(V) reduction with hydrazine was tested in the set of solutions prepared based on 2.84 M  $HNO_3$ . This acidity was used as it is well known [4] that the fraction of the hydrolyzed form of Tc(IV) could be important in the solutions with smaller acidity thus leading to its smaller catalytic activity.

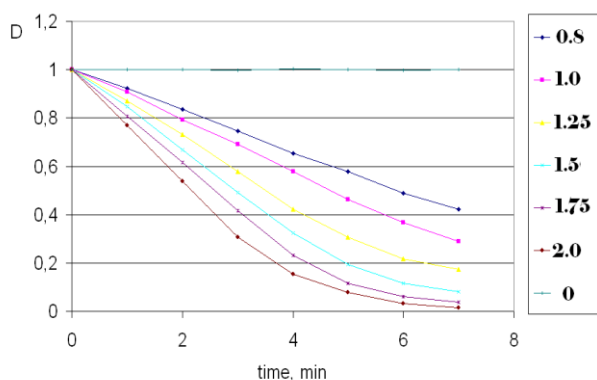


Fig. 8. Np(V) reduction with 0.052 M  $H_2N_5NO_3$  catalyzed by Tc(IV) added at different concentration: (0.8, 1.0, 1.25, 1.5, 1.75, 2.0  $\times 10^{-4}$  M) in 2.84 M nitric acid.

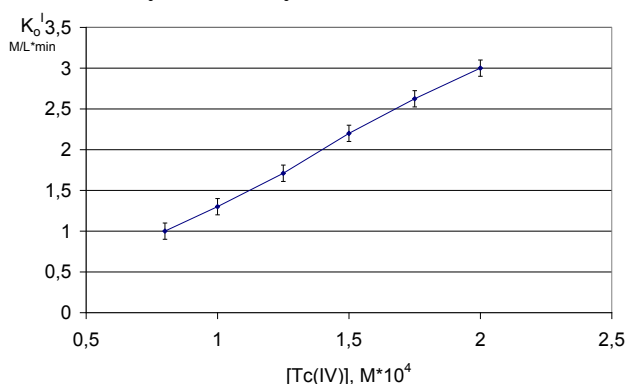


Fig. 9. Effective reaction constant  $K_o^I$  for Np(V) reduction with 0.052 M  $H_2N_5NO_3$  catalyzed by Tc(IV) as a function of different Tc concentration (0.8, 1.0, 1.25, 1.5, 1.75, 2.0  $\times 10^{-4}$  M) in 2.84 M nitric acid.

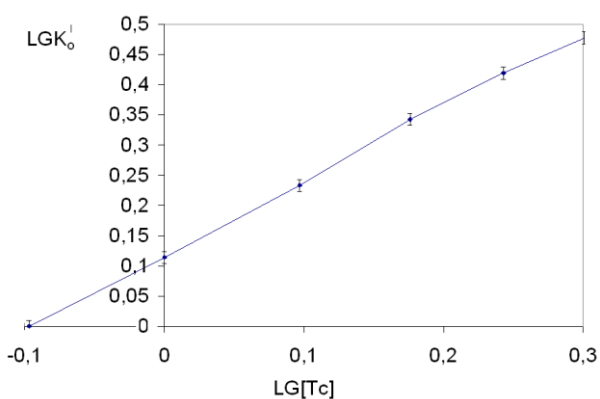


Fig. 10.  $Lg K_o^I$  as a function of different  $Lg [Tc]$  (for  $[Tc^{(IV)}]_{init} = 0.8, 1.0, 1.25, 1.5, 1.75, 2.0 \times 10^{-4}$  M) in 2.84 M nitric acid.

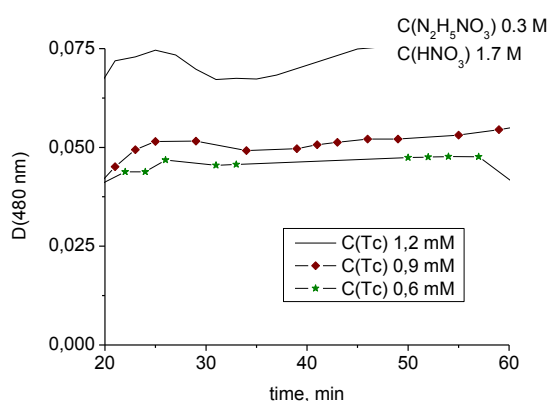


Fig. 11. The evolution in the spectra optical density ( $\lambda = 480 \text{ nm}$ ) in the region of Tc(IV+V) species at 50 °C for different total Tc concentrations.

As follows from Fig 10, the reaction order for Np(V) reduction with  $H_2N_5NO_3$  catalyzed by Tc(IV) over [Tc] is equal to 1. After the reduction of Np(V) to Np(IV) is complete the evolution in the spectra optical density at  $\lambda = 480 \text{ nm}$  has indicated very small changes in Tc(IV) to Tc(V) species concentration ratio during the first hour of storage even at 50 °C (Fig. 11).

So, the kinetics equations for the Np(V) reduction with  $\text{H}_2\text{N}_5\text{NO}_3$  catalyzed by Tc(IV) could be drawn as:

$$- (d[\text{Np(V)}]/dt = K_o[\text{Tc(IV)}][\text{HNO}_3]^2, \\ \text{where } K_o = K_o^1 / ([\text{Tc}][\text{HNO}_3]^2 = 14.8 (2) * 10^{-2} \text{ M}^{-2} * \text{min}^{-1}$$

It is important to note that in this report the effect of nitric acid on the  $K_o^1(\text{Np(V)})$  was not divided for the separate effects of  $[\text{H}^+]$  and  $[\text{NO}_3^-]$  although we may predict from the known chemical properties of Np(V) that the latter dependence should be of higher importance. This study was not the special task of this report but it is under way and will be completed in the nearest future.

An important item of the Np(V) catalytic reduction driven with Tc(IV) is the hydrazine concentration. The reduction of Tc(V) to Tc(IV) in high excess of hydrazine is a comparatively fast reaction.

When the reduction of Np(V) is complete, the latter is stable for 0,5-1,5 hours depending on the temperature of the solution. The further reduction of Tc (probably to Tc(III)) causes the hydrazine catalytic decomposition and then – partial back oxidation of Np(IV). For longer terms the considerable fraction of Tc is oxidized back to Tc(VII) that was confirmed by liquid – liquid extraction tests and the EXAFS spectra registered on the aged solutions.

When Tc(VII) is added to the Np(V) solution containing hydrazine, the induction period is needed for the startup of Np(V) catalytic reduction. In case when Tc(V) was added no induction stage is observed. The previously prepared Tc(IV) being added to Np(V) in 1.5- 3.5 M nitric acid – hydrazine nitrate solutions) causes the Np(V) catalytic reduction with hydrazinium to Np(IV) without any induction period. The Np(V) reduction with  $\text{N}_2\text{H}_5^+$  is catalyzed by Tc(IV) ions and follows the kinetics being zero order in  $[\text{Np(V)}]$ , 1-st order in  $[\text{Tc(IV)}]$ , 2-nd order in  $[\text{HNO}_3]$ , with  $\square E_{\text{activ}} = 41.9(3) \text{ J/M}$ .

When the reduction of Np(V) is complete, the latter is stable for 0,5-1,5 hours depending on the temperature of the solution. The further reduction of Tc (probably to Tc(III)) causes the hydrazine catalytic decomposition and then – partial back oxidation of Np(IV).

The technetium reduction by hydrazine nitrate and hydroxylamine chloride in the presence of Th(IV) and Zr(IV) was investigated. The experimental procedures of this work involved conventional spectrophotometric methods for the kinetics measurements of Tc. The initial concentration of Tc was varied as 0,4 – 1,52 mmol/l,  $C(\text{Th}) = 0 – 6,32 \text{ mmol/l}$ ,  $C(\text{N}_2\text{H}_5\text{NO}_3) = 0,255 \text{ M}$ . The temperature was about  $55^\circ\text{C}$ . The reactions were carried out in thermostatic quartz cells. A typical sequence of spectral changes in one experiment is given at Fig. 12. To get the equilibrium state more than 2 hours were needed. As can be seen the reaction consists of 3 stages. On addition of hydrazine to Tc-Th solution in nitric acid the reaction first proceeds as a Tc(VII) reduction to Tc(IV) thus developing the shoulder at 400 nm and following the zero order kinetics, initiating the hydrazine decomposition with gas evolution, then decomposition of Tc(IV) takes place in similar zero order kinetics with formation of unidentified Tc(X) species, then finally forming pink or brown (depending on Tc concentration) Tc(Y)-Th(IV) complex characterized with a peak at 470-475 nm in first order kinetics. The later is supposed to be Tc(V)-Th(IV) complex which is stable for several days at  $55^\circ\text{C}$ .

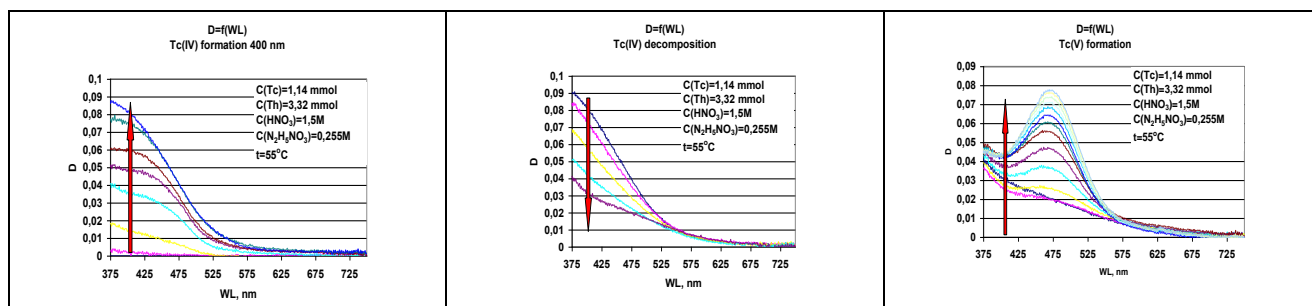


Fig. 12. Reduction of Tc with hydrazine in presence of Th

The conditions providing intermediate Tc species stabilization in presence of four valence actinides were found giving an evidence that at least three reduced Tc species (Tc(IV), TcX and Tc(V)) are appearing and disappearing in the course of the consequent reactions (Fig. 13). Two different technetium species exist simultaneously. The reaction of Tc(V) complex formation in presence of Th(IV) can be turned back to Tc(IV) formation when a new portion of hydrazine is added.

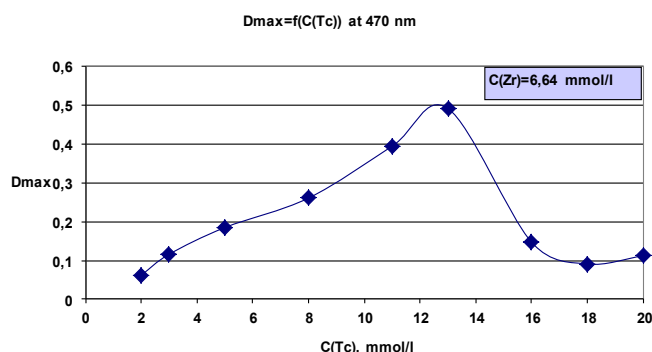
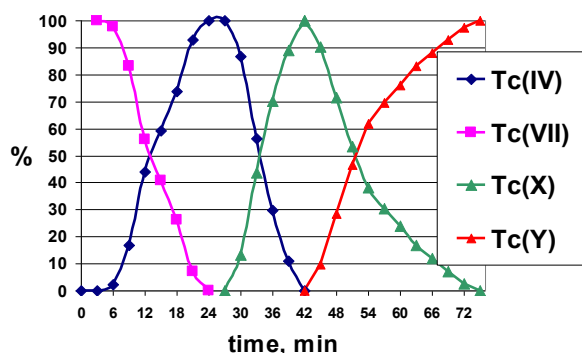


Fig. 13. Change in content of reduced Tc species. Fig. 14.  $D=f(c(Tc))$  for equilibrated solutions in presence of Zr(IV).

It was found that the final complex of Tc with Th (Zr) at 470 nm by hydrazine and at 500 nm by hydroxylamine reduction has the ratio of two to one accordingly (Fig. 14).

It was found that Th and Zr produce clear stabilizing effect onto several reduced Tc species. Tc(V) forms stable complexes with redox inactive d- and f-elements like Th(IV) and Zr(IV) in nitric acid in presence of reducing N-derivatives (with the ratio between Tc and Zr is 2 to 1).

## References

1. Campbell D.O., Burch W.D. The chemistry of fuel reprocessing: present practices, future trends. *J. Radioanal. Nucl. Chem., Art.*, 1990, v.142, No. 1, p.303 - 320.
2. Phillips C. Uranium - plutonium partitioning by pulsed column in the first cycle of the three cycle thermal oxide reprocessing plant. *Waste'92, Proceedings (1992)* 1041- 1045.
3. J. A. Rard, M. H. Rand, G. Anderegg, H.Wanner. *Chemical thermodynamics 3. Chemical Thermodynamics of Technetium*. Edited by M.C.A. Sandino and E. Östhols, OECD NEA - Data Bank. 1999, Elsevier Pbl.
4. V.S.Koltunov, R.J.Taylor, T.V.Gomonova, O.A.Savilova, G.I.Zhuravleva, I.S.Denniss // *Radiochim. Acta* 88, 425-430 (2000).
5. N.Boukis, B.Kannellakopoulos // *Radiochimica Acta* 49. 141-145, (1990).
6. Zelvert A.: *Rapport CEA-R-5443*, (1988).
7. D.N.Tumanova, K. E. German, Ph. Moisy, M. Lecomte, V. F. Peretruxhin. In: *Abstracts of the 6-th International Symposium on Technetium and Rhenium – Sciences and Utilization*. NMMU - Port Elizabeth, 7-10 October 2008, p.46.
8. K. E. German, Ya. A. Obruchnikova, Ph Moisy , M. Lecomte, V. F. Peretruxhin. In: *6-th International Symposium on Technetium and Rhenium*. NMMU-Port Elizabeth, 7-10 October 2008, p.29.
9. K.E.German. *The Fourth Adv.-ORIENT Cycle Seminar. "New Resource Strategy Pioneered by Advanced Nuclear Science and Technology"*. Rokkasho-mura, Aomori, Japan, July 30, 2010. *Abstracts and presentations*, 2010 - Rokkasho-mura Nuclear Research Centre. Pp.1- 6.
10. K. German, A. Melentiev, V. Misharin et all. *Nucl. Med. Biol.* V. 37, No 6, (2010), P. 678.
11. K. German, A. Melentiev, V. Misharin et all. Tc-DTPA sediments formed in Tc-hydrazine-DTPA-nitric acid solutions. *Proceedings of the International Symposium on Technetium and Other Radiometals in Chemistry and Medicine – Forum Brixen – Bressanone Congress Center (Italy)* September 8-11, (2010). pp. 47 - 50.

12. C. S. Gong, W. W. Lukens, F. Poineau, K. R. Czerwinski. *Inorg. Chem.*, (2008), 47 (15), pp. 6674–6680.



ISTR2011 Delegates in Red Hall and Winter Garden of Presidium RAS



A. Maslennikov



2.6.

## COMPOSITION AND CATALYTIC PROPERTIES OF TECHNETIUM-BASED SEDIMENTS AND INTERPHASE SUBSTANCES FOUND IN THE URANIUM-PLUTONIUM SEPARATION STAGE OF THE PUREX PROCESS

D.N. Kolupaev<sup>1</sup>, A.B. Melentev<sup>1</sup>, A.N. Mashkin<sup>1</sup>, V.A. Misharin<sup>1</sup>, A.V. Ananyev<sup>2</sup>,  
V.P. Shilov<sup>2</sup>, K.E. German<sup>2</sup>, I.G. Tananaev<sup>2</sup>

<sup>1</sup>FSUE “PA“Mayak”, Lenin st., 31, Ozersk, Russian Federation, 456780, mayak@po-mayak.ru

<sup>2</sup>Institution of Russian Academy of Sciences – A.N. Frumkin Institute of Physical Chemistry and Electrochemistry of RAS, Leninskiy prosp., 31-4, Moscow, Russian Federation, 119071

**KEYWORDS:** technetium complexes, sedimentation, spent nuclear fuel, hydrazine

### ABSTRACT

This paper represents results of study of the composition and properties of sediments and interphase substances (IS's), found in the uranium/plutonium reductive separation apparatus, used in the Purex-type extraction reprocessing of VVER-440 and BN-600 spent nuclear fuel (SNF) on the RT-1 facility. It was found, that both sediments and IS's are based on the compounds of technetium and palladium and accumulate beta- and gamma-active nuclides. Frequency factors were obtained for the homogeneous and heterogeneous reactions of hydrazine and tetravalent uranium catalytic oxidation in presence of sediments and IS's. The polyaminocarboxylic nature of Tc compounds in sediments and IS's was shown with the methods of spectral analysis.

### INTRODUCTION

The SNF reprocessing by Purex requires extraction of U and Pu to the 30% TBP solvent in the HA extraction apparatus. The largest part of fission products (FP) remain in the aqueous stream and are directed to HA waste. Although, some FP's are extractable, and among them Tc should be noted as the element extracted close to 99% [1]. The flow of the loaded solvent (containing U, Pu, Tc, some other elements) goes to the most important and at the same time - very complicated operation of U/Pu separation.

The separation of U from Pu in the extraction reprocessing of VVER-440 and BN-600 SNF on the RT-1 facility of PA «Mayak» is achieved by using the reductive agent, containing U(IV), hydrazine, and the complexing agent (DTPA) for stabilizing purposes. As a result of this operation, Pu is reduced to trivalent inextractible state and U remains in solvent stream. The simplified flowsheet of the HA extraction cycle (incorporating the U/Pu separation apparatus) is shown on fig.1.

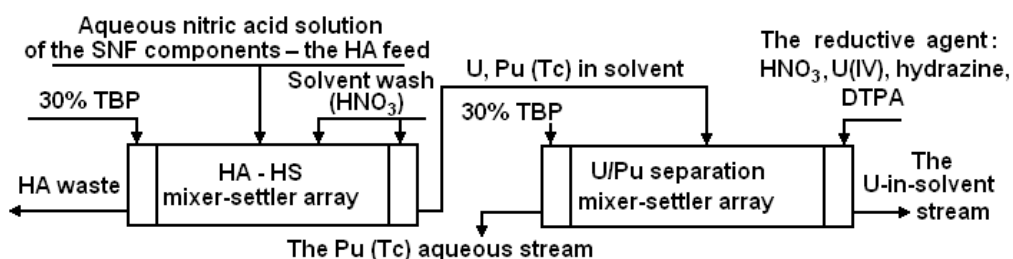


*Figure 1 – The flowsheet of the HA cycle*

Generally the extraction process functions properly, but sometimes the rapid consumption of reductive agents is observed at the U/Pu separation stage, and this leads to the malfunction of Pu re-extraction. The causes of these incidents remained unclear.

During the investigation of the problem the presence of sediments at the interphase boundaries and at the bottom of some stages of the the U/Pu separation mixer-settler array was uncovered, and samples were taken for research [2].

## EXPERIMENTAL

The samples of sediments and IS's were obtained from the stages of the industrial mixer-settler array with the peristaltic pump. Dissolution of sediments and IS's was carried out at 70-80°C in 6-7 M HNO<sub>3</sub> with addition of some H<sub>2</sub>O<sub>2</sub>. The inorganic components in solutions were determined by spectroscopy. UV-vis spectra were obtained with Varian Cary 50 and Perkin Elmer LAMBDA 35, gama-ray spectra - with SEG analyzer, and x-ray fluorescence spectra - with BHV-7 X-ray tube.

Processes leading to sedimentation and formation of IS's were studied using modeled HNO<sub>3</sub>-N<sub>2</sub>H<sub>5</sub>NO<sub>3</sub>-Tc-DTPA-UO<sub>2</sub>(NO<sub>3</sub>)<sub>2</sub> solutions, representing the systems typical for the operation of U/Pu reductive separation. IR spectra of the modeled precipitates which were formed in these systems, were acquired with Specord M80 and Thermo Nicolet Nexus, XRD - with DRON-3, and ESR with Bruker ESP 300. [Tc] was determined by beta-scint. counting at Beckman 6500 and with UV-vis spectroscopy.

For kinetics studies portions of sediments and IS's were placed in thermostatically controlled vials, HNO<sub>3</sub> solutions containing hydrazine were added. A row of kinetics experiments was also carried out with two phase systems where the aqueous HNO<sub>3</sub> phase contained the tetravalent uranium along with hydrazine, and the organic phase was 30% TBP in hydrocarbon diluent. Constant mixing was applied to these systems with the overhead stirrer. U(IV) and hydrazine content in the solutions were analyzed by titration at the exact time intervals.

## RESULTS AND DISCUSSION

### *The composition of sediments and IS's*

The sediments and IS's were located in mixer-settler array stages from 2 to 7 (this zone of the extraction apparatus prior to the feeding stage serves for the Pu re-extraction), and varied in density, color and quantity, with darker and more dense formations being found in stages 3, 7.

Elemental analysis had shown that the inorganic macrocomponents of sediments and IS's are Tc and Pd, and their content may exceed 30 and 6 g/dm<sup>3</sup>, respectively. Some steel corrosion products like Fe, Ni and Cr were detected. Uranium was also present, but it was not strongly associated to the sediments and IS's, probably being just mixed with the samples during the extraction process. Further research revealed that the total deposits of Tc in the extraction array may reach up to 520 g, deposits of Pd – up to 200 g. The content of non-organic components in samples is given in table 1.

Table 1 – Components of sediments and IS's found in the stages of mixer-settler array

Stage №	Phase	Component, g/dm <sup>3</sup>					
		U	Tc	Pd	Fe	Cr	Ni
3	IS	0,30	9,09	1,88	0,60	-	-
	Sediment	-	30,10	6,25	425	-	-
4	IS	0,30	5,92	0,62	0,30	-	-
	Sediment	1,75	27,14	4,30	-	0,75	0,40
7	IS	0,10	9,00	0,54	0,05	-	-
	Sediment	1,00	8,83	1,39	6,38	1,75	0,70
8	IS	-	4,87	1,41	-	-	-

Analysis has also shown that the sediments and IS's absorbed and concentrated the beta- and gamma-active nuclides (table 2). The most part of their activity is determined by <sup>106</sup>Ru, <sup>125</sup>Sb and <sup>134</sup>Cs. <sup>137</sup>Cs came second. The significant presence of <sup>95</sup>Zr and <sup>233</sup>Pa was also detected.

Table 2 - Activity of radionuclides in samples and accompanying phases for the 3rd stage of U/Pu separation mixer-settler array

Phase	Exposure dose, $\mu\text{R}/\text{sec} \cdot \text{dm}^3$	Nuclide activity, $\text{Bq}/\text{dm}^3$				
		<sup>233</sup> Pa	<sup>125</sup> Sb	<sup>106</sup> Ru	<sup>137</sup> Cs	<sup>95</sup> Zr
Solvent	0,022	$4,4 \cdot 10^4$	$5,3 \cdot 10^4$	$2,1 \cdot 10^7$	$2,0 \cdot 10^4$	$4,2 \cdot 10^3$
IS	7,1	-	$6,1 \cdot 10^7$	$7,8 \cdot 10^9$	$5,6 \cdot 10^7$	$1,5 \cdot 10^7$
Aq.	0,021	$3,0 \cdot 10^5$	$2,3 \cdot 10^5$	$1,5 \cdot 10^7$	$3,6 \cdot 10^5$	$8,7 \cdot 10^4$
Sediment	14,7	$1,2 \cdot 10^8$	$1,5 \cdot 10^8$	$1,6 \cdot 10^{10}$	$3,2 \cdot 10^7$	$2,6 \cdot 10^7$

According to table 2 both sediments and IS's are very active compared to the aqueous and organic phases, taken from the same mixer-settler. Concentration factors for gamma-emitting nuclides in the samples were calculated as a ratio of nuclides activity in sample to the activity in accompanying phase (aqueous for sediments and organic for IS's). These factors, varying from 10 to  $10^3$  (depending on the stage of mixer-settler array) are presented in table 3. The largest consecration factors were calculated for Cs and Ru in formations at the stage 3 of the extraction array.

Table 3 - Accumulation factors for radionuclides in sediments and IS's

Stage №	Phase	Nuclide accumulation factor				
		<sup>233</sup> Pa	<sup>125</sup> Sb	<sup>106</sup> Ru	<sup>137</sup> Cs	<sup>95</sup> Zr
3	IS	-	1150	370	2800	360
	Sediment	400	650	1060	890	300
4	IS	-	60	40	130	-
	Sediment	140	640	1350	20	440
7	IS	10	190	30	-	-
	Sediment	480	110	610	20	550
8	IS	-	90	50	270	-

### The causes for sedimentation

Palladium may become included in sediments and IS's dew to its fast reaction with the  $\text{HN}_3$  (the decomposition product of hydrazine) forming the insoluble Pd diazide, which in the presence of the organic phase (30% TBP) turns to a thick interphase film capable of absorbing different solid particles [3]. The reduction of Pd to metal by U(IV) may also contribute to this element accumulation in the extraction array [4], and it was shown that sediments containing Pd may form the IS's because of the azide formation even if there is no available Pd in aqueous phase [5]. But no data was available about the possible formation of insoluble Tc compounds causing the accumulation of this element in the extraction apparatus under the conditions of the U/Pu separation. In order to find out the reason for Tc deposition, modeled solutions imitating the aqueous phase of the extraction system were studied, and it was found that formation of sediments, fine flakes and thin films on the sides of reaction vessels takes place, although the process is not fast.

Sedimentation occurs within the large interval of  $[\text{HNO}_3]$  (from 0,5 to 3 M) and is accompanied with catalytic decomposition of hydrazine in presence of Tc, and only if DTPA or EDTA complexing agents are present in the solution.

On the initial stage of hydrazine-Tc interaction fast reduction of highly extractable septivalent form of technetium along with the decrease of free DTPA content was observed, but no sediments

were found at this stage (figure 2). Intensive sedimentation was detected visually and by the decrease of overall Tc content in solution along with the reoxidation of reduced Tc, and the gradual increase of [Tc(VII)]. Tc reoxidation occurred after the residual concentration of hydrazine in the studied solutions fell below 10% of the initial concentration. The presence of  $[\text{UO}_2(\text{NO}_3)_2]$  (0.21 mol/l) and increase of acidity speeded up the hydrazine decomposition and provided conditions for more rapid sedimentation.

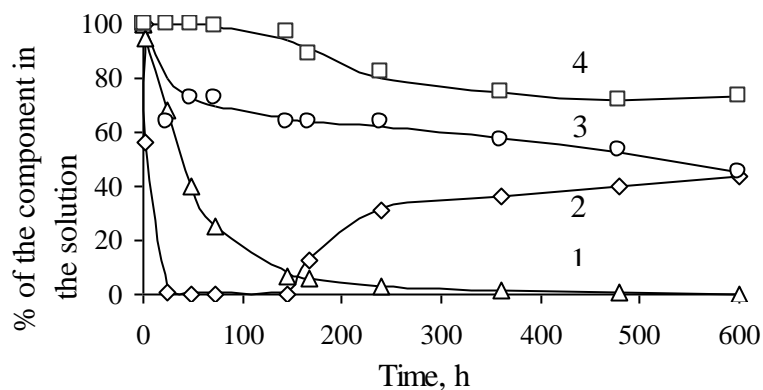
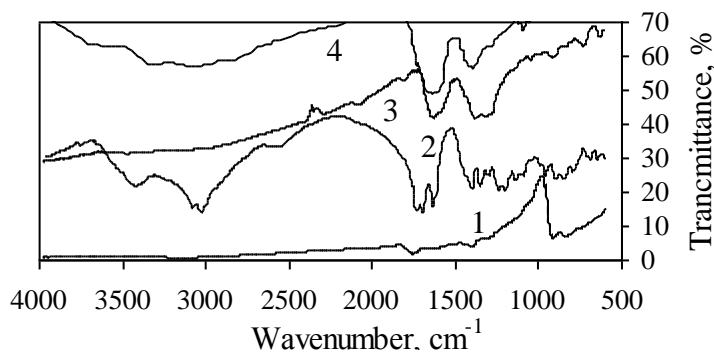


Figure 2 – Behavior of the modeled solution components  
 $[\text{Tc}]_0 = 2 \cdot 10^{-3} \text{ M}$ ;  $[\text{DTPA}]_0 = 0,5 \cdot 10^{-2} \text{ M}$ ;  $[\text{HNO}_3] = 1 \text{ M}$ ;  
 $[\text{N}_2\text{H}_5\text{NO}_3]_0 = 0,63 \text{ M}$ ;  $25^\circ\text{C}$   
 1 –  $\text{N}_2\text{H}_5\text{NO}_3$ ; 2 – Tc(VII); 3 – DTPA; 4 – Tc (total)

The Tc-DTPA precipitates were isolated from mother solutions and studied with a variety of methods (IR, ESR, XRD). The precipitate was completely X-ray amorphous. The IR spectrum of the precipitate (figure 3) demonstrated clearly that it is not  $\text{TcO}_2$  and gave evidence for the presence of strongly coordinated DTPA. Characteristic absorption shapes in  $1350\text{-}1600 \text{ cm}^{-1}$  and  $\sim 1040 \text{ cm}^{-1}$  shifted towards lower wavenumbers (compared to pure DTPA) indicate that there are carboxylic groups and nitrogen complexed to metal within the structure of the studied compound.

Figure 3 - The IR spectra of the modeled Tc precipitate (1), DTPA (2),  $\text{TcO}_2$  (3) and solid U-DTPA complexonate (4), as studied in [6]



Similar IR spectrum was obtained for the solid uranium-DTPA complexonate known from literature [6]. ESR gave evidence of tetravalent Tc present in the compound. The Tc - DTPA ligand ratio was found to be close to 1:1. Further investigation was carried out utilizing EXAFS and XANES methods on the K-edge of Tc, and the possible structure of the compound – the polynuclear oxo-bridged Tc polyaminocarboxylate, was proposed [7].

#### Catalytic properties of sediments and IS's

Due to the high Tc and Pd content (both elements being well known for their catalytic activity), the study was carried out for catalytic reactions of oxidation of the reducing agents used in the extraction reprocessing of SNF in presence of modeled and really isolated sediments and IS's. The frequency factors ( $K'$ ) for the reaction of hydrazine oxidation were obtained at variable temperatures and  $[\text{HNO}_3]$ .

With the heterogeneous catalyst (sediments or IS's) the induction period typical for the reaction was not distinguishable, but  $K'$  in all such systems was found to be lower, then in presence of the homogeneous catalyst – the  $\text{HTcO}_4$  (table 4). The catalytic activity of modeled sediments was more significant compared to the activity of the really isolated ones, which may be explained by the possible passivation of real sediments during their continuous contact with the environment of the U/Pu separation apparatus.

The studied catalytic process became more active upon heating. The rise of temperature from  $40$  to  $60^\circ\text{C}$  increased the  $K'$  for the real sediments more than tenfold.

Table 4 - Catalytic decomposition of hydrazine in presence of different Tc-containing compounds

Tc added to solutions as*	t, °C	[HNO <sub>3</sub> ], mol/L	Half decomposition of hydrazine, h	K' of hydrazine decomposition, h <sup>-1</sup>	Duration of fast reaction period, h	
HTcO <sub>4</sub>	40	0,5	2,5	0,307	4,5	
		1,0	1,4	0,454	1,5	
Modeled sediment		0,5	3,2	0,186	-**	
		1,0	2,3	0,303	-**	
Real sediment		0,5	> 6	0,035	-**	
		1,0	> 6	0,058	-**	
IS		1,0	4,0	0,180	-**	
HTcO <sub>4</sub>		60	0,5	0,7	1,320	1,0
			1,0	0,4	2,500	0,5
Modeled sediment			0,5	0,5	1,830	0,5
	1,0		0,45	1,950	0,5	
Real sediment	0,5		1,5	0,494	1,5	
	1,0		0,9	0,757	1,0	

\* - [Tc] in all systems = 1 · 10<sup>-3</sup> mol/l  
 \*\* - fast reaction period was not distinguishable

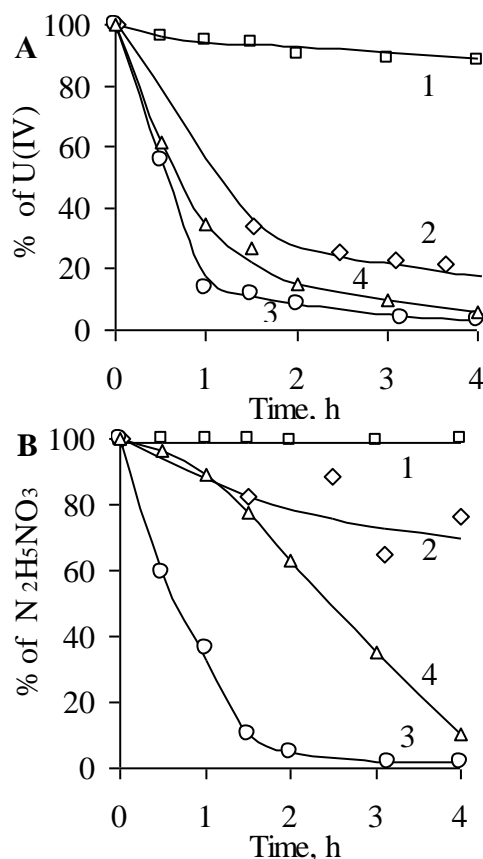
For more precise imitation a row of experiments was carried out with two phase systems and the U(IV) was added to the aqueous phase along with hydrazine. In these systems the constant mixing was applied using the overhead stirrer (figure 4).

Figure 4 - Oxidation of U(IV) (A) and hydrazine (B) in a two-phase system (HNO<sub>3</sub> - 30% TBP/ dodecane) in presence of HTcO<sub>4</sub>, Pd<sup>2+</sup> and Tc-containing sediment; [HNO<sub>3</sub>] = 1 M; [N<sub>2</sub>H<sub>5</sub>NO<sub>3</sub>] = 0,24 M; [U(VI)] = 0,336 M; [U(IV)] = 0,022 M; 40 °C; phase ratio 1:1; Catalyst added: 1 – non; 2 – [Pd] = 2 · 10<sup>-4</sup> M; 3 – [Tc] = 2 · 10<sup>-3</sup> M; 4 – modeled sediment ([Tc] = 2 · 10<sup>-3</sup> M upon complete dissolution)

A system with no catalytic additives has shown only a minor decrease in U(IV) content because of complex autocatalytic reactions in the organic phase, there the protective influence of hydrazine is absent [8]. In a system there Pd in a form of PdCl<sub>2</sub> was added, U(IV) oxidation was significant and some hydrazine was consumed. Formation of flakes (metal Pd) was observed within 40 min from the beginning of the experiment. With Tc added as HTcO<sub>4</sub> the rate and yield of oxidation of both U(IV) and hydrazine exceeded these parameters of all other systems.

The K' for the reaction of U(IV) oxidation were 0,026; 0,42; 1,74 and 0,69 h<sup>-1</sup> for the two-phase systems without any additives, with PdCl<sub>2</sub>, with HTcO<sub>4</sub> and with modeled Tc-based sediment, respectively.

It was also found that the catalytically active components may be leached from the sediments and the IS's into the solution adding the homogeneous factor to the heterogeneous catalytic process. Along with the rapid changes of temperature or HNO<sub>3</sub> content, the Tc (Pd) transfer to liquid phase becomes significantly more intensive, although the complete dissolution of sediments does not occur at the extraction process operating conditions (figure 5).





At  $[\text{HNO}_3] < 1,5 \text{ M}$  the effect of temperature on the dissolution of samples was insignificant. At  $60^\circ\text{C}$  less than 60% of Tc, and at  $40^\circ\text{C}$  – about 50 % were leached from the

samples within one hr. But with increase of acidity in solution from 1,5 to 3,0 M the raising of temperature from  $40^\circ\text{C}$  to  $60^\circ\text{C}$  caused almost complete leaching of Tc from the sediments. In 10 M  $\text{HNO}_3$  Tc was leached to 99% at all temperatures, although there was still some undissolved material left in the test sell.

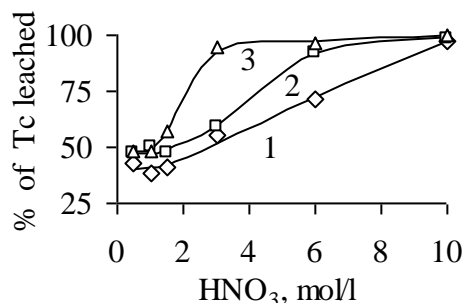


Figure 5 - Dissolution of the modeled Tc sediment at different temperatures and  $[\text{HNO}_3]$ ; Temperature: 1 –  $25^\circ\text{C}$ ; 2 –  $40^\circ\text{C}$ ; 3 –  $60^\circ\text{C}$

Increase of  $[\text{HNO}_3]$  or temperature in the industrial scale extraction process may lead to the dissolution of sediments and burst runout of catalytically active components to the aqueous phase. The described effects occurring in presence of sediments and IS's may be one of the possible reasons for the malfunctioning of the extraction process characterized by rapid destruction of reducing agents and the rise of temperature.

## CONCLUSION

The composition of sediments and IS's formed in the stage of U/Pu separation of the RT-1 flowsheet was defined. Tc and Pd are the major components of these sediments and IS's. It was found, that sediments and IS's collect and transport corrosion products and  $\beta$ ,  $\gamma$  – emitting nuclides ( $^{106}\text{Ru}$ ,  $^{125}\text{Sb}$ ,  $^{137}\text{Cs}$ ,  $^{233}\text{Pa}$ ,  $^{137}\text{Cs}$ ). The accumulation factors for some of these nuclides were found to be as high as  $10^3$ .

In the system Tc- $\text{HNO}_3$ -hydrazine-DTPA within the large interval of  $[\text{HNO}_3]$  Tc forms an individual insoluble compound – Tc polynuclear polyaminocarboxilate. This compound is formed mainly on the final stage of Tc-hydrazine reaction when Tc(IV) is slowly oxidized and most part of hydrazine is expended.

The Tc (Pd) containing sediments and IS's have an explicit catalytic effect on the process of hydrazine and U(IV) oxidation in  $\text{HNO}_3$  aqueous solutions. Increase of temperature or acidity speeds up the oxidation and initiates Tc leaching to aqueous phase. These factors may lead to fast consumption of reducing agents and malfunction of the U/Pu split apparatus.

## ACKNOWLEDGMENTS

The work was supported by RFBR grant 09-08-00153-a.

## REFERENCES

1. A.N.Mashkin, K.K. Korchenkin, N.A. Svetlakova et al, Radiokhimiya. 44: 34-40 (2002).
2. A.B. Melent'ev, V.A. Misharin, A.N. Mashkin, I.G.Tananaev, K.E.German. Abstracts of the 6-th Russian conference on radiochemistry, 12-16 Oct. 2009. Moscow.- Ozersk, FSUE Mayak, 2009, p. 209.
3. B.Ya.Zilberman, A.N. Mashkin, G.A. Lelyk et al, Radiokhimiya. 32: 45-49 (1990)
4. V.S.Koltunov, A.S. Kostikov, K.M. Frolov, Radiokhimiya. 32: 60-66 (1990).
5. D.N.Kolupaev, A.N. Mashkin, A.B. Melent'ev, I.G. Tananaev, Radiation Safety Problems. №1: 9-16 (2011).
6. G.I. Petrjak, G.S. Lojkina, S.S. Zelentsov, Radiokhimiya. 16: 386-390 (1974).
7. K.E.German, A.B. Melent'ev, Ya.V. Zubavichus et al, Radiokhimiya. 53: 155-161 (2011).
8. V.I. Marchenko, V.S. Koltunov, K.N. Dvoeglazov, Radiokhimiya. 52: 97-110 (2010).

2.7.

## INTERACTION OF MICROORGANISMS AND RADIONUCLIDES

T.V. Khijniak

Winogradsky Institute of Microbiology of RAS (Prospect 60-letiya Oktyabrya 7/2, Moscow, Russian Federation)

**Keywords:** sediments, bacterial reduction of radionuclides,  $^{99}\text{Tc}$ ,  $^{237}\text{Np}$ ,  $^{239}\text{Pu}$ ,  $^{244}\text{Cm}$

### Abstract:

Interaction of microorganisms with metals and radionuclides is quite complex and includes biosorption, bioaccumulation, bioleaching, biomineralisation and biotransformation. The microbial activity affects the red/ox state of elements and therefore affects their mobility in the environment. The reduction of long-lived radionuclides including Pu(V,VI), Np(V) and Tc(VII) is reviewed and the biogeochemical mechanisms of reduction are discussed.

### Introduction

Pollution of environment by toxic materials such as heavy metals and radionuclides is an important problem facing the postindustrial society. The radioactive wastes were intensively produced in course of fission materials production during 50 past years and it will be increasingly generated by various plants of nuclear fuel cycle. Safe treatment of the wastes of this type is an imperative to further nuclear cycle development. The laboratory studies show that during underground storage of waste 95-97% of radionuclides (Sr, Ru, Cs, Ce) precipitated. Remained solution contains long-lived elements (Tc, Pu, Np, U), which can migrate with pore water and therefore radioactive contaminated area enlarged. Microbial metal reduction results in the precipitation of a low valence, reduced form of the element, and have therefore been proposed as a strategy to treat contaminated waters.

There are many papers about using of biotechnological techniques for purification from uranium, strontium, cesium and iodine. In this study we paid attention to radionuclides of higher importance with respect to long-term radioactive waste control. Technetium-99, neptunium-237, plutonium-239, curium-244 are long-lived and mobile radionuclides and have high potential for biological uptake. The cases of penetration of those radionuclides to the environment were reported. However, published data on biological and physico-chemical mechanisms of actinide sorption by lake sediments and on kinetics of these processes are incomplete. We chose two lakes with different trophic types to test behavior of radionuclides ( $^{99}\text{Tc}$ ,  $^{237}\text{Np}$ ,  $^{239}\text{Pu}$ ,  $^{244}\text{Cm}$ ) in case of its penetration of water reservoirs as a result of catastrophes. Several low-valence forms of radionuclides are possible and it is important, therefore, to identify the products accurately so that the long-term stability and environmental mobility of microbially reduced species can be predicted.

### Results and Discussion.

Two typical fresh water lakes were chosen according to different biological productivity: highly productive eutrophic lake (Beloye Kosino, Moscow region, Russia) and a dystrophic lake (Shatura region, Russia) where organic matters present as humic and fulvic acids.

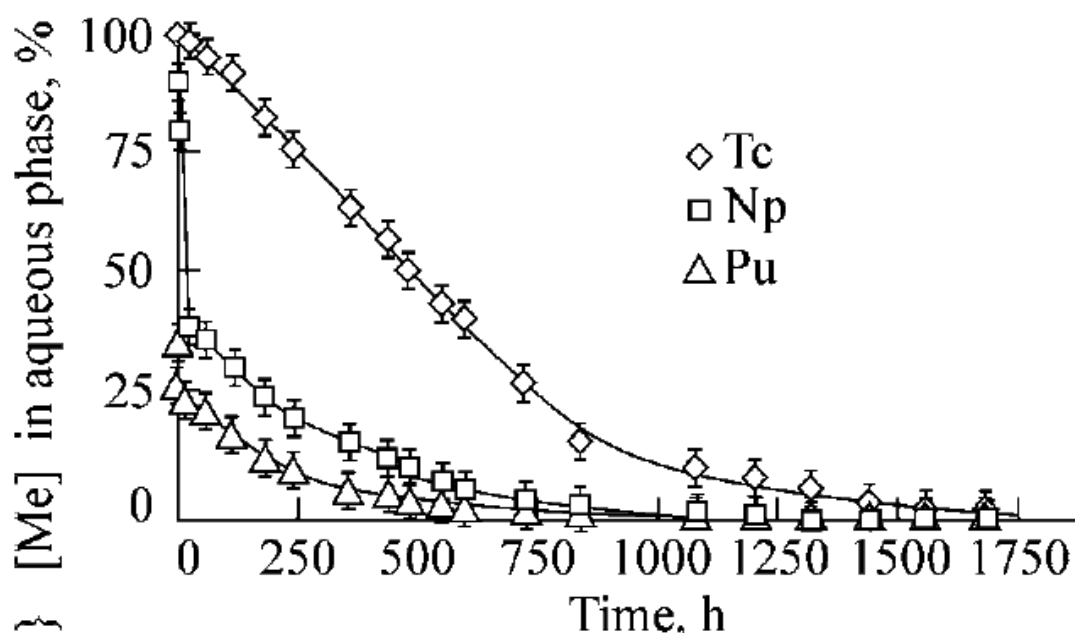


Fig.1. Uptake of long-lived radionuclides by sediments of eutrophic lake Beloe, Moscow region.  $[Tc]_0 = [Np]_0 = [Pu]_0 = 10^{-5} M$ .

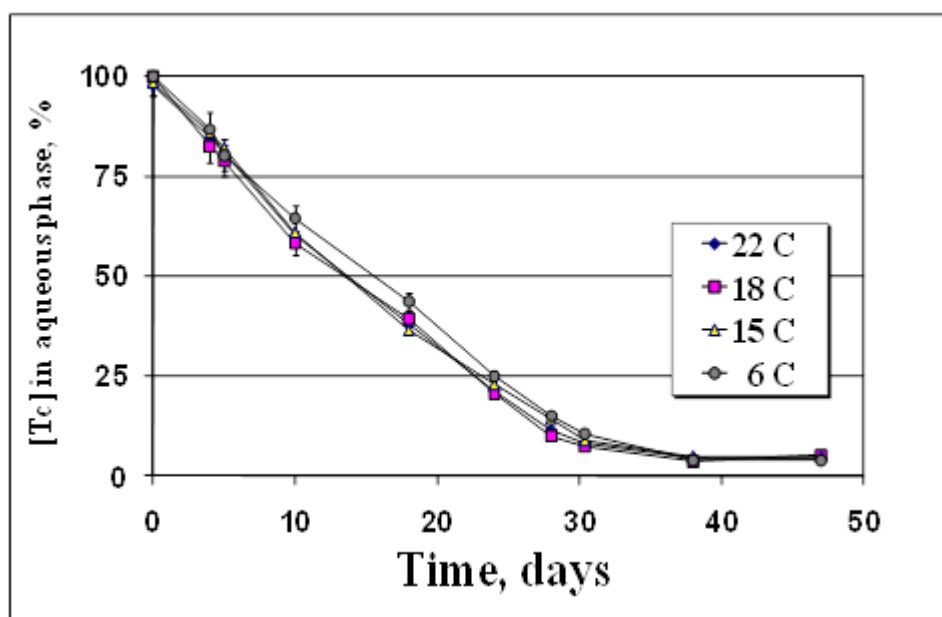


Fig.2. Temperature influence on Tc-99 uptake by eutrophic sediment.

The initial concentrations of radionuclides were  $10^{-5} - 10^{-4} M$ . Our laboratory model experiments indicate that uptake of radionuclides reached 98-99% during one summer season and biological processes play the significant role [1,2]. Our results shown that uptake of actinides from water should be considered as two-phase process – physico-chemical and biological phases (Fig.1) [2]. First phase was very fast (during 1-2 hours) and could be described as a sorption of actinides on the sediment particles. Neptunium sorption had fast uptake during first hour when 60% and 50% of initial input was sorbed by sediment of eutrophic and dystrophic lakes, and a slow bioaccumulation period when neptunium uptake was completed in 1 and 2 months for eutrophic (Fig.1) and

dystrophic lakes, respectively [3, 4]. In case of plutonium and curium, the first phase takes in 1 hour also, but sorption of radionuclides reached only 34-38% [2, 5]. The Tc uptake rate was almost constant, the time of half-uptake being 0.5-0.6 and 1 month for eutrophic and dystrophic lakes [2, 6-9]. The complete Tc accumulation by sediment took place after 1 and 2,5 months, respectively. Temperature dependence of radionuclides uptake was investigated also [3, 10]. Temperature dependence of Tc uptake rate was not very high, the uptake halftimes increasing from 16 to only 18 days with the temperature decrease from 15 °C to 6 °C (Fig.2). The microflora of lake played important role in the accumulation and reduction of some radionuclides [6, 11]. The additional donor or acceptor of electron can change uptake rate of Tc. Lactate or cut reed as the electron donors increase technetium bioaccumulation rate in case of sediments from eutrophic lake. The time of half-uptake take place in 10 days instead of 20 (Fig.3). Addition of sulfate or nitrate decreases the rate of Tc accumulation due to competition relationships between  $\text{SO}_4^{2-}$  or  $\text{NO}_3^-$  and  $\text{TcO}_4^-$  - the time of half-uptake of technetium prolong up to 30 days instead of 20 days (Fig.3) [3, 10]. In case of dystrophic lake organic matter decompose very slowly and not complete and form a lot of humic and fulvic acids. These acids have very high molecular weight, complex structure and can made complex with many elements, with heavy metals in particularly. Our experiments show that being added to water phase of dystrophic lake finally about 3% of Tc and 30% Np were bounded in water soluble complexes with natural humic acids precipitating on acidifying water to pH 1 (concentration of humic acids was up to 0,5%) [10, 12]. In the eutrophic lake water, the humic acid concentration was below 0,005% and the fraction of Np bound to them was no more than 1% [10, 13, 14].

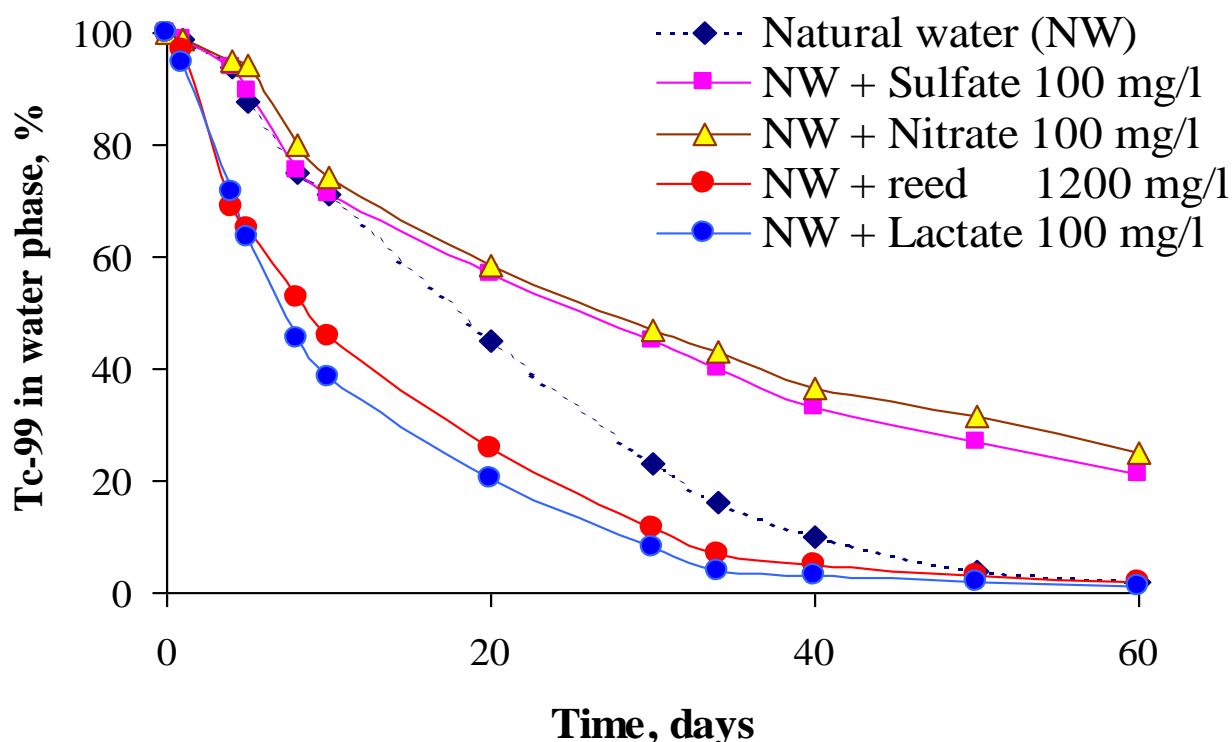


Fig.3. Substrate impact on Tc-99 uptake by eutrophic sediment.

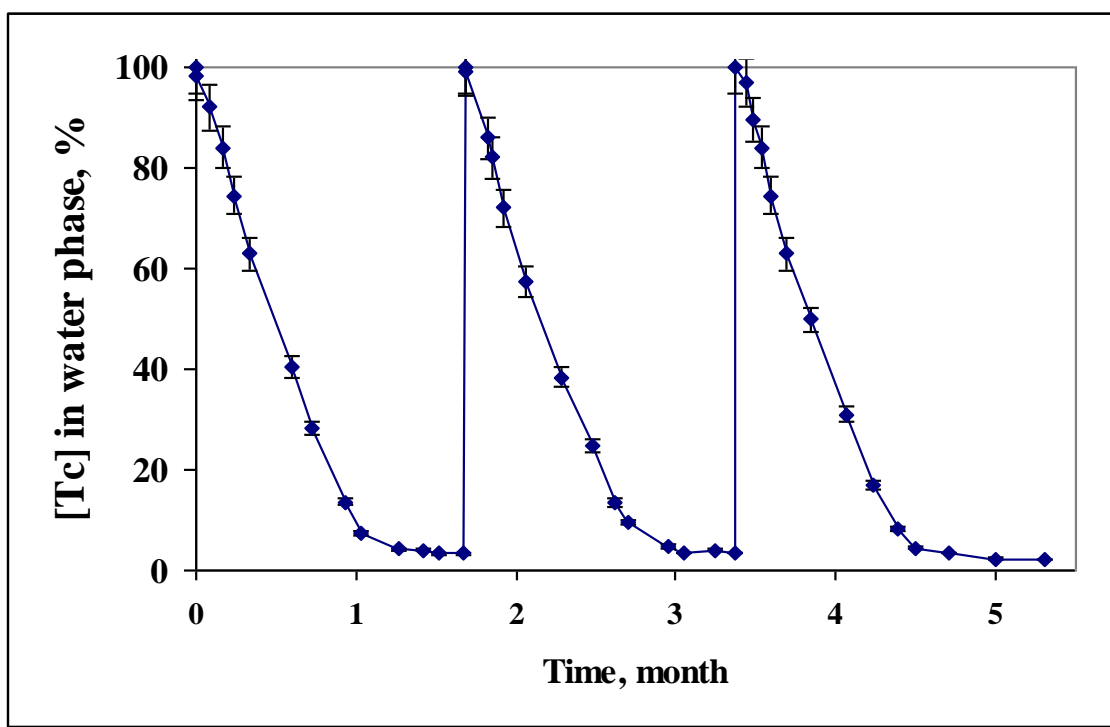


Fig.4. Multiple addition and uptake of Tc-99 by eutrophic sediment

The desorption of technetium was carried out with H<sub>2</sub>O, 1M HCl, 1M NaClO<sub>4</sub> or 15% H<sub>2</sub>O<sub>2</sub>. The desorption factors were 0.05, 0.05, 0.08 and more 0.99 thus indicating the technetium was sorbed by sediments as a reduced forms, which were generated by microorganisms. Thus, bacterial reduction of Tc is the main mechanism controlling the Tc transport to bottom sediments.

Microbial metal reduction results in the precipitation of a low valence, reduced, form of the element, and has therefore been proposed as a strategy to treat contaminated waters [16]. Sulfate-reducing bacteria *Desulfovibrio desulfuricans* (Fig.5) [17], metal-reducing bacteria *Shewanella putrefaciens* [18] and *Geobacter sulfurreducens* [19], *Escherichia coli* [20] and thermophilic archaea and bacteria *Thermoterrabacterium ferrireducens*, *Tepidibacter thalassicus* [21] were found to be capable of reducing Tc(VII) at neutral pH. In this case very soluble pertechnetate was reduced to insoluble TcO<sub>2</sub> via direct enzymatic reaction. Under acidic conditions, *Acidithiobacillus ferrooxidans* and *Acidithiobacillus thiooxidans* can also reduce Tc(VII) to low-valency forms with formation of brown colloid [22]. Some haloalkaliphilic bacteria (identified as *Halomonas*) isolated from soda lakes and soils were capable to reduce Tc(VII) under the alkaline anaerobic conditions (Fig.6) [23]. Several reduced species, including Tc(V), Tc(IV) and Tc(III) were identified under such conditions (Fig.7). The results of extraction clearly show that after 4 days of incubation under anaerobic alkaline conditions, an average of 76% of the 0.25 mM of pertechnetate had been reduced by haloalkaliphilic cultures to Tc(IV) and Tc(V) species. Within the pH range from 8 to 11, the anionic complex Tc<sup>IV</sup>O(OH)<sub>3</sub>(CO<sub>3</sub>)<sup>-</sup> is the dominant one.



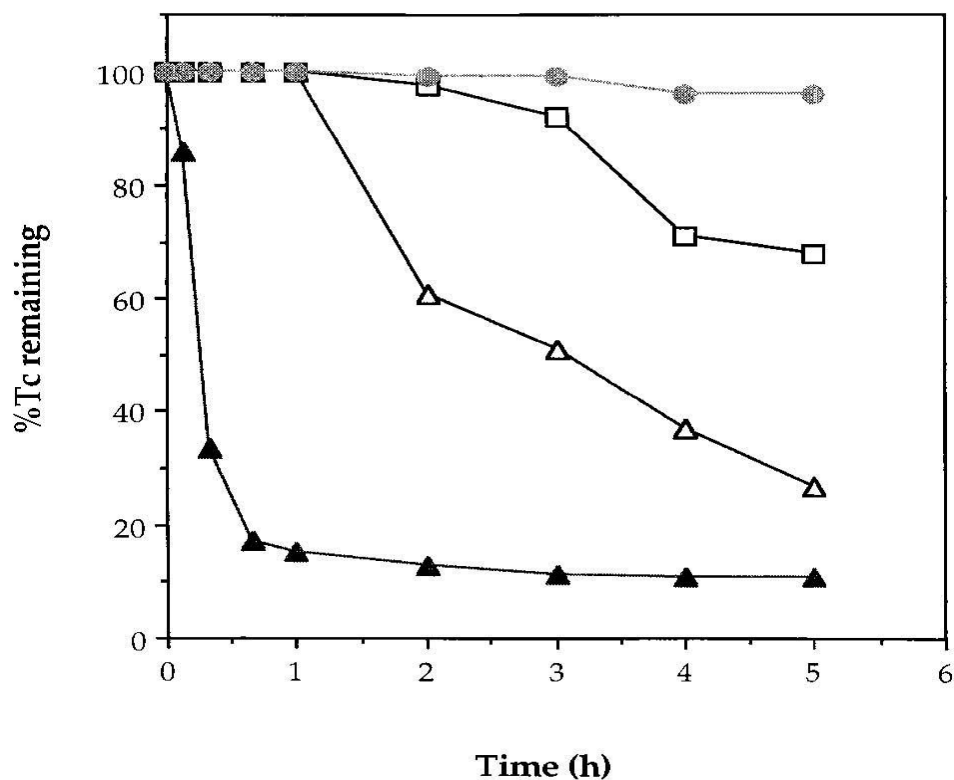


Fig.5. The reduction of pertechnetate by *Desulfovibrio desulfuricans*.  $[Tc]_0 = 0,25$  mM. 1- control, 2- lactate, 3- formate, 4- H<sub>2</sub>.

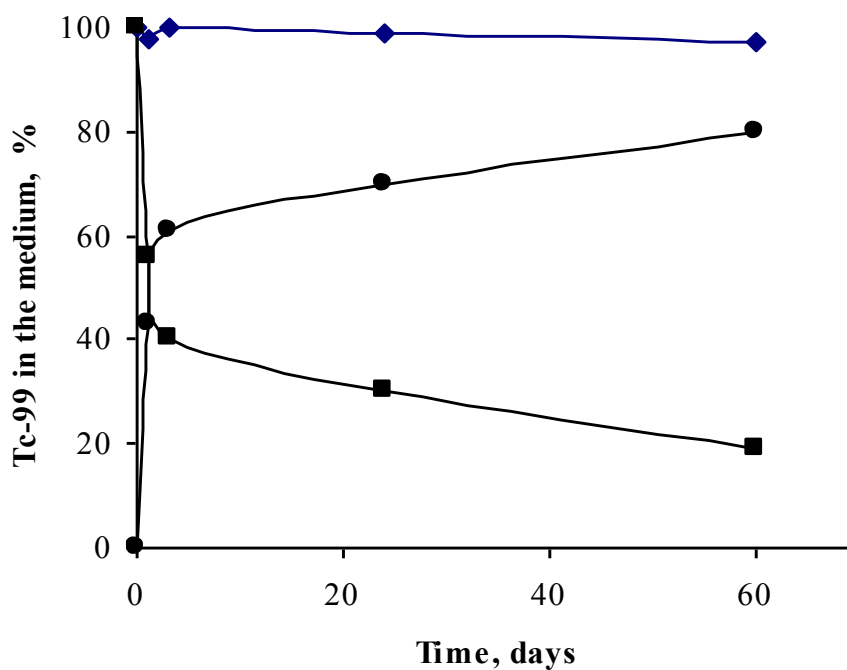


Fig.6. The reduction of pertechnetate by haloalkaliphilic bacteria.  $[Tc]_0 = 0,25$  mM, 1- control, 2 – Tc(IV), 3 – Tc(VII).

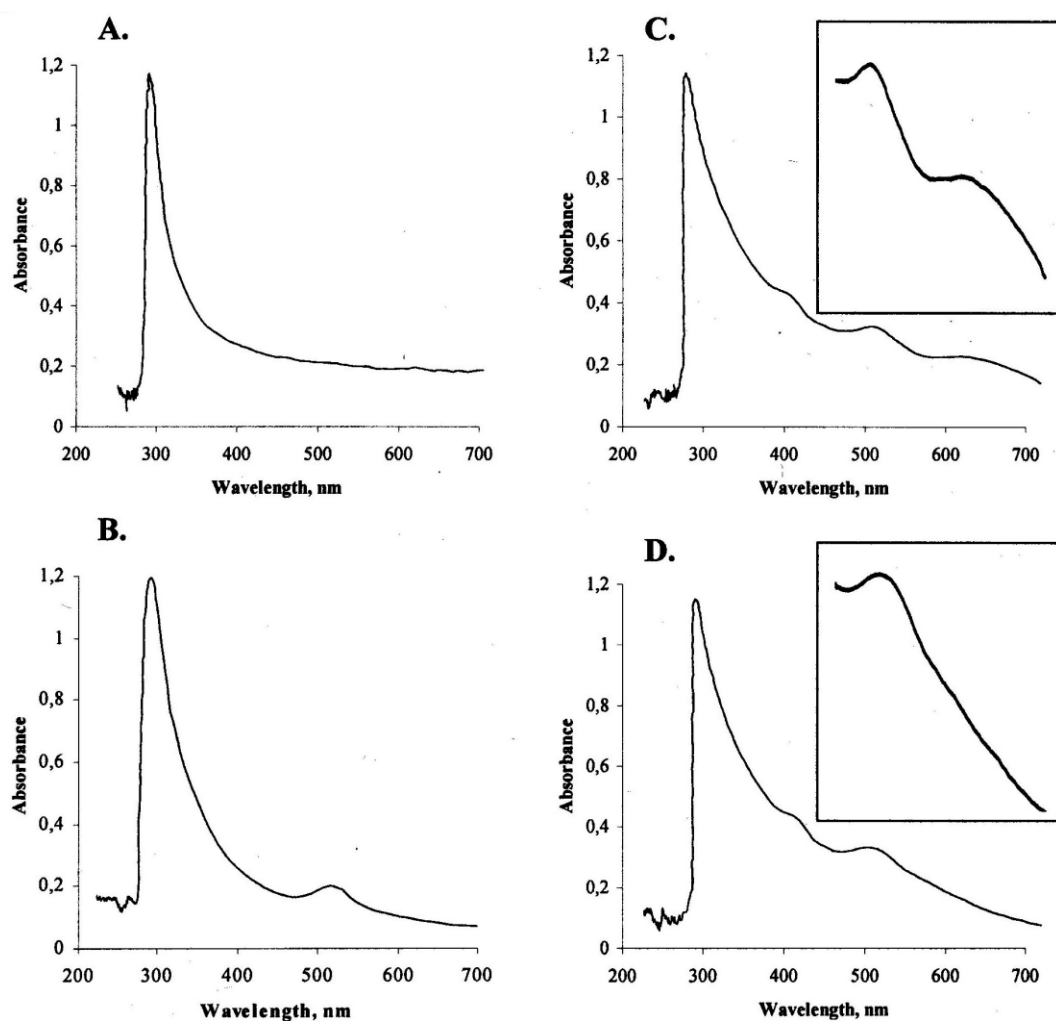


Fig.7. Spectrophotometric analysis of bacterial spent medium under alkaline condition.  $[Tc]_0 = 0,25 \text{ mM}$ ,  $\text{pH} 9.8$ ,  $t = 30$ . A - 0 hour, Tc(VII) at 290 nm, B- 3 days, Tc(VII) and Tc(IV) at 512 nm, C- 12 days, Tc(VII), Tc(IV) and Tc(III) at 628 nm, D – Tc(III) disappeared with addition of  $O_2$ .

The results of this research may be important for the fate and transport of technetium in the environment. Haloalkaliphilic heterotrophic microorganisms could provide a perspective for the biotechnological treatment of low level radioactive waste. Our isolates were capable of using formate, acetate, lactate, methanol and ethanol as electron donors and pertechnetate, nitrate, selenite, selenate, tellurite, chromate and elemental sulfur as electron acceptors [23]. This wide variety of substrates and resistance to high concentration of technetium make such bacteria attractive for biotechnological applications. However, the formation of highly electronegative soluble Tc(IV) carbonate complexes indicates that it may be necessary to reassess current concepts of Tc transport in anaerobic, carbonate enriched ground waters, where Tc mobility has been considered to be controlled by the low solubility of  $TcO_2$ .

## Conclusions.

Microbial reduction provides a great potential for remediation of low level radioactive wastes.

**Acknowledgments:** The work was supported by Russian Foundation for Basic Research grant 10-04-01500a.

## References.

1. German K.E., Khizhnyak T.V., Lyalikova N.N., Peretrukhin V.F. In: Russian Radiochemical Conference, Dubna, Abstracts, p.144 (1994).
2. Peretroukhin V.F., Khizhnyak T.V., Lyalikova N.N., German K.E. *Radiochemistry (Russ)*. **38/5**: 471-475 (1996).
3. Khijniak T.V., German K.E., Firsova E.V., Peretrukhin V.F., Medvedeva-Lyalikova N.N. *Ecological Chemistry (in Russ)*. **10/4**: 233-237 (2001).
4. Peretroukhin V.F., German K.E., Firsova E.V., Khijnyak T.V., Lyalikova N. N. Oral presentation at the 2-d Russian conference on radiochemistry. Dimitrovgrad, 27-31 October 1997. Extended abstracts, p.144-145.
5. Firsova E.V., German K.E., Peretroukhin V.F., Khijniak T.V. Fourth International Symposium and Exhibition on Environmental Contamination in Central and Eastern Europe. 1998. Abstracts, p.160.
6. German K.E., Khizhnyak T.V., Lyalikova N.N., Peretrukhin V.F. 5-th Annual Conference of the Nuclear Society, Moscow. Nuclear energy and Industry. Obninsk, 27 June - 1 July 1994, p. 498 - 499.
7. Khizhnyak T.V., German K.E., Lyalikova N.N., Peretrukhin V.F. The role of microorganisms, algae and organic remains of sediments in the behaviour of technetium in fresh water lakes. In: Abstracts 5-th Intern. Conf. on Chemistry and migration behaviour of actinides and fission products in the geosphere. MIGRATION'95. Saint-Malo, France, Sept. 10 - 15 , 1995, p.107 - 108.
8. Khizhnyak T.V., Lyalikova N.N, German K.E., Peretroukhin V.F.Uptake of technetium by bottom sediment of fresh water lakeand role of microorganisms in this process. Papers of Russian - Japanese Seminar on Technetium, July 1-5, 1996. p.38 - 39.
9. German K.E., Khijnyak T.V., Peretroukhin V.F., German E.S., Firsova E.V. Behaviour of technetium in eutrophic and dystrophicfresh water lakes. The second Japanese-Russian Seminar on Technetium. Shizuoka, Japan, Nov. 29 - Dec.2. 1999. Abstracts, pp.50-51.
10. German K.E., Firsova E.V., Peretroukhin V.F., Khijnyak T.V., Simonoff M. *Radiochemistry (Russ)*. **45/3**: 229-235 (2003).
11. German K.E., Khizhnyak T.V., Lyalikova N.N., Peretrukhin V.F. Technetium bioaccumulation by microorganisms. *Journ. of Nuclear Biology and Medicine*. **38/3**: 406 (1994).
12. German E., Firsova E., Khijnyak T., Lyalikova N., German K., Peretroukhin V. Studies of neptunium behavior in fresh water eutrophic and dystrophic lakes. Journees des actinides, 1999, 15-17 april , Luso, Portugal, Abstracts, pp.39-40.
13. Khijnyak T.V., German K.E., Firsova E.V., Medvedeva-Lyalikova N.N. Natural analog studies of Tc and Np behaviour in freshwater eutrophic and dystrophic lakes. Migration'99, Abstracts, Seventh International Conference on the Chemistry and Migration Behavior of Actinides and fission Products in the Geosphere. Incline Village, Lake Tahoe, Nevada, USA, September 26- October 1, 1999, p.48.
14. German K.E., Firsova E.V., Peretrukhin V.F., Khijnyak T.V. Simonoff M. Bioaccumulation of Tc-99, Pu-239 and Np-237 by bottom sediments of freshwhater lakes of Moscow Region. Extended synopses of reports. The 3-rd Russian-Japanese Seminar on Technetium, (Dubna, June 23 – July 1). – Dubna: JINR, 2002 – ISBN 5-85165-706-5. P. 14-16.
15. Barinova F.A., Bugaeva N.G., German K.E., Peretrukhin V.F. MODEL EXPERIMENTS ON BIOACCUMULATION OF TECHNETIUM AND THORIUM BY BOTTOM SEDIMENTS OF EUTROPHIC LAKES OF MOSCOW AND UDOMLYA REGIONS. International Symposium on Technetium - Science and Utilization - Oarai, Japan, May 24 - 27, 2005.

16. Lloyd J.R. *FEMS Microbiol. Rev.* **27**: 411-425 (2003)
17. Lloyd J.R., Ridley j., Khizniak T.V., Lyalikova N.N., Macaskie L.E. *Appl. Environ. Microbiol.* **65**: 26-91-2696 (1999)
18. Wildung, R.E., Gorby, Y.A., Krupka, K.M., Hess, N.J., Li, S.W., Plymale, A.E., McKinley, J.P., Fredrickson, J.K. *Appl. Environ. Microbiol.* **66**: 2451–2460 (2000)
19. Lloyd J.R., Sole V.A., Van Praagh C.V.G., Lovley D.R. *Appl. Environ. Microbiol.* **66/9**: 3743-3749 (2000).
20. Lloyd, J.R., Cole, J.A., Macaskie, L.E.. *J. of Bacteriology* **179**: 2014–2021 (1997)
21. Chernyh N.A., Gavrillov S.N., Sorokin V.V., German K.E., Sergeant C., Simonoff M., Robb F., Slobodkin A.I. *Appl. Microbiol. Biotechnol.* **76/2**: 467 – 472 (2007).
22. Medvedeva-Lyalikova N.N., Khijniak T.V. *Mikrobiologiya*, **65 (4)**: 533-539 (1996).
23. Khijniak T.V., Medvedeva-Lyalikova N.N., Simonoff M. *FEMS Microbiol. Ecol.* **44/1**: 109-115 (2003)



At the Poster Session (G.Sidorenko, A. Miroslavov and H. Braband)

2.8.

## LAYERED HYDRAZINIUM TITANATE: REDUCTIVE ADSORBENT FOR IRREVERSIBLE IMMOBILIZATION OF TECHNETIUM

S.N. Britvin, Y.I. Korneyko<sup>1</sup>, S.V. Krivovichev, W. Depmeier<sup>2</sup>.

Department of Crystallography, Geological Faculty, St. Petersburg State University (Universitetskaya Nab. 7/9, St. Petersburg, Russian Federation)

<sup>1</sup> - V.G. Khlopin Radium Institute (2-nd Murinsky Ave. 28, St. Petersburg, Russian Federation)

<sup>2</sup> - Institute for Geosciences, University Kiel (Olshausenstr. 40, Kiel, Germany)

Layered Hydrazinium Titanate - 9 Å (LHT-9) is a new nanohybrid compound related to a family of lepidocrocite-type layered titanates. Its chemical composition corresponds to the formula  $(\text{N}_2\text{H}_5)_{0.5}\text{Ti}_{1.87}\text{O}_4 \cdot \text{aq}$ . LHT-9 combines redox functionality of hydrazine, ion exchange properties of layered titanate and high specific surface area due to its quasi two-dimensional crystallites [1]. Superposition of reductive and ion exchange properties allows using LHT-9 as effective adsorbent capable of uptake of more than 50 elements of the Periodic system, with adsorption loadings approaching 20 wt. %. Ions of completely diverse chemical behavior, like pertechnetate anion  $\text{TcO}_4^-$  and cationic cesium  $\text{Cs}^+$  can be simultaneously adsorbed by LHT-9 involving reduction and ion exchange mechanisms, respectively. Herein we describe the adsorption properties of LHT-9 relative to the problem of  $^{99}\text{Tc}$  fixation [2]. Reductive precipitation is considered as the best way for fixation of Tc [3]. The proposed reductants (Fe(0), Fe(II),  $\text{NaBH}_4$ , sulfides, bioreduction), however, possess obvious drawbacks including (1) rather narrow pH working range and (2) inapplicability of adsorption products for long-time disposal of Tc. Hydrazine is well known reductant for pertechnetate, but the reduction products have strong tendency to retain unprecipitated in the parent solution [3]. LHT-9 overcomes this problem by irreversible *in-situ* adsorption of Tc(IV) onto nanocrystalline layered titanium dioxide matrix. Having rather wide working range from pH 1 to 10, LHT-9 is capable of Tc uptake from acid ( $\text{HTcO}_4$ ), neutral ( $\text{KTcO}_4$ ) and alkaline ( $\text{KTcO}_4 + \text{KOH}$ ) solutions, with uptake capacities up to 10 wt. %. It is even more important that adsorption products are therefore ready-to-use precursors for inexpensive one-pot preparation of stable Synroc-type titanate ceramics. Tc was found to incorporate into rutile  $(\text{Ti,Tc})\text{O}_2$ , hollandite  $\text{K}(\text{Ti,Tc})_8\text{O}_{16}$  and metallic Tc phases, the latter being considered as the most durable form for long-time Tc disposal [4]. Besides of removal of Tc from concentrated HLW solutions, LHT-9 can be used as effective additive into cementous waste forms allowing long-time disposal of Tc from low-level nuclear wastes containing trace amounts of pertechnetate ion.

**Acknowledgments:** The work was supported by Russian Federal Programme “Cadres” (contract 02.740.11.0326) and internal budget grant of St. Petersburg State University (no. 3.37.84.2011).

### References.

1. S. N. Britvin, S. V. Krivovichev, W. Depmeier, O. I. Siidra, D. V. Spiridonova, V. V. Gurzhiy, A. A. Zolotarev, *Patent Application* PCT/EP2010/001864 (2010).
2. N. N. Popova, I. G. Tananaev, S. I. Rovnyi, B. F. Myasoedov, *Russ. Chem Rev.* **72**: 101-121 (2003).
3. B. Gorski, H. Koch, *J. Inorg. Nucl. Chem.* **31**: 3565-3571 (1969).
4. N. P. Laverov, S. V. Yudintsev, B. I. Omel'yanenko, *Geology of Ore Deposits* **51**: 259-274 (2009).



2.9.

## Re AND Tc IN CERMET WASTE FORMS

S.V. Yudintsev\*, E.E. Konovalov\*\*, B.S. Nikonov\*

\* IGEM RAS, 119017 Moscow, Staromonetny 35, syud@igem.ru

\*\* FSUE «SRC RF – IPPE», 249033 Obninsk, Bondarenko 1

Method of producing matrices for joint immobilization of actinides and Tc by self-sustaining high-temperature synthesis, SHS has been suggested. More than 20 samples consisting of REE-Al-garnet (a target phase for actinides) and alloy (host for Tc) were obtained and studied. At the first stage radionuclides were replaced by Sm or Nd (imitator of REE-actinides fraction) and Re (Tc), one experiment was carried out with addition of technetium-99 along with Re.

Main phases of these ceramic – metal waste forms (or cermets) were REE-Al-garnet (60-70 vol.%), glass (15-20 vol.%), and alloy (10–15 vol.%). Sm and Nd enter into the garnet and glass, Re forms alloys with iron group elements or molybdenum. In spite of high temperature Re and Tc did not evaporate during SHS. Compositions of the metallic inclusions in cermets and partitioning of the elements of interest (Re, Tc) between co-existing phases were analyzed.

The results are compared with published data on (Re,Tc)-containing alloys prepared by sintering or melting in high-temperature Joule-heated furnaces and by arc melting route. Compositions of the Re-containing alloys in cermets and equilibrium phases in the Fe-Re and Mo-Re systems are discussed. Alternate method for synthesis of alloys with Tc is inductive melting in a cold crucible.

Special attention was paid to analysis of conditions for the Tc-containing forms safe geological disposal. The repositories should be located in crystalline rocks at depth of 500 m or below with slightly alkaline (pH ~ 8) and reducing (Eh < 0) properties of the underground waters. Indicator of such a geochemical media is a presence of minerals of Fe (II). In these environments Tc (IV) will be stable with a very low solubility of its solid phases –  $TcO_2 \cdot 2H_2O$  or  $TcO(OH)_2$ .

2.10.

## ELECTROCHEMICAL AND SPECTROELECTROCHEMICAL INVESTIGATIONS OF $\text{TcO}_4^-$ ELECTROREDUCTION IN ACIDIC MEDIA

M. Chotkowski, A. Czerwiński

Faculty of Chemistry, University of Warsaw (Pasteura 1, 02 – 093 Warsaw, Poland)

Despite many years of research on  $\text{TcO}_4^-$  ions electroreduction in the acidic solutions the mechanism of this process is still not fully understood [1]. Recent studies [2] indicate that in the highly concentrated  $\text{H}_2\text{SO}_4$  solutions the  $\text{TcO}_4^-$  ions transform into  $\text{TcO}_3(\text{OH})(\text{H}_2\text{O})_2$ . Generally, in the acidic solutions multistep mechanism is postulated. As a result of the subsequent steps of the  $\text{Tc(VII)}$  ions electroreduction the different forms of Tc at lower oxidation states [3-5] are formed. The aim of our study was to elucidate the mechanism of the  $\text{Tc(VII)}$  ions electroreduction on different surfaces (Au, Pt, RVC - reticulated vitreous carbon) and in a wide range of sulfuric acid concentrations (0.5-12M). Our study were carried out using electrochemical techniques (such as cyclic voltammetry, chronoamperometry coupled with UV-Vis spectroscopy and rotating ring disc electrode technique (RRDE)). The best characterised electrochemical waves are observed for gold surface. In strongly acidic solutions are recorded two main cathodic waves. Spectroelectrochemical measurements show that in the first step of discussed process one-electron, reversible reduction of  $\text{TcO}_4^-/\text{TcO}_3(\text{OH})(\text{H}_2\text{O})_2$  to  $\text{Tc(VI)}$  is observed. In the next step the formation of  $\text{Tc(III,IV)}$  ( $\lambda_{\text{max}} = 505 \text{ nm}$ ) is observed. The results indicate the mixed chemical(disproportionation) and electrochemical pathways for generation of  $\text{Tc(IV)}$  species.  $\text{Tc(IV)}$  ions can be reversibly reduced to the  $\text{Tc(III)}$  ions ( $\lambda_{\text{max}} = 670 \text{ nm}$ ). The stability of  $\text{Tc(IV)}$  and  $\text{Tc(III)}$  ions increase with increasing concentration of  $\text{H}_2\text{SO}_4$  in the solution. Further measurements using the rotating ring disk electrode allowed to provide us with additional informations regarding this process. In the hydrodynamic conditions two currents were recorded. The activation energy of the electroreduction process calculated for limiting current recorded at potentials lower than 0.4V vs. SHE in 4M  $\text{H}_2\text{SO}_4$  was  $12.30 \pm 1.14 \text{ kJ} \cdot \text{mol}^{-1}$ .

**Acknowledgments:** The work was financially supported by Faculty of Chemistry UW (BW – 191202).

### References.

1. Rard, J. A.(ed.); *Chemical Thermodynamics of Technetium*, Elsevier: New York, 1999, pp. 74-96.
2. F. Poineau, P.F. Weck, K. German, A. Maruk, G. Kirakosyan G., W. Lukens, D.B. Rego, A.P. Sattelberger, K.R. Czerwinski, *Dalton Trans.* **39(37)**: 8616-8619 (2010)
3. G. Horányi, I. Bakos, *J. Electroanal. Chem.* **370**: 213-218 (1994).
4. O.Courson, C. Le Naour, F. David, A. Bolyos, A. Maslennikov, N. Papadopoulos, *Czech. J. Phys.* **49**., 687-694 (1999).
5. B. Pihlar, *J. Electroanal. Chem.*, **102**: 351-365 (1979)

2.11.

## STABILIZATION OF RHENIUM (VI) COMPOUNDS IN SOLUTION AND USING THEM IN ANALYSIS

L.V.Borisova,<sup>1</sup> V.V.Minin<sup>2</sup>

<sup>1</sup>Vernadsky Institute of Geochemistry and Analytical Chemistry Russian Academy of Sciences, Kosygin str. 19, Moscow, 119071 Russia  
e-mail: [borisova19@yandex.ru](mailto:borisova19@yandex.ru)

<sup>2</sup>Institute of General and Inorganic Chemistry RAS, Moscow 119071, Leninsky str. 31. Russia.

**Keywords** : rhenium (VI), complex compounds, stabilization in solution, analysis

### Abstract :

The usage of the compounds with “unusual” oxidation states of rhenium (VI) is mainly determined by the possibility of their stabilization in solution. The stable Re(VI) oxohalide complexes ( $\text{ReOCl}_5^-$ ,  $\text{ReOBr}_4$ ) and series complexes with S-containing organic ligands in different systems ( $\text{ReO}_4^-$ ,  $\text{ReOCl}_5^-$ ,  $\text{ReOBr}_4 - \text{HCl}$  ( $\text{H}_2\text{SO}_4$ ) – L – solv.) has been established. The S-containing organic ligands ( dithionaphtol (DTN), monothiophenols and others) forms a stable brown-violet complexes with rhenium, which characterized by specific electron (UV-VIS) and magnetic (ESR) properties. On the basis of the properties of Re(VI) compounds a number of high specificity and sensitive methods ( ESR and ESP) of rhenium determination have been developed . Methods were used for determination of rhenium concentration in different natural and technical materials.

### Introduction

Rhenium, being a typical transition element, is characterized by a whole series of states of oxidation ( from +7 to –1), which it realizes in its compounds , manifesting differing reactivity and specific properties. Among them a special place is occupied by Re(VI), having one unpaired electron  $5d^1$ , exhibiting paramagnetism and characterized by specific parametric resonance (ESR) spectra in its compounds. They have not been used in practice, because of the absence of simple methods for obtaining of them in solution under usual conditions. The use of Re(VI) compounds deals with the possibility of their stabilization in solutions.

To improve the stabilization of the compounds of Re (VI) and create systems with stable forms of Re(VI), we studied the interaction of the Re(VII) and oxohalogenide complexes of Re(VI) with the nitrogen- and sulfur-containing organic ligands. The optimal conditions of complexes formations and ESR spectrum parameters have been determined. The quantitative formation of stable, paramagnetic Re(VI) complexes in acid, neutral and organic solution, equilibrium diagrams of Re compounds, their properties (redox, complex formation, catalytic, etc), mechanism of kinetic reactions were studied by us with the use of UV/VIS, IR, ESR, kinetic spectroscopy and other methods [1]. The cycle of our works on the stabilization of the compounds of Re(VI) in solutions made it possible to identify several systems where these compounds had adequate stability in the solutions and in the air, which made it possible to use their properties to develop the first quantitative methods for determining rhenium - photochemical, catalytic, ESR (and ESR spin-trap) and others methods [ 1 ] and apply them to analysis of rhenium- containing materials.

In this work we investigated complex of Re(VI) with sulfur –containing organic ligands in the systems: ( $\text{ReO}_4^-$ ), ( $\text{ReOCl}_5^-$ ), ( $\text{ReOBr}_4$ ) – HCl ( $\text{H}_2\text{SO}_4$ ) – L –  $\text{CHCl}_3$  and used them in analysis .

### Experimental

Reagents:  $\text{HReO}_4$ ,  $\text{KReO}_4$ , hydrochloric and sulphuric acids – analytical grade.  $\text{ReOCl}_5^-$  and  $\text{ReOBr}_4$  were prepared earlier [ 2 ], as it is shown below. Oxomonothiophenols and dithionaphtol have been synthesized in Inst. of Physical Chemistry ( AS Azerbaijan ). 0.1 M solutions of this

ligands was prepared by dissolving them in CHCl<sub>3</sub>. Apparatus: UV – Vis spectra were taken at Specord M- 40, ESR spectra – with Bruker E- 680X “ELEXYS”.

### The oxochloride complexes of rhenium (VI)

Rhenium (VI) oxochloride complex ReOCl<sub>5</sub><sup>-</sup>, stable in solutions, is formed in the following systems: ReOCl<sub>5</sub><sup>2-</sup>, (ReO<sub>2</sub>.aq), (ReO<sub>4</sub><sup>-</sup>) -H<sub>2</sub>SO<sub>4</sub>(H<sub>4</sub>P<sub>2</sub>O<sub>7</sub>) -HCl [ 3- 5 ], and the optimum conditions of its formation have been determined. It was also shown that solutions of the complex had a typical light absorption spectrum with an intensive band in the visible spectral range in contrast Re ( IV, V ) chloride complexes and ReO<sub>4</sub><sup>-</sup> ion, the intensive bands of which lie in the UV-range. The spectra parameters are given in Table 1.

Table 1. Parameters of electron spectra of some rhenium ions

Ions	λ max. ( ε max.)	Ions	λ max. ( ε max.)
ReO <sub>4</sub> <sup>-</sup>	230 ( 3.6.10 <sup>3</sup> )	ReOCl <sub>5</sub> <sup>2-</sup>	240 (5.6.10 <sup>3</sup> ), 410 (31), 480 (26), 750 (23)
ReOCl <sub>5</sub> <sup>-</sup>	275 (6.0.10 <sup>3</sup> ), 430 (4.0.10 <sup>3</sup> ), 560 (800)	ReCl <sub>6</sub> <sup>2-</sup>	281.5 (1.13.10 <sup>4</sup> )

Compounds of Re(VI), having one unpaired electron on the next-to-last 5d-electron shell ( 5d<sup>1</sup>, s=1/2) exhibiting paramagnetism and characterized by specific ESR spectra. The parameters of ESR spectrum of Re(VI) oxide chloride ( ReOCl<sub>5</sub><sup>-</sup> in H<sub>2</sub>SO<sub>4</sub> ) complex are following:

$$\begin{array}{cccc} g_{\parallel} & g_{\perp} & A_{\parallel} \times 10^{-4}, \text{ cm}^{-1} & A_{\perp} \times 10^{-4}, \text{ cm}^{-1} \\ 2.01 & 1.76 & 640 & 329 \end{array}$$

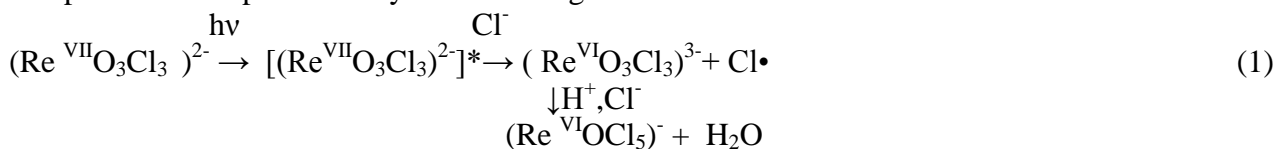
The presence of specific electron and ESR spectra has made it possible to develop a number of quantitative methods of rhenium determination on the basis of the formation of the oxopentachloride complex of rhenium.(VI) [ 6 ].

The quantitatively formation of ReOCl<sub>5</sub><sup>-</sup> complex have been established in following system, containing Fe( II ) as the reducer: Re(VII)-(H<sub>2</sub>SO<sub>4</sub>+HCl)-Fe(II) [ 7 ].

The use of iron (II) as a reduction agent allows to quantitatively reduce Re(VII) to Re(VI) in practically no time. It means that the formed compound is characterized by an intensive absorption band at 430 nm, reaching the maximum at Re(VII) : Fe(II)=1:1.

### Systems Re(VII)- HCl- hv ; Re(VII)-(HCl+H<sub>2</sub>SO<sub>4</sub>)-hv

We studied the photochemical reduction of rhenium (VII) to Re<sup>VI</sup>OCl<sub>5</sub><sup>-</sup> in the hydrochloric acid media and in mixtures of conc.HCl and H<sub>2</sub>SO<sub>4</sub> [ 8 ]. The mechanism of the changes in solutions was studied with the use of flash photolysis [ 9 ]. The formation of rhenium (VI) oxochloride complex can be represented by the following scheme:



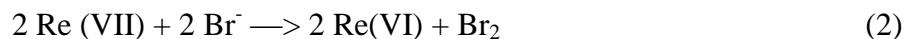
The quantitative formation of a stable complex of ReOCl<sub>5</sub><sup>-</sup> was achieved by irradiation of the 98% H<sub>2</sub>SO<sub>4</sub> and 2% HCl solution, containing rhenium (VII), in quartz cells (l=1 cm) with the UV-light of lamp BUV-15 (ν<sub>max</sub> =39400 cm<sup>-1</sup>).

It is shown that the solutions achieve stable optical density, when irradiation does not exceed 20-30 min. The formation of this complex was also confirmed by characteristic ESR spectra. Spectrophotometric and ESR methods for rhenium determination, based on photochemical production Re(VI) in conc. H<sub>2</sub>SO<sub>4</sub> have been developed with limit determination 1 μg /ml.

Thus, the photochemical reduction of rhenium (VII) to rhenium (VI) enables conducting reduction without introducing special reagents – reducers, and that is the priority of the method.

### System Re(VII), Re(V) – H<sub>2</sub>SO<sub>4</sub>- Br<sup>-</sup>

The formation of rhenium (VI) oxobromide complex was established in the systems: Re(VII) – H<sub>2</sub>SO<sub>4</sub> – Br<sup>-</sup>, Re(VII) – H<sub>2</sub>SO<sub>4</sub> – Br<sup>-</sup> - Solv. [10,11]. Complex ReOBr<sub>4</sub> in system ReO<sub>4</sub><sup>-</sup> - H<sub>2</sub>SO<sub>4</sub> – Br<sup>-</sup> is based on the reaction:



and has the advantages (a) readily, stable, perrhenate as starting material, (b) a quantitative and rapid reduction at room temperature, (c) after removal of bromine, ReOBr<sub>4</sub> can be quantitatively extracted into organic solvent and (d) product will not be subject to hydrolysis or oxidation in contact with the acid. Optimal conditions for ReOBr<sub>4</sub> formation have been chosen. It has been shown that ReOBr<sub>4</sub> forms in conc. H<sub>2</sub>SO<sub>4</sub> (> 16 M), Re: Br<sup>-</sup> ratio from 1:20 to 1:50, in 20-30 min after adding KBr, and remains stable for 2 hr and more. Absorption spectra of ReOBr<sub>4</sub> solution in sulphuric acid has the following parameters:  $\epsilon = 2200 \pm 140$  ( $\nu = 18000 \text{ cm}^{-1}$ ) and  $2050 \pm 100$  ( $\nu = 15300 \text{ cm}^{-1}$ ).

The ESR spectrum has the following parameters:  $g_{\parallel} = 2.17 \pm 0.005$ ,  $g_{\perp} = 1.765 \pm 0.005$ ,  $A_{\parallel} = 495 \pm 10 \text{ Gc}$ ,  $A_{\perp} = 340 \pm 10 \text{ Gc}$  [12-14]. No impurity ions practically complicate the determination by the ESR technique. Thus, fast and high selectivity spectrophotometric and ESR methods for rhenium determination, based on the formation of rhenium (VI) oxobromide complex are suggested.

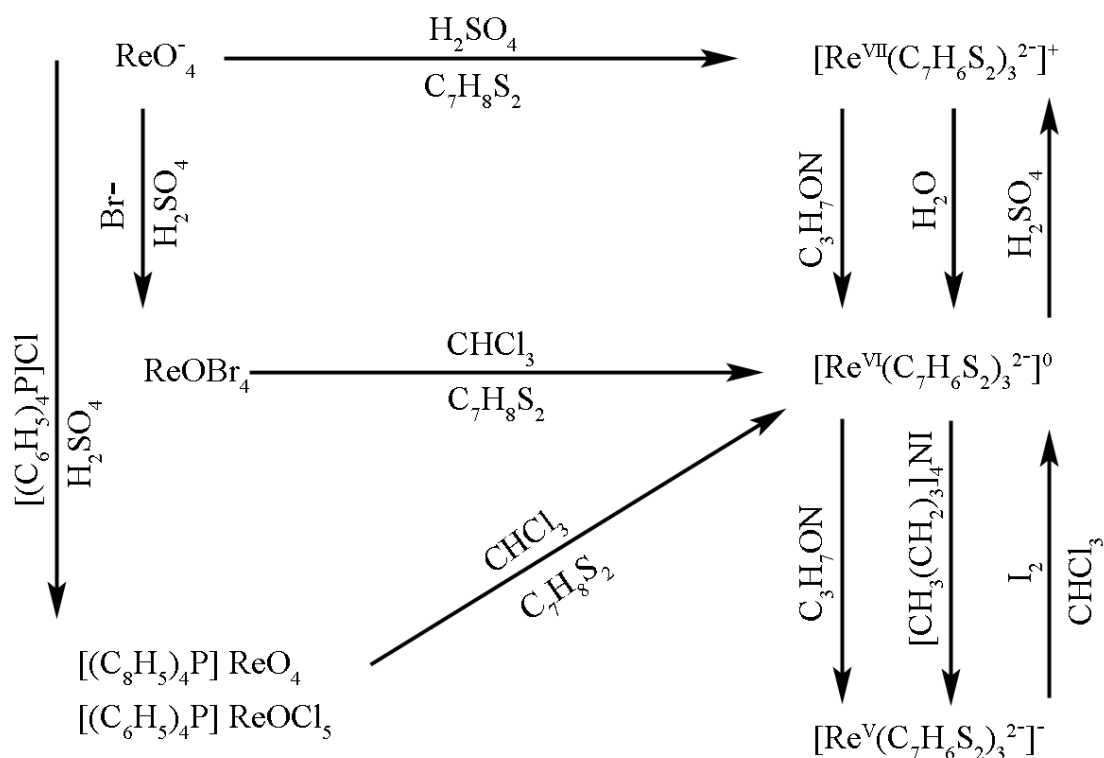
Rhenium (VI) oxotetrabromide is quantitatively extracted by chloroform, toluene and other solvents [11]. The Beer's law is valid for the ReOBr<sub>4</sub> extract in toluene within the rhenium concentration range of  $(2.5-50) \cdot 10^{-4} \text{ M}$ . The specific conditions of ReOBr<sub>4</sub> formation and the possibility to separate it from impurities by extraction have enabled the development of a high selectivity method of rhenium quantitative determination both in the spectrophotometric version and the ESR.

## Results and Discussion.

### Systems ReO<sub>4</sub><sup>-</sup>, (ReOCl<sub>5</sub><sup>-</sup>), (ReOBr<sub>4</sub>) – H<sub>2</sub>R

A number of organic sulphur-containing compounds form complexes with Re(VI), the chromophorous properties of which provide the possibility to use them in analysis. The high sensitivity reactions of rhenium with toluene-3,4-dithiol (H<sub>2</sub>Tdt), quinoxaline-2,3-dithiol (H<sub>2</sub>QS<sub>2</sub>) and thiophenoles in systems ReO<sub>4</sub><sup>-</sup>, (ReOCl<sub>5</sub><sup>-</sup>), ReOBr<sub>4</sub> – H<sub>2</sub>R - solv. by the spectrophotometric and ESR methods have been studied. The primary rhenium (VI) compounds were obtained with the use of the above methods in mixtures of sulphuric and hydrochloric (hydrobromic) acids. Various organic solvents, such as chloroform, chloric methylene, toluene, etc., were used as extractants. Tetraphenylphosphonium and tetraphenylarsonium chlorides were added to maintain the full transfer of the rhenium (VI) oxopentachloride complex into the extract. As it has been shown earlier, the transfer of ReOBr<sub>4</sub> into the extract is quantitative and fast. That simplifies the procedure and makes it more efficient for the analysis. The reactions can be represented by the following scheme (for example with C<sub>7</sub>H<sub>8</sub>S<sub>2</sub> – H<sub>2</sub>Tdt) [15]:





System  $\text{ReOBr}_4\text{-H}_2\text{Tdt-chloroform}$  was used to develop a high sensitivity and selective method of rhenium determination in the spectrophotometric version [16].

It was established that when  $\text{H}_2\text{Tdt}$  in chloroform is added to the  $\text{ReOBr}_4$  chloroform extract, a green complex with an intensive absorption band at  $14500\text{ cm}^{-1}$  ( $690\text{ nm}$ ,  $\epsilon = 2.4 \cdot 10^4$ ) is formed. The optimum conditions is the 20-30-fold excess of the reagent. The formed complex achieves the most intensive colour in 30-40 min, and it is stable for 10 or more days even when it contacts with water. The elemental analysis and spectrophotometric method corresponded to the composition  $\text{Re}:\text{H}_2\text{Tdt}=1:3$ .

The measurement of the molecular electroconductivity in the chloroform solution has shown that the complex is not electrolyte. In the IR-spectrum of the complex there were no bands typical for the  $\text{Re-O}$  in the range of  $800 - 1000\text{ cm}^{-1}$ . Solutions of the complex had ESR spectra. It was established that the ESR spectrum has the following parameters:  $g_1 = 2.044$ ,  $g_2 = 2.016$ ,  $g_3 = 1.999$ . On the basis of the obtained data was shown that the complex has the following composition:  $\text{Re}^{\text{VI}}(\text{Tdt})_3$  with a trigonal-prism structure, where  $(\text{Tdt})^{2-}$  is the bidentate ligand.

Unlike the galogenide solutions those of the dithiolate complex are characterized by a high stability in the air, enabling the development of a high efficiency extractational-spectrophotometric method of rhenium determination applied to the analysis of the concentrated technical sulphuric acid solutions. Under the optimum conditions of the complex formation the calibration diagram preserves its straight linearity in the rhenium concentration range of  $1 \cdot 10^{-5} - 1 \cdot 10^{-4}\text{ M}$ .

#### System $\text{Re}^{\text{VII}}\text{O}_4^- - \text{HCl} (\text{H}_2\text{SO}_4) - \text{dithionaphthol (monothiophenols)} - \text{CHCl}_3$

The quantitative formation of stable rhenium (VI) complexes with sulfur-containing organic ligands (L), such as dithionaphthol (DTN), mono-thiophenols (their derivatives) has been established in the systems, containing perrhenate- ion in acid (HCl or  $\text{H}_2\text{SO}_4$ ) and organic ligands in  $\text{CHCl}_3$  (and also in system  $\text{ReOBr}_4 - \text{CHCl}_3 - \text{L}$ ) with stirring in combination with UV/ VIS, IR, ESR and other methods. Complexes of rhenium with dithionaphthol and butylthiophenol have stability in solution in air and specific absorbance spectra with intense bands in the visible region of the spectrum and the electron spin resonance (ESR) spectrum characteristic of rhenium (VI).

Optimal conditions of complex formation in the system  $\text{Re (VII)} - \text{HCl} - \text{DTN} - \text{CHCl}_3$  are the 100 - 200 - fold excess of DTN, 11.5 M HCl,  $V_{\text{org}} = V_{\text{aq}}$ ,  $\tau = 40\text{-}50\text{ min}$  (stable for 2 or more

days). Optimal conditions of complex formation in the system  $\text{ReOBr}_4 - \text{CHCl}_3 - \text{DTN}$  are the 5-fold excess of DTN in  $\text{CHCl}_3$ ,  $\tau = 5$  min (stable for 5 or more days).

The composition of complex corresponded to the ratio  $\text{Re} : \text{DTN} = 1 : 2$ , as it was determined by molar ratio methods (Fig.1). Formula of complex can be described as  $[\text{Re}^{\text{VI}}\text{O}(\text{C}_{10}\text{H}_5\text{OHS}_2)_2]^0$ .

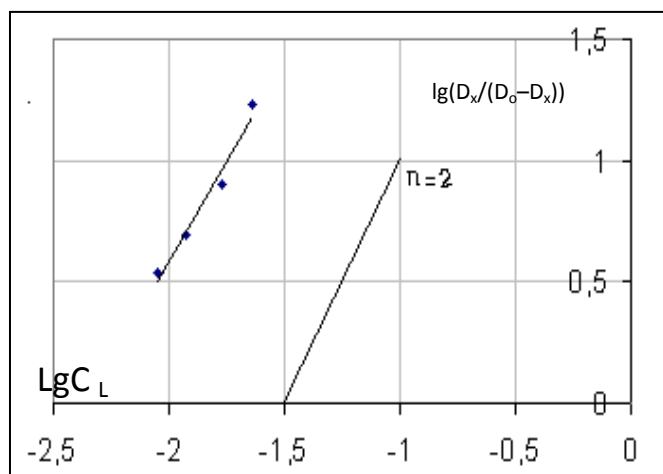


Fig.1. The composition of complex rhenium with oxidithionaphthol

The extract of this compound is characterized by absorption spectrum with the parameters -  $\lambda_{\text{max}} = 505 \text{ nm}$ ,  $\varepsilon_{\text{max}} = 1.5 \times 10^4$  (Fig. 2). Solutions of the complex had ESR spectra (Fig. 3). It was established that the ESR spectrum has the following parameters:  $g_{\parallel} = 2.059$ ,  $g_{\perp} = 1.979$ ,  $A_{\parallel} = 446 \text{ G}$ ,  $A_{\perp} = 34.9 \text{ G}$ .

After treatment of complex extract by 0.5 M  $\text{NH}_4\text{OH}$ , all elements (except Re complex) pass in aquatic-alkaline solution. No impurity ions practically complicate the determination by the ESR technique.

The specificity of the electronic spectra of rhenium (VI) complexes and their ESR spectra made it possible to develop quantitative methods for the determination of rhenium.

System  $\text{Re(VII)} - \text{HCl}_{\text{conc.}} - \text{DTN} - \text{CHCl}_3$  and  $\text{ReOBr}_4 - \text{DTN} - \text{CHCl}_3$  were used to develop a high selective methods of rhenium determination by spectrophotometry and ESR spectroscopy. For the determination of rhenium the main line in ESR spectrum was used.

The limit of detection for rhenium is  $0.15 \mu\text{g} / \text{ml}$ . The methods are applicable to the determination of rhenium in industrial sulfuric acid and several alloys (Fe-Ni-Re, Mo-Re, W-Mo-Re and other), in fumarole deposits (volcano Kudriavyy, Iturup isl., Kuril arc), ground water, plants samples under field conditions.

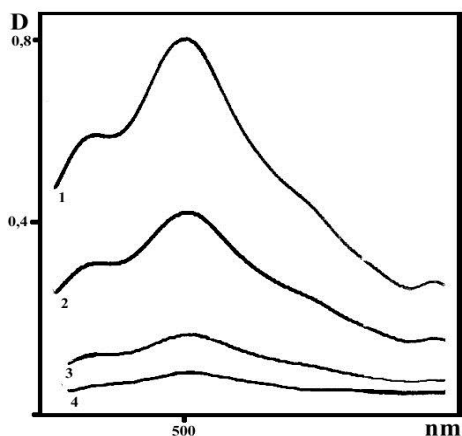


Fig. 2. Absorbance spectra of complex rhenium with oxidithionaphthol  $D=f[\text{Re}]$ .

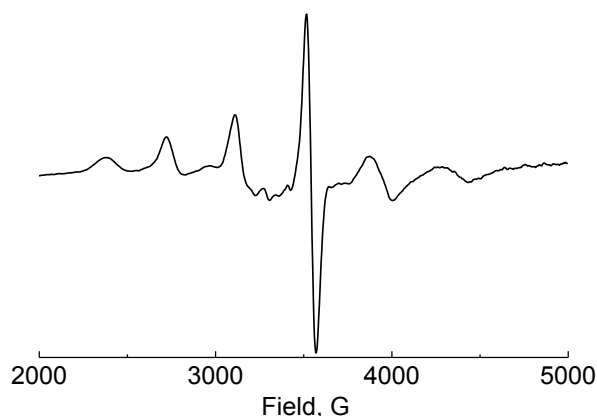


Fig. 3. ESR spectrum of rhenium (VI) with oxidithionaphthol.

## Conclusions.

Thus, the stabilization complexes of the unconventional oxidation state of rhenium with S-containing organic ligands (in the systems, where the oxohalogenide complexes of  $\text{Re(VI)}$  or perrhenate-ion used as starting materials) leads to develop the high selectivity and stability methods of rhenium determination (in the spectrophotometric version and the ESR) in contrast to

oxohalogenide complexes, which are sensitive to the action of water and atmospheric moisture (oxygen).

## References

1. L.V.Borisova . *Trends in Inorganic Chemistry* , review, , 2011 ( in press).
2. L.V.Borisova. *Analiticheskaya Khimiya redkih elementov*. M.:”Nauka” (1988), p. 169.
3. L.V.Borisova, A.N.Ermakov, O.D.Prasolova.*Dokl. AN SSSR* ( in Russian).**215**: 589 (1974).
4. O.D.Prasolova, I.I.Antipova-Karataeva, L.V.Borisova, A.N.Ermakov. *Zh. Neorg. Khim.* **25**:991 (1980).
5. L.V.Borisova,A.N.Ermakov, O.D.Prasolova. *Dokl. AN SSSR* ( in Russian) .**218** : 581 (1974).
6. I.N.Marov, L.V. Borisova, A.N.Ermakov. *Zh. Neorg. Khim.* **20** : 741 (1975).
7. L.V.Borisova, A.N.Ermakov, O.D.A.Prasolova. *Zh. Analit. Khim.* **31**: 504 (1976).
8. M.V.Koroleva, G.I. Romanovskaja, L.V.Borisova, A.K.Chibisov. *Khimiya visokih energii.* **18** : 47 (1984).
9. L.V.Borisova, M.V.Koroleva, A.K.Chibisov, Y.N.Dubrov. *Mikrochim. Acta.* **1**: 57 (1986).
10. L.V.Borisova, E.I.Plastinina, A.N. Ermakov. *Dokl. AN SSSR* ( in Russian)**223**: 609 (1975).
11. E.I.Plastinina, L.V.Borisova, O.M.Petruchin, *Zh. Neorg. Khim.* **27**: 457 (1982).
12. L.V.Borisova, A.N.Ermakov, E.I.Plastinina, O.D.Prasolova, *Analyst.***107**:.500 (1982).
13. L.V.Borisova, E.I.Plastinina, A.N.Ermakov,I.N.Marov,V.I. Zhukov. *Zh. Analit. Khim.* **33** : 978 (1982).
14. I.N.Marov,L.V.Borisova,E.I.Plastinina,V.E.,Zhukov. *Zh. Neorgn.Khim.* **21**: 1641 (1976).
15. L.V.Borisova,E.I.Prasolova,G.I.Evtikova,I.N.Marov. *Zh.Neorg.Khim.***35**:944 (1990).
16. O.D.Prasolova, L.V.Borisova. *Zh. Analit. Khim.* **44**: 346.(1989).



Excursion about Vorobiev Hills, Moscow (M.Ozawa, K.German, F. Poineau, W. Kerlin)

2.12.

## **NOVEL APPROACH TO THE MASS-SPECTROMETRIC DETERMINATION OF TRACE AMOUNTS OF RHENIUM USING ITS COMPLEXES WITH ORGANIC REAGENTS**

A.A.Grechnikov, L.V.Borisova, V.A.Ryabukhin

Vernadsky Institute of Geochemistry and Analytical Chemistry of Russian Academy of Sciences, Kosygin str., 19, 119071 Moscow, Russia.

**Keywords:** SALDI, mass spectrometry, rhenium complexes, quantitative analysis.

### **Abstract**

Novel approach to the determination of trace levels of rhenium has been presented. It involves the formation of rhenium complexes with organic ligands and the subsequent determination of obtained complexes using surface assisted laser desorption/ionization (SALDI) technique. A lab-built, linear time-of-flight mass spectrometer with a rotating ball interface was used in this work. Two different systems were studied: 1) Re complexes with thiourea or its derivatives, and 2) Re complex with 8-mercapto-quinoline. SALDI mass spectra of rhenium complexes were obtained in positive ionization mode. The detection limit of studied complexes was estimated to be less than 1 pg of analytes deposited on the ion emitter, with a potential for improvements.

### **Introduction**

Surface assisted laser desorption ionization (SALDI) is a novel method of ionization of organic and bioorganic compounds which has been under intensive development over the last decade. In SALDI the gas-phase ions are formed from molecules deposited on a particular surface substrate that is irradiated with a pulsed laser [1]. This process does not require the entrainment action of an added matrix compound for desorption and ionization. A variety of inorganic materials in the form of powders or monolithic plates were studied as a possible platform for SALDI, and it was found, that only a few selected substrates have the ability to strongly promote ion formation. Among them, silicon materials have been and still are the most commonly used as ion emitters in SALDI due to their high ionization efficiency and relatively soft ionization process. One of the prominent examples is amorphous silicon obtained by RF sputtering [2]. When compared to other forms of silicon materials, deposited amorphous films have a number of advantages, such as easy and controllable method of fabrication, greater uniformity over large areas, higher purity and good reproducibility.

Traditional field that SALDI has been applied to is the determination of organic and bioorganic compounds including drugs, natural products and peptides. Typically, SALDI sample preparation entails pipet deposition of a several  $\mu\text{L}$  droplet of the analyte solution on the surface of the SALDI-active substrate. The droplet is dried and the substrate inserted into the vacuum chamber for analysis. The main problem with this approach is very poor repeatability from substrate to substrate. Recently, the rotating ball SALDI interface with electrospray deposition for rapid, convenient and reproducible analysis of analytes in liquid solutions was developed [3].

In this paper we demonstrate that SALDI technique can be successfully used for elemental analysis. The focus of the present work is on the identification and quantitation of trace levels of rhenium using rotating ball SALDI interface.

## Experimental

The experimental setup has been described in detail earlier [3].

A lab-built, linear time-of-flight instrument with a 0.60m flight tube was used in this work. The free flight tube was biased at 2 kV and the rotating ball and substrates were grounded. The detector signal was processed by a 1 GS/s ADC averager. Two SALDI-active substrates, each 3x3mm, were installed on opposite sides of the ball. One side of the ball was exposed to atmospheric pressure and the other to the vacuum in a mass spectrometer. Analytes were applied using electrospray deposition to a silicon substrate on the atmospheric side, the ball was rotated 180°, and the analyte molecules were ionized and desorbed using laser irradiation. In order to utilize the analyte more efficiently, the laser focus was scanned over a 1×2 mm<sup>2</sup> sample deposition area using a computer-controlled dual-mirror scanner.

A diode-pumped Nd:YAG-laser with 355 nm wavelength (third harmonic), 0.5 ns pulse duration and 300 Hz repetition rate was used for the desorption-ionization. The laser pulse energy was varied in the range of 10-30 μJ using an attenuator.

Amorphous Si ( $\alpha$ -Si) films were deposited on monocrystalline silicon by standard RF sputtering of Si in a low pressure (10<sup>-3</sup> Torr) Ar atmosphere [2]. The thickness of the deposited film was approximately 0.5 nm.

All chemicals were obtained commercially and used without further purification. Rhenium complexes with thiourea and its derivatives were synthesized by method referenced in [4]. To 1 mL of HReO<sub>4</sub>, containing 1 g Re firstly was added 10 mL of 8 M HCl and then thiourea (Thio) at such a quantity to obtain Re:Thio = 1:10. The mixture was stirred for 3-4 h at room temperature, during which time a dark brown crystalline precipitate formed. This was filtered off, washed with cold water and then air-dried. The synthesized complexes were dissolved in methanol-chloroform (1:1) solvent.

Rhenium complexes with 8-mercapto-quinoline were synthesized by method referenced in [5]. To 8 mL of HReO<sub>4</sub>, containing 1 g Re was added 37 mL of concentrated HCl and 5 mL of 6% solution of 8-mercapto-quinoline in concentrated HCl. After warming at water bath, the reaction mixture was cooled and the synthesized complex was extracted in chloroform. The solutions of analyte in methanol-chloroform (1:1) were used for further SALDI analysis.

## Results and Discussion

The developed method for the determination of trace levels of rhenium is based on a formation of rhenium complexes with organic reagents and the subsequent determination of obtained complexes by SALDI technique. The main specific feature of organic reagents is that they should contain at least two essentially different functional groups. One of such group has the ability to form thermally stable complexes with Re while another one provides high effective ionization for subsequent mass-spectrometric detection.

Two different systems were studied in a view of possible applications for Re determination: 1) Rhenium complexes with thiourea and its derivatives, and 2) Rhenium complexes with 8-mercapto-quinoline.

All studied complexes are characterized by relatively high ionization efficiency. Also the relatively high mass spectrometric selectivity is obtained as a relatively high resolution,  $m/\Delta m$ , of ~800 is realized in mass spectrometer due to a short desorbing laser pulse and to a well defined ionization zone, located on the active surface of  $\alpha$ -Si substrate.



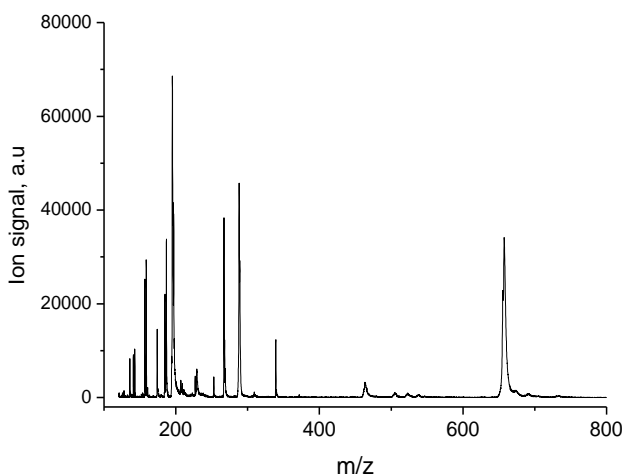


Fig.1. SALDI mass-spectrum of Re complex with phenylthiourea

amu was observed, as it is seen from Fig.1. On the one hand this yields structural information about studied complexes, but on the other hand, can strongly complicate the determination of Re complexes in the multicomponent mixtures.

For successful discrimination of a targeted analyte from interfering chemical noise mass spectra should be “clean” with low chemical background and with no or very specific fragmentation of ions of analytes. Such spectra were observed for another studied complex. Fig.2 shows a SALDI mass spectrum of 5 ng of Re complex with 8-mercapto-quinoline deposited on the  $\alpha$ -Si surface from a 500 ng/ml solution. The base peak in the mass spectrum corresponds to the molecule ions, and only two minor fragment ion peaks are observed.

Fig.3A demonstrates the molecular ion peak derived from the mass spectrum presented in Fig.2. It should be mentioned, that a relatively high mass-spectrometric resolution makes it possible to easily distinguish M and (M+1) peaks. It is seen from Fig.3A that the molecular ion peak consists of several isotopic lines. Among them the isotopic lines at  $m/z=521$  and  $m/z=519$  are the most abundant. It is well known that naturally occurring rhenium is 37.4%  $^{185}\text{Re}$  and 62.6%  $^{187}\text{Re}$ . The ratio of the areas of the peaks at  $m/z = 519$  and at  $m/z=521$  is 37.5/62.5 that is very similar to the Re isotopic composition. High accuracy of molecular mass determination in mass spectrometer as well as measured isotopic distribution makes it possible to determine the composition of the synthesized complex. Fig. 3B shows the isotopic distribution of the

Fig. 1 shows a typical SALDI mass-spectrum of about 50 ng of rhenium complex with phenylthiourea deposited on the  $\alpha$ -Si surface from a 10  $\mu\text{g/ml}$  solution. The peak with the maximal  $m/z$  value in the mass spectrum corresponds to the molecular ions and hence gives the information about the composition of the synthesized complex. According to the mass spectrum, the composition of these ions is  $(\text{ReOL}^1_3)^+$ , where  $L^1$  is phenylthiourea ligand. The ability of ionization technique to obtain the intensive molecular ion is very useful in practical mass spectrometric analysis.

However, the extensive fragmentation of desorbed ions in the mass region of 150-350

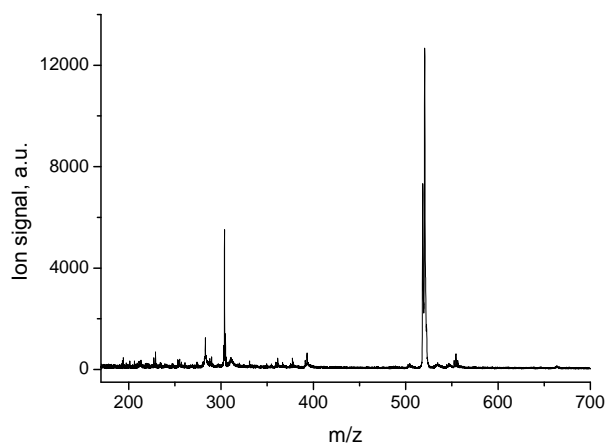


Fig.2. SALDI mass-spectrum of Re complex with 8-mercapto-quinoline

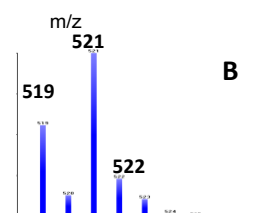


Fig.3. Molecular ion peak of Re complex with 8-mercapto-quinoline: A) - derived from the mass spectrum presented in Fig.2, B) – calculated.

molecular ion peak calculated for complex composition  $(\text{ReOL}^2_2)^+$ , where  $\text{L}^2 = \text{C}_9\text{NSH}_6$  (8-mercapto-quinoline – H). One can see that the measured molecular peak coincide with the calculated one, within the error of measurements.

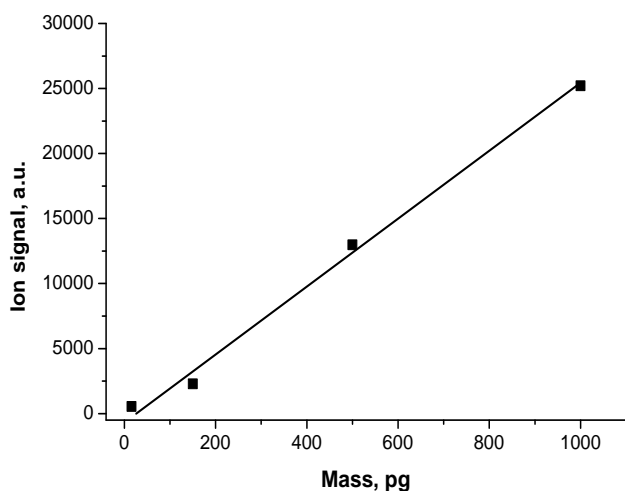


Fig.4. Analyte ion signal plotted against the mass of Re complex with 8-mercapto-quinoline deposited on the  $\alpha$ -Si surface

Rotating ball interface allows for deposition of controlled amounts of analytes. The SALDI ions signal was measured for different amounts of Re complexes with 8-mercapto-quinoline over a range of two orders of magnitude by changing the concentration of the solutions deposited. A typical dependence of the analytical signal on the mass of Re complex deposited on the  $\alpha$ -Si surface is illustrated in Fig. 4. The dependence is seen to be linear over the studied range. The relative standard deviation with 7 replicate analyses was less than 10%. These results clearly demonstrates that proposed technique can be successfully used for the quantitative analysis of Re. Limit of detection was estimated to be less than 1 pg of deposited analyte, with a potential for improvements.

## Conclusion

Novel approach to the determination of trace levels of Re, including the formation of Re complexes with organic ligands and the subsequent determination of obtained complexes by SALDI method has been presented. The reported results demonstrate that SALDI technique possesses high analytical potential for determination of Re in natural and technogenic samples.

## Acknowledgments

The authors are grateful for financial support from the Federal Agency for Science and Innovation Programs (grant № 02.522.12.2012) and the Russian Foundation for Basic Research Programs (grant №11-03-01080-a).

## References

1. IUPAC Project 2003-056-2-500.  
URL:[http://amitpatel745.files.wordpress.com/2010/10/iupac\\_ms\\_terms\\_second\\_draft1.pdf](http://amitpatel745.files.wordpress.com/2010/10/iupac_ms_terms_second_draft1.pdf)
2. S.S. Alimpiev, A.A Grechnikov., J. Sunner, V.A. Karavanskii, S.N. Zhabin, Ya.O. Simanovsky, S.M. Nikiforov. *J.Chem.Phys.* **128**: 014711 (2008).
3. S. Alimpiev, A.A Grechnikov., J. Sunner, V.A. Karavanskii, Ya.O. Simanovsky, S.M. Nikiforov. *Rapid Commun. Mass Spectrom.* **25**: 140–146 (2011).
4. L.V. Borisova , A.N.Ermakov . *Analytical chemistry of rhenium*, M., Nauka, 1974, p.99 (in russian).
5. Yu.A. Bankovsky, A.F. Ievinsh, Z.E. Liepinya, *Zhurn. analit. khimii* **15**: 78 (1960).

2.14.

## METHOD FOR HEXAMMINECOBALT (III) PERRHENATE SYNTHESIS FROM PERRHENIC ACID

K. Leszczynska-Sejda, G. Benke, K. Anyszkiewicz, A. Chmielarz, S. Cupial

Instytut Metali Niezależnych, 44-100 Gliwice ul. Sowinskiego 5, Poland

A method for production of high purity  $[\text{Co}(\text{NH}_3)_6](\text{ReO}_4)_3 \cdot 2\text{H}_2\text{O}$  from perrhenic acid obtained by ion exchange method was presented. The perrhenic acid production is based on sorption of ammonium ions on acid cation-exchange resin – Purolite C160(H) and regeneration of the ionite with 32% solutions of nitric(V) acid. In the result of thickening of the solution, which is generated after sorption, perrhenic acid is produced, containing 300-900 g/L Re and Ca < 0.001 %, K < 0.001%, Mg < 0.0001 %, Cu < 0.0001 %, Na < 0.0001 %, Mo < 0.0001%, Ni < 0.0001%, Pb < 0.0001%, Fe < 0.0001%,  $\text{NH}_4^+$  < 0.0003 %.

Studies into production of dihydrate of hexamminecobalt(III) perrhenate were conducted with application of  $[\text{Co}(\text{NH}_3)_6]\text{Cl}_3$  (by Acros Organics) as a source cobalt compound. Also substitution of the commercial product  $[\text{Co}(\text{NH}_3)_6]\text{Cl}_3$  with the produced in laboratory hexamminecobalt(III) chloride was examined as well as possibilities for direct precipitation of  $[\text{Co}(\text{NH}_3)_6](\text{ReO}_4)_3 \cdot 2\text{H}_2\text{O}$  from cobalt containing ammonia solutions.

It was found out that precipitation of  $[\text{Co}(\text{NH}_3)_6](\text{ReO}_4)_3 \cdot 2\text{H}_2\text{O}$  should be conducted from solution of Co content at the level of 50 g/L, in room temperature, with 60 % excess of rhenium vs. cobalt. It is important to use aqueous solution of perrhenic acid where rhenium concentration is over 100 g/L. The combined solutions should be intensively mixed for half an hour so the cobalt concentration in the solution after precipitation of  $[\text{Co}(\text{NH}_3)_6](\text{ReO}_4)_3 \cdot 2\text{H}_2\text{O}$  is <0.001 g/L. Solubility of the produced compound in water and in selected organic solvents was examined. It was established that  $[\text{Co}(\text{NH}_3)_6](\text{ReO}_4)_3 \cdot 2\text{H}_2\text{O}$  is slightly soluble in water (solubility in 25 °C – 0.3 g/L, and in 80 °C – 4.1 g/L) and in classical organic solvents such as ethanol, acetone. It is, however, readily soluble in DMSO and *N,N*-dimethylformamide. The solubility in room temperature was 500 and 600 g/L, respectively. It was established that the examined substance is stable in the temperature range up to 60 °C. In the temperature of 80 °C some mass loss was observed which prove removal of one water molecule. The temperature increase to 100 °C resulted in removal of the next water molecule. In the temperature range 100-180 °C a stable anhydrous hexamminecobalt(III) perrhenate was formed.

Application of the developed method resulted in production of  $[\text{Co}(\text{NH}_3)_6](\text{ReO}_4)_3 \cdot 2\text{H}_2\text{O}$  with efficiency of over 97 %, of following composition: 10.77 %  $\text{NH}_4^+$ , 6.22 % Co, 58.93 % Re and containing less than 150 ppm of impurities, such as sodium, chlorine, iron, nickel, chromium, potassium, magnesium and lead.

2.15.

## **MODERN X-RAY ANALYTICAL INSTRUMENTS OF BRUKER AXS**

D. Golovanov

Bruker Ltd., Moscow, Russia  
e-mail: [dg@bruker.ru](mailto:dg@bruker.ru)

Bruker company is widely pronounced manufacturer of industrial and scientific research instruments. Bruker AXS designs and manufactures analytical X-ray systems for elemental analysis, materials research and structural investigations. On the CIS region company is represented by Bruker Ltd. located in Moscow, Russian federation.

Bruker AXS produces wide range of X-ray diffractometers and spectrometers for different areas of application. Mentioned systems are installed in the most of leading research and industrial centers all over the world. That allows one to adopt produced equipment and to develop software for any urgent request from the customer.

For the “common” phase analysis of small amount of samples we offer table top diffractometer D2 Phaser. System allows one to do quantitative phase analysis and structure determination. Diffractometer comes fully equipped with evaluation and measurement software. In addition system equipped with Topas program suite for Rietveld based profile analysis. Diffractometer is fully self-contained and require no external water cooling or extra units for operation but only 220 V plug.

For higher level research we offer D8 Advance system. It can be equipped with a set of thermal chambers and X-ray optics. Diffractometer allows operation in different modes: Bragg-Brentano, parallel beam, several types of focusing geometry and others. One of the advantage of the D8 Advance is a wide set of detectors: scinti, line position sensitive detectors – solid state and gaseous, energy dispersive and 2-dimensional area detectors. Specially designed mounts allows changes in configuration without complicated alignment.

The rest of investigation areas can be accomplished with D8 Discover. Diffractometer features high resolution measurement and micro-analysis. System equipped with a wide set of precise X-ray optics and can be configured with rotating anode, microfocus source or sealed tube on demand.

Bruker Ltd company serves for all kind of customer relation. Our specialists develop a certain methodic for your measurements. Among sales activity we fully cover guarantee and service issues for all Bruker AXS customers.

2.16.

## PREPARATION OF $^{95m,g}\text{Tc}$ , $^{96}\text{Tc}$ BY IRRADIATION OF MOLYBDEN WITH ALPHA-PARTICLES AND DEUTRONS

R.A. Aliev

Lomonosov MSU

A method is proposed to produce the short-lived radionuclide  $^{95g}\text{Tc}$  via formation of the parent  $^{95}\text{Ru}$ . To produce  $^{95}\text{Ru}$ , the bombardment of molybdenum target of natural isotopic composition with  $\alpha$ -particles and the irradiation of ruthenium of natural isotopic composition with bremsstrahlung photons were used.

Irradiation of natural molybdenum stack foil target for 15 min with alpha particle beam (1  $\mu\text{A}$ ) followed by radiochemical separation yields 140 kBq of  $^{95g}\text{Tc}$  and 9 kBq  $^{96}\text{Tc}$ .

The  $^{95g}\text{Tc}$  obtained is of considerably higher purity than those formed by common ways (niobium or molybdenum irradiation with alpha particles). The main radionuclide impurity (that could not be avoided) is a small amount ( $9.1 \times 10^{-2} \%$ ) of long-lived  $^{95m}\text{Tc}$  isomer.

Attention was also paid to the production of side products such as  $^{95m}\text{Tc}$ ,  $^{96}\text{Tc}$  and  $^{97,103}\text{Ru}$ , in order to utilize optimally the energy of the alpha particle beam.



ISTR2011 participants in the Winter Garden of Presidium RAS



## 2.17.

### **MODERNIZATION METHOD FOR PRODUCTION OF FISSION Mo-99 FROM LOW-ENRICHED-URANIUM FOIL (LEU-FOIL)**

Sami M. Alwaer; Jalal; Basim

Tajoura Nuclear Research Center (TNRC)  
P.O.Box: 30878, Tripoli – Libya  
samiwaer@yahoo.com

#### **ABSTRACT**

Tajoura Nuclear Research Center (TNRC), Libya, will implement the technology for <sup>99</sup>Mo isotope production using LEU-foil target (This target is made of a LEU metallic uranium foil inserted between two concentric aluminium cylinders), to obtain new revenue streams for the TNR-reactor and desiring to serve the Libyan hospitals by providing the medical radioisotopes. Korean target will be used in this work which will be irradiated for 72 hours in the reactor core at flux equal to  $1.0 \times 10^{14}$  N/Cm<sup>2</sup>.S. The target will stay 10 h. in the reactor pool for cooling before disassembling it inside a hot cell located in the reactor building. The LEU-foil will be transferred to chemical hot cell pneumatically. A special set up has been designed for the processing of LEU-foil. The set up consists of the dissolver with controlled pressure, nitric acid will be used for dissolution, cold trap cooled in liquid nitrogen for removing the fission gases, precipitation of Mo-99 by fresh 2% alpha-benzoin-oxime will be done and purification of the final product by using two chromatographic columns: the first one contains AgC ( carbon coated with silver nitrate) and the second one is a combined column with C, HZO-1 (hydro zirconium oxide) and AgC. The final product of Mo-99 solution will be filtered with 0.22 µm filter. The final radioactivity of Mo-99 expected to be >150 Ci and 95% purity.

#### **INTRODUCTION**

Technetium-99m, the daughter product of Molybdenum-99 (Mo-99), is the most commonly utilized medical radioisotope in the world, used for approximately 20-25 million medical diagnostic procedures annually, comprising some 80% of all diagnostic nuclear medicine procedures [1,2]. National and international efforts are underway to shift the production of medical isotopes from HEU to Low Enriched Uranium (LEU) targets [3]. A small but growing amount of the current global Mo-99 production is derived from the irradiation of LEU targets. The IAEA became aware of the interest of a number of developing Member States that are seeking to become small scale, indigenous producers of Mo-99 to meet local nuclear medicine requirements. The IAEA initiated Coordinated Research Project (CRP) T.1.20.18 “Developing techniques for small-scale indigenous production of Mo-99 using LEU or neutron activation in order to assist countries in this field [4]. The more significant world crises are related to the availability of the <sup>99</sup>Mo/<sup>99m</sup>Tc generator, because of its extensive use and the short half life precluding significant anticipation [5]. Tajoura Reactor is a pool type reactor, moderated and cooled by light water located at the Tajoura Nuclear Research Center (TNRC). The reactor was designated to carry out experiments in field of nuclear physics and nuclear engineering, neutron activation analysis, solid state physics and isotope production. The reactor was put into operation at a power level of 10 MW in September 1983. [6]. The reactor was completely converted to Low Enriched Uranium (LEU, 19.7% of <sup>235</sup>U) fuel of type IRT-4M at the end of 2006; the new fuel is an alloy (matrix) of aluminum and uranium-dioxide (UO<sub>2</sub>-Al) with aluminum cladding.

## Experimental

### Annular Target Assembly Instructions [7]

#### 1.0 Prepare the Target Tubes:

Machine the inner and outer tubes the dimensions identified. Clean-off machining fluids from tubes using standard machine shop method.

1.1 Obtain dimensions of the inner and outer tubes prior to assembly.

a. Measure and record the I.D. and O.D. of the inner tube.

b. Measure and record the I.D. of the outer tube.

1.2 Clean the tubes, use powder-free latex gloves to handle the tubes to prevent particulate contamination of the weld faying surfaces.

1.3 Place in ultrasonic cleaner containing a solution of detergent for ~10 minutes at ~ 90°C, thoroughly rinse tubes in running water.

1.4 Bright Dip consists of 90 vol% concentrated H<sub>3</sub>PO<sub>4</sub> / 5 vol% H<sub>2</sub>SO<sub>4</sub> / 5vol% HNO<sub>3</sub>, thoroughly rinse tubes in running water.

1.5 Hot-air dry tubes for at least ten minutes at ~ 125°C using a heat gun (Fig. 1).



Fig.1. Inner and outer tubes

2.0 Prepare the Uranium Foil for Annular Target Assembly, two Ready targets have been prepared with LEU-foils with different sizes Table. 1. shows the measurements for LEU foils.

Table. 1. Measurements for LEU foils

ID No. of foil	Width (mm)			Length (mm)	Thickness (micron)			Av. Thickness (µm)	Weight (g)	Weight (U235)
	W1	W2		L	t1	t2	t3			
1	44.1	44.1	44.1	76	154	142	159	152	8.20	1.63
					124	156	105	128		
					167	162	176	168		
2	44.2	44.0	44.2	76.1	169	180	126	158	8.41	1.67
					120	157	194	157		
					155	122	166	148		

2.1 Envelope the uranium foil with the precut nickel-foil fission recoil barrier (Fig. 2).

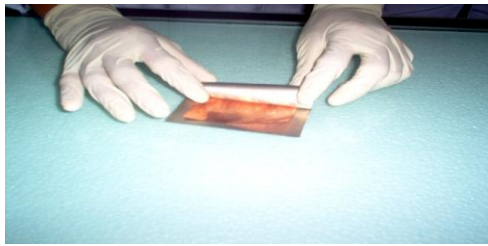


Fig. 2 Envelope LEU-foil with Nickel barrier

### 3.0 Annular Target Assembly

- 3.1 Coat the inside of the inner tube with “dry graphite”, this will act as a lubricant for the draw plug and prevent the inner tube from galling when drawing the inner/outer tubes together.
- 3.2 Clean the outer surface of inner tube ends to remove any excess graphite lubricant using a lint-free cloth moist with acetone.
- 3.3 Make a longitudinal permanent marker/ scribe mark on the outer tube to identify foil gap position, wrap the uranium/nickel foil around the inner tube, slide the inner tube into the outer tube and ensure that the foil gap is lined up with the scribed mark on the outer tube (Fig. 3).



Fig. 3 Target assembly

### 3.4 Electron Beam (EB) weld target ends and Helium leak test the assembled target, Fig.4.

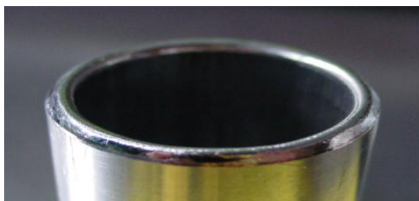


Fig.4 weld the ends

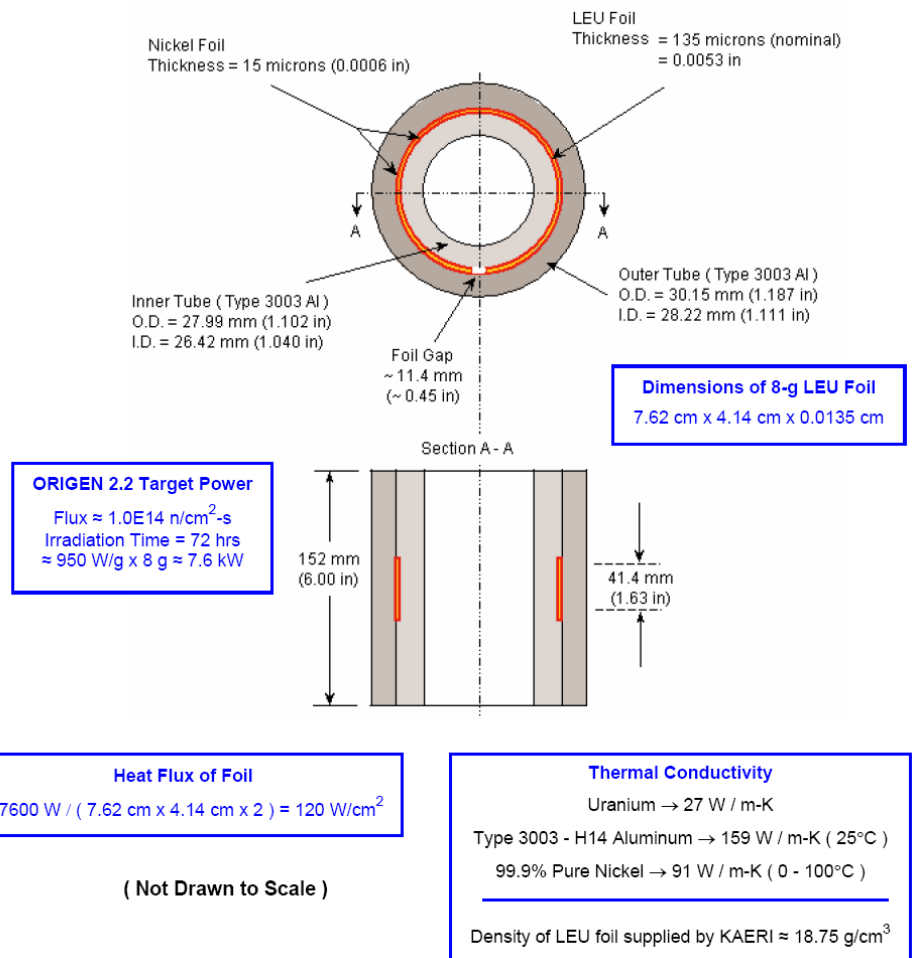
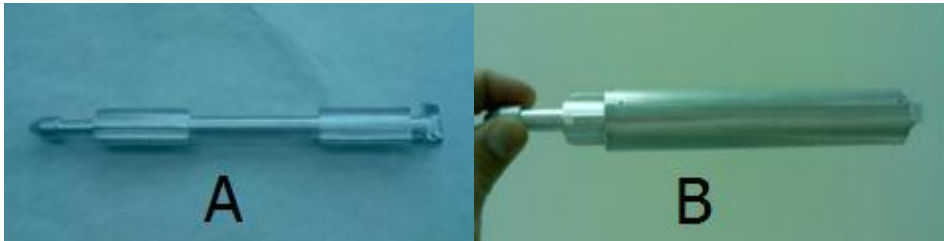


Fig. 5. LEU Target Horizontal, Vertical Cross Sections, and Dimensions.

3.5 Fig. 5 shows the LEU Target Horizontal, Vertical Cross Sections, and Dimensions [8].

### Target Irradiation

The ready target will be irradiated in the Reactor for 72 h. at a flux equal to  $1.0 \times 10^{14}$  n/cm<sup>2</sup>.S. and a special Rig has been made to handel the target during the irradiation, Fig. 6.



*Fig. 6 (A) the rig, (B) the rig with the target*

### Disassembling the LEU target

After irradiation, the target will be cooled in the reactor pool for 10 h. then the target will be transfered to a hot cell in the reactor bulding. Finally the target will be transfered to another hot cell which is just near the first one where the target will be dsassembled by using a special cuter (Fig. 7).



*Fig. 7. LEU target cuter*

Special toole has been made to determine the edges of the LEU target during the disassembling, another particular piece was manufactured for the purpose of the expansion of the shear longitudinal tube,( Fig. 8 & 9) respectively [9].



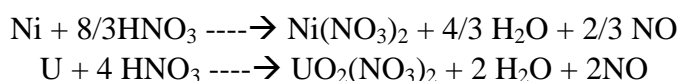
*Fig. 8*



*Fig. 9*

## LEU-foil processing

1. Calculate the concentration of nitric acid needed for 40 mL of dissolver solution. This calculation is based on the grams of total uranium and grams of nickel fission barrier for the target to be processed [10].



2. Remove foil from target and prepare for processing, place the foil in the dissolver, and verify it is setting directly on the bottom (use push tool if necessary).
3. Attach the dissolver to the vacuum pump (using the septum), open the valve between the septum and the dissolver, and evacuate the air from the dissolver (Fig. 10).



Fig. 10. Evacuate the air from the dissolver

4. Use the syringe to inject a 40 mL of dissolver solution which will be added to the dissolver through the dissolver septum. Heat the dissolver by using the heat gun (Fig. 11).



Fig.11. Heating the dissolver

5. When dissolution is complete, stop heating, allow dissolver to cool for 10 minutes and connect it to the cold finger. A special electric machine has been used for connecting the dissolver to the cold finger (Fig. 12).





*Fig.12. Connecting the dissolver and cold finger*

6. By a special crane inside the hot cell the connected dissolver and cold finger have been handled up and transferred to a special stand to insert the cold finger into the LN-Dewar, and liquid nitrogen flows to the Dewar (Fig 13). Allow the pressure to stabilize, and then slowly open the cold-finger and dissolver valves. Keep the cold finger in the liquid nitrogen and allow it to draw off the gas phase for 30 minutes. Close all valves and disconnect the dissolver from the cold finger by the same machine described in (Fig. 12). The vacuum inside the dissolver should be measured with a pressure/vacuum gauge.



*Fig.13 Cold finger in LN-Dewar*

7. Set the dissolver upright and vent it through a hypodermic needle. Invert the dissolver and fix it in its place in the setup and drain the solution into an evacuated double-ended bottle labeled “Raw Fission No. 1” through a 2-way “Luer-Lok” valve (Fig.14). Inject 25 mL of 1M HNO<sub>3</sub> into the dissolver and agitate it with the manipulators, making sure the acid solution wets the entire inner surface of the dissolver, Drain the rinse solution from the dissolver into the “Raw Fission bottle.”



*Fig. 14 drain the solution into an evacuated double-ended*

8.0. Add NaI carrier, Add 10% AgNO<sub>3</sub> in 0.1M HNO<sub>3</sub>, shake, a white precipitate should form, Add 1.0 M HCl additional Precipitate should form and Add Mo carrier.

9.0. A sample of ~0.5 mL should be collected to measure Mo-99 content of the sample for calculating process yield.

10.0. Pass the solution through 0.3μm and 0.2μm filter assembly into another bottle (Fig. 15).



*Fig. 15 Pass the sol. through 0.2μm filter*

11.0 Add 2.5% KMnO<sub>4</sub> solution slowly to the raw fission liquor until a deep pink color holds for ~30 seconds, Add 1.5 mL of Rh carrier to the raw fission liquor, and shake, Add Ru carrier and shake, Add fresh 2% alpha-benzoin-oxime in 0.4M NaOH to the raw fission liquor, shake well. Wait about one minute. A white, flocculent precipitate should form.

12.0 Filter the precipitate through a 51-mm fritted-glass column. Make sure all liquid is drained from the column. Wash the precipitate in the column five times with 10 mL of 0.1M HNO<sub>3</sub>; shaking the column well after each wash is injected. Drain these washes into the “Acid Wash” bottle (Fig 16).



*Fig. 16 Mo-99 ppt. filtration*

13.0 To dissolve the precipitate, inject 0.4M NaOH sol. with ~1% H<sub>2</sub>O<sub>2</sub> into the column, vent through a charcoal filter, Heat the column that contains the solution with forced hot air until the solution begins to boil, drain the dissolved precipitate into a bottle.

14.0 Pass the dissolved precipitate through the AgC column. Gravity controlled flow through the column allows a flow rate of 1 - 3 mL/minute. Rinse the AgC column with 0.2M NaOH (Fig. 17). The sol. should appear clear and colorless. Add NaI carrier to the bottle and add 10% AgNO<sub>3</sub> in 0.1M HNO<sub>3</sub> solution to the bottle. Shake well, and wait ~5 minutes.

15.0 The slurry in the bottle is fed to the AgC/ZrO/AC combination column. Gravity will allow a flow rate of 1 -3 mL/minute.



*Fig. 17 Ag/C column or AgC/ZrO/AC combination column*

16. Using a one-mL syringe, remove ~0.5-mL sample from the bottle and introduce it through the septum into the QC sample vial.

17. Pass product solution through the .02 μm filter into the final product bottle (Fig. 18).

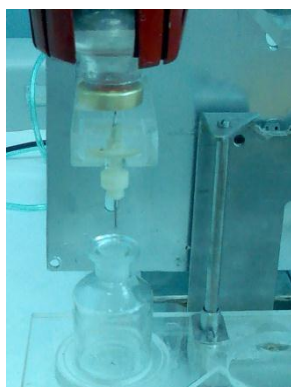


*Fig. 18 Filtration the final product solution through 0.02 μm filter*

18. All the steps have been explained in this paper combined in one setup as shown in (Fig. 19).



*Fig. 19 Combined setup for Mo-99 production*

## CONCLUSIONS

This paper briefly presents the major activities on production of a fission Mo-99 by LEU-foil target as new scientific achievements in TNRC. A special combined setup has been designed for all the chemical processes.

## ACKNOWLEDGMENT

Alhamdulillah for giving me the strength and health for completed this project work until it done. Not forgotten to TNRC administration for providing everything to this project work. Then I would like to thank Mr. Ira Goldman and Ed Pradly from the IAEA for guiding and supporting me through the many meetings throughout this project. Last but not least, I would like to thank Prof. George Vandegrift from ANL Institution (USA) how was sharing our ideas. He was helpful that when we combined and discussed together, we had this task done.

## REFERENCES

- [1] Preliminary Report on Supply of Radioisotopes For Medical Use And Current Developments In Nuclear Medicine, SANCO/C/3/HWD (2009) Rev. 8, 30 October 2009
- [2] Report on Molybdenum-99 Production for Nuclear Medicine 2010 – 2020, Association of Imaging Producers and Equipment Suppliers (AIPES), November, 2008.
- [3] The 26th Annual Radiology Conference was arranged in Karachi on 29th – 31st October, 2010 at Sheraton Hotel Karachi
- [4] The IAEA initiated Coordinated Research Project (CRP) T.1.20.18 'Developing techniques for small-scale indigenous production of Mo-99 using LEU or neutron activation' **Vienna, 2005**
- [5] H. Bonet: 13th RRFM, Vienna, Austria, 22-25.March, 2009, Transactions pp 70-74
- [6] KNOW-HOW DOCUMENTATIONS: "*Tajoura Nuclear Research Design*", Building 1, Design Features of the Control Rod Arrangement in the Reactor Ensuring Replacement with the Fuel Charge Pattern in the Core, 622-1-KH-151 (9), 1979.
- [7] Leyva, Argentina. "Assembly Procedures for Annular LEU Target". Workshop on "LEU Foil Target Fabrication, Irradiation, and Chemical Processing using Modified Cintichem Technique", BATAN, Indonesia, 2-6 March, 2006.
- [8] Production of Fission Product Mo-99 Using the LEU-Modified Cintichem Process. Feasibility Study-Part 1. University of Missouri Research Reactor. TDR-0102. July 2006.
- [9] Bakel, Allen; Vandegrift, George. "Target Disassembly". Workshop id. BATAN, Indonesia, 2-6 March, 2006 [7].
- [10] Vandegrift, George. "ANL LEU-Modified Cintichem Process". Workshop id. BATAN, Indonesia, 2-6 March, 2006 [7].

2.P1.

## **<sup>99</sup>Tc TRANSMUTATION TARGET HETEROGENEITY FOR THE ARTIFICIAL STABLE RUTHENIUM PURIFICATION FROM <sup>106</sup>Ru**

A.A. Kozar<sup>1</sup>, V.F. Peretrukhin

Frumkin Institute of Physical Chemistry and Electrochemistry of RAS,  
31/4 Leninsky prosp., Moscow, 119071, Russia, [kozar@ipc.rssi.ru](mailto:kozar@ipc.rssi.ru)

<sup>99</sup>Tc transmutation can be the source of artificial stable ruthenium <sup>100–102</sup>Ru. Radioactive <sup>106</sup>Ru ( $T_{1/2} = 369$  days) can not be generated by <sup>99</sup>Tc transmutation, however it will appear in the target as fission product from actinide impurities.

The total (U+Pu) impurity is usually about  $5 \cdot 10^{-8}$  g per gram of Tc, isolated from spent fuel by modified Purex process and selective precipitation of tetraalkylammonium pertechnetate. The fission of all actinide nucleus-impurities is complete during the transmutation, because of the cross sections of ( $n, f$ ) actinide reactions are higher in 1 – 2 orders of magnitude than that of <sup>99</sup>Tc neutron capture.

Therefore the artificial stable ruthenium, prepared from Tc homogeneous target, is contaminated by <sup>106</sup>Ru, which prevents the practical use of the product in non-nuclear field during ~10 year up to its complete decay.

<sup>106</sup>Ru can not be removed from artificial stable ruthenium by chemical methods. However there is the possibility to remove fission product <sup>106</sup>Ru from transmutation products <sup>100–102</sup>Ru during the irradiation of technetium by thermal neutrons using the physical phenomenon of recoil after nuclear transformations.

The kinetic energy and recoil range of fission fragments, including <sup>106</sup>Ru, are higher than those of transmutation products <sup>99</sup>Tc( $n, \gamma$ )<sup>100</sup>Tc( $\beta^-$ )<sup>100</sup>Ru.

If technetium target is manufactured from Tc metal powder with the particles whose size is compared with the recoil range of <sup>106</sup>Ru (about 8 mkm), this radionuclide can escape the Tc particle.

<sup>106</sup>Ru yield from Tc-Ru spherical particle with radius R is following:

$$Y = \frac{3 \bar{R}}{4 R} - \frac{1}{16} \left( \frac{\bar{R}}{R} \right)^3 \text{ if } R \geq \bar{R}/2 \text{ and } Y = 1 \text{ if } R \leq \bar{R}/2,$$

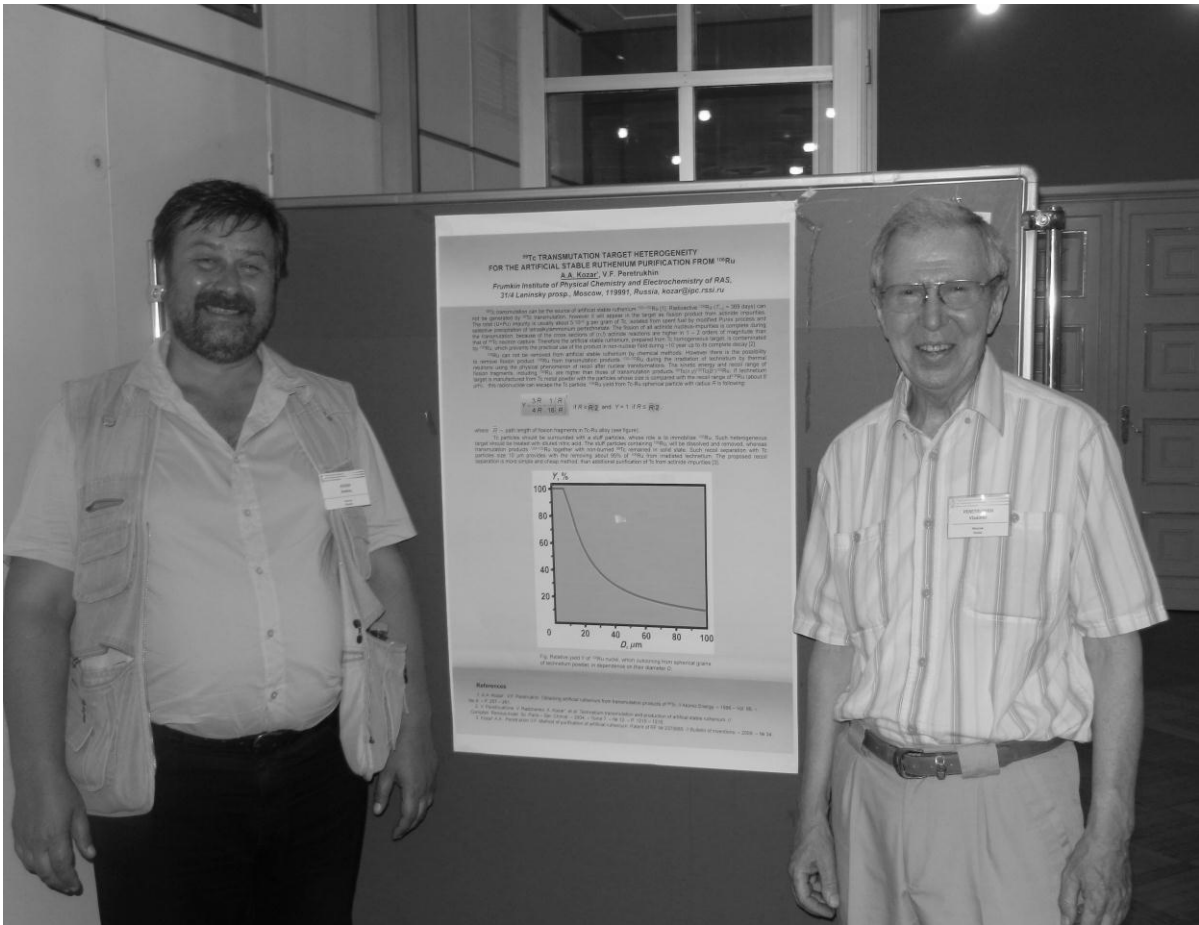
where  $\bar{R}$  – path length of fission fragments in Tc-Ru alloy.

Tc particles should be surrounded with a stuff particles, whose role is to immobilize <sup>106</sup>Ru. Such heterogeneous target should be treated with diluted nitric acid.

The stuff particles containing <sup>106</sup>Ru, will be dissolved and removed, whereas transmutation products <sup>100–102</sup>Ru together with non-burned <sup>99</sup>Tc remained in solid state. Such recoil separation with Tc particles size 10 mkm provides with the removing about 95% of <sup>106</sup>Ru from irradiated technetium.



The proposed recoil separation is more simple and cheap method, than additional purification of Tc from actinide impurities.



Poster Session (A. Kozar and V. Peretruchin)



G.Shteinberg, B.Bryskin, A. D. Besser, I.D.Troshkina, A.M. Chekmarev, E.A.Ospanov

2.P2.

## THE BEHAVIOR OF TECHNETIUM, AMERICIUM AND NEPTUNIUM IN THE SPENT FBR (U, Pu)N FUEL AFTER FAST NEUTRON IRRADIATION AS A FUNCTION OF THE TEMPERATURE AND BURN-UP

G.S. Bulatov, K.N. Gedgovd, D.Yu. Lyubimov<sup>1</sup>.

Institution of Russian Academy of Sciences – A.N. Frumkin Institute of Physical Chemistry and Electrochemistry of RAS (Leninsky prosp. 31-4, Moscow, Russian Federation)

<sup>1</sup>ENTERPRISE OF “ROSATOM” - FEDERAL STATE UNITARIAN ENTERPRISE “SCIENTIFIC RESEARCH INSTITUTE SCIENTIFIC INDUSTRIAL ASSOCIATION “LUCH” (24, Zheleznodorozhnyay st., Podolsk, Moscow region, Russian Federation)

**Keywords:** uranium – plutonium nitride, fast neutrons, fission products, technetium, americium, neptunium, partial pressures

### Abstract:

The thermodynamic analysis of chemical and phase compositions and parameters of evaporation of the uranium - plutonium nitride  $U_{0.8}Pu_{0.2}N$  was carried out depending on burn up (up to 14%) after irradiation by fast neutrons at temperatures 900 – 2000 K.

It was shown, that accumulation of fission products results in formation of a multicomponent solid solution on a basis of uranium plutonium nitride containing Np, Am, Zr, Y and lanthanides, and also separate condensed phases:  $U_2N_3$ , BaTe, CeRu<sub>2</sub>, LaSe, Rh<sub>3</sub>Te<sub>2</sub>, USe, Ba<sub>3</sub>N<sub>2</sub>, CsI, Sr<sub>3</sub>N<sub>2</sub>, pure metals: Tc, Mo, Ru, Ba and intermetallic compounds: U (Ru, Rh, Pd)<sub>3</sub>. The amount and composition of these phases is defined at various temperatures and burn up.

Partial pressures of technetium, americium and neptunium above  $U_{0.8}Pu_{0.2}N$  have been calculated at various temperatures and burn up.

### Introduction

The development of new generation of nuclear power reactors previews the utilization of nitride base fuel, including mixed uranium – plutonium nitride [1]. This kind of fuel may be also used for the incineration of military plutonium, minor actinides and some fission products before the final disposal [2].

### Calculations

To obtain new data on the behavior of (U,Pu)N under fast neutron irradiation thermodynamic analysis of the composition of condensed and gas phases of  $U_{0.8}Pu_{0.2}N_{0.995}$  was carried out using ASTRA-4 software [3] as a function of temperature and burn-up up to 14 %.

### Results and Discussion

Irradiation brings to the formation of a complex structure including solid solution based on uranium-plutonium nitride with dissolved americium and neptunium, zirconium, yttrium and lanthanides and some separate condensed phases, namely  $U_2N_3$ , CeRu<sub>2</sub>, BaTe, Ba<sub>3</sub>N<sub>2</sub>, CsI, Sr<sub>3</sub>N<sub>2</sub>, LaSe, Rh<sub>3</sub>Te<sub>2</sub>, USe as well as Mo metal, Tc metal and intermetallic compounds U(Ru, Rh, Pd)<sub>3</sub>. The content of the mentioned and its change as a function of the irradiation temperature and burn-

up values was determined (tables 1 and 2). It was found that the content of Tc, Am, Np at 13.6 % burn-up was 0.253; 0.126; 0.018 % wt. correspondingly.

Table 1. Phase composition and concentrations (% wt.) of condensed compounds in  $U_{0.8}Pu_{0.2}N_{0.995}$  at 900 K and different burn-up

Condensed phase	Burn-up, % (U+Pu)		
	4.5	9	13.6
(U, Pu, Np,Am,Me) $N_z$ *)	92.6840	84.9070	77.0780
U <sub>2</sub> N <sub>3</sub>	4.4189	9.270	14.145
CeRu <sub>2</sub>	0.47278	1.0036	1.5517
UPd <sub>3</sub>	0.39886	0.86637	1.3635
Mo	0.3360	0.6929	1.0321
Tc	0.0902	0.1747	0.2533
URh <sub>3</sub>	0.1771	0.3541	0.5208
BaTe	0.1488	0.3013	0.4571
Ba <sub>3</sub> N <sub>2</sub>	0.0739	0.1625	0.2708
URu <sub>3</sub>	0.1479	0.1864	0.2111
CsI	0.0794	0.1471	0.2080
Sr <sub>3</sub> N <sub>2</sub>	0.0569	0.1107	0.1619
LaSe	0.0148	0.0297	0.0446
Sum of phases	99.0996	98.1964	97.2967

\*) Solid solution, were Me=Zr+Y+lantanides, z=N/(U+Pu+Np+Am+Me)

Table 2. Phase composition and concentrations (% wt.) of condensed compounds in  $U_{0.8}Pu_{0.2}N_{0.995}$  at 1900 K and different burn-up

Condensed phase	Burn-up, % (U+Pu)		
	4.5	9	13.6
(U, Pu, Np, Am, Me) $N_z$ *)	97.045	94.056	91.041
CeRu <sub>2</sub>	0.3876	0.8968	1.4263
UPd <sub>3</sub>	0.3989	0.8664	1.3635
Mo	0.3360	0.6929	1.0321
Tc	0.0902	0.1747	0.2533
Rh <sub>3</sub> Te <sub>2</sub>	0.1584	0.3207	0.4864
URu <sub>3</sub>	0.2377	0.2990	0.3433
USe	0.0177	0.0349	0.0518
URh <sub>3</sub>	0.0236	0.0432	0.0491
Sum of phases	98.6950	97.3746	96.0455

\*) Solid solution, were Me=Zr+Y+ lantanides, z=N/(U+Pu+Np+Am+Me)

The values of partial pressures for certain gas phase components over irradiated  $(U_{0.8}Pu_{0.2})N_{0.995}$  were calculated for the same range of temperatures and burn-up 13.6% (Fig.1) The empiric equations describing the changes of Tc, Am and Np partial pressures (atm.) with temperature were deduced:

$$\lg(P_{Tc})=7.55 - 35194/T + 33139/T^2 \quad (1500 - 2000K)$$

$$\lg(P_{Am})=9.43 - 38550/T + 10000000/T^2 \quad (1000 - 2000K)$$

$$\lg(P_{Np})=6.10 - 37230/T - 319050/T^2 \quad (1500 - 2000K)$$

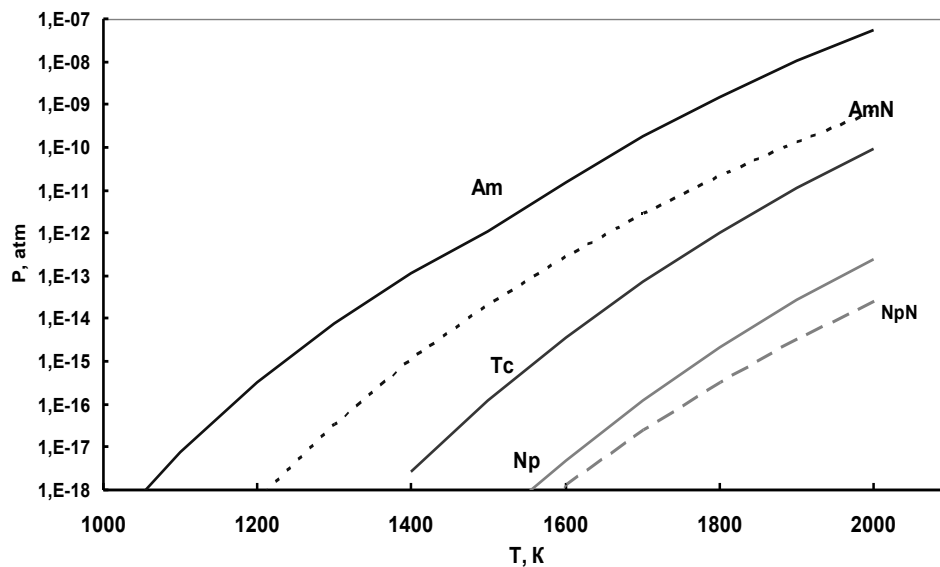


Fig.1. Partial pressures (atm.) of Tc, Am, Np, AmN, NpN depending on temperature at 13,6% burn-up

### Conclusions

The presented results may be used in the design of fast breeder reactors using nitride based fuel, for the estimation of the risks associated with the behavior of (U,Pu)N in the accidental situation and in the development of the spent nitride fuel.

### References

1. F.G. Reschetnikov, *Atom. Energ.* **91**: 453-458, (2001).
2. R. Thetford, M. Mignanelli, *J. Nucl. Mater.* **320**: 44-53, (2003).
3. Sinjarev G.B., Vatolin N.A., Trusov B.G., Moiseyev G.K *Application of the COMPUTER for thermodynamic calculations of metallurgical processes*. Science: Moscow, (1982), 267p.



D.V. Drobot, G.S. Shteinberg, I.D. Troshkina in the Red Hall





N.G. Kravchenko, E.O. Nazarov, T.I.A. Gerber, E.S. German and A.M. Chekmarev



Int. adv. Committee: throw lots onto balance for 2014 – Chicago or Las Vegas?



2.P3.

## COMPOUNDS OF CURIUM WITH TECHNETIUM

E. Pichuzhkina, S. Tomilin

Joint Stock Company “State Scientific Center-Research Institute of Atomic Reactors”, Dimitrovgrad, Ulyanovsk region, ryabinin@niar.ru

For the last years RIAR has pursued investigations on synthesis of the TPE compounds, specifically, curium and americium with other elements of the periodic system. The paper provides the primary results of production and identification of compounds of curium-244 with technetium which refer to the complex oxides.

The samples of the technetium compounds with curium were obtained during condensation of the curium metal vapours on the technetium substrate and investigated by the X-ray diffractometry (a DRON-7 diffractometer) at room temperature.

The investigations performed allowed us to obtain the new curium compounds which were not known before:

- complex oxide  $\text{Cm}_6\text{TcO}_{12}$  that has a hexagonal lattice of the  $\text{Ho}_6\text{MoO}_{12}$  type and the crystal lattice parameters (CLP)  $a = 10,552(3) \text{ \AA}$ ,  $c = 9,879(5) \text{ \AA}$ ;

- complex oxide  $\text{Cm}_3\text{Tc}_2\text{O}_{10}$ , the isostructural  $\text{La}_3\text{Mo}_2\text{O}_{10}$ , with the cubic crystal lattice and the CLP  $a = 5,592(1) \text{ \AA}$ .

It is noted that curium remains insoluble in the hexagonal closed-packed technetium lattice.

2.P4.

## **EXTRACTION-CHROMATOGRAPHIC PURIFICATION OF URANIUM EXTRACT FROM TECHNETIUM**

V.I. Volk, K.N. Dvoyeglazov, V.L. Vidanov, L.N. Sergeeva.

Open Joint Stock Company “Academician A.A. Bochvar High-Tech Research Institute of Inorganic Materials”, 5a,  
Rogova str., Moscow  
e-mail: vitya@bochvar.ru

Uranium purification from technetium in the process of spent nuclear fuel reprocessing is one of the most complex problems.

Uranium reclaim for separating plant is to be extremely decontaminated from Tc because of the problems at the sublimation stage caused by volatile  $TcF_6$  formation during uranium recycling process.

There is a conflict between Thorp plant requirements for uranium product after the second extraction cycle (Tc content 4 mg/kg U [1]) and ASTM C787-03 standard, which requires Tc content in uranium hexafluoride less than 0.5 mg/kg U and in some cases [2] the level of uranium decontamination from Tc in this product should be less than 1.6 mkg/kg U. This conflict could be resolved by uranium reclaim additional radiochemical reprocessing for supplying purified product to the sublimation plant. It is evident that such technology makes reprocessing process rather expensive.

The aim of the research work was to find and work out such a process, that can provide effective and not expensive deep uranium purification from Tc on the basis of extraction spent fuel reprocessing technology.

The solution of mentioned problem is an extraction-chromatographic purification of uranium extract by usage of aqueous reducing agents solution as a purifying stream. These agents reduce Tc (VII) to nonextractable Tc (IV).

The process of purifying is carried out in cyclically-countercurrent feed mode of purified and purifying streams in a column filled with porous excipient (charged with aqueous purifying stream).

It is shown that depending on composition of the aqueous phase concentration factor varies from 40 and above. These conditions provide practically complete treatment of uranium extract.

### **References**

1. Kopyrin A.A., Karelin A.I., Karelin V.A. “Technology of the production and radiochemical reprocessing of nuclear fuel” M, Atomizdat, 2006, p. 226
2. Timofeev S.V., Belyaev V.D., Karpov A.A., Shishkov S.U. “ Improving the evaluation control of technetium-99 in the chemical reprocessing technology of NFC natural and recycled uranium”. Youth NFC: Science, production, ecological safety, URL:<http://conf.atomsib.ru/archive/conf2008/section1/17.doc>, date - March 4, 2011.

2.P5.

## METAL-THERMAL IMMOBILIZATION OF HIGH-ACTIVE TECHNETIUM WASTE INTO MATRICES BASED ON METAL GLASS CRYSTALLINE COMPOSITES

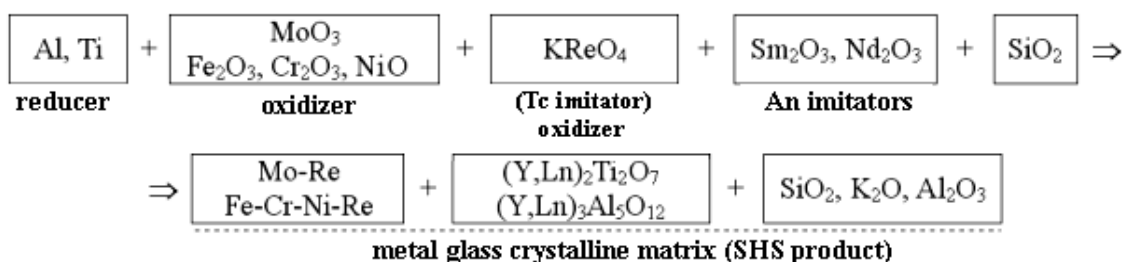
E.E. Konovalov, T.O. Mishevets, S.S. Shulepov, Yu.D. Boltoev

FSUE «SSC RF – IPPE», Obninsk, Kaluga region, Russia  
[mishto@ippe.ru](mailto:mishto@ippe.ru)

In the framework of recycling fuel cycle the problem of high-active waste (HW) treatment should involve solution of the three major process stages: liquid HW fractionation; calcination (crystallizing) of radionuclides of these fractions predominantly on inorganic sorbents and immobilization of produced dry sorption-crystal concentrates into chemically and thermally resistant mineral-like matrix materials suitable for ecologically safe disposal. To synthesize such matrices, it is recommended to use metal-thermal self-propagating high-temperature synthesis (SHS) where Al and Ti are the fuel elements (reducers), and molybdenum oxide and iron oxide are mainly oxidants.

To provide further progress in this direction, the problem of immobilization of technetium as most environmentally dangerous product of nuclear fuel fission is considered in this report. Technetium imitator representing its nearest chemical analog – rhenium in the form of potassium perrhenate is used in investigations.

When treating high-active waste, Tc-fraction can contain actinides impurities. Therefore the matrix composite materials synthesized in SHS conditions should incorporate phases efficiently immobilizing both technetium (rhenium) and actinides (An). To imitate the last-named, lanthanides (Ln) are used. SHS-produced metallic phases where rhenium-molybdenum (Mo-Re) and Fe-Cr-Ni-Re alloys are dissolved with ease have been produced as matrix material for rhenium immobilization (see the diagram). Matrix materials being simultaneously synthesized on the basis of stable aluminate or titanate complex oxides like pyrochlor  $(Y, An...)_2Ti_2O_7$  or Y-Al garnet  $(Y, An...)_3Al_5O_{12}$  are used to immobilize An.



The present authors are grateful to S.V. Yudintsev and B.S. Nikonov, IGEM RAS\* experts, for identification of interaction SHS products and analysis of their structure.

\* The Institute of Geology of Ore Deposits, Petrography, Mineralogy, and Geochemistry, Russian Academy of Sciences

2.P6.

## APPLICATION OF MODIFIED WOOD MATERIALS FOR EXTRACTION OF TECHNETIUM (VII) FROM AQUEOUS MEDIUM

N.N. Popova, G.L. Bykov, I.G. Tananaev, B.G. Ershov

A. N. Frumkin Institute of Physical Chemistry and Electrochemistry, Russian Academy of Sciences,  
building 4, 31 Leninsky prosp., 119071 Moscow, Russian Federation.  
E-mail: popovann@gmail.com

**Keywords:** technetium, sorption, wood materials, carbonized of wood, nanomaterial "Taunit"

### Abstract:

It is investigated sorption ability of some carbon vegetative materials, namely: the charcoal formed at electron beam processing of vegetative materials; the oxidized coal received at soft oxidation of wood carbonized and aspen sawdust (wood) in relation to Tc(VII). Influence of introduction in a carbon matrix of various modifying additives on the efficiency of sorption of Tc(VII) ions is investigated. Modifying of samples was carried out by urea, a phosphoric acid, thiourea and potassium thiocyanate. The possibility of Tc(VII) extraction from the solutions modeling underground waters in area of lake Karachaj (FGUP "PO" Maiak»), sea water, etc is shown. The samples synthesized by us have shown high sorption properties, even from solutions with a high salt background.

### Introduction.

Working out of effective methods of concentration and extraction of the Tc(VII) of various water environments is actual [1]. At a sorbent choice it is necessary to consider not only its chemical and mechanical stability, but also such factors, as simplicity of reception and availability of initial materials. In this connection, recently for extraction of Tc(VII) the modified natural materials and technological products are more and more used [2]. Therefore search of cheap, accessible and effective materials for sorption Tc(VII) ions from a liquid radioactive waste and environments was the purpose of our work.

Influence of various modifying additives on sorption ability of some carbon materials in relation to the Tc(VII) is studied.

### Experimental.

As objects of research were are taken: (1) coal formed at electron beam processing of vegetative materials; (2) carbonized of wood; (3) the oxidized coal received at soft oxidation carbonized of wood by oxygen of air, and also the initial and modified (4) wood (aspen sawdust); (5) activated coal FAS-E and (6) carbon nanomaterial "Taunit".

For improvement sorption properties concerning the Tc(VII) carbon materials have been modified by processing by phosphoric acid, urea (thiourea) and potassium thiocyanate.

Coal was impregnated with KCNS solutions, was dried up and got warm at 140°C within 1 hour. Other sample was impregnated urea (thiourea) and got warm within 1 hour at 200°C.

The oxidized coal was made of aspen sawdust in two stages. At the first stage sawdust charred at temperature 250-300°C, at the second stage received carbonized was oxidized air at 250-300°C.

### Result and Discussion.

It has been shown that oxidizing processing carbonized of wood (2) improves it sorption properties. It is possible to explain this fact, education on a surface of coal participating in anionic exchange of carbonyl and carboxyl groups at processing on air.

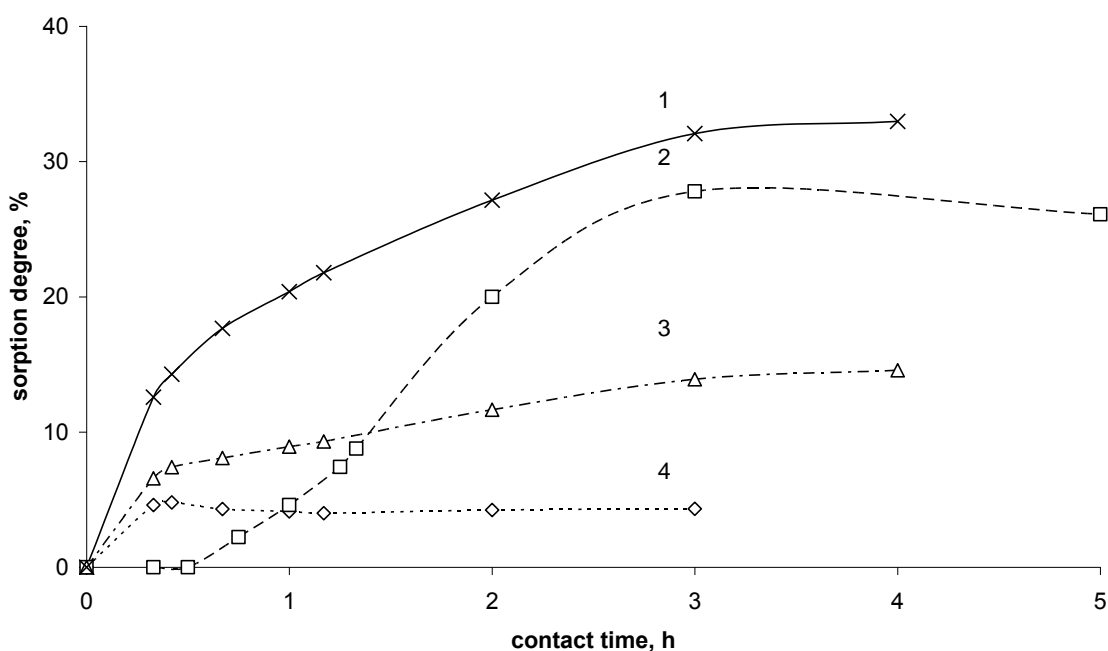


Fig.1. Dependence of sorption degree of Tc(VII) from contact time for  $10^{-3}$  M  $HNO_3$  and following sorbents: 1 – the coal modified thiourea; 2 – the wood modified by phosphoric acid; 3 – the coal modified potassium thiocyanate; 4 – the wood modified by urea.

It is received, that at use of the modified carbon materials the Tc(VII) is taken practically completely within the first 30 minutes of contact of phases. Studying of influence medium pH on efficiency of sorption of the Tc(VII) modified materials has shown, that maximum high sizes of distribution coefficients are observed at pH 3 on all studied samples.

It is shown that in the acidic medium (pH <4) the Tc(VII) is most effectively taken by the wood modified by urea ( $K_d = 1,3 \cdot 10^2$   $sm^3/g$  from 2M  $HNO_3$ ). In the subacidic and neutral environment (Fig.1) is the most effective than the Tc(VII) it is taken by the coal modified thiourea ( $K_d = 58,64$   $sm^3/g$  from  $10^{-3}$  M  $HNO_3$ ). In the alkaline environment is better the wood modified by phosphoric acid ( $K_d = 76$   $sm^3/g$  proves at pH 9).

It is found that samples FAS-E modified by urea and  $H_3PO_4$  effectively takes the Tc(VII) of subacidic solutions  $HNO_3$  (Fig.2, 3) with  $K_d$  equal  $2,4 \cdot 10^4$  and  $1,7 \cdot 10^4$   $sm^3/g$ , accordingly. Modified by urea or  $H_3PO_4$  samples of "Taunit" (Fig.3) take the Tc(VII) in the same conditions with  $K_d$  equal 400 and 73  $sm^3/g$ , accordingly.

Also sorption properties received by us modified samples of "Taunita" and FAS-E concerning extraction of the Tc(VII) from the modeling solution of technogenic changed ground waters of area of the lake Karachaj have been tested (Fig.2). It has appeared that FAS-E, modified by urea, effectively extracts ions of the Tc(VII) from modeling solutions of complicate structure ( $K_d = 71,1$   $sm^3/g$ ), and sorption balance also is reached during 30 minutes after the beginning of contact of phases.



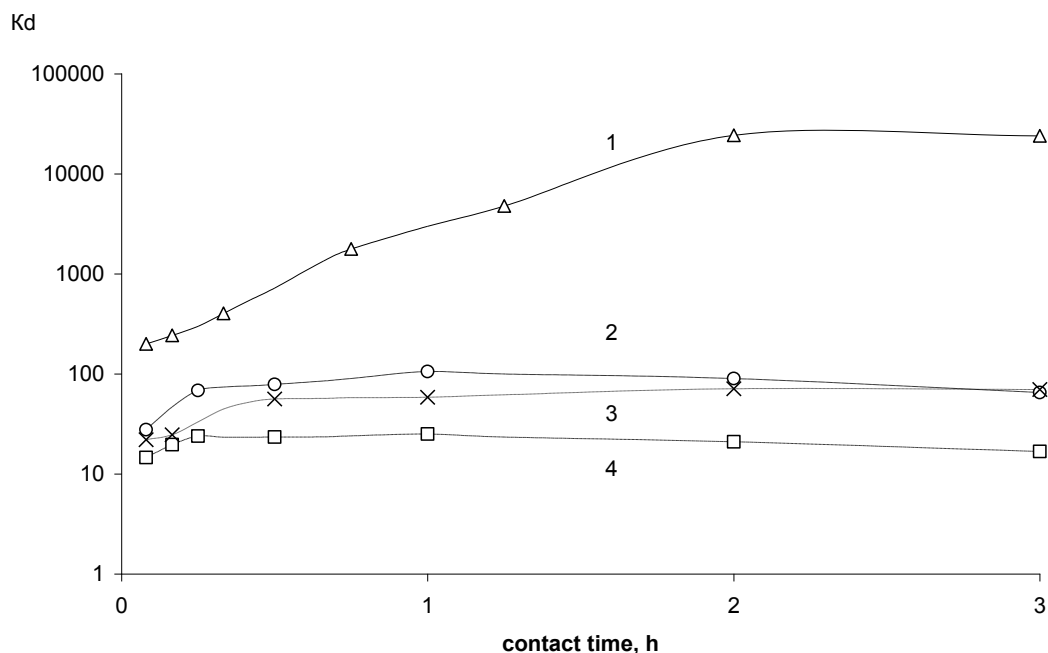


Fig.2. Kinetics of sorption Tc(VII) on FAS-E, modified by urea at 300°C from various environments (the data on distribution factors is presented in a logarithmic scale): 1 –  $10^{-3}$  M  $HNO_3$ ; 2 - 0,1 M NaOH; 3 – lake Karachaj water; 4 – 2 M  $HNO_3$ .

The mechanism of sorption, consisting in localization Tc(VII) on a surface of samples as a result of course of competing processes - reduction of the Tc(VII) to Tc(IV) being in the sample by means of  $NH_2$ -groups at the expense of its modifying by urea, and also fixing of formed complexes with participation of this element.

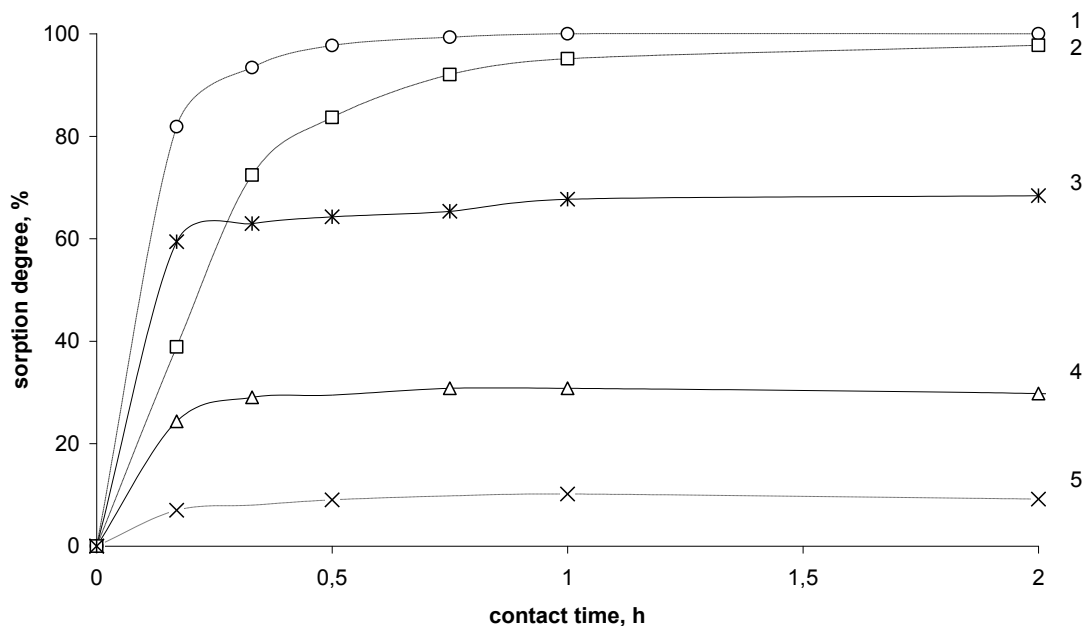


Fig.3. Kinetics of sorption Tc(VII) from  $10^{-3}$  M  $HNO_3$  and  $V/m=200$   $cm^3/g$  ( $V=5$  ml,  $m=25$  mg) with use: FAS-E, modified by urea (1) and phosphoric acid (2); «Taunit», modified by urea (3) and phosphoric acid (4); not modified «Taunit» (5).

### **Conclusion.**

Thus, researches have shown that as a whole modifying of wood and carbon materials improves their sorption properties in relation to technetium (VII). Important that the modified carbon materials possess concerning high sorption abilities in relation to Tc(VII) at its extraction from the natural (technogenic) objects possessing difficult salt structure. Thus, presence of extraneous impurity practically does not interfere with extraction of a purposeful element technetium the modified sorbents synthesized by us on the basis of carbon materials.

### **References:**

1. N.N. Popova, I.G. Tananaev, S.I. Rovniy, B.F. Miyasoedov, *Russian Chemical Reviews*, 2003, **72**, № 2, 115.
2. G.V. Miyasoedova, V.A. Nikashina, *Mendeleev Chemistry Journal*, 2006, т.Л, №5, с.55-62.

2.P7.

## STRUCTURE AND PROPERTIES OF INSOLUBLE TECHNETIUM COMPOUNDS FORMED IN TECHNETIUM - HYDRAZINE - DTPA - NITRIC ACID- SOLUTIONS

K.E. German, A.B. Melentev<sup>1</sup>, Ya. V. Zubavichus<sup>2</sup>, S.N. Kalmykov<sup>3</sup>,  
A.A. Shiryaev, I.G. Tananaev

Institution of Russian Academy of Sciences – A.N. Frumkin Institute of Physical Chemistry and Electrochemistry of  
RAS, Moscow, guerman\_k@mail.ru

<sup>1</sup>FSUE “PA “Mayak”, Ozersk, melentev74@mail.ru

<sup>2</sup>RRC “Kurchatov Institute”, Moscow

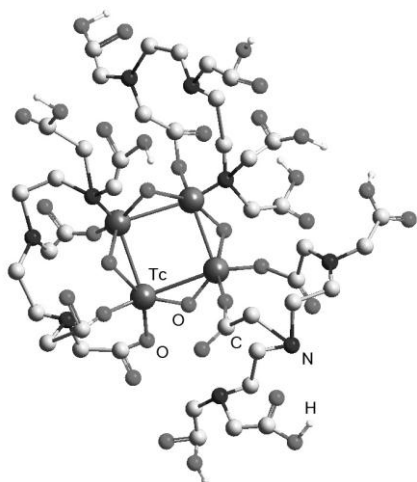
<sup>3</sup>Lomonosov MSU, Moscow

The paper presents the results of the study of low-soluble technetium compounds with diethylenetriaminepentaacetate (DTPA), which finds use as a stabilizing agent in the extraction reprocessing of spent nuclear fuel. The Tc sediments were studied by chemical analyses, XRD, IR, Raman and UV-VIS, EXAFS and ESR spectroscopy. The role of the Tc reduction process by hydrazine in mother solutions prior to precipitation was also evaluated.

It was shown, that the precipitation of Tc occurs when the reduced Tc(IV) is partially back-oxidized to Tc(VII) with a possible formation of intermediate Tc species after the most part of hydrazine is expended. The studied precipitate was defined as the Tc polyaminocarboxilate of both polynuclear and polymeric nature. Tc-DTPA ratio was found to be close to 1:1, the huge part of Tc in the polymeric sediments being in Tc(IV) valent state. Both carboxylic and amino-groups of the DTPA participate in the formation of the Tc compound and the coordination of functional groups from one DTPA molecule to multiple Tc atoms is highly possible. The Tc-DTPA chelates tend to form large and more complex ensembles with Tc-Tc bonds and bridging oxo ligands.

Possible structure of the Tc-DTPA compound was modeled (fig. 1) and some ways for exclusion of the Tc precipitation during SNF reprocessing were proposed.

*Fig. 1 - The model of the possible structure of Tc-DTPA core*



The work was supported by RFBR grants 09-08-00153-a and 09-02-12257-ofi\_m

2.P8.

## THE BEHAVIOR OF THE TECHNETIUM - HYDRAZINE - NITRIC ACID - TBP SYSTEM IN PRESENCE OF THE COMPLEXING AGENTS

A.B. Melentev, A.N. Mashkin, O.V. Tugarina, K.E. German<sup>1</sup>, I.G. Tananaev<sup>1</sup>

FSUE “PA “Mayak”, Ozersk, melentev74@mail.ru

<sup>1</sup>Institution of Russian Academy of Sciences – A.N. Frumkin Institute of Physical Chemistry and Electrochemistry of RAS, Moscow

The extraction properties of one of uranium fission products – technetium - are of a major importance for the spent nuclear fuel reprocessing by PUREX-process. Tc(VII) possess significant distribution coefficient in TBP/HNO<sub>3</sub> system thus following the U and Pu at the first extraction step. Later it may seriously interfere with the U-Pu reductive separation by catalyzing undesirable red-ox reactions and increasing the decomposition rate of hydrazine, used as a stabilizer. Different complexing agents may be used to reduce the negative influence of Tc and to control its extraction behavior.

This paper presents the experimental results on the extraction behavior of Tc and the decomposition of hydrazine in presence of complexing agents - DTPA and oxalic acid. It was shown that DTPA did not render significant impact on the hydrazine decomposition in the modeled hydrazine-containing nitric acid Tc solutions during the 6 hours hold out at temperature of 45 °C, but the rate of the Tc(IV) reoxidation decreased in presence of DTPA. After the hydrazine was spent, the yield of Tc(VII) as a result of reoxidation process was found to be significantly lower, compared to the DTPA-free systems. Upon increase of acidity the chelating properties of DTPA weakened, so this agent may have limited usability for stabilizing reduced technetium in fuel reprocessing.

Oxalic acid was shown to be more efficient protecting agent for both hydrazine and Tc(IV). In presence of H<sub>2</sub>C<sub>2</sub>O<sub>4</sub> hydrazine decomposition rate was slow; the remaining concentration of hydrazine after 6 hours exceeded 50% of the initial quantity, and only insignificant oxidation of reduced Tc(IV) was observed. It should be noted, that the initial reduction of Tc(VII) by hydrazine was slower, than in solutions not containing the complexing agents. The ability to bind Tc(IV) increased for H<sub>2</sub>C<sub>2</sub>O<sub>4</sub> with the rise of HNO<sub>3</sub> content. It was also found, that azide products of hydrazine decomposition play an important role in the process of stabilizing the systems both with and without complexing agents.

The authors are grateful to Prof. B.Ya. Zilberman for useful discussion of the results. The work was supported by RFBR grant 09-08-00153-a.

2.P9.

## TECHNETIUM(VII) EXTRACTION WITH HYBRID PHOSPHOR-NIROGENATED DERIVATIVE LIGANDS

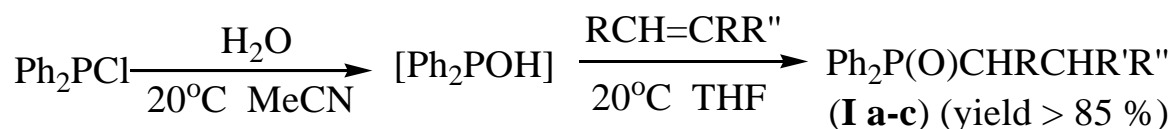
A.M. Safiulina<sup>1</sup>, K.E. German<sup>1</sup>, E.I. Goryunov<sup>2</sup>, I.B. Goryunova<sup>2</sup>, E.E. Nifantiev<sup>2</sup>, I.G. Tananaev<sup>1</sup>, B.F. Myasoedov<sup>1</sup>

<sup>1</sup> Institution of Russian Academy of Sciences - A.N. Frumkin Institute of Physical Chemistry and Electrochemistry of RAS (Moscow, Russia)

<sup>2</sup> Institution of Russian Academy of Sciences - A.N. Nesmeyanov Institute of Elementoorganic Compounds of RAS (Moscow, Russia)

A new simple “one-pot” synthetic method based on the reagents that are commercially available is elaborated as a route to prepare hybrid phosphor-nitrogenated derivative ligands like Ph<sub>2</sub>P(O)CHRCHR'R'' (**I a-c**; **a** R = Ph, R' = R'' = CN; **b** R = Ph, R' = CN, R'' = COOEt; **c** R = R' = H, R'' = 2-pyridyl), being the substances of potential bioactivity.

The synthetic route is given by the sequence:



Thus obtained compounds were tested with respect to technetium liquid-liquid extraction (Organic phase: 0.05 M Ph<sub>2</sub>P(O)CHRCHR'R'' in CCl<sub>3</sub>H, aqueous phase contained 10<sup>-5</sup> M KTcO<sub>4</sub> in 0.05-0.5M NaOH or 0.05-5.5M HNO<sub>3</sub>).

Very small distribution coefficients were measured for Tc(VII) extraction from the basic solutions for the 0.05-0.5M NaOH concentration range studied.

Extraction from nitric acid solutions was notable, with 2-[2-(diphenylphosphoryl)ethyl]pyridine (**I c**) being the most effective for 0.7 – 1.5 M HNO<sub>3</sub> range.

The data indicate that **I**-type phosphoryl-nitrogenated derivatives functionalization is prospective approach to Tc(VII) extraction.

Extraction tests for reduced Tc with the hybrid phosphor-nitrogenated derivative ligands like Ph<sub>2</sub>P(O)CHRCHR'R'' (**I b-c**; **b** R = Ph, R' = CN, R'' = COOEt; **c** R = R' = H, R'' = 2-pyridyl) indicate the necessity of temperature pretreatment and the importance of reducing reagent excess in the aqueous phase.

The work was partially supported by the Program P-17 (Elaboration of new methods for chemical synthesis and design of new materials) of Presidium RAS.



2.P10.

## **New materials for immobilization of rhenium, technetium containing waste for the purpose of their isolation from environment**

Murat Abdulakhatov<sup>1</sup>, Sergey Bartenev<sup>2</sup>, Mikhail Goikhman<sup>3</sup>, Alexander Gribanov<sup>3</sup>, Valery Guselnikov<sup>1</sup>, Nikolai Firsin<sup>2</sup>, Yuri Novikov<sup>1</sup>, Yuri Sazanov<sup>3</sup>, Mikhail Zykov<sup>2</sup>

<sup>1</sup> Petersburg Nuclear Physics Institute (PNPI), Gatchina, Russia, e-mail: [amk@pnpi.spb.ru](mailto:amk@pnpi.spb.ru)

<sup>2</sup> V.G. Khlopin Radium Institute (KRI), Saint-Petersburg, Russia

<sup>3</sup> Institute of Macromolecular Compounds (IMC), Saint-Petersburg, Russia

### **Summary**

Conditions for immobilization of rhenium and technetium in carbon matrices were investigated. It is shown that the carbon matrices incorporating the above elements can be produced by carbonization of composites with ITA-31 polyimide binder, investigated elements and carbon fabric as reinforcing component. The elements under investigation were used both in the form of salts or oxides and in the form of their complexes with ion-exchange resins. The produced composites were carbonized in inert gas (argon) or in vacuum. The physical-chemical properties of the samples were studied. It was revealed that the resultant matrices meet the requirements imposed on waste storage and disposal or for transmutation.

### **1. Introduction**

Further development of nuclear power over the world depends to a great extent on solving two main problems: safety of nuclear power and industrial facilities as well as ecologically reliable and economic disposal of radioactive waste (RAW) containing long-lived alpha-, beta- and gamma radionuclides. Hence, the long-term isolation of RAW from biosphere is an important problem responsible for further development of nuclear power. Of prime attention is the question on management of long-lived radionuclides because of their serious hazard if they escape into the environment. The point is that the radioactivity of fission products (<sup>99</sup>Tc, <sup>129</sup>I) and minor actinides such as <sup>237</sup>Np and <sup>241</sup>Am remains practically at the same level over a period of thousand hundreds years.

Two variants are best suited to handle these long-lived radionuclides. One of them consists in elaborating a method for immobilization of radionuclides into matrices of high thermal, chemical and radiation resistance for subsequent long-term storage or final disposal [1]. Another variant is transmutation of long-lived radionuclides into short-lived or stable isotopes in special nuclear reactors or Accelerator Driven Systems (ADS) [2-3]. It should be emphasized that the both variants involve production of matrices possessing some properties suitable for prolonged storage or disposal and transmutation of long-lived radionuclides. The different research centres carry out research on the development of new techniques for production of reliable matrices. One of such techniques consists in production of carbon matrices. Carbon matrices can be obtained by carbonization of organic substances. To meet the requirements placed on the properties of carbon matrices being obtained, some composites on the basis of polyimide binder ITA-31 were developed [4]. By producing the carbon matrices it is extremely important to bind nuclides being immobilized by ion-exchange resins (IER) and complexing agents, which may be used then as components in synthesis of polymer materials. For attaining the stated goal, different materials may be used. In this work several commercial IER with high thermal, chemical and radiation stability were chosen. The

conditions for production of the carbon matrices incorporating rhenium, stable iodine and stable europium as the chemical analogues of  $^{99}\text{Tc}$ ,  $^{129}\text{I}$  and  $^{241}\text{Am}$ , respectively, were investigated.

## 2. Methodology

### 2.1 Initial materials and reagents

Polyimide binder ITA-31 with the following composition was used: dianhydride of 3,3',4,4'-benzophenonetetracarboxylic acid - 50% and tetraacetyl derivative of 4,4'-diaminodiphenyl ether - 50%. During composite synthesis the binder was mixed with IER containing rhenium in the form of perrhenate-ion ( $\text{ReO}_4^-$ ), iodine in the form of iodide-ion ( $\text{I}^-$ ) and europium in the form  $\text{Eu}^{+3}$ . The strongly basic anionites like AV-17, VP-1AP, VPB, Amberlite IRA-400 and Dowex 1×4 were used for preliminary sorption of rhenium and iodine. For preliminary sorption of europium the Russian IER SF-5 and KB-10 were applied. The carbon fabric of ELUR type was used in composite synthesis as reinforcing addition for higher strength of matrices.

### 2.2 Synthesis of composites and their carbonization

Synthesis of composites was carried out in two stages [5]. At the first stage the composite-1 incorporating ITA-31 binder and the IER containing a corresponding nuclide at the ratios of ITA-31:IER 8:1 ÷ 1:1 was synthesized. ITA-31 and IER were mixed at 260 – 280°C. Then the carbon fabric ELUR was added to the resultant composite-1 for its higher strength to afford its mass content from 20 to 60% in end product (composite-2). The process for production and pressing of composite-2 was conducted at 280-320°C and under excess pressure of 20 – 250 atm., while the carbonization process proceeded at 600 – 650°C.

### 2.3 Determination of leach rates

The procedures recommended by International standards were used for determination of leach rates of rhenium, iodine and europium from obtained matrices [6-7]. ICP MS and emission spectral analysis was used for determining I, Re and Eu leach rates.

## 3. Results

### 3.1 Thermal stability of composites

Taking into account that the radioactive waste containing long-lived radionuclides may be heated-up due to radioactive decay, special attention should be given to thermal resistance of matrices used for long-term storage or final disposal of RAW. In the previous works conducted by the authors it was shown that the carbonization process of the composites containing polyimide binders is an efficient method for production of heat-resistant carbon-plastics and carbon-carbon materials on their basis [4]. However, it was unknown which properties would be typical for the composites based on ITA-31 and other components of produced matrices. Such components may involve, for instance, the IER containing the elements under investigation. In the early stage of investigations some experiments to measure thermal resistance of initial components and related composites were performed. In Fig. 1 the data are given of differential thermogravimetric analysis (DTA) of VP-1AP in different chemical forms, including that containing the stable iodine as  $\text{I}^-$ . For correlation purposes there are also presented the DTA individual results on the ITA-31 and composite containing ITA-31 and VP-1AP in  $\text{I}^-$  form.

The thermal experiments have demonstrated that the IER containing chemical analogues of investigated elements enter into chemical reactions with polyimide binders like ITA-31 and it is possible in such a manner to produce the heat-resistant matrices for incorporation of the above elements in the course of subsequent carbonization process. In the range of 600 - 1000°C no significant losses of rhenium and europium are observed and only some marked losses of iodine occur due to lower melting point of its compounds.

### 3.2 Synthesis of composites incorporating ITA-31 binder and elements under study

The technology for production of carbon-plastics elaborated in the previous works [4] involved the ITA-31 synthesis, the procedure for impregnation of a required number of carbon-fabric layers, the pressing at 300°C for 1 hour under excess pressure of 0.1 – 0.5 atm. The mass ratio between binder and carbon fabric was 1:1.

The composite (prepreg) being converted into carbon-plastic state was then subjected to carbonization in vacuum or inert medium in the temperature range of 20 - 600°C at a rate of 7 °/min. It should be noted that both prepreg and carbon-plastic produced in accordance with this technology possess high mechanical and thermal strength. The properties of the carbon-plastics produced by incorporation of IER (for example VP-1AP) into their composition at various ratios between components are shown in the Table 1.

As it is seen from the results obtained, the strength values of carbon-plastics remain rather high over a wide range of ratios between ITA-31 and IER. These values meet the requirements of the Russian and International standards for RAW incorporating matrices.

However, by using such carbon-plastic molding technique a partial loss of composite occurs due to its flowing out of press mold. In production practice of carbon-plastics containing no harmful chemical and radioactive substances these losses can be collected and returned into the process without any technical difficulties. However, in the case of producing the carbon-plastics (matrices) containing radioactive substances the composite flowing from press-mold may lead to non-controlled contamination of equipment and work places.

Other variants of molding matrices were elaborated in this work, which could prevent the non-controlled losses of RAW during molding.

In the first case the preliminarily prepared prepreg containing ITA-31 and ELUR was crushed to sizes of 5 – 10 mm and mixed on heating with the resin saturated by element being investigated. At the bottom of the heated press-mold the PM film (polyimide film) was placed and above it the mixture of crushed prepreg and resin. Pressing was conducted at 5 - 250 atm.

Another variant envisaged mixing of crushed carbon with the resin containing the elements under study; then, molten binder was added on heating and stirring; the resulting mixture was transferred into the heated press-mold. Pellets were pressed at 300°C for 1 hour.

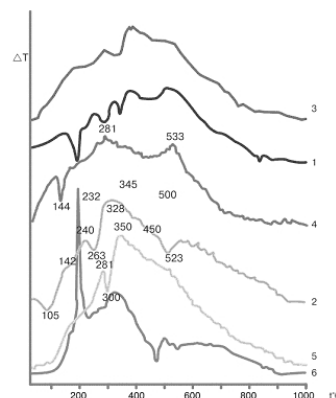


Figure 1 Results of DTA

1 – ITA-31; 2 – VP-1AP (OH<sup>-</sup>); 3 – ITA-31+VP-1AP(OH<sup>-</sup>); 4 – ITA-31+VP-1AP(OH<sup>-</sup>)+ELUR; 5 – VP-1AP (NO<sub>3</sub><sup>-</sup>); 6 – VP-1AP (I)

It was found that among three variants of matrix production the third one is most feasible; in this case no prepregs should be preliminarily prepared. This method allows to avoid the non-controlled losses of investigated elements and to obtain sufficiently strong pellets. Besides, one can introduce nuclides in a carrier (ion-exchange resin, fullerene soot) as well as in any other solid chemical form, for example oxide.

Table 1. Properties of composites containing VP-1AP

Ratio of ITA-31: VP-1AP	Properties of C-C composite		
	Compression strength, MPa	Modulus of elasticity, GPa	Mass loss on carbonization, %
8 : 1	84	90	12
6 : 1	79	82	14
4 : 1	80	81	16
2 : 1	54	57	17

### 3.3 Leach rates of investigated elements

Alongside the thermal and strength characteristics the leach rates of immobilized radionuclides or their chemical analogs are of significance in defining the chemical stability of matrices. In this work the leach rate was determined in accordance with the recommendations of the International standards. Distilled water was used as liquid phase; open surface area for different samples was 1.2 – 2.0 cm<sup>2</sup>. It is determined that the leach rates of rhenium from sample prepared on the basis of rhenium-saturated resin VP-1AP are  $6.8 \times 10^{-5} - 1.7 \times 10^{-7}$  g/cm<sup>2</sup>×day upon leaching during 1 – 90 days; of europium from sample prepared on the basis of SF-5 resin saturated with europium are  $2.5 \times 10^{-5} - 1.6 \times 10^{-7}$  g/cm<sup>2</sup>×day on leaching within the same time interval; of iodine from sample prepared on the basis of AB-17 saturated with iodide-ion are  $4.8 \times 10^{-5} - 2.7 \times 10^{-6}$  g/cm<sup>2</sup>×day.

### 3.4 Radiation stability of matrices.

It is shown that irradiation of the matrices by neutrons and gamma-irradiation in research reactor VVR-M in PNPI at neutron-flux density  $\sim 4 \cdot 10$  n/cm<sup>2</sup>·s and integral flow  $\sim 10^{18}$  n does not render the essential influence on their mechanical properties and leach rates of investigated elements. The values of these parameters for the samples after irradiation practically such, either as for samples before irradiation.

## 4. Conclusions

The chemical analogues of such long-lived radionuclides as <sup>99</sup>Tc, <sup>129</sup>I, and <sup>241</sup>Am were immobilized. Rhenium, stable iodine and europium were used as the corresponding analogs, respectively. It was shown that the samples carbonized at temperatures up to 600-650°C possess high thermal stability. The produced samples exhibit high mechanical strength. Their compression strength varies from 47 to 84 MPa, the modulus of elasticity from 49 to 90 GPa. The leach rates of rhenium, iodine and europium for different samples range between  $2.5 \times 10^{-5} - 1.7 \times 10^{-7}$  g/cm<sup>2</sup>×day. On the basis of the results obtained in this work strong matrices of high thermal, chemical and radiation stability for disposal of long-lived radionuclides can be developed. In our opinion the developed carbonization method can be used for reprocessing of spent IER and other organic complexing components, containing of radionuclides and hazardous heavy metals.

## 5. Acknowledgments

The work was carried out under financial support of International Science and Technology Centre (ISTC), Moscow (Project #2391).

## 6. Proposals and Suggestions

The authors of this paper are open to cooperation on mutually acceptable terms.

## References

- [1] «Management of radioactive waste and spent nuclear fuel», MINATOM, Information and Analytical Collection, Moscow, 2000, issue 2, p. 90.
- [2] A.Fernandez et al. "Fuel/Target Concepts for Transmutation of Actinides". Proc. 6<sup>th</sup> OECD/NEA Information Exchange Meeting on Actinide and Fission Product P&T (Madrid, Dec. 11-13, 2000).
- [3] Michael W. Cappiello, Dana C. Christensen «The Role of LANSE in the Nuclear Energy Future», Los Alamos Science, Number 30, 2006
- [4] M.Ya.Goykhman et al. "Study of the mechanism high-temperature curing of polyimide ITA binders". Acta Montana, Series B , No 7 (1997) 9-19.
- [5] Invention with the patent № 2340968 «Method of immobilization for long-lived radionuclides» Patent holder - PNPI RAS (RU). Patent Application № 2007105656. Priority from February 14, 2007. Registered in State register Russian Federation at December 10, 2008. Period of validity February 14, 2027. Authors: Abdulakhatov M.K., Bartenev S.A., Goikhman M.Ya., Gribanov A.V., Guselnikov V.S., Zykov M.P., Firsin N.G.
- [6] ASTM Standard. C 1220-92, Standard Test Method for Static Leaching of Monolithic Waste Forms for Disposal of Radioactive Waste
- [7]. ASTM Standard. C 1285-94, Standard Test Method for Determining Chemical Durability of Nuclear Waste Glasses: The Product Consistency Test (PCT)



2.P11.

## TECHNETIUM SULFIDES – ROLE IN CHEMISTRY AND ECOLOGY

German K.E., Peretrukhin V.F., Tumanova, D.N., A.Yu. Tsivadze

Institution of Russian Academy of Sciences A.N. Frumkin Institute of Physical Chemistry and Electrochemistry RAS, Moscow, Russia, e-mail: [german@ipc.rssi.ru](mailto:german@ipc.rssi.ru)

**Keywords:** technetium-99, sulphide, environmental chemistry,

### Abstract

Sulfur is an element of high of high environmental importance, especially for understanding of many different metals behavior. Tc – S system is not an exclusion in this respect. The sulfur, its different compounds and their derivatives are often present in the natural waters, minerals and rocks and being leached by dissolution mechanism or microbiological transformation affect drastically the Tc environmental dissipation or concentrating routs. For better understanding the Tc behavior in the different natural environments we need quantitative data for the composition and properties of Tc sulfide species that could be formed. This review is aimed to analyze the progress in the field of Tc-S system with the principle focus to its environmental value.

### Historical data and its reconsideration.

So-called technetium heptasulfide was among the first synthesized Tc compounds [1-2] because it was considered as a convenient route for Tc separation from aqueous solutions. Already in the first works its composition was established as  $Tc_2S_7$ , thus supposing that Tc is present in its higher oxidation state. This experimental data were sufficiently precise although rather surprising in view of Tc(VII) redox potentials being in contradiction with those of  $S^{2-}$ . Spitsyn and Kuzina in IPCAS, Moscow, as well confirmed this composition [3]. Meanwhile the crystallographic characterization of technetium heptasulfide was not possible as the precipitate was completely X-ray amorphous. All the attempts of recrystallization in solution failed and no explanation of the composition and the structure was available for more than 45 years [4].

Lee and Bondietti in 1979-83 studied the effects of Fe(II) and of  $S^{2-}$  on Tc solubility having found out that, in the absence of  $S^{2-}$ , the pertechnetate was reduced by Fe(II) and Tc(IV) hydroxide precipitated from the solution [5-6]. Meanwhile, in the presence of  $S^{2-}$ ,  $Tc_2S_7$  precipitated, and the authors concluded that Tc(VII) was not reduced with this ion [6]. When both Fe(II) and  $S^{2-}$  were present, Tc was reduced and coprecipitated with a FeS phase as a carrier.

Amorphous Tc(IV) sulfide was also described by Boyd having been prepared while heating  $Tc_2S_7$  in the absence of  $O_2$  [7]. Crystalline  $TcS_2$  in turn was prepared by chemical transport reaction along a temperature gradient (1423-1353 K) in a sealed tube. According to [8] the presence halogen as a carrier gas, improved transport efficiency [8]. This  $TcS_2$  formed triclinic crystals.

Sodium thiosulphate or thioacetamide were shown being able to produce  $Tc_2S_7$  in treatment of acidic Tc(VII) solutions [9, 10].

Important Tc accumulation by some sulfide minerals was observed [11-13], the most effective sorbents being the sulfides with higher solubility or possessing reducing metal ions. The mechanism for Tc sorption differed for different minerals [13].

The  $Tc_2S_7$  solubility was investigated based on the measurements of Tc concentration in the aqueous solutions equilibrated with the previously precipitated and washed technetium sulfide [13]. No reasonable value was possible to establish because of its complicated hydrolyses behavior under the applied conditions as described in [3, 13] and references therein.

Formation kinetics was studied spectrophotometrically [14] providing with the data on the Tc(VII) reaction with sulfide reaction while the further colloidal particle size speciation studies supported with ultramicrocentrifuge technics [15-16] provided with the reliable information on Tc concentration dependences.

The  $TcO_4^-$  and  $S_2^{2-}$  solutions have important absorbances in the UV region, being completely transparent in the region of visible light. In course of the reaction of the pertechnetate with  $S_2^{2-}$ , the brown color of the solution develops, the corresponding spectrum being attributed to the technetium sulfide formation [14]. For the kinetic studies in [14] the  $\lambda = 450$  nm was chosen (Fig.1 – 2). Some kinetic curves registered for solutions with different with initial  $[TcO_4^-]_0$ ,  $[Na_2S]$  and pH are illustrated at Fig. 2-4.

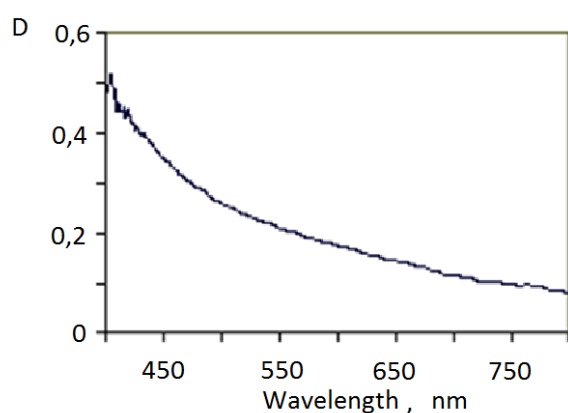


Fig.1. Typical spectrum for technetium sulfide formed after exposition for  $t = 4560$  s, in the solution with initial  $[TcO_4^-]_0 = 1 \cdot 10^{-4}$  M,  $[Na_2S] = 0,27$  M and  $pH = 11,8$ .

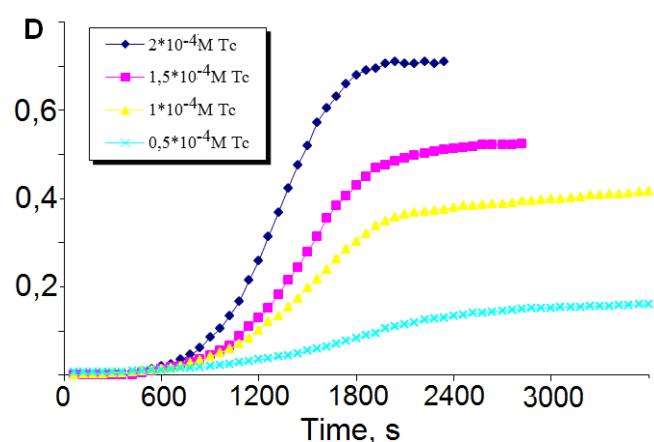


Fig. 2. Kinetic curves registered at 450 nm for the reaction of pertechnetate with sodium sulfide:  $[TcO_4^-]_0 = (0,5 - 2) \cdot 10^{-4}$  M,  $[Na_2S] = 0,27$  M,  $pH = 11,8$ .

As the pH of the solution could be affected by hydrolyses and sulfide oxidation, some tests were conducted in buffer solutions [14]. In all cases the pH was kept within  $pH = 8 - 12$  region as lower pH are favorable for hydrolyses of sulfide and hydrosulfide ions and conversion of elementary sulfur formed in the reaction into disulfide ion. The typical kinetics for phosphate buffers is demonstrated in the Fig. 3.

Three stages are characteristic for this reaction, the first one being induction period (from 13500 and up to 35000 s (= 9.7 h) dependent on the pH) its duration being dependent on the initial accumulation of disulfide ion, the second – intermediate reduction of pertechnetate to mixed Tc oxosulfide(V,IV) (14000 – 50000 s dependent on the pH) and the third – final formation of trinuclear Tc disulfide [14-15]. The colloidal solutions of the technetium sulfide thus formed were rather stable. Similar solutions were described by T. Sekine and co-authors in [16]. The composition of the precipitate separated from this solution by 10 kD ultramicrocentrifuge membranes was determined by chemical analyses and by Rutherford back scattering (CENBG Bordeaux-Gradingan in collaboration with Lab. Pierre Sue, Saclay) and was equal to  $Tc:S = 2 : 6,73(25)$  [15]. This precipitate was analyzed by EXAFS studies at ESRF, Grenoble the results (see Fig. 4.) had confirmed its identity with the technetium sulfide studied by different authors [17-18].

The rate constant  $K_1$  for the initial step of Tc(VII) reduction with sulfide (producing Tc(IV) and polysulfide ions) was determined as  $7.0 \cdot 10^{-6} \text{ cek}^{-1}$  while  $K_2$  constant for the final formation of technetium sulfide (in fact trinuclear technetium(IV) polysulfide) as shown in [17]) was  $2.0 \cdot 10^{-4} \text{ cek}^{-1}$ , being by 2 orders of magnitude higher than  $K_1$ .

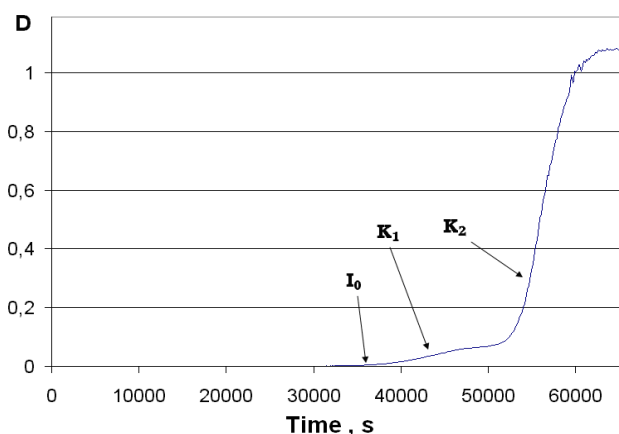


Fig. 3. Technetium sulfide formation kinetics (registered at 450 nm) in the reaction of pertechnetate with sodium sulfide at constant pH provided with buffer solution:  
 $[TcO_4^-]_0 = 1.57 \cdot 10^{-4} \text{ M}$ ,  $[Na_2S] = 0.09 \text{ M}$ ,  
 buffer solution  $[HPO_4^{2-}]/[H_2PO_4^-] = 3/1$ ,  
 $[PO_4]_{\Sigma} = 0.19 \text{ M}$ ,  $pH = 8.2$

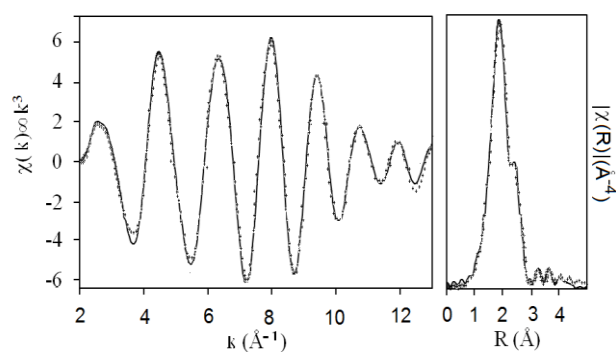


Fig.4. Tc K-edge EXAFS spectra (left) and their Fourier transforms (right) of the Tc sulfide colloidal solution corresponding to the reaction of pertechnetate with sodium sulfide for  $[TcO_4^-]_0 = 2,0 \cdot 10^{-4} \text{ M}$ ,  $[Na_2S] = 0,27 \text{ M}$ ,  $pH = 11,8$ .

The influence of initial technetium(VII) concentration (within the range of  $(0,57-2,66) \cdot 10^{-4} \text{ M}$   $KTcO_4$  and constant  $[Na_2S] = 0.3 \text{ M}$ ) on the reaction rate of Tc and sulfide was determined from the data shown in Fig. 2. The rate constant was practically lineary dependent on the technetium concentration within the range  $(0,57 - 2,66) \cdot 10^{-4} \text{ M}$ .

The kinetics data recalculated from concentration to conversion degree axes are presented at the Fig5. Under the listed conditions the reaction of Tc(VII) with sulfide was also characterized with induction period and the kinetics dependent on the  $[Na_2S]$  in the solution and the pH of the solution. Reaction of  $NaTcO_4$  with  $0,3 \text{ M}$   $Na_2S$  was completed within 2000 s, the further development of the precipitate was due to aging effects. The S/Tc ratio in the sediment was obtained by chemical analyses as 3.36(7) on a macroammount of the precipitate and confirmed by RBS (Fig.6) [15].

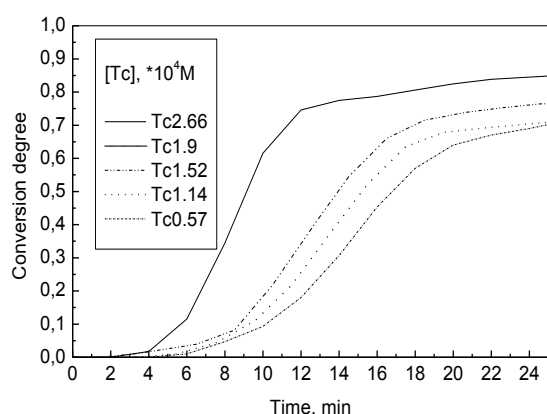


Fig.5. Reaction kinetics of  $NaTcO_4$  with  $0,3 \text{ M}$   $Na_2S$ ,  $pH=11.8$ ,  $t=20^\circ C$  [15]

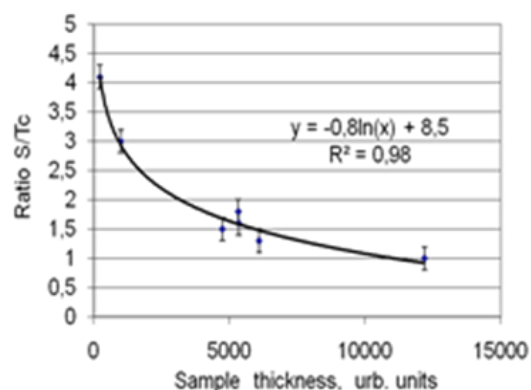


Fig. 6. RBS determination of S/Tc ratio in technetium sulfide [10]

Particle growing processes were investigated for technetium(VII) sulfide ( $Tc_2S_7$ ) colloids produced in a mixture of  $Na_2S$  and  $TcO_4^-$  solutions by laser-induced photoacoustic spectroscopy (LPAS). Analysis of the LPAS signal intensities indicated that the particle size increased in the solution with an increase of standing time, while the number of particles remained constant. It was revealed that the size of colloid particles increased by deposition of  $Tc_2S_7$  on the particle surfaces, not by coagulation of colloid particles. The formation mechanism and growing process of the colloids are

discussed based on the LaMer model, which deals with nucleation processes. In the aging process of Tc-S colloid system, the size of colloid particles was shown to increase by deposition of Tc sulfide on the particle surface, not by coagulation of the particles [11].

The final ideas for explanation of Tc – S system became possible only based on EXAFS studies [12]. It was demonstrated that -S-S- disulfide ligands are present in the structure thus explaining the reduction mechanism for Tc(VII) to Tc(IV) with no notable change in Tc:S stoichiometric ratio that remained close to the value within the interval of 3,3 – 3,5.

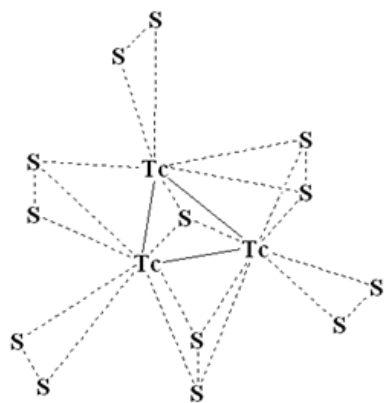


Fig.7. Structure unit fragment  $Tc_3S_{13}$  for technetium sulfide acc. to EXAFS studies[17]

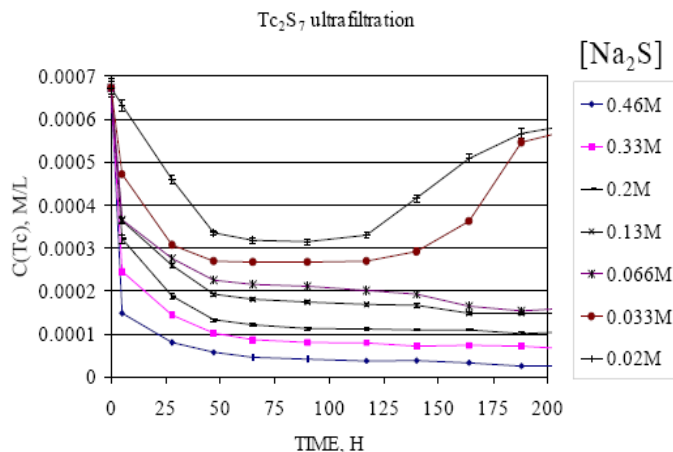


Fig.8. Concentration of free Tc species as fractionized with separation of ionic or nanocolloidal particles with 5 kD "Sartorius" ultramicrocentrifuge tubes [15]

At the same time the presence of  $S_2^{2-}$  ligand in the compound explains some other properties that was not well understood before. The determination of the concentration of free Tc species as fractionized with separation of ionic or nanocolloidal particles with 5 kD "Sartorius" ultramicrocentrifuge tubes [15] gave evidence on the  $Tc_3S_{10}$  nanosulfide formation (Fig.3) similar to that observed in [17].

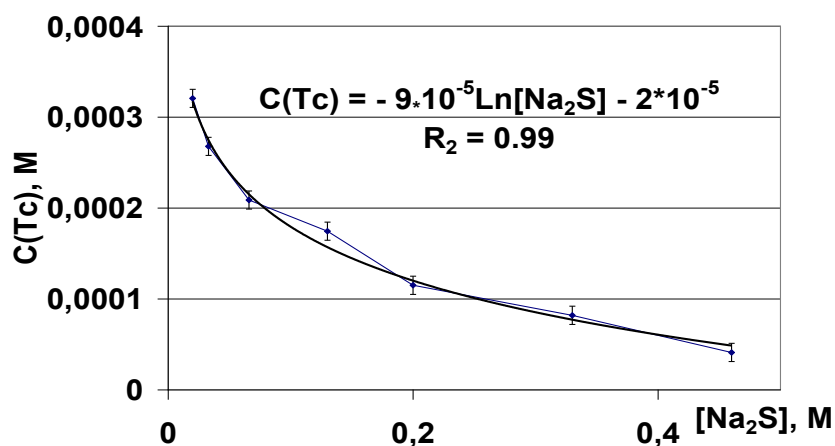


Fig. 9. Solubility of Tc sulfide at  $\tau = 75 - 110$  h as evaluated for different  $[Na_2S]$  by separation of nano-colloidal particles with 5 kD "Sartorius" ultramicrocentrifuge tubes [15]

The stability of  $Tc_3S_{10}$  in the resulting solution was dependent of the  $S^{2-}$  concentration in it. When higher than 0.06M  $Na_2S$ , further growth of Ts sulfide particles occurred for  $\tau \geq 150$  h similar to observations made in [11]. For  $[Na_2S] \leq 0.04$  M, the  $Tc_3S_{10}$  was reoxidized by present air to Tc(VII) within 175-200 hours thus being resolubilized.

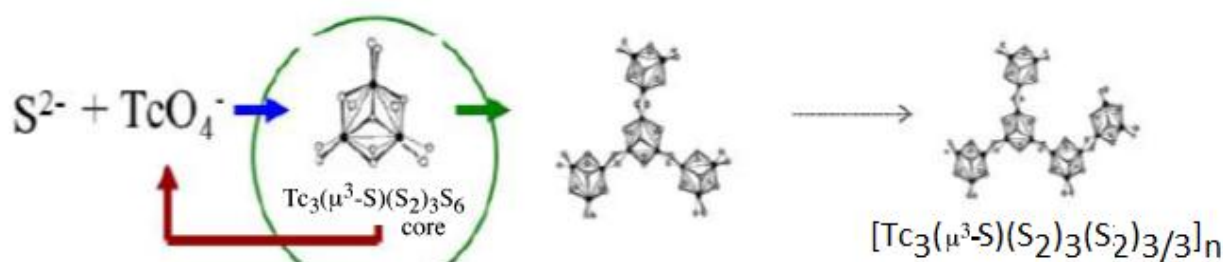


Fig. 10. The scheme of Tc reaction with sulfide describing precipitation and ultracentrifugal speciation tests the follows the ideas drawn based on the results of Lukens et al. , Sekine et all and German et all [15 - 17].

The determination of the free Tc species concentration with separation of ionic or nanocolloidal particles with 5 kD “Sartorius” ultramicrocentrifuge tubes [10] (Fig. 4) gave evidence on the  $Tc_3S_{10+x}$  nanosulfide formation similar to that observed in [12]. The equation for the Tc sulfide solubility based on these figures was evaluated.

The stoichiometry of technetium sulfide precipitated from aqueous solutions by sulfide action was recently confirmed by Liu, Tery and Jurisson in [18]. Some important data on the FeS effect onto Tc environmental behavior was reported by the same authors in [19]. Although the proposed technetium dioxide formula applied in [19] for the processing of the EXAFS data differs in the number of water molecule bounded to the  $TcO_2$  from the recommended value (that is 1.6  $H_2O$  according to [4], and very similar to 1.5  $H_2O$  observed earlier for Re(IV) hydroxide), the results of [18,19] support in principle the evidence for the formulation of common technetium sulfide established by Lukens and co-workers [17]. Also the results of [20] are not in contradiction with [17]. Therefore we consider that the latter work provide a correct and important description of technetium sulfide is the compound is formed from water solutions by reaction of pertechnetate with sulfide/polysulfide source.

#### Acknowledgments:

The work was carried out in part as the statutory work of the A.N. Frumkin Institute of Physical Chemistry and Electrochemistry of RAS within the grant No.8 with the Department of Chemistry and Material Sciences (Russian Academy of Sciences). We also highly acknowledge the fruitful discussions with Dr. W. Lukens and the provided supplementary EXAFS and XANES data on  $Tc_3S_{10}$ .

#### References.

1. Cobble, J. W., Nelson, C. M., Parker, G. W., et al., *J. Am. Chem. Soc.*, **74** (1952) 1852.
2. Rulfs, C. L., Meinke, W. W. *J. Am. Chem. Soc.*, **74** (1952) 235–236.
3. Spitsyn, V. I., Kuzina, A. F., “Investigation of weighable amounts of technetium”, *Proc. Acad. Sci. USSR Chem. Sect.*, **124** (1959) 103–105.
4. Rard J.A., Rard M.H., Anderegy G., Wanner H. // "Chemical Thermodynamic of Technetium.", by Ed. Sandino M.C.A., Osthls E., OECD NEA, Data Bank , Issy-les-Moulineaux, France, 1999
5. Bondietti, E.A., Francis , C.W. *Science*, **203** (1979) 1337-1340.
6. Lee, S. Y., Bondietti, E. A., In: “Sci. Basis Nucl. Waste Manage. VI, held Nov. 1982 in Boston”, (Brookins, D. G., ed.), New York: North-Holland, 1983, pp. 315–322.
7. Boyd, G. E., “Technetium and promethium”, *J. Chem. Educ.*, **36** (1959) 3–14.
8. Wildervanck, J. C., Jellinek, F., “The dichalcogenides of technetium and rhenium”, *J. Less-Common Met.*, **24** (1971) 73–81.
9. Eckelman, W. C., Levenson, S. M., “Radiopharmaceuticals labeled with technetium”, *Int. J. Appl. Radiat. Isot.*, **28** (1977) 67–82.



10. Anders, E., The radiochemistry of technetium, Washington D.C.: Department of Commerce, 1960, 50 p.,
11. Winkler A., Bruhl H., Trapp, Ch., Bock W.D. *Radiochim. acta* , **44/45** (1988), 183-186.
12. K.E. German, V.F. Peretrukhin, L.I. Belyaeva, O.V.Kuzina. In: "Technetium and Rhenium Chemistry and Nuclear Medicine 4, (Bressanone-Bolzano-Italy, Sept. 12-14, 1994, (Nicolini M., Bandoli G., Mazzi U.- Eds.) SGEEditoriali, pp. 93- 97
13. S.El-Waer, K. E.German, V. F.Peretrukhin. *J. Radioanal. Nucl. Chem.*, **157** (1992) 3–14.
14. M. Simonoff, K. E. Guerman, G. Simonoff. In: Abstracts of the 2<sup>nd</sup> Japanese-Russian Seminar on Technetium, Shizuoka, 1999, p. 25
15. M. Simonoff, K. E. Guerman, C. Sergeant et all. *Journee Radiochimie 2000*, Gif-sur-Yvette, 28-29 September, 2000, France.
16. Y. Saiki, M. Fukuzaki, T. Sekine et all. *J. Radioanal. Nucl. Chem.* **255** (2003) 101–104.
17. W. W. Lukens, J. J. Bucher, D. K. Shuh, N. M. Edelstein. *Environ. Sci. Technol.*, **39** (2005) 8064-8070.
18. Y. Liu, J. Terry, S. Jurisson. Per technetate immobilization in aqueous media with hydrogen sulfide under anaerobic and aerobic environments. *Radiochimica acta.* **95** (2007) 717 - 727.
19. Y. Liu, J. Terry, S. Jurisson. Per technetate immobilization with amorphous iron sulfide. *Radiochimica acta.* **96** (2008) 823-833.
20. M.J. Wharton, B. Atkins, J.M. Charnock, F.R. Livens, R.A.D. Patrick, D. Collison. An X-ray absorption spectroscopy study of the coprecipitation of Tc and Re with mackinawite (FeS). *Applied Geochemistry* 15 (2000) 347-354.

2.P12.

## TECHNETIUM LIMNOLOGY AS FRAME FOR ITS ECOLOGY AND THE KEY FOR UNDERGROUND STORAGE

K.E. German, T. V. Khijniak, V.F., Peretrukhin

Institution of Russian Academy of Sciences A.N. Frumkin Institute of Physical Chemistry and Electrochemistry RAS, Moscow, Russia, e-mail: [german@ipc.rssi.ru](mailto:german@ipc.rssi.ru)

Winogradsky Institute of Microbiology of RAS  
Prospect 60-letiya Oktyabrya 7/2, Moscow, Russian Federation

Radionuclides' accumulation by natural associations of microorganisms is important item for comprehension of their behavior in natural and technogenic water ecosystems. Different microorganisms are shown to exhibit different concentration factors from very low to very high, and the situation is complicated when we analyze the behavior of natural sediments composing of the association of some about 100 microbial species with some mineral. Tc transfer factors from water to sediments were analysed in some works [1-3 and ref. therein]. The influence of natural water composition onto radionuclides sorption by lake sediments is not thoroughly studied.

Here we overview the results of model laboratory study of the bioaccumulation of the long-lived radionuclides [4-5]. The isotopes were introduced as pertechnetate solution ( $^{99}\text{Tc}$  (VII)) or nitrate solution ( $^{234}\text{Th}$  (IV) - as a tracer for typical behavior of four-valent actinides) into batch samples containing lake water and sediments taken from the 3 eutrophic lakes 1) Belye Kosino (Moscow reg.), 2) l. Kezadra and 3) l. Navolok, both - Udomlya reg., near from Kalininskaya NPP). The initial concentrations of Tc have been adjusted to  $10^{-6}$ - $10^{-7}$  M and that of  $^{234}\text{Th}$  (IV) to 3000 cpm per initial aliquote. Eutrophic lake Belye Kosino sediment was mainly formless organic detritus, gray colored,  $\text{H}_2\text{S}$  odoriferous. Udomlya reg. lakes sediment were 30% organic detritus and humics, 60% sand and 10% ( $\text{Fe}_2\text{O}_3$  and other inorganic minerals).

*Table.1. Main eutrophic lake Navolok sediment and water phase content*

Microorganism	Cells' number N/ml	Comments
		Ratio in batch: $V_{\text{sediment}} : V_{\text{liquid}} = 1:3$
<i>Microalgae</i>	$10^6$	Total = $2 \cdot 10^9$ bacteria/g, pH = 7.0 (stable); Eh = -0.20V NHE (inner sediment part); water phase: $[\text{HCO}_3^-] = 1 - 4$ mg-C/l; $[\text{HSO}_4^-] = 0 - 50$ mg/l, $[\text{Cl}^-] = 35$ mg/l.
<b><i>Bacteria:</i></b>		
Sulphate reducing	$10^4$	
Methanogenic	$10^4 - 10^5$	
Nitrifying	$10^3 - 10^4$	
Denitrifying	$10^5$	

Two equilibration modes were modeled (overhead agitation and hipolimnionic Tc transfer to sediment). Centrifuge MPW-210 (48G, 15 min), and microfilterfuge tubes – (5 kD “Sartorius” ) were used for phase separation. No more than 5 % of water phase was sampled during the experiments in total. More than 95% of Tc-99 were truly dissolved species of  $\text{TcO}_4^-$  in water phase all time through the experiment. The kinetics' analysis of data from Fig.1 has shown that the half-time values of the initial content removal from the water-phase form 400h for Tc. Two different uptake rates were characteristic for Tc sorption for some samples from Udomlya reg. : fast uptake during the first 2 hours when 40% of initial input was sorbed by eutrophic river/lake sediment, and a slow bioaccumulation period when Tc uptake was completed in 11 days.

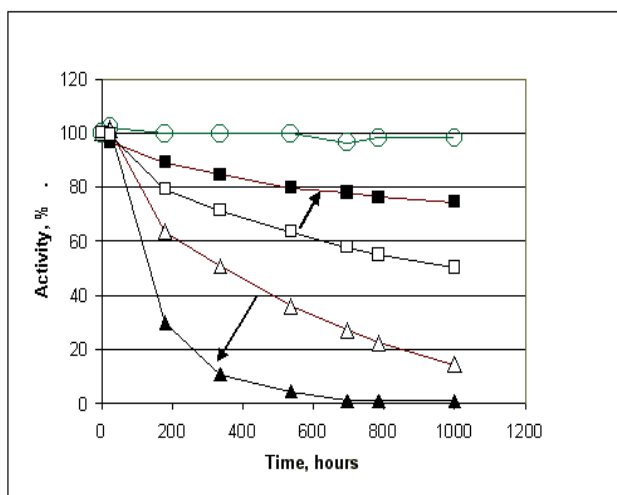


Fig.1. Tc uptake by Lake Sediments: O – steril sample; □-Torfyanoe, ∇ - Beloe; white points - sedimentation; black points – agitated in overhead

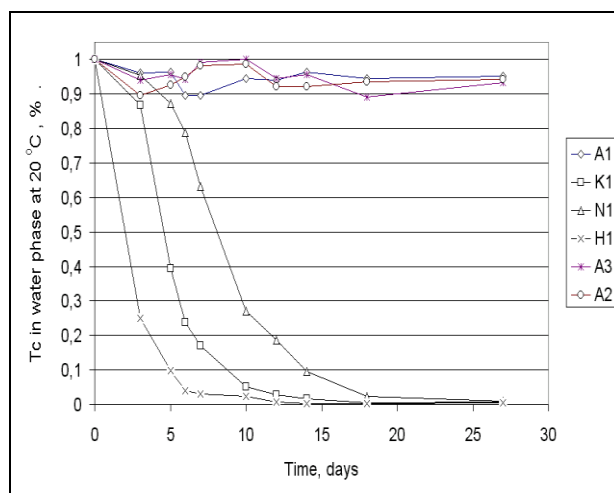


Fig.2. Tc uptake by Lake Sediments A1 – steril sample; K1 – Kezadra, N1- Navolok; H1- Homutovka

The Tc uptake rate differed for different lakes sediments, the time of half-uptake being  $\frac{1}{2}$  month for eutrophic lake Belye Kosino (Moscow reg.) and much less (4-7 days) for the two lakes of Udomlya reg. Concentration factors at 1600 hours of equilibration of Tc with sediments and natural water were 1710 ml/g for eutrophic lake Belye Kosino and 1850 ml/g for the two lakes of Udomlya reg. The complete Tc accumulation by sediment took place after 1.0 months and 0.8 month respectively. Speciation by centrifuging at 10000 rpm, ultrafilterfuging or filtration through 0.05 - 0.22  $\mu\text{m}$  membranes, has shown that the Tc fraction remaining in water phase was present as truly ionic species up to 90%. The microflora of lake played important role in the accumulation and reduction of radionuclides. Some microorganisms (being able of anaerobic respiration) had competition relationships between  $\text{SO}_4^{2-}$  or  $\text{NO}_3^-$  and  $\text{TcO}_4^-$  so that the additions of  $\text{SO}_4^{2-}$  or  $\text{NO}_3^-$  decreases the rate of Tc accumulation by the sediment.

Reduction of Tc(VII) to Tc(IV) and sorption of hydrolyzed species are the main mechanisms for Tc accumulation in this biosystem. We suppose that Tc(VII) reduction and further uptake by the lake sediment is due to microbial activity of the sediment components, most probably to sulfate-reducing bacteria, that are known to reduce Tc(VII) [5]. The difference in the uptake rate is associated with the higher chemical stability of  $\text{TcO}_4^-$ . This mechanism is supported by Tc uptake rate slowing down when concurrent anions like sulfate or nitrate are injected into the water phase.

The sediments from freshwater lakes have a considerable sorption capacity. The consecutive sorption runs have demonstrated only small decrease of Tc uptake rate. The desorption of technetium was carried out with  $\text{H}_2\text{O}$ , 1M HCl, 1M  $\text{NaClO}_4$  or 15%  $\text{H}_2\text{O}_2$  and gave the desorption factors of 0.05, 0.05, 0.08 and more 0.99 thus indicating the oxidative stripping mechanism and contrary - the bioreduction of technetium to be the main mechanism of its uptake.

Thorium (IV) uptake by the sediments of both types was complete in 3 to 5 hours due to much more important sorption affinity of four-valent elements. About 20 % was sorbed by

microparticulated organic matter and were removed only by microfilterfuge tubes ultrafiltration (5 kD “Sartorius”).

The analyses of the new experimental results and its comparison with the literature data unambiguously indicate that some important ideas well developed in conventional limnology could be applied with success to the modeling and the forecast of radionuclide migration in the mixed mineral-sediment-aquatic natural environment both surfacial and deep underground. The known dependencies of season variations of temperature, oxic conditions and hydrodynamics could be useful for these purposes. Some chemosynthetic and thermophilic bacteria species impact could be discussed also with respect to the recent accidents at the seaside environments (p.e. Fukushima accident).

### References

1. M.J. Keith-Roach, P. Roos. The transport of Tc to the sediments of stratified fjords. Int. Conference Migration'2001. Bregenz, Austria, Sept 2001. Abstracts, PA5-05
2. Blaylock B.G., Frank M.L., Hoffman F.O., Deangelis D.L. Behaviour of technetium in fresh-water environment. In: Technetium in Environment. Edited by G.Desmet, C.Myttenaere. Elsevier Applied Science Publishers. London, New York, 1986, p.79-90.
3. G.M. Milton, R.G. Cornett, S.J. Kramer, A. Vezina. The transfer of iodine and technetium from surface waters to sediments. *Radiochimica acta*, 58/59 (1992) 291-296. .
4. Lloyd, J. Khijnyak T.V., Macascie L., and Lyalikova N.N. Reduction of technetium by Disulfo-fibriio desulfuricans: Biocatalyst Characterisation and use in a flowthrough bioreactor. *Appl. Environm. Microbiol.*1999, v.65, No.6. pp.2691-2696.
5. Guerman K.E., Khijnyak T.V., Peretroukhin V.F., German E.S., Firsova E.V. Behaviour of technetium in eutrophic and dystrophic fresh water lakes. The second Japanese-Russian Seminar on Technetium. Shizuoka, Japan, Nov. 29 - Dec.2. 1999. Abstracts, pp.50-51.

2.P13.

## **KASSITERITE AS A DURABLE HOST-PHASE FOR TECHNETIUM IMMOBILIZATION**

Yu.I. Korneyko, V.M. Garbuzov, B.E. Burakov.

V.G. Khlopin Radium Institute, 194021 Russia, Saint-Petersburg,  
2nd Murinsky Avenu, 28,  
e-mail : [yuliakorneyko@mail.ru](mailto:yuliakorneyko@mail.ru)

Kassiterite, SnO<sub>2</sub>, is well-known accessory mineral with high mechanical and chemical durability.

Solid solution of Tc in kassiterite, (Sn,Tc)O<sub>2</sub>, was suggested as a durable host-phase for technetium immobilization. Starting precursor was obtained by co-precipitation from aqueous solution (SnCl<sub>2</sub> + KTcO<sub>4</sub>) using ammonium hydroxide.

Reduction of Tc valence state from (7+) to (4+) was observed during precursor preparation. Then precursor was calcined in air at 800°C, ground in agate mortar and cold pressed. Ceramic synthesis was carried out at 1100°C in argon.

No essential evaporation of Tc was detected during synthesis.

Crystalline ceramic doped with 5% wt. Tc was obtained. All the samples obtained were studied using optical and scanning electron microscopy (SEM); powder X-ray diffraction (XRD) and microprobe analysis (EMPA).

Ceramic physical and chemical properties are discussed.

It was concluded that Sn-Tc-containing precursor obtained in air might be used for synthesis of Tc-doped ceramic based on kassiterite.

This is in contrast with all other precursors obtained before in reducing or inert atmosphere only.



2.P14.

**ELECTROCHEMICAL INVESTIGATION OF CORROSION AND  
DISSOLUTION OF METALLIC TECHNETIUM AND  
Tc-Ru ALLOYS IN 0,5 – 6,0 M HNO<sub>3</sub>**

A.G. Maslennikov<sup>1</sup>, K.V. Rotmanov<sup>2</sup>, N.G. Kravchenko<sup>1</sup>, V.M. Radchenko<sup>2</sup>,  
M.V. Kormilitsyn<sup>2</sup>, V.F. Peretrukhin<sup>1</sup>

<sup>1</sup> A.N. Frumkin Institute of Physical Chemistry and Electrochemistry RAS

<sup>2</sup> Joint Stock Company “State Scientific Center – Research Institute of Atomic Reactors”, Dimitrovgrad, Ulyanovsk region, [ryabinin@niiar.ru](mailto:ryabinin@niiar.ru)

The electrochemical oxidation of metallic technetium and Tc-Ru alloys in 0,5 – 6,0 mol/l HNO<sub>3</sub> was studied. The quantitative characteristics of the corrosion and dissolution processes were determined.

It was found that at the concentration of the nitric acid in the electrolyte less than 2,0 mol/l and at potentials less than 650 mV / Ag/AgCl the metal surface is passivated due to the formation of the slightly soluble hydrated Tc(IV) dioxide. The potential increase leads to the transition of the technetium metal into the transpassive state. In solutions containing more than 2,0 mol/l HNO<sub>3</sub> hydrated Tc(IV) dioxide loses its passivating properties.

It is shown that oxidation of Tc(IV)/Tc(V) is the main reaction that effects the corrosion rate. The results of the corrosion rates obtained from the measurements suggest that technetium metal can be quantitatively dissolved in nitric acid if its concentration exceeds 4,0 – 6,0 mol/l.

Comparison of the repassivation potentials of Tc-Ru alloys with the repassivation potentials using the pure Tc and Ru electrodes shows that the values of the alloy repassivation potential are intermediate between the repassivation potentials using the pure Tc and Ru electrodes. As in the case with pure metals, the values of the alloy repassivation potentials increase with increasing the HNO<sub>3</sub> concentration in the solution.

2.P15.

## **Tc-99 DETERMINATION IN CONTAMINATED GROUNDWATER**

R.A.Aliev<sup>1</sup>, S.N. Kalmykov<sup>1</sup>, I.G. Tananaev<sup>2</sup>, I.A. Ivanov<sup>3</sup>.

1- <sup>1</sup> Lomonossov Moscow State University,  
(Leninskie gory, 1, Chem. Dept., Moscow, Russian Federation)  
2 - Institution of Russian Academy of Sciences A.N. Frumkin Institute of Physical  
Chemistry and Electrochemistry RAS, Moscow, Russia,  
3 - PA Mayak, Ozersk, Russia

As a result of long-term operation of industrial ponds V-9 and V-17 as reservoirs for liquid nuclear wastes at PA “Mayak” the significant contamination of groundwater system by radionuclides occur. During several years the distribution and migration of <sup>90</sup>Sr, <sup>137</sup>Cs, <sup>60</sup>Co, <sup>3</sup>H and long-lived alpha-emitting isotopes in subsurface horizons was studied while no data is available concerning the behaviour of <sup>99</sup>Tc. This study presents the first experimental results on <sup>99</sup>Tc distribution in groundwater near V-9 and V-17 reservoirs. The samples were collected from different depths.

The analytical determination of <sup>99</sup>Tc included precipitation of Fe(III) hydroxide to co-precipitate some of the interfering radionuclides that form cationic species, then technetium was reduced to Tc(IV) by adding Fe(II) and co-precipitated with its hydroxide. The precipitate was separated by centrifugation and then dissolved in diluted nitric acid with addition of H<sub>2</sub>O<sub>2</sub> to oxidize Fe(II). Finally technetium containing solution was purified by anion exchange. The radioactivity of <sup>99</sup>Tc was determined using liquid scintillation spectrometry, the chemical yield was determined using <sup>99m</sup>Tc tracer.

It is shown that <sup>99</sup>Tc activity varies between 1 and 2300 Bq/l with the tendency of increase of its concentration with depth. The last fact could be explained by the high density of waste solutions in V-9 and V-17 and gravitational exclusion of groundwater by contaminated solution.

2.P16.

## **SORPTION OF Tc-99 AND Np-237 BY DEPLETED UO<sub>2</sub>**

O. Batuk<sup>1</sup>, S.N. Kalmykov<sup>1</sup>, E.V. Zakharova<sup>2</sup>.

<sup>1</sup> Lomonosov Moscow State University, (Leninskie gory, 1, Chem. Dept., Moscow, Russian Federation)

2 - Institution of Russian Academy of Sciences A.N. Frumkin Institute of Physical Chemistry and Electrochemistry RAS, Moscow, Russia

Alteration of spent nuclear fuel (SNF) upon storage in deep geological repositories under oxidizing conditions will likely result in formation of secondary phases on UO<sub>2</sub> surface. This may influence the solubility of SNF and release of radionuclides to the environment. On the other hand precipitated phases may limit the leaching of other radionuclides and prevent SNF from further oxidation. The goal of this work was the study solubility, secondary phase formation and Np(V) retention on the surface of UO<sub>2+x</sub> sample during hydrothermal treatment in simulated oxic groundwater.

The UO<sub>2</sub> sample was characterized by X-ray powder diffraction (XRD) and X-ray photoelectron spectroscopy (XPS) to determine bulk and surface phase composition that were UO<sub>2</sub> and UO<sub>2.25</sub> respectively. The hydrothermal experiments were performed at 25°C, 70°C and 150°C during 6 months in the presence of about 1·10<sup>-5</sup> M of Tc(VII) and Np(V). For room temperature experiments the retention of Tc(VII) Np(V) by UO<sub>2</sub> sample was also studied as a function pH in batch mode. Solid phase and solution aliquots were taken periodically for various analyses: determination of technetium and neptunium concentrations in solutions, for XRD, XPS, SEM and TEM analyses of solid phases. Neptunium sorption was almost quantitative for all studied temperature conditions after one week of equilibration while technetium sorbed only at pH<2. Uranium solubility increased in time and reached the equilibrium values typical for U(VI) also in about one week. The progressive oxidation of the sample with formation of U(VI) alteration phases were detected by XPS, XRD and TEM for samples treated at 70 °C and 150 °C.

For Np sorption experiments that were done at room temperature the reduction of Np(V) to Np(IV) was observed at pH<4.5 while technetium stayed as Tc(VII) that explains its low sorption affinity towards UO<sub>2+x</sub>. Neptunium reduction was possible either due to its interaction with the surface that had a stoichiometry close to UO<sub>2</sub> at low pH as determined by XPS or through the reduction by U(IV) present in solution. Upon the increase of pH the UO<sub>2</sub> surface became more oxidized and its stoichiometry became close to UO<sub>2.25</sub> as determined by XPS. At pH>4.5 neptunium was present in pentavalent and was sorbed by the surface complexation mechanism.

The work was partly supported by the ISTC project No. 2694.

2.P18.

## ReO<sub>4</sub><sup>-</sup> AND TcO<sub>4</sub><sup>-</sup> ION-SELECTIVE BUBBLE-THROUGH FLOW CELLS

Yu.I. Urusov<sup>1</sup>, K.E.German<sup>2</sup>, A.V.Kopytin<sup>3</sup>, A.F.Zhukov<sup>1</sup>

<sup>1</sup> D.Mendeleev Russian Chemical-Technology University, Miusskaya sq.9, Moscow, 125047, Russia

<sup>2</sup> Frumkin Institute of Physical chemistry and electrochemistry, Leninsky pr.31-4, Moscow, Russia

<sup>3</sup> Kurnakov Institute of General and Inorganic Chemistry Leninsky pr.31-1, Moscow, Russia

**Keywords:** Flow system; Bubble-through flow cell; Chloride; perrhenate; pertechnetate; Ion-selective electrodes.

### Abstract

A fast-response flow cell with ion-selective electrodes was constructed for continuous-flow measurements in air-segmented streams without debubbling. The flow system was optimized for perrhenate and pertechnetate determinations. With a flow-rate of 4 ml min<sup>-1</sup> a sampling rate of 480 h<sup>-1</sup> was achieved for ion determinations; the average relative standard deviation in all instances was better than 3%. In order to eliminate the operation of removing bubbles with debubbler and to obtain the rapid sampling rates in conventional air-segmented system, bubble-through flow cells without different bubble-gating methods have been proposed in this report for Tc and Re tetraoxometallate anion determination.

### Introduction

The object of present work is a development and an investigation of ion-selective electrodes for ReO<sub>4</sub><sup>-</sup> and TcO<sub>4</sub><sup>-</sup> determination in flow continuous analysis. As electrode active substances in ion-selective electrodes were used quaternary alkylammonium salts.

Quaternary alkylammonium and phosphonium salts are widely used for preparation of the membranes giving a response to different ions. The selectivity of ion determination depends on hydration energy of ion and on the nature of membrane solvent.[1] With this approach to a creation of new ion-sensitive sensors some electrode membranes for different anions and acidocomplexes determination have been developed [ 2-5 ].

The system with the rotary valve was used for studying the dependence of the cell response on the flow-rate.[ 6]

### Experimental

**Membranes preparation.** The ionophore ((C<sub>12</sub>H<sub>25</sub>)<sub>4</sub>NReO<sub>4</sub>), plasticizer (o-nitrophenyloctyl ether, Fluka) and high molecular weight polyvinylchloride (Aldrich) were dissolved in the appropriate volume of cyclohexanone and mechanically stirred. All membrane cocktails were cast in glass rings placed on glass plates. Solvent from PVC membrane was allowed to evaporate at room temperature. The thickness of the resulting membranes was about 0.2 - 0.3 mm.

The electrochemical properties of the electrodes were investigated in the conventional configuration. Small disks were punched from the cast membranes and mounted in electrode bodies. The external reference electrode was a double-junction Ag/AgCl reference electrode OP-8020 P (Radelkis). The potential was measured using pH/ion analyzer OP-300 (Radelkis, Hungary).

Potassium perrhenate (pertechnetate) solutions in 1M Li<sub>2</sub>SO<sub>4</sub> were used for the electrode response function determination. The selectivity coefficients were determined by the separate solution method (SSM) using 0.01 M potassium or sodium salts of the anions.

The influence of pH on the electrode response was examined by adjusting the pH of the measured solution with 1M sodium hydroxide and hydrochloric acid.

### Flow cell construction

All the measurements were done with a flow cell of modified wall-jet design (Fig. 1).

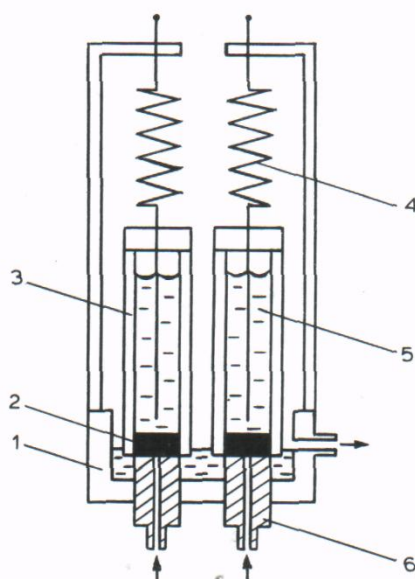


Fig. 1. Bubble-through flow cell. (1) Cell body; (2) membrane; (3) ion-selective electrode; (4) steel spring; (5) inner reference solution; (6) sample guide.

The body of the cell is fabricated from a Plexiglas cylinder, 5 cm in diameter and 2 cm long. Two Teflon sample guides are screwed into the bottom of the cell body, each having a narrow inlet channel (0.4 mm in diameter). The indicator and reference electrodes are supported in a vertical position by steel springs serving also as connecting wires for the mV/pH meter. The electrodes rest on the flat top surfaces of the sample guides, the diameter of sensing membranes being equal to that of the sample guides (5 mm). To reduce the pressure built up in the system, supporting springs are adjusted so that the electrodes rest on the surface of the sample guides with 1-3 g force. The electrodes are positioned so that the flow is introduced at the centre of the membrane face and is forced to exit between the membrane face and the top surface of the sample guide around the membrane perimeter into the reservoir. The liquid level in the reservoir is kept constant (ca. 0.5 mm above the membrane surface) by differential pumping. Air bubbles passing quickly between the membrane face and the surface of the sample guide never collect under the membrane covering the whole sensing surface, so the contact between indicator and reference electrodes is never broken. Reference electrode on the basis of a composition of  $\text{Ag}_2\text{S-AgCl}$  was used.

### Apparatus

A Reihelt E 25/WM K10 peristaltic pump was used for pumping the solutions. The sampler was Contiflo OL-601/11 with a laboratory-made programming device, allowing different sampling rates and sample-to-wash ratios to be maintained. The potentials were measured at room temperature with a Radelkis OP-208 pH/mV meter and recorded by an  $x-t$  recorder. Tygon tubing (0.7 and 1.65 mm i.d.) was used to construct the manifold.

A schematic diagram of the cell response rate measuring system is shown in Fig. 2.



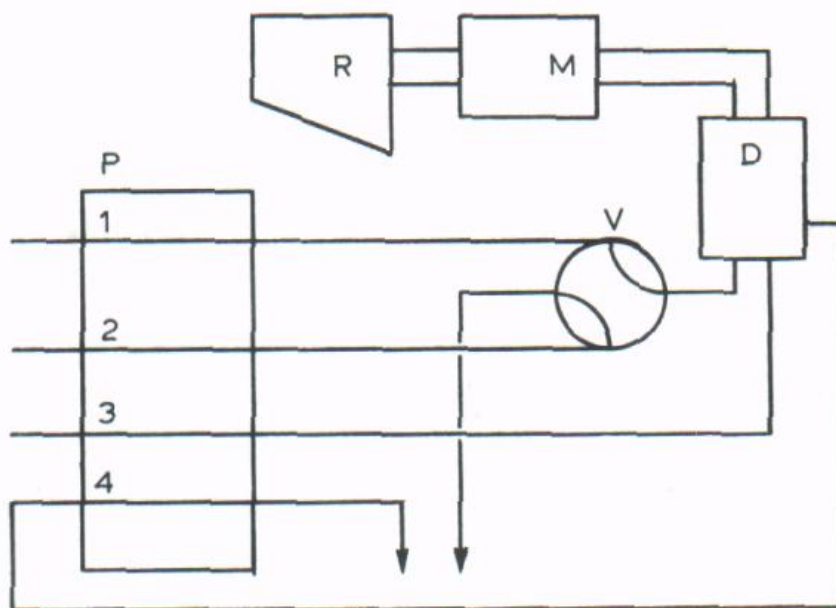


Fig. 2. Schematic diagram of the cell response rate measuring system. (P) Peristaltic pump; (V) rotary valve; (D) flow cell; (M) mV/pH meter; (R) x-t recorder; (1), (2) standard solutions, flow-rate 1-12 ml min<sup>-1</sup>; (3) reference solution, flow-rate 2 ml min<sup>-1</sup>; (4) to waste, flow-rate 14 ml min<sup>-1</sup>.

A Teflon rotary four-way valve was used to interchange the solutions flowing through the cell. The channels of the valve were 0.8 mm i.d.; the inlet port of the cell was connected to the valve outlet port by a 1-cm length of 0.76 mm i.d. Tygon tubing. With manual operation of the valve, sharp concentration jumps were obtained; in any event the dispersion of the solutions was kept constant throughout all the measurements.

Figure 3 shows a schematic diagram of the automated analysis flow system. The analyzer includes no special devices for either the air segmentation (air-bar) or the debubbling.

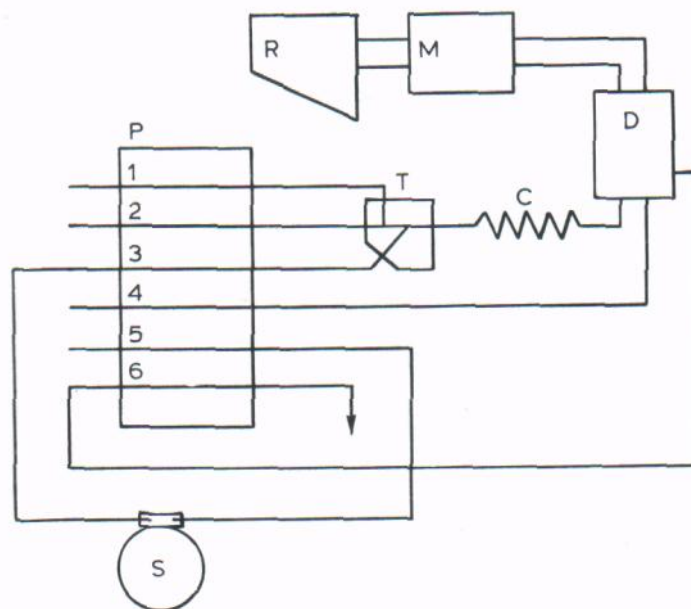


Fig. 3. Schematic diagram of the automated analysis flow system. (P), (D), (M), (R) as in Fig. 2; (T) T-connector; (C) mixing coil; (S) sampler; (1) air, flow-rate 2.6 ml min<sup>-1</sup>; (2) buffer solution, flow-rate 2 ml min<sup>-1</sup>; (3) sample/wash, flow-rate 2 ml min<sup>-1</sup>; (4) reference solution, flow-rate 2 ml min<sup>-1</sup>; (5) wash (distilled water), flow-rate 3 ml min<sup>-1</sup>; (6) to waste, flow-rate 7.5 ml min<sup>-1</sup>.

## Results and discussion

The response for  $\text{ReO}_4^-$  and  $\text{TcO}_4^-$  electrodes are shown in fig.4.

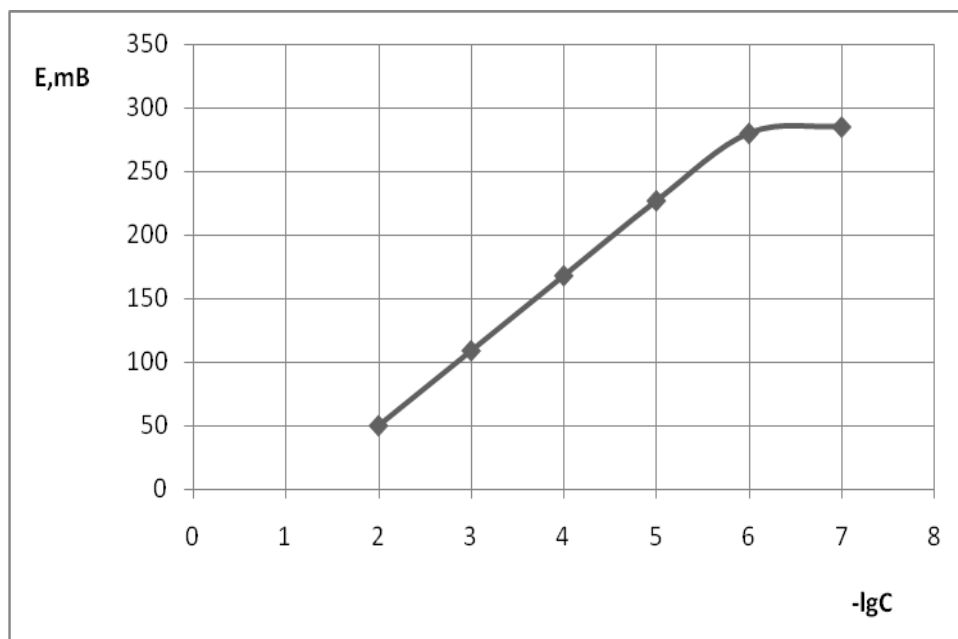


Fig.4 Responses  $\text{ReO}_4^-$  and  $\text{TcO}_4^-$  selective electrodes.

For all these electrodes response function is linear in the range  $10^{-6}$  -  $10^2$  M with the slope equal to  $59 \pm 2$  mV/pTc at  $25^\circ\text{C}$ .

Almost the same results have been obtained with tetradodecylammonium perrhenate (pertechnetate).

High potentiometric selectivity to  $\text{ReO}_4^-$  and  $\text{TcO}_4^-$  of the ISEs against the main anions was found for all the ISEs developed (see Table 1).

Table 1. Selectivity of  $\text{ReO}_4^-$  and  $\text{TcO}_4^-$  electrodes.

ion electrode	$\text{F}^-$	$\text{SO}_4^{2-}$	$\text{H}_2\text{PO}_4^-$	$\text{Cl}^-$	$\text{NO}_3^-$	$\text{BF}_4^-$	$\text{ClO}_4^-$	$\text{TcO}_4^-$	$\text{ReO}_4^-$
$\text{ReO}_4^-$	$2 \cdot 10^{-5}$	$3 \cdot 10^{-5}$	$1 \cdot 10^{-5}$	$1 \cdot 10^{-4}$	$9 \cdot 10^{-4}$	$7 \cdot 10^{-2}$	0.1	1.2	1
$\text{TcO}_4^-$	$1 \cdot 10^{-5}$	$3 \cdot 10^{-5}$	$9 \cdot 10^{-6}$	$1 \cdot 10^{-4}$	$1 \cdot 10^{-3}$	$6 \cdot 10^{-2}$	0.1	1	0.9

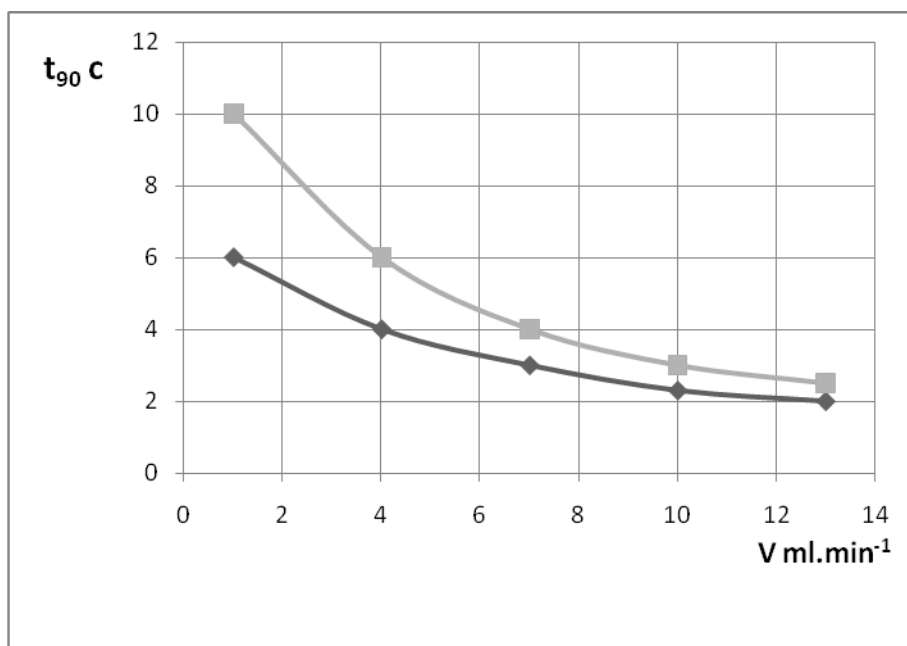


Fig.4. Dependence of time of the response on speed of submission of a solution  
 1.  $1.10^{-2}M \rightarrow 1.10^{-4}M$ ; 2.  $1.10^{-4}M \rightarrow 1.10^{-2}M$

### Cell response rate

The system with the rotary valve (Fig. 2) was used for studying the dependence of the cell response on the flow-rate. The cell response time  $t_{90}$ , the time to reach 90% of the steady-state potential for both the  $\text{ReO}_4^-$  and  $\text{TcO}_4^-$  electrodes, was observed to improve when the flow-rate was increased in the range 1-7 ml min<sup>-1</sup>, as shown in Fig. 4

Further increases in flow-rate had no significant effect on the cell response time; a flow-rate of 4 ml min<sup>-1</sup> was chosen for operation of the automated analyzer. The increase in a range of determined concentration leads to increase in a relative standard deviation.(fig. 5)

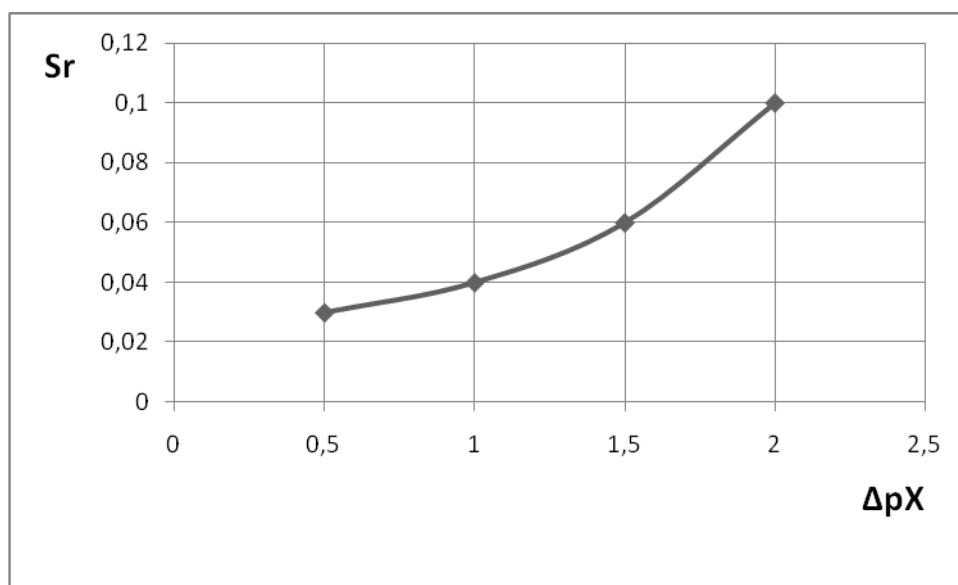


Fig. 5. Dependence of a relative standard deviation on a range of determined concentration

### Automated analysis

The mixing coil dimensions and the air flow-rate were optimized during preliminary experiments. Ten turns of a 50-cm length of glass tubing with i.d. 1.5 mm were sufficient for adequate mixing of the two streams, each having a flow-rate of 2 ml min<sup>-1</sup>. Changes in the air flow-rate from 2 to 3 ml min<sup>-1</sup> had no effect on the noise level and the sample dispersion; an air flow-rate of 2.6 ml min<sup>-1</sup> was chosen for operation of the analyzer.

Mixing between the sample and the wash slugs as they pass through unsegmented zones of the CF system, i.e., from the tip of the sample probe through the pump to the T-connector, contributes considerably to the dispersion in the flow system. To reduce this mixing effect in the sample line, the introduction of two air segments at the leading edge of each sample and wash slug by rapid repetitive insertion and withdrawal of the sample probe ("pecking") was used [7]. This pecked sampling technique significantly reduced carry-over and allowed the sampling rate to be increased.

With ion-selective electrodes used in flow analysis, the wash (or carrier) stream electrolyte is usually spiked with the ion to be measured to stabilize the baseline and improve the response [8,9]. More often this is adopted when FIA is used, as a variable baseline may affect significantly the recorded peak-height value. When the CFA technique is involved, i.e., a steady-state or close to steady-state detector signal is measured, the baseline is not always necessary. For the automated determination of  $\text{ReO}_4^-$  and  $\text{TcO}_4^-$  1M  $\text{Li}_2\text{SO}_4$  was used as the wash electrolyte; this reduced the cell wash time and allowed the sampling rate to be increased.

For Ion determinations the sampling and wash times were 4 s, the sampling rate being  $450 \text{ h}^{-1}$ . A typical recording for the analysis of aqueous Ion standards is shown in Fig. 6. The percentage of the peak height observed with respect to the peak height of the steady-state response (98-99%) is acceptable when the CFA technique with ion-selective electrodes is used [10-12]. The calibration graph is linear in the concentration range employed (0.001-0.0001 M) and has a slope of 59 mV, which did not change during 3 months of continuous use.

For  $\text{ReO}_4^-$  and  $\text{TcO}_4^-$  determinations the sampling time was 3.5 s and the wash time was 4 s, the sampling rate being  $480 \text{ h}^{-1}$ . Calibration runs and analysis standard samples for  $\text{ReO}_4^-$  are shown in Fig. 7.

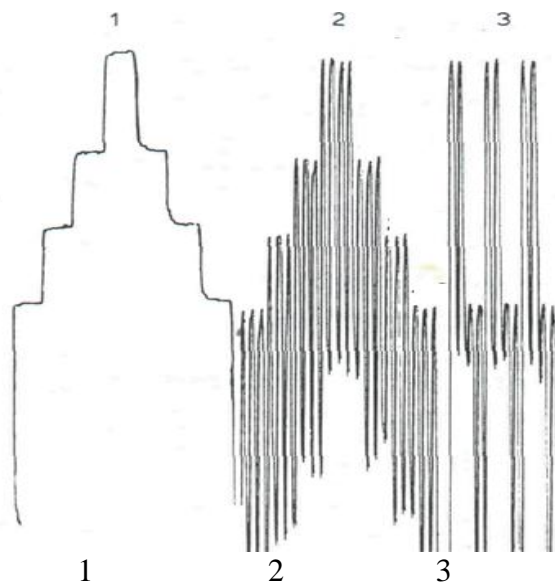


Fig.7. Rhenium determinations in standard solutions.  
 (1) A series of steady-state measurements ( $10^{-4}$ - $10^{-3}$  M);  
 (2) calibration runs;  
 (3) sequential analysis of aqueous standards containing  $10^{-3}$  and  $10^{-4}$  M.

The calibration graph is linear in the concentration range used (0.0001-0.001 M) with a slope of 57.5 mV. The average relative standard deviation in all instances was better than 3%.

Changing the analyzer operation mode from  $\text{ReO}_4^-$  and  $\text{TcO}_4^-$  determination took less than 5 min, involving only sampler reprogramming and replacement of electrodes and reagent bottles.

As an increase in the sampling rate is an important factor, this work was intended to demonstrate, using a simple example, the possibilities of the air-segmented technique and its advantages (higher sampling rate with simpler equipment) compared with the non-segmented approach.

## Conclusion

Have been offered and studied electrodes for quantitative definition of  $\text{ReO}_4^-$  and  $\text{TcO}_4^-$ . Electrodes can be applied to the analyses of  $\text{ReO}_4^-$  and  $\text{TcO}_4^-$  in some kinds of solutions flow analysis. The system with the rotary valve was used for studying the dependence of the cell response on the flow-rate.

## References

1. N. Lakshminarayanaiah. Membrane electrodes. Academic Press. New York, San Francisco, London. 1976.-360p.
2. Fu B., Bakker E., Yun J. H., Yang V.C., Meyerhoff M.E. Analytical Chemistry. 66, 2550 (1994).
3. T. Ito, H. Radecka, M. Kataoka, K. Tohda, E. Kimura, K. Odasima, Y. Umezawa. J. Am. Chem. Soc. **120**, №13, 3049 (1998).
4. A. Schwake, K. Cammann, A.L. Smirnova, S.S. Levitchev, V.L. Khitrova, A.L. Grekov, Yu. G. Vlasov. Anal. Chim. Acta. **393**,19 (1999).
5. Rakhimenko EM., Prilutskaya, Yakimenko T.M., Yakimenko O.V. II Proceedings of the National Academy of Sciences of Belarus. Series of Chemical sciences, №1 (2000), 18-23.
6. J. Ruzicka and E.H. Hansen, Flow Injection Analysis, Wiley, New York, 1981.
7. C.J. Patton, M. Rabb and S.R. Crouch, Anal. Chem., 54(1982) 1113.
8. K. Toth, J. Fucsko, E. Lindner, Zs. Feher and E. Pungor, Anal. Chim. Acta, 179 (1986) 359.
9. J. Ruzicka, E.H. Hansen and E.A. Zagatto, Anal. Chim. Acta, 88 (1977) 1.
10. M. Vandeputte, L. Dryon and D.L. Massart, Anal. Chim. Acta, 91 (1977) 113.
11. P.W. Alexander and P. Seegopaul, Anal. Chem., 52 (1980)2403.
12. T.K. Christopoulos and E.P. Diamandis, Analyst, 112(1987) 1293.



## Re Hydrometallurgy



The chairman of the 3<sup>rd</sup> section I.D. Troshkina and G.S. Schteinberg

## 3.1.

**RHENIUM IN NUCLEAR FUEL CYCLE**

I.D. Troshkina

D. Mendeleev University of Chemical Technology of Russia,  
(Miusskaya Sq. 9, Moscow, Russian Federation)**Keywords:** rhenium, nuclear fuel cycle, uranium mining, rhenium alloys, rhenium –188.

Nuclear-power complex, as is known, includes a number of some production cycles: the recovery of uranium from mineral resources, production of its pure compounds by using its chemical engineering, isotope enrichment, nuclear fuel production, fuel use in nuclear reactors to generate steam and electricity, as well as work on disposal of radioactive waste.

This review covers the following areas of location and use of rhenium in the nuclear fuel cycle (NFC).

1. Rhenium recovery in uranium mining and hydrometallurgical processing.
2. Rhenium-containing alloys – structural material of high-temperature nuclear reactors.
3. Rhenium as isotope production for nuclear medicine.
4. Rhenium - a simulator of technetium in research investigations.

**1. Rhenium recovery in uranium mining and hydrometallurgical processing.** Implementation of the first stage of the nuclear fuel cycle (NFC) – uranium mining at the present stage is accompanied by a strengthening of the role of complex processing [1,2].

Rhenium, an important strategic metal, has a special place among the other by-product metals due to the high profitability of its recovery. Rhenium is usually obtained mainly from molybdenum and copper ores [1]. In 2009, production of primary rhenium was more than 40 tons. Nearly two-thirds of the primary rhenium was made in Chile, the other major producing countries are the United States, Poland, China and CIS countries (Kazakhstan, Uzbekistan and Armenia). Data on the primary and secondary production of rhenium, the deficit and surplus, stocks and demand from 2000 to 2009 are presented in the Fig. 1.

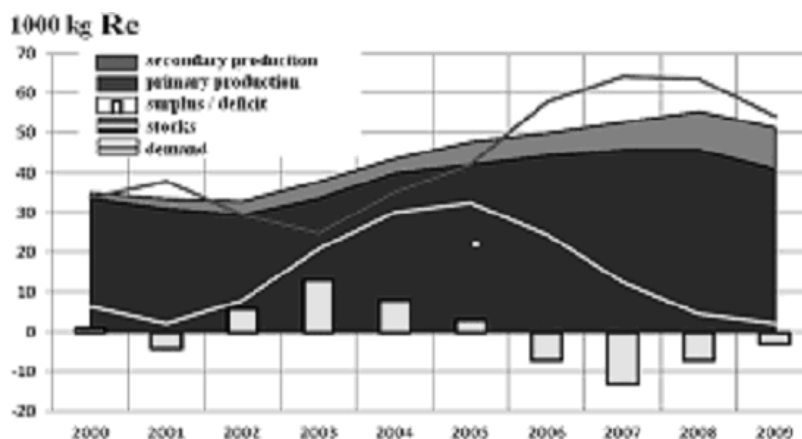


Fig. 1. The dynamics of the rhenium global market [3].

Stocks are not available. Demand for rhenium is higher than supply. The annual consumption of rhenium in 2015 will reach more than 70 t under the influence of demand in the production of rhenium-containing alloys for the aerospace industry.

Rapid increasing demand of rhenium superalloys is the reason of intensive processing of uranium ores.

*Background.* For the first time rhenium was obtained from uranium ores in 1969 in the United States of America. Beginning about 1969, significant quantities of rhenium were recovered as by-product of the uranium ores produced in the Falls City, Texas area by Susquehanna Corporation. The rhenium was recovered in dilute solution and shipped by railroad tank cars to Shattuck Chemical in Denver. There it was integrated into the Shattuck system for production of ammonium perrhenate. Rhenium was obtained up to 1974 [4].

In the former USSR rhenium was first discovered in 1978 during the operation of uranium deposits in Central Asia (Bukinayskaya group) in the productive solutions of underground leaching [2].

Increased content of rhenium is observed in uranium deposits of the sedimentary type, as well as stratum-infiltration exogenous deposits. For example in the USA the rhenium content is (0,5 - 3,0 g/t) for the ores of sedimentary deposit situated at the Colorado Plateau and up to 50 g/t for stratum-infiltration molybdenum-grade uranium ores in the South Dakota.

Geochemical relationship of rhenium with uranium and molybdenum is the characteristic feature of uranium ores. The rhenium in the molybdenum-uranium deposits of the exogenous type present as heptaoxide.

In the former Soviet Union stratum-infiltration exogenous epigenetic deposits, developed a progressive method of underground leaching, are concentrated within a few ore-bearing provinces: Central Kyzyl Kum, Syr Darya, Chu-Sarysu, Ili, which form the largest uranium province of the world – Prityanshanskaya [2]. Ancient reservoir zone of oxidation and the associated uranium deposits with associated Re-known in the Turan plate complex platform within Prityanshanskoy U-ore province. First of all, it is well-known deposits of Kazakhstan and Uzbekistan.

An important feature of polymetallic ores is a distinct correlation to the power of rhenium and uranium, which allows to predict the content of rhenium reserves, using parameters of the uranium ore.

In accordance with a reserve of rhenium per unit area in the deposit plan (the productivity) rhenium-uranium ores are divided into very poor (up to 1 g/m<sup>2</sup>); low-productivity (1-5 g/m<sup>2</sup>), ordinary (5-10 g/m<sup>2</sup>) and high-yield (10 g/m<sup>2</sup>) [2].

*Leaching.* Uranium ore, depending on the composition of processed according to the schemes of acid or alkali leaching.

Assessment of the underground leaching of rhenium can be made based on the results of thermodynamic calculations of dominance fields of its compounds in the liquid and solid phases with separation of geotechnical regimes of selection (Fig. 2).

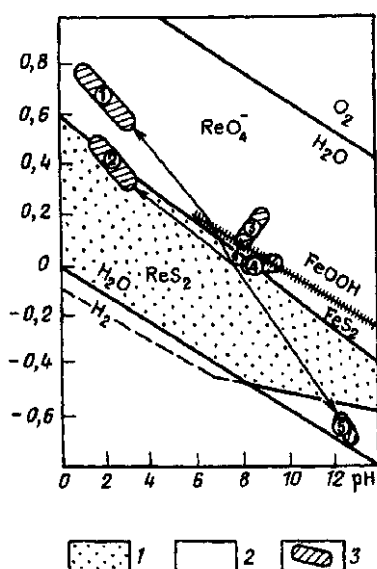
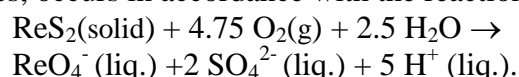


Fig.2. Fields of rhenium predominance (temperature - 25 °C, pressure - 1 bar, concentration of sulfate-ions – 10<sup>-1</sup> mol/l, concentration of carbon dioxide – 10<sup>-1.5</sup> mol/l, concentration of rhenium – 10<sup>-5.8</sup> mol/l) [2]:

- 1 - fields of solid phases;
- 2 - fields of liquid phase;
- 3 - geotechnological fields

Interaction of leaching solutions with rhenium disulfide – the most likely compound of rhenium in uranium ores, occurs in accordance with the reaction



The nature of the medium does not affect on the thermodynamic characteristics of this reaction. It requires the presence of oxygen or other oxidants to its implement. As can be seen from Fig.2, sulfuric acid and carbonate with an oxidizer geotechnological environment, located in a vast field of perrhenate ion are favorable for the leaching of rhenium. Under these conditions, rhenium can be recovered from ores with molybdenum and uranium. The special role of oxidant to convert rhenium from a solid to a liquid phase was confirmed.

Using chemicals and produced water without oxidizer degree of recovery of rhenium does not exceed 20-30%; in the presence of oxygen, regardless of the type of agent (including the application of produced water) - 50-60% or more. The use of hydrogen peroxide in an amount equivalent to the oxygen concentration of 100-500 mg/l, increases the degree of recovery up to 70-95%. The average concentration of rhenium in output solutions, depending on the initial content in the ore varied from 0.15 to 2.5 mg/l.

Comparison of the leaching kinetics of rhenium and uranium shows that rhenium is recovered first from uranium ore (Fig.3).

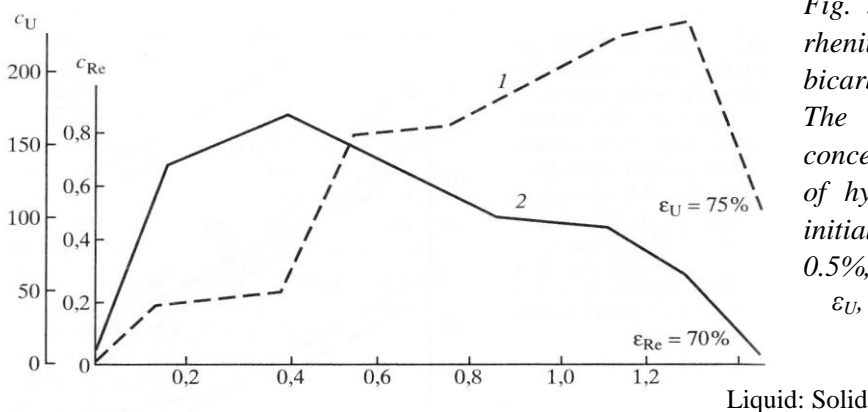


Fig. 3. Diagram of uranium (1) and rhenium (2) filtration leaching by using bicarbonate solution with oxidant [2]. The ammonium bicarbonate concentration – 2 g/l, the concentration of hydrogen peroxide – 0.6 g/l, the initial content of uranium in the ore – 0.5%, initial content of rhenium – 1 g/t.  $\epsilon_U$ ,  $\epsilon_{Re}$  – the degree of uranium and rhenium leaching, %.

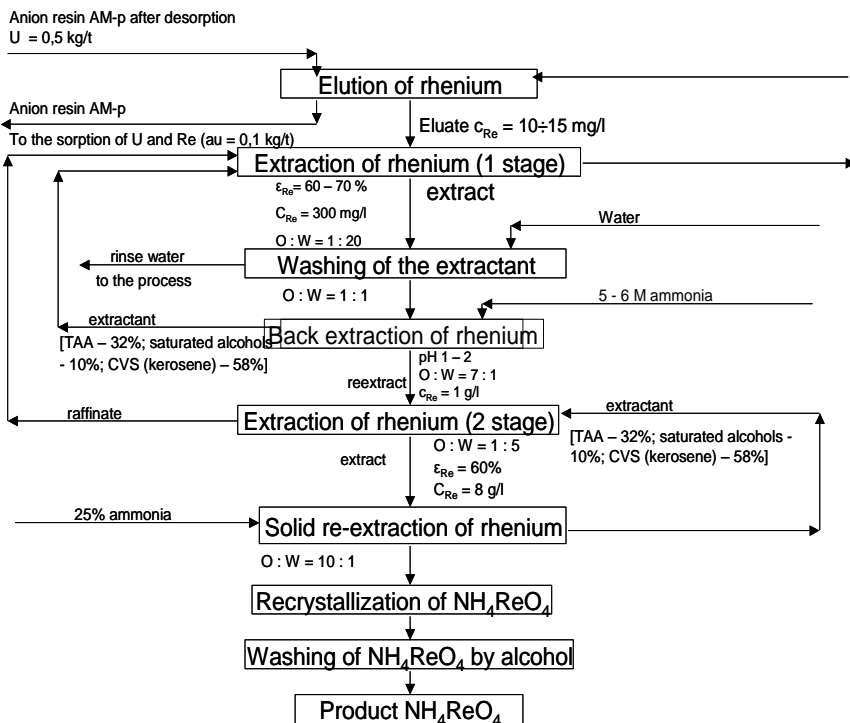


Fig. 4. The process flow diagram of rhenium recovery from uranium ore leaching solutions [2].

During sulfuric acid leaching rhenium begins to actively move to the solution, as soon as the oxidizing agent (including atmospheric oxygen introduced to the reagent) reaches the ore.

Recovery of rhenium is considered economically feasible for complex processing of ore to produce molybdenum.

The process flow diagram of rhenium recovery from uranium ore leaching solutions is shown in Fig. 4.

The recovery of rhenium from solutions of underground leaching of uranium is carried out by sorption method. Rhenium and uranium are sorbed from productive sulfuric acid solutions by

strong-base anion exchanger (for example AM-p or other [1,2,5,6]). Selective desorption of rhenium is carried out by acidic solutions containing nitrate ions ( $\text{NO}_3^-$  – 80-90 g/l,  $\text{HNO}_3$  – 4-4.5%). Rhenium is extracted from the eluates (10-15 mg/l Re) by the solution of trialkylamine fraction of  $\text{C}_7$ - $\text{C}_9$  in kerosene with the addition of decanol as a modifier. Content of rhenium in the extract is up to 8 g/l, which allows to carry out the back extraction of rhenium in solid form by the ammonia solution.

Rhenium can be precipitated from the nitrate-sulfate eluates by water-soluble polyelectrolytes [7]. The sorption of rhenium with uranium anion exchangers AN-21 and AMP is observed from the *bicarbonate solution*. In this case, the sorption of uranium anions is completed much earlier than rhenium. Applied to fields in the Northern Bukinay (Uzbekistan) scheme for processing of bicarbonate solutions using an oxidant includes: sorption of uranium and rhenium anions; solid-phase desorption by solutions of sodium bicarbonate and ammonium carbonate; selective desorption of rhenium by ammoniacal solution of ammonium thiocyanate (1-2 mol/l  $\text{NH}_4\text{SCN}$  + 1%  $\text{NH}_4\text{OH}$ ), precipitation of crystals of ammonium perrhenate by evaporation of desorbate (at 80°C) [2].

Under the scheme of acid leaching slightly carbonate ores (mine Ambrosia Lake, Gas Hills, etc.) are processed. 1 ton of rhenium per year was produced from sulfuric acid solutions at all US refineries. And the degree of rhenium recovery was 50%. Scheme of alkali leaching is used for processing of high carbonate uranium ore (mine Ambrosia Lake, Front Reynd, etc.) [1].

For the associated extraction of rhenium from productive solutions of underground leaching alternative biological methods are developed.

Along with uranium and rhenium molybdenum, vanadium, selenium, yttrium, rare earth metals, scandium can be recovered from multicomponent solutions of underground leaching. Sorption and extraction methods are developed for processing of these complex composition solutions [2].

For the recovery of rhenium from sulfuric acid solutions obtained by underground leaching, along with well-known, synthetic granular nanostructured styrene-acrylate resins of new generation have been successfully tested [8].

The complex processing of productive solutions can increase profitability mining of low-grade ores. Despite the low value of the share price of rhenium in the product, significant amounts of recycled productive solutions allow to get tons of rhenium. Since the basic and operational costs for underground leaching include the cost of extracted principal components - uranium, the cost of associated rhenium and other metals will consist of operating and capital costs for their recycling, which reach 10-15% of the cost of the final product. Indicative techno-economic calculation of complex processing of productive solutions allows justify the concentration of rhenium in waste solutions after sorption: when the initial concentration of rhenium is 0.2 mg/l, residual concentration may be 0.1 mg/l. In this case, the profitability of extraction of rhenium is very high - 540%, indicating the possibility of an effective recycling of solutions with lower initial concentrations of rhenium.

## **2. Rhenium-containing alloys – structural material of high-temperature nuclear reactors.**

Tungsten-rhenium alloys as structural materials of equipment operate at high temperatures (1000–1200 °C). W-alloys are used as plasma facing components in fusion reactors [9]. Neutron irradiation induces significant transmutation of tungsten into rhenium and osmium. Precipitation of these alloying elements could dramatically modify the properties of the initial material. Using atom-probe tomography, it was showed that neutron irradiation could trigger the precipitation of nanoscale precipitates of the  $\sigma$  and  $\chi$  phases in W-10 and 25 at. % Re alloy irradiated between 575 and 675 °C to 8.6 dpa (Fig. 5).



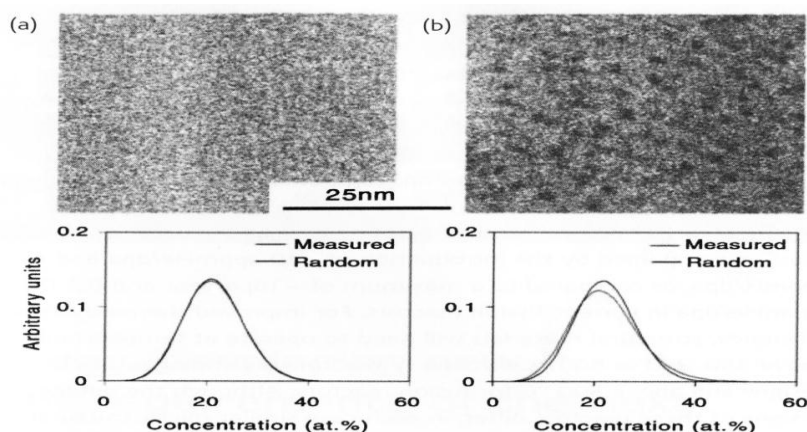


Fig. 5. 5 nm thick slices through atom-probe tomography reconstructions obtained from a W-25 at. % Re alloy. Only Re atoms are shown. (a) Re is in solid solution before implantation (a) and (b) clustered after implantation by 2 MeV W ions at 500 °C to 2.8 dpa. (b) The concentration distributions confirm the random Re distribution before implantation and non-random one after implantation [9].

More observations of precipitation in irradiated tungsten alloys revealed the onset of phase separation at low doses. Fig. 5 shows 3D reconstruction of a W-25 at. % Re alloy before and after implantation revealing the formation of nanometer-scale Re-rich clusters after only 2.8 dpa at 500°C. Understanding of irradiation –induced precipitation in W alloys is still inadequate, in great part due to the lack of knowledge of the phase diagram. While the high temperature part of the W-Re phase diagram predicts complete solid-solution up to 22 at. % Re, the lower part of the diagram ( $T < 1500^{\circ}\text{C}$ ) cannot be assessed experimentally for kinetic reasons. Systematic atomic-scale experimental and theoretical work may pave the way towards a better understanding. Precipitation of these alloying elements could dramatically modify the properties of the initial material.

Rhenium is intended for use in high-temperature nuclear power plants to improve efficiency and safety of their work. The interaction of nuclear fuel – uranium mononitride with the material cladding – rhenium in the temperature range 1800-2200K was investigated [5].

Rhenium-molybdenum alloy large tubing was developed for nuclear reactor control [5].

**3. Rhenium as isotope production for nuclear medicine.** Actively being introduced into medical practice a generator of rhenium-188 is obtained from the stable isotope of tungsten-188 produced at enterprises NFC. Isotope of rhenium-188 is used in nuclear medicine for diagnostics of some illnesses [5].

#### **4. Rhenium - a simulator of technetium in research investigations.**

This field of Re using in NFC is connected due to the similarity of rhenium and technetium properties. So rhenium substitutes technetium in the modeling process to generate predictions of the nuclear fuel cycle. However it should be taken into account that investigation of technetium behavior in a variety of complexes in multicomponent NFC solutions cannot be always possible. According to modeling method for creating predictions for the nuclear fuel cycle, proposed by International Atomic Energy Agency, rhenium can substitute technetium in solid products, for example, in sludge.

#### **Conclusions.**

In the implementation of the nuclear fuel cycle traditional features of associated recovery and use of rhenium are being saved:

- As a trace element rhenium is extracted from uranium multicomponent raw materials.
- As a metal, having high refractoriness, it is used in the heat-resistant alloys for the manufacturing of high-temperature reactors.

## References.

1. A.A. Palant, I.D. Troshkina, A.M. Chekmarev, *Metallurgy of Rhenium*, Science: Moscow (2007). 298 p. (rus.)
2. *In-Situ Leaching of Ores*, Academy of Mining Sciences, Publishing House: Moscow (1998). 446 p. (rus.)
3. [www.roskill.com/reports/minor-and-light-metals/rhenium](http://www.roskill.com/reports/minor-and-light-metals/rhenium), 2010.
4. Proceedings of the International symposium on rhenium and rhenium alloys: TMS annual meeting. Orlando (Florida), 1997. 826 p.
5. 7<sup>th</sup> International Symposium on Technetium and Rhenium – Science and Utilization. Book of abstracts. July 4-8, 2011, Moscow, Russia. 204 p.
6. A. Zagorodnyaya, Z. Abisheva, E. Ponomaryova, V. Bobrova, *Non-ferrous metals*. **8**: 59 – 62 (2010).
7. A. Chekmarev, I. Troshkina, Y. Nesterov et al., *Chemistry for Sustainable Development*. **1 (11)**: 113-117 (2004).
8. I. Troshkina, N. Balanovsky, A. Shilyaev et al., *Chemical Technology*. **6**: 337-341 (2011).
9. E. Marquis, J. Hyde, D. Saxey, S. Lozano-Perez et al., *Materialstoday*. **12 (11)**: 32 (2009).

3.2.

## **RHENIUM OF KAZAKHSTAN (REVIEW OF TECHNOLOGIES FOR RHENIUM RECOVERY FROM MINERAL RAW MATERIALS IN KAZAKHSTAN)**

Z. S. Abisheva, A. N. Zagorodnyaya

Centre of Earth Sciences, Metallurgy and Ore Beneficiation (Shevchenko, 29/133, Almaty, Kazakhstan)

**Keywords:** rhenium, sorption, desorption, wash sulfuric acid, underground leaching solutions

### **Abstract:**

Results of the study on sorption technology development for rhenium recovery from new composition of wash sulfuric acid solution from Kazakhstan copper smelter and from underground leaching solutions of Kazakhstan uranium deposit using A170 and A172 weak basic anionites (by Purolite) are presented in the paper. Effect of parameters typical for rhenium sorption and desorption was studied. Optimum parameters for rhenium recovery were selected. It was shown that good performance for rhenium recovery from the solutions could be achieved with use of A170 ionite only. Flow sheet are proposed for the solutions.

### **Introduction**

Rhenium in Kazakhstan has been recovered as a by-product during copper and molybdenum concentrate processing obtained from Kounrad, Sayak and Zhezkazgan ore deposits. The first commercial production of rhenium in Kazakhstan was organized in the 1940s originally from molybdenite concentrate roasting dust and later from solutions of the trapping system and from wash sulfuric acid solutions of metallurgical gas cleaner after electro-smelting and matte conversion at the Balkhash copper smelter. In early nineties rhenium production was suspended due to lack of raw materials, at the smelter. Currently, it is recovered only from wash sulfuric acid of the Zhezkazgan copper smelter during Zhezkazgan copper ore concentrate processing. Also rhenium partially goes to dust and slime transferred to the lead smelter. It should be noted that rhenium containing lead and zinc concentrates are also produced from Zhezkazgan copper ore. Lead concentrate and dust from copper concentrate processing are used at lead smelter along with other lead-containing materials. During lead processing rhenium goes mainly to the dust and partially to the wash solutions. A number of technologies have been developed for rhenium recovery from dust leach solutions and from gas clean solution.

Thus, processing of copper and lead concentrates produces rhenium-containing solutions, dust and slime. Commercial production of ammonium perrhenate from the solutions has been organized at the copper and lead smelters. Technologies for rhenium recovery from the dust and the slime have been developed and tested at the smelters. Although quite good results were achieved during the tests the technologies were not implemented in commercial production due to some reasons.

In 2008, Balkhash copper smelter recommenced processing of Zhezkazgan copper concentrates and resumed sulfuric acid production. So, it is necessary to resume production of ammonium perrhenate at the smelter. Previously sorption technology by the Institute of Metallurgy and Ore Concentration of Kazakh Academy of Sciences (now Centre of Earth Sciences, Metallurgy and Ore Beneficiation) was used. Since composition of the wash solutions now is different from the wash solutions of 1970<sup>th</sup> - 1980<sup>th</sup> and new anionites available in the market it is necessary to study rhenium recovery from the wash solutions.

Kazakhstan uranium ore also contains significant quantities of rhenium. The ore is mined with use of underground leaching method. No rhenium recovery from such solutions has been undertaken yet, despite some readily available technologies.

The issues of rhenium recovery from wash solutions of copper and lead smelters and from uranium underground leach solutions were presented at the symposium and also discussed in detail in the publications [1]. In this paper we present the results of sorption technology development for rhenium recovery from wash sulfuric acid of different composition and from underground uranium ore leach solutions using weakly basic anionites (by Purolite). Optimum conditions for sorption and desorption were selected and principal technologies for rhenium recovery were developed on the basis of the study.

## Experimental

**Reagents.** Anionites: AN-21 (Russia), A170 and A172 (Purolite). Industrial wash sulfuric acid solutions (WSAS) from Balkhash copper smelter (BCS), underground leach solutions (ULS) and filtrates after uranium sorption (UF) from a KAZATOMPROM enterprise. Sulfuric acid (chemically pure, GOST 4204-77); hydrochloric acid (chemically pure, GOST 3118-77); nitric acid (chemically pure, GOST 4461-72); sodium hydroxide (chemically pure, GOST 4328-77); and ammonium hydroxide (chemically pure, GOST 3760-64).

**Pretreatment of ionites.** Anionites were cleaned from iron and synthesis products using sodium hydroxide and hydrochloric acid solutions [2]. The A170 anionite was converted into chloride, sulfate, hydrosulfate and nitrate forms under dynamic conditions according to the conventional method [2] by washing it with 2 mol/dm<sup>3</sup> solutions of the acids. To prevent hydrolysis of hydrosulphate ions, the saturated anionite was washed with dehydrated ethanol until negative reaction to sulfate ions is achieved. Transformation of the ionite in HSO<sub>4</sub><sup>-</sup> form into sulfate form was made by washing of the ionite with water.

**Methods of analysis.** Rhenium in solutions was analyzed using atomic emission spectrometry (AES Optima 2000 DV, PerkinElmer, USA) and in column effluents using colorimetric method [3]. Uranium was analyzed using method [4]. Anionites in different salt forms were studied using IR-spectroscopy method according to [5].

**Experimental method.** Experiments were carried out under dynamic conditions in temperature-controlled columns with fixed anionite layer. Flow rate of solutions was 2 - 6 specific volumes per hour during sorption phase and 1 specific volume per hour during elution phase. The flow rate of the solutions was controlled every hour. Rhenium sorption was carried out at room temperature and elution at 40 °C. Daily filtrates were put together, mixed and analyzed for rhenium and uranium. Before elution the anionite was washed with distilled water to pH=4. Column effluents were collected every hour in a separate container and analyzed for rhenium.

## Results and Discussion

**Rhenium recovery from wash sulfuric acid of Balkhash copper smelter.** It was found earlier by scientists of the Institute of Metallurgy and Ore Enrichment (Kazakh Academy of Sciences) that rhenium during concentrate smelting in Vanukov furnaces is distributed as follows: up to 70 % goes to the gas, 10 to 15 % - to the matte, 7 to 8 % - to the dust, and 16 to 17 - to the slag [6].

Due to absence of circulation the volume of wash sulfuric acid is growing, which affects adversely rhenium concentrations in it. Monitoring of rhenium and H<sub>2</sub>SO<sub>4</sub> concentrations in wash sulfuric acid solution showed that concentration of sulfuric acid in the wash solution is from 30 to 192 g/dm<sup>3</sup> (mainly 60 to 80 g/dm<sup>3</sup>) and rhenium concentration is from 11 to 34 mg/dm<sup>3</sup> (mainly 12 to 14 mg/dm<sup>3</sup>). The total quantity of rhenium is commercially viable. In the future rhenium quantity would be increased due to processing of rhenium-bearing ores from Aktogai and Bozshekul deposits. Similar solutions are used in Poland at KGHM plant for rhenium recovery using sorption technology [7].

Previously rhenium was recovered from wash sulfuric acid solutions at the Balkhash copper smelter using anionite AN-21 in the form of gel and later in the form of porous material [8, 9]. Concentration of rhenium in the solution was from 40 to 185 mg/dm<sup>3</sup> and sulfuric acid - from 100 to 300 g/dm<sup>3</sup>.

In this work weakly basic anionite A170 with macro-porous structure was used. Effect of solution flow rate (2, 4 and 6 specific volumes per hour) and salt form of the anionite (hydroxide, chloride, sulphate, hydrosulphate and nitrate) were studied. Also, parameters of rhenium elution from the ionite were studied. Rhenium sorption was carried out from industrial wash sulfuric acid solution containing 13 mg/dm<sup>3</sup> of rhenium, 60.5 g/dm<sup>3</sup> of sulfuric acid and sediments of the lead-containing slime. Therefore, the acid solution was filtered. Some times red sediment appeared in the solution. It was established using different physical and chemical methods that the sediment is selenium of red modification.

In order to reduce duration of the experiments with different flow rates and anionite forms affecting sorption characteristics, some rhenium was added to the wash sulfuric acid solution to get rhenium concentration at 186 mg/dm<sup>3</sup>.

According to the experimental data (Figures 1 and 2), rhenium is sorbed from the solution quite well. This is confirmed by the quantity of the solution passed through the anionite and by the quantity of rhenium sorbed. After 3000 volumes of the solution per volume of anionite have passed through the anionite column rhenium concentrations in the column effluents is 95 % of the original one. One cubic centimeter of the anionite sorbs 27 mg of rhenium.

Presence of selenium in kind of a halo ring on the surface of the anionite in the column was detected in experiments. Similar selenium behavior was found in the past during rhenium recovery with AN-21 anionite from wash sulfuric acid solutions at the Balkhash copper smelter.

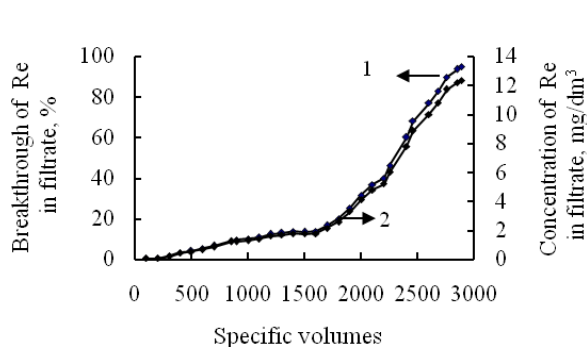


Fig. 1. Rhenium sorption curves from industrial wash solution on A170: 1 – Re share in filtrate, 2 – Re concentration in filtrate

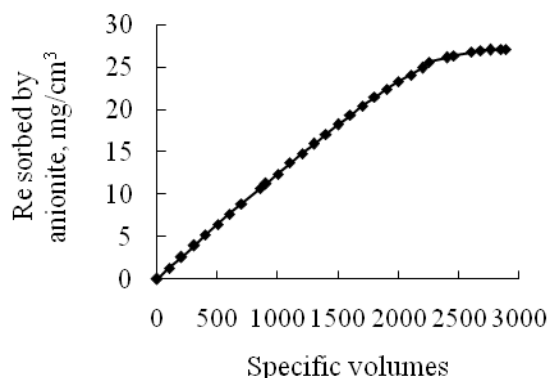


Fig. 2. Quantity of absorbed rhenium from wash solution per 1 cm<sup>3</sup> of the anionite

It was established that follow rate of the solution through the column in the studied interval (2, 4 and 6 volumes per volume per hour) affects rhenium sorption: share of rhenium in the filtrate after the column and rhenium sorbed per 1 cm<sup>3</sup> of the swelled anionite. However, when 150 volumes

Table 1. Influence of the solution flow rate to sorption characteristics of A170 anionite

Specific volumes	Flow rate of solution, sp.vol./h					
	2		4		6	
	Breakthrough of Re in filtrate, %	Re, sorbed by anionite, mg/sm <sup>3</sup>	Breakthrough of Re in filtrate, %	Re, sorbed by anionite, mg/sm <sup>3</sup>	Breakthrough of Re in filtrate, %	Re, sorbed by anionite, mg/sm <sup>3</sup>
100	2.15	18.37	2.15	18.26	2.96	18.04
200	3.20	36.39	3.96	36.21	5.91	35.78
300	6.00	53.91	6.45	53.65	8.17	53.08
400	15.10	69.94	20.92	68.65	34.41	66.72
500	21.20	84.70	24.32	82.90	51.61	76.02
600	26.50	98.69	27.05	96.65	59.46	83.81
700	37.45	111.02	67.57	103.43	70.27	89.88
800	52.50	120.96	80.40	107.54	80.29	94.18
900	77.30	126.24	88.95	110.00	90.35	96.43
1000	87.40	129.03	95.50	111.09	97.50	97.10



of the solution per volume of the anionite have passed through the column with flow rate 2, 4 and 6 volumes per volume per hour rhenium share in the filtrate is ~ 3 %, and the quantity of sorbed rhenium is 27 mg/cm<sup>3</sup> approximately (Table 1).

Influence of flow rate became more obviously during increasing of quantity of solution passed through anionite. When 1000 volumes of the solution per volume of the anionite have passed through the column sorption characteristics depend on the flow rate. At 2 specific volumes per hour flow rate rhenium share in the filtrate is 87.4 %, and quantity of the sorbed rhenium is 129 mg/cm<sup>3</sup>; at 4 specific volumes per hour flow rate rhenium share in the filtrate is 95.5 % and quantity of the sorbed rhenium is 111.1 mg/cm<sup>3</sup>; at 6 specific volumes per hour flow rate rhenium share in the filtrate is 97.5 % and quantity of the sorbed rhenium is 97.1 mg/cm<sup>3</sup>. The revealed regularity is quite explainable: first rhenium sorption takes place at the surface of anionite grains. In this case steric hindrances for diffusion of hydrated perrhenate ions to ionogenic groups of the ionite are minimal; therefore flow rate of the solution has no effect to the sorption characteristics. In time sorption proceed in deeper layers of the grain, where access of perrhenate ions to ionogenic groups is hindered. This is the reason for deterioration of sorption characteristics of the anionite with increase of the flow rate.

It was established that the salt form of the anionite does not affect its sorption characteristics (Figure 3).

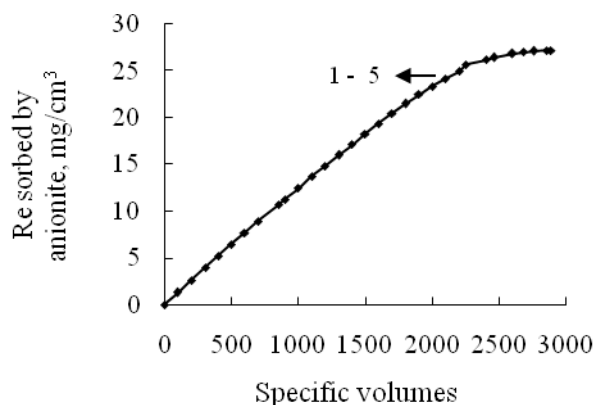


Fig. 3. Influence of salt form of anionite on Re sorption: 1 – hydroxide, 2 – chloride, 3 – hydrosulfate, 4 – sulfate, 5 – nitrate

(Figure 3). Therefore, all studied anionite forms are suitable for rhenium recovery from sulfur acid solutions.

The results of rhenium elution with ammonia solution from the anionite containing 27 mg of rhenium per 1 cm<sup>3</sup> of swelled anionite (saturated with wash sulfuric acid solution from the Balkhash copper smelter) demonstrate high performance of this process (Figure 4). Maximum concentration of rhenium in the column effluent was 7.7 g/dm<sup>3</sup>, and minimum concentration - 0.022 g/dm<sup>3</sup>. More than 96 % of rhenium is recovered from the anionite with four specific volumes of the eluent. The average rhenium concentration in 4 combined volumes of column effluent was 5.44 g/dm<sup>3</sup>. It is possible to produce ammonium perrhenate from column effluents with the above said rhenium concentrations via evaporation of the solutions factor 10 to 12 times. This technique is used in sorption technologies for rhenium recovery from solutions of non-ferrous metallurgy [7, 9, 10]. For almost complete elution of rhenium it is sufficient to use six volumes of eluent per volume of ionite.

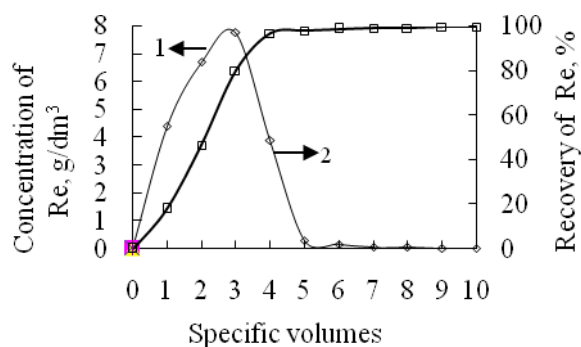


Fig.4. Rhenium elution profile for eluant (3 mole/dm<sup>3</sup> ammonia): 1 – concentration in eluate, 2 – recovery from anionite.

**Rhenium recovery from underground leach solution and effluents of uranium sorption.** Sorption-extraction technology for rhenium recovery from such solutions using highly basic anionite for sorption and eluents for uranium extraction are described in [11]. More effective sorption technology with use of weakly basic anionite AN-21 was also developed. It was reasonable to determine if widely advertised weakly basic anionites by Purolite could compete with AN-21. Experiments were carried out with A170, A172 and AN-21 anionites for comparison. Sorption capacity of the anionites was evaluated when breakthrough of rhenium in the column effluent is at 100 %. The following criteria for comparison were used: quantity of wash sulfuric acid passed through, time required for full saturation of the ionite, quantity of sorbed metals per ton of dry anionite (full dynamic capacity (FDC) of anionite). Composition of the solutions is shown in Table 2.

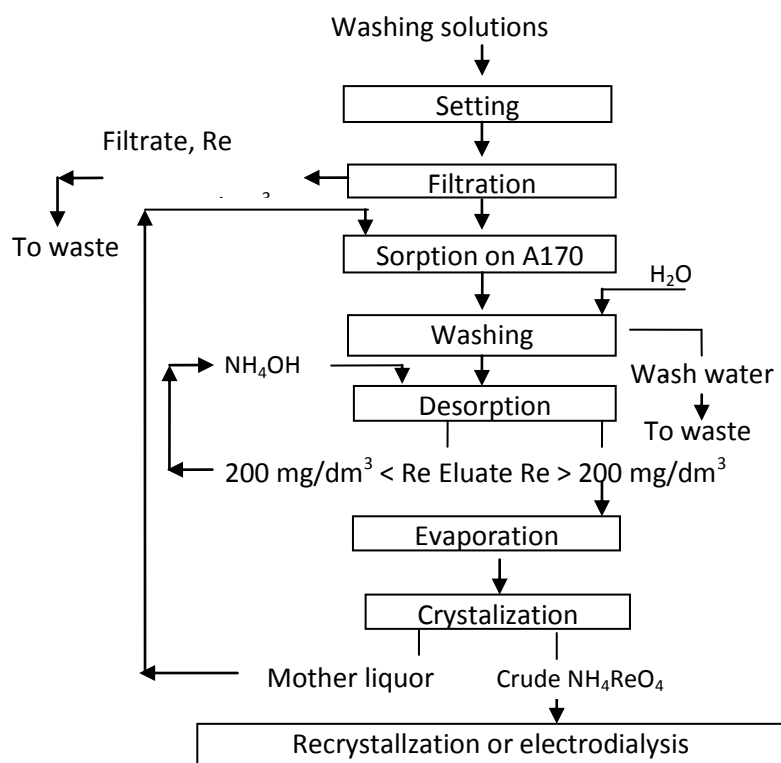


Fig. 5. Flow sheet for recovery of Re from washing solutions of BCM

Four volumes are intended for evaporation to produce ammonium perrhenate and two volumes are intended for preparation of effluent for subsequent rhenium elution. The study showed that rhenium could be recovered with high performance from industrial wash sulfuric acid solutions of the Balkhash smelter using A170 anionite. Process flow sheet for rhenium recovery including rhenium sorption, anionite washing, elution, evaporation of ammonia column effluents, crystallization of crude ammonium perrhenate and production of commercial salt using re-crystallization or electro-dialysis methods are shown on Figure 5.

According to the table the difference between ULS and UF uranium solutions is only in uranium concentration and slightly in concentrations of nitrate-, chloride- and sulfate ions. It is seen from Table 2 that rhenium and uranium are sorbed together from the solutions with all the anionites.

In accordance with the evaluation criteria the row of anionites is AN-21, A170 > A172 for uranium sorption from the underground leach solution and A172 > AN-21, A170 for rhenium sorption from the same solution. Full dynamic capacity regarding to uranium is 26.66 (AN-21), 27.5 (A170), 8.73 (A172) kg per ton, and regarding to rhenium 1.67, 1.77, 6.74 kg per ton respectively. Saturation of the anionites with uranium is achieved 14 – 25 times faster than that for rhenium. The number of specific volumes of the solution per volume of swelled anionite is 200 (AN-21), 230 (A170), 770 (A172) for uranium and 5100, 4900, 11344 for rhenium respectively.

According to the criteria the row of anionites is AN-21, A170 > A172 regarding to uranium sorption from the uranium filtrates. For rhenium the row of anionites is the same for both solutions. Full dynamic capacity of the ionites for sorption from column effluent is smaller for uranium (5.0 kg per ton (AN-21), 5.6 kg per ton (A170), 0.8 kg per ton (A172)) and bigger for rhenium (3.76; 3.95; and 13.82 kg per ton respectively) as compared to that for the underground leach solutions.

Table 2. Recovery of Re and U from solutions of UL and UF by anionites AN-21, A170, A172

Parameters	Anionites					
	AN-21		A170		A172	
	Re	U	Re	U	Re	U
<b>Underground leaching solutions (ULS)</b>						
Concentration, mg/dm <sup>3</sup> : 0.48 Re, 60 U, 14000 SO <sub>4</sub> <sup>2-</sup> , 210 Cl <sup>-</sup> , 150 NO <sub>3</sub> <sup>-</sup> , 144 SiO <sub>2</sub> , 264 Fe <sup>3+</sup> , 1156 Fe <sup>2+</sup> , 427 Ca <sup>2+</sup> , 547 Mg <sup>2+</sup> , 964 Al <sup>3+</sup>						
Breakthrough of metals in filtrate, %	100	95.3	98.0	99.0	100.0	97.12
Time of ionites saturation, days	42	2	41.0	2	91	4
Average flow rate of solution, sp. vol./h	5.2		5.3		5.2	
Quantity of passed solutions before breakthrough of metals in filtrate, sp.vol.	5100	200	4900	230	11344	770
Full dynamic capacity (FDC) of anionite), kg/per ton of dry anionite	1.67	26.66	1.77	27.5	6.74	8.73
<b>Filtrates after sorption of uranium from underground leaching solutions (UF)</b>						
Concentration, mg/dm <sup>3</sup> : 0.48 Re, 1 U, 13800 SO <sub>4</sub> <sup>2-</sup> , 160 Cl <sup>-</sup> , 120 NO <sub>3</sub> <sup>-</sup> , 140 SiO <sub>2</sub> , 260 Fe <sup>3+</sup> , 1150 Fe <sup>2+</sup> , 425 Ca <sup>2+</sup> , 550 Mg <sup>2+</sup> , 970 Al <sup>3+</sup>						
Breakthrough of metals in filtrate, %	97.0	96.0	98.5	98.3	97.9	96.0
Time of ionites saturation, days	56	42.0	57	52	165	47
Average flow rate of solution, sp. vol./h	5.0		5.1		5.3	
Quantity of passed solutions before breakthrough of metals in filtrate, sp.vol.	6740	5010	7020	6300	19820	2000
Full dynamic capacity (FDC) of anionite), kg/per ton of dry anionite	3.76	5.0	3.95	5.6	13.82	0.8

Due to low metal concentrations in these solutions (0.48 mg/dm<sup>3</sup> Re and 1.0 mg/dm<sup>3</sup> U) the volume of the solutions passed through ionites is big and the saturation time is long (Table 2).

According to the experimental data A172 anionite is better than the others for rhenium sorption from both solutions. AN-21 and A170 anionites are almost identical on their sorption characteristics.

Preliminary experiments on rhenium elution from A172 with aqueous ammonia showed that rhenium cannot be recovered from the ionite. Since AN-21 and A170 are practically identical in their sorption characteristics all further experiments were carried out with A170 anionite saturated from both solutions.

As it is shown above, rhenium and uranium are sorbed collectively from the solutions and can be separated at elution stage. Referring to the literature data ammonia solution was selected as eluent for rhenium and sulfuric acid solution was selected as eluent for uranium. The eluents were passed through anionite at flow rate 1 specific volume per hour. The experiments were carried out with the anionites saturated from ULS containing 3.02 kg/ton of rhenium and 40.0 kg/ton of uranium and saturated from UF containing 6.44 kg/ton of Re and 2.1 kg/ton of U.

Rhenium elution was carried out at 50 °C with 3 mol/dm<sup>3</sup> ammonia solution concentration. Elution was stopped when rhenium concentration in the column effluent is 8 mg/dm<sup>3</sup>. No uranium was detected in the ammonia column effluents. The results are shown on Figure 6. Second specific volume of effluent has maximum rhenium concentrations (330 and 187 mg/dm<sup>3</sup>). In eight specific volume of eluent the concentration goes down steeply and then gradually. First eight specific volumes of column effluent contain ~ 50 % of the total anionite capacity and 30 specific volumes, from 70 to 80 % of the total anionite capacity. The remaining quantity of rhenium in the anionite is considered a circulating load. Different concentrations of rhenium in the column effluents depend on different rhenium content in the anionites.

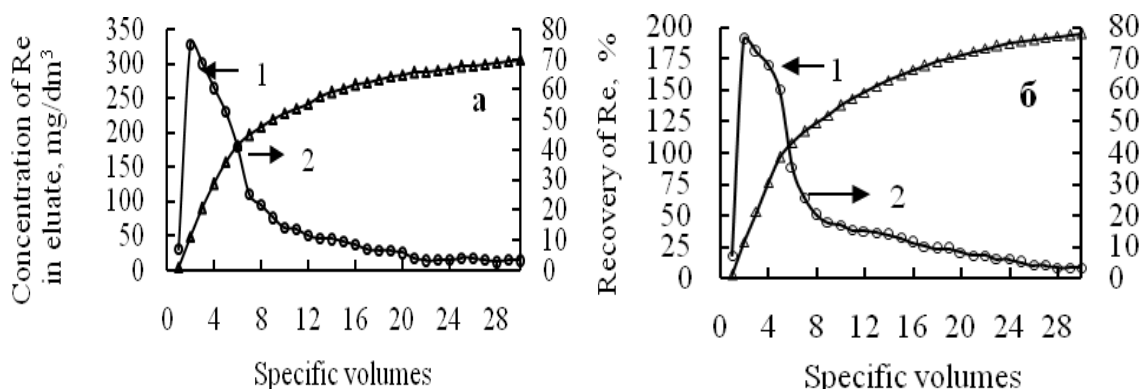


Fig. 6. Rhenium elution profile by ammonia (1) and recovery of Re from anionite A170 (2), saturated by rhenium from ULS and UF. Content of rhenium, mg/g: a – 6.44, b – 3.86

After rhenium desorption the anionite containing 2.1 kg per ton of uranium was washed with water. Uranium elution was carried out with sulfuric acid solution ( $100 \text{ g/dm}^3$ ) and with acidic solution of ammonium nitrate (pH – 0.45) at room temperature. It is shown (Figure 7) that uranium is almost completely eluted with 8 specific volumes of nitrate-containing effluent and 15 specific volumes of sulfuric acid solution.

Thus, solutions containing only rhenium or uranium can be obtained using different eluents. Due to the low concentration of rhenium in the ammonia column effluents second phase of concentration is necessary. Liquid solvent extraction with triallylamine and tributylphosphate mixture is described in [12, 13]. We used A170 weakly basic ionite for secondary concentration. Since weakly basic anionites do not work in alkaline media

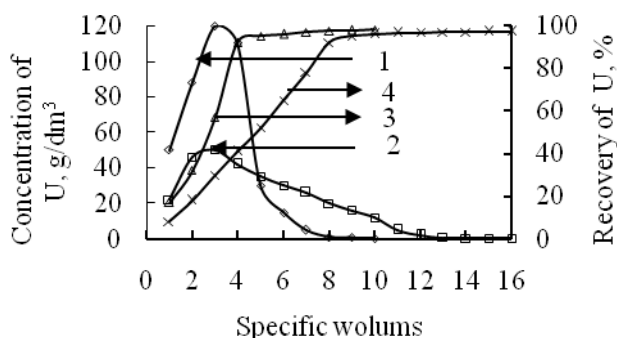


Fig. 7. Uranium elution profile by nitrate (1) and sulfate (2) solutions and recovery of U from anionite (3, 4) correspondingly

rhenium-bearing column effluents were neutralized with inorganic acids to weakly acidic state and ammonium was distilled off.

Referring to the fact that nitric and hydrochloric acids are strong depressants for perrhenate ions, sulfuric acid was used for neutralization.

The ammonia column effluents contained  $54 \text{ mg/dm}^3$  of rhenium,  $2370 \text{ mg/dm}^3$  of nitrates,  $170 \text{ mg/dm}^3$  of sulfates, and  $1 \text{ mol/dm}^3$  of ammonia.

The flow rate was 4 specific volumes of solution per hour. Sorption was carried out at room temperature.

Every 50 specific volumes column effluents were assayed for rhenium. Saturated anionites were washed with water, collected together and rhenium was recovered from it in dynamic conditions with  $3 \text{ mol/dm}^3$  ammonia solutions at  $50 \text{ }^\circ\text{C}$  and one specific volume per hour flow rate.

The results of rhenium sorption from two types of neutralized ammonium column effluents and Re desorption from the anionite are shown on Figures 8 (sorption) and 9 (elution).

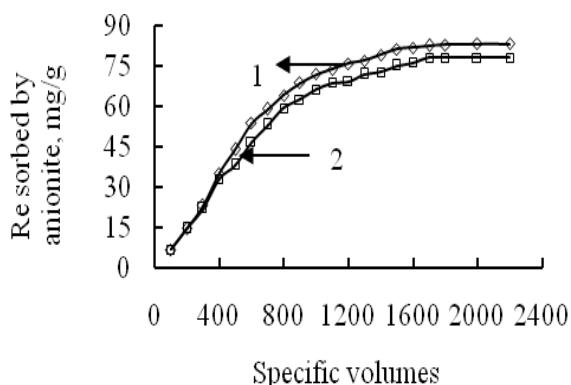


Fig. 8. Rhenium elution profile from evaporated (1) and neutralized (2) eluates

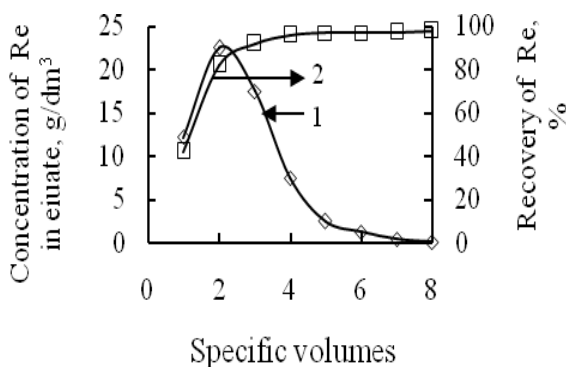


Fig. 9. Rhenium elution profile (1) and its recovery from anionite (2)

It is seen from Figure 8 that pretreatment of the solution does not affect sorption characteristics. One ton of dry anionite absorb 83 kg of rhenium from the evaporated solutions and 78 kg of rhenium from the neutralized solutions at 2200 and 1800 specific volumes of the solution respectively.

Rhenium is eluted well with ammonia (Figure 9). Five specific volumes of ammonia recover 95 % of rhenium with maximum concentration of 22.3 g/dm<sup>3</sup>. The average rhenium concentration in

combined column effluents was 4 g/dm<sup>3</sup>.

Crude ammonium perhenate can be obtained from such solution using evaporation and cooling operations similar to the operations used in nonferrous metallurgy for rhenium recovery.

A process flow sheet for NH<sub>4</sub>OH production from uranium sorption filtrates (Figure 10) is proposed on the basis of the study. The flow sheet is more environmentally safe (due to elimination of toxic triallylamine and tributyl phosphate, flammable kerosene and higher alcohol), more efficient (2 rhenium concentration operations instead of 3), ionite capacity regarding to rhenium is higher as

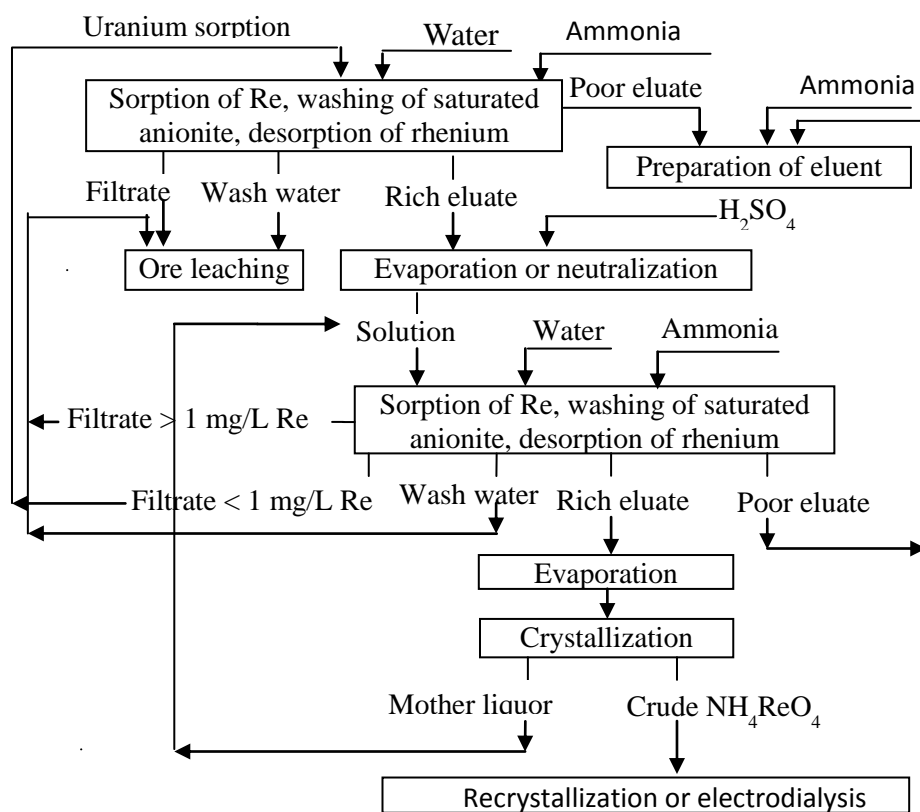


Fig. 10. Flow sheet for recovery of rhenium recovery from uranium sorption filtrates

compared to other options, it uses less aggressive eluent and cheaper.

### Conclusions

On the basis of the results of the study on rhenium sorption from industrial wash sulfuric acid solutions from the copper smelter with low Re concentrations and from Kazakhstan uranium ore underground leach solutions with ultra-low Re concentrations using A170 and A172 weakly basic



anionites and rhenium desorption from A170 ionite depending on the criteria of the processes the flow diagrams were developed.

## References

1. Z. S. Abisheva, A. N. Zagorodnyaya, N. S. Bekturganov. Review of technologies for rhenium recovery from mineral raw materials in Kazakhstan// Hydrometallurgy, 2011, vol. 109 N 1-2, P. 1 - 8.
2. Ionites. Methods of test preparation. GOST 10897-64.
3. L. V. Borisova, A. V. Yermakov Analytical chemistry of rhenium. Moscow (1974), p. 319
4. Method for determination of uranium mass concentration. TU 640-38229886-3AO-02-2000.
5. K. Nakomoto, Infrared and Raman Spectra of Inorganic and Coordination Compounds, Moscow (1991), p. 536
6. K. N. Scherban, V. V. Bobrova. In: Chemistry, technology and analytical control for rhenium. Moscow (1990). p. 230 - 232.
7. A. Chmlearz Benke, G. Leszczynska-Segda, A. Anyszkiewicz, K. Litwinionek. Copper 2010. Hamburg (2010). V. 5. p. 1803 – 1814.
8. A. A. Egizarov, L.I. Mekler. In: Extraction and sorption in metallurgy of molybdenum, tungsten and rhenium. Moscow (1971). p. 17 - 24.
9. K.B. Lebedev, L. I. Mekler, E. I. Kryukova. Non-ferrous metals. Issue 2, p. 79 – 83 (1976).
10. Ionites in non-ferrous metallurgy / edited by K.B. Lebedev. Moscow (1975). 352 p.
11. A. N. Zagorodnyaya, Z.S. Abisheva, E.I. Ponomaryova, V. V. Bobrova. Non-ferrous metals. Issue 8, p. 59 – 62 (2010).
12. I. S. Ortikov, V.P. Nebera. Non-ferrous metals. Issue 3, p. 72 – 75 (2010).
13. V. P. Volkov, N. V. Nikitin, M. A. Kikhailenko et al. In: Proceedings of the 5th International Basic and Applied Scientific Conference. Actual issues of uranium industry. Almaty. 2008, p. 353.

### 3.3.

## **DEVELOPMENT OF THE TECHNOLOGY FOR PRODUCTION OF HIGH-PURITY AMMONIUM PERRHENATE AT BALKHASH COPPER SMELTER, REPUBLIC OF KAZAKHSTAN**

E.A. Ospanov, E.I. Gedgagov\*, N.A. Ospanov, S.V. Zakharyan

BALKHASH COPPER SMELTER, REPUBLIC OF KAZAKHSTAN

\*FSUE "GINTSVETMET Institute",

13, Acad. Korolyov Street, 129515, Moscow, Russia, e-mail: gin@gintsvet.msk.ru

The Republic of Kazakhstan is within five world's largest rhenium producers. The main source of rhenium in Kazakhstan is copper ore and Kazakhmys is virtually copper monopolist in Kazakhstan. The copper concentrate is processed in electric furnace (Zhezkazgan smelter) and Vanyukov furnace (fluidized bed furnace, Balkhash smelter). During smelting and converting processes the rhenium sublimates with the gas which goes through dry ESP, cooling and washing processes and finally fed to the Acid plant to produce strong sulfuric acid. At this stage up to 70% of initial rhenium in the feed is reported to the washing sulphuric acid (weak acid).

The weak acid produced at Zhezkazgan copper smelter is supplied as a rhenium-containing feed to Zhezkazganredmet (Zhezkazgan rare metals plant) being 50% owned by Kazakhmys and 50% by the Government. The technology used at the plant is solvent extraction (SX) with followed by trialkylamine re-extraction with ammonia solution and crystallization.

The weak acid produced at the Balkhash commissioned in 2007 acid plant is the primary potential source of rhenium. It is the low rhenium grade at comparatively large flow determined the selection of the extraction method – sorption in resin-based water-insoluble ion-exchangers. The weak acid produced at Balkhash acid plant is featured by presence of selenium.

The purpose of this article is to give idea about the technology used for processing the sulfuric acid solutions produced at Balkhash acid plant, based on industry tested sorption processes featuring high rhenium and selenium recoveries and producing high-grade ammonium perrhenate and metallic selenium.

The total process flowsheet includes two stand-alone sorption sections. The first one provides for complete rhenium extraction. The rhenium-free solution containing the remaining selenium produced by the main rhenium sorption is fed to the same stand-alone selenium sorption process as well. The second stage sorption producing elemental selenium.

A special attention in the development of the sorption-based technologies should be paid to preventing the impurities from poisoning the ion exchanger as well as to development of the ion exchanger regeneration technologies.

Thus, implementation of the developed Balkhash acid plant solutions processing flowsheet will allow significant increase in high-quality APR-0 grade ammonium perrhenate production.

3.4.

## USE OF ION-EXCHANGE RESINS FOR PRODUCING HIGH-PURITY AMMONIUM PERRHENATE IN PROCESSING OF CRUDE ORE AND MANMADE RHENIUM-CONTAINING RAW MATERIALS

E. I. Gedgagov\* and N. E. Nekhoroshev\*\*

\*GINTSVETMET Institute, ul. Akademika Koroleva 13, Moscow, Russia  
e-mail: gin@gintsvet.msk.ru

\*\*ZAO VR, ul. Radio 7, Moscow, Russia  
e-mail: nk@pzcm.com

**Keywords:** perrhenate, crude ore, rhenium wastes, rhenium sorbents

### Introduction

The Flowsheets used for processing crude ore and manmade rhenium-containing raw materials differ from those for processing the other metals by a wide variety of processes intended for manufacturing commercial ammonium perrhenate for the following reasons. On the one hand, rhenium recovery is relatively easy because perrhenate anion is the major rhenium species in aqueous solutions almost over the entire range of hydrogen ion concentrations; and on the other, this low-hydrated anion has no rivals in absorption, except for anions of the strongest acids known hitherto. One more reason for diversified technologies is small production volumes, and a pilot-scale sorbent batch of no more than several hundred liters in volume is sufficient for filling sorption apparatuses. Another aspect of the problem is the selection of a sorbent to desorb the absorbed perrhenate anion to a vanishingly low residual capacity easily and with a small volume of ammoniac solution. Such properties are intrinsic to low-basicity anion exchangers or amphoteric sorbents, and to reach all required properties of sorbents is not an easy task. Before assessing the recent advances in synthesis of sorbents, it is expedient to carry out a retrospective review of sorption recovery methods.

### Retrospective review

The first industrial low-acidity styrene-divinylbenzene anion exchangers, for example, AN-21, were unable to recover rhenium at high acidities, and it was recommended to dilute these acid solutions with water. However, this was not the only drawback of the then-existing low-basicity anion exchangers. Passage of considerable amounts of an ammoniac desorbent was required for rhenium to be desorbed from anion exchanger AN-21, so that eluates were diluted many times over. The idea of crosslinking resins (that is, providing a polystyrene matrix with high divinylbenzene percentage in the form of crosslinked chains) with the goal of causing a sieve effect at the ion-exchange phase boundary, was first embodied in anion exchanger AN-21x14 (by K.B. Lebedev); this anion exchanger was intended to be used in purifying rhenium from molybdenum in molybdenum-rhenium concentrate processing flowsheets [1]. Upon sorption from scrubber solutions, perrhenate anion easily penetrates the depth of ion-exchanger grains, while bulky molybdenum polyanions remain in solution for the reason that the resin matrix has a rigid structure. The Pobedit plant also employed resin AN-82x14 for recovering rhenium from molybdate solutions; this resin was synthesized using the known idea of crosslinking to create a rigid ion-exchanger framework [3]. At the All-Russia Research Institute of Chemical Technology (by N.G. Zhukova and A.I. Zorina), a 2-methyl-5-vinylpyridine matrix was used to create a rhenium resin; but unlike AN-21, this new resin belonged to the class of ampholytes, and this was only in order to

improve the conditions for rhenium desorption by weak ammoniac solutions [9]. In this way, the plant in Dneprodzerzhinsk produced a pilot lot of VP-14KR (a known ampholyte) [3], and it was later modified to VP-18KR. The major drawback of those resins consisted of acidity limitations; that is, they were low efficient at acidities above 100 g/l of sulfuric acid, but the ammoniac desorption of rhenium was over after the passage of no more than two or three specific volumes of the desorbent. Despite a limited range of available resins, the practice of using ion exchangers in rhenium sorption finally culminated in commercialization at the Pobedit Plant [2], at the Chimkent Lead Plant (in sorption from zinc–cadmium sulfate solutions) [4], at the Skopino Mining and Metallurgical Plant (in sorption from post-molybdenum-sorption solutions), at the Severonikel Plant, at the Uzbekistan Plant of Refractory and Heat-Resistant Metals [3], and at the Kirgiz Ore Mining Plant [5]. A characteristic example of employing a sorption method in the absence of a large-scale production of special sorbents was the commercialization [7] of technology for reprocessing aluminum–platinum–rhenium spent catalysts at the Severonikel Plant (by N.E. Nekhoroshev). Ampholyte VP-1K was employed for recovering rhenium; this ampholyte had been designed for recovering tungsten polyanions, but was used for rhenium not only because of the low basicity of its functional groups but also following the then-known principle of "being available off the shelf." Despite this principle, the tungsten ampholyte demonstrated acceptable rhenium sorption values, and this was not barred by the propensity of the ampholyte to swelling with a coefficient exceeding 5.5 ml/g resin and the associated considerable dilution of rhenium-containing eluates. Certainly, more recent studies carried out by scientists from the St.-Petersburg Technological Institute (A.A. Blokhin) in collaboration with specialists from the Purolite company (M.A. Mikhailenko) provided an optimal version of sorbent synthesis for recovering rhenium from solutions after leaching rhenium-containing catalysts, namely, anion exchanger Purolite A170 [8].

The range of resins for rhenium is not confined to low-basicity ion exchangers that have been used in acid media. Neutral and alkaline solutions, for example, carbonate–bicarbonate systems of underground uranium leaching, can be reprocessed to recover rhenium only with the use of strongly basic anion exchangers. These anion exchangers have high rhenium sorption capacities compared to the low-basicity ion exchangers over a wide range of hydrogen ion concentrations, but inasmuch as rhenium desorption from them was extremely difficult, the vector of research was redirected to the selection of reagents providing the most efficient sorption, frequently without worrying about detrimental phenomena, such as chemical destruction and poisoning of ion exchangers. At different times, proposed were solutions of ammonium thiocyanate, nitric acid, hydrochloric acid, and various combinations thereof, with or without heating, in a dynamic mode or under stirring in a batch mode. Moreover, a variant of extractive desorption has been proposed for separating rhenium and molybdenum (at GINTSVETMET). According to this technology, a strongly basic resin saturated with rhenium and molybdenum is contacted with a tertiary amine extractant. As a result, the rhenium is quantitatively transferred to the extractant phase (from which it can easily be desorbed by a weak ammoniac solution) whereas molybdenum, which is sorbed in the form of large polyanions, practically all remains in the resin and can also be desorbed by ammonia--salt mixtures, but without rhenium. The rhenium/molybdenum separation factors are very high, which helps reduce hardware design and one-time downloads of resins used for the separation.

Processes with rhenium microconcentrations have become a very important line in rhenium recovery technologies. In particular, this will help come close to solving the long-standing problem of recovering rhenium from an unusual system such as fumarolic gases from the Kudryavy Volcano on the island of Etorofu of the Kuril Chain, where the yearly rhenium amount is estimated at several tons. Presumably, upon water entrainment of rhenium heptoxide from fumarolic systems, solutions can form where rhenium concentrations will be such that to require the use of flowsheets with rhenium microconcentrations. Very important studies intended to find sorbents suitable for operating with rhenium microconcentrations (these sorbents are necessary for finding other alternative sources of rhenium) are now underway at the Russian University of Chemical Technology (by I.D. Troshkina), at the St.-Petersburg State Technological Institute (A.A. Blokhin),

at GINTSVETMET (by E.I. Gedgagov), and at other scientific centers. Underground uranium leaching solutions are a real source of rhenium. In this context, there are increasing suggestions to carry out the associated recovery of rhenium by sorption from underground uranium leaching solutions, where rhenium contents are less than 0.5 mg/l. Uranium–rhenium solutions are not a new system. As early as in 1986, a sorption–extraction combination technology for underground leaching solutions of uranium ores was commercialized at the Fifth Mining Group of the Leninabad Mining and Chemical Plant (by A.N. Zagorodnyaya). Strongly basic anion exchanger AM, which was proposed for recovering rhenium from solutions containing rhenium in amounts of 0.25 mg/l on average, provided a high degree of rhenium recovery (70%) along with extractive preconcentration from eluates. Attempts have also been made (at GINTSVETMET) to recover rhenium by sorption from the clarified portion of the sludge field of the Uzbekistan Plant of Refractory and Heat-Resistant Metals, tailings of the Erdenet plant (in Mongolia), and settling sumps of the beneficiation cycle at the beneficiation plant of the Dzhezkazgan Mining and Metallurgical Plant [6]. In all of these cases, evidently, processes for recovering rhenium from solutions with 0.1–0.2 mg/l have quite a different hardware design. Apparatus with a stationary resin bed should have been substituted by pressurized columns with the highest linear rates hitherto unknown in nonferrous metallurgy, and if it were so, rhenium recovery technology could have become a replica of underground leaching technology for uranium. And given the persistently rising prices and shortage of supply, we cannot rule out that this scenario is quite realistic for rhenium.

### **Recent advances in synthesis of sorbents**

The current situation in the synthesis of resins in Russia is such that, for rhenium, in the near future here will be need to purchase ion exchangers produced by the leading companies abroad, and this work has been already started. Studies on the synthesis of sorbents, specifically, for rhenium, are now underway in other companies, too, for example, Lanxess (Germany), Rohm & Haas, and Dow Ch. (both in the USA), and others.

The Russian Federation does not have significant sources of rhenium-containing ore material; however, there are some measures that can help achieve a substantial progress in the provision of Russia with rhenium (which is certainly the metal of future progress in aerospace science), namely: careful attention to technologies for reprocessing all possible waste (superalloy, spent catalyst, binary alloy, and other waste), solving the problem of reprocessing systems with rhenium microconcentrations (volcanic eruptions, underground leaching of uranium solutions, and so on), as well as attention from the government to the creation of the domestic industry for the synthesis of sorbents and multilateral scientific and practical discussion of the achievements at various conferences.

### **References.**

- [1]. Lebedev, K.B., et al., *Ion Exchangers in Nonferrous Metallurgy*, Moscow: Metallurgiya, 1975.
- [2]. Korneeva, S.G., "Recovery of Rhenium in Processing of Molybdenite Concentrates at the Pobedit Plant," in *Collected Works of GINTSVETMET*, 1990, pp. 85--87.
- [3]. Rumyantsev, V.K., Vol'dman, S.G., and Kulakova, V.V., "Associated Rhenium Recovery in Processing of Molybdenite Concentrates," *Tsvet. Metally*, No. 7, 1991, pp. 33--39.
- [4]. Abisheva, Z.S., Zagorodnyaya, A.N., and Ponomareva, E.I., "The State and Prospect of Rare-Metal Industry in Kazakhstan," *News of Science of Kazakhstan*, 2000, No. 2, pp. 7--10.
- [5]. Gedgagov, E.I., and Besser, A.D., "The Russian Federation as Part of the World's Market for Refractory Metals Raw Materials," *Khim. Tekhnol.*, 2000, No. 1, pp. 15--24.



- [6]. Volk, V.I., Vakhrushin, A.Yu., and Besser, A.D., "Technology for Recovering Rhenium from Solutions with Extremely Low Rhenium Concentrations," *Tsvet. Met.*, 1999, Vol. 35, No. 6, pp. 16--19.
- [7]. Gedgagov, E.I., "Development of Scientific Rationale and Commercialization of Molybdenum, Tungsten, and Rhenium Sorption on High-Porosity Ion Exchangers," Abstract of Doctoral Dissertation., 1989, 380 pp.
- [8]. Blokhin, A.A., Mal'tsev, E.E., et al., "Ion-Exchange Recovery of Rhenium from Molybdenum-Containing Sulfuric Acid Solutions," *Tsvet. Met.*, No. 2, 2005, pp. 59--62
- [9]. Baskakov, A.N., et al., "Copolymers of Vinylpyridine, Divinylbenzene, and Vinylphenylacetic Acid and Methods for Their Preparation," USSR Author's Certificate No. 969006, June 22, 1982.

3.5.

## **PUROLITE<sup>®</sup> ION EXCHANGE RESINS FOR RECOVERY AND PURIFICATION OF RHENIUM**

Mikhaylenko, M.

Purolite International Limited, Representation office in the CIS, Lusinovskaya 36, Moscow, 115093, Russia,  
[purolite\\_mm@co.ru](mailto:purolite_mm@co.ru)

Rhenium supply in the world market is fed from two main sources: processing of different ores and recycling of secondary materials.

Hydrometallurgical methods are used for processing the rhenium feed. Often the SX, precipitation and membrane separation techniques are used to recover and purify rhenium from other elements. However in many practical cases application of rhenium selective resins provide the most direct and simplest, and consequently the most economical way to produce ammonium perrhenate of high grade.

Purolite<sup>®</sup> manufactures two rhenium selective resins: Purolite<sup>®</sup> A170 and A172. Both resins are weak base anion exchange resins made of polystyrene-divinylbenzene polymer, but the first one is macroporous and the second is gel type. Effective desorption of rhenium can be done by either sodium or ammonium hydroxide. Enrichment coefficient in desorbate can be as high as  $10^3$  order of magnitude.

The A170 resin is perfect for recovery of rhenium from solutions comprising of 1 to several hundred ppm of rhenium, up to several hundred grams per liter of sulfuric acid, high chloride. The rhenium recovery is very selective in regards of common alkali, alkali earth and base non-ferrous metals. Such solutions are commonly generated by copper smelters and two large smelters have already installed this resin.

The A172 resin is tailored for selective separation of rhenium from molybdenum. This technical task is quite difficult due to very similar chemical properties of perrhenate and molybdate compounds in aqueous solutions. Such solutions are obtained at processing of molybdenite concentrates.

Other application of the A170 resin is rhenium recovery from low grade solutions. An example is sulfuric uranium PLS where rhenium concentration is typically 0.5 to 3 ppm. This resin has been installed at Navoi GMK, Uzbekistan to recover rhenium from uranium barren solutions, i.e. after sorption of uranium by strong base anion exchange resin, and has been successfully operating for several years.

Finally, the A170 resin can be effective for recovery of technetium from acidic solutions.

### 3.6.

## PHYTOMINING OF RHENIUM - AN ALTERNATIVE METHOD FOR RHENIUM PRODUCTION

Ognyan Bozhkov<sup>1</sup>, Christina Tzvetkova<sup>1</sup>, and Ludmila Borisova<sup>2</sup>

<sup>1</sup>Institute of General and Inorganic Chemistry, Bulgarian Academy of Sciences,  
Acad. G. Bontchev str., bl. 11, Sofia, 1113 Bulgaria,  
e-mail: bozhkov@svr.igic.bas.bg

<sup>2</sup>Vernadsky Institute of Geochemistry and Analytical Chemistry, Russian Academy of Sciences, Kosygina str. 19,  
Moscow, 119071 Russia

**Keywords:** rhenium, phytomining, plant hyperaccumulators, ammonium perrhenate

### Abstract:

Phytomining is the uptake and preconcentration of bioavailable metal species from the environment into the plant biomass in a natural way. Rhenium possesses the unique property to accumulate and concentrate as perrhenate in the green parts of all terrestrial and aquatic plants in amounts many times exceeding its natural occurrence, which is a precondition for its phytomining. Our approach for Re phytomining from soils and waters was as follows: a) carrying out regional investigations on Re distribution in the vegetation around the copper mine „Asarel”- Bulgaria and locating areas with industrial importance of Re concentration in the vegetation; b) discovering plant species, which are rhenium hyperaccumulators; c) developing a procedure for efficient Re extraction from the plant mass and obtaining pure  $\text{NH}_4\text{ReO}_4$ . As a result of the application of our approach: a) we found the points in the area around the copper mine „Asarel”- Bulgaria which are of industrial importance as regards the Re concentration in the vegetation; b) we discovered four plant species as new hyperaccumulators of Re suitable for its phytomining; c) we developed two procedures for quantitative extraction of Re from the plant mass and a simple procedure for purification of the leachate from the main ash elements such as K, Ca Mg and Cu. The final solution contains 98.2 % of Re and only 1.8 % of impurities as a sum of the main ash elements.

### Introduction

The phytoextraction of metals or mining with plants (phytomining) is the uptake and preconcentration of water-soluble metal compounds (bioavailable species) from the environment into the plant biomass. The plants absorb metals through the root system and store them in the root biomass and/or transport them up into the stems and/or leaves [1, 2]. A living plant may continue to absorb substances until harvested. The main advantage of phytoextraction is its environmental friendliness. Another benefit of phytoextraction is that it is less expensive than any other method for recovery of metals from polluted soils without damage of the environment [1, 2]. Enough is the contaminated area to be plants with the crop and after plant development to harvest the green mass. The further step is to extract the metal from the plant mass, usually by incineration of the latter.

In our previous studies it was found that the plant biosphere is a natural extractor and concentrator of rhenium from soils and waters [3]. A basic feature of Re is that this metal is preferably accumulated (more than 98%) in the green over ground parts of all kinds of plants. It was established that the plant biosphere in the vicinity of copper mines and copper processing factories was enriched with rhenium in amounts exceeding its natural abundance in Earth's crust by a factor of 214 to  $1.98 \times 10^6$  [3,4]. Therefore, phytomining is appropriate to be applied in those areas, where conventional methods for extracting the metals are not cost-effective. We also proved that the different plant species have different capacity for rhenium accumulation and that the bioavailable species of rhenium in the surface environment is the  $\text{ReO}_4^-$  ion [3, 4 and 5].

Our approach for Re phytorecovery from soils and waters [4] was as follow: a) carrying out regional investigations on Re distribution in the vegetation of the copper mine „Asarel”- Bulgaria; b) locating the areas with industrial importance of Re concentration in the vegetation; c) discovering plant species, which are rhenium hyperaccumulators (able to accumulate 1000 g Re/t dry mass or more; d) developing a procedure for efficient Re extraction from the plant mass and obtaining pure  $\text{NH}_4\text{ReO}_4$ .

In this work we summarize the results of the application of our approach for Re phytorecovery from soils and waters of copper mining areas with alfalfa.

## Experimental

The Re content in all plant samples was analyzed by incineration of the dry plant mass, followed by Re extraction from the ash with alkaline solution and its determination according to the spectrophotometric catalytic method for determination of ng amounts of Re with N,N-dimethyldithiooxamide (DMDTO), developed by us [6]. For field determination of the Re content in the vegetation we used the DMDTO spot test after Re extraction from the plant mass with ethanol [6, 7]. The spectrophotometric determination of Re was carried out on the double beam UV-VIS spectrophotometer Evolution 160, Thermo Scientific. Flame AAS determinations were carried out on the Thermo SOLAAR M5 Dual AA Spectrometer, Thermo Scientific. The samples (copper concentrates, a soil sample and a solid sample from the tailings) were analyzed by melting with an oxidation mixture of  $\text{Na}_2\text{O}_2$  and  $\text{Na}_2\text{CO}_3$  at  $520^\circ\text{C}$  and treating the melt with water for leaching of Re [8]. In the obtained alkaline leachates the Re content was determined according to the highly selective and sensitive catalytic method using DMDTO [6].

## Results and discussion

### Regional investigation on Re distribution in the vegetation in the area around the open-air copper mine „Asarel”

Our preliminary autumn investigations in October 2006 on the degree of rhenium accumulation in the vegetation of soils from the „Asarel” mine were insufficient to throw light on the real Re distribution in plants from this region [3]. Nevertheless, the experiments showed that Re was not uniformly distributed in the vicinity of the „Asarel” mine and helped us to mark several sampling points for the subsequent regional summer investigations, e.g., close to the open mine, at the spoils, at the installation for copper concentrate production, at the shore of the lake collecting the waste mining waters, etc. The autumn investigations showed that acacia and birch were good collectors of rhenium. To find the best plant biocollector of Re it was necessary to expand the plant species sampling. The summer sampling was carried out in the second half of June 2007 [4]. We analyzed the Re content of 22 samples, collected from 5 main points in the vicinity of the „Asarel” mine: 15 plant samples from 10 different plant species, 3 water samples, 2 samples of copper concentrates produced in the enrichment installations of the „Asarel” mine, 1 soil sample and 1 solid sample from the tailings [4]. The Re content in the vegetation was analyzed according to the procedures described above [7]. The sampling points of our summer regional investigation are marked on Fig. 1 and the results of the analysis are shown in Table 1.

The summer regional investigation on rhenium distribution in the vegetation [4] showed that the content of rhenium in plants growing on the territory of restored spoils was lower than that in the vegetation growing near the open-air mine „Asarel” (compare the results in Table 1, points S1 and S5). These results could be explained by the lowest concentration of rhenium in soils of the spoils because of their restoration. Analysis of the vegetation growing on the shore of the Gelev Chuchur Lake confirmed our previous findings [4] that waterside plants can extract and concentrate rhenium from waters [3]. On the other hand, it is apparent that different plants have a different capacity for Re bioaccumulation (the sampling distance between the different plant species from the shore was maximum 15 m). It could be presumed that plant species with a well developed root system would suck more water from the lake and hence, accumulate more rhenium (see the results in Table 1, S2, leaves of oak and bush).

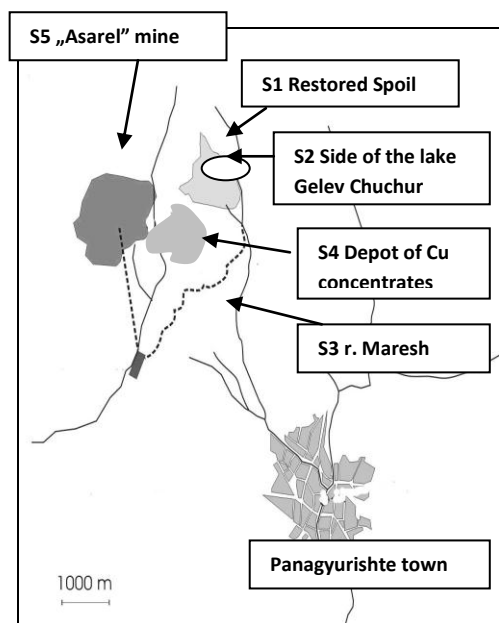


Fig. 1. Map of the surroundings of „Asarel” coppers mine.

Sampling site, Sample type	C <sub>Re</sub> μg/g ash	Ratio C <sub>Re</sub> /Clark *
S1, leaves of flowering clover	2.30	3 286
S1, leaves of acacia	0.59	843
S2, leaves of oak	7.20	10 286
S2, leaves of bush	2.44	3 491
S2, drainage water from lake	0.12 μg/ml	171
S3, river water	0.04 μg/ml	57.1
S3, elder leaves	30.8	44000
S4, flotation copper concentrate	1.0	1 429
S4, cementation copper concentrate	135	192 857
<b>S4, leaves of acacia, 5 m from depot</b>	<b>1686</b>	<b>2.41x10<sup>6</sup></b>
S4, soil – 5 m from depot	5.0	7143
S4, waste water with bacteria, pH=1.5	0.06	86
S5, leaves of acacia	13.2	18 857
S6, tailing sample	0.05	71

\*The Clark of Re in the Earth’s crust is 0.7 ng Re/g

The rhenium concentration in the lake water was about three times higher than that in the River flowing from the lake (see S2 and S3 water samples) because of the high water of river Maresh near the town of Panagyurishte. The results of the sampling points in the area of the installation for copper concentrate production and the depot of copper concentrate (see S4 in Table 1) are very interesting. The concentrate which contains more than 50 g Re per ton is of industrial importance. The average Re content in the copper concentrates varies between 1 and 3 g Re/t [9]. „Asarel” mine produces two kinds of copper concentrates: flotation and cementation concentrates. The flotation concentrate contains the expected amount of rhenium (1 g Re/t) while the cementation concentrate contains an extremely high amount of rhenium (135 g Re/t) [4]. It is known that the molybdenum concentrate has the highest rhenium content [9]. What is more interesting, is that the vegetation (acacia) growing close to the depot of cementation copper concentrate is able to bioaccumulate in its leaves up to 1686 g Re/t ash in a natural way [4]. This value is of industrial importance and is commensurable with the richest in Re molybdenum concentrates (USA, state Nevada -1030 g Re/t, South-West Africa – 2300 g Re/t, ex USSR territory-1930 g Re/t and Stavanger, Norway-3100 g Re/t [9]).

It is very probable that part of rhenium in the cementation concentrate is in the form of the easily assimilated by plants  $\text{ReO}_4^-$  species. Since oxide copper concentrate is produced by bioleaching of Cu from poor copper ores with the aerobic bacteria *Acidithiobacillus ferrooxidans* in  $\text{H}_2\text{SO}_4$  solution in presence of  $\text{Fe}^{3+}$  ions, it is very likely that during this process part of  $\text{ReS}_2$  is also oxidized to  $\text{ReO}_4^-$ . The role of the bacteria consists of oxidation of  $\text{Fe}^{2+}$  to  $\text{Fe}^{3+}$ , as well as sulphur to soluble sulphate [10].

As the cementation copper concentrate is stored under atmospheric conditions, it is probable that the rainfalls wash out part of the perrhenate ions from the concentrate and thus rhenium penetrates



the soil and is then extracted by plants. The results also evidence that the Re concentration in leaves of acacia growing 5 m away from the store concentrate is 12.5 times higher than that in the concentrate [4]. As a result of the regional investigation [3, 4] we found the points of industrial importance of rhenium content in the vegetation – the one close to the installation for producing cementation copper concentrate and the other - to the depot of copper concentrate (Table 1., S4). The regional investigation showed again that the acacia leaves are the best plant biocollector of rhenium. However, to develop a procedure for real Re phytorecovery from soils we need a plant biocollector which should:

- be unpretentious for cultivation and grow fast with a well developed root system;
- have a great quantity of green mass which is a precondition for hyperaccumulation of rhenium;
- be easy for harvesting and grow again after cutting.

Taking into account these considerations, we chose alfalfa (*Medicago*), white clover (*Trifolium Repens*), mountain-spinach (*Atriplex hortensis*) and buck-wheat (*Polygonum Fagopyrum*) for our further experiments [12, 13].

### **Study of the capacity of the abovementioned four plant species for Re phytoextraction from soils spiked with $\text{ReO}_4^-$ at laboratory conditions**

The experiments were carried out as follows [13]. In four portions of 2.5 kg dry soil (in pots), we put seeds of alfalfa, white clover, mountain spinach, buck-wheat and regularly watered them. After two weeks, the seeding plants grew and developed leaves. Then each soil was spiked with 0.3218 g Re as  $\text{KReO}_4$  solution. The concentration of Re in the soil was 128.72  $\mu\text{g/g}$  soil. The plants were regularly watered. Monitoring of the bioaccumulated Re in the samples of vegetation was carried out in different periods after the spiking of soil. The plant samples were dried to constant weight under atmospheric conditions. An exactly weighed quantity of dry plant mass was incinerated at 480°C and the rhenium content was determined according to the procedures described above [6, 7].

The results of the analysis showed that alfalfa is a new efficient plant hyperaccumulator of Re from soils [11]. It was established that after 7 days the content of Re in alfalfa growing on soil spiked with  $\text{ReO}_4^-$  ( $C_{\text{Re}} = 128.72 \mu\text{g Re/g soil}$ ) increased up to 46 586  $\mu\text{g Re/g dry mass}$  (4.66% Re) alfalfa, respectively 294 289  $\mu\text{g Re/g ash}$  (29.43% Re) and did not further increase with time. The enrichment factor was 362 for dry mass, respectively 2286 for ash. In this way, for the first time we prepared rhenium phytoconcentrate at laboratory conditions. The investigations showed that also white clover (*Trifolium Repens*) is hyperaccumulator of rhenium from soils spiked with perrhenate [12, 13]. It was established that 22 days after spiking the soil with  $\text{ReO}_4^-$  ( $C_{\text{Re}} = 128.72 \mu\text{g Re/g soil}$ ) the content of Re in the clover growing on this soil increased up to 35 090  $\mu\text{g Re/g dry clover}$  (3.51% Re), resp. 226 553  $\mu\text{g Re/g ash}$  (22.66% Re). The enrichment factor was higher than 272 for dry mass, respectively 1760 for ash. The other two plant species - mountain-spinach (*Atriplex hortensis*) and buck-wheat (*Polygonum Fagopyrum*) accumulated up to 3150  $\mu\text{g Re/g dry mass}$  or 9130  $\mu\text{g Re/g dry mass}$ , respectively, which is a low capacity for rhenium bioaccumulation. Hence, these species are not perspective for practical rhenium phytoextraction from soils [13]. The significance of rhenium hyperaccumulation by alfalfa and white clover is evidenced by the Re content in them - 4.66% of Re in the dry mass of alfalfa, respectively 29.43% of Re in the ash and 3.51% of Re in the dry mass of white clover, respectively 22.66% of Re in the ash. For comparison, the Re concentration in the richest molybdenum concentrates is maximum 0.1-0.2 % of Re [9]. Another significant difference between these two Re containing materials is that the phytoconcentrates are obtain in a natural way (only through watering of the plants and using their metabolism) with minimum resources, while the ore concentrates, are obtain by sophisticated high-cost technologies.

As a result of our experiments we found four plant species, which are new Re hyperaccumulators. For all further experiments, we chose the alfalfa with known Re content obtained at laboratory conditions [13].

### Purification of the Re containing leachate from the main ash elements

In our previous study [14] we developed two procedures for 100% rhenium extraction from the green mass as follows:

- Direct incineration of the plant mass at 480°C in oxidation atmosphere, followed by alkaline extraction of rhenium from the ash;
- Ethanol extraction of rhenium from the green mass, evaporation (or distillation) of the ethanol followed by incineration of the dry organic residue at 480°C and extraction of rhenium from the remaining ash by an alkaline solution.

The concentration of Re in the leachate was determined according to the catalytic DMDTO method [6]. The concentrations of K, Ca, Mg, and Cu in the leachate were determined by FAAS. The experiments showed [14] that the alkaline leachate obtained after direct incineration of alfalfa contains 52.79% of Re and 47.21% of K, Ca, Mg, and Cu (sum of the main ash elements). The leachate obtained after ethanol extraction of Re from alfalfa contained 67.4% of Re and 32.6% of the above mentioned main ash elements [14]. It is evident that the leachates obtained according to these two procedures are not sufficiently purified from the main ash elements and are not suitable for obtaining pure ammonium perrhenate. In our previous studies, we found that the rhenium species in the alkaline leachate was  $\text{ReO}_4^-$  [5, 7]. On the other hand, the main ash elements - K, Ca, Mg and Cu, are cations. The usual way for removing cations from solutions is *via* cation exchange resins [15]. We chose the strongly acidic cation exchange resin Dowex 50W×8 in  $\text{H}^+$  form with a total capacity of  $5.2 \pm 0.3$  meq per dry gram [11]. In our experiments, we used the batch method of sorption because of its simplicity of performance. To find the optimal time for sorption of the cations on the Dowex 50W×8 resin we carried out preliminary experiments with rhenium containing alfalfa obtained at laboratory conditions. The investigation showed [11] that after 1 hour of dynamic contact between the liquid phase and the resin, the degree of sorption of the cations was about 89%, after 2 hours the degree increased up to 95% and after 3 hours, it reached 99%. In all further experiments with alfalfa for purification of leachates, the batch method was performed for 3 hours. The experiments were carried out as follows [11]:

Two portions of raw alfalfa (1 g each) were treated by the two methods developed by us for extraction of rhenium from the plant mass: by direct incineration of raw alfalfa and by ethanol extraction of rhenium from the green mass [14]. Both 20-ml ammonia leachates were analysed for the Re content by the catalytic DMDTO method and for K, Ca, Mg and Cu by FAAS [11].

Two portions of dry Dowex50W×8 (1 g each) were soaked in distilled water overnight to allow the resin to swell. The swollen resin was separate from the water and was add to the 20-ml alkaline leachates containing rhenium and the main ash elements. The experiments were carrying out in 50-ml polypropylene flasks with stoppers. The sorption was performing by the batch method on a shaking machine for 3 hours. The resin was separating from the solution by filtration through a paper filter. The resulting solutions were analysed for Re, K, Ca, Mg and Cu [11].

### Results and discussion

The results of the experiments [11] showed that the leachate obtained after direct incineration of the plant mass, purified by treatment with Dowex 50W×8, contains 95.3 % of Re and only 4.7% of the sum of main ash elements. The leachate obtained after ethanol extraction of Re from alfalfa and its purification with Dowex 50W×8 contains 98.2 % of Re and only 1.8 % of impurities of main ash elements. The comparison of the results of the two procedures for Re extraction from the plant mass revealed that after ethanol extraction of Re from alfalfa a higher degree of purification of the Re containing leachate from the main ash elements was achieved than after direct incineration of alfalfa [11]. These results are in accordance with our previous study [14]. As a result of our experiments, we developed a simple procedure for purification of the Re containing leachate from the main ash elements such as K, Ca, Mg and Cu by cation exchange on the Dowex 50W×8 resin.  $\text{NH}_4\text{ReO}_4$  is

easily obtaining from the final solution after its alkalization with  $\text{NH}_4\text{OH}$ , preconcentration by evaporation and crystallisation of  $\text{NH}_4\text{ReO}_4$  [16].

## Conclusions

As a result of our investigations we developed a low-cost and environmentally friendly technological scheme for real phytorecovery of Re dispersed in the soils of ore dressing areas by alfalfa which includes:

1. Regional investigation of Re distribution in the vegetation of the copper ore dressing areas and finding the points with industrial importance for Re phytomining;
2. Cropping these areas with alfalfa and obtaining of Re phytoconcentrate;
3. Harvesting the alfalfa and extraction of Re from the green mass;
4. Purification of the Re containing leachate by a simple procedure developed by us and obtaining of  $\text{NH}_4\text{ReO}_4$  - the commercial product of Re on the world market.

## Acknowledgments:

The authors acknowledge the financial support of the National Science Fund of Bulgaria (National Centre for New Materials UNION, Contract No DCVP-02/2/2009).

## References:

1. M. M. Lasat, *Journal of Hazardous Substance Research*, **2**: 5-25, 2000.
2. V. Sheoran, A. S. Sheoran, P. Poonia, *Minerals Engineering*, **22**, 1007-1019, 2009.
3. O. Bozhkov, Chr. Tzvetkova and T. Blagoeva, Proceedings of the 1st International Conference on Waste Management, Water Pollution, Air Pollution, Indoor Climate (WWAI'07), Published by WSEAS Press, ISBN: 978-960-6766-09-1, Arcachon, France, October 13-15, 2007, pp. 257-261.
4. O. Bozhkov, Chr. Tzvetkova and T. Blagoeva, Proceedings of the 2<sup>nd</sup> WSEAS International Conference on Waste Management, Water Pollution, Air Pollution, Indoor Climate, (WWAI'08) Published by WSEAS Press, ISBN:978-960-474-017-8, Corfu, Greece, October 26-28, 2008, pp. 262-265.
5. O. Bozhkov, Chr. Tzvetkova, L. Borisova, V. Ermakov and V. Ryabukhin, *Trends in Inorganic Chemistry*, review, Vol. **9**, 1-10, 2006.
6. O. Bozhkov and L.V. Borisova, *Anal. Communications*, **33**, 133-135, 1996.
7. O. D. Bozhkov and L. V. Borisova, *Intern. J. Environ. Anal. Chem.*, vol. **83**, N 2, 135-141, 2003.
8. O. D. Bozhkov, N. Jordanov, L. V. Borisova, Yu. I. Fabelinskii, *Fresenius Z. Anal. Chem.*, **321**, 62- 64, 1985.
9. L. Borisova and A. Ermakov, *Analytical Chemistry of Rhenium (in Russian)*, Nauka, Moscow, 1974.
10. M.A. Askari Zamani, N. Hiroyoshi, M. Tsunekawa, R. Vaghar, M. Oliazadeh, *Hydrometallurgy*, **80**, 23-31, 2005.
11. Chr. Tzvetkova and O. Bozhkov, Proceedings of the 2nd International Conference on Waste Management, Water Pollution, Air Pollution, Indoor Climate (WWAI'08) Published by WSEAS Press, ISBN:978-960-474-017-8, Corfu, Greece, October 26-28, 2008, pp. 82- 85.
12. Chr. Tzvetkova and O. Bozhkov, Proceedings of the 7<sup>th</sup> WSEAS International Conference on Environment, Ecosystems and Development (EED '09), Published by WSEAS Press, ISBN: 978-960-474-142-7, Puerto De La Cruz, Tenerife, Canary Islands, Spain, December 14-16, 2009, pp. 123-126.
13. O. Bozhkov, Chr. Tzvetkova, Proceedings of the 7<sup>th</sup> WSEAS International Conference on Environment, Ecosystems and Development (EED '09), Published by WSEAS Press, ISBN: 978-960-474-142-7, Puerto De La Cruz, Tenerife, Canary Islands, Spain, December 14-16, 2009, pp. 127-131.

14. Chr. Tzvetkova, O. Bozhkov and E. Russeva, Proceedings of the 1st International Conference on Waste Management, Water Pollution, Air Pollution, Indoor Climate(WWAI'07), Published by WSEAS Press, ISBN: 978-960-6766-09-1, Arcachon, France, October 13-15, 2007, 253-256.
  15. N. Petrov, M. Pavlova, O. Bozhkov, Method for Extracting Rhenium and Tungsten from Wastes of Rhenium-Tungsten Alloys, *United States Patent*, 4, 278, 641, Jul. 14, 1981.
- Z.S. Abisheva, A.N. Zagorodnyaya, *Hydrometallurgy*. **63** 55–63, 2002.

## 3.7.

## INDUSTRIAL SORPTIVE RECOVERY OF RHENIUM FROM CIRCULATING SOLUTIONS OF URANIUM IN SITU LEACHING OPERATION

V.P. Volkov, N.M. Mescheryakov

ZAO NPO "GPS", Moscow

[npogps@mail.ru](mailto:npogps@mail.ru)

There are many researches devoted to the problem of the incidental sorptive recovery of Rhenium from the situ leaching solutions of Uranium. However due to the set of techno-economical reasons they didn't have any industrial use. Until 2002 Navoi Mining-Metallurgical Combine (NGMK) has periodically attempted to recover Rhenium from the Ionite AMP after its stripping from Uranium. Though the very expedience of this method remains questionable for the reason of the low sorptive capacity of AMP Ionite for Rhenium, inconvenient conditions of its regeneration (composition of the stripping solution – 3,0 - 3,5% HNO<sub>3</sub> + 6 - 7% NH<sub>4</sub>NO<sub>3</sub>, regenerate commodity output makes 20 volumes to one of Ionite, with 10-15 mg/l Rhenium concentration, temperature amounting 50 C°) and the complexity of further extraction of Rhenium from the desorbates (2 cycles of extraction – re-extraction).

In 2003 the research workers of ZAO NPO «GPS» carried out preproduction tests of the Purolite Int. Ltd.' Ionite KEP-100 during the Rhenium sorption from the model solutions, imitating the composition of manifold after Uranium sorption from PV RU-5 NGMK solutions [1]. The results of tests show high sorptive properties of the Ionite: Rhenium capacity accounts for 1,86 mg/ml (AMP capacity in the conditions is 0,3 – 0,55 mg/ml).

On the ground of the received results the decision was made to set up an experimental-industrial plant on the RU-5 NGMK. It is designed to provide the test cycles of the Rhenium sorption processes from the industrial in-situ leaching solutions and the regeneration of the Rhenium-enriched Ionites.

This experimental-industrial plant was worked out by the research workers of ZAO NPO «GPS». It was mounted by 2004. It consists of two columns, connected by the pipelines, feeding the columns on the poor Uranium solutions (bottom-up) and stripping (bottom-up) with corresponding pumps and valving fittings

There were conducted 5 cycles of sorption and regeneration altogether in the column with Ionite KEP-200. Ionite KEP-100 tests were suspended since the productivity for solutions reduced (fine granulation) and the capacity of Rhenium fell considerably in further cycles.

The composition of solutions before the sorption (concentration given in mg/L): Re – 0,95; Mo – 0,56; U – 2,0; P – 44,0; Fe – 400,0; Al – 377,0; Si – 48,4; SO<sub>4</sub> – 9627; NO<sub>3</sub> – 54,0; pH – 2,0. Test results are given in the table below\*

№	Technological properties	Unit	KEP-100	KEP-200
1	Volumes of the solution treated for one cycle	m <sup>3</sup>	5500	7340
2	Elapsing time of a sorption cycle	hour	735	790
3	Re concentration in the solution after sorption	g/L	0,16	0,40
4	Capacity of Rhenium-enriched Ionite	kg/m <sup>3</sup>	6,88	5,95
5	Re concentration in the end product regenerates	kg/m <sup>3</sup>	1,21	1,42
6	Quantity of Re recovered in the product regenerate	kg	14,52	20,87

\* - average rates during the tests



The composition average rates of the product regenerates from the KEP-200 Ionite' regeneration (concentration given in g/m<sup>3</sup>): Re – 1,43; Mo – 1,74; U – 4,1; P – 2,52; Fe - < 0,15; A; - < 0,25; Si – 96,0; Cr - < 0,5; Mn - < 0,2.

According to the test results basic data was developed for the creation of the industrial plant by mounting of two sorptive columns with 30 m<sup>3</sup> of Ionite in each [2].

The production of the high-clean ammonium perrhenate of AP-0 brand after the launch of the first column exceeded the quantity of 3 tones.

The technology described above is protected by the patent of the RF [3].

#### **References:**

1. Report on the subject: «The development of the new technology of Re recovery from the in-situ leaching solutions of Uranium, using the compositional extract polymer KEP-100». Moscow. 2003, ZAO NPO «GPS» funds
2. Report on the research on the subject: «The development of the technology of Re recovery from the in-situ leaching solutions using the composite extract polymer KEP-100. The development of the methods of the experimental-industrial test on a section of in-situ leaching». By the contract of KEP-100, 30.10.2002
3. Volkov V.P, Mescheryakov N.M. et al. «The method of Rhenium recovery from solutions». Patent of the RF № 2294392, 24.05.2005

3.8.

## **RHENIUM(VII) SOLVENT EXTRACTION BY MIXTURES OF TERTIARY AMINE AND OXYGEN-CONTAINING EXTRAGENTS FROM SULPHATE MEDIA**

A.G. Kasikov, A.M. Petrova

Institution of Russian Academy of Sciences – I.V.Tananaev Institute of Chemistry and Technology of Rare Elements and Mineral Raw Materials of the Kola Science Centre of RAS  
Akademgorodok, 26a, Apatity, Murmansk reg., Russian Federation

**Keywords:** rhenium, solvent extraction, tertiary amine, aliphatic alcohol and ketone

### **Abstract**

Solvent extraction of rhenium(VII) from sulphate media, involving mixtures of tertiary amines and octyl alcohol or ketone in an aliphatic diluents, has been investigated. Increasing  $H_2SO_4$  concentration from 0.5 to 7 mol/L was noted to diminish the rhenium(VII) distribution coefficients  $D_{Re}$  regardless of both the mixture composition and temperature. Maximum  $D_{Re}$  values were observed at pH=1-2. It was found that in response to octyl alcohol addition to the extraction mixture the  $D_{Re}$  diminished slightly. As for octyl ketone, it somewhat promoted rhenium(VII) extraction. The latter was probably due to different solvation effects of alcohol and ketone on TiOA.

### **Introduction**

Tertiary aliphatic amines  $R_3N$  with hydrocarbon radicals of the  $C_8$ - $C_{10}$  fraction are widely used in rhenium technology. In particular, they can be turned into commercial agents to extract rhenium from scrubbing sulphuric acid solutions of the gas purification system at copper smelters (Zhezkazganredmet, Kazakhstan).

At the same time, efforts are being made to develop new extracting compositions to improve rhenium recovery. In this work, we have examined parameters affecting the process of rhenium(VII) extraction from sulphate media by solutions of different-structured tertiary amines in a solvent containing octyl alcohol or ketone as modifiers.

### **Experimental**

In this work, the reagents were tri-n-octylamine (TOA) solutions of the “pure” grade, a technical-grade mixture of tertiary amines with hydrocarbon radicals of normal structure  $C_8$ - $C_{10}$  (TAA) or an imported technical-grade reagent tri-iso-octylamine (TiOA) of Hostarex A324 brand (no less than 95% of the main substance and up to 5% of primary and secondary amines) in the Escaid 100 diluent with addition of 20-70 vol.% aliphatic alcohols (2-ethyl-hexanol-1) or ketone (2-octanone) of pure grade.

The extracting agent was first converted into a salt by bringing in contact with a  $H_2SO_4$  solution of the same concentration as a solution of rhenium, from which the extraction was performed. Model rhenium-containing solutions were prepared by dissolving ammonium perrhenate in distilled water, adding a certain amount of chemically pure sulfuric acid.

The extraction process took place in separatory funnels at a volume ratio of the organic to aqueous phase equal to 1:25, at room temperature for 5 min, which allowed to attain equilibrium in the system.

Rhenium(VII) content in the aqueous phase was determined by using spectrophotometry, tracing the changing color intensity of the rhenium(IV) thiourea complex formed in the presence of Sn(II) as reducer. The light absorption was measured with a KFK-3 photoelectric colorimeter at a wavelength of  $\lambda = 390$  nm [1] or by the atomic-emission method on a Plazma 400 spectrometer.

The content of rhenium in the organic phase was calculated from the difference of its contents in the aqueous phase before and after extraction.

### Results and Discussion

The parameters essential for the process were the type and concentration of both amine and modifier, as well as acidity of the aqueous phase. In terms of structure and extractive ability towards rhenium, these amines can be arranged in the following series: TiOA>TOA>TAA. Most of the experiments involved TiOA as the best reagent for rhenium(VII) extraction.

Fig.1 shows that the distribution coefficients of rhenium(VII) extraction diminish considerably as the aqueous phase acidity increases in the interval of 0.5-6 mole/L. The latter is usually associated with the competitive process of sulphuric acid extraction.

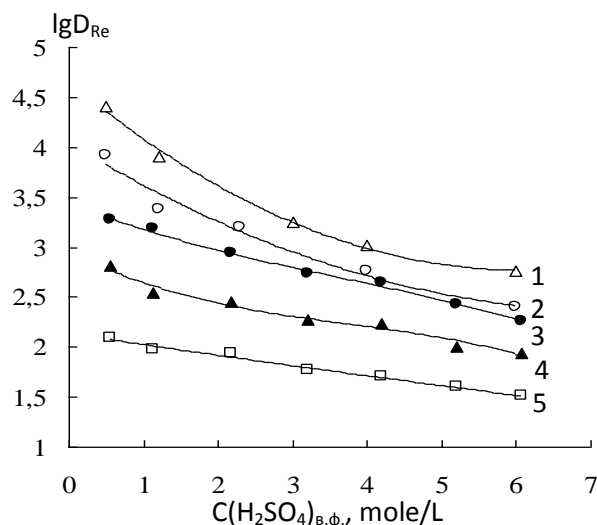


Fig. 1 the effect of  $H_2SO_4$  concentration and extractant composition on rhenium(VII) extraction.  $C_{init.}(Re)=10^{-3}$  mole/L,  $O/W=1/25$ , extractant composition, v/v %:  
 1,  $\Delta$  – 30% TiOA+20% 2-ethylhexanol-1 in kerosene; 2,  $\circ$  – 30% TiOA in 2-ethylhexanol-1;  
 3,  $\bullet$  – 5% TiOA in octanone-2; 4,  $\blacktriangle$  – 5% TiOA +20% octanone-2 in kerosene;  
 5,  $\square$  – 5% TiOA+20% 2-ethylhexanol-1 in kerosene.

In inter-phase distribution studies, the pH region has revealed an extraction maximum by tertiary amines at pH=1-2 (Fig. 2). When the pH increased to 7-9, rhenium(VII) extraction by an amine-alcohol mixture becomes totally suppressed. By using amine-ketone mixtures, rhenium(VII) can be effectively extracted at pH~5-7.

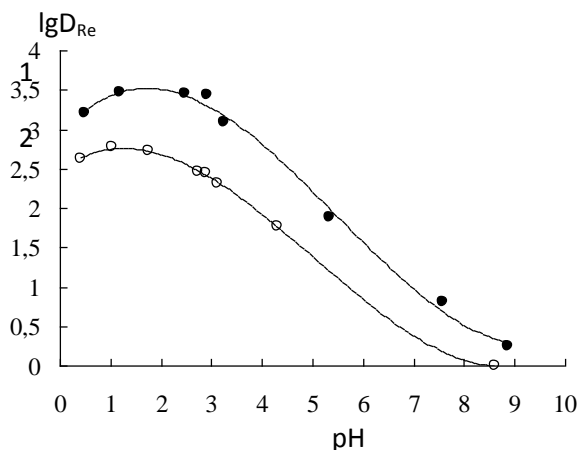


Fig. 2 Effect of pH and extractant composition on rhenium(VII) extraction.  $C_{init.}(Re)=10^{-3}$  mole/l,  $O/W=1/25$ , extractant composition, v/v % :  
 1,  $\bullet$  – 5% TiOA in octanone-2; 2,  $\circ$  – 5% TiOA+20% 2-ethylhexanol-1 in kerosene.

It is also obvious from Fig.1 that both the type and concentration of a modifier in the extragent affect its extractive properties appreciably. In the case of ketone as modifier, a synergetic effect was observed (Fig. 1, 2), and also differently directed effects of increasing modifier concentration in the organic phase when using alcohols and ketones (Fig. 3). In the case of increasing octyl alcohol concentration in extragent, the rhenium(VII) distribution coefficients diminished, whereas with octanon-2, these coefficients increased.

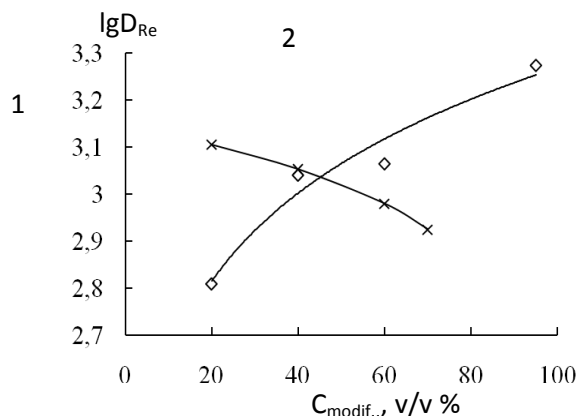


Fig. 3 The effect of modifier type and its concentration on rhenium(VII) extraction with a TiOA-based extragent.

$C_{init.}(Re)=10^{-3}$  mole/l,  $O/W=1/25$ , extragent composition, v/v%:  
1, x – 30% TiOA+2-ethylhexanol-1; 2, o – 5% TiOA+octanon-2.

The fact that alcohol and ketone influence dissimilarly the amine extraction ability may be explained by the difference in their solvatic behavior when interacting with TiOA. Being an electron-seeking reagent, alcohol solvates the anion part of the amine salt producing relatively stable solvate of the  $(R_3NH)_2SO_4 \cdot 2ROH$  [2] type, thus reducing its basicity and, consequently, its extractive ability. Unlike alcohol, ketone is a more nucleophilic reagent solvating the electron-acceptor component of the extragent, i.e. the amine salt cation. This enhances the electron density of the amine functional group and improves its extraction ability.

## Conclusions

It has been found that, by varying the modifier nature, it is possible to affect the extractive ability of tertiary amine-containing extragents. For commercial applications, mixtures of a tertiary amine in either ketone or aliphatic alcohol can be recommended, depending on the nature and composition of the feed rhenium-containing solution.

## References

6. L. V. Borisova, A. N. Ermakov, Analytical chemistry of rhenium (Rus), Nauka: Moscow (1974).
1. Schmidt, V.S., Solvent Extraction with Amines (Rus), Moscow: Atomizdat, 1970.

### 3.9.

## INTERPHASE SUBSTANCES OF RHENIUM EXTRACTION CIRCUIT ARE A SOURCE FOR PRODUCTION OF RHENIUM AND RADIOGENIC OSMIUM

A.N. Zagorodnyaya, Z.S. Abisheva, S.E. Sadykanova

Centre of Earth Sciences, Metallurgy and Ore Beneficiation, Almaty, Kazakhstan  
e-mail: alinazag39@mail.ru

**Keywords:** interphase substances, composition, rhenium, isotope osmium-187, technology.

#### Abstract:

It has been determined that the reason for the formation of interphase substances (IS) during rhenium extraction is the presence of a black-colored fine precipitate in the feed solution. The elemental composition of the interphase substances has been determined, including the content of trialkylamine (TAA). The behavior of a IS in solvent extraction technology of rhenium is studied. The technology of complex recovery of TAA and osmium-, rhenium-containing deposit from IS and rhenium from TAA has been developed and introduced in manufacture. The combined method of selective recovery of rhenium from the deposit resulting in production of ammonium perrhenate and osmium-, rhenium-containing concentrate suitable for obtaining from it of isotope osmium-187 by a known technology has been developed. It was established that in 3% rhenium and osmium is lost with IS (from entering with the charge in copper production).

#### Introduction

Sorption or solvent extraction technology of rhenium recovery from solutions of Kazakhstani metallurgical enterprises is accompanied by the formation of black sediment, which differs in their consistency. Sediment of sorption technology - friable, solvent extraction - the dough-like or black oil-like [1, 2]. At the one of the copper plants in Kazakhstan, rhenium is recovered from acidic solutions resulting from the washing of metallurgical smelter gases (sulfuric wash acid). A schematic

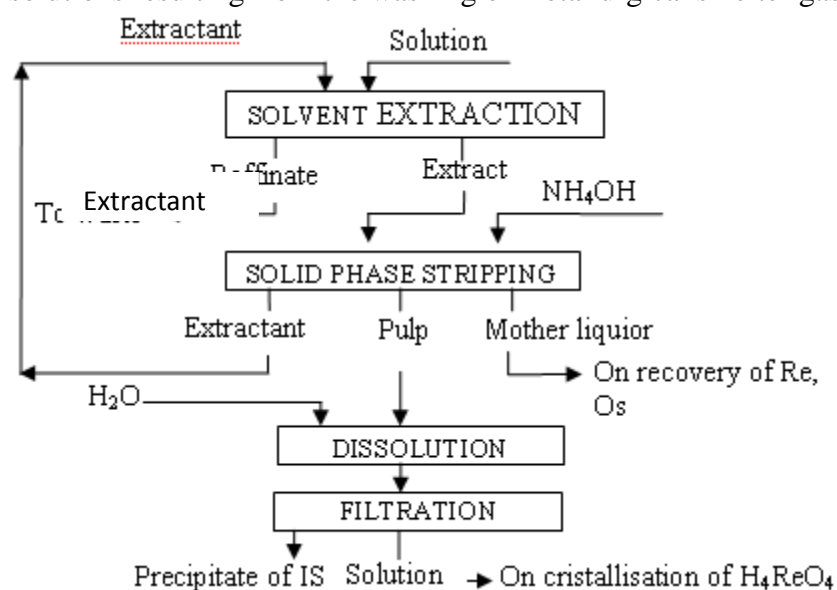


Fig. 1. Schematic flow-chart of rhenium extraction from wash sulfuric acid

flow-chart consists of the following operations: rhenium solvent extraction, solid-phase stripping [3] (Fig. 1).

The extractant is a mixture, % (vol.): 15 TAA, 2-ethylhexanol, and 75 kerosene. Stripping was performed by ammonia at high ratios of organic and aqueous phases giving a basic amount of rhenium precipitates in the form of ammonium perrhenate, which partly captures the extractant and mother liquor (pulp). The study of the rhenium extraction

technology over many years has demonstrated that a black-colored fine precipitate accumulates in an extract. At the stage of the solid-phase stripping, the precipitate distributes between the salt of  $\text{NH}_4\text{ReO}_4$ , the mother liquor and the organic phase. During the isolation of ammonium perrhenate from the pulp, the black precipitate is



recovered as an independent fat dough-like or black oil-like product (hereinafter referred to as interphase substance IS). It is established that the IS contained up to 10 % (wt.) of rhenium and 0.5 % (wt.) of isotope osmium -187. The lost of rhenium and osmium with IS is in 3 % from entering with the charge in copper production [4].

A significant amount of IS of different consistency has accumulated in the enterprise because of lack of processing technology of IS. It was a matter of considerable interest to determine the elemental composition of this product and develop technology for it processing.

## Experimental

**Study of the composition of IS:** for several years, samples of IS of various consistency were taken from the ammonium perrhenate production cycle for the analysis. During this time, some processes and the composition of the raw materials had changed. This paper presents the summarized findings of the long-term production monitoring (Tabl 1).

Table 1. Characteristic of probes

Number of probe	Technological change	Consistency	Color
1	The operation of the sulfur afterburning unit	Fat dough-like	Black
2	None unit	Fat dough-like	Black
3	None unit, new raw material	Oil-like	Black
4	None unit, new raw material	Oil-like	Grey

A weighed sample of interphase substance was thoroughly washed out with hot distilled water to remove rhenium-containing solution. Rhenium cleanliness was controlled by qualitative reaction with ammonium thiocyanate [5]. Then the precipitate of IS was repulped in heptane at room temperature at the ratio of S:L=1:20 and vacuum filtered [1]. The filtered residue was washed with the heptane until color was eliminated. The content of TAA in IS and concentration of Re in TAA was calculated based on the TAA concentration in heptane. After removing TAA from the precipitate, its consistency changed to become fluffy, crumbly and easily ground. The washed precipitate was dried until it reached the constant weight, weighed and examined with various physicochemical methods of analysis.

The composition of IS was determined by infrared — spectroscopic, X-ray diffraction (XRD), spectral and chemical analyses. Infrared Fourier spectrometer “Avator CsJ 370” was used for reading infrared spectra. A Bruker D8 Advance diffractometer using Co radiation at 40 kV and 35 mA was used to perform XRD characterization. The compounds were identified based on spectrograms and X-ray photographs according to [6, 7]. The concentrations of rhenium were determined by the well-known methods [5].

**Development of technology for processing of IS:** recovery of extractant from IS was performed by repulping in sealed cells with a jacket, mixing was performed with a mechanical stirrer; the temperature was supported by a thermostat. On the same set of experiments on hydrometallurgical leaching of precipitate recovered from the IS, and leaching of sintering cake were conducted. Experiments on the sintering of the precipitate with calcium oxide (charge) was carried out in a muffle furnace at 650 °C. The charge was prepared by thoroughly mixing of the precipitate with CaO at a given ratio.

## Results and Discussion

**IS and precipitate.** The samples washed by water were initially analyzed by infrared spectroscopy. The interpretation of spectrograms demonstrated that all interphase substances contained the following: TAA (absorption bands: 2968, 2932, 2875 cm<sup>-1</sup>); ReO<sub>4</sub><sup>-</sup> (912 cm<sup>-1</sup>), ReO<sub>2</sub> and ReO<sub>3</sub> (1400 cm<sup>-1</sup>), BiO<sub>3</sub> (312, 430, 470 cm<sup>-1</sup>), Bi<sub>2</sub>O<sub>3</sub> (360, 410, 450, 534 cm<sup>-1</sup>); PbSO<sub>4</sub> (600, 625, 969, 1055, 1108, 1170 cm<sup>-1</sup>), H<sub>2</sub>O (3440 cm<sup>-1</sup>), crystalline hydrate H<sub>2</sub>O (1616 cm<sup>-1</sup>); OsO<sub>4</sub> (960, 322 cm<sup>-1</sup>); H–N groups (3490 cm<sup>-1</sup>), C=O (1800 cm<sup>-1</sup>), C=C (1513 cm<sup>-1</sup>), rings of aromatic hydrocarbons contained in humate ions. Samples No.3 and No.4 contained

kerosene ( $\text{CH}_3$ ,  $\text{CH}_2$  — 2956, 2998, 2284, 2800, 1380, 1450–1468  $\text{cm}^{-1}$ ); sample No.4 contained  $[\text{Cd}(\text{NH}_3)_4](\text{ReO}_4)_2$  (3339, 3263, 1598, 917, 902  $\text{cm}^{-1}$ ),  $[\text{Cu}(\text{NH}_3)_4]\text{Cl}_2$  (3263, 1598, 1241  $\text{cm}^{-1}$ ). The presence of  $\text{Hg}(\text{CH}_3)_2$  (551  $\text{cm}^{-1}$ ) is also possible.

In the IR-spectra of precipitates washed by heptane, the absorption bands of TAA, kerosene and  $\text{ReO}_4^-$  were absent. But they were present in the heptane solutions after washing the precipitates. The absence of absorption bands for  $\text{ReO}_4^-$ , and the high concentration of rhenium in TAA, indicates that during the dissolution of the pulp, rhenium transfers to solution and is extracted by the released TAA. The presence of TAA and kerosene is the result of the extraction reagent captured by ammonium perrhenate during rhenium stripping. When the pulp was subjected to thermal dissolution in water or in rhenium-containing solutions, a suspension consisting of the extraction reagent and the fine precipitate was recovered in an independent phase. When solutions were evaporated until the required concentration of rhenium was obtained, kerosene and heptane volatilizes and TAA remains in solution (Table 2).

Table 2. Content of TAA and Re in of probes of IS

Content	Fat dough-like		Oil-like	
	Number of probe			
	1	2	3	4
TAA, mole in 1 kg IS	1.2	1.0	0.6	0.6
Re in TAA, $\text{g}/\text{dm}^3$	80.0	86.2	86.1	75.6
Output of precipitate, %	35.2	13.4	20.8	18,5

The quantitative content of elements in IS was specified by chemical analyses (Table 3). The data in

Table 3. Chemical composition of IS

Number of probe	Content, % (mass.)												
	S	Bi	Re	Cd	Fe	Ca	Zn	Se	Pb	Hg	Si	Os	As
1	66	1.2	8.00	2.00	2.30	1.10	1.20	0.80	0.50	0.01	0.41	0.21	0.45
2	9.1	24.8	6.75	1.70	1.65	1.10	0.80	1.10	0.77	0.01	0.37	0.42	0.28
3	9.1	25.1	5.65	1.58	1.00	0.76	0.98	0.73	0.80	0.01	0.38	0.37	0.28
4	8.5	3.25	5.70	4.45	1.50	1.00	0.98	0.92	0.80	13.6	0.40	0.52	0.42

Notes: content, % (mass): Mg, Ti, Ni, Na —  $\leq 0.2$ ; Mn, Cr, K —  $\leq 0.06$ ; Ag, Sn —  $\leq 0.01$

Table 3 show that all IS are identical respect to the elements present, irrespective of some process changes. IS, containing the whole percentages of rhenium and tenth parts percentages of osmium could be considered as additional raw material for the production of rhenium and isotope osmium-187. However, the quantitative amounts of some of the individual elements vary substantially. The content of sulfur varies from 66 to 8.5 % (mass.); bismuth varies from 1.2 to 25.1 % (mass.); cadmium from 1.7 to 4.45 % (mass.); mercury from 0.01 to 13.6 % (mass.).

The cause of the high content of sulfur in sample No.1 is a carryover of elemental sulfur from the afterburning unit into the gas scrubber whilst that of bismuth and mercury is caused by the composition of raw materials. The cause of higher content of cadmium (as a complex salt  $[\text{Cd}(\text{NH}_3)_4](\text{ReO}_4)_2$ ) is an insufficient washing of the extract and the conditions of pulp dissolution. It is well-known that cadmium and zinc contained in the solution are extracted in the form of chloride anions and are stripped with ammonia. The complex salt  $[\text{Cd}(\text{NH}_3)_4](\text{ReO}_4)_2$  is white, therefore its presence has influenced the color of sample No.4.

Based on these data, it was assumed that the precipitate comes from the leaching solution of sulfuric acid. A careful visual examination of acid indicated on the presence of very small amounts of black sludge in the form of a light mist.

The content of the precipitate and its distribution generated in rhenium solvent extraction in the original solution, raffinate, extract, and extraction reagent after rhenium stripping was determined by the methods we developed [8]. Table 4 shows the average values over three years.

*Table 4. Content of precipitate and its distribution through the products of rhenium recovery from wash sulfuric acid by solvent extraction*

Name of product	Content, g/sm <sup>3</sup>	Recovery of precipitate, %	Note
Initial solution	0.0160	100.0	Content in precipitate: Os - 0,63, Re – 10.4 % (mass.)
Raffinate	0.0014	8.7	
Extract	0.4732	91.3	
Extractant	0.0494	9.5	
Pulp	22.921	47.5	
Mother liquor	2.3200	34.4	

As it was shown from table 4 content of precipitate in wash sulfuric acid is 0.016 g/dm<sup>3</sup>. During rhenium extraction 91 % of the precipitate is accumulated in the extract and its content in the extract 0.4732 g/dm<sup>3</sup>, the stage of rhenium solid phase stripping 81,8 % of the precipitate is recovered, 47,5 % of which co-precipitates with ammonium perrhenate and 34,4 % passes into mother liquors. Its content in the ammonium perrhenate pulp is 22.921 g/dm<sup>3</sup>, in the mother liquore -2.32 g/dm<sup>3</sup>. Content of Os in the precipitate is 0,63, Re - 10.4 % (mass). Causes of osmium, rhenium-containing sediment formation are described in [9].

Osmium-, rhenium-containing precipitate is extracted from the mother liquors by water-soluble compounds with production from them a metallic osmium isotope-187 and ammonium perrhenate according the technology, described in [10].

**Development of technology for processing of IS.** Our investigations have shown that IS - a very valuable by-product with high content of isotope osmium-187, rhenium, extractant, which can be considered as an additional source of Re and Os-187. In addition, up to 10 % of the volume of extractant involved in the process have lost with IS monthly. The presence of the extractant in the IS is not permit to process IS according the technology [10]. In this regard, it was necessary to develop a universal technology permitted to recover the extractant and contained in it rhenium and produce a powdery residue suitable for production from it ammonium perrhenate and metal osmium-187 isotope. In the base of technology laid the ability of TAA dissolved in organic solvents. This permit to recover TAA from IS by repulpatation. When choosing an organic solvent guided by the following criteria: time of phase separation, filtration, sediment texture, the concentration of rhenium. Ketones, alcohols, paraffin hydrocarbons, mixtures of a paraffin hydrocarbons and alcohol in different ratios, mixture of ammonia and organic solvent, a mixture of a solvent with polyethylene polyamine (PEPA), a mixture of the ketone with ammonia, a mixture of a solvent with ammonia solution and PEPA were tested as solvents. The effect of S:L (1:2 ÷ 10, S - weight of sample of IS, L - solvent,), duration (0.5 - 5 h) and temperature (30 - 60 °C) of repulpatation, volume ratio of ammonia to the solvent (0.5 - 4) on the process indicators by chosen solvent has been studied. The optimal conditions that enable to extract TAA from IS and produce powdery residue has been established. Experiments on the release of ammonium perrhenate from ammonia solution by combination of processes of evaporation and crystallization have been carried out. Extraction of rhenium from industrial solutions by TAA, recovered from IS has been conducted under the conditions stipulated by the technical documentation of company. The resulting crude salt of ammonium perrhenate is identical to salt of the existing technology. Multicyclical experiments on the extraction-stripping of rhenium have shown the possibility of circulation of the TAA in the main process.

A complex of experiments on the recovery of rhenium and osmium from precipitate resulting in repulpatation of IS has been performed. As it mentioned above, the rhenium and osmium are present in precipitate as slightly soluble compounds in acid solutions (do not have oxidizing properties), and alkaline solutions. On the basis of research on the interaction of rhenium oxides and sulfides

with hydrogen peroxide in sulfuric acid and ammonium media [11, 12] as leaching reagent was selected aqueous solution of hydrogen peroxide. According to the experiments on the effect of hydrogen peroxide concentration (2 - 16 mol/dm<sup>3</sup>), the ratio S:L (1:2 ÷ 20), time (1 - 6 h), temperature (20 - 90 °C) was chosen optimal conditions under which in the solution is extracted only 80 % of rhenium, and 40 % of osmium distilled into the gas phase. As it was established by XRD method rhenium is found in the precipitate in the form of Bi<sub>3</sub>ReO<sub>8</sub>. The unsatisfactory results of hydrometallurgical methods have led to development of combined method, the essence of which is concluded in sintering of precipitate with calcium oxide at 650 °C, followed by leaching the cake with water (S:L = 1:4, temperature 80 °C, time (1 h). At the optimum content of calcium oxide in the mixture in the solution is extracted 93 % of rhenium, the cake is almost completely Bi<sub>3</sub>ReO<sub>8</sub>. Osmium is practically completely left in the cake, from which it can be recovered by the technology [10]. Rhenium-containing solutions can be either send to the dissolution of the pulp or processed independently with production of ammonium perrhenate. Based on the complex of conducted

investigations the technology of processing of IS (Fig. 2) was proposed, which was tested in pilot-industrial scale at a plant in Kazakhstan.

Eight operations with cumulative and current IS of different texture with some correction of regime of repulping was conducted.

Ammonia solutions of all the operations were combined and evaporated three

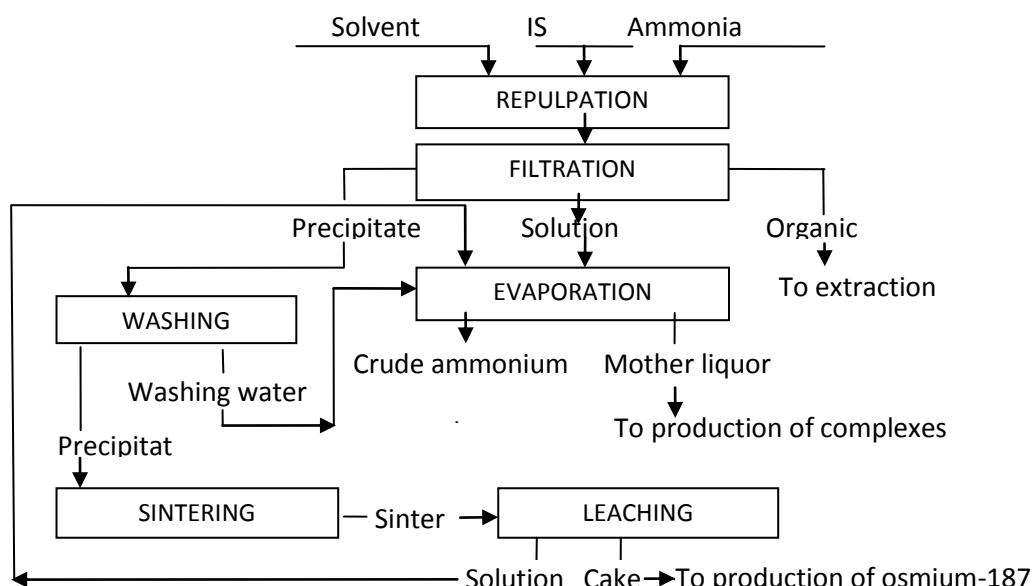


Fig.2. Technological flow sheet for processing of IS with production of ammonium perrhenate, TAA and osmium-, rhenium-containing precipitate

times. after cooling was obtained.

Crude ammonium perrhenate of white colour after cooling was obtained. Extractant from all operations have been also joined, corrected for the concentration of the TAA and on the equipment of shop in accordance with the existing technological regimes had been conducted multiple solvent extraction-stripping of rhenium. Results for repulping of IS presented in Table 5.

The following results were obtained:

- TAA and rhenium are extracted from IS almost completely. The concentration of rhenium in the extractant is 0.026 - 0.104 g/dm<sup>3</sup>;
- concentration of TAA in the solvent is 0.117-0.287 mol/dm<sup>3</sup>;
- concentration of rhenium in an ammonia solution is 17.9 – 42.2 g/dm<sup>3</sup>; osmium - 0.0025 – 0.0042;
- yield of precipitate is 10.65 - 23.5 %;
- rhenium content in the sediment is 2.0 - 4.64 % (mass.), Os - 0.53 – 2.0;
- the crude ammonium perrhenate with rhenium content 67.9 % (by weight) and very low content of potassium 0.001 was obtained from ammonia solutions. The pure salt of trade mark AR-0 was produced by recrystallization of crude ammonium perrhenate;
- trialkylamine selected from IS extracted and re-extracted rhenium without complications.

Table 5. - The results of pilot-industrial scale test of technology IS processing

Organic solution			conet TAA in 1 kg precipitate, mol/dm <sup>3</sup>	Ammonia solution		Cake			Content of soluble Re in IS, % (mass.)
concentration				concentration, g/dm <sup>3</sup>		output, %	content, % (mass.)		
Re, g/dm <sup>3</sup>	Os, mg/dm <sup>3</sup>	TAA, mol/dm <sup>3</sup>	Re	Os	Re		Os		
Content in fat dough-like, % (mass.): Re – 12,6, Os – 0,064									
0.043	0.0002	0.166	0.83	24.0	0.0028	13.50	4.00	1.28	8.00
0.029	0.0001	0.179	0.86	28.8	0.0031	14.20	3.85	1.76	7.20
0.026	0.0001	0.287	1.43	35.0	0.0025	13.80	4.19	1.42	8.75
0.096	0.0002	0.206	1.03	32.0	0.0030	14.40	4.64	2.00	8.00
0.054	0.0001	0.127	0.84	36.6	0.0025	13.55	3.94	1.98	9.15
0.061	0.0001	0.152	0.76	42.2	0.0042	10.65	3.75	1.34	1.55
Content in oil-like, % (mass.): Re – 4,63, Os – 0,091									
0.048	0.0001	0.117	0.59	27.20	0.0066	21.9	2.15	0.56	7.55
0.104	0.0001	0.132	0.66	17.90	0.0050	23.5	2.00	0.53	6.71

Currently, technology of IS processing introduced into production, resulting in increasing of rhenium recovery from wash sulfuric acid on 2 % and to reduce consumption by of TAA on 10 %. Recovery of rhenium and osmium from precipitate by combined method will be carried out periodically as precipitate accumulates in such quantities that capable to support the productivity of shop equipment.

### Conclusions

Qualitative and quantitative compositions of IS was determined. The technology of recovery of trialkylamine, rhenium and osmium-, rhenium-containing precipitate from IS has been developed and implemented in production. A combined method for selective recovery of rhenium and osmium concentrate, suitable for production of metal isotope osmium-187 according the previously developed and implemented technology was developed.

### References

1. A. N. Zagorodnyaya, Z. S. Abisheva, E. I. Ponomareva, V.V. Bobrova, A. S. Sharipova. Kompleksnoe ispol'zovanie mineral'nogo syr'ya, 1: 52 – 31 (2000).
2. S. E. Sadykanova, A. N. Zagorodnyaya, Z. S. Abisheva, V.V. Bobrova. Abstracts of the international conference on chemical technology, 17 - June, 2007. Moscow. - 2007, Vol. 4, p. 229 - 232.
3. A. A. Palant, I. D. Troshkina and A. M. Chekmarev; Metallurgy of Rhenium. Nauka: Moscow, 2007, 298 p.
4. A. N. Zagorodnyaya, Z. S. Abisheva, S. E. Sadykanova, V.V. Bobrova, A. S. Sharipova. Non-ferrous metals, 11: 74 – 77 (2005).
5. L.V. Borisova, A.V. Yermakov; Analytical Chemistry of Rhenium. Nauka: Moscow, 1974, 319 p.
6. K., Nakamoto; Infrared and Raman Spectra of Inorganic and Coordination Compounds. Mir: Moscow, 1991, 536 p.
7. Powder diffraction file, Search Manual. Hanawalt Method. Inorganic. International Center for Diffraction Data. 1987.
8. S. E. Sadykanova, A. N. Zagorodnyaya, Z. S. Abisheva. Kompleksnoe ispol'zovanie mineral'nogo syr'ya, 1: 75 – 80 (2005).
9. A. N. Zagorodnyaya, Z. S. Abisheva, S. E. Sadykanova, V.V. Bobrova, A.S. Sharipova. Hydrometallurgy 104: 308 – 312 (2010).
10. Z. S. Abisheva, A. N. Zagorodnyaya, T. N. Bukurov. Platinum Metals Review, vol. 45, 3: 132 – 135 (2001).
11. S. E. Sadykanova, A. N. Zagorodnyaya, Z. S. Abisheva. Proceedings of the international practical conference, 18 – 19 May, 2006. Karaganda, 252 – 255.
12. S. E. Sadykanova, A. N. Zagorodnyaya, Z. S. Abisheva, V. V. Bobrova. Kompleksnoe ispol'zovanie mineral'nogo syr'ya, 6: 54 – 66 (2010).



3.10.

## **ELECTRODEPOSITION OF RHENIUM ALLOYS IN FORM OF POWDERS AND COATINGS FROM WATER SOLUTIONS BY MEMBRANE ELECTROLYSIS**

L. Ya. Agapova, Z. S. Abisheva, S. K. Kilibayeva, I. A. Sapukov

Centre of Earth Sciences, Metallurgy and Ore Beneficiation,  
(Shevchenko str. 29/33, Almaty, Republic of Kazakhstan)

**Keywords:** rhenium alloys, electrolytic coatings, powders, complexes of rhenium, tungsten and nickel, membrane electrolysis, microhardness

### **Abstract:**

Alloys on the basis of refractory rhenium have a number of unique physicochemical and mechanical properties allowing essentially improve parameters of some devices. Homogeneous structure of rhenium alloys obtained from water solutions by electrolysis under given conditions with properties essentially differ from properties of these alloys produced by thermal methods. Electrochemical processes in water solutions differ by their high efficiency and need neither aggressive reagents nor high temperatures. The basic problem is stability of anodes. All materials, except platinum, may decompose and contaminate deposited alloys during electrolysis. Application of ionite membranes in electrolyzers allows to prevent of cathodic and anodic reactions' products mixing and to obtain a pure final product without application of expensive platinum electrodes. The possibility of Re-W, Re-Ni, Re-W-Ni alloys deposition in the form of powders and coatings on the copper and steel base plates in membrane electrolyzer with the graphite anode has been shown. As electrolytes sulfate-ammonium and sulfuric solutions with citric acid, sodium fluoride and glycerin additives were used. The Re-W, Re-Ni, Re-W-Ni coatings are alloys in the form of solid solutions on Re, W and Ni base. Alloys are nanostructured because their crystallization occurs with isolation of fine-dispersed phases having 2-20 nanometers size of grains. Microhardness of the coatings deposited on copper plate can reach 8270 MPa for Re-Ni, 35000 MPa for Re-W, 14808 MPa for Re-Ni-W coatings depending on electrolysis parameters. Re-W coatings corrosion resistance is higher than Re-Ni coatings corrosion resistance.

### **Introduction**

This paper is devoted to electrodeposition of rhenium alloys in the form of powders and coatings from water solutions in conditions membrane electrolyses. Alloys of rhenium with tungsten and nickel have especially valuable properties: a fusion heat, chemical firmness at heats and are used in the space-rocket techniques, aircraft, atomic engineering, instrument making, radio electronics [1]. The scientists in the former USSR execute the big complex of researches of physical and chemical interaction of rhenium with the metals formed a theoretical basis of creation of new alloys with the set properties [2-5]. The basis for carrying out of these investigations was our researches on recycling of a technological waste of the electronic industry formed in the course of manufacture of tungsten- rhenium alloys and products them have served. This waste alkaline solutions obtained after electrochemical processing, in our opinion, can serve as a basis of electrolyte for deposition by a method electrolyses of tungsten- rhenium coverings or powders. The electrolyses method enables to obtain alloys of homogeneous structure with the set properties. In the case of drawing of coatings provides uniformity of a coating, its strong coupling with the basic metal and possibility to have a

coat layer of a necessary thickness. The properties of electrolytic alloys essentially differ from the properties of the same alloys obtained by thermal methods. Micro hardness, plasticity, thermal stability electrolytic alloys can be above several times [6]. It is connected by that formation electrolytic deposits passes in no equilibrium conditions. As a result on the cathode met stable crystal phases are formed. Many works devoted to electrolytic deposition of rhenium alloys with tungsten are known. In all these works, as a rule, for of rhenium alloys obtaining the process of electrolyses conduct at high density of a current (5000-20000 A/m<sup>2</sup>) with use of platinum anodes. The electrochemical processes are highly effective in water solutions requiring neither aggressive reactants nor high temperature conditions. The most challenging problem consists in anodes stability. All materials, platinum excepted, may be attacked in electrolysis process resulting in contamination of deposited alloys. This problem may be solved using ion-exchange electrolyze membranes which prevent potential mixing of cathode and anode reactions products when the super purity alloys are produced without application of expensive platinum electrodes [7].

### Experimental

Properties of electrolytes containing ions of rhenium, tungsten and nickel studied by conductometry, voltammetry, infrared spectroscopy, electro dialysis. For obtaining of rhenium containing powders and coverings four-chamber membrane electrolyzer with graphite anode was used. During process current density, temperature of solutions, their structure and a cathode material were changed. As a substrate material stainless steel, copper are used. The cathode with a deposit washed out with distilled water, dried with alcohol, weighed on analytical scales, counted a thickness of a covering. Alloys sediments are analyzed by electron-spectroscopic, X-Ray and chemical methods. Microhardness of rhenium containing coverings measured by microhardness meter PMT-3, pressing a diamond pyramid by loading of 50 or 100g.

### Results and Discussion.

The introduction of additives in electrolyte pulls together potentials of metals restoration (see Table 1). It does possible their joint deposition on the cathode in the metal form in an alloy.

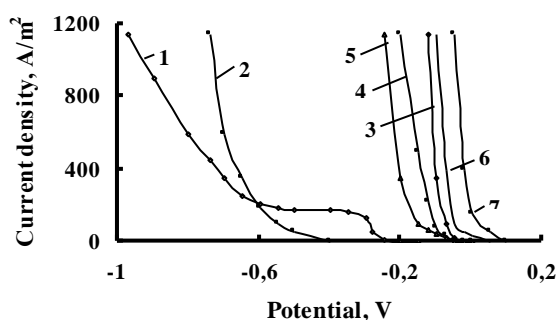


Fig.1. Cathodic polarization curves on a Pt-electrode in Re-,W-containing solutions. The electrolyte, g/dm<sup>3</sup>: 1 – 5 Re; 2 – 9 W; 3 – 5 Re, 9 W, 40 H<sub>2</sub>SO<sub>4</sub>; 4 – 5 Re, 9 W, 40 H<sub>2</sub>SO<sub>4</sub>, 5 NaF; 5 – 5 Re, 9 W, 80 H<sub>2</sub>SO<sub>4</sub>, 5 NaF; 6 – 5 Re, 9 W, 100 (NH<sub>4</sub>)<sub>2</sub>SO<sub>4</sub>; 7 – 5 Re, 9 W, 100 (NH<sub>4</sub>)<sub>2</sub>SO<sub>4</sub>, 100 citric acid

Kinetic studying of cathodes restoration of ions Re, W and Ni from ammonium-sulfate citric acid and fluoride-sulfate electrolytes by the methods of voltamperimeter (Fig.1) and volumeter has shown, that process of restoration irrespective of electrolyte structure is accompanied by competing process of allocation of hydrogen. Speed of process of metals ions restoration is defined by the chemical polarization passing in concentration and then in the phase. The speed of process, as a whole, is limited by the slowest stage - electro crystallization of cathodes sediment.

Table 1. Measurement data on the equilibrium potential of Pt-electrode in Re-, W-, Ni- containing solutions (25°C)

The electrolyte, g/dm <sup>3</sup>	Potential, V (n.h.e.)	The electrolyte, g/dm <sup>3</sup>	Potential, V (n.h.e.)
NH <sub>4</sub> ReO <sub>4</sub> (5 Re)	+0,806	Na <sub>2</sub> WO <sub>4</sub> (9 W)	+0,441
NH <sub>4</sub> ReO <sub>4</sub> (5 Re), 100 (NH <sub>4</sub> ) <sub>2</sub> SO <sub>4</sub>	+0,687	Na <sub>2</sub> WO <sub>4</sub> (9 W), 100 (NH <sub>4</sub> ) <sub>2</sub> SO <sub>4</sub>	+0,397
NH <sub>4</sub> ReO <sub>4</sub> (5 Re), 100 citric acid	+0,848	Na <sub>2</sub> WO <sub>4</sub> (9 W), 100 citric acid	+0,756
NH <sub>4</sub> ReO <sub>4</sub> (5 Re), 100 (NH <sub>4</sub> ) <sub>2</sub> SO <sub>4</sub> , 100 citric acid	+0,767	Na <sub>2</sub> WO <sub>4</sub> (9 W), 100 (NH <sub>4</sub> ) <sub>2</sub> SO <sub>4</sub> , 100 citric acid	+0,795
NH <sub>4</sub> ReO <sub>4</sub> (5Re), 5 NaF	+0,607	Na <sub>2</sub> WO <sub>4</sub> (9 W), 5 NaF	+0,459
NH <sub>4</sub> ReO <sub>4</sub> (5 Re), 40 H <sub>2</sub> SO <sub>4</sub>	+0,938	Na <sub>2</sub> WO <sub>4</sub> (9 W), 40 H <sub>2</sub> SO <sub>4</sub>	+0,911
NH <sub>4</sub> ReO <sub>4</sub> (5Re), 40 H <sub>2</sub> SO <sub>4</sub> , 5 NaF	+0,901	Na <sub>2</sub> WO <sub>4</sub> (9W), 40 H <sub>2</sub> SO <sub>4</sub> , 5 NaF	+0,884
NH <sub>4</sub> ReO <sub>4</sub> (5 Re), Na <sub>2</sub> WO <sub>4</sub> (9 W), 100 (NH <sub>4</sub> ) <sub>2</sub> SO <sub>4</sub> , 100 citric acid	+0,773	NH <sub>4</sub> ReO <sub>4</sub> (5Re), Na <sub>2</sub> WO <sub>4</sub> (9 W), 40 H <sub>2</sub> SO <sub>4</sub> , 5 NaF	+0,866
NH <sub>4</sub> ReO <sub>4</sub> (5 Re), 40 H <sub>2</sub> SO <sub>4</sub> , 10 NaF	+0,906	8,4 H <sub>2</sub> WO <sub>4</sub> , 40 H <sub>2</sub> SO <sub>4</sub> , 10 NaF	+0,659
NH <sub>4</sub> ReO <sub>4</sub> (5 Re), 40 H <sub>2</sub> SO <sub>4</sub> , 10 NaF, 8,4 glycerin	+0,651	8,4 H <sub>2</sub> WO <sub>4</sub> , 40 H <sub>2</sub> SO <sub>4</sub> , 10 NaF, 8,4 glycerin	+0,650
20 NiSO <sub>4</sub> , 40 H <sub>2</sub> SO <sub>4</sub>	+0,673	20 NiSO <sub>4</sub> , 40 H <sub>2</sub> SO <sub>4</sub> , 40 H <sub>2</sub> SO <sub>4</sub> , 10 NaF, 8,4 glycerin	+0,659
20 NiSO <sub>4</sub> , 40 H <sub>2</sub> SO <sub>4</sub> , 40 H <sub>2</sub> SO <sub>4</sub> , 10 NaF	+0,651		

The formation of anion complexes of tungsten and rhenium with citric acid and sodium fluoride in ammonium-sulfate citric acid and fluoride-sulfate ammonium-sulphate electrolytes was shown by the methods of conductor meter, the IR-spectroscopy, an electro dialysis. The *stehio* meter structure of rhenium and tungsten complex ions is defined; free energy of formation and instability constants are calculated (see Table 2). It is shown, that process of formation of complexes passes in steps through intermediate, less steady complexes. Tungsten and rhenium with citric acid and sodium fluoride form anionic complexes, presumably [WO<sub>2</sub>C<sub>6</sub>H<sub>5</sub>O<sub>7</sub>]<sup>-</sup>, [ReO<sub>3</sub>(OH)F<sub>2</sub>]<sup>2-</sup> или [ReO<sub>2</sub>(OH)(HF<sub>2</sub>)<sub>3</sub>]<sup>-</sup>, [ReO(H<sub>2</sub>Cit)(OH)<sub>4</sub>]<sup>2-</sup>, HWO<sub>3</sub>F<sub>2</sub><sup>-</sup>. Tungsten Rhenium more than inclined to form complexes, and the formation of fluoride complexes of tungsten can pass through the intermediate sulfate complex, presumably [WO<sub>3</sub>SO<sub>4</sub>]H<sup>-</sup>. The fluoride complexes of rhenium and tungsten are steadier, than citric acids ones, and complexes of tungsten stronger the rhenium ones [8].

Table 2. The values of the instability constants (K<sub>i</sub>) and free energies of formation (ΔG) complex ions of Re and W

The ratio of Me: ligand in the complex	Rhenium		Tungsten	
	K <sub>i</sub>	ΔG, kJ / mol	K <sub>i</sub>	ΔG, kJ / mol
Fluoride complexes				
1:1	3.80×10 <sup>-3</sup>	13.79	1.33×10 <sup>-4</sup>	22.11
1:2	6.22×10 <sup>-7</sup>	35.39	2.20×10 <sup>-8</sup>	43.66
1:3	2.00×10 <sup>-8</sup>	43.90	3.88×10 <sup>-9</sup>	47.91
Citrate complexes				
1:1	7.20×10 <sup>-3</sup>	12.22	1.29×10 <sup>-3</sup>	16.48
1:2	1.33×10 <sup>-4</sup>	22.11	1.90×10 <sup>-6</sup>	32.62
1:3	6.22×10 <sup>-7</sup>	35.38	2.38×10 <sup>-8</sup>	43.47

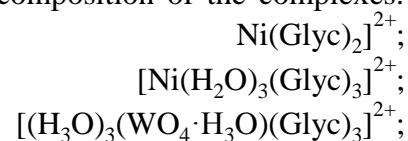
is besiege, taking root in a crystal lattice of rhenium. The double layer concentration decreasing with complex ions of tungsten leads to sedimentation rhenium and so on. Two variants of electrolytic obtaining of W-Re coatings of high quality on stainless steel cathode are proposed based on the carried out experiments [9]. The first variant includes productions of these types of coatings from electrolytes of the following composition, g/dm<sup>3</sup>: 7.2 NH<sub>4</sub>ReO<sub>4</sub>; 16.0 Na<sub>2</sub>WO<sub>4</sub>; 3.0-8.0 NaF; 30-80 H<sub>2</sub>SO<sub>4</sub>, at current density of 1000-2000 A/m<sup>2</sup> and 20-25°C of solution temperature.

According to the second variant, thin bright covers are produced from electrolyte composing of, g/dm<sup>3</sup>: 5.0-20.0 NH<sub>4</sub>ReO<sub>4</sub>; 8.0-16.0 Na<sub>2</sub>WO<sub>4</sub>; 100 (NH<sub>4</sub>)<sub>2</sub>SO<sub>4</sub>; 100 citric acid. This electrolysis process is carried out during 3 hours with graded increase of current density of 500-750-1000 A/m<sup>2</sup> per 1 hour. The glycerol additive in fluoride-sulfate electrolyte positively influences on the quality of Re-W and Re-Ni coverings, as it was shown by our subsequent researches. The glycerol is preferable because of its well dissolution in water, formation complexes with some metals and surface-active properties that are why we have chose it as the additive. It is established, that in fluoride-sulfate and ammonium-sulfate electrolytes with glycerol additives rhenium does not form, and tungsten and nickel form with glycerol cat ion complexes. The stehiometer structure and values of constants of instability of W and Ni

Table 3. The values of the instability constants (K<sub>i</sub>) and free energies of formation (ΔG) of complex compounds of Ni and W with glycerol

The ratio of Me: ligand in the complex	Nickel		Tungsten			
			Na <sub>2</sub> WO <sub>4</sub> ·2H <sub>2</sub> O		H <sub>2</sub> WO <sub>4</sub>	
	K <sub>i</sub>	ΔG, kJ / mol	K <sub>i</sub>	ΔG, kJ / mol	K <sub>i</sub>	ΔG, kJ / mol
3:4	1.70·10 <sup>-8</sup>	44.32				
3:6 (1:2)	2.07·10 <sup>-8</sup>	43.84				
3:8	5.78·10 <sup>-8</sup>	41.29				
1:2			0.44	2.03		
1:3			0.18	4.25		
4:2 (2:1)					2.60·10 <sup>-6</sup>	31.86
4:3					2.58·10 <sup>-6</sup>	31.88

with glycerol complexes are defined (see Table 3). The steadiness of complexes of glycerol increases in the line: (complexes with W in solutions Na<sub>2</sub>WO<sub>4</sub> < complexes with W in solutions of H<sub>2</sub>WO<sub>4</sub> < complexes with Ni). With increasing of glycerol concentration in solutions of steadiness Ni-complexes decreases, and W, on the contrary, raises. The estimated composition of the complexes:



[(H<sub>3</sub>O)<sub>2</sub>(H<sub>2</sub>WO<sub>4</sub>)<sub>2</sub>(Glyc)]<sup>2+</sup>. Kinetic laws of cathodes restoration Re, Ni and W from fluoride-sulfate and ammonium-sulfate electrolytes with glycerol additives are revealed. The calculated values of seeming energy of activation (6,9-54,6 kJ/mol) testify diffusion-kinetic mode of restoration process proceed. As a whole the speed of cathodes metals restoration process at investigated electrolytes raises among: nickel-rhenium-tungsten. Higher speed of formation of a cathodes deposit under these conditions is marked for rhenium, the greatest influence of the glycerol additive render for speed of cathodes restoration of tungsten. The mechanism of process of cathodes restoration of ions of rhenium, nickel and tungsten to alloy from fluoride-sulfate solutions with glycerol additives is offered. First of all on the cathode cat ion glycerol tungsten and nickel complexes, and then anion fluoride rhenium and tungsten complexes are discharged. It is established, that glycerol additives in the fluoride-sulfate solution at parity in it of concentration rhenium, tungsten and the glycerol 1:1.2 : (1.5-1.9) ratios (g/dm<sup>3</sup>) lead to increase of microhardness of besieged coatings [10]. The glycerol additive influences on the quality of the coating. Its surface becomes more dense and fine-grained. The chemical analysis of deposits of coatings has shown that the glycerol additive in fluoride-sulfate electrolyte promotes increase of the maintenance of tungsten in the alloy. The results of measurements of micro hardness of the Re-W-coverings besieged from fluoride-sulfate of electrolyte without and with additives of glycerin, and the calculated values of their thickness depending on concentration of glycerin in electrolyte are presented in Table 4. The microhardness of coverings Re-W (Fig. 2) besieged from fluoride-sulfate of

Table 4. Effect of the glycerin added in fluoride-sulfate electrolytes based on tungsten acid ( $H_2WO_4$ ) on the thickness and microhardness of deposited Re-W coatings

Re-W coatings properties	Glycerol concentrations in fluoride-sulfate electrolyte, g/dm <sup>3</sup>				
	0	4.2	8.4	12.7	16.9
Thickness, $\mu\text{m}$	17.24	21.77	23.08	23.86	21.51
Microhardness, Mpa	15407	16860	35851	32769	10946

electrolytes on the basis of tungsten acid ( $H_2WO_4$ ) with the additive of glycerol makes 35851 MPa. In the Table 5 the speed of anode corrosion of deposits of coverings in ammonium-alkaline solutions depending on structure of electrolytes of their sedimentation is shown. The obtained data enables to draw a conclusion on direct interrelation

of the microhardness values of the coverings with their corrosion steadiness. The investigations on Re-W coverings obtaining under the conditions of membrane electrolyses made in modeling of Re-W-containing solutions. However the researches carried out by us testify to possibility of

Table 5. Effect of electrolyte composition on the thickness, microhardness and corrosion resistance of deposited Re-W coatings (current density 1500 A/m<sup>2</sup>, temperature 20°C, duration of electrolysis 5h)

Re-W coatings properties	The electrolyte, g/dm <sup>3</sup>			
	10NaF; 40H <sub>2</sub> SO <sub>4</sub> 7.2 H <sub>4</sub> ReO <sub>4</sub> ; 8.4 H <sub>2</sub> WO <sub>4</sub>	10NaF; 40H <sub>2</sub> SO <sub>4</sub> 7.2 NH <sub>4</sub> ReO <sub>4</sub> ; 8.4 H <sub>2</sub> WO <sub>4</sub> ; 8.4 glycerol	10NaF; 40H <sub>2</sub> SO <sub>4</sub> 2Na <sub>2</sub> SO <sub>4</sub> ; 7.2NH <sub>4</sub> ReO <sub>4</sub> 8.4 H <sub>2</sub> WO <sub>4</sub>	10NaF;40H <sub>2</sub> SO <sub>4</sub> 2Na <sub>2</sub> SO <sub>4</sub> ; 7.2NH <sub>4</sub> ReO <sub>4</sub> ; 8.4H <sub>2</sub> WO <sub>4</sub> ; 8.4 glycerol
Thickness, $\mu\text{m}$	17.24	23.08	19.28	19.48
Microhardness, MPa	15407	35851	19896	30952
Corrosion resistance, g/sm <sup>2</sup> ·min	$7.18 \cdot 10^{-5}$	$5.7 \cdot 10^{-5}$	$7.22 \cdot 10^{-5}$	$8.04 \cdot 10^{-5}$

sedimentation of Re-W of coverings from the solutions obtained at recycling of W-Re of a waste of the electronic industry. The updating of the solutions' structure after anode dissolution W-Re of waste under certain conditions enables to besiege from these solutions the qualitative W-Re electrolytic coverings at low density of a current (to 3000 A/m<sup>2</sup>). The coverings Re-Ni in conditions of membrane electrolyses on the copper cathode from

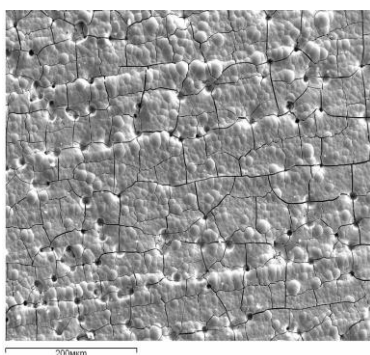


Fig. 2. The microphotography of Re-W alloy surface, deposited on copper plate from fluoride sulfuric solution with additional of glycerol

sulfate acid ammonium-sulfate solutions with glycerol are besieged. Under conditions of membrane electrolyses with use of not platinum electrodes double and threefold alloys on a basis of Re as in the form of powders, and coverings can be obtained. The dense brilliant thin coverings of Re-Ni-W on a copper substrate from citric acid ammonium-sulfate electrolytes with the maintenance in them of citric acid 100 g/dm<sup>3</sup> at graduate increase of density with a current from 500 to 1000A/m<sup>2</sup> are besieged. At the smaller maintenance of citric acid the covering are thicker, but porous. The expediency of carrying out of the coverings heating operation in argon atmosphere at temperature 400°C, when the corrosion firmness leads to increase and microhardness of coverings on 8-10 % is established. By data X-ray analysis of the cathodes deposits represent the alloys in the form of firm solutions on the basis of Re,

W and Ni. The firm solutions on the basis of Re have hexagonal lattice, on the basis of Ni - cubic. In the Re-Ni-W alloys as a result of complicated isomorphic replacement of rhenium atoms on the Ni and W atoms the firm solution which has hexagonal lattice is formed. The character of X-ray



analyses enables to speak about crystallization of the Re-Ni, Re-W and Re-Ni-W alloys with allocation of the small disperse phases with the size of grains 2-20 nanometers. The size of particles makes a great impact on microhardness that is connected with the Hall-Petcha law [6]. In crystal coverings the growth of micro hardness with reduction of the size of grain is explained by the increase of the total area of the borders of grains which are the obstacle for dislocations. The crystallization of the Re-Ni alloys from ammonium-sulfate sulfate acid electrolytes occurs with allocation of small disperse phases with the size of grains of 16 nanometers, therefore the microhardness of Re-Ni coverings is lower (7871 MPa) in comparison with the coverings on the basis of Re-W alloys (to 35851 MPa), with the size of grains from 1,7 to 2 nanometers. For comparison, the microhardness of pure heated Re, W and Ni makes accordingly 1300, 2100 and 1000 MPa [6].

### Conclusions.

The possibility of Re-W, Re-Ni, Re-W-Ni alloys deposition in the form of powders and coatings on the copper and steel base plates in membrane electrolyzer with the graphite anode has been shown. As electrolytes sulfate-ammonium and sulfuric solutions with citric acid, sodium fluoride and glycerin additives were used. The Re-W, Re-Ni, Re-W-Ni coatings are alloys in the form of solid solutions on Re, W and Ni base. Alloys are nanostructured because their crystallization occurs with isolation of fine-dispersed phases having 2-20 nanometers size of grains. Microhardness of the coatings deposited on copper plate can reach 8270 MPa for Re-Ni, 35000 MPa for Re-W, 14808 MPa for Re-Ni-W coatings depending on electrolysis parameters. Re-W coatings corrosion resistance is higher than Re-Ni coatings corrosion resistance. Possibility of electrodeposition from water solutions electrolytes of nanostructured alloys on the basis of refractory rare metals (rhenium, tungsten) in the form of coatings with the improved constructional and physicochemical properties was established.

### References.

1. Proc. Inter. Symp. on Rhenium and Rhenium Alloys. 9-13 Feb., 1997. Orlando, Florida / Ed. B. D. Bryskin. – Orlando (Fla.): TMS, 1997.
2. Physical and chemical properties of rhenium alloys. Ed. E. M. Savitsky, M. A. Tylkina. – Nauka: Moscow, 1979. p. 215.
3. E. M. Savitsky, M. A. Tylkina, A.M. Levin, *Rhenium alloys in electronics*, Energya: Moscow, 1980. p. 216.
4. Yu. V. Lakhokin, A.I. Krasovskiy, *Rhenium-tungsten coatings*. Moscow, 1989. P.120-122.
5. V.V. Povetkin, I.M. Kovenskiy, Yu.I. Ustinovschikov, *Electrolytic alloys structure and properties*, Moscow, 1992, p. 255.
6. Yu. D. Gamburg, *Electroplating. Guide to use*, Tekhnosfera: Moscow, 2006. p. 216.
7. E.I. Ponomareva, L.Ya. Agapova, Z.S. Abisheva, S.K. Kilibayeva, S.N. Aitekeeva, *Tsvetnie metalli*, 4: 39-44 (2010).
8. S.K. Kilibayeva, L.Ya. Agapova, Z.S. Abisheva, *Komplexnoe ispolzovanie mineralnogo cyria*, Almaty, Kazakhstan, 3: 95-106 (2010).
9. L.Ya. Agapova, S.N. Aitekeyeva, E.I. Ponomaryova, Z.S. Abisheva, Method of rhenium-tungsten coatings electrodeposition. Patent #10216, 2004, Republic of Kazakhstan.
10. L.Ya. Agapova, Z.S. Abisheva, S.K. Kilibayeva, V.V. Bobrova, Method of rhenium-tungsten coatings electrodeposition. Patent #22227, 2010, Republic of Kazakhstan.

3.11.

## APPLICATION OF ELECTRODIALYSIS METHOD FOR HIGH PURITY METAL RHENIUM OBTAINING

Z.S. Abisheva, L.Ya. Agapova, E.I. Ponomareva, Z.T. Abdrakhmanova

Centre of Earth Sciences, Metallurgy and Ore Beneficiation,  
(Shevchenko str. 29/33, Almaty, Republic of Kazakhstan)

**Keywords:** ammonium perrhenate, electro dialysis, membranes, rhenium acid, temperature reduction, powder, metal rhenium

### Abstract:

High-temperature reduction of ammonium perrhenate by gaseous hydrogen is widespread method for powdery metal rhenium obtaining. Purity of metal rhenium produced by this method is generally determined by purity of initial ammonium perrhenate obtained by re-crystallization of crude ammonium perrhenate or by electro dialysis of its solutions. Metal rhenium produced from marketable AR-0 grade ammonium perrhenate (weight %: Re - 69,2; K -  $3.0 \cdot 10^{-3}$ ; Na -  $1.1 \cdot 10^{-3}$ ; S <  $2.0 \cdot 10^{-4}$ ; P <  $1.0 \cdot 10^{-3}$ ; Si <  $4.0 \cdot 10^{-5}$ ; Mg -  $4.0 \cdot 10^{-5}$ ; Mn -  $2.0 \cdot 10^{-5}$ ; Al -  $2.0 \cdot 10^{-4}$ ; Fe -  $6.0 \cdot 10^{-5}$ ; Ca -  $2.0 \cdot 10^{-3}$ ; Mo -  $1.0 \cdot 10^{-4}$ ; Ni -  $1.0 \cdot 10^{-4}$ ; Cu <  $5.0 \cdot 10^{-5}$ ) by method of high-temperature reduction with gaseous hydrogen at 800-900° C contained no more than 99.981 % of the basic metal. Initial ammonium perrhenate purification was carried out on industrial electro dialysis apparatus with using specially purified water for increase of metal rhenium purity in industrial conditions. In the process of electro dialysis was obtained rhenium acid. The content of impurities in ammonium perrhenate besieged from this acid was on 1-2 order lower than in initial salt. Metal rhenium powder, produced by high-temperature reduction with gaseous hydrogen of ammonium perrhenate, preliminary purified by electro dialysis method, exceeds on degree (order) by basic metal content (not less than 99.9970 %) the rhenium, obtained by reduction of AR-0 grade ammonium perrhenate.

### Introduction

On copper manufacture in Zhezkazgan a method of recrystallization crude ammonium perrhenate a commodity product of mark AR-0 is produced. It is thus formed rhenium containing product enriched with potassium less than 1 %. The outcome of this salt makes 6 - 10 % from a commodity output. Earlier this salt directed to a process head on solvent extraction, and now processes by electro dialysis method [1-3]. The electro dialysis method favourably differs by its simplicity from known methods of clearing [4-5]. However its use for rhenium acid obtaining restrained in the absence of corrosion-proof anode materials. The most stable anode material is platinum, at anode polarization in solutions of rhenium acid it is exposed to destruction and pollutes a final product. Besides, a high cost and deficiency of platinum limit its application. In the Institute of Metallurgy and ore Beneficiation (now “the Center of sciences about the Earth, Metallurgy and ore Beneficiation”) the theoretical and applied researches on electro dialysis application to technologies of Re were carried out for many years [6-8]. The device is designed and regime parameters of rhenium acids production, the basic product for other rhenium products are worked out [7-9]. In the method and an electro dialyzator design for high pure rhenium acid obtaining the difficulties with a choice of an anode material have been overcome at the expense of application of isolating chambers and barrier membranes. Such design of the device enables to use the cheap anode materials

(graphite, alloys on the basis of the lead, etc.), excludes pollution of acid by an anode material that is the important condition for obtaining of its solutions of high purity. For expansion of the let out nomenclature commodity rhenium production at the “Center” the investigations of metal rhenium obtaining from commodity ammonium perrhenate AR-0 carried out by a method of its high-temperature restoration by gaseous hydrogen at 800-900°C. The obtained metal Re contained no more than 99.981 % of the basic metal. For higher purity metal Re obtaining the initial ammonium perrhenate of mark AR-0 was cleared from present impurity industrially on industrial installation with use of specially cleared water.

### Experimental

The investigation was carried out in a seven-chamber electrolysizer with a graphite anode and stainless cathode. The electrolysizer consists of three sections: first section includes anodic, first barrier chamber and separating them cation-exchange membrane; second – includes second barrier, concentration and buffer chambers and separating them cation-exchange and anion-exchange membranes; third – cathodic, demineralization chambers and separating them cation-exchange membrane. The design of the seven-chamber electrolysizer eliminates the usage of platinum electrodes. MK-40 and MA-40 ionite heterogeneous membranes used for this study were produced by firm “Azot” (Russia). The cation-exchange membrane MK-40 and anion-exchange membrane MA-40 have the change capacity 2.6 meq/g and 3.8 meq/g correspondingly. Solutions of hydrochloric acid with concentrations of 10 and 1 g/dm<sup>3</sup> were fed into the anode and cathode chambers. The essence of electrolysizer method of rhenium acids production consists in the following. To the electrolysator desalting chamber submit a solution of rhenium salts. The cations of salt and impurities contained in a solution migrate under the influence of an electric current to cathodes space, and perrhenate ions through anion exchanging membranes - to the chamber of concentration (Fig.1). The process has been made continuously. The obtained rhenium acid with certain speed is constantly deduced from the chamber of concentration to special vessel for storage. The concentration acid degree depends on a speed of carrying over of perrhenate-ions to the chamber of concentration. The rhenium acid should satisfy not only purity requirements, but also concentration - not less than 20 % of Re. The more Re concentration in acid, the purer salt of

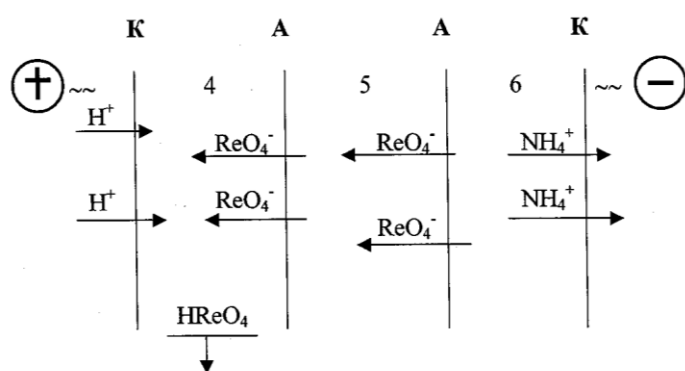


Fig.1. Scheme of ion transport of rhenium from the desalting chamber (6) through the buffer chamber (5) in a cell concentration (4) rhenium acid.

Membranes: A - anion, and K - cation.

ammonium perrhenate it is possible to besiege from rhenium acid [9]. From obtained rhenium acid by an ammonia solution neutralization the ammonium perrhenate salt besieges. The salt washed out and dried up in the portions processed on laboratory installation for restoration of ammonium perrhenate by hydrogen.

### Results and Discussion.

The researches of the concentrated rhenium acid obtaining process are carried out by the electrolysizer method [9]. The laws of rhenium acid concentrating process depending on a

current density (Fig.2), temperature (see Table 1), rhenium concentration in an initial solution (Fig.3), speed of a channel of an initial solution for the rhenium acid concentration speed in seven-chamber electrolysizer with ionic heterogeneous membranes MK-40 and

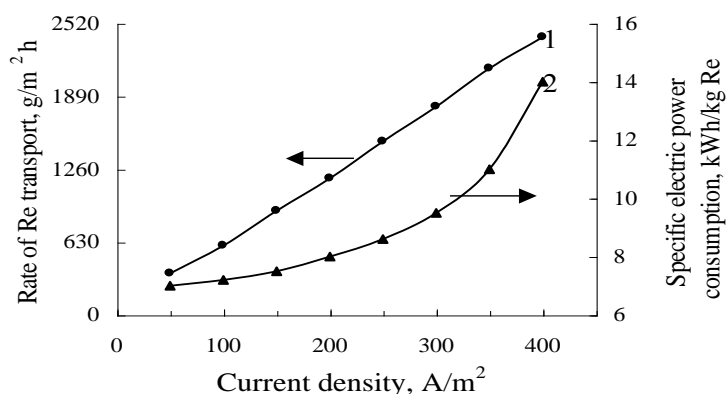


Fig.2. Effect of current density on rhenium transport to concentrating chamber (1) and specific electric power consumption (2)

For successful membrane operation the optimum solution temperature in electrolysers has not to be over 50°C. Taking into account the degree of rhenium ions' transport, the best parameters of the electrolysis process were obtained at 400 A/m<sup>2</sup> current density. However, at this current density the specific electric power consumption is high and the solutions temperature is high, requiring significant heat removal from the system. Taking all these factors into account the optimum current density was identified as 300 A/m<sup>2</sup>. One of the basic factors influencing transport of rhenium through membranes in the process of electrolysis is solution temperature. The results of investigation of temperature effect on rhenium ions transport using electrolysis of a saturated solution of potassium perrhenate are presented in Table 1. Rhenium transport into the concentration chamber increases significantly with increase of temperature. However, as noted, the increase of solutions temperature higher than 50°C

Table 1. Effect of temperature on rhenium transport for electrolysis of potassium perrhenate solution (experiment time is 60 minutes)

Current density, A/m <sup>2</sup>	Solution temperature, °C	Rhenium transport to the electrolyzer concentration chamber, g/m <sup>2</sup> ·h	Rhenium current efficiency, %
250	30	114.0	6.3
250	40	169.0	9.4
250	50	389.0	22.4
350	30	415.0	16.8
350	40	468.0	18.8
350	50	630.0	25.2
400	30	428.0	15.0
400	40	477.0	16.8
400	50	640.0	22.4

is undesirable because ionite membrane selectivity decreases and mechanical strength is abruptly decreased. Fall in solutions temperature to 25°C and lower leads not only to decrease of rhenium ions' transport into the concentration chamber but also to precipitation of perrhenate salts in electrolysis chambers because of decrease of their solubility. Solubility of ammonia and potassium perrhenates decreases two-fold with the decrease of the temperature from 50°C to 30°C [10]. Experiments on production of rhenium acids by electrolysis were carried out at current density of 100 A/m<sup>2</sup> from solutions of ammonia perrhenate within the range of 5-45 g/dm<sup>3</sup> concentration. Effect of rhenium concentration in initial solution of ammonia perrhenate on specific electric power consumption and current efficiency is shown in Fig. 3. Specific electric power consumption abruptly increased and current efficiency decreased in solutions with less than 15 g/dm<sup>3</sup> rhenium concentration. Concentration polarization, electrical resistance of solutions and quantity of heat are increased during the process of electrolysis at low rhenium content in solutions. Concentration polarization of membranes was not observed at

MA-40 are defined. The reaction temperatures of solution in the first and second barrier chambers are increased at 200, 300 and 400 A/m<sup>2</sup> current densities and were on average 47, 64 and 87°C, respectively. To determine optimal current density three factors were taken into account. They were the rate of rhenium ions transport, specific power consumption and maximum permissible temperature of solutions in barrier chambers.

is undesirable because ionite membrane selectivity decreases and mechanical strength is abruptly decreased. Fall in solutions temperature to 25°C and lower leads not only to decrease of rhenium ions' transport into the concentration chamber but also to precipitation of perrhenate salts in electrolysis chambers because of decrease of their solubility. Solubility of ammonia and potassium perrhenates decreases two-fold with the decrease of the

rhenium concentration of higher than 15-17 g/dm<sup>3</sup>. Inconsiderable increase of current efficiency and a slight decline of specific electric power consumption is only explained by increasing specific conductivity of solution and therefore by decrease of electric power consumption for heating. Characteristics of the electrolysizer under these conditions are near their extreme values limiting the rate of rhenium transport from the demineralization chamber into the concentration chamber for the given electrolysis parameters. Thus, the best conditions of rhenium acid concentration are obtained when the process is carried out with saturated or close to saturated solutions of rhenium salts. However, it is necessary to note that the selectivity of ion exchange membranes is decreased with the increase of concentration of external solution [11]. It has been identified that the optimum conditions of perrhenic acid

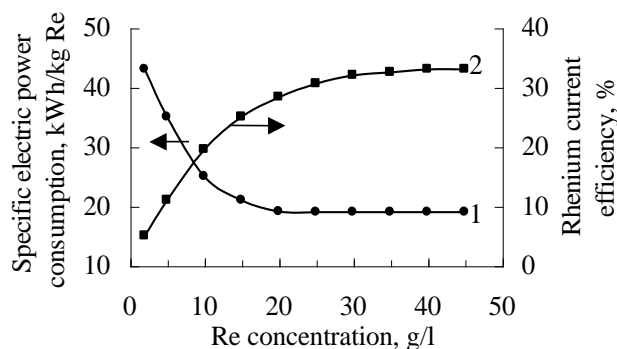


Fig.3. Effect of rhenium content in initial solution of ammonia perrhenate on specific electric power consumption (1) and current efficiency (2)

concentration by electrolysis of ammonia and potassium perrhenate solutions are the following: 300 A/m<sup>2</sup> current density, 50°C solution temperature in electrolysizer's chambers, 35-40 g/dm<sup>3</sup> rhenium concentration in initial solution, 0.67-0.83 volume of chamber/min flow rate of initial solution in a demineralization chamber [9]. Concentration of rhenium acid in these conditions is 300 g/dm<sup>3</sup> and higher. However, higher concentration of produced rhenium acid is inadvisable because the selectivity and mechanical strength of ionite membranes are decreased. The transformation of rhenium in rhenium acid from the initial quantity rhenium

has been 99 %. The basic rhenium losses (0,2 %) with anode and cathodes chambers waste solutions occur. The outcome on a current of rhenium has made 60 %, the expense of the electric power on 1 kg Re - 6 κVt/h. From obtained rhenium acid by an ammonia solution neutralization the ammonium perrhenate salt besieges, weights, containing. %: Re - 69,2; K<1.0·10<sup>-3</sup>; Na - 1.0·10<sup>-4</sup>; S - 2.0·10<sup>-3</sup>; P <1.0·10<sup>-4</sup>; Si <1.0·10<sup>-4</sup>; Mg <1.0·10<sup>-4</sup>; Mn <1.0·10<sup>-4</sup>; Al <1.0·10<sup>-4</sup>; Fe <5.0·10<sup>-4</sup>; Ca <1.0·10<sup>-3</sup>; Mo <5.0·10<sup>-4</sup>; Cu <5.0·10<sup>-5</sup> and corresponding ammonium perrhenate of mark AR-0. For higher purity metal rhenium obtaining the initial ammonium perrhenate of mark AR-0 was cleared from present impurity industrially on industrial installation with use of specially cleared water. Produced rhenium acid contained, weight %: Re -27,5; K- 4.0·10<sup>-5</sup>; Na - 8.0·10<sup>-5</sup>; Fe - 2.0·10<sup>-4</sup>; SO<sub>4</sub><sup>2-</sup>-0.01; Cl—0.06; mechanical impurities were not determined. The ammonium perrhenate besieged from this acid by ammonia contained, mass. %: Re-69.2; K<2.0·10<sup>-4</sup>; Na - 6.0·10<sup>-5</sup>; S<2.0·10<sup>-4</sup>; P<1.0·10<sup>-3</sup>; Si< 4.0·10<sup>-5</sup>; Mg - 8.0·10<sup>-6</sup>; Mn - 4.0·10<sup>-6</sup>; Al - 1.0·10<sup>-4</sup>; Fe -5.0·10<sup>-6</sup>; Ca - 3.0·10<sup>-4</sup>; Mo - 1.0·10<sup>-4</sup>; Ni <1.0·10<sup>-4</sup>; Cu <5.0·10<sup>-5</sup>. The maintenance in ammonium perrhenate of such impurity as potassium, sodium, magnesium, manganese, iron were on 1-2 order lower than in initial salt. The salt washed out and dried up in the portions processed on laboratory installation for restoration of ammonium perrhenate. The products of high-temperature ammonium perrhenate restoration process by hydrogen were: a powder metal of rhenium, the absorbing solutions containing rhenium, a deposit on a quartz pipe. The extraction of rhenium in a metal powder has made from 93.4 to 98.2 %. Rhenium transformation in absorbing solutions was from 0.07 to 0.37 %. The X-ray analysis of the obtained metal powder has shown full rhenium restoration to metal and absence of oxides in it. The maintenance of impurity in a powder metal rhenium was defined by the quantitative spectral method. The rhenium maintenance is calculated as a difference of the impurity sum and has made not less than 99.9962-99.9970 % (see Table 2, tests № 2-6).



Table 2. The maintenance of impurity in metal rhenium \*

The maintenance, weights. %	Tests metal rhenium					
	1	2	3	4	5	6
K	$9.0 \cdot 10^{-3}$	$<1.0 \cdot 10^{-3}$	$<1.0 \cdot 10^{-3}$	$<1.0 \cdot 10^{-3}$	$<1.0 \cdot 10^{-3}$	$<1.0 \cdot 10^{-3}$
Na	$2.5 \cdot 10^{-3}$	$3.0 \cdot 10^{-4}$	$3.0 \cdot 10^{-4}$	$7.0 \cdot 10^{-4}$	$1.0 \cdot 10^{-3}$	$3.0 \cdot 10^{-4}$
Ca	$5.0 \cdot 10^{-3}$	$<1.0 \cdot 10^{-3}$	$<1.0 \cdot 10^{-3}$	$<1.0 \cdot 10^{-3}$	$<1.0 \cdot 10^{-3}$	$<1.0 \cdot 10^{-3}$
Si	$4.2 \cdot 10^{-4}$	$3.2 \cdot 10^{-4}$	$2.2 \cdot 10^{-4}$	$1.8 \cdot 10^{-4}$	$2.8 \cdot 10^{-4}$	$2.4 \cdot 10^{-4}$
Al	$4.3 \cdot 10^{-4}$	$1.8 \cdot 10^{-4}$	$1.3 \cdot 10^{-4}$	$1.0 \cdot 10^{-4}$	$5.0 \cdot 10^{-5}$	$8.0 \cdot 10^{-5}$
Fe	$6.0 \cdot 10^{-5}$	$8.0 \cdot 10^{-5}$	$5.0 \cdot 10^{-5}$	$5.0 \cdot 10^{-5}$	$6.0 \cdot 10^{-5}$	$5.0 \cdot 10^{-5}$
Mg	$7.0 \cdot 10^{-4}$	$1.8 \cdot 10^{-4}$	$1.0 \cdot 10^{-4}$	$1.5 \cdot 10^{-4}$	$1.7 \cdot 10^{-4}$	$2.0 \cdot 10^{-4}$
Ni	$1.0 \cdot 10^{-4}$	$1.0 \cdot 10^{-4}$	$1.0 \cdot 10^{-4}$	$1.0 \cdot 10^{-4}$	$1.0 \cdot 10^{-4}$	$1.0 \cdot 10^{-4}$
Mo	$<1.0 \cdot 10^{-4}$	$<1.0 \cdot 10^{-4}$	$<1.0 \cdot 10^{-4}$	$<1.0 \cdot 10^{-4}$	$<1.0 \cdot 10^{-4}$	$<1.0 \cdot 10^{-4}$
Cu	$6.0 \cdot 10^{-5}$	$2.0 \cdot 10^{-5}$	$2.0 \cdot 10^{-5}$	$2.0 \cdot 10^{-5}$	$3.0 \cdot 10^{-5}$	$1.0 \cdot 10^{-5}$
Re not less than	99.9806	99.9967	99.9970	99.9969	99.9962	99.9969

\*1 test metal rhenium is obtained from ammonium perrhenate of mark AR-0;  
2-6 tests metal rhenium are obtained from the cleared ammonium perrhenate.

Thus, electro dialysis clearing branded ammonium perrhenate AR-0 before its high-temperature restoration by gaseous hydrogen enables to raise 10 times cleanliness of the obtained powder of metal rhenium.

### Conclusions.

The seven-chamber electro dialyzator and technology of electro dialysis clearings, concentrating and obtaining of rhenium containing products (rhenium acid, perrhenate salts) from industrial rhenium containing solutions are developed [12-13]. The device design enables to use the cheap anode materials (graphite, alloys on the basis of lead, etc.), excludes pollution of rhenium acid by anode material that is the important condition for the obtaining solutions of high purity. The technology of rhenium acid electro dialysis obtaining has been introduced in manufacture at Zhezkazgansky copper factory in 1991 and it functions at the present time. The electro dialysis method for obtaining of a commodity output from sub-standard ammonium perrhenate which went earlier to a process head is used. The rhenium maintenance in a sub-standard product fluctuates from 66.5 to 69.2 %, potassium - from 0.1 to 0.85 %. From these products by electro dialysis method the rhenium acid with rhenium concentration from 25.5 to 30.5 %, potassium - less than 0.001 % is made. The transformation of rhenium in rhenium acid from the initial quantity rhenium was 99 %. The basic rhenium losses (0.2 %) with anode and cathodes chambers waste solutions occur. The outcome on a current of rhenium has made 60 %, the expense of the electric power on 1 kg Re - 6 kVt/h. The optimum conditions of electro dialysis rhenium acid concentration process conducting from the ammonium perrhenate and potassium solutions are: the density of a current - 300 A/m<sup>2</sup>, temperature of solutions in electro dialyzators chambers - 50°C, rhenium concentration in an initial solution - 35-40 g/dm<sup>3</sup>, speed of an initial solution channel in the desalting chamber – 0.67 -0.83 volumes/minutes. Under these conditions the 300 g/dm<sup>3</sup> and above of rhenium acid concentration is reached. Metal rhenium produced from marketable AR-0 grade ammonium perrhenate by method of high-temperature reduction with gaseous hydrogen at 800-900°C contained no more than 99.981 % of the basic metal. Metal rhenium powder, produced by high-temperature reduction with gaseous hydrogen of ammonium perrhenate, preliminary purified by electro dialysis method, exceeds on

degree (order) by basic metal content the rhenium (not less than 99.9970 %), obtained by reduction of AR-0 grade ammonium perrhenate.

### References.

1. Z.S.Abisheva, A.N. Zagorodnyaya, N.S.Bekturganov, *Hydrometallurgy*, **109**(N 1-2): 1-8 (2011).
2. Z.S.Abisheva, A.N. Zagorodnyaya, *Tsvetnie metalli*, **5**: 70-73 (2005).
3. Z.S. Abisheva, E.I. Ponomareva, L.Ya. Agapova, A.M. Bikineev, Z.T.Abdrakhmanova, *Tsvetnie metalli*, **5**: 73-75 (2005).
4. K.V. Marunova, M.A. Stepanova, *Rhenium. Chemistry, technology, analysis*, M.: Nauka, 1976, P. 87-89.
5. K.V. Marunova, A.V. Stepanov, *Tsvetaya metallurgiya*, **18**: 25-27 (1977).
6. N.A.Chokanov, A.M. Bikineev, L.V. Olenina, M.T. Dgumagaziev, *Komplexnoe ispolzovanie mineralnogo cyria (Combine usage of mineral resources)*, Almaty, Kazakhstan, **11**: 91-93 (1988).
7. S.N. Orazbaev, I.Ya. Sadchikov, Ch.T. Masenov, E.I. Ponomareva, *Komplexnoe ispolzovanie mineralnogo cyria*, Almaty, Kazakhstan, **10**: 57-61 (1990).
8. E.I. Ponomareva, A.M. Bikineev, Z.S.Abisheva, L.Ya. Agapova, *News of Science of Kazakhstan. Express information. Series: The development of modern science. The future of science*. Almaty, Kazakhstan, **3**: 35-36 (1996).
9. L.Ya Agapova., E.I. Ponomareva , Z.S. Abisheva, *Hydrometallurgy*, **60**: 117-122 (2001).
10. K.B.Lebedev. *Rhenium* (in Russian). Metallurgizdat, Moscow ( 1963) 208 p.
11. *Demineralization by electrodialysis*, Edited by J.R.Wilson. Butterworths scientific publications, London (1960) 351 p.
12. L.Ya Agapova., Z.S. Abisheva, Z.T.Abdrakhmanova, T.N. Bukurov, Patent RK № 15026, Method of producing metal powder of high purity rhenium, publ. 15.09.2007, Bulletin of Inventions № 9.
13. A.M. Bikineev, Z.S.Abisheva, E.I. Ponomareva, L.Ya. Agapova, V.V. Bobrova, Patent RK № 20323, Method for production of rhenium acid in multiple electrodialyzers, publ. 17.11.2008, Bulletin of Inventions № 11.

3.12.

### **THE ELECTROLYTIC SUBSIDENCE OF RHENIUM FROM ACID ELECTROLYTES**

E.A. Salahova, V.A. Majidzade, F.S. Novruzova, A.F. Qeybatova, P.E. Kalantarova

M. F. Nagiyev Institute of Chemical Problems of Azerbaijan NAS

e-mail: [elza\\_salahova@mail.ru](mailto:elza_salahova@mail.ru)

The future development of science and technology is possible through the study of materials with new features and development of new equipments that would meet up-to-date requirements based on these materials. From this view point the electrochemical acquisition of rhenium covers is of great importance. The fact that rhenium has high melting temperature and anti-corrosion durability allows utilizing these covers in various fields of modern technology. There are numerous electrolytes for the subsidence of rhenium in acid solutions. The main feature of the below abstract include the methods on the electrochemical acquisition of thin layers of rhenium covers from various electrolytes, as well as the selection of the optimal regime and electrolyte for the utilization of the acquired covers in the technology. For this purpose the process of the electrolytic subsidence of rhenium from sulfate, chloride-sulfate and chloride-borate solutions has been studied through the application of modern electrochemical methods. Platinum, rhenium and copper electrodes have been utilized as cathodes and platinum electrode has been utilized as anode; silver-chlorine electrode has been utilized as comparison electrode. The affects of thickness, temperature, acidity of solution, currency density, thickness of active surface elements, change speed of the potential, stirring, etc. on the process of electrolytic subsidence of rhenium have been studied. Through the controlled potential and cycle polarization curves revealed that the rhenium reduction in sulfate and chloride-sulfate solutions happens in several stages alongside with the acquisition of interim products (Re oxides). In this regard, each stage is characterized with certain electrode potential. Because rhenium reduction happens in acid environment the potential grade of its reduction depend upon the acidity as well. The impact of the electrolytic acidity on the electrolytic subsidence process shows that as the acidity increases the interim elements passivate the surface of the electrode to certain degree which hinders the subsidence of rhenium. With the change of the acidity of the electrolyte the yield of rhenium as per currency changes as well and its value ranges between 50-60%. In order to clarify the kinetic and mechanical features of the subsidence process the cathode and anode curves of rhenium were drawn and their nature of their polarization in the given electrolytes was studied. It was determined that under smaller values of the currency rhenium subsides through electrochemical polarization, under the barrier currency through diffusion and under next densities through mixed polarization.

3.P1.

## **SORPTION RECOVERY OF RHENIUM FROM ACIDIC SULFATE AND MIXED NITRATE-SULFATE SOLUTIONS CONTAINING MOLYBDENUM**

A.A. Blokhin<sup>1</sup>, E.E. Maltseva<sup>1</sup>, M.A. Pleshkov<sup>2</sup>, Ju.V. Murashkin<sup>1</sup>,  
M.A. Mikhaylenko<sup>3</sup>

<sup>1</sup> Saint-Petersburg State Institute of Technology (Technical University),  
Saint-Petersburg, blokhin@list.ru;

<sup>2</sup> Science Research Center Hydrometallurgy, Saint-Petersburg,  
pleshkov@gidrometall.ru;

<sup>3</sup> The Purolite representative office in the CIS, Moscow, purolite\_mm@co.ru

**Keywords:** rhenium, molybdenum, molybdenites, sulfuric acid, nitric acid, solutions, anion exchange resins, sorption, stripping, separation, concentration

### **Abstract:**

The possibility of rhenium recovery from the molybdenite concentrates processing solutions by means of macroporous and gel anion exchange resins Purolite A170 and Purolite A172 (referred below as A170 and A172) has been investigated. It has been found, that A170 macroporous resin, unlike A172 gel resin, loaded both rhenium and significant amounts of molybdenum. Due to this effect, the rhenium capacity of A170 lower than that of A172 by 20–30% on terms of the sorption from the molybdenum containing solutions. At the same time, ammoniac solutions readily striped rhenium from A170 resin for any resin saturation of rhenium, as in the case of A172 resin acceptable stripping occurred only for high resin saturation of rhenium. Rhenium stripping was not complete when low rhenium saturation of A172 resin obtained. Therefore, A172 resin is proposed for the rhenium recovery from the acidic sulfate solutions from the roasting gas treatment system, and A170 is proposed for the rhenium recovery directly from the pregnant solutions of autoclave leaching molybdenite concentrates with nitric acid. Both A170 and A172 resins are applicable for the secondary concentration of rhenium from primary eluates if optimal pH conditions would be provided. Above recommendations have been experimentally proved on the model and real solutions.

### **Introduction**

Molybdenites are the richest natural source of rhenium. Oxidizing roasting and leaching in nitric acid (usually pressure leaching in the presence of oxygen) are the most common ways for the molybdenite concentrates processing [1]. Acidic sulfate solutions from the roasting gas treatment system contain, g/l: Re – 0,3–0,7; Mo – 3–6; Cu, Zn, Fe – in 1–2; H<sub>2</sub>SO<sub>4</sub> 50–120. Pregnant solutions from the nitric acid pressure leaching contain, g/l: Re – 0,01–0,04; Mo – 8–15, Fe, Cu, Zn – in 2–5; H<sub>2</sub>SO<sub>4</sub> 100–150; HNO<sub>3</sub> 10–30.

Preliminary experiments have shown that iron and nonferrous metals did not affect the rhenium sorption from the acidic solutions with anion exchange resins. While, at the same conditions molybdenum is readily absorbed with the resin, and may essentially decrease rhenium loading. Therefore, rhenium and molybdenum separation is the main problem in the processing of the solutions involved.

The possibility of rhenium recovery from the molybdenite concentrates processing solutions by means of macroporous and gel anion exchange resins Purolite A170 and Purolite A172 has been investigated.

## Experimental

The anion exchange resins preliminary were converted to  $\text{SO}_4^{2-}$ -form. The experiments on studying the sorption and stripping of rhenium were carried out in the static and dynamic conditions.

The determination of the values of the rhenium and molybdenum capacities of the anion exchange resins (Q) and the distribution coefficients (D) of these metals was carried out by bath equilibration. Samples of the anion exchange resins (0,2 g in a count on mass of the absolutely dry resin) were treated by 20 ml of a solution of one or another composition. The mixture was shaken for 48 h until equilibrium was attained. Then the rhenium and molybdenum concentrations in the solution were determined. The amount of adsorbed metals was determined from the difference between their initial and final concentrations. The values of mass capacity of the anion exchangers (mg of rhenium or molybdenum on g of dry the anion exchanger) were counted taking into account the specific volume of the anion exchanger on the values of by volume capacity (mg of rhenium or molybdenum on ml of the swelled anion exchanger). In a number of experiments the values of the molybdenum capacity of the anion exchangers were determined parallel on the analysis of desorbates. Samples of the anion exchangers after the saturation were separated from workings solutions, carefully washed with distilled water and treated by 20 ml of the 1 M NaOH solution containing 1 mole/l of  $\text{NaNO}_3$ . The mixture was shaken for 48 h. Then the rhenium and molybdenum concentrations in the desorbates were determined.

The D values were calculates in the usual manner.

In the stripping experiments after the resin reached equilibrium with the solution, it was separated from the solution and washed with distilled water. The washed resin was then stripped using 6 M ammoniac solution. Both the equilibrium solution and the stripped solution were sampled and analysed.

The experiments in the dynamic conditions were carried out in a glass column with a bed volume (BV) of 20 ml and  $H : D = 10 : 1$ . The flow rate maintained about 1,0 bed volumes per hour (BV/h) during sorption and 0,5 BV/h during stripping.

The concentrations of rhenium and molybdenum were determined by photocolorimetric methods [2, 3] on the photoelectric colorimeter CFC-2MP. In column experiments with a real pregnant solution of nitric acid pressure leaching of molybdenite concentrate the rhenium and molybdenum concentrations were determined by atomic-emission method on the Thermo Scientific iCAP 6200 ICP Spectrometer.

## Results and Discussion

### 1. Preliminary study

#### 1.1. Sorption

The presence of molybdenum in acidic sulfate solutions did not remarkably affect the sorption of rhenium with A172 gel resin and resulted in decrease of rhenium loading in the case of A170 macroporous resin (Figure 1).



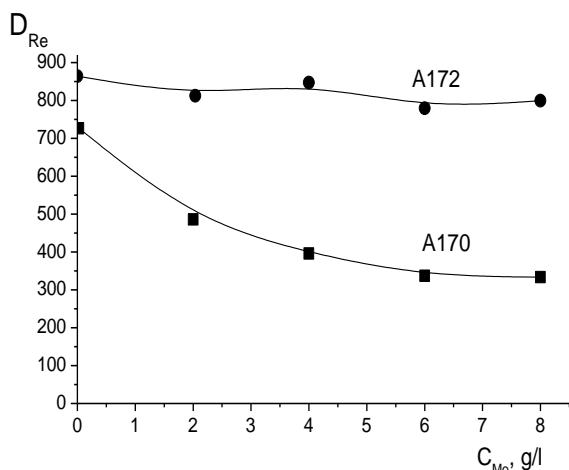


Figure 1. Molybdenum influence on rhenium sorption from the solution, containing 1M  $H_2SO_4$  with initial rhenium concentration of 1 g/l

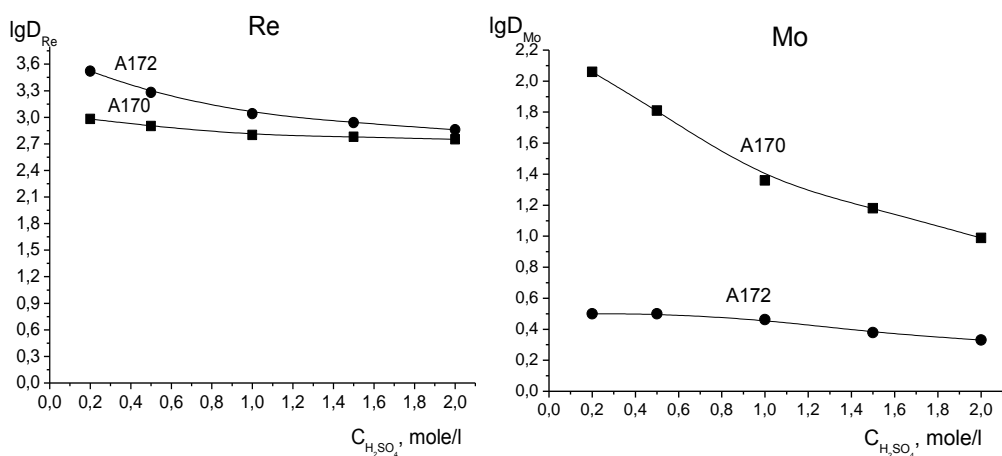


Figure 2. The influence of  $H_2SO_4$  on the rhenium and molybdenum distribution (Initial rhenium concentration of 0,6 g/l, molybdenum of 2 g/l)

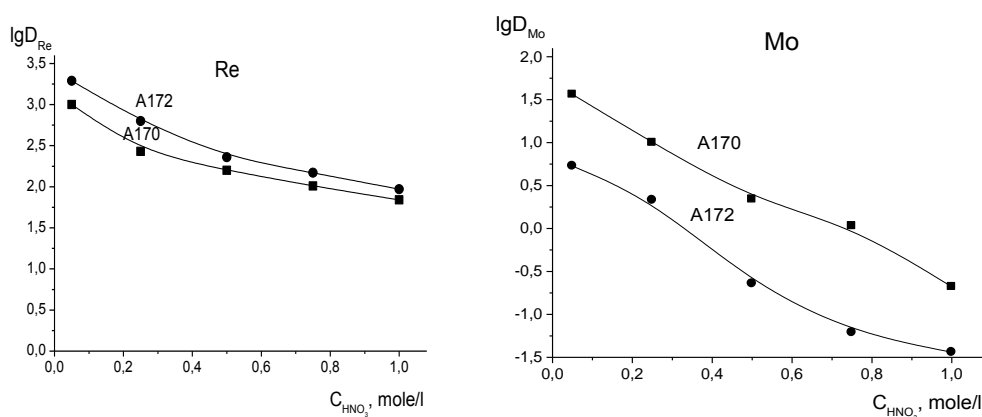


Figure 3. The influence of  $HNO_3$  on rhenium and molybdenum distribution (initial rhenium concentration of 0,1 g/l, initial molybdenum concentration of 2 g/l, sulfuric acid concentration of 1 mol/l)

A170 macroporous resin, unlike A172 gel resin, loaded both rhenium and significant amounts of molybdenum. Rhenium loading capacity slightly depended upon sulfuric acid concentration both for macroporous and for gel resin, with essential molybdenum capacity decreasing in the case of A170 macroporous resin (Figure 2).

For any resin tested both rhenium, and molybdenum loading capacity decreased in the presence of nitric acid, being more distinguish for molybdenum (Figure 3).

### 1.2. Rhenium stripping

Ammoniac solutions readily striped rhenium from A170 resin for any resin saturation of rhenium, as in the case of A172 resin acceptable stripping occurred only for high resin saturation of rhenium. Rhenium stripping was not complete when low rhenium saturation of A172 resin obtained (Figure 4).

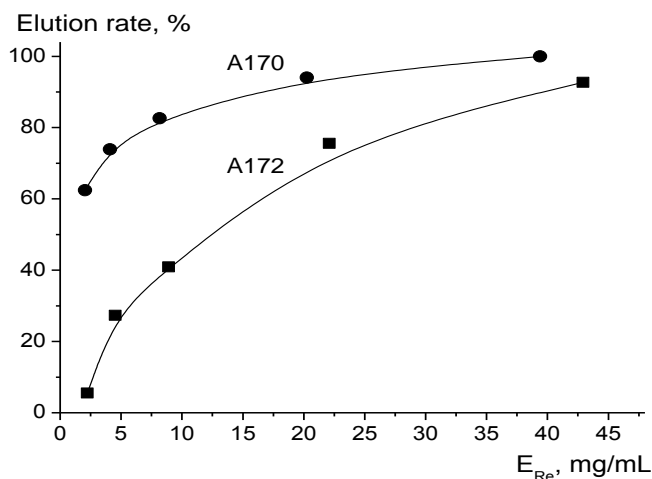


Figure 4. The dependence of the rhenium elution rate upon the resin saturation (Stripping solution: 6M ammonia)

### 2. Rhenium recovery from acidic sulfate solutions from the roasting gas treatment system

Obtained adsorption and elution curves for rhenium and molybdenum are shown on the Figures 5 and 6, and some calculated characteristics are in the Table 1.

According to the data given A172 gel resin is more suitable for the rhenium recovery from the solutions involved.

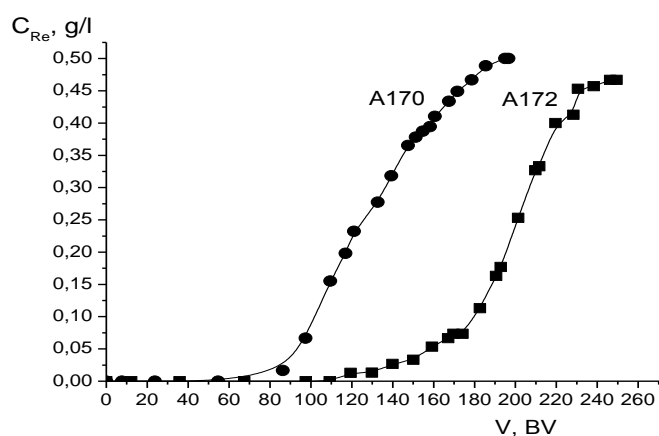


Figure 5. Rhenium adsorption curves from the model solution containing Re of 0,5 g/l, Mo of 4 g/l and  $H_2SO_4$  of 100 g/l

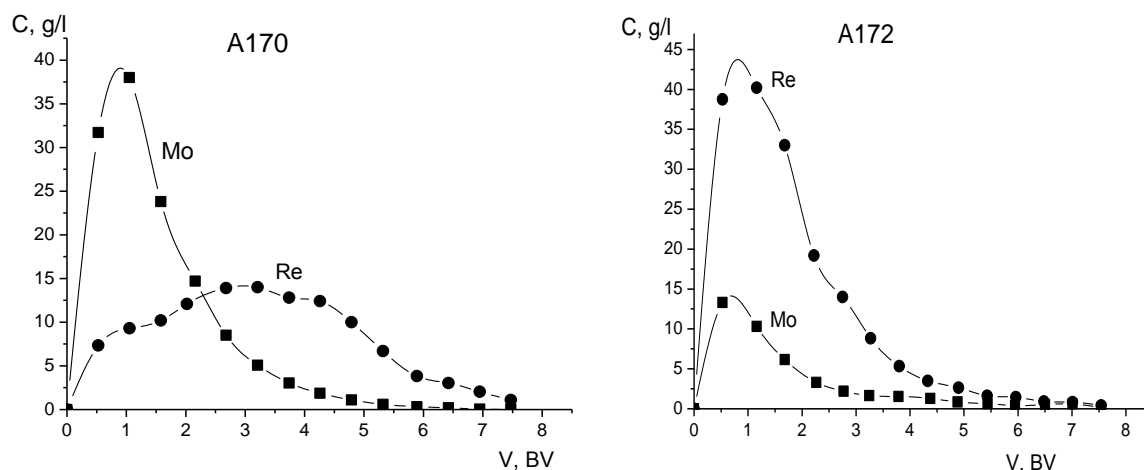


Figure 6. Rhenium and molybdenum elution curves by 6M ammonia

To reduce molybdenum content in the rhenium eluates a selective stripping of molybdenum using saline solutions was proposed. Rhenium and molybdenum elution curves from preprocessed resin one can see on the Figure 7, and some calculated characteristics are in the Table 1.

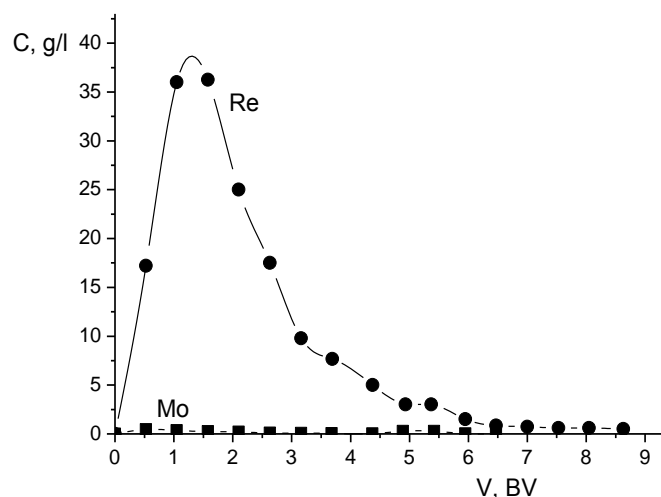


Figure 7. Rhenium and molybdenum elution curves from A172 loaded resin by 6M ammonia after molybdenum scrubbing

Table 1. Sorption and elution characteristics of rhenium and molybdenum recovery according to the column experiment with A170 and A172 resins

Resin	Re in loaded resin, mg/ml resin	Mo scrubbing, mg/ml resin		Re stripping, mg/ml resin		Re:Mo ratio		Re K Mo
		Re	Mo	Re	Mo	feed	eluate	
A170	64,0	—	—	63,3	68,7	0,125	0,92	7,36
A172	98,9	—	—	94,4	23,5		4,02	32,2
A172	97,3	3,0	16,3	87,1	1,1		79,2	633,5

### 3. Rhenium recovery from pregnant solutions of molybdenite concentrates nitric acid pressure leaching

A basic difficulty in rhenium recovery from pregnant solutions of molybdenite concentrates autoclave pressure leaching in the presence of nitric acid is caused by low rhenium concentration and depressing effect of nitrate ions on the rhenium adsorption. As one can see on the Figure 8, both resins appeared to be quite rhenium selective, with A172 gel resin having higher rhenium capacity.

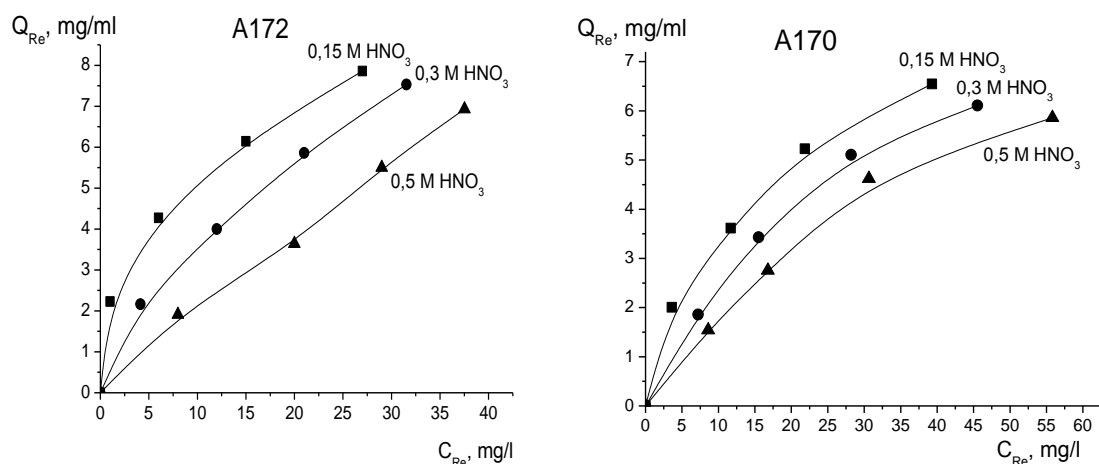


Figure 8. Rhenium adsorption isotherms from mixed nitrate-sulfate solutions containing Mo of 8 g/l and H<sub>2</sub>SO<sub>4</sub> of 100 g/l

Unfortunately, rhenium stripping was found to be incomplete when low rhenium saturation of A172 resin obtained (Table 2).

Therefore, just A170 resin was proposed for the direct rhenium recovery from pregnant solutions of molybdenite concentrates autoclave pressure leaching in the presence of nitric acid.

Table 2. Rhenium elution characteristics for A170 and A172 resins

Resin	Re in loaded resin, mg/ml resin	Stripping conditions	Re in eluate, mg/ml resin	Elution rate, %	Re in striped resin, mg/ml resin
A170	5,36	6 M ammonia, 19°C	5,13	95,7	0,23
A172	5,24	6 M ammonia, 19°C	1,83	34,9	3,41
A172	5,24	6 M ammonia, 50°C	2,55	48,7	2,69

In column experiments we used A170 resin and a real pregnant solution of nitric acid pressure leaching of molybdenite concentrate. It contained, g/l: Re– 0,0096; Mo– 9,0; Fe– 1,3; Cu– 0,5; H<sub>2</sub>SO<sub>4</sub> ~ 100; HNO<sub>3</sub> ~ 10; Se ~ 0,015. Obtained adsorption and elution curves for rhenium and molybdenum are shown on the Figures 9 and 10, and some calculated characteristics are in the Table 3.

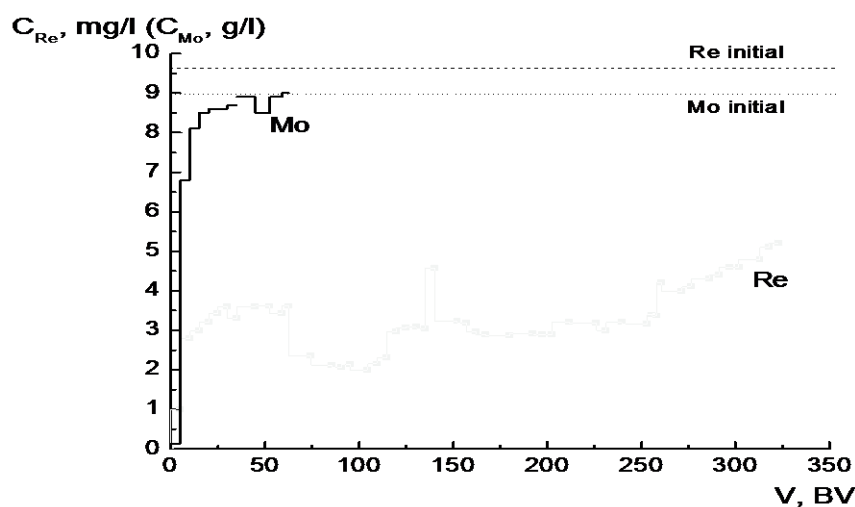


Figure 9. Rhenium adsorption curves from a real solution for A170 resin

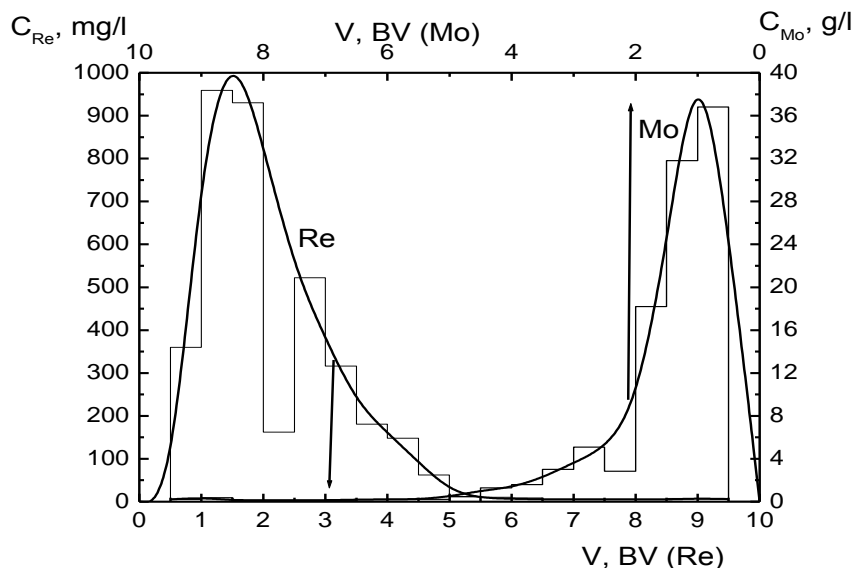


Figure 10. Rhenium and molybdenum elution curves from loaded A170 resin by 7 M ammonia

Rhenium concentration in the eluates appeared to be low. So, the second stage of rhenium ion-exchange concentration following by the ammonia distillation from the primary eluates is needed for the rhenium recovery. Both A170 and A172 resins are applicable for the secondary rhenium concentration from primary eluates, if optimal pH conditions would be provided (Figure 11, 12; Table 3).

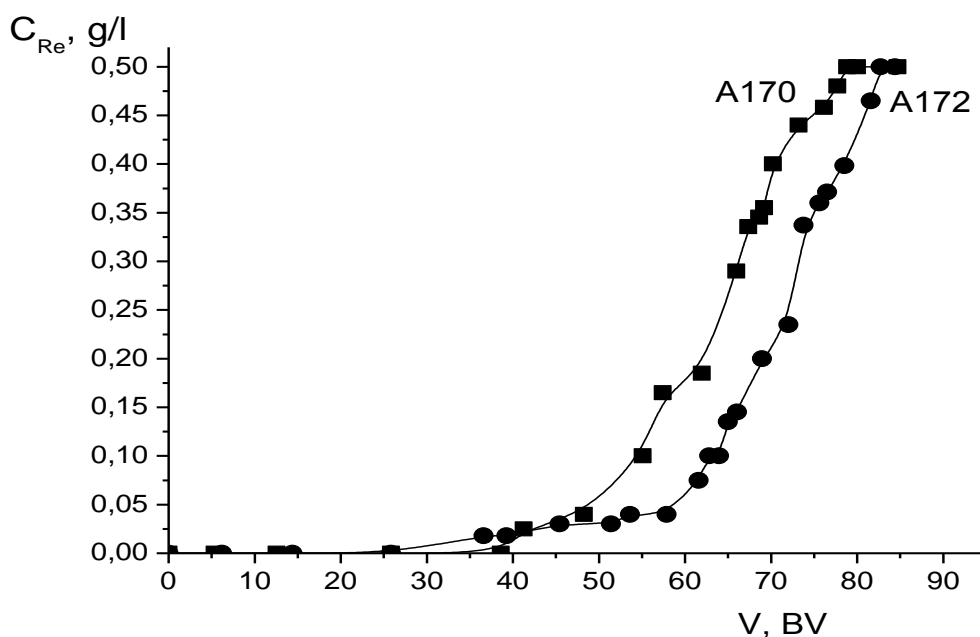


Figure 11. Re and Mo adsorption curves on secondary rhenium concentration (Initial Re concentration of 0,5 g/l, Mo of 15 g/l, and  $\text{NH}_4\text{NO}_3$  of 0,35 mole/l)



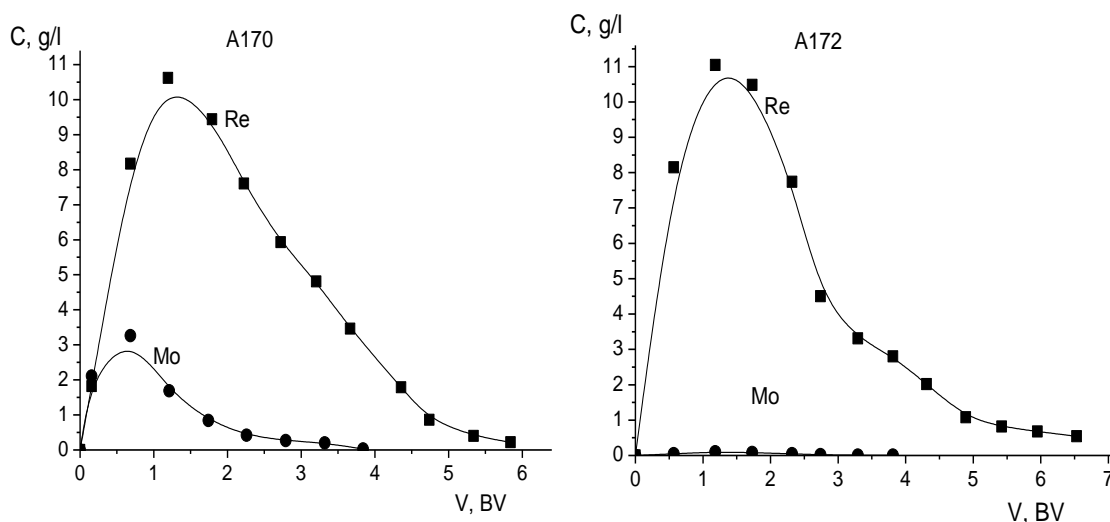


Figure 12. Re and Mo elution curves on secondary rhenium concentration by 6 M ammonia

Table 3. Sorption and elution characteristics of rhenium and molybdenum recovery according to the column experiment with A170 and A172 resins

Stage	Resin	Re in loaded resin, mg/ml resin	Re stripping, mg/ml resin		Re:Mo ratio		K <sub>Re</sub> / K <sub>Mo</sub>	K <sub>Re conc.</sub>
			Re	Mo	feed	eluate		
I	A170	2,0	1,85	51,0	0,00107	0,036	33,9	37,5
II	A170	31,5	28,5	3,9	0,033	7,3	221,2	10,36
Σ I+II	A170	–	–	–	–	–	6822	540
II	A172	34,8	30,1	0,17	0,033	177,1	5365	9,26
Σ I+II	A170(I)+ A172(II)	–	–	–	–	–	165514	482

## Conclusions

The possibility of rhenium recovery from the molybdenite concentrates processing solutions by means of macroporous and gel anion exchange resins Purolite A170 and Purolite A172 has been investigated. As a result A172 resin is proposed for the rhenium recovery from the acidic sulfate solutions from the roasting gas treatment system, and A170 is proposed for the rhenium recovery directly from the pregnant solutions of autoclave leaching molybdenite concentrates with nitric acid. Both A170 and A172 resins are applicable for the secondary concentration of rhenium from primary eluates if optimal pH conditions would be provided.

## References

1. A.N. Zelikman, B.G. Korshunov. Metallurgiya redkih metallov. Moscow: Metallurgiya, 1991. 432 p.
2. L. V. Borisova, A.N. Ermakov. Analiticheskaya chemia reniya. Moscow: Nauka, 1974. 319 p.  
A.I. Busev, V.G. Tintsova, V.M. Ivanov. Rukovodstvo po analiticheskoy chemii redkih metallov. Moscow: Chemia, 1978. 423 p.

3.P2.

## RHENIUM PHYTOMINING BY ALFALFA (*MEDICAGO*) FROM SOILS OF ORE DRESSING REGIONS AT LABORATORY CONDITIONS

Christina Tzvetkova<sup>1</sup>, Ognyan Bozhkov<sup>1</sup> and Ludmila Borisova<sup>2</sup>

e-mail:icho68@abv.bg

<sup>1</sup>Institute of General and Inorganic Chemistry, Bulgarian Academy of Sciences,  
Acad. G. Bontchev Str., bl. 11, Sofia, 1113 Bulgaria

<sup>2</sup>Vernadsky Institute of Geochemistry and Analytical Chemistry, Russian Academy of Sciences, Kosygina str. 19,  
Moscow, 119071 Russia

**Keywords:** rhenium, phytomining, alfalfa, soils, copper mines

### Abstract:

Rhenium is dispersed in surface environment of copper ore dressing and work processing regions as a  $\text{ReO}_4^-$  and volatile  $\text{Re}_2\text{O}_7$  that is converted to  $\text{ReO}_4^-$  in contact with water. The unique property of rhenium to accumulate as a  $\text{ReO}_4^-$  in the green over ground parts of vegetation could be used for its collection from the environment of these regions, i.e., for phytomining. The present work deals with the application of discovered by us Re hyperaccumulator -alfalfa (*Medicago*) for collection of dispersed Re from the soil near the depot of Cu concentrate of the mine Asarel – Bulgaria. Laboratory experiments for Re extraction with alfalfa from soil of mine Asarel were carried out. The results showed that 35 days after sowing the Re concentration in alfalfa reached the maximum value of 4870 g Re/t ash. Simple calculations show that 1t alfalfa ash could be obtained from 2937 m<sup>2</sup> alfalfa crop and that the profit for the producers will be around 20 000 \$. Moreover phytomining of Re with alfalfa leads to remediation of exhausted soils of mine regions.

### Introduction

Current technologies for the production of rhenium containing concentrates and subsequent rhenium recovery are not effective enough. During these processes, part of the rhenium is lost and dispersed as  $\text{ReO}_4^-$  in the waste industrial solutions and waters and as volatile  $\text{Re}_2\text{O}_7$  that is converted to  $\text{ReO}_4^-$  in contact with water in the surrounding soils. The unique property of rhenium to accumulate in the green over ground parts of vegetation could be used for collection of the rhenium scattered in the environment of copper ore dressing and work processing regions, i.e., for phytomining [1,2]. The best plant hyperaccumulators of Re discovered by us at laboratory conditions are alfalfa (*Medicago*) containing 4.66 % Re in the dry mass and white clover (*Trifolium repens*) – 3.51 % Re in the dry mass [3, 4].

The present work deals with the application of alfalfa (*Medicago*) for collection of the rhenium scattered in the soil near the depot of Cu concentrate of the mine Asarel - Bulgaria.

### Experimental

We took the soil sample near to the depot of copper concentrate of mine Asarel. The bio available form of rhenium in the surface environment is the soluble perrhenate ion ( $\text{ReO}_4^-$ ). An aqueous extract from the soils was made for determination of Re [5]. The pH of the leaching aqueous solution was 8.5-9.0. This indicates that the soil is alkaline. The Re content in the leaching solution was determined by the highly selective and sensitive catalytic method with N, N-dimethyl-dithiooxamide (DMDTO) developed by us [6]. The results of the analysis show that  $C_{\text{Re}} = 5 \mu\text{g Re/g dry soil}$ . The further experiments were carried out as follow:

One plastic plate with soil sample was planted with alfalfa and regularly watered. Three days after seeding, the alfalfa sprouted and further developed small leaves within thirty days. Probably the soil was very exhausted and the plant did not get sufficient nutrient ions for its growth. However, the green mass was harvested on 10 and 35 days after sowing and dried at 70°C in an oven. The dry plant mass was exactly weighed and incinerated at 480° C in a crucible furnace. Re was extracted from the ash by an alkaline solution [7]. The content of Re was determined by the DMDTO method [6]. The results are shown in Table 1.

## Results and discussion

The results of table 1 show that, although the alfalfa species is undeveloped, it accumulates extracts and concentrates Re from contaminated soil. The Re concentration in alfalfa (4869  $\mu\text{g Re/g ash}$ ) exceed around three times that in acacia leaves (1682  $\mu\text{g Re/g ash}$ ) growing on the same soil [8]. The undeveloped alfalfa may be due to the exhausted soil and its alkalinity. It is known that the optimum pH range of soil for alfalfa growing is pH= 6-7 [9], while the exhausted soil from mine Asarel is with pH=8.5-9. The laboratory experiments show that the Re phytoextraction from contaminated and exhausted soils from ore dressing region is really possible. For field experiments agronomists should be consulted with a view to optimize the conditions for development of alfalfa. This includes preconditioning of soil, optimization of the depth of ploughing, the quantity of seed per 1000m<sup>2</sup>, the depth of sowing, and the quantity of fertilizer, watering and other [9]. Our opinion is that the well developed alfalfa will accumulate more rhenium.

Tab.1. Rhenium accumulation by undeveloped alfalfa from exhausted soils of mine Asarel ( $C_{\text{Re}}=5\mu\text{g Re/g dry soil}$ )

Plant species	Sampling time after sowing	$C_{\text{Re}}$ $\mu\text{g Re/g dry mass}$	F	$C_{\text{Re}}$ $\mu\text{g Re/g ash}$	F
alfalfa	10 days	593	119	2778	556
alfalfa	35days	1381	276	4869	974
F – Enrichment factor = $C_{\text{Re}}$ in plant/ $C_{\text{Re}}$ in soil					

alfalfa growing is pH= 6-7 [9], while the exhausted soil from mine Asarel is with pH=8.5-9. The laboratory experiments show that the Re phytoextraction from contaminated and exhausted soils from ore dressing region is really possible. For field experiments agronomists should be consulted with a view to optimize the conditions for development of alfalfa. This includes preconditioning of soil, optimization of the depth of ploughing, the quantity of seed per 1000m<sup>2</sup>, the depth of sowing, and the quantity of fertilizer,

watering and other [9]. Our opinion is that the well developed alfalfa will accumulate more rhenium.

## Conclusions

We can conclude that:

1. Alfalfa is suitable for real collection of scattered rhenium from soils of ore dressing regions.
2. Simple calculations show that 1t alfalfa ash could be obtained from 2937 m<sup>2</sup> alfalfa crop. With Re concentration = 4870 g Re/t ash at a current price of Re = 4 500\$/kg, the profit for the producers will be around 20 000 \$, after deducting the cost of production.
3. Cultivation of alfalfa on the exhausted soils of mine regions leads to their remediation. For example, after being sowed with alfalfa for three years, 1000 m<sup>2</sup> soil was enriched with 7 kg P<sub>2</sub>O<sub>5</sub>, 12 kg Ca, 20 kg N<sub>2</sub> and 9 kg K<sub>2</sub>O. This exceeds the average norm for fertilization of agriculture soils [10].
4. Application of Re phytomining in ore dressing regions would result in remediation and purification of the environment in these districts.

## References

1. O. Bozhkov, Chr. Tzvetkova and T. Blagoeva, Proceedings of the 1st International Conference on Waste Management, Water Pollution, Air Pollution, Indoor Climate(WWAI'07), Published by WSEAS Press, ISBN: 978-960-6766-09-1, Arcachon, France, October 13-15, 2007, pp. 257-261.
2. O. Bozhkov, Chr. Tzvetkova, L. Borisova, V. Ermakov and V. Ryabukhin, *Trends in Inorganic Chemistry*, review, **9**, 1- 10, 2006,.
3. Chr. Tzvetkova and O. Bozhkov, Proceedings of the 2nd International Conference on Waste Management, Water Pollution, Air Pollution, Indoor Climate(WWAI'08) Published by WSEAS Press, ISBN:978-960-474-017-8, Corfu, Greece, October 26-28, 2008, pp. 82- 85.
4. Chr. Tzvetkova and O. Bozhkov, Proceedings of the 7<sup>th</sup> WSEAS International Conference on Environment, Ecosystems and Development (EED '09), Published by WSEAS Press, ISBN: 978-960-474-142-7, Puerto De La Cruz, Tenerife, Canary Islands, Spain, December 14-16, 2009, pp. 123-126.
5. O. Bozhkov, Chr. Tzvetkova, Proceedings of the 7<sup>th</sup> WSEAS International Conference on Environment, Ecosystems and Development (EED '09), *Published by WSEAS Press*, ISBN: 978-960-474-142-7, Puerto De La Cruz, Tenerife, Canary Islands, Spain, December 14-16, 2009, pp. 127-131.
6. O. Bozhkov and L.V. Borisova, *Anal Communications*, **33**, 133-135, 1996.
7. Ognyan D. Bozhkov and Luydmila V. Borisova, *Intern. J. Environ. Anal. Chem.*, **83**, N 2, 135-141, 2003.

8. O. Bozhkov, Chr. Tzvetkova and T. Blagoeva, Proceedings of the 2<sup>nd</sup> WSEAS International Conference on Waste Management, Water Pollution, Air Pollution, Indoor Climate, (WWAI'08) Published by WSEAS Press, ISBN:978-960-474-017-8, Corfu, Greece, October 26-28, 2008, pp. 262-265.
9. Alison M. Bowman, W. Smith and J. Brockwell, *Soil Biology and Biochemistry*, **36**, 8, 1253-1260, 2004.
10. L. Talgre<sup>1</sup>, E. Lauringson<sup>1</sup>, H. Roostalu, A. Astover, *Agronomy Research*, **7**(1), 125-132, 2009.

3.P3.

## RHENIUM RECOVERY FROM GAS-PURIFICATION WASTES OF THE KOLA MINING COMPANY

A.G. Kasikov, A.M. Petrova, N.S. Areshina, A.A. Blokhin, E.E. Maltseva

Institution of Russian Academy of Sciences – I.V.Tananaev Institute of Chemistry and Technology of Rare Elements and Mineral Raw Materials of the Kola Science Centre of RAS  
(Akademgorodok, 26a, Apatity, Murmansk reg., Russian Federation)

**Keywords:** rhenium recovery, gas-purification wastes, solvent extraction, ion exchange sorption

### Abstract

Several variants of hydrometallurgical processing of gas-purification wastes resulting from a copper-nickel process, whereby rhenium is extracted and purified, are proposed. For dust- and gas purification solutions, a complex solvent technology based on rhenium, osmium and H<sub>2</sub>SO<sub>4</sub> solvent extraction by tertiary amines has been developed. From gas-purification fine dust, rhenium can be extracted by aqueous leaching, whereupon it is isolated from solution by using solvent extraction or ion-exchange sorption.

### Introduction

As the result of pyrometallurgical digesting of sulphide copper-nickel minerals of the Kola MMC JSC (Murmansk region, Russia) vast volumes of sulphur dioxide enriched in some volatile compounds, including Re<sub>2</sub>O<sub>7</sub> are turned out. When the gas is purified, rhenium mostly concentrates in solutions of the wet gas purification system (GPS) and, partly, in fine dust of the GPS electric precipitators. At Severonikel JSC (Kola MMC), the rhenium content in wet GPS solutions achieves 8-15 g/L. In view of sizable volumes (~10000 m<sup>3</sup> per year), these wastes can be regarded as a considerable source of rhenium. The fine dust captured by electric filters in the GPS may contain as much as 30-40 g/t Re, which is also attractive for commercial extraction. Nowadays, however, rhenium is not extracted from these wastes being lost during their utilization.

### Experimental

In this work, we used industrial specimens of the GPS system at Severonikel Plant (Kola MMC JSC) – washing sulphuric acid solutions containing, g/L: 300-500 H<sub>2</sub>SO<sub>4</sub>, 1-5 Ni, 1-3 Fe, 1-5 Cu, 0.05-0.2 Zn, 0.003-0.01 Os, 0.002-0.015 Re; acidic discharge of flue ducts (“flue sludges”), containing, g/L: 1300-1700 H<sub>2</sub>SO<sub>4</sub>, 0.5-1.0 Se, 0.015-0.02 Os, 0.001-0.01 Re; and also fine converter dust of the GPS of the Pechenganikel Plant (Kola MMC JSC). By examining the dust phase composition, we found that fairly high rhenium contents can pass to solution by way of aqueous leaching during 1 h at the temperature of T~80°C (S:L=1:5). The resulting solution contained, g/l: 8.0 Ni, 4.9 Cu, 13.0 As, 13.7 Fe, 6.3 Zn, 0.017 Mo, 0.005 Re, pH=0.8.

Large-scale laboratory testing of rhenium solvent extraction from process solutions was carried out at a laboratory cascade of mixer-settler extractors designed and made at ICTREMRM KSC RAS. As a reagent, TiOA solutions of Hostarex A324 brand admixed with “pure”-grade 2-octanol were employed.

The sorption experiments proceeded under dynamic conditions in a glass column filled with a weakly basic macroporous anionite Purolite of A170 brand, in which the ratio of the anionite layer height to the column inner diameter was 10:1.



## Results and Discussion

For rhenium extraction from wet GPS solutions, we developed a complex technology providing for  $H_2SO_4$ , Re and Os extraction. Since solvent extraction of solutions containing  $>850$  g/L  $H_2SO_4$ , is of little effect, it was proposed to undertake rhenium extraction from the strongly acidic flue sludges after they are diluted with washing acid, so that the GPS solutions were processed simultaneously. The extragents in this case were 30% TiOA in 2-octanol and pure 2-octanol. As can be seen from Fig.1, the mixture with tertiary amines is more effective.

Moreover, the 30% TiOA and 2-octanol mixture effectively extracts  $H_2SO_4$  from gas-purification solutions, which is obtained after aqueous re-extraction. Rhenium and osmium accumulate in the circulating organic phase. The rare metal-rich extragent should be regularly subjected to deep re-extraction with alkalis. After osmium separation and additional extractive concentration, a marketable ammonium perrhenate can be obtained. A schematic diagram of the complex extraction technology for wet GPS solutions, yielding rhenium, is presented in Fig. 2.

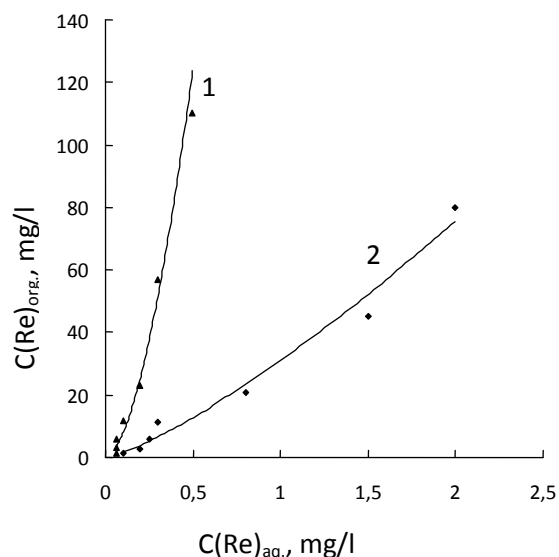


Fig. 1. Isotherm of rhenium(VII) extraction from wet gas purification system solution  
1 – 30% TiOA+70% 2-octanol;  
2 – 2-octanol;

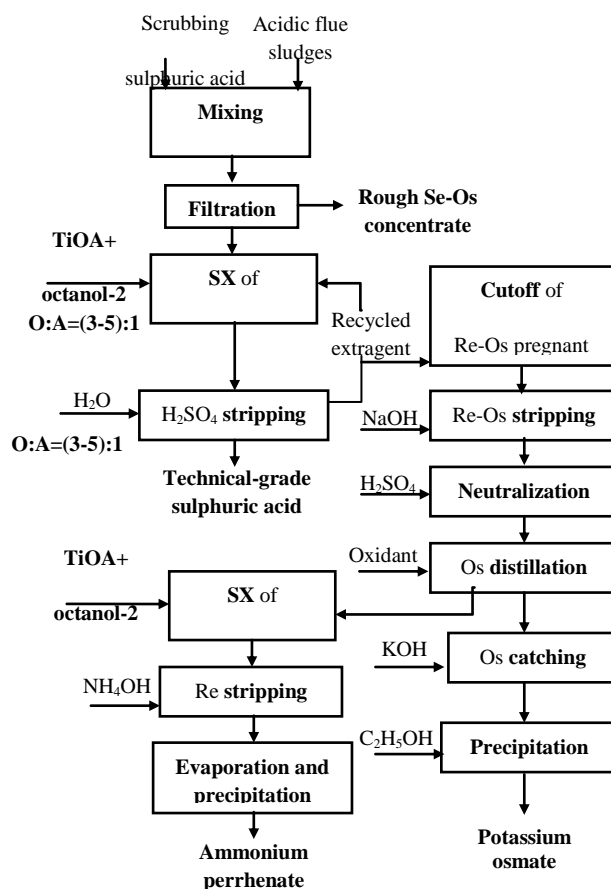


Fig. 2 Comprehensive Solvent Extraction technology of the wet gas purification system wastes of "Severonikel" Plant of Kola MMC JSC.

During the large-scale laboratory testing of the new technology, the scrubbing sulphuric acid from Severonikel Plant was processed at a extractor cascade as the result of which ~70% H<sub>2</sub>SO<sub>4</sub> and about 80% Re and 60-70% Os were recovered.

For extracting and concentrating of rhenium from leaching solutions of GPS fine dust, solvent extraction and ion-exchange technologies were applied. The schematic flow-sheet is shown in Fig.3.

Due to very low rhenium concentrations in dust leaching solutions, we have tried pre-concentrating rhenium by using a highly selective Purolite ionite of the A170 brand. 15 L of solution were processed to obtain a desorbat containing 0.2 g/L rhenium and 0.016 g/L molybdenum. The level of Re sorbed out was comparable with that after solvent extraction, but the process selectivity was higher. For practical realization, we recommend the flow-sheet presented in Fig.3, providing a very high Re concentration and removal of most of impurities. Pre-concentration in this case can be done through either solvent extraction or sorption.

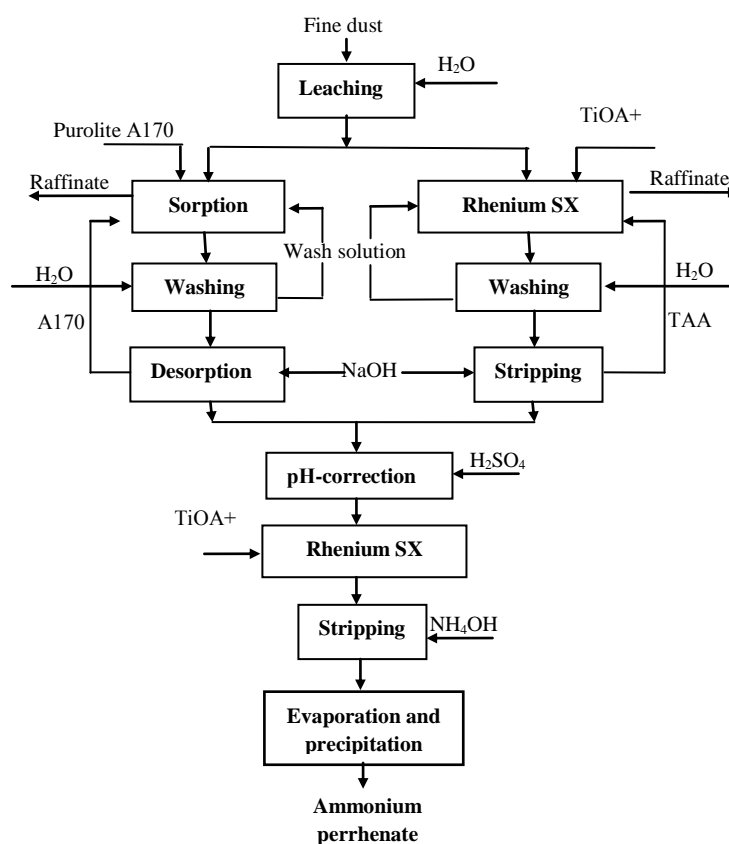


Fig. 3 Hydrometallurgical technology of rhenium recovery from fine dust of the gas purification system of “Pechenganikel” Plant of Kola MMC JSC.

### Conclusion

The aim of this work was to find methods for rhenium extraction from wastes of dust-and-gas purification systems at copper-nickel smelters. As the result, several variants of hydrometallurgical processing have been proposed.

3.P4.

## SOLVENT EXTRACTION OF RHENIUM(VII) FROM ACID SOLUTIONS WITH HIGH-MOLECULAR ALIPHATIC ALCOHOLS

A.G. Kasikov, A.M. Petrova

An Institution of the Russian Academy of Sciences - I. V. Tananaev Institute of Chemistry and Technology of Rare Elements and Mineral Raw Materials of Kola Science Centre of RAS (Akademgorodok 26a, Apatity, Murmansk reg., Russian Federation)

**Keywords:** rhenium, solvent extraction, high-molecular alcohols, acid solutions

### Abstract:

Rhenium(VII) extraction by high-molecular aliphatic alcohols C<sub>8</sub>-C<sub>12</sub> from HCl and H<sub>2</sub>SO<sub>4</sub> solutions, including the effect of alcohol structure and aqueous phase acidity on rhenium(VII) distribution coefficient, have been investigated. As efficient extracting agents, secondary aliphatic alcohols C<sub>8</sub>-C<sub>12</sub> are proposed. A new solvent-extraction method for extracting rhenium(VII) from acidic solutions by using secondary aliphatic alcohols has been developed and pilot-scale tested.

### Introduction

High-molecular aliphatic alcohols have been widely used for solvent extraction of metals from acidic solutions [1]. Regarding their physicochemical properties, aliphatic alcohols containing 7–10 carbon atoms in the hydrocarbon chain satisfy the major requirements posed on commercial extractants (poor solubility in aqueous phase, high flash point, low density, and low viscosity, providing both a fast phase segregation and chemical stability). In terms of extracting ability to rhenium(VII), alcohols rank below amines and organophosphorus compounds, but exhibit better selectivity, at the same time being less expensive. Furthermore, with such alcohols, there is no need to use any diluents and modifiers, which simplifies extraction systems.

In this work, rhenium(VII) extraction by C<sub>8</sub>-C<sub>12</sub> alcohols from acidic sulphate and chloride solutions has been investigated.

### Experimental

In this work, we used the following higher aliphatic alcohols produced in Russia: 1-heptanol, 2-heptanol, 4-heptanol, 1-octanol, 2-DL-octanol, 1-nonanol, 1-decanol, 4-decanol, 2-dodecanol of the “pure” brand, as well as the imported undiluted 3-octanol of the 97.8% “for synthesis” brand. The extractants were saturated with the respective mineral acid to preclude its extraction in the process of rhenium(VII) extraction. The acidic rhenium(VII) model solutions were prepared by diluting the initial NH<sub>4</sub>ReO<sub>4</sub> solution prepared from a salt of the “pure” brand together with certain amounts of a high-purity mineral acid.

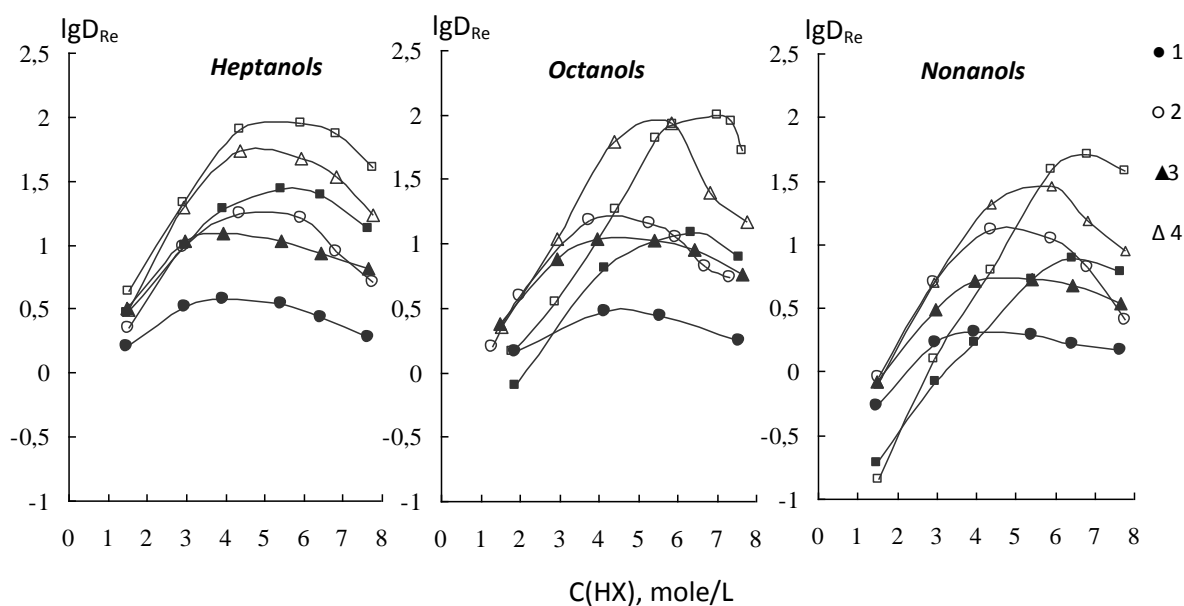
Extraction was performed in 0.05 L in size, plugged calibrated cylinders which were agitated manually at room temperature (T=20±1°C). The phase ratio during the extraction was A/O=1 and the contact time was 5 min, which allowed to achieve equilibrium.

The rhenium(VII) content in the aqueous phase was determined by the color intensity of the Re(IV) thiourea complex forming in the presence of reducing SnCl<sub>2</sub> by measuring the light absorption at λ=390 nm [2]. The rhenium(VII) concentration in the organic phase was calculated by the difference between the contents in the aqueous phase before and after extraction. Mineral acid concentrations in solutions were determined by titrimetrically.

### Results and Discussion

It has been established that, notwithstanding the satisfactory performance of C<sub>10</sub>-C<sub>12</sub> alcohols during the rhenium(VII) extraction from acidic solutions, the increasing hydrocarbon radical length tends to promote etherification with mineral acid, creating compounds with surfactant properties in the

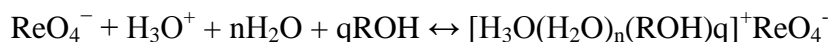
organic phase. This hinders separating of the phases in the aqueous-organic systems, especially at the alkali stripping stage. Therefore alcohols like 1-decanol and 2-dodecanol can hardly be acceptable as extractants from acidic solutions. The extracting ability of C<sub>7</sub>-C<sub>9</sub> alcohols with regard to rhenium(VII) is shown in Fig. 1.



$C_{init.}(Re)=10^{-3}$  mole/l,  $O/W=1/1$ , extraction from  $HCl$  (1, 3, 5) and  $H_2SO_4$  (2, 4, 6).  
Heptanols: 1-heptanol (1, 2), 2-heptanol (3, 4), and 4-heptanol (5, 6);  
Octanols: 1-octanol (1, 2), 2-octanol (3, 4), and 3-octanol (5, 6);  
Nonanols: 1-nonanol (1, 2), 2-nonanol (3, 4), 4-nonanol (5, 6).

Fig. 1. Rhenium(VII) distribution coefficient  $D_{Re}$  vs. mineral acid concentration in the aqueous phase  $C(HX)$  during the extraction from  $HCl$  and  $H_2SO_4$  solutions with aliphatic alcohols  $C_7-C_9$ .

For all these alcohols, rhenium distribution coefficients  $D_{Re}$  are greatly dependent on the mineral acid concentration in the aqueous phase with an extraction maximum at approximately 4-7 mole/L, depending on the alcohol type. Initially,  $D_{Re}$  increases with increasing solution acidity due to the presence of  $H^+$  participating in extraction according to the hydrate-solvate mechanism:



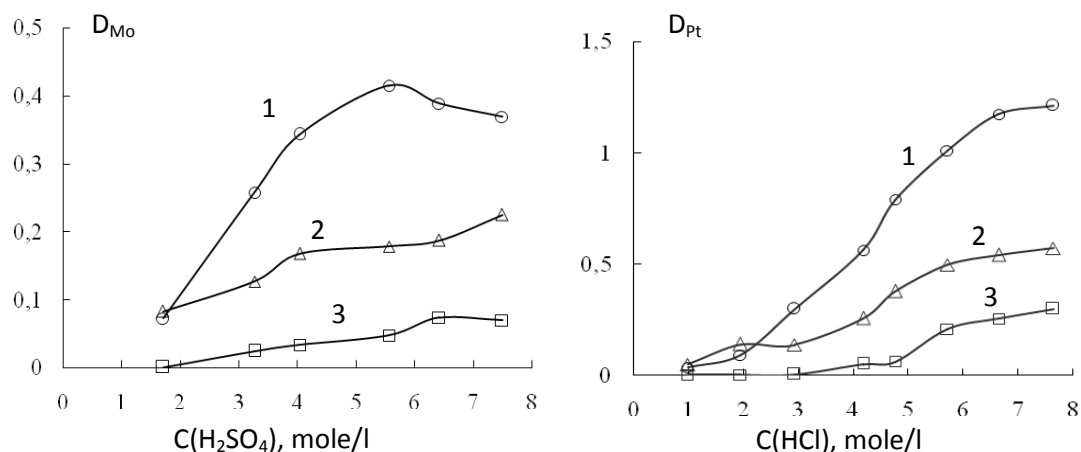
It is evident that, due to increasing  $H^+$  concentration, the equilibrium shifts to the right.

The  $D_{Re}$  diminishes in the more acidic region in response to the competing process of mineral acid extraction by alcohol.

On transition from primary to secondary alcohols, their extractive ability regarding rhenium(VII) enhances. This must be caused by the fact that the basicity of secondary alcohols is higher than that of primary alcohols due to intensifying +I inductive effect exerted by the alkyl substituent when changing from primary to secondary alcohols having the OH-groups in positions 2, 3, and 4.

Simultaneously, this dependence on the alcohol structure was observed when extracting single-charged complex anions from sulphate and chloride solutions; at the same time, the double-charged anion complexes were better extracted by primary alcohols.

For instance, during the extraction of double-charged  $MoO_2(SO_4)_2^{2-}$  и  $PtCl_6^{2-}$  anion complexes from acidic solutions using octyl alcohol isomers an inverse relationship between the  $D_{Mo}$  and  $D_{Pt}$  distribution coefficients and the alcohol structure was observed (Fig.2):



$C_{init.}(Me)=10^{-3}$  mole/l,  $O/W=1/1$   
 1-octanol (1), 2-octanol (2), and 3-octanol (3);

Fig. 2. The effect of octyl alcohol structure on molybdenum(VI) and platinum(VI) distribution coefficient  $D_{Mo}$  and Re/Mo separation coefficient  $K_{Re/Mo}=D_{Re}/D_{Mo}$  in solvent extraction from sulphuric acid media.

Apparently, these dependencies are the result of steric complications emerging when multiply charged complexes are extracted by secondary alcohols. The dissimilar ability of primary and secondary alcohols to extract differently charged metal complexes can be harnessed to separate rhenium(VII) from platinum(VI) and molybdenum(VI) while processing secondary rhenium-containing raw materials.

### Conclusion

Our research findings were used to develop a new extraction method for selective recovery of rhenium(VII) with secondary aliphatic alcohols as extractants, which is covered by an RF patent [3].

### References

- Z. I. Nikolotova, N. A. Kartashova, Handbook of Solvent Extraction. Solvent Extraction with neutral organic compounds (Rus), Atomizdat: Moscow (1976) vol. I.
- L. V. Borisova, A. N. Ermakov, Analytical chemistry of rhenium (Rus), Nauka: Moscow (1974).
- RF Patent 2330900, MPK S22V 61/00, S22V 3/26. A method for rhenium (VII) extraction from an acid solution / A.G.Kasikov, A.M.Petrova (RF) – №2006142845/02; Appl. 04.12.06; Publ. 10.08.08. Bull. № 22.



3.P5.

## **PRODUCTION OF THE HIGH PURITY NH<sub>4</sub>REO<sub>4</sub> USING ELECTRODIALYSIS METHOD**

A.A. Palant, O.M. Levchuk, A.M. Levin, O.V. Reshetova

IMET RAS, Moscow, reshetovaolga@list.ru

At the last years in Europe it was passed new high standards to the NH<sub>4</sub>ReO<sub>4</sub> quality.

Our long-termed experience shows that standard method of recrystallization doesn't produce NH<sub>4</sub>ReO<sub>4</sub> of high quality. The objective of this work was the investigation of the ability of the ultra pure NH<sub>4</sub>ReO<sub>4</sub> producing. For this problem solution the process flowsheet was used: NH<sub>4</sub>ReO<sub>4</sub> – electro dialysis synthesis – NH<sub>4</sub>ReO<sub>4</sub> by ammonia precipitation.

In this paper NH<sub>4</sub>ReO<sub>4</sub>, which contains next impurities, %: Na, Mg, Mn, Al, Ni, S – 0.002, Mo – 0.01, Cu, Fe – 0.01, was studied. The investigations were carried out in the three-cell electro dialysis apparatus, which have included two membranes: the first was MA-41IL and the second was MK-40. At the first time it was added 5 g/l of the HNO<sub>3</sub> to the anodic cell, where bidistilled water was, and 100 g/l of the HNO<sub>3</sub> to the cathodic cell. NH<sub>4</sub>ReO<sub>4</sub> was periodically added to the middle cell. It was producing the pregnant solution of the HReO<sub>4</sub> with C<sub>Re</sub>=400 g/l as a result of electro dialysis. From this solution NH<sub>4</sub>ReO<sub>4</sub> was precipitated by NH<sub>4</sub>OH using standard method.

The process conditions were: I=2.5-5.0 A, U=18-25 V, temperature in the anodic cell was 20-30°C, in the middle cell 25-40°C.

NH<sub>4</sub>ReO<sub>4</sub> crystals contain next impurities, %: Fe – 0.00008 (0.0005), Al – 0.0001(0.0001), Cu – 0.00005 (0.0001), Mo – 0.00005 (0.0005), Ni – 0.00005 (0.0001), Mn – 0.00005 (0.0001), Mg – 0.00005 (0.0001), Ca – 0.00016 (0.0005), Na – 0.00006 (0.0005), K – 0.00004 (0.0005), Cr – 0.00005 (0.0001) (in parentheses it are maximum permissible concentration of the impurities in accordance with new European regulations).

3.P6.

## REGULARITIES OF RHENIUM SALTS OXIDIZING LEACHING

R. Dj. Allabergenov, H. T. Sharipov, R.H. Sharipov, A. A. Niyazmatov

SE «The Central laboratory» under The State Committee of the Republic of Uzbekistan on Geology and Mineral Resources - The Tashkent institute of chemical technology

**Keywords:** rhenium heptasulfide, oxidation, hydrogen peroxide, sodium nitrite oxidation-reduction potential

### Abstract:

In the article are presented mechanism and results of kinetic researches of rhenium oxidizing leaching from sulfide raw materials. The main processing factors, allowing to provide maximal rhenium extraction are determined.

### Introduction

The basic forms of rare metals composing a sulphide concentrate, extracted from the molybdenum production solutions, are rhenium heptasulfide and molybdenum and tungsten trisulfides. The heptasulfide form of rhenium ( $\text{Re}_2\text{S}_7$ ) constituent concentrate — black substance, almost insoluble in water, hydrochloric acid, 50 % sulfuric acid; dissoluble in hydrogen peroxide, nitric acid, mixture of caustic soda or ammonia water with hydrogen peroxide. The  $\text{Re}_2\text{S}_7$  disoxidates to metal during red-heating in hydrogen flow, and when heating in air it ignites generating  $\text{Re}_2\text{O}_7$  and  $\text{SO}_2$  [1-3]. It is the first experience of technological estimation of rhenium sulphide concentrate oxidative catalytic leaching in sulfuric medium in the presence of sodium nitrite and oxygen in conditions of rarefication.

In this connection, and considering that it is necessary to utilize rhenium heptasulfide, resulting in process of the molybdenum production tails utilization, and study of regularities of this leaching form is actual. There are scientific novelty and practical use perspectives. Investigations were conducted by means of the rhenium sulphide concentrate leaching method in a way of disperse phases dissolution. This way is the closest to real technological conditions and allows to receive necessary data on optimum parameters of process, suitable for industrial scaling, immediately during experiments.

### Experimental

The analysis of rhenium concentration was carried out by ICP/MS «Agilent-700» and atomic-absorption spectrophotometer «Zeenit-700», the redox potential in solutions was measured by Ionmeter-74.

### Results and Discussion.

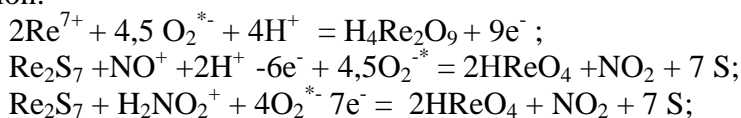
According to the data presented in literature and results of investigations, leaching in acid solutions in oxidizing conditions in the presence of sodium nitrite and oxygen allows to obtain maximal decomposition of various thrust raw materials. By way of examples of various raw materials leaching (table № 1) with maximal decomposition of the basic component is shown, that for breakage of the strongest type of bond - covalent bond - increased oxidation-reduction potential of media (above 740 millivolt) is required, and for breakage of ionic bond - the main bonding power in minerals and sediments - oxidation-reduction potential of media can be more lower than 720 millivolt.

Table 1. Optimum experimental values of oxidation-reduction potential for real hydrochemical systems (The technological mode of experiments is resulted on fig. №1)

№	Raw material	The basic mineral of raw material	Bond type in base minerals of raw material	Crystal structure	Experimental oxidation-reduction potential of raw material full decomposition, millivolt by chlorine-silver electrode
1	Nickel matte	Alloy of Ni, NiS, CuS	Basically covalent	Lump fritted material	780-800
2	Cement cooper	$\text{Cu}^0 + \text{Zn}(\text{OH})_2$	Basically covalent	Metallized material in the form of a powder	740-760
3	Molybdenic end product	$\text{MoS}_2$	ionic bond	Hexagonal layer structure, trigonal prisms	720-740
4	Rhenium concentrate	$\text{Re}_2\text{S}_7$	ionic bond	Amorphous black powder	700-720
5	Cooper concentrate	$\text{CuFeS}_2$	ionic bond	In structure tetrahedrons $[\text{Cu}^{\text{I}}\text{S}_4], [\text{Fe}^{\text{III}}\text{S}_4], [\text{SCu}_2\text{Fe}_2]$	690-710
6	Sulfur concentrate	$\text{FeS}_2$	ionic bond	Type of lattice - cubic	605-625
7	Vanadium catalysts	$\text{NaVO}_3, \text{KVO}_3, \text{VOSO}_4$	ionic bond	Crystal salts	490-520
8	Nickel accumulators	$\text{Ni}(\text{OH})_2$	ionic bond	Amorphous sediment	490-510
9	Fine powder of copper smeltery	$\text{CuSO}_4 \text{ CuS}$	ionic bond	Crystal salts	385-400

This makes it possible to draw a conclusion that different minerals decomposition is actually defined by uniform parameter - oxidation-reduction potential of leaching solution. Simplicity of the process parameters control and possibility to predict its results are advantages of the revealed regularity which proves, that oxidation-reduction potential is the effective characteristic allowing to minimize search of an optimal technological mode of leaching. For this purpose it is recommended to model system «acid-water-oxygen-sodium nitrite», used as leaching media which should provide oxidation-reduction potential in the presence of one or another raw material in specified interval, that guarantee high parameters of process acidic oxidative catalytic leaching.

It is necessary to maintain pulps oxidation-reduction potential on a defined level depending on mineralogical and chemical composition of raw material. Control of oxidation-reduction potential should be implement according to consumption of reagents, providing necessary hydrodynamic regime in a non-standard leaching reactor with deep gasmain for oxygen and simultaneous contact of solid, liquid, steam and gas phases by means of the original mechanism of agitation. Observance of the specified requirements provides realization of oxidation-reduction processes in a working space of the reactor, excluding any emissions to surrounding environment. This data are of scientific and practical interest for recycling and processing of various thrust mineral raw materials. Behaviour of rhenium in these conditions can be described by the following chemical model. This model demonstrates reactions of formation super rhenium  $\text{H}_4\text{Re}_2\text{O}_9$  and rhenium  $\text{HReO}_4$  of acids in solution:



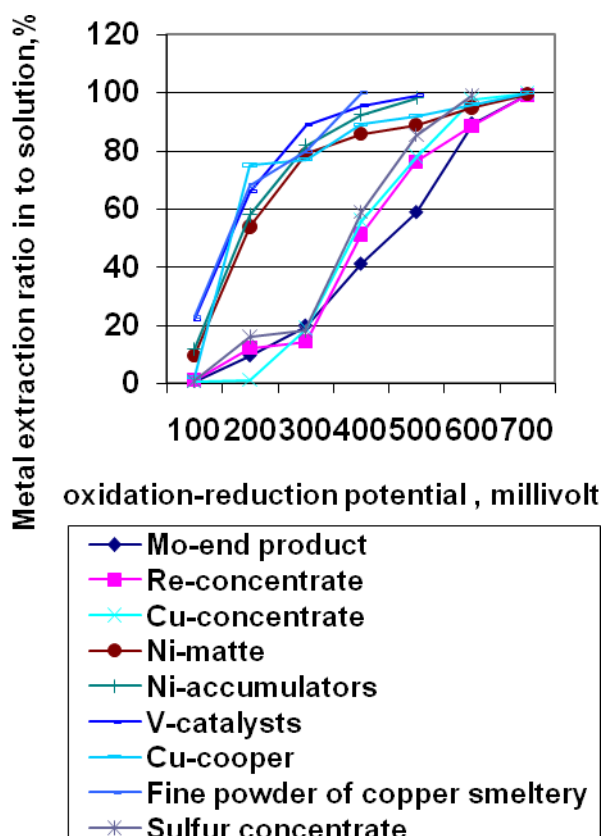
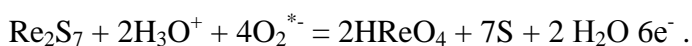


Fig. 1. Influence of oxidation-reduction potential of sulfuric solution (200 g/l  $\text{H}_2\text{SO}_4$ ) in the presence of  $\text{NaNO}_2$  (0,7 g/l) and oxygen (partial pressure 80 pascal or  $0,8 \cdot 10^{-3} \text{ atm.}$ ) on rate of metals extraction from different raw materials; temperature 75-80°C; S:L = 1:4-5; duration of mixing - 60 minutes; number of revolutions - 600 per minute; pH-1,5; rarefication -10-60 millimeter of water (below atmospheric).

The active beginning and the motive force of these processes are radicals: nitrosonium ( $\text{NO}^+$  or  $\text{H}_2\text{NO}_2^+$ ), superoxide oxygen ( $\text{O}_2^{*-}$ ) and oxonium ion ( $\text{H}_3\text{O}^+$ ). These radicals are generated in a working space of a leaching reactor and serve for rhenium extraction in to solution through the mechanism of oxidation-reduction. The oxidation-reduction mechanism consists in a process when sulphur is oxidising to atomic  $\text{S}^{2-} - 2\text{e}^- = \text{S}$ , nitrosonium ion is reducing to nitrogen oxide  $\text{NO}^+ + 1\text{e}^- = \text{NO}$ , and nitrogen oxide is oxidising to dioxide  $\text{NO} + 1\text{O}_2^{*-} + 1\text{e}^- = \text{NO}_2$  which in aqueous medium forms nitrogenous acid - a source of active radicals. In formation of 4 molecules of nitrogenous acid in a liquid phase participate 5 moles of gas ( $4\text{NO} + \text{O}_2 + 2\text{H}_2\text{O} = 4\text{HNO}_2$ ). Consequently the absolute pressure of a gas phase over a solution declines. This provides rarefication in a reactor. As reaction of nitrogenous acid regeneration is irreversible its rate grows with fall of absolute pressure, and consequently, rate of oxygen consumption with formation of active radicals grows.

Characteristic feature of oxidative catalytic leaching is combination of two processes in one reactor: regeneration of active oxidizers-radicals and their simultaneous consumption. In other words, there is a multiple regeneration of nitrogen oxides directly in a working space of a

reactor at the expense of oxygen. As a result allocation of a gas phase outside the reactor is ruled out and full consumption of oxygen and oxidizers-radicals is provided.

Studying of kinetic mechanisms of rhenium sulfide oxidative leaching indicated, that formation of rhenium and super rhenium acids in sulfuric solution is possible in wide range of oxidation-reduction potential and pH values of leaching media. Oxidation-reduction potential is conditioned by acidity of media, presence of oxygen and sodium nitrite: perceptible oxidation starts at pH-1 and lower, then initiates oxygen consumption, regeneration of nitrogenous acid and growth of metal extraction in to solution. It confirms data about participation of hydroxonium in reactions of active radicals formation in acidic medium which is not enough in the subacidic media.

For maintenance of the maximum regeneration of nitrogenous acid initial acidity should be not lower 100 g/l of sulfuric acid; by pH 0-1 in solutions with oxidation-reduction potential above 600 millivolt decomposition of rhenium heptasulfide occurs without kinetic difficulties; Low initial acidity of sulfuric solution (pH 2-3) not allows to exceed amount of nitrogenous acid regeneration more than 20 % from the initial content; the reason is weak interaction of sodium nitrite and the subacidic media. In this conditions rhenium practically is not oxidised, nitrogen oxide from solution it is not allocated, oxygen is not consumed; in the area of low acidity (pH 3-4) and low concentration of nitrite-ion (0,6-0,7 g/l) raw material oxidation is not observed at all; meanwhile

rate of rhenium leaching linearly increases proportionally to agitating intensity increase. A condition of effective oxidation-decomposition with high rate of nitrogenous acid regeneration is intensive agitation of a pulp by means of a mixer with number of revolutions 600-800 per minute with maintenance rarefaction in a reactor-10-50 millimeters of water; The further increase of revolutions causes decelerating of process rate that apparently is attributed to transient condition of regeneration process.

Dependence of rhenium dissolution rate and nitrite concentration is complicated: up to concentration=0,7 g/l rate of leaching increases; from 0,7 to 2,8 g/l of sodium nitrite - a transient condition; more than 3,5 - g/l rate of rhenium leaching is stabilised.

Rate of rhenium leaching in conditions of initial increasing acidity of media in the range of 5-50 g/l of sulfuric acid increases linearly and a proportionally; when acidity exceeds 50 g/l process rate decreases approximately in the same dependence.

In conditions of oxygen lack in system rate of acid regeneration reaction decreases and rarefaction in reactor reduces to values less than 10 millimeters of water rarefaction degree depends on two factors: amount of nitrogen oxides in a gas phase and rate of oxygen feed in to a reactor. Nitrogen oxides are the catalyst of the oxidising process which function consists in assimilation, i.e. of oxygen solubility increasing.

With temperature growth in an interval 25-100<sup>o</sup>C and moderate decrease of leaching rate is observed; when acidity and temperature of media increasing the rate of leaching increases. However, by acidity is more than 100 g/l of sulfuric acid and temperature is more than 120<sup>o</sup>C leaching process inhibition is observed, probably to result from accludation of elemental sulfur creating diffusive impediments for rhenium leaching and process turns in to intradiffusive area, where rhenium leaching rate characterizes by the rate nitrosonium radical diffusion through a layer of elementary sulphur.

At temperature 60<sup>o</sup>C and initial concentration of sulfuric acid 250 g/l and sodium nitrite concentration 0,7 g/l rhenium leaching proceeds in a kinetic mode without any diffusion difficulties. Oxidation-reduction potential makes 620-630 millivolt [by chlorine-silver electrode]. All other things being equal, but at concentration of sodium nitrite - 2,8 g/l, oxidation-reduction potential of media increases to 700 millivolt, and rhenium leaching rate decreases, that testifies to transition of leaching process in to intra-diffusion area.

Provision of active hydrodynamic regime of leaching is the indispensable condition for technological efficiency of oxidising catalytic leaching of sulphide raw materials. This regime provides maximal contact of all phases of media: «raw material – water – acid - sodium nitrite - oxygen». To this effect are recommended special devices with ejection-circulating agitation or mechanical high-speed agitator with diffuser.

### Conclusions.

Thus, rhenium sulphide concentrate oxidative catalytic leaching in acidic medium in the presence of oxygen and catalyst sodium nitrite in conditions of rarefaction allows to attain maximal rhenium extraction in to solution - 98-99 %. Extraction completeness is provided with amount of oxidising potential of solution which is supported by low concentration of sodium nitrite in the presence of oxygen and by oxidative regime of leaching. The process regime is regulated by technological parameters: acidity, temperature, concentration of sodium nitrite and oxygen and agitation intensity.

### References:

1. R.D. Allabergenov, R. K. Akhmedov, H. S. Sabirov, C. V. Mikhailov, H. R. Sharipov. Main sources of raw materials and ways of rhenium extraction. *Geology and Mineral Resources* 2010 № 5 p.43-48
2. A.A. Polant, I.D. Troshkina, A.M. Chekmarov. Rhenium Metallurgy. Moscow. 2009, 187.
3. G.I. Abashin. Recovery of rhenium from waste non-ferrous alloys, 1960 № 5 p.69-70.





E. Johnstone, A. Nadykto, Ya. Obruchnikova, B. Bryskin, N. Kravchenko, E. Nazarov



3.P7.

## RHENIUM SORPTION FROM URANIUM-CONTAINING SOLUTION BY NANOSTRUCTURED IONITES

I.D. Troshkina, A.V. Shilyaev, N.V. Balanovskiy \*, A.M. Chekmarev, O.A. Chernyadyeva

D. Mendeleev University of Chemical Technology of Russia,  
Miusskaya Sq. 9, Moscow 125047, Russian Federation. E-mail: [tid@rctu.ru](mailto:tid@rctu.ru)  
Federal State Unitary Enterprise Leader Research Institute of Chemical Technology,  
33, Kashirskoye shosse, Moscow 115409, Russian Federation.  
E-mail: [tid@rctu.ru](mailto:tid@rctu.ru)

**Keywords:** rhenium, sorption, acid solution, nanostructured ionites.

### Abstract.

Rhenium is traditionally obtained as by-product in the processing of molybdenite and copper ores concentrates. Limited resources of traditional raw materials in Russia are responsible for the searching of new sources of rhenium. Uranium-containing polymetallic raw material is additional source of rhenium [1]. Rhenium was recovered from uranium ores in USA from 1969 to 1974 (Texas, Susquehanna Corporation).

Effective method of uranium ores processing is the underground leaching. Productive solutions of uranium contain 0.1-0.5 mg/l Re. Rhenium as by-product is recovered by sorption.

The aim of this study is the rhenium recovery in processing of model productive solution of underground leaching of uranium. The sorption of rhenium by nanostructured ionites was used in this paper. The model solution contained: sulfate-ion – 10 g/l; chloride-ion – 1 g/l; rhenium (perrhenate-ion) – 20 mg/l.

Sorption characteristic are investigated in static and dynamic conditions. The equilibrium, kinetic and dynamic data are obtained.

Nanostructured ionites are recommended for rhenium recovery from of productive uranium-containing sulfuric acid solution obtained in processing of ores by underground leaching.

### Introduction

Uranium-containing ores as an additional source of rhenium is known till 1950<sup>th</sup> when rhenium was obtained from molybdenum-uranium ores in amount about 1000 kilos in the USA [2]. In CIS area stratified infiltrative exogenous deposits exploited by underground leaching method are situated in world's biggest uranium province near the Tien Shan region. Rhenium content in ores of this province is from 0.02 to 2 g/1000kg [2].

The possibility of rhenium extraction from mineralized sulfuric solutions imitating the content of underground leaching solutions by new nanostructured styrene-acrylate based ionites was investigated. The synthesis of those ionites was realized in Leader Research Institute of Chemical Technology by N. Balanovskiy and A. Zorina.

### Experimental

On microphoto of ionite's grain cleavage obtained by electron microscopy one can see 200-400 nm sized spheric grains (Fig.1) and 100 nm sized pores between them (Fig.2).

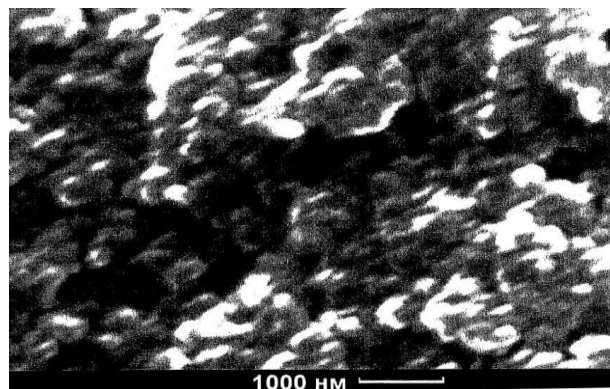


Fig.1. The surface of styrene-acrylate base nanostructured ionite's cleavage

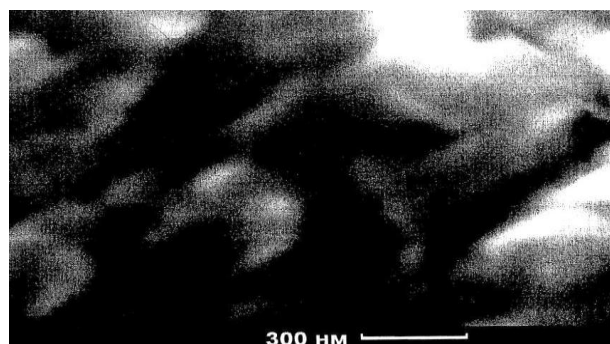


Fig.2. The surface of styrene-acrylate base nanostructured ionite's cleavage with 100 nm pores predominance

Rhenium sorption by nanostructured ionites was produced from model solution [3] containing 20 mg/l of rhenium, 10 g/l of sulfate-ion, 1 g/l of chloride-ion (pH 2). The model of solution concentrations was based on data of underground leaching solution content. Rhenium concentration in those solutions is higher than one in productive underground leaching solutions. The choice of this concentrations is conditioned by sensitivity of photocolometric analysis method based on formation of colored thiocyanate complexes of rhenium in hydrochloric acid solutions [4].

### Results and Discussion.

The results of rhenium sorption by nanostructured ionites from sulfuric solutions are shown in Table1.

Table 1. Rhenium sorption by nanostructured ionites from sulfuric solutions

Ionite	Sorption capacity,		The degree of sorption, %	The distribution coefficient of rhenium, ml/g
	mg/g	mmol/g		
Rossion –25	10,8	0,058	54,2	1181
Rossion –25-35	8,7	0,047	43,5	771
Rossion –25-65	12,6	0,068	63,0	1699
Rossion –62	16,6	0,089	83,2	4939
Rossion –510	16,1	0,087	80,6	4147
Rossion –511	14,8	0,080	74,1	2860
Rossion –610	15,5	0,084	77,7	3488
Rossion –611	14,8	0,079	73,8	2822

Sorption isotherms were obtained by method of alternating portions at room temperature with Rossion-62 and Rossion-510 ionites from sulfuric solutions (pH 2) (Fig.3,4). The linear character of the isotherms obtained (Fig. 3,4) allows to apply the Henry equation to describe.

Henry's constants calculated with least square technique have the following meanings  $(1,48 \pm 0,13) \cdot 10^3$  ml/g for Rossion-62 ionite with correlation coefficient 0.91 and  $(1,88 \pm 0,13) \cdot 10^3$  ml/g for Rossion-510 ionite with correlation coefficient 0.93.

Rhenium sorption dynamic data were performed from solution containing 1.5 mg/l of rhenium by Rossion-62 ionite in column of 7 mm internal diameter and 7 cm length. The flow rate of solution was 1 ml/min. The breakthrough curve is shown on Fig.5.

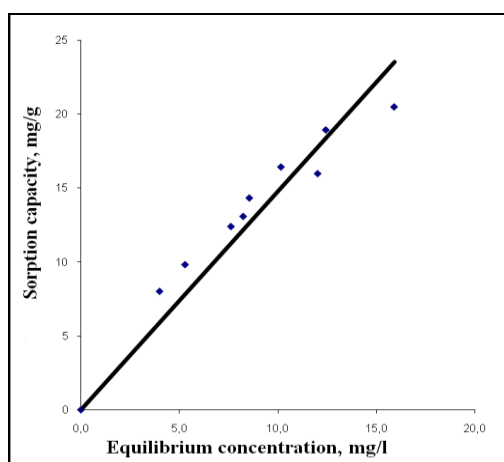


Fig.3. Sorption isotherm of rhenium by ion exchanger Rossion – 62 from sulfuric acid solutions.

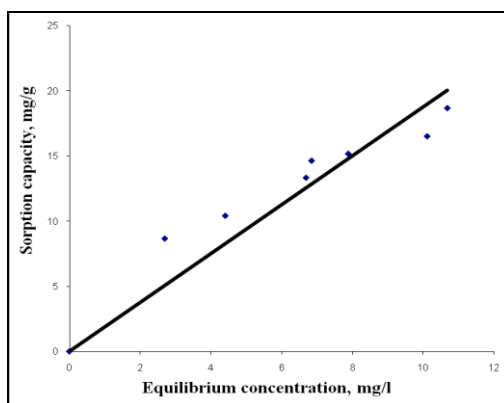


Fig.4. Sorption isotherm of rhenium by ion exchanger Rossion -510 from sulfuric acid solutions.

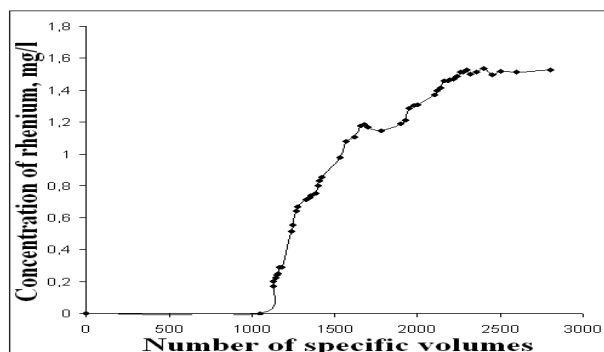


Fig.5. Breakthrough curve of rhenium sorption by Rossion-62 ionite from sulfuric acid solution.

The calculated dynamic parameters of rhenium sorption are shown in Table 2.

Table 2. Calculated dynamic parameters of rhenium sorption

Number of specific volumes to breakthrough solution of rhenium	Number of specific volumes of solution to saturation of the rhenium resin	Total dynamic exchange capacity on rhenium, mg/g
1130	2300	6,8

As can be seen from Fig. 5 and Table 2 rhenium breakthrough occurs after passing 1130 column volume of solution. Complete saturation of the ionite by rhenium occurs by passing through the ionite layer 2300 column volumes of the initial solution. The total dynamic capacity was found to be 6.8 mg/l.

### Conclusions.

On the basis of finding equilibrium and dynamic rhenium sorption data from mineralized sulfuric solutions the applicability of the new nanostructured styrene-acrylate based ionites Rossion-62 and Rossion-510 for rhenium sorption from uranium ores's underground leaching solutions was shown.

### References

1. V.Paretsky, A.Besser, E.Gedgagov, *Non-ferrous metals*. **10**: 17-21 (2008).
2. A.A. Palant, I.D. Troshkina, A.M. Chekmarev, *Metallurgy of Rhenium*, Science: Moscow (2007). 298 p. (rus.)
3. *In-Situ Leaching of Ores*, Academy of Mining Sciences, Publishing House: Moscow (1998). 446 p. (rus.). P. 203.
4. L.V. Borisova, A.N. Ermakov, *Analytical chemistry of rhenium*. M.: Chemistry, 1974. 318 p. (rus.).



3.P8.

## **SORPTION OF PALLADIUM FROM THE RHENIUM-CONTAINING SULFURIC ACID SOLUTION**

A. A. Abdusalomov<sup>1</sup>, I. D. Troshkina<sup>1</sup>, A. M. Chekmarev<sup>1</sup>, N. P. Ismailov<sup>2</sup>

<sup>1</sup> D. Mendeleev University of Chemical Technology of Russia  
(9 Miuskaya sq., Moscow 125047, Russian Federation; tid@rctu.ru)

<sup>2</sup> Tashkent Chemical-Technological Institute  
(32 Navoi str., Tashkent 100011, Republic of Uzbekistan; abdulomov@mail.ru)

**KEYWORDS:** sorption, palladium, rhenium, sulfuric acid solution, ion exchange resins, recovery.

### **ABSTRACT**

Solutions formed during the preparation of sulfuric acid from metallurgical gases of copper and molybdenum production are the main source of rhenium. The possibility of palladium recovery from sulfuric acid solutions by commercial sorbents was studied. The distribution coefficient of palladium sorption is in the range  $3.8 \cdot 10^1 \div 4.0 \cdot 10^4$  cm<sup>3</sup>/g decreasing in the order: TP 214 > D 4384 (Aliquat 336) > TP 207 > AN-105 > CS-PTFE > A170 > MN 202 (TAA) > MP 62 > VP-14KR. Ammonia (8%) and/or hydrochloric acid (4 mol/l) were used to elution of Pd(II) from all of the sorbents examined. Based on data of sorption and elution for the effective associated recovery of palladium from rhenium containing sulfuric acid solutions sorbents Lewatit MonoPlus TP 207 (Lanxess) and Purolite D 4384 can be recommended.

### **INTRODUCTION**

Rhenium is traditionally obtained as by-product in the processing of molybdenite and copper ores concentrates [1].

Rhenium raw materials of Uzbekistan have high complexity with known in recent years a significant share of the platinum metals. The source of the associated recovery of rhenium and platinum group metals is copper-molybdenum deposit of Almalyk's ore field. Its special feature is the presence of radiogenic isotopes of osmium-187 – a product of the decay of rhenium-187, as well as appreciable amounts of palladium, platinum, iridium, ruthenium, rhodium.

New mineral of Uzbekistan's ores - telluride palladium and platinum - the Merenskyite (Fig. 1) was defined [2].

In the smelting of copper concentrates from 6.7 up to 13.2 % of each of the platinum group goes from the gas phase in the dust, caught in a dust chamber and electric filter [3]. Solutions formed during the preparation of sulfuric acid from metallurgical gases of copper and molybdenum production are the main source of rhenium. They contain the sulfuric acid (up to 150 grams per liter), chloride- and fluoride-ions, arsenic, lead, iron, copper, bismuth, zinc and rhenium [4].

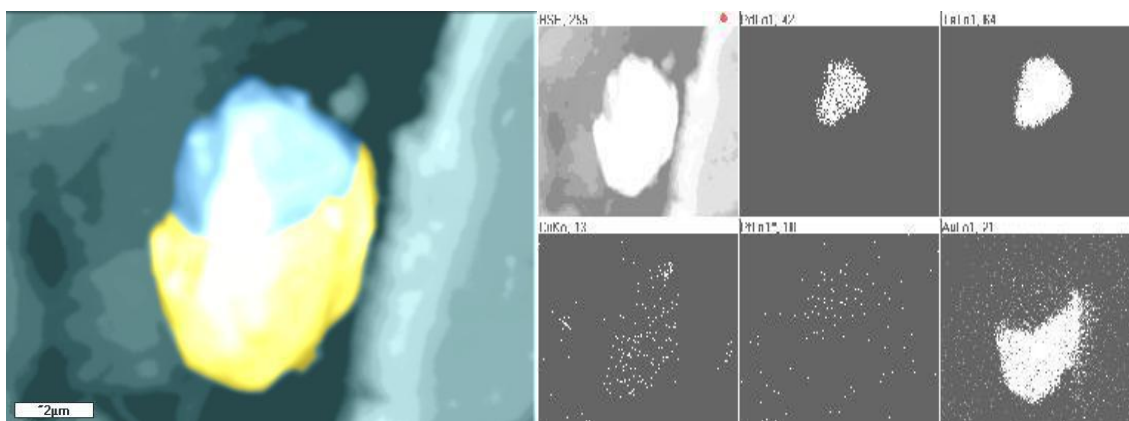


Fig. 1: Coalescence of merenskyite ( $PdTe_2$ ) with virgin gold in molybdenum concentrates of AMMC. Photograph in the electrons reflected and the characteristic X-radiation Pd, Te, Cu, Pt and Au. Increase in 9000x [2].

## EXPERIMENTAL

The aim of this paper is to investigate the possibility of sorption and preconcentration of palladium from rhenium-containing sulfuric acid solutions. As sorbents were used: a low basic anion exchanger AN-105, ampholyte VP-14KR, ion exchange resins with different basicity of the company Purolite (A 170, MN 202 and D 4384), as well as the company Lanxess (Lewatit MP 62, MonoPlus TP 207 and MonoPlus TP 214), carbon sorbent, modified by polytetrafluoroethylene (CS-PTFE) (Table 1).

Table 1. Characteristic of the sorbents

Sorbent	Type	Structure	Functional group
MP 62	Weak base	Macroporous	Tertiary amine
TP 207	Chelating	Macroporous	Iminodiacetic acid
TP 214	Chelating	Macroporous	Thiourea
A 170	Weak base	Macroporous	Secondary amine
D 4384 (Aliquat 336)	Composition anionite	Impregnate	Quaternary amine
MN 202 (TAA)	Composition anionite	Impregnate	Tertiary amine
AN-105	Weak base	Gel	Cyclohexylamine
VP-14KR	Ampholyte	Gel	Pyridine and carboxyl
CS-PTFE	Carbon sorbent, modified by the polytetrafluoroethylene		

Sorption of palladium was carried out in batch conditions for 3 days from the solution of the following composition: palladium - 24 mg/l, sulfuric acid - 100 g/l. The phase ratio of the sorbent to the solution was 1:500. Desorption of palladium was carried out also in batch conditions at a ratio of 1:60 using ammonia (8%) and/or hydrochloric acid (4 mol/l).

## RESULTS AND DISCUSSION

The results showed that the distribution coefficient of palladium in the sorption of the material under study is located within  $3.8 \cdot 10^1 \div 4.0 \cdot 10^4$  cm<sup>3</sup>/g decreasing in the order: TP 214 > D 4384 (Aliquat 336) > TP 207 > AN-105 > CS-PTFE > A170 > MN 202 (TAA) > MP 62 > VP-14KR (Table 2).

Table 2. Sorption of palladium by different ionites

Sorbent	Concentration of palladium in the solution after the sorption		Capacity on palladium, E <sup>Pd</sup>		Distribution coefficient K <sub>d</sub> , cm <sup>3</sup> /g	Degree of the sorption, %
	mg/l	·10 <sup>-3</sup> mmol/l	mg/g	·10 <sup>-3</sup> mmol/g		
MP 62	21.5	202.2	1.4	12.7	63	11.2
TP 207	< 0.3	2.8	11.9	112.3	39830	98.8
TP 214	0.3	2.8	12.0	112.3	39833	98.8
A 170	16.7	157.0	3.8	35.2	224	30.9
D 4384 (Aliquat 336)	< 0,3	2.8	11.9	112.3	39833	98.8
MN 202 (TAA)	18.6	174.8	2.8	26.3	150	23.1
AN-105	7.5	70.5	8,3	78.5	1113	69.0
VP-14KR	22.5	211.5	0,8	7.9	38	7.0
CS-PTFE	9.1	85.5	7.5	70.9	829	61.9

The best results were observed for the palladium desorption from composition anionite D 4384 (Aliquat 336) by ammonium hydroxide solution (distribution coefficient – 31.7 g/cm<sup>3</sup>) and from ionite TP 207 by hydrochloric acid (distribution coefficient – 38.9 g/cm<sup>3</sup>) (Table 3,4).

Table 3. Desorption of palladium from different ionites by hydrochloric acid

Ionite	Initial capacity on palladium		Residual capacity on palladium		Concentration of palladium in the eluate		Distribution coefficient K <sub>d</sub> , g/cm <sup>3</sup>	Degree of the desorption, %
	mg/g	·10 <sup>-3</sup> mmol/g	mg/g	·10 <sup>-3</sup> mmol/g	mg/l	·10 <sup>-3</sup> mmol/l		
MP 62	1.4	12.7	1.1	10.5	3.9	36.4	3	17.2
TP 207	11.9	112.3	3.6	33.6	139.5	1311.1	39	70.1
TP 214	12.0	112.3	11.9	111.8	<0.1	0.9	0	0.05
A 170	3.8	35.2	3.5	32.9	4.1	38.9	1.1	6.6
D 4384 (Aliquat 336)	11.9	112.3	10.2	95.8	29.2	274.4	2.8	14.7
MN 202 TAA	2.8	26.3	1.5	14.2	21.6	203.0	14	46.3
AN-105	8.3	78.5	7.1	66.6	21.1	198.3	2.9	15.2
VP-14KR	0.8	7.9	0.8	7.5	0.9	8.2	1.1	6.2
CS-PTFE	7.5	70.9	6.9	65.0	10.6	99.6	1.5	8.4

Table 4. Desorption of palladium from different ionites by ammonia

Ionite	Initial capacity on palladium		Residual capacity on palladium		Concentration of palladium in the eluate		Distribution coefficient $K_d$ , g/cm <sup>3</sup>	Degree of the desorption, %
	mg/g	$\cdot 10^{-3}$ mmol/g	mg/g	$\cdot 10^{-3}$ mmol/g	mg/l	$\cdot 10^{-3}$ mmol/l		
MP 62	1.4	12.7	0.6	5.4	12.8	120.1	22	56.8
TP 207	11.9	112.3	11.9	112.2	<0.1	0.9	-	-
TP 214	12.0	112.3	11.4	106.8	9.9	93.0	0.8	4.9
A 170	3.8	35.2	3.3	31.3	7.0	65.8	2.1	11.2
D 4384	11.9	112.3	4.1	38.7	130.5	1226.5	31.0	65.5
MN202	2.8	26.3	2.7	25.6	1.2	10.9	0.4	2.5
AN-105	8.3	78.5	6.7	63.4	26.6	250.3	4.0	19.2
VP-14KR	0.8	7.9	-	-	33.7	317.2	-	-
CS-PTFE	7.5	70.9	7.1	67.2	6.7	63.4	0.9	5.3

## CONCLUSION

Thus, based on data of sorption and elution for the effective associated recovery of palladium from rhenium containing sulfuric acid solutions sorbents MonoPlus TP 207 and Purolite D 4384 can be used.

## REFERENCES

1. A.A. Palant, I.D. Troshkina, A.M. Chekmarev, *Metallurgy of Rhenium*, Science: Moscow (2007). 298 p. (rus.)
2. S. K. Smirnova, V. V. Kozlov, etc. *Mining J. of Uzbekistan*, **3**: 13-26 (2005).
3. L. M. Rabicheva, V. N. Morozov, et al., *Tsvetnye Metally*, **12**: 54-55 (1981).
4. I. F. Popov, L. I. Mekler, et al. *Scientific works of the Central Asia Research Institute of Nonferrous Metals*, **11**: 59-98 (1975).

3.P9.

## ULTRAFILTRATION SEPARATION OF RHENIUM AND URANIUM USING NITROGEN-CONTAINING POLYELECTROLYTES

I. D. Troshkina, T. G. Abdrakhmanov, N. A. Smirnov, A. B. Mayboroda,  
K. I. Potapova, A. M. Chekmarev

D. Mendeleev University of Chemical Technology of Russia,  
Miusskaya Sq. 9, Moscow 125047, Russia. E-mail: [tid@rctu.ru](mailto:tid@rctu.ru)

**KEYWORDS:** ultrafiltration separation, uranium, rhenium, polyelectrolyte

### ABSTRACT

Membrane techniques have been proven for selective recovery and separation of rhenium and uranium from complex multi-component effluents, in particular, the method of complexing ultrafiltration. The laboratory installation involved standard ultrafilter with semipermeable polymer membrane (polysulfone fiber). The effects of external factors (ratio of nitrogen-containing polyelectrolytes Praestol 658, Praestol 859, KF-99 and PGHA to rhenium and uranium, pH value, concentration of nitrate-ion) on the separation characteristics of the process were studied. The optimal conditions of polyelectrolytes regeneration were found.

### INTRODUCTION

Uranium mines is one of the rhenium sources. Hydrometallurgical treatment of them produces solutions where rhenium concentration is tenth of mg/l [1,2]. Large quantities productive solutions and high market value of rhenium are the base for its reasonable recovery.

Baromembraneous techniques (reversible osmosis, ultrafiltration, microfiltration) widely use for the separation of solutions. The method of selective concentration combining ultrafiltration with preliminary complex formation (CF-UF method) is known since 1968 (Michaels A.S., 1968). High capacity at low power in combination with high selectivity of the separation allow to use the CF-UF method for the recovery of valuable or pollutant components from industrial effluents [3,4]. The ultrafilter used in the CF-UF process passes low-molecular components of solution, but retards high-molecular polyelectrolytes (PE) connecting the ions of constituent. Selective connection is provided by introducing of functional groups in the PE molecule having high affinity to metal ion. An important advantage of the CF-UF method for mostly used systems is a high velocity of process, that favourably compares it with sorption method widely used in the processing of dilute solutions. Method of complexing ultrafiltration was used for rhenium recovery from water solutions [4-6].

The possibility of recovery and separation of rhenium and uranium by the CF-UF method with nitrogen-containing polyelectrolytes Praestol 658, Praestol 859, KF-99 and PGHA was investigated in this work.

### EXPERIMENTAL

In this work following soluble synthetic nitrogen-containing polyelectrolytes Praestol 658 and 859 (Degussa, Germany), KF-99 and PGHA (China) were used.

The rhenium concentration in solution was determined by photocolometric method [7].

The CF-UF characteristics of rhenium recovery have been studied at the laboratory installation involved standard ultrafilter with semipermeable polymer membrane (polysulfone fiber with nominal cut-off molecular mass -40000 amu prepared by phase inversion) [6]. Pore sizes in the dense selective layer are 10–40 nm. Ultrafiltration module used in this study is a cylindrical device, which is placed inside the bundle of hollow fibers as set forth in the ends of the shell polymer compound. Ultrafilter on the basis of hollow fibers is a flow-type apparatus, so after the addition of polyelectrolyte to a



solution containing metal ions, filtration was carried out at the circulation of the solution, maintaining at the entrance to the membrane module excess pressure 0.5 atm.

Selectivity of the membrane has been studied for uranium and rhenium depending on the concentration of various polyelectrolytes.

The selectivity of the membrane on metal ( $\phi$ ,%) was determined from the relation:

$$\phi = \left(1 - \frac{S_P}{S_I}\right) \cdot 100\%$$

where  $S_I$  and  $S_P$  - metal concentration in the initial solution and permeate, mg/dm<sup>3</sup>, respectively.

The separation factor of uranium and rhenium was calculated by analogy with the coefficient of separation of the components of gas or organic compounds.

## RESULTS AND DISCUSSION.

The selectivity of the membrane by using polyelectrolyte Praestol 859 reaches 90% at its concentration of 0,017%, Praestol 658 – from 0,1%, KF-99 – from 0.03%. The selectivity of the membrane in the case of PGHA reaches a plateau, (85% at its concentration of 0.05%).

Minimum concentration of polyelectrolyte in a solution of uranyl sulphate ( $[U] = 50 \text{ mg / dm}^3$ ) is determined, at which the value of the selectivity reaches 90%, according to this dependence. The selectivity of the membrane reaches 90% by using polyelectrolyte Praestol 859 at its concentration of 0.017%, while in the case Praestol 658 - from 0,06%.

The effect of nitrate anions and pH value on the process of complexation - ultrafiltration for both metals was studied at the chosen concentration of polyelectrolytes.

The data obtained shows that the optimal concentration of sodium nitrate for the elution of perrhenate ions from the polyelectrolyte Praestol 859 is 0.05 mol/dm<sup>3</sup>; from Praestol 658 - 0.1 mol/dm<sup>3</sup>; from KF-99 - 0,03 mol/dm<sup>3</sup>. In this case, on the one site, a high degree of regeneration (98%) is reached, which provides a wealth of permeate. On the other site, a relatively low concentration of nitrate ions in solution facilitates processing of the permeate by hydrometallurgical methods.

The effect of nitrate ions on the selectivity of the polysulfone membrane on uranium was studied using polyelectrolyte Praestol 658. Experiments were conducted by joint and separate extraction of uranium and rhenium from solutions based on the above experimental data on the working pH range and the influence of the content of nitrate ions on the selectivity of polysulfone membranes on rhenium and uranium. The optimal parameters allowing to selectively concentrate each of the components, or both simultaneously were determined (Table).

Table. The parameters of membrane separation of uranium and rhenium\*

Condition	$\phi$ Re, %	$\phi$ U, %	Separation factor Re/U	Separation factor U/Re
pH 7,4	91	92	-	1,2
pH 6,9; 0,1 mol/l NO <sup>3-</sup>	1	92	-	12,0
pH 4,1	96	11	25,8	-

\* initial uranium concentration - 50 mg/dm<sup>3</sup>, initial rhenium concentration - 20 mg/dm<sup>3</sup>, concentration of polyelectrolyte Praestol 658 - 0,1 % (mas.)

## CONCLUSION

The possibility of recovery and ultrafiltration separation of uranium and rhenium in water solution using 0.1% solution of polyelectrolyte Praestol 658 was shown. The selectivity of the polysulfone membrane with selective concentration of uranium is 92% (pH 6.9, the concentration of nitrate ions 0.1 mol/l), of rhenium - 96% (pH 4.1).

## REFERENCES

1. A.A. Palant, I.D. Troshkina, A.M. Chekmarev, *Metallurgy of Rhenium*, Science: Moscow (2007). 298 p. (rus.)
2. *In-Situ Leaching of Ores*, Academy of Mining Sciences, Publishing House: Moscow (1998). 446 p. (rus.)
3. G.I.Tokareva, N.I. Tokarev, J.I.Djitnerskij, et al., *Selective concentration of metals in solutions by polymeric connection and ultrafiltration*, VIEMS: Moscow (1988), 60 p. (rus.).
4. S.M. Moldabekov, N.V. Kotshergin, A.A. Kamshibaev, U.B.Besterekov. Abstracts of the IV Conference on the membrane methods of mixture separation, 1987. Moscow, NIITECHIM, 1987, p. 44-45.
5. I.D. Troshkina, A.M. Chekmarev, S.B. Mayboroda, N.S. Smirnov, Abstracts of the Intern. Symposium on technetium – science and utilization: IST-2005. May 24-27, 2005. Oarai (Japan), 2005, p. 37.
6. N.S. Smirnov, I.D. Troshkina, A.B. Mayboroda, A.M. Chekmarev, *Chemical Technology*. **8(10)**: 468-471 (2007)
7. L.V. Borisova, A.N. Ermakov, *Analytical chemistry of rhenium*. M.: Chemistry, 1974. -318 p.

3.P10.

## RECOVERY OF RHENIUM FROM AQUEOUS SOLUTIONS BY FIBROUS MATERIALS

I.D. Troshkina, L.A. Zemskova\*, A.M. Chekmarev, A.V. Plevaka,  
Aye Minn, A.V. Shilyaev, A.V. Voit\*, D. N. Tumanova

D. Mendeleev University of Chemical Technology of Russia,  
Miuskaya Sq. 9, Moscow 125047, Russia. E-mail: [tid@rctu.ru](mailto:tid@rctu.ru)

\*Institute of Chemistry, Far Eastern Branch of Russian Academy of Sciences, 159, pr. 100- letiya Vladivostoka,  
690022, Vladivostok, Russia.  
E-mail: [zemskova@ich.dvo.ru](mailto:zemskova@ich.dvo.ru)

**KEYWORDS:** rhenium, sorption, fibrous materials FIBAN, carbon fibers, modified fibers

### ABSTRACT

The possibility of rhenium recovery from aqueous solutions by fibrous materials was investigated. Sorption characteristics of the following fibrous materials: carbon fibers (Busofite and Actylene), carbon fibers modified by electrochemical and chemical method (adsorption on the surface of natural polyelectrolyte – chitosan) and acrylic fibers FIBAN having the following anion-exchange groups:  $-N(CH_2COO^-)_2$  (FIBAN A-6) and  $=NH$ ,  $-NH_2$ ,  $-COOH$ ,  $\equiv N$  (FIBAN AK-22) have been studied. The best capacity parameters for modified carbon materials prepared in the anodic region and at the open-circuit potential are observed. The half-conversion time  $\tau_{0.5}$  (3-10 min.) for them is much less than that for original carbon fibers ( $\tau_{0.5}$ –60-65 min). The degree of rhenium sorption by the ionites FIBAN A-6 and AK-22 was equal 70.8 and 97.0 % accordingly. Elution characteristics for sorbent FIBAN AK-22 are better than for ionite FIBAN A-6.

### INTRODUCTION

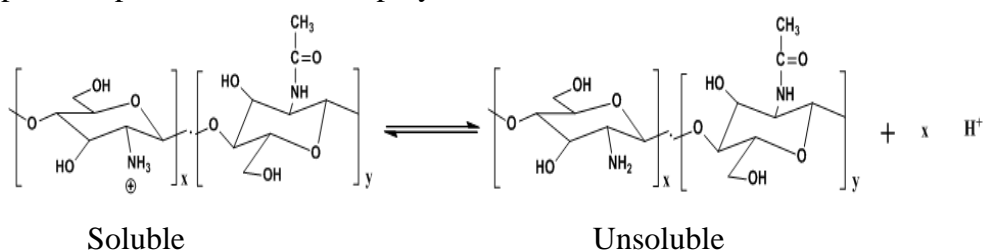
Granular nitrogen containing anionites and complexing ionites as well as amino containing impregnates are used for sorption of rhenium. The possibility of rhenium recovery from aqueous solutions by fibrous materials was investigated. The main advantage of them as compared with granular ionites is a high sorption rate.

### EXPERIMENTAL

Sorption characteristics of the carbon fibers (Busofite and Actylene) modified by electrochemical and chemical method (adsorption on the surface of natural polyelectrolyte – chitosan) and acrylic fibers FIBAN (A-6 and AK-22) are studied.

FIBAN-sorbents contain the following anion-exchange groups:  $-N(CH_2COO^-)_2$  (FIBAN A-6);  $=NH$ ,  $-NH_2$ ,  $-COOH$ ,  $\equiv N$  (FIBAN AK-22). The synthesis of these ionites was described by authors [1].

Chitosan, a natural organic polymer containing amino groups can adsorb  $ReO_4^-$  and sorption depends on the ionic strength and pH values of its solutions. Specifically, chitosan has primary amino groups that have  $pK_a$  values of about 6.3. At pH below  $pK_a$  most of the amino groups are protonated making chitosan a water-soluble, cationic polyelectrolyte. At pH above the  $pK_a$  chitosan amino groups are deprotonated, and this polymer becomes insoluble [2]:



These properties of chitosan were used for obtaining new sorption materials (Table 1).

Carbon clothes with high specific area ( $\sim 700\text{-}800\text{ m}^2/\text{g}$ ) were used as initial material for obtaining the sorbents. Carbon fibers were modified with chitosan by means of electrochemical process and adsorption on the carbon cloth. Thus, the three types of the sorption materials were obtained by the following ways: by cathodic and anodic polarization (in potentiostatic regime) and at open-circuit potential in electrolyte solution. The amount of chitosan precipitate depends on the treatment method at the same concentration.

The determination of the types of nitrogen containing groups was carried out by the X-ray photoelectron spectra. The X-ray photoelectron N 1s spectra of all the samples were recorded. Deconvolution of these spectra gives two peaks corresponding to nitrogen of the initial and protonated amino groups (Fig. 1).

Table 1. Regime of obtaining and characteristics of modified carbon fibers.

Sorbent	Potential, mV	Potential immersion, mV*	Specific surface, $\text{m}^2/\text{g}^{**}$
Base – Busofite (BHUM)			
BHUM-1	-900	+60	872
BHUM-2	-700	+70	887
BHUM-3	-500	+50	886
BHUM-4	-200	+70	890
BHUM-5	-100	+80	902
BHUM-6	+100	+50	1015
BHUM-7	+600	+290	1278
BHUM-8	without polarization	+230	1145
Base - Actylene (AHUM)			
AHUM-1	-100	+150	716
AHUM-2	-500	+90	628
AHUM-3	-900	+70	593
AHUM-4	+100	+180	749
AHUM-5	-900	+50	615
AHUM-6	without polarization	+300	852
AHUM-7	+900	+580	945
AHUM-8	+900	+620	918
AHUM-9	+600	+450	965
AHUM-10	+900	+540	941
AHUM-11	+900	+450	950
AHUM-12	+900	+450	950

\* - The potential of immersion is defined in 0.9% NaCl solution.

\*\* - The specific surface area is calculated by measuring of the HUM electrochemical capacity in the formation of the electrical double layer.

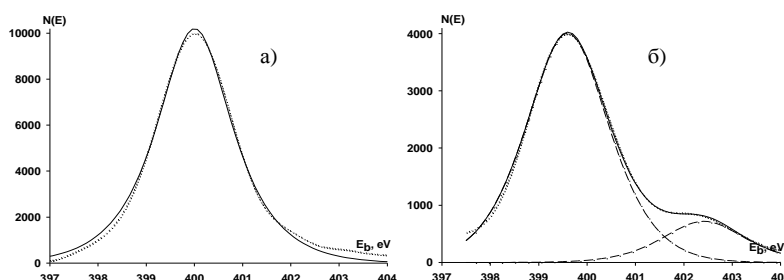


Fig. 1. X-Ray photoelectron N 1s spectra of carbon fibers (Busofite) modified with chitosan by cathodic (a) and anodic (b) polarization.

It was determined that chitosan precipitated at the negative electrode had much less amount of protonated amino groups.

The surface of the original and the modified fibers was investigated by scanning electron microscopy (Fig. 2).

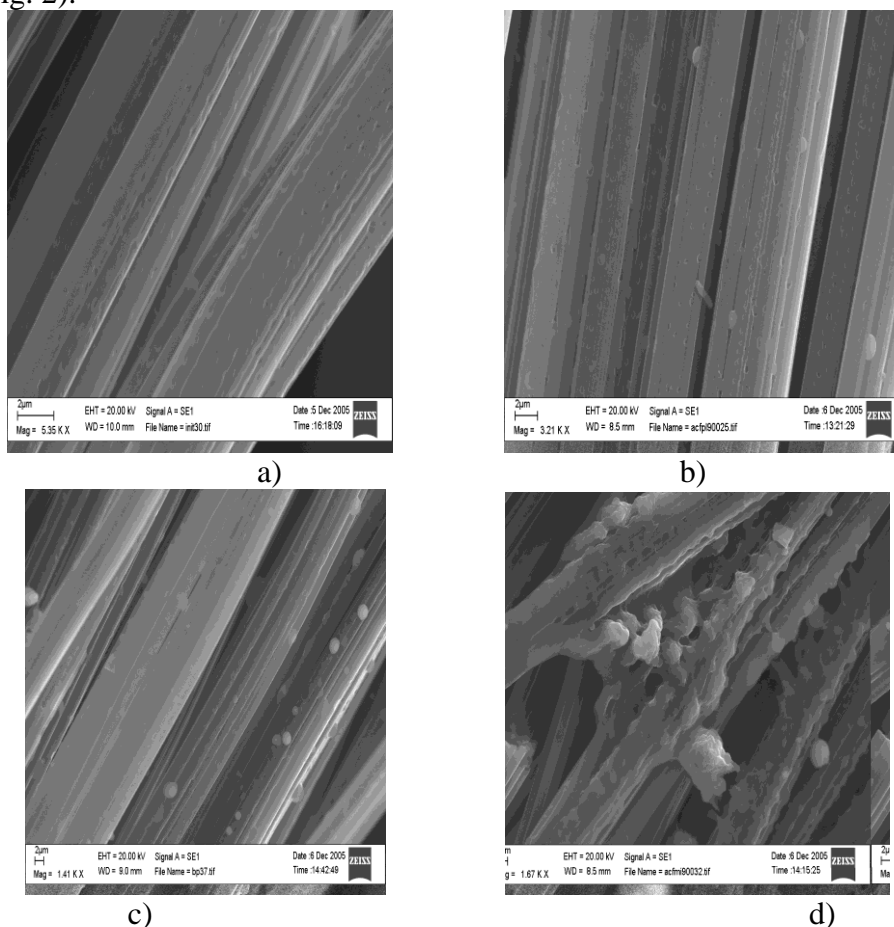


Fig. 2. Photos surface of the carbon fibers obtained by *e*-force microscopy: a) original fiber, and b) BHUM (anodic polarization, 900 mV), c)BHUM (without polarization), d)BHUM (cathodic polarization, -900 mV).

The surface of the fiber source (the width of the fibers from 3 microns to 10 microns) is smooth and covered with well-developed network of pores (Fig. 1a). Round and oval pores with diameters close to the boundary between meso- and macropores, ie, ~ 50-200 nm are visible. During the electrochemical deposition of chitosan in the anode potential biopolymer film is deposited in the form of particles or hemispherical shape, which is located on the borders of macropores (Fig. 1b). Chitosan which chemically deposited on the fiber surface exists in various forms: as a film or spherical particles with a thickness of 500 nm to 2000 nm (Fig. 1c). Probably, by the swelling the molecule of polymer fibers is introduced between the fibrils and filled the space. In the cathodic modification (Fig. 1d) chitosan film coats the fibers, forming growths of complicated form on the surface. In places with quiet relief the film has a surface with multiple bulges. On the surface of the fibers macropores from 100 nm to 600 nm are developed. The film thickness on flat ground is approximately 200-250 nm.

The equilibrium and kinetic characteristics of rhenium sorption by modified fibrous carbon materials treated electrochemically with recovery potentials varying from – 900 to +600 mV from aqueous solutions in the presence of natural biopolymer chitosan.

The rhenium sorption by fibrous materials was carried out in batch conditions. The ammonia solution was used for rhenium elution.



## RESULTS AND DISCUSSION.

### *Rhenium sorption on fibrous carbon materials and carbon fibers modified by electrochemical and chemical method*

Investigation of sorption properties of the HUM materials obtained as regards to perrhenate ion was carried out. The highest rhenium capacity is observed for the material prepared at the recovery potential +600 mV (Table 1,2).

Table 2. Rhenium sorption and desorption characteristics of modified carbon fibers BHUM and AHUM.

HUM	Sorption			Desorption	
	Capacity of Re, mg/g	Distribution coefficient, cm <sup>3</sup> /g	Degree of sorption, %	Distribution coefficient, g/cm <sup>3</sup>	Degree of desorption, %
BHUM-7	18.5	11600	92.3	23700	82.3
AHUM-6	19.5	39000	97.5	8900	78.3
AHUM-9	19.8	66000	98.8	38000	93.9
AHUM-10	19.0	17300	94.8	7200	73.5

Isotherms of rhenium for sorbents BHUM-7 and AHUM-9 have a convex shape. They are described by the Langmuir equation. The Langmuir constants in the equation were equal  $(7.3 \pm 0.8) \cdot 10^{-2}$  l/mg and  $(1.9 \pm 0.3)$  l/mg, respectively.

It was found that the modified sorption materials (BHUM-7 and AHUM-9) had higher sorption capacity as compared to the initial material. The results of this investigation are shown in Fig. 3.

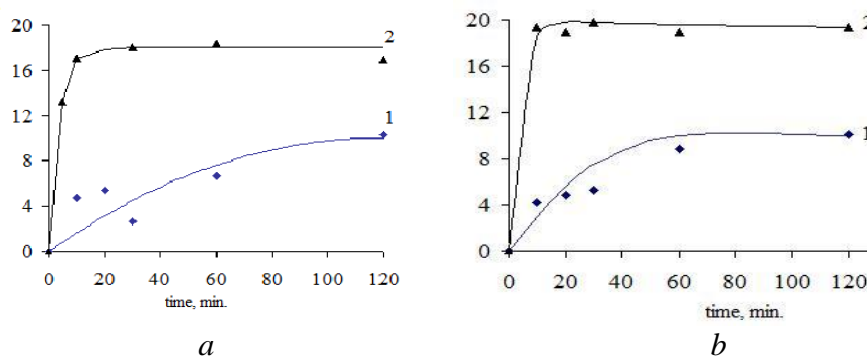


Fig.3. Integral kinetic curves of rhenium sorption from aqueous solution: 1a - Busofite; 2a - BHUM-7; 1b - Actylene; 2b - AHUM-9.

It was established that the kinetic characteristics of the sorbents BHUM-7 and AHUM-9 are comparable (Fig. 3). Best kinetic properties are observed for the sorbents BHUM-7 and the AHUM-6 (no polarization). The half-conversion time  $\tau_{0.5}$  is 3.0 min. and 7.5 min. respectively. It was found that the rate of rhenium sorption by modified HUM significantly higher than by the original carbon fiber (for Busofite, for example,  $\tau_{0.5}$  is equal 65 min.).

#### **The following model to describe experimental results can be possible [3,4]:**

- carbon porous materials modified with chitosan in anodic area have a large number of protonated amino groups.

- large number of amino groups in protonated form can interact with the negatively charged perrhenate anion  $\text{ReO}_4^-$  via electrostatic interaction as in [3].

Possible types of interaction perrhenate-ion sorption by chitosan-carbon materials are:

*With carbon fiber materials:*

- physical adsorption in the pores;

- **electrostatic adsorption of perrhenate ion, due to the positively charged surface of the carbon material;**

**- ion exchange of perrhenate ion with the surface oxygen anion groups (OH<sup>-</sup>).**

*Due to the electrochemical processing:*

- electrostatic adsorption of perrhenate ion, due to the positively charged surface of carbon material (anode region).

*Through modification of chitosan:*

- interaction of perrhenate ion with protonated amino groups of chitosan adsorbed from a solution of carbon material;
- interaction of perrhenate ion by protonated amino groups of chitosan deposited on the surface during the electrochemical process in the cathode region.

*Rhenium sorption by FIBAN-ionites.* The degree of rhenium sorption was 70.8 and 97.0 % for the ionites FIBAN A-6 and AK-22 accordingly (Table 3).

Table 3. Rhenium sorption from sulfuric acid solutions at FIBAN-sorbents\*

FIBAN	Degree of rhenium sorption, %	Capacity of rhenium, mg/g
A-6	70.8	1.8
AK-22	97.0	2.4

\* ratio of sorbent to solution = 1:50 (g: ml), the Re concentration –50 mg/l, pH 2.

Elution characteristics for sorbent FIBAN AK-22 are better than for ionite FIBAN A-6 (Table 4).

Table 4. Elution of rhenium from FIBAN-sorbents\*

FIBAN	Degree of desorption after 1 <sup>st</sup> contact, %	Degree of desorption after 2 <sup>nd</sup> contact, %	Total degree of desorption, %
A-6	56.5	63.4	84.7
AK-22	55.1	93.6	97.1

\* ratio of sorbent to solution = 1:20 (g: ml), concentration of ammonia in solution – 8 %.

## CONCLUSION.

Rhenium sorption has been studied from aqueous solutions on fibrous materials of two types: chitosan-modified carbon material (in the cathodic and anodic polarization regions and at the open-circuit potential) and acrylic ionites FIBAN.

- The best capacity parameters for HUM materials prepared in the anodic region and at the open-circuit potential are observed. The sorption behavior of the materials depends on the number of the protonated amino groups. The highest rhenium capacity of BHUM-7 was 18.5 mg/g and for AHUM-9 - 19.8 mg/g (without polarization). The rhenium sorption isotherm has a convex shape. The calculated Langmuir constants were equal  $(7.3 \pm 0.8) \cdot 10^{-2}$  l/mg and  $(1.9 \pm 0.3)$  l/mg, respectively.
- Kinetic characteristics of rhenium sorption from aqueous solutions by modified HUM have been studied. The half-conversion time  $\tau_{0.5}$  (3 - 10 min.) is much less than that for original carbon fibers ( $\tau_{0.5}$  – 60-65 min).
- The possibility of rhenium sorption by fiber ionites FIBAN was shown. The degree of rhenium sorption by ionite FIBAN AK-22 (97 %) is more than for ionite AK-6 (70.8 %).

## REFERENCES.

1. V. S. Soldatov, G.I. Sergeev, *GWChO*. **1**: 101-106 (1990).
2. Li-Qun Wu, Anand P.Gadre, Hyunmin Yi, et. al., *Langmuir*, **18**: 8620-8625 (2002).
3. E. Kim, M.F. Benedetti, J. Boulegue. *Water Research*. **38**: 448-454 (2004).
4. A.V. Plevaka, I.D. Troshkina, L.A. Zemskova, A.V. Voit, *J. of Inorg. Chem.* **54(7)**: 1229–1232 (2009).

3.P11.

## **RHENIUM RECYCLING FROM HEAT-RESISTANT RHENIUM-CONTAINING NICKEL-BASED SUPERALLOYS**

A.G. Kasikov, A.M. Petrova, P.B. Gromov, V.T. Kalinnikov

An Institution of the Russian Academy of Sciences – I.V.Tananaev Institute of Chemistry and Technology of Rare Elements and Mineral Raw Materials of the Kola Science Centre of RAS  
(Akademgorodok, 26a, Apatity, Murmansk reg., Russian Federation)

**Keywords:** rhenium, recycling, heat-resistant nickel alloy, waste

### **Abstract**

Two new flow-sheets of rhenium recycle technology from nickel-based heat-resistant alloys (HRA) have been investigated. By the first variant, the nickel base of HRA is leached by a mineral acid, with rhenium pre-concentrated in the residue, followed by rhenium high-temperature distillation as  $\text{Re}_2\text{O}_7$ . After dissolution and hydrometallurgical purification of sublimate, technical-grade ammonium perrhenate is obtained. The second variant incorporates waste leaching with acid under oxidizing conditions, transferring more than 95% of rhenium to solution. Rhenium is selectively recovered by solvent extraction with secondary alcohol. After the extractant washing, a pure perrhenate ammonium solution and a technical-grade rhenium salt are produced. The proposed schemes have been tested on an enlarged laboratory scale.

### **Introduction**

It is known that heat-resistant alloys (HRA) of the latest generations contain 4-9% rhenium, so both their treatment and operation wastes can be regarded as fairly rich rhenium sources. Although the amount of such wastes, annually turned out in Russia, is ~25-35 t (according to FSUE “VIAM” data), only a small part of them is currently recycled.

Rhenium recycling has recently become a burning issue. This is due to many factors, the principal one being runaway prices resulting from disbalance of supply-demand at the rhenium market. Peaking at 2008 (USD 10560 /kg), the Re prices remain fairly stable (6600 /kg) [1], notwithstanding the ongoing economic crisis.

However, according to A. Lipmann, an authority in the “minor-metal” issues, the industrial application of the methods for HRA processing is limited due to their high cost (1 kg of secondary rhenium costs ~3000 USD/kg) and low effectiveness (the yield is ~70%) [2]. Hence the necessity to develop effectual technologies of rhenium recovery from HRA.

### **Results and Discussion**

Since HRA are multicomponent, the metals from them are conventionally extracted by hydrometallurgical methods [3]. One of the problems arising here is crushing of extremely hard large HRA lumps (such as turbine blades and other elements weighing up to several kg). Based on our experience of hard nickel alloys processing [3], we proposed that lumpy HRA wastes of the ZhS-32 type should be crushed by high-temperature melting with aluminium granules. After melting for 0.5 h in an induction furnace at 1500-1700°C we obtained a homogeneous alloy of ~4kg charge mixture with a mass ratio of  $m(\text{alloy}):m(\text{Al}) \sim 5:1$ . The nickel base of HRA was converted to aluminide  $\text{Ni}_3\text{Al}$ , easily broken at low temperatures, so that the cooled melt could be ground in standard facilities such as a jaw crusher and disc attritor. The resulting material had the grain size of about 315  $\mu\text{m}$  (~95 w/o), most of which (81.6%) was 200-315  $\mu\text{m}$ . Table 1 demonstrates the chemical analyses of the initial and dispersed products.

Table 1. Chemical composition of initial and ground HRA wastes.

Product	Content of elements, mass %								
	Ni	Co	Cr	Mo	W	Re	Al	Ta	Nb
Initial HRA	61.0	9.0	4.9	1.0	8.5	2.6	5.9	2.1	1.6
Ground HRA	48.0	6.3	3.1	0.9	6.5	1.5	32.0	1.1	0.7

We have tested two variants of acidic leaching of rhenium-containing HRA wastes: in oxidizing conditions (whereby rhenium passes directly to solution) and without an oxidizer, resulting in rhenium concentration in leaching residue.

For acidic leaching of the alloy base without an oxidizer, sulphuric and hydrochloric acids were used. The process was carried out for 3-6 hours at  $T=80^{\circ}\text{C}$  until completion of the reaction of metal components with mineral acid. When 2-5 mole/L  $\text{H}_2\text{SO}_4$  solutions and 5-6 mole/L  $\text{HCl}$  solutions were used, more than 90 mass.% of the nickel base was dissolved, with but a small part of rhenium passing to solution (1.2-5%). The solid phase diminished by 80-90 mass.%, which made possible to concentrate much of rhenium in the insoluble residue, where its content was about 10 mass.%.

It should be noted that hydrochloric acid is preferable in this case because at later stages the non-ferrous metals are easy to separate in chloride media. In particular, solvent extraction can be applied to hydrochloric solutions containing 5-6 mole/L  $\text{Cl}^-$  to isolate cobalt with tertiary amines.

It has been proposed to isolate rhenium from the leaching residue (solid-phase rhenium concentrate), mostly containing Re, Nb, Ta and W, by using high-temperature distillation of  $\text{Re}_2\text{O}_7$ . The best result in  $\text{Re}_2\text{O}_7$  distillation in an oxygen flow was achieved at  $950^{\circ}\text{C}$ , when 99.1% Re was extracted in 1 hour. After 3 hours, up to 99.8 Re was extracted. Since the sublimate also contains molybdenum, it can be dissolved in water and separated by solvent extraction methods with di-2-ethylhexylphosphoric acid (D2EHPA).

Rhenium extraction to solution is considerably improved by adding an oxidizer at the stage acidic leaching. Since subsequent Re extraction from solution is best performed in a sulphuric acid medium, the leaching was conducted in the presence of an oxidizer by 5-6 mole/L  $\text{H}_2\text{SO}_4$  at  $\text{S:L}=1:15$  and the temperature of  $70-80^{\circ}\text{C}$ . During the first 2-3 hours the process occurred without an oxidizer, which was added after the bulk of metal components had reacted with  $\text{H}_2\text{SO}_4$  (for 1.5-3 h). The oxidizer solution was fed by batches using a peristaltic pump at a rate sufficient to maintain the desired ORP value measured relatively a saturated chlorine-silver electrode.

Additional experiments on optimizing the oxidizer consumption have shown that efficient Re extraction requires hydrogen peroxide in amounts needed to maintain the ORP system at the level of 0.55-0.75 V for 2-3 h, resulting in diminishing of  $\text{H}_2\text{O}_2$  consumption compared to tentative experiments.

Fairly concentrated  $\text{H}_2\text{SO}_4$  solutions are needed for effective leaching of the non-ferrous metal base and also for obtaining of solutions acidic enough to selectively extract rhenium by solvent extraction with secondary aliphatic alcohols [4].

In particular, we have tested 2-octanol, a reagent made in Russian. Reagents of this type feature high capacitance in rhenium ( $\sim 100$  g/L) selectively extracting it in sulphuric acid media in the presence of molybdenum and other non-ferrous metals, which allows to isolate Re from solutions of complex salt composition.

Laboratory experiments on extraction from leaching solutions were conducted in glass separating funnels (0.25-0.5 L) under mechanical agitation at room temperature ( $20\pm 2^{\circ}\text{C}$ ). To prevent additional acid extraction from leaching solution, the extragent was initially saturated with  $\text{H}_2\text{SO}_4$ . The time of phase contact at all operations was 5 min, the O:A ratio was 1-5:1 depending on operation. As the result of the laboratory experiments, extraction from leaching solution of HRA wastes containing, g/L: Ni-21.8; Co-3.0; Al-15; Cr-1.4; Mo-0.36; W-0.25; Re-0.75 and 3.7 mole/L  $\text{H}_2\text{SO}_4$ , at one stage at the O:A ratio equal to 1:1 yielded 97.3% Re and 19.4% Mo to the organic phase. By single washing at O:A=5:1, 61.9% molybdenum and a greater part of co-extracted  $\text{H}_2\text{SO}_4$  were stripped, together with an insignificant quantity of rhenium. So, stripping with a 3 mole/L  $\text{NH}_3$

solution produced a purified rhenium-containing solution with Re concentration of 0.5 g/L and molybdenum concentration of 0.03 g/L. The level of Re extraction to ammonium concentrate was ~80%.

Apparently, rhenium losses with wash water can be prevented by returning it to the process, either to the extraction stage or to the stage of leaching solution preparation.

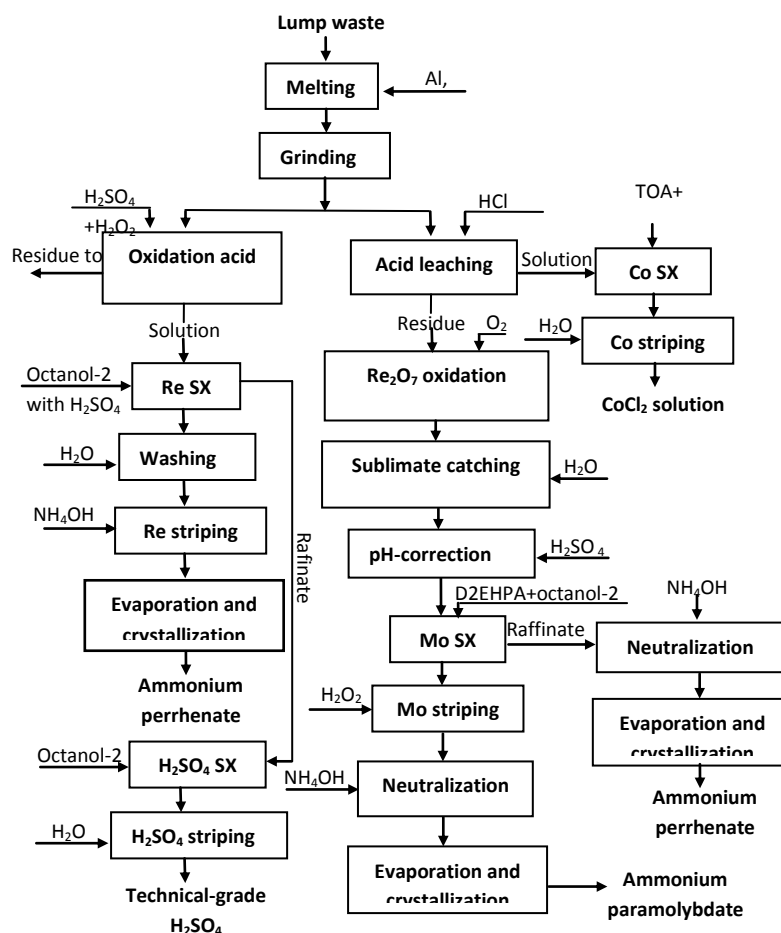


Fig. 1 Hydrometallurgical technology of rhenium- containing lump HRA wastes

By carrying out extraction at a laboratory cascade of mixer-settler extractors made in ICTREMRM KSC RAS in the counter-flow regime, with wash water returned to extraction, we managed to increase the rhenium yield from leaching solutions of rhenium-containing alloys. Extraction was conducted at a 3-stage cascade at O:A=1:2, whereupon the extract was washed with an acidified water solution (stage1) at O:A = 5:1. Re-extraction was carried out by a 3 mole/L NH<sub>3</sub> solution at O:A=3:1. From about 5 L of leaching solution containing, g/L: Ni-30.2; Co-4.2; Cr-3.1; Mo-0.6; W-0.01; Re-2.0 and 4.5 mole/L H<sub>2</sub>SO<sub>4</sub>, an ammonium re-extract containing 12 g/L Re was produced. After evaporation, the resulting NH<sub>4</sub>ReO<sub>4</sub> was purified from main impurities.

Our testing has revealed the possibility of selective solvent extraction of rhenium from leaching solutions of HRA resulting in a purified ammonium perrhenate. This hydrometallurgical technology of rhenium recycling from HRA waste has been covered by an RF patent [5].

### Conclusion

As the result of this work, 2 variants of rhenium recycling from Re-containing HRA wastes, providing for not only rhenium extraction but also a possibility of comprehensive processing of wastes have been proposed. The schematic diagram of these processes is presented in Fig.1.



## References

1. <http://www.catalysts.basf.com>
2. <http://www.lipmann.co.uk>
3. A. G. Kasikov, A. M. Petrova Rhenium recycling from heat-resistant and special alloy wastes (rus). *Tekhnologiya Metallov*. **2**: 2-12, (2010).
4. RF Patent 2330900, MPK S22V 61/00, S22V 3/26. A method for rhenium(VII) extraction from an acid solution / A. G. Kasikov, A. M. Petrova (RF).– №2006142845/02; Appl. 04.12.06; Publ. 10.08.08. Bull. № 22.
5. RF Patent 2412267, MPK S22V 61/00. A method for rhenium recovery from metallic wastes of nickel-containing heat-resistant alloys / A. G. Kasikov, A. M. Petrova, E.G. Bagrova, N. V. Serba, V. T. Kalinnikov (RF).– №2009145364/02; Appl. 07.12.09; Publ. 20.02.11. Bull. № 5.

3.P12.

## **INSTALLATION FOR LIQUID-LIQUID EXTRACTION CONCENTRATING AND RECOVERY OF RHENIUM FROM AQUEOUS SULFATE SOLUTION**

A.M. Safiulina, K.E. German, N.N. Popova, M.Yu. Burtsev.

Academinvestservice Ltd., JSC NPO Innovation and development

Liquid-liquid extraction is a powerful method for separation of rare metals in course of its hydrometallurgical reprocessing. It is widely used in course of technetium separations in the reprocessing of spent nuclear fuel. Its application for the separation of rhenium – a close neighbor of Tc in the Periodic Table – is considerably less abundant as the sorptive technologies are well developed [1].

Although less abundant, the extraction separations of Re are also known and used for example in the case of separation of Re from W in its nucleus generator [2].

Here we present an installation that could be applied to liquid-liquid extraction concentrating and recovery (LLEC-I) of Re from aqueous sulfate solution.

The principle blocks of the LLEC-I include the clarification blocks (CS 1, 3), LLE and stripping block (LLESB, 2), precipitation block (PB, 4). In a special installation modification LLEC-I-C the conversion block (CB, 5) is adopted.

The CS block is based on a know-how spiral principle. The LLESB is a conventional extractor, while PB is presented by two modifications (C – a conventional one, and M – equipped with a melter of special design with know-hows and a patent providing with the possibility of melted organic perrhenate separation.

### **References**

1. Pallant A.A., Troshkina I.D., Chekmarev A.M. *Rhenium metallurgy*. M.: Nauka Publ.. 2007. 298 p.
2. M.P.Zykov, A.T.Filyanin, G.E.Kodina, A.Yu.Tsivadze, V.N. Romanovsky et.all., 2011, This issue.

3.P13.

## RECOVERY OF RHENIUM FROM OIL SHALE

I. D. Troshkina, M.V. Vazchenkov, A. M. Chekmarev

D. Mendeleev University of Chemical Technology of Russia,  
Miusskaya Sq. 9, Moscow 125047, Russia. E-mail: [tid@rctu.ru](mailto:tid@rctu.ru),

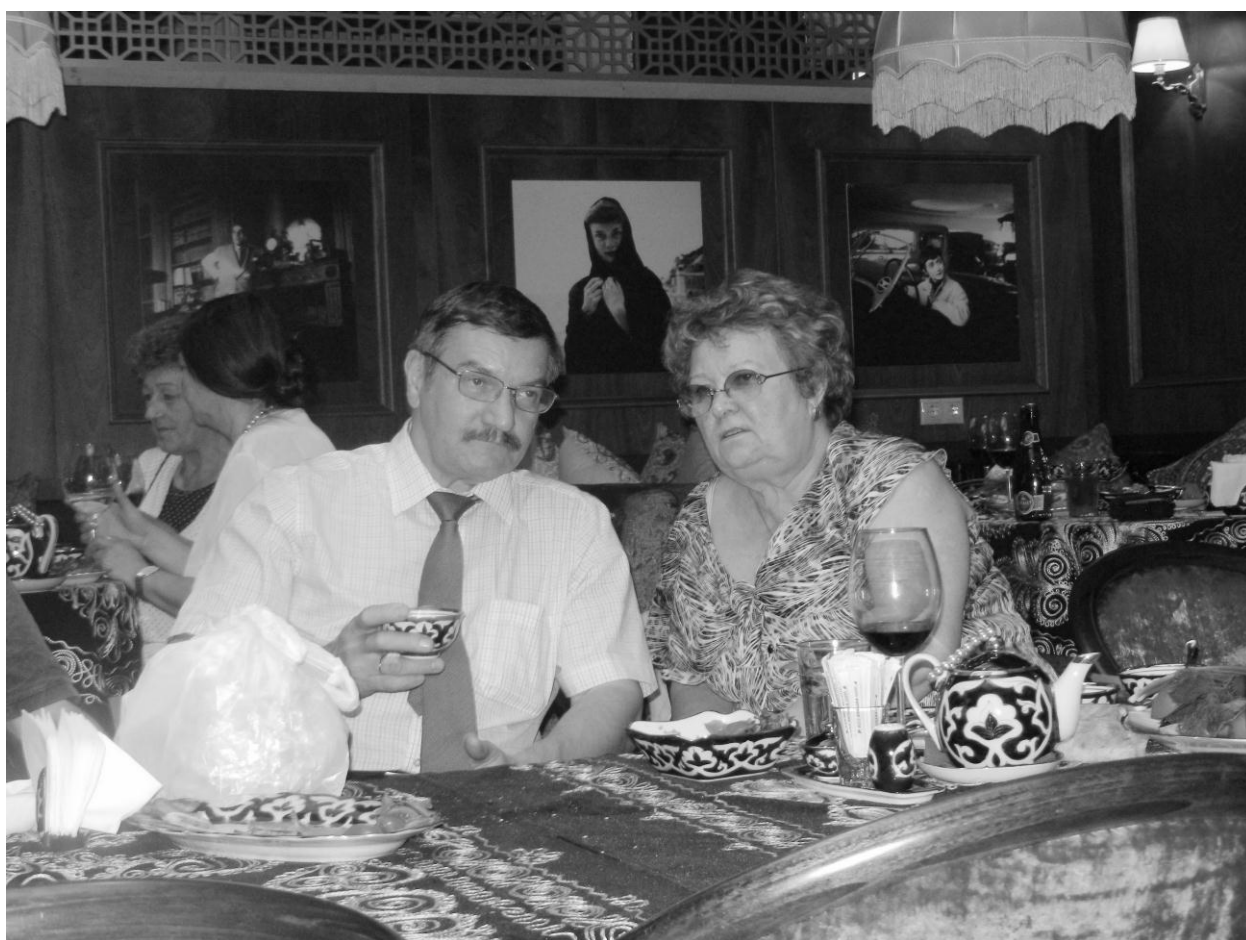
Carbonaceous source which is represented by a large group of minerals, such as oil, bitumen, carbon, oil shale (OS) is a non-traditional potential raw material of rhenium. Since the deposits of these minerals run into milliards of tons, the rhenium resources in them are great, in spite of the relatively low rhenium concentration. Data on rhenium content in carbonaceous raw materials are relatively scarce and contradictory, although all of them considerably exceed its abundance ratio in the crust ( $7 \cdot 10^{-4}$  g/t by A.P.Winogradov).

Rhenium is found in solid combustible minerals enriched with Mo, V, Cu and U. This complex of microelements is more characteristic of oil shale than of the coal. Comprehensive energy-technological processing of metalliferous oil shale with complete utilization of organic and mineral parts includes their thermal treatment for production of electric and heat energy, chemical products, metals, and building materials. Traditional methods for the thermal treatment of OS are pyrolysis, semicoking, heat dissolution.

Rhenium distribution at high temperature combined processing of oil shale (OS) - oxidizing pyrolysis and the semicoking was studied. The semicoking of OS (Uzbekistan) was performed at the pilot device with solid heat-transport medium at 750°C, the pyrolysis –in the reactor at universal device. The oxidizing pyrolysis of OS at 750-800 °C results in extensive decomposition of the organic substances, which presumable incorporate rhenium. Rhenium heptaoxide, which is a highly volatile compound, passes into the gaseous phase and concentrates in the coke (84.7%). During the semicoking, the main part of rhenium also concentrates in the solid product-semicoke (60.0 %).

Rhenium recovery from the coke was investigated. The rhenium leaching from the coke by water was carried out. Rhenium is successfully recovered from obtained solutions by sorption on active carbon, modified active carbon and anionite. The sorption degree of rhenium was reached 50 % (active carbon BAU), 94.6 % (modified active carbon) and 99.4 % (anionite).

## Tc and Re in Nuclear Medicine



The chairman of the 4<sup>th</sup> Section G.E. Kodina and K.E. German at the social dinner – short time to relax

4.1.

## Tc-99m AND Re-188 IN RUSSIAN NUCLEAR MEDICINE

G.E.Kodina

Burnazyan Federal Medical Biophysical Center of FMBA Russia;  
123182, Moscow, Zhyvopisnaya,46; e-mail: [gkodina@yandex.ru](mailto:gkodina@yandex.ru)

The main tendency of modern nuclear medicine is substantial growth of radiopharmaceuticals (RP) using for therapy, first of all in oncology, but at a proceeding expansion of diagnostic RP. Thus, despite of rapid development of PET quantity of diagnostic procedures with  $^{99m}\text{Tc}$  SPECT and SPECT/CT also continue to grow.

New line for fission  $^{99}\text{Mo}$  production started at the end of 2010 in RIAR (Dimitrovgrad). It has allowed to liquidate a problem of  $^{99}\text{Mo}$  deficiency in Russia and a significant amount is already exported. There are 3 enterprises on  $^{99m}\text{Tc}$ -generators (chromatographic type) production in our country – at IPPE and BPCI (Obninsk) and at PTI (Tomsk). New manufacture of the generators on GMP requirements is projected in Obninsk at the near future. Extraction generators providing centralized deliveries of a  $\text{Na}^{99m}\text{TcO}_4$ -solution work in Moscow, St.-Petersburg and Tomsk. Capacities of operating manufactures are quite sufficient for full satisfaction of the Russian clinics and capable to increase release of generators significantly. Growth of volumes of release restrains with lack of the equipment in hospitals as well as unsatisfactory schemes and time of delivery to some Russian regions.

$^{99m}\text{Tc}$ -kits are let out by DIAMED Ltd. (Moscow), certificated according to requirements GMP. The enterprise during 20 years completely satisfies needs of domestic and NM-departments and also is capable to increase volumes of release significantly. It is necessary to note, that to 2008 the volume of kits supplied to domestic clinics has returned on a level which has been reached up to a default (1998r.), but is not observed growth (for the reasons specified above) not looking at expansion of the nomenclature further. Nowadays the list includes 13 positions. Analysis of changes in  $^{99m}\text{Tc}$ -kits usage for diagnostics of various diseases is resulted in the report.

Among last development of new  $^{99m}\text{Tc}$ -RP, introduced in manufacture or clinical trials it is necessary to note « Resoscan,  $^{99m}\text{Tc}$  » (for osteoscintigraphy, on the base of zoledronic acids) and «Nanotech,  $^{99m}\text{Tc}$  » (nanocolloid for sentynel lymph nodes visualization).

$^{188}\text{Re}$ -Generators are let out by IPPE (Obninsk). R&D on  $^{188}\text{Re}$  production in a centrifugal extractor are spent in KRI (St.-Petersburg) in collaboration with IPCE RAS (Moscow).

Preclinical trials of «Zoleren,  $^{188}\text{Re}$ » ( $^{188}\text{Re}$ -zoledronic acid for therapy of bone metastasises) are starting in June, 2011 and then clinical trials will be held in 2012. The RP was developed in FMBC under the order of JS-Company «Pharm-Sintez». The R&D program on creation of  $^{188}\text{Re}$ -RP for radiosynovectomy is begun this year.

As a whole it is possible to conclude, that in Russia there are necessary and sufficient conditions for progress and development of new technologies for nuclear medicine with use both  $^{99m}\text{Tc}$ , and  $^{188}\text{Re}$ . Researchers and manufacturers of generators and RP on the basis of these radionuclides hope, that realization of the Federal program «Development of the pharmaceutical and medical industry of the Russian Federation for the period till 2020 and the further prospect» as well as the Project «Progress of nuclear medicine in the Russian Federation » will allow to expand significantly researches and to increase volumes of release of already existing and new radiopharmaceuticals.



4.2.

## THE *fac*-{TcO<sub>3</sub>}<sup>+</sup> CORE – A CHALLENGE FOR HIGH-VALENT TECHNETIUM CHEMISTRY

H. Braband

Institute of Inorganic Chemistry, University of Zurich, Winterthurerstr. 190, 8057 Zurich, Switzerland

**KEYWORDS:** Radiopharmacy, Labeling, Cycloaddition, Biodistribution, Glucose**ABSTRACT:**

We report a protocol for the synthesis of [<sup>99m</sup>TcO<sub>3</sub>(tacn)]<sup>+</sup> (**[1]**<sup>+</sup>) that is suitable for clinical translation. Bioconjugates containing pharmacophores ([TcO(NO<sub>2</sub>-Imi)(tacn)]<sup>+</sup> **[2]**<sup>+</sup>), artificial amino acids ([TcO(Fmoc-allyl-His)(tacn)]<sup>+</sup> **[3]**<sup>+</sup>), and glucose derivatives ([TcO(allyl-tetraacetylglucose)(tacn)]<sup>+</sup> **[4]**<sup>+</sup>) were synthesized by cycloaddition strategies and fully characterized (<sup>99</sup>Tc and <sup>99m</sup>Tc). These new Tc complexes are stable at neutral pH and demonstrate the potential and flexibility of the (3+2) cycloaddition labeling concept. In addition to the synthetic work, the first biodistribution study of **[1]**<sup>+</sup> was completed. The biodistribution study suggests the stability of this complex *in vivo*. Further it could be demonstrated that the high hydrophilicity of the [<sup>99m</sup>TcO<sub>3</sub>(tacn)]<sup>+</sup> building block is a complement to the complexes of the *fac*-{Tc(CO)<sub>3</sub>}<sup>+</sup> core.

**INTRODUCTION:**

The site specific conjugation of a metalloradionuclide like <sup>99m</sup>Tc to a targeting vector in a manner in which the product retains the affinity of the parent is challenging.

To address this issue, one can take advantage of the rich coordination chemistry of technetium. Coordination of radio-metals to an appropriate and strong chelator, conjugated to a targeting biomolecule (peptides, oligonucleotides or small molecules) is the most frequently applied labelling strategy and known as the bifunctional chelator (BFC) approach.<sup>1</sup> The BFC approach conveniently enables screening of a large number of targeting molecules with one particular metal core for which the chelator is designed. In the field of technetium chemistry, Tc<sup>V</sup> and Tc<sup>I</sup> cores have been widely explored to prepare molecular imaging probes.<sup>2-5</sup>

The ability to create new Tc synthons paves the way for the development of new and effective imaging probes that overcome the challenges of introducing a metal complex into a vector.

In this context, the Tc<sup>VII</sup> core, *fac*-{TcO<sub>3</sub>}<sup>+</sup> came into the focus of our recent research because it is compact and can be coordinated to tripodal ligands. Besides the small size, complexes with the *fac*-{TcO<sub>3</sub>}<sup>+</sup> core display a unique reactivity, particularly in water, that can be used as a creative route to preparing novel molecular imaging probes. With alkenes, complexes of the *fac*-{TcO<sub>3</sub>}<sup>+</sup> core undergo metal-mediated, vicinal *cis*-dihydroxylation reactions (alkene-glycol interconversion) via a (3+2) cycloaddition reaction.<sup>6</sup> *cis*-Dihydroxylation reactions with [OsO<sub>4</sub>] have been known for a long time,<sup>7, 8</sup> with *fac*-{TcO<sub>3</sub>}<sup>+</sup> complexes this reaction type enables a ligand-centered labeling strategy as recently shown with a proof-of-principle study.<sup>9</sup> However, *fac*-{TcO<sub>3</sub>}<sup>+</sup> complexes are uncommon<sup>10-20</sup> and their syntheses in water remained unknown until recently.<sup>21</sup> To utilize the *fac*-{TcO<sub>3</sub>}<sup>+</sup> core for preparation of molecular imaging probes, a one step synthesis of the [<sup>99m</sup>TcO<sub>3</sub>(L<sup>3</sup>)]<sup>+</sup> precursor is required. To address this need [<sup>99m</sup>TcO<sub>3</sub>(tacn-R)]<sup>+</sup> (tacn-R = 1,4,7-triazacyclononane or derivatives) were synthesized in moderate overall yield by the reaction of [<sup>99m</sup>TcO<sub>4</sub>]<sup>-</sup> with phosphines and tacn or tacn derivatives.<sup>9</sup> We report a protocol for the synthesis of [<sup>99m</sup>TcO<sub>3</sub>(tacn)]<sup>+</sup> and the preparation of bioconjugates using cycloaddition strategies. In addition to the synthetic work, the biodistribution study of [<sup>99m</sup>TcO<sub>3</sub>(tacn)]<sup>+</sup> was completed.

## EXPERIMENTAL:<sup>22</sup>

### Synthesis of <sup>99</sup>Tc complexes

**[<sup>99</sup>TcO<sub>3</sub>(NO<sub>2</sub>-Imi)(tacn)]Cl ([2]Cl):** Complex [1]Cl (20 mg, 0.06 mmol) was dissolved in 4 ml of distilled water and 1-allyl-4-nitro-imidazol (9.8 mg, 0.06 mmol) was added. While stirring at 65°C, the yellow reaction solution turned deep blue in a couple of minutes. After 2 h, heating was stopped and the solvent evaporated to dryness by a slow nitrogen stream. Compound [2]Cl can be isolated as analytically pure micro crystals. Yield: 28 mg (98%).

**[<sup>99</sup>TcO<sub>3</sub>(Fmoc-allyl-His)(tacn)](BPh<sub>4</sub>) ([3](BPh<sub>4</sub>)):** Complex [1]Cl (11 mg, 0.04 mmol) was dissolved in 1 ml of distilled water and the Fmoc-protected 1-allyl-histidine (20 mg, 0.05 mmol) was added. The reaction solution was stirred for 2 h at 60°C. Compound [3](BPh<sub>4</sub>) was precipitated from the reaction solution by addition of Na(BPh<sub>4</sub>) (14 mg, 0.04 mmol). Yield: 38 mg (95%).

**[<sup>99</sup>TcO<sub>3</sub>(allyl-tetraacetylglucos)(tacn)]Cl ([4]Cl):** [1]Br (17 mg, 0.05 mmol) was dissolved in a mixture of water and acetonitrile (1:1, 3 ml) and the protected monosaccharide allyl 2,3,4,6-tetra-O-acetyl-β-(D)-glucopyranoside (19 mg, 0.05 mmol) was added. The reaction mixture was stirred overnight at ambient temperature. Blue crystals, suitable for X-ray diffraction analysis, were obtained by the addition of Na(PF<sub>6</sub>) (8.4 mg, 0.05 mmol) to the reaction mixture and slow evaporation of the solvent. Yield: 28 mg, 86%.

### Synthesis of <sup>99m</sup>Tc complexes

**[<sup>99m</sup>TcO<sub>3</sub>(tacn)]Cl ([1]Cl):** Polymer (10 mg) [Nova Syn<sup>®</sup> amino resin (90 μm), coupled to tris(2-carboxy-ethyl)phosphine hydrochloride (≈ 0.3 mmol·g<sup>-1</sup> resin) by standard SPPS technique] was transferred with 1,4,7-triazacyclononane trihydrochloride (23.5 mg, 10<sup>-4</sup> mol) to a vial, tightly closed and flushed with N<sub>2</sub> for 10 min. [<sup>99m</sup>TcO<sub>4</sub>]<sup>-</sup> (1 mL) eluate was added and the reaction mixture heated for 1 h at 95°C. The reaction solution was cooled, the resin filtered and the solution neutralized by the addition of NaOH (0.1 M). Based on the exact amount of used NaOH (≈ 90 μl) the amount of distilled water was calculated and added to the [<sup>99m</sup>TcO<sub>3</sub>(tacn)]Cl solution to obtain a physiological NaCl concentration. 5 mg DOWEX 1 resin were activated in three times 1 ml of saline solution until the solution was not acidic anymore. The resin was filtered and added to the [<sup>99m</sup>TcO<sub>3</sub>(tacn)]Cl solution. After 10 min at room temperature the resin was filtered and the [<sup>99m</sup>TcO<sub>3</sub>(tacn)]Cl solution was used for further biological studies. Radiochemical purity was measured by HPLC. Yield 10 – 15%, radiochemical purity > 99%.

**[<sup>99m</sup>TcO(tacn)(NO<sub>2</sub>-Imi)]Cl ([2]Cl):** Compound [1]Cl (<sup>99m</sup>Tc) was prepared by the method described above. 1-Allyl-4-nitro-imidazol (15 mg, 0.1 mmol) was added to the physiological solution of [1]Cl. The reaction mixture was heated to 60°C for 30 min. Compound [2]Cl was isolated by semi-preparative column chromatography using PBS as mobile phase. Radiochemical purity was measured by HPLC. Yield: 30%, radiochemical purity > 99%.

**[<sup>99m</sup>TcO<sub>3</sub>(tacn)(Fmoc-allylHis)]Cl ([3]Cl):** Compound [1]Cl (<sup>99m</sup>Tc) was prepared by the method described above. The Fmoc-protected 1-allyl-histidine (41 mg, 0.1 mmol) was added to the physiological solution of [1]Cl and the reaction solution was stirred for 2 h at 60°C. Radiochemical purity was measured by HPLC. Yield: 72%.

**[<sup>99m</sup>TcO<sub>3</sub>(tacn)(allyl-tetraacetylglycos)]Cl ([4]Cl):** Compound [1]Cl (<sup>99m</sup>Tc) was prepared by the method described above. The protected monosaccharide allyl-2,3,4,6-tetra-O-acetyl-β-(D)-gluco-

pyranoside (39 mg, 0.1 mmol) was added to the reaction solution and the mixture was stirred for 19 h at 40°C. Radiochemical purity was measured by HPLC. Yield: 96%.

## RESULT AND DISCUSSION:

The chemical properties of  $[^{99m}\text{TcO}_3(\text{tacn})]^+$  [**1**]<sup>+</sup> are attractive for developing molecular imaging probes because of its small size, hydrophilicity, serum stability and its reactivity with alkenes.<sup>9</sup> To evaluate the biological behaviour of [**1**]<sup>+</sup> and to evaluate its suitability for preparing bioconjugates via cycloaddition reactions, a protocol for the synthesis of [**1**]<sup>+</sup> suitable for clinical translation was developed. An immediate challenge was the very high hydrophilicity of [**1**]<sup>+</sup> and its separation from unreacted  $[^{99m}\text{TcO}_4]^-$ . After the preparation of [**1**]<sup>+</sup> from  $[^{99m}\text{TcO}_4]^-$  with 1,4,7-triazacyclononane and a polymer bound phosphine (figure 1), the solution was neutralized and diluted with water to obtain an isotonic NaCl solution. Addition of a strong anion exchange resin (DOWEX 1) removed residual  $[^{99m}\text{TcO}_4]^-$  quantitatively within 10 min at room temperature. This convenient procedure allowed the isolation of compound [**1**]<sup>+</sup> with a radiochemical purity higher than 99% (figure 1).

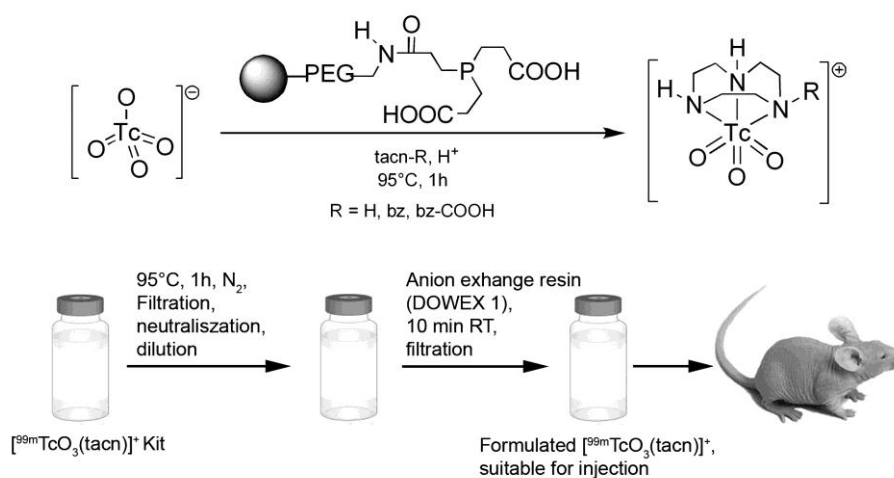


Figure 1: Synthesis of  $[^{99m}\text{TcO}_3(\text{tacn})]\text{Cl}$  and its formulation for biological applications.

With this protocol for the synthesis of [**1**]<sup>+</sup> it was possible to characterize the biological profile of  $[^{99m}\text{TcO}_3(\text{tacn})]^+$  (figure 2) and to evaluate its suitability for preparing bioconjugates via cycloaddition reactions.

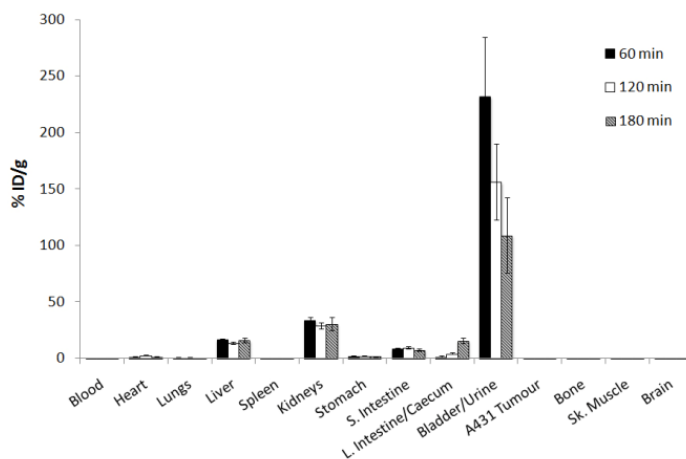
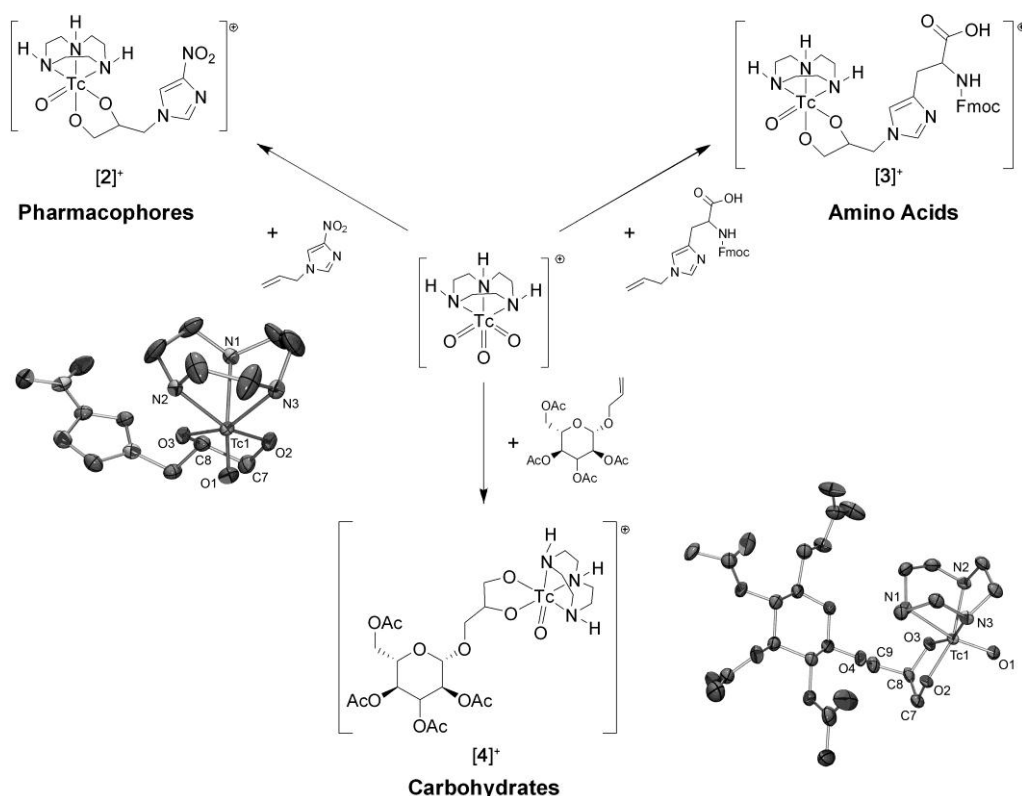


Figure 2: Biodistribution of [**1**]<sup>+</sup> in A431 tumor xenograft bearing mice.

The biodistribution of  $[1]^+$  suggests the stability of this complex *in vivo* since decomposition to  $[TcO_4]^-$  would result in thyroid and stomach/gut accumulation which was not observed. The bio-profile of  $[1]^+$  corroborates the high hydrophilicity of the  $[^{99m}TcO_3(tacn)]^+$  building block because it shows rapid clearance of  $[1]^+$  and the product resides mainly in the bladder and urine with some uptake and retention in the kidneys and liver. Thus  $[^{99m}TcO_3(tacn)]^+$  is a complement to the *fac*- $[Tc(H_2O)_3(CO)_3]^+$  core which binds to blood pool proteins, thereby inhibiting a fast clearance from the body.<sup>23</sup>  $[1]^+$  shows a similar route of excretion compared to the small *fac*- $[Tc(CO)_3]^+$  complex  $[Tc(tacn)(CO)_3]^+$  reported by Suzuki *et al.* although  $[1]^+$  appears to be retained in the liver and kidney to a higher degree over three hours.<sup>24</sup>

To explore the potential and general utility of the new bioconjugation strategy, three classes of vectors were bound to the *fac*- $[^{99m}TcO_3]^+$  framework via a simple (3+2) cycloaddition: 4-Nitroimidazole as a hypoxia imaging agent,<sup>25</sup> histidine to create a non-natural amino acid that can be incorporated into peptides and radiolabeled and a simple glucose derivative (scheme 1). Glucose is a particularly interesting biomolecule because of the search for  $^{99m}Tc$ -based carbohydrates as a complement to 2-deoxy-2- $(^{18}F)$ fluoro-D-glucose ( $^{18}F$ -FDG).<sup>26-28</sup>

These reactions and the stability of the products demonstrate the flexibility and suitability of this new labeling strategy. *In vivo* studies with these new compounds and the preparation of other new radiopharmaceuticals derived from this core are currently under way.



Scheme 1: Labeling of 1-allyl-4-nitroimidazole, 1-allyl-L-histidine and allyl-2,3,4,6-tetra-O-acetyl- $\beta$ -(D)-glucopyranoside with  $[^{99m}TcO_3(tacn)]^+$  via (3+2)-cycloaddition.

## CONCLUSION:

The preparation of  $[^{99m}TcO_3(tacn)]^+$  in high radiochemical purity introduces a new synthon for the preparation of molecular imaging probes. The *in vivo* study with the parent  $[^{99m}TcO_3(tacn)]^+$  demonstrated that the compound is stable *in vivo* and is rapidly excreted, in contrast to the pharmacokinetic profile observed for  $[^{99m}Tc(H_2O)_3(CO)_3]^+$ . The reactivity of  $[^{99m}TcO_3(tacn)]^+$

towards alkenes represents a convenient and efficient technique for labelling biomolecules through a (3+2) cycloaddition. To exemplify the versatility of the labelling procedure, three principally different biomolecules were linked to the *fac*- $\{^{99m}\text{TcO}_3\}^+$  core. These include a hypoxia targeting pharmacophore, an amino acid analogue and a glucose derivative. We demonstrated that the high hydrophilicity of the  $[\text{TcO}_3(\text{tacn})]^+$  building block is a complement to the complexes of the *fac*- $\{\text{Tc}(\text{CO})_3\}^+$  core which are generally hydrophobic.

It has to be emphasized that the high-valent chemistry of technetium is not only relevant from a radiopharmaceutical point of view, but also with respect to the significant amounts of long lived  $^{99}\text{Tc}$  produced in world's nuclear power plants. The possibility of binding *fac*- $\{\text{TcO}_3\}^+$  compounds via (3+2)-cycloaddition covalently to a substrate, such as surface modified nanoparticles or resins, without a ligand replacement reaction could pave the way for new opportunities in the field of technetium immobilization. Therefore, the direct activation of  $[\text{TcO}_4]^-$  and its efficient transformation into water stable *fac*- $\{\text{TcO}_3\}^+$  compounds is of great interest.

#### ACKNOWLEDGMENT:

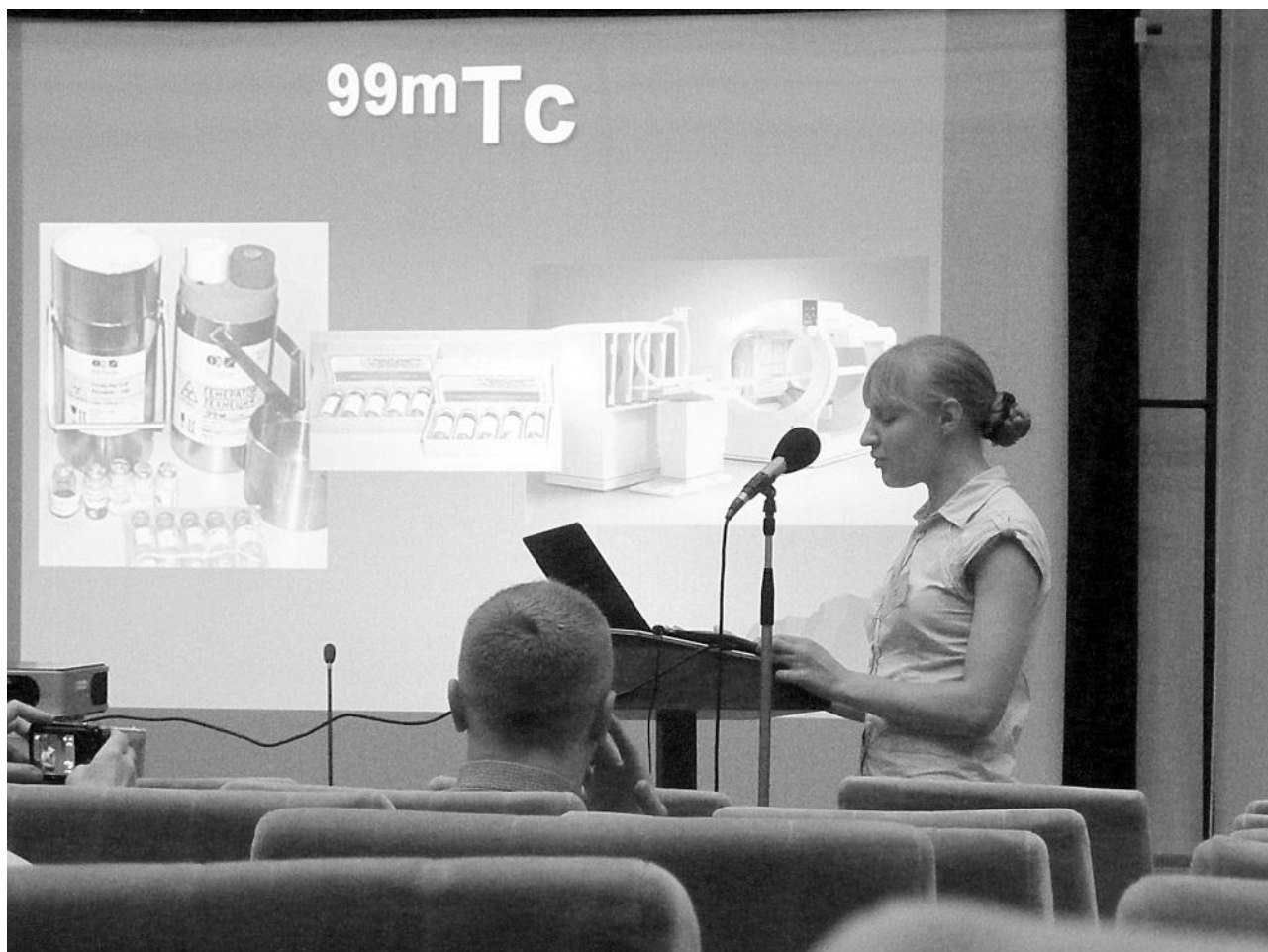
H. Braband acknowledges financial support from the Swiss National Science Foundation, Ambizione project PZ00P2\_126414.

#### REFERENCES:

- Blower, P., *Dalton Trans.* **2006**, 1705.
- Alberto, R.; Abram, U., *Handbook of Nuclear Chemistry*. Kluwer Academic Publishers: 2003; Vol. 4, p 211.
- Liu, S.; Edwards, D. S., *Chem. Rev.* **1999**, 99, 2235.
- Jurisson, S. S.; Lydon, J. D., *Chem. Rev.* **1999**, 99, 2205.
- Dilworth, J. R.; Parrott, S. J., *Chem. Soc. Rev.* **1998**, 27, 43.
- Pearlstein, R. M.; Davison, A., *Polyhedron* **1988**, 7, 1981.
- Kolb, H. C.; VanNieuwenhze, M. S.; Sharpless, K. B., *Chem. Rev.* **1994**, 94, 2483.
- Schroeder, M., *Chem. Rev.* **1980**, 80, 187.
- Braband, H.; Tooyama, Y.; Fox, T.; Alberto, R., *Chem. Eur. J.* **2009**, 15, 633.
- Thomas, J. A.; Davison, A., *Inorg. Chim. Acta* **1991**, 190, 231.
- Oehlke, E.; Alberto, R.; Abram, U., *Inorg. Chem.* **2010**, 49, 3525.
- Tooyama, Y.; Braband, H.; Spingler, B.; Abram, U.; Alberto, R., *Inorg. Chem.* **2008**, 47, 257.
- Supel, J.; Hagenbach, A.; Abram, U.; Seppelt, K., *Z. Anorg. Allg. Chem.* **2008**, 634, 646.
- Supel, J.; Abram, U.; Hagenbach, A.; Seppelt, K., *Inorg. Chem.* **2007**, 46, 5591.
- Thomas, J. A.; Davison, A., *Inorg. Chem.* **1992**, 31, 1976.
- Du Preez, J. G. H.; Gerber, T. I. A.; Gibson, M. L., *J. Coord. Chem.* **1990**, 22, 33.
- Herrmann, W. A.; Alberto, R.; Kiprof, P.; Baumgärtner, F., *Angew. Chem. Int. Ed.* **1990**, 29, 189.
- Banbery, H. J.; Hussain, W.; Evans, I. G.; Hamor, T. A.; Jones, C. J.; McCleverty, J. A.; Schulte, H.-J.; Engles, B.; Kläui, W., *Polyhedron* **1990**, 9, 2549.
- Nugent, W. A., *Inorg. Chem.* **1983**, 22, 965.
- Davison, A.; Jones, A. G.; Abrams, M. J., *Inorg. Chem.* **1981**, 20, 4300.
- Braband, H.; Abram, U., *Inorg. Chem.* **2006**, 45, 6589.
- Braband, H.; Tooyama, Y.; Fox, T.; Simms, R.; Forbes, J.; Valliant, J. F.; Alberto, R., *Chem. Eur. J.* **2011**, in press.
- Egli, A.; Alberto, R.; Tannahill, L.; Schibli, R.; Abram, U.; Schaffland, A.; Waibel, R.; Tourwe, D.; Jeannin, L.; Iterbeke, K.; Schubiger, P. A., *J. Nucl. Med.* **1999**, 40, 1913.
- Suzuki, K.; Shimmura, N.; Thipyapong, K.; Uehara, T.; Akizawa, H.; Arano, Y., *Inorg. Chem.* **2008**, 47, 2593.



25. Chu, T.; Hu, S.; Wei, B.; Wang, Y.; Liu, X.; Wang, X., *Bioorg. Med. Chem. Lett.* **2004**, *14*, 747.
26. Alberto, R.; Braband, H.; N'Dongo, H. W. P., *Current Radiopharmaceuticals* **2009**, *2*, 254.
27. Bowen, M. L.; Orvig, C., *Chem. Comm.* **2008**, 5077.
28. Schibli, R.; Dumas, C.; Petrig, J.; Spadola, L.; Scapozza, L.; Garcia-Garayoa, E.; Schubiger, P. A., *Bioconjugate Chem.* **2004**, *16*, 105.



Alesya Maruk presenting her report on  $^{99\text{m}}\text{Tc}$  radiopharmaceuticals

#### 4.3.

### **NEW RADIOPHARMACEUTICALS BASED ON TECHNETIUM-99m WITH BIFUNCTIONAL CHELATING AGENTS**

A.Ya. Maruk, A.B. Bruskin, G.E. Kodina

Burnazyan Federal Medical Biophysical Center of FMBA Russia;  
123182, Moscow, Zhyvopisnaya,46; e-mail: [amaruk@list.ru](mailto:amaruk@list.ru)

Currently,  $^{99m}\text{Tc}$  is radionuclide of choice for the preparation of SPECT-radiopharmaceuticals (RP) in the whole world.  $^{99m}\text{Tc}$  is eluted from the generator in the form of a solution  $\text{Na}^{99m}\text{TcO}_4$ , and then subjected to reduction and complexation with ligands. The complexity of technetium chemistry makes it necessary to search for new, improved and multifunctional complexing agents. Particular attention is paid to ligands that can not only bind technetium, but also can be linked to biomolecules such as peptides or monoclonal antibodies. Among these ligands, called bifunctional chelating agents (BCA), best results are showed by DTPA (Diethylene triamine pentaacetic acid),  $\text{MAG}_3$  (Mercaptoacetyltriglycine), and HYNIC (6-Hydrazinopyridine-3-carboxylic acid).

Published data on the synthesis and application of some peptides labeled with  $^{99m}\text{Tc}$  using HYNIC, and DTPA and  $\text{MAG}_3$  are reviewed. There were found changes in the behavior of conjugates with the same peptide using different BCA. This suggests that the choice of BCA should be the first stage of planning the development of each new BCA RP with technetium-99m.

As a biological basis for the creation of conjugates with different radionuclides ( $^{111}\text{In}$ ,  $^{68}\text{Ga}$ ) octreotide is often taken. Octreotide is an analogue of the somatostatin which is accumulated in cancer cells of neuroendocrine nature. It was found that the conjugates with  $^{99m}\text{Tc}$ -octreotide are not effective enough, and the peptide has been modified. The most successful results of such modifications are Vapreotid (RC-160) and tyrosine-Octreotide (TOC).

When comparing DTPA,  $\text{MAG}_3$  and HYNIC most researchers coincide that preference over the other two BCA is given to HYNIC, which is caused, first of all, by its more suitable pharmacokinetic properties. Nevertheless, data on biodistribution of all three BCA conjugates still remain controversial.

The report also discusses published data on the choice soligand to HYNIC. The following soligands are considered: tricine (1,1-bis(hydroxymethyl)ethyl)glycine), EDDA (Ethylene diamine diacetic acid) and the mixture tricine with nicotinic acid. All these soligands provide obtaining of peptides labeled with  $^{99m}\text{Tc}$ , in good yield and stability. According to some reports, the best pharmacokinetics (accumulation in tumors, the rapid excretion via the kidney) was detected in the RP with EDDA as soligand. With the data presented, it is clear that not only conjugates known soligands (mostly tricine and EDDA) should be further developed, but also new ones should be looked for. The peptide most advisable to use is TOC.

4.4.

## **“Rezoskan, <sup>99m</sup>Tc” IN THE DIAGNOSIS OF METASTATIC BONE LESIONS**

V.N. Korsunsky, V.N. Oshchepkov, S.V. Shiryaev, E.Z. Rabinovich

A.I. Burnazyan FMBC,  
N.N.Blokhin RCRC, Institute of Urology, "Farm-Sintez" Inc.

“Rezoscan, <sup>99m</sup>Tc” is the first kit used in the domestic and international practices for commercial radiopharmaceuticals (RP) based on zoledronic acid, being intended for the diagnostic of bone pathology by Single Photon Emission Computed Tomography (SPECT).

Our clinical studies provided with the data on the high diagnostic value of the drug enabling to identify metastatic bone cancer patients. The primarily observed pharmacokinetic characteristics of the drug, compared with those applied in the clinic counterparts, indicate that it is characterized with more rapid RP elimination from the body, low accumulation in organs and tissues at high tropism to sites of metastasis in the skeleton. It provide with higher sensitivity and resolution in detecting metastatic lesions of the skeleton of variable nature.

Due to favorable pharmacokinetics, the “Rezoscan, <sup>99m</sup>Tc” SPECT examination is possible 1 - 1.5 hours after administration of the radiopharmaceutical, whereas all the existing RP require at least 3 hours waiting period before the patient bone scan examination. This ensures high economic and technological efficiency and lower patient irradiation dose rates.

Using “Rezoscan, <sup>99m</sup>Tc” it was possible to identify both blastic, mixed, and, most important, the lytic metastases in primary bone scan, that were not detected by commonly used radiopharmaceuticals in clinics. It should be noted that in recent medical practice there were no other radioisotope diagnostic products providing with the possibility to detect lytic metastases in the skeleton.

The investigation conducted on a selected group of patients has shown that bone scanning with “Rezoscan, <sup>99m</sup>Tc” allows control of skeletal metastases by means of therapy with zoledronic acid combined with chemotherapy.

Based on the foregoing, we conclude that the drug “Rezoscan, <sup>99m</sup>Tc” significantly differs from the previous generation of diagnostic radiopharmaceuticals and it has prospects for wider use in clinical practice.

4.5.

## OBTAINING TECHNETIUM-99M LABELED NANOCOLLOIDS BASED ON ALUMINUM OXIDE FOR MEDICAL DIAGNOSTICS

V.S. Skuridin, V.L. Sadkin, E.S. Stasiuk, N. V. Varlamova,  
A.C. Rogov, E.A. Nesterov

National Research Tomsk Polytechnic University  
634050, Russia, Tomsk, Lenina, 30. E-mail: [svs1946@rambler.ru](mailto:svs1946@rambler.ru)

In recent years, labeled with technetium-99m ( $^{99m}\text{Tc}$ ) nanosized colloids of various compositions are widely used in medicine for the diagnosis of inflammatory processes, the identification of "sentinel" lymph nodes in cancer patients, for labeling autoleukocytes etc. Presupposition for using aluminum oxide as a "carrier"  $^{99m}\text{Tc}$  label is its relatively low toxicity, combined with good adsorption properties, availability and low cost. As the object of research, we used gamma- $\text{Al}_2\text{O}_3$  nanopowder with a particle size of 7 nm obtained from aluminum hydroxide by cyclic heating to 500°C.

In order to obtain stable compounds of  $^{99m}\text{Tc}$  with  $\text{Al}_2\text{O}_3$  oxide there was previously studied the effect of acid activation of oxides on the value of their sorption capacity in relation to  $^{99m}\text{Tc}$  which has different degrees of oxidation in static conditions for adsorption. As a reducing agent tin (II) chloride dehydrate ( $\text{SnCl}_2 \cdot 2\text{H}_2\text{O}$ ) was used. As a result, it was found that the maximum adsorption of  $^{99m}\text{Tc}$  is observed on oxides  $\text{Al}_2\text{O}_3$ , treated with HCl solution on the basis of  $2 \cdot 10^{-4}$  mole per 1 g of oxide, which corresponds to pH 5.6 colloid. In these conditions the adsorption of  $^{99m}\text{Tc}$  (VII) ions is about 30%, and of reduced ions of  $^{99m}\text{Tc}$  (IV) – more than 90%. The method of filtering the resulting product through a filter with a pore diameter of 100 nm revealed that in the latter case, the output of labeled nanocolloid exceeds 98%. In this case, adsorbed on oxide  $^{99m}\text{Tc}$  (IV) is not washed off with saline (0.9% solution of NaCl), which indicates the stability of the compound. The investigation of the chromatograms showed in the resulting product apart to  $^{99m}\text{Tc}$  (VII) the presence of two reduced forms of  $^{99m}\text{Tc}$ . Perhaps one of them is  $^{99m}\text{Tc}$  (V).

Medicobiological tests of  $^{99m}\text{Tc}$  labeled oxide  $\text{Al}_2\text{O}_3$  were conducted on "Vistar" line white male-rats with weight 300-350 g. Inguinal lymph node in all the animals clearly visualized in 15 minutes, when it accumulated from 1,2 to 2,1% of introduced amount of labeled colloid. This shows the principal possibility of using the obtained compound for conducting lymphoscintigraphy.

4.6.

## **RECEIVING OF NANOSIZED COLLOIDS BASED ON MODIFIED DTPA MOLECULE LABELED WITH TECHNETIUM-99m**

E.A. Nesterov, V.S. Skuridin, M.L. Belyanin, J.V. Nesterova,  
V.L. Sadkin, A.S. Rogov, I.V. Chikova

National Research Tomsk Polytechnic University, Russia, Tomsk, Lenin Avenue, 30, [nesterov\\_evgeny@mail.ru](mailto:nesterov_evgeny@mail.ru)

Currently, the significantly intensification of interest to use of radioactivity colloid nonmaterial's in medicine is note all around the world. Radioactivity nanocolloid application in oncology is based on quick and effective ability of «sentinel» lymph nodes detection.

Optimal method of «sentinel» lymph node detection is consider in use of colloid nonmaterial's marked by technetium-99m for scintigraphic or radiometric detection of node localization. Rich coordination chemistry of technetium can obtain on its basis the various simple and complex, biologically active coordination compounds with desired properties.

As a result of the spent researches the methods of receipting of new nanocolloid based chemical systems on basis of modification of diethylene triamine pentaacetic acid (DTPA) molecule has been worked out. The main factor, which is affect on using DTPA as chelator of radioactive mark, was molecule or one's derivative ability to form enough stable complexes with different radioactive metals including combination of technetium-99. The DTPA molecule hydrophilic and that's why one can't form colloidal particles. Hydrophilic fragments addition gave the ability to receive insoluble's modified complex of DTPA.

Preliminary research of compound transmission density, show's that the middle radius of generated colloids is near 100 nanometers. But the middle radiochemical emission of nanocolloid, which have the diameter less than 100 nanometers, is about 80%, and this is closed to foreign analogs rate.

The result of dynamic scintigraphic research showed, that after being injected, the preparation goes to lymphatic system very active. Eventually one can say that modify nanocolloids are functionally suitable for lymphoscintigraphy and « sentinel» node visualization.

That work has been carried out in the network of federal program «Scientific and scientific-pedagogical manpower of innovated Russia for 2009-2013»



4.7.

## **SYNTHESIS AND COMPLEX ANALYSIS OF BIOLOGICALLY ACTIVE POLYMERS (POLY-N-VINYLPYRROLIDON) WITH THE $\text{Re}(\text{CO})_3$ SPECIES.**

N. I. Gorshkov<sup>1</sup>, A. Yu. Murko<sup>1</sup>, Yu. I. Zolotova<sup>1</sup>, O. V. Nazarova<sup>1</sup>, I. I. Malakhova<sup>1</sup>, V. D. Krasikov<sup>1</sup>, R. Schibli<sup>2</sup>

<sup>1</sup>Institute of Macromolecular Compounds RAS, St.-Petersburg, 1999004, Bolshoi pr VO, 31, Russia

<sup>2</sup>Institute for Pharmaceutical Sciences ETH Hönggerberg, HCI H425 Wolfgang-Pauli-Strasse 10 CH.8093 Zurich, Switzerland

**Key words:** bioactive synthetic polymers (BASP), rhenium, radiopharmaceuticals, HPLC, spectroscopy

### **Abstract**

Poly-N-vinylpyrrolidone derivatives with attached iminodiacetic groups were prepared in a wide range of molecular masses (9 000 – 30 000 Da). Labeling of polymer carriers with the “cold”  $\text{Re}(\text{CO})_3^+$  species were performed under mild conditions. Metallo-polymeric conjugates were comprehensively characterized by means of spectroscopic methods (IR, NMR, ESI-MS) and also with HPLC. Special attention was paid to the choice of stationary and liquid phases for HPLC procedure, because it is extremely important for the further analysis of radiolabeled polymeric systems.

### **Introduction**

Over the last 15 years chemistry of organometallic species,  $\text{M}(\text{CO})_3^+$  ( $\text{M} = \text{Tc}, \text{Re}$ ) was intensively studied. This interest grew up due to promising properties of this organometallic fragment: relatively small size and low metal charge of metal atom (+1) [1]. Potentially, these parameters should not disturb biological properties of organometallic biocojugates. However, worldwide practice of synthesis of low molecular compounds labeled with the  $\text{M}(\text{CO})_3^+$  fragment and biodistribution studies demonstrate significant decreasing of specific site transport of conjugates and accumulation of radioactivity in non target organs. More successful was introducing of organometallic species into macromolecular native biomolecules (antibodies, proteins) [2].

Targeted delivery of effector functions and moieties to diseased sites in the human body for diagnostic or therapeutic purposes is a hallmark of modern drug development. Monoclonal antibodies (MAb) has become an indispensable tools in this respect. However, the development and production of such macromolecules is extremely expensive and as a consequence such drugs are growing burden for the health system. Hence, less costly alternatives have to be developed and investigated which combine the positive biological and pharmacological features of antibodies with the lower costs of development of small molecules. Possible alternatives could be biologically active synthetic polymers (BASP).

The major advantages of BASP in contrast to natural macromolecules (e.g. antibodies) are: (i) the possibility synthesis of polymers with relative narrow molecular mass distribution, (ii) possibility of regulation sites for attaching of biological vector and (iii) to attach one or several radiometal fragments to bioconjugate (if desired to achieve high specific activity) (iv) low cost and possibility to perform radiolabeling in one step procedure without complicated additional purification. Last point is urgent for routine clinical application.

In the work we present an approach for labeling of biologically active synthetic polymers (BASP) with the  $\text{M}(\text{CO})_3^+$  fragment. To our knowledge literature data for radiolabeling of grafted BASP are scarce.

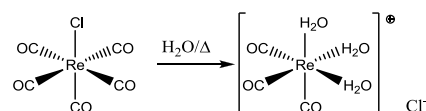
We propose combination of macromolecular pharmaceutical chemistry and radiopharmaceutical chemistry for the development of novel, more efficient and less expensive targeted radio-polymers (BASP) useful for tumor diagnosis and therapy. Polymer-carrier poly-N-vinylpyrrolidone was chosen due to its known pharmacological properties [3]. Polymers with attached chelation iminodiacetate (IDA) groups were synthesized in a wide range of molecular masses (9 000 -30 000 Da). IDA is known as effective chelation system for linking of  $M(\text{CO})_3$  species [4]. Special attention was paid for chromatographic analysis of metallo-polymeric conjugates, due to it is a single method for determination of radiochemical purity of resulting radiopharmaceuticals.

## Experimental.

All chemical reagents have pure and HPLC grade quality and were purchased from (Neva-Reactiv, Cryochrom, Reachim (Russia) and Sigma-Aldrich, Merck (Germany).

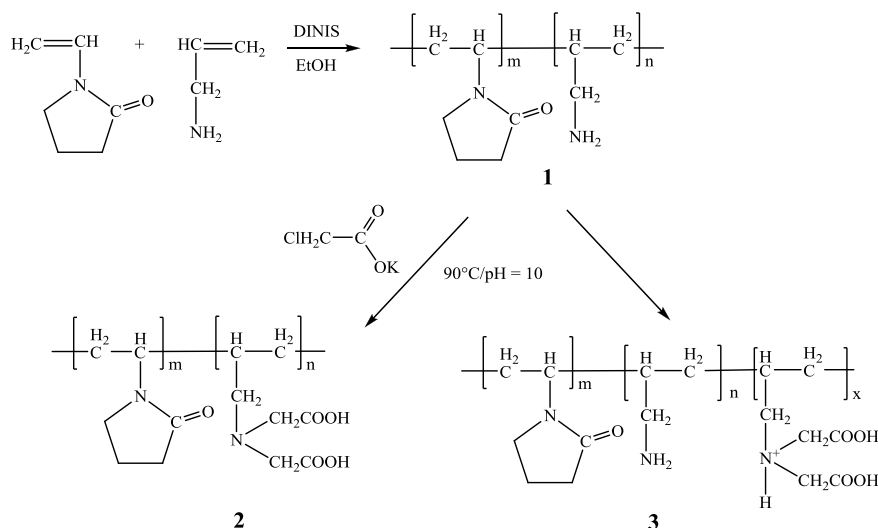
Spectral measurements were performed on IR FSM 201 unit (Russia), NMR spectrometer Bruker AM 500 (Germany), pilot ESI MS unit (Institute of Analytical Instrument-Making RAS, Russia). Chromatographic analysis was performed on the multidetector HPLC system (Knauer, Germany). Ultrashort monolithic CIM (Convective Interaction Media) columns (Austria) were used as a stationary phase, elution system - 0.1% TFA aqueous buffer, flow rate – 0.3 ml/min, detection: 210, 230, 254, 280 nm, RI.

Synthesis of aqueous solution of  $[\text{Re}(\text{CO})_3(\text{H}_2\text{O})_3]\text{Cl}$  was performed according to the previously described procedure [5] (scheme 1).



Scheme 1: Synthesis of the organometallic precursor  $[\text{Re}(\text{CO})_3(\text{H}_2\text{O})_3]^+.$ [2]

Synthesis of iminodiacetate-poly-N-vinylpyrrolidone was done according to previously developed procedure [3] (scheme 2)



Scheme 2: Preparation of PVP comprising exclusively the metal chelating system IDA (**2**) and the synthesis of mixed PVP comprising free primary amine functionalization (**3**) - for subsequent attachment of targeting molecules and formation of biologically active synthetic polymers (BASP) - and the metal chelating system IDA

Contents of free aminogroups in co-polymers were performed by means of potentiometric titration with the 0.1M HCl. Data on characteristic viscosity were obtained in 0.1 M sodium acetate

aqueous solution at 25°C. Molecular masses were evaluated according to Mark-Howink constants for unmodified PVP. (Tables 1, 2)

Table 1. Polymerization conditions and characteristics of polymers obtained at Stage I

№	Polymerization conditions				Mass. %	Characteristics of amino co-polymers			
	[VP] : [AA]		[DINIS], vass. % from mon.	Conc. %		[η], dl/g	M <sub>η</sub>	[VP] : [AA]	
	Mass. %	Mol. %						Mol. %	
1	66 : 34	50 : 50	1	50	20	0,10	13000	93,7 : 6,3	88,4 : 11,6
2	82 : 18	70 : 30	1	50	43	0,16	30000	97,1 : 2,9	94,4 : 5,6
3	66 : 34	50 : 50	1	50	20	0,08	9000	93,8 : 6,2	88,5 : 11,5

Table 2. Polymerization conditions and characteristics of PVP-IDA copolymers obtained at Stage II

Starting amino-co-polymer				Resulting PVP-IDA co-polymer		
№	[AA], Mol. %	[η], dl/g	M <sub>η</sub>	№	[IDA], Mass. %	[IDA], Mol %
1	11,6	0,10	13000	4	5,8	6,6
2	5,6	0,16	30000	5	5,7	6,5
3	11,5	0,08	9000	6	5,8	6,6

Metall-polymeric conjugates were synthesized under various conditions: at ambient temperature (2-3 days), 60-70 C (2-3 hrs), microwave activation (3 min, 450 Wt), at pH≈7. Final product was purified by membrane dialysis, lyophilic drying and characterized by spectral and chromatographical methods.

## Result and Discussion

On the preliminary stage of our research we concentrated our efforts on organic synthesis of model poly-N-vinyl pyrrolidone (PVP) biofunctionalized with metal chelating systems suitable for (radio)labeling with organometallic precursors of the element technetium and rhenium ( $[M(CO)_3(H_2O)_3]^+$  M = Tc, Re). This water soluble precursor has been reported to coordinate with a wide variety of metal chelating systems comprising various donor groups. The organometallic precursor  $[Re(CO)_3(H_2O)_3]^+$  was prepared starting from commercially available  $Re(CO)_5Cl$  according to the literature data [5]. This procedure was chosen in order to avoid presence of undesirable salts (e.g.  $NEt_4Cl$ ), in contrast to the traditional  $[Re(CO)_3Br_3][NEt_4]_2$  precursor [1], which could impair the subsequent reaction with the polymers and would be difficult to separate for the desired product. The synthetic route is given in scheme 1.

In order to exclude any unwanted and unspecific labeling of PVP with the organometallic precursors via the lactone groups we studied the coordinative behaviour of the nonmodified PVP

with  $[\text{Re}(\text{CO})_3(\text{H}_2\text{O})_3]^+$ . Reactions were followed by HPLC and products were purified by membrane dialysis and lyophilic drying. The isolated product was characterized by IR. The IR spectra revealed extremely weak bonding of organometallic precursor to PVB backbone. The characteristic signals of the metal carbonyl were very weak indicating that the lactone rings appeared to be weak chelating agents and are not able to efficiently form complexes with  $\text{Re}(\text{CO})_3$ -moiety.

For functionalization of PVP with metal chelating systems N-vinyl pyrrolidone was reacted with allylamine according to scheme 2. The corresponding PVP (1) were reacted with chloro acetic acid at 90°C at pH 10 for N-alkylation to form the bifunctional derivative (2). The iminodiacetate (IDA) derivative 3 was obtained in good yields. The range of attached IDA chelation groups varied from 2 to 6 mass %. The purification was performed by dialysis and lyophilic drying. The polymers were characterized by  $^1\text{H}$ - $^{13}\text{C}$  2D NMR, viscosimetry, and IR spectroscopy. MS analysis further revealed that the size distribution of the PVP ranged from 9 000 -30 000 Da (optimal range of masses for the target biological transport).

In a parallel strategy we prepared modified PVP contained both IDA chelators and free amino groups for further coupling of (tumor) targeting of small peptides (scheme 2).

In a second step we labelled the derivatives 2 and 3 with the organometallic precursor. The reaction conditions have been optimized. Syntheses were carried out under different conditions: at ambient temperature (2-3 days), 60-70 C (2-3 hrs), microwave activation (3 min, 450 Wt). Complexation of organometallic complex was followed by HPLC fig.1. It could be shown, that reaction strongly depends on pH (optimal value was estimated as  $\text{pH} \approx 7$ ). The labelled polymers were purified in order to remove undesired traces of buffer salts dialysis and lyophilized. The products  $[\text{Re}(\text{CO})_3(2/3)]$  were characterized by  $^1\text{H}$  NMR, IR spectroscopy (fig.1).

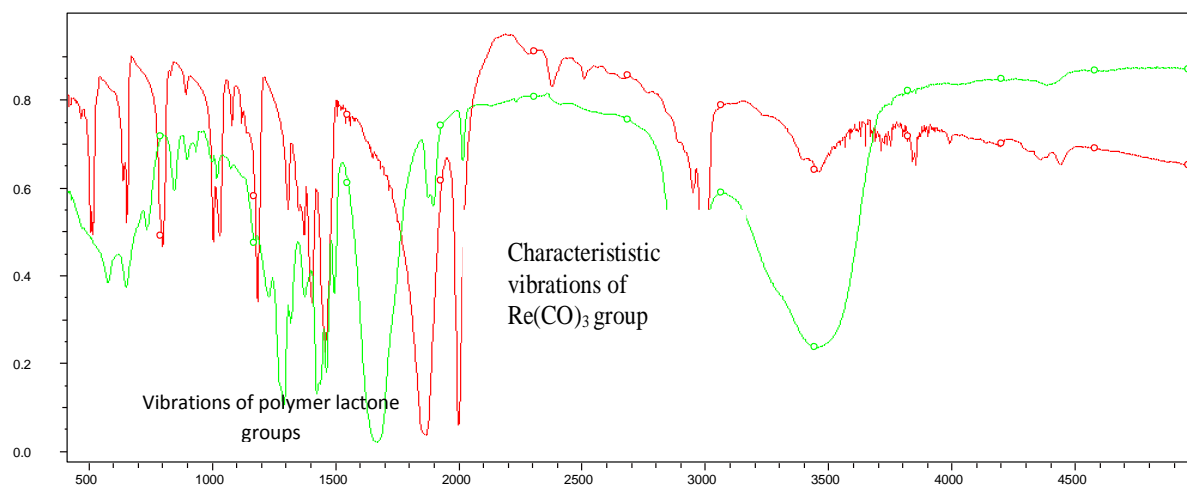


Fig.1. IR characterization of conjugated PVP-IDA- $\text{Re}(\text{CO})_3$  co-polymers, KBr pellets. Red –  $[\text{Re}(\text{CO})_3\text{Br}_3][\text{NEt}_4]_2$  (as a reference), green- PVP-IDA- $\text{Re}(\text{CO})_3$  conjugate (sample 13 000 Da)

According to the presented data it is clear, that valent vibrations of noncoordinated  $\text{Re}(\text{CO})_3^+$  are significantly shifted contrastly to metallo-conjugated polymer with the  $\text{Re}(\text{CO})_3^+$  species. Moreover, decreasing of vibrations of  $\text{Re}(\text{CO})_3^+$  in contrast to vibrations lactone rings confirms quantitative linkage of metallorganic fragment to polymeric matrix. This tendency was observed to all range of studied conjugates and in the good agreement for published data for low molecular compounds, labeled with  $\text{M}(\text{CO})_3$  fragment [3].

Data of ESI mass spectrometry also confirms formation of metallo-polymeric conjugate (fig.3)

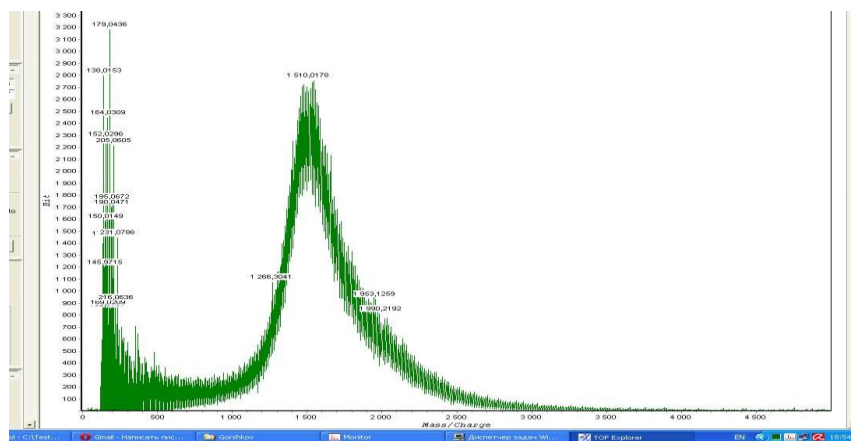


Fig. 3. ESI-MS for the PVP-IDA-Re(CO)<sub>3</sub> conjugate (starting PVP-IDA -MW = 13 000 Da + 2 000 Re(CO)<sub>3</sub>) Mz ≈ 15 000 Da.

Special attention was paid for chromatographical analysis of reaction mixtures and final BASP with incorporated Re(CO)<sub>3</sub> species. It is well known, that chromatographic methods for analysis and purification of radiolabeled compounds are the very effective tool. Therefore, a separate task of current work was to find an optimal conditions for separation using HPLC and HPTCL. At the moment, for fast and efficient separation of reaction products (high and low weight molecular components) ultra-short monolithic CIM (Convective Interaction Media, BiaSeparations, Austria) exhibited most efficient properties. However, despite extremely short times of analysis (5 min), this type of columns cannot provide information about the distribution of the analyths according to their molecular mass. In contrast, the originally prepared monolithic and silica modified HPTLC plates have capability for identification all reaction products online. Furthermore, it was estimated that employing traditional SEC HPLC on a known sorbents previously prepared in our group allows separating polymeric species in a wide range of molecular masses. Typical chromatogram of reaction mixture is presented below (fig. 4).

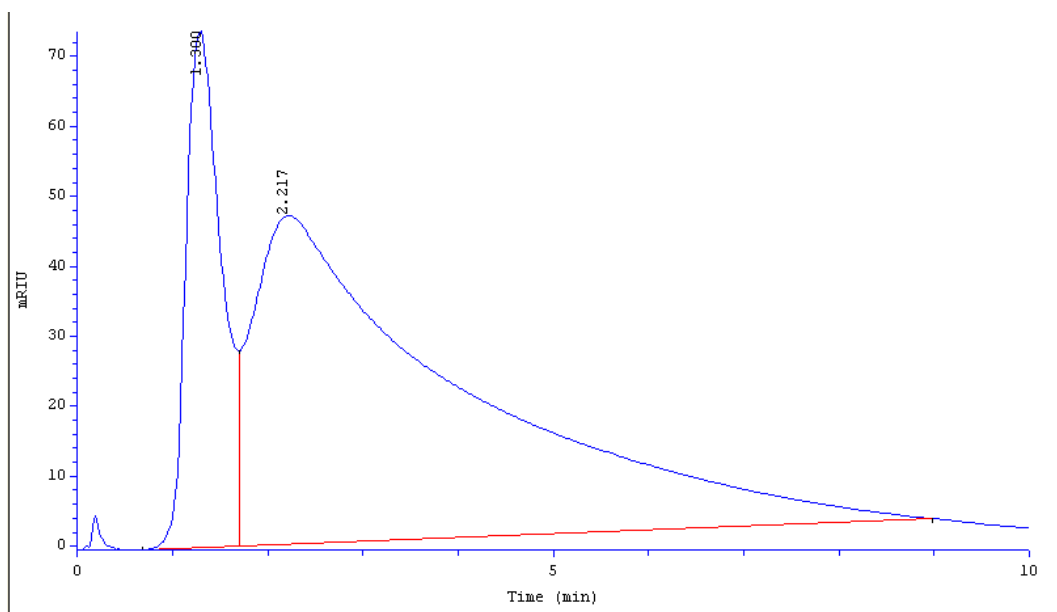


Fig. 4. Separation of artificial mixture of copolymer PVP-IDA-Re(CO)<sub>3</sub> and Re(CO)<sub>3</sub>(H<sub>2</sub>O)<sub>3</sub> on the CIM-CM ultrashort column Elution system (0/1% TFA/methanol 50:50), UV detection (diode array) (210, 230, 260, 310 nm), RI detection, flow -0.3 ml/min (absorption maximum of conjugate -210 nm). **First sharp peak corresponds to PVP-IDA-Re(CO)<sub>3</sub> conjugate; second broad peak - Re(CO)<sub>3</sub>(H<sub>2</sub>O)<sub>3</sub>**



## CONCLUSIONS

It was demonstrated that organometallic species are fully trapped by IDA chelation system and produce stable metallo-polymeric conjugates. Moreover, it should be noted, that both types of polymers, **2** and **3**, have the same coordinative properties, thus the free primary amine in derivative **3** does not seem to participate in the metal coordination (according to NMR and IR data).

HPLC system for separation of organometallic precursor and target polymeric conjugate, based on CIM technology, was developed.

## ACKNOWLEDGMENTS

This work is supported by SCOPES Project No. IZ73Z0\_128443 and RFBR N 10-08-00963

## References

1. Alberto et al. *J. Am. Chem. Soc.* **120**: 7987-7988 (1998);
2. Kirsch U. E., poly-N-vinylpyrrolidone and other poly-N-vinylamides, , Moscow, Nauka (*in Russian*) (1998)
3. M. Welch, C. S. Redvanly. Handbook of Radipharmaeuticals.Wiley, (2003).
4. Schibli et al. *Bioconjugate Chem.* **13**, 750-756. (2002)
5. N. Gorshkov et. al *Radiochemistry* **42**, 231-235(2000).

6. 4.8.

## **DEVELOPMENT OF DOSIMETRIC SUPPORT AND PLANNING OF RADIONUCLIDE THERAPY WITH RADIOPHARMACEUTICAL LABELED $^{188}\text{Re}$**

A.N. Klyopov<sup>2</sup>, V.V. Krylov<sup>1</sup>, Y.A. Kurachenko<sup>2</sup>, Eu.S. Matusovich<sup>2</sup>, Eu.V. Snigirev<sup>2</sup>, O.P. Aleksandrova<sup>2</sup>

<sup>1</sup>Medical Radiological Research Centre of Ministry of Health, krylov@mrrc.obninsk.ru

<sup>2</sup>Obninsk Institute for Nuclear Power Engineering of National Research Nuclear University MEPhI

Now in MRRC of Ministry of Health of Russian Federation is realized the program of skilled-technological and preclinical tests perspective radiopharmaceutical labeled  $^{188}\text{Re}$ . For some of them carrying out of a phase of clinical researches in the near future is planned. With a view of increase of efficiency of medical technologies by employees INPE together with MRRC the complex of development in the field of individual dosimetric support and planning radionuclide therapies of some diseases with radiopharmaceutical on the basis of  $^{188}\text{Re}$  is carried out. They include: 1) development of techniques for dosimetry of critical organs (kidneys, bladder, blood, red bone marrow, etc.) and target organs (tumours or metastasises) which, in turn, lean on offered optimum, and sparing for patients, protocols for clinical researches of radiopharmaceutical pharmacokinetics (with light invasive and noninvasive techniques); the criterion of an optimality here means use minimally necessary number of time measurements and an opportunity of restoration of data about accumulation of radiopharmaceutical in those organs in which it is impossible direct to carry out radiometry; 2) a substantiation and development of techniques for mathematical (multichamber) modelling of radiopharmaceutical metabolism in an organism of patients, and realization of numerical identification of corresponding kinetic parameters - with the purpose of restoration continual dependences of radiopharmaceutical dynamics, carried out on the basis of the limited volumes of skilled data; 2) development of techniques of carrying out of single-photon emission images in a problem of identification of activity  $^{188}\text{Re}$ , accumulated in amazed and healthy organs of patients; in particular, development of mathematical models for target organs - the bone structures allowing with certain accuracy to restore distribution of activity in view of factors of degradation single-photon emission images; 3) mathematical modelling of fields of absorbed doses by a method of Monte-Carlo in the volumes of tumors and critical organs; 4) development of Radiation Safety recommendations under scripts of patient's contact with relatives after their extract from hospital.

Results of numerical calculation of fields of absorbed doses in phantoms of tumours and also results of variational modelling of radiopharmaceutical pharmacokinetics with  $^{188}\text{Re}$  in an organism of patients with bone metastasises are resulted.

## 4.9.

### EDUCATION AND TRAINING IN NUCLEAR MEDICINE, RADIOPHARMACY, MEDICAL PHYSICS AND MOLECULAR IMAGING: THE INSTN EXPERIENCED APPROACH

A. Hammadi

Atomic Energy Commission, Saclay Research Center, National Institute for Nuclear Science and Technology, 91191 Gif-sur-Yvette, France – [akli.hammadi@cea.fr](mailto:akli.hammadi@cea.fr)

Nuclear medicine, radiopharmacy, molecular imaging or related fields combine advanced engineering in chemistry, nuclear science, molecular biology and physiology together with state-of-the-art technology for non invasive *in vivo* imaging. This field contributes immensely to biomedicine because it is the major technology that can explore and measure the chemistry of life in a non invasive manner. It is thus a key for the development of new diagnostics and therapeutics. Considering the rapid development of technologies, there is an urgent need of specific educational programs in these fields. Physicians, researchers and chemists must be well qualified and appropriately trained to adapt themselves to these new technologies. This must be achieved through suitable and updated trainings.

Since 1974, the National Institute for Nuclear Science and Technology (INSTN) within the French Atomic Energy Commission (CEA) has been responsible for organising the theoretical training of medical doctors, pharmacists, chemists and physicists in **nuclear medicine**, **radiopharmacy** and **medical physics**. This Institute is recognised by the European Association of Nuclear Medicine (EANM) as a training centre in radiopharmacy. The INSTN provides solutions to satisfy needs in nuclear medicine, radiopharmacy and molecular imaging training in the requirements from professionals. To do so, the institute is in charge of organising short trainings for professionals (Life-Long Learners). It also brings training solutions to special needs for national and/or international trainings. At last, the INSTN is deeply involved in the academic field.

Among the training courses provided by the INSTN, the new **European Master in Molecular Imaging** (EMMI) offers an international program entirely dedicated to **molecular imaging**. Supported by the European Commission under the SOCRATES programme, this two years interdisciplinary curriculum is brought together by prominent European molecular imaging research groups, with the objective to prepare students for both academic and industrial positions.

Courses are held in parallel at the partners Institutions: the INSTN (Saclay, France) – coordinating, and the Universities of Paris Sud 11 (France), Antwerp (Belgium), Crete (Greece) and Turin (Italy). The curriculum includes courses on the basics of physics, chemistry, biology and physiology for Molecular Imaging, advanced courses on each imaging technology (PET, SPECT, MRI, OI, and ultrasound) as well as a full time six months immersion in one of over forty industrial or academic partner laboratories around the world. In just two years, EMMI students acquire full theoretical and practical competences in all molecular imaging modalities. The master programme is entirely held in English, built for students with a bachelor degree in biology, biomedical sciences but also in physics, chemistry and computer science as optional bridging courses are offered in physiology and biology.

Those highly specialized theoretical and practical courses, which are recognized by professionals, are open to students and employees willing to improve their professional qualification in these fields. It would be clever to ask one or many Universities in order to face the setting up of a middle-term academic training allowing the training of the future radio pharmacists. Thus, Russia could be inspired by the trainings (INSTN) made for these professionals in France at the present time.

4.10.

## HIGH SPECIFIC ACTIVITY RADIONUCLIDES IN NCA FORM: Re-186g PRODUCED BY CYCLOTRON

M.L. Bonardi<sup>1</sup>, F. Groppi<sup>1</sup>, E. Lapshina<sup>2</sup>, S. Manenti<sup>1</sup>, L. Gini<sup>1</sup>

<sup>1</sup> Università degli Studi di Milano, UNIMI and Istituto Nazionale di Fisica Nucleare, INFN,  
L.A.S.A., Radiochemistry Laboratory, Via F.lli Cervi 201, I-20090 Segrate, MI, ITALY

<sup>2</sup> Institute for Nuclear Research, 60th October Anniversary Prospect, 7A Moscow, 117312, RUSSIA

The <sup>186g</sup>Re is a double purpose  $\beta$  and  $\gamma$  emitter, that, thanking to its suitable chemical and nuclear properties:  $T_{1/2} = 90.64$  h;  $E_{\beta}^{\max} = 1069.5$  keV (74.3%) and 932.3keV (18.8%); main  $\gamma$ s at 137.155 (8.22%) and 122.58 (0.56%) keV, is presently used in metabolic radiotherapy with palliative pain elimination of bone metastases but it is a good candidate to be used in metabolic radioimmuno-therapy (RIT) combined with molecular imaging devices (i.e. theragnostics). Unfortunately this radionuclide cannot be used yet in RIT therapeutic procedures, because its present production route - by radiative neutron capture on moderately enriched <sup>185</sup>Re in thermal nuclear reactor - leads to a relatively low specific activity  $A_S$ , in carrier-added (CA) form. The possibility to improve the use of this radionuclide is strictly linked to the possibility of increasing the  $A_S$ , approaching the theoretical carrier-free (CF) value of 6.88 GBq  $\mu\text{g}^{-1}$ . A way is its production by proton or deuteron bombardment on tungsten-186 targets via either (p,n) or (d,2n) nuclear reactions.

In order to assess the effectiveness of the  $W(p,n)^{186g}\text{Re}$  and/or  $W(d,2n)^{186g}\text{Re}$  nuclear reactions to produce <sup>186g</sup>Re in no-carrier-added (NCA) form, new sets of thin target excitation functions and experimental thick-target yields for each RN were measured, at variable proton energies up to  $22.0 \pm 0.2$  MeV and deuteron energies up to  $19.0 \pm 0.2$  MeV [1-3]. The experiments were carried out at first by using W targets of natural isotopic composition. This leads to a production of a range of Re radioisotopes and to an effective <sup>187</sup>W “internal spike”. A first conclusion is that natural W is not a suitable target due to the low  $A_S$ (NCA) and radioisotopic purity achievable, caused by the production of several other stable and radioactive nuclides of Re and secondly that the production by deuteron beam is envisaged, due to the substantially higher yield. Besides, a suitable radiochemical separation of Re isotopes from W and <sup>186</sup>W targets and from <sup>183</sup>Ta by-product was set up for both proton and deuteron bombardments. A single radiochromatography method based on activated acidic aluminum oxide (AAO) was adopted. The radiochemical recovery yield obtained in each separation is greater than 98 % within the first 12.5 mL and the values reach 100 % within 15 mL of solution for a 100 mg W metal target. For W target weights up to 500 mg, the solution and column volumes have been scaled-up. NAA and ET-AAS have been adopted for determination and quality control of chemical purity and  $A_S$ (NCA).

**Acknowledgments:** Special thanks are devoted to the staff of JRC-Ispra (VA, Italy) of EC for cyclotron irradiations, INFN-GrV for financial support and Doctorate School in Physics, Astrophysics and Applied Physics of the Università degli Studi di Milano.

### References

1. Z.B. Alfassi, E. Persico, F. Groppi, M.L. Bonardi, *Appl. Radiat. Isot.*, **67**:240–242 (2009).
2. M.L. Bonardi, F. Groppi, S. Manenti, E. Persico, L. Gini, *Appl. Radiat. Isot.*, **68**:1595-1601 (2010).
3. M. Bonardi, F. Groppi, E. Persico, S. Manenti, K. Abbas, U. Holzwardt, F. Simonelli, Z.B. Alfassi, *Radiochim. Acta*, **99**:1-11 (2011).

4.11.

## OPTIMIZATION OF PARAMETERS OF THE <sup>188</sup>RE OBTAINING PROCESS IN A CENTRIFUGAL EXTRACTOR

M.P.Zykov<sup>1</sup>, A.T.Filyanin<sup>2</sup>, G.E.Kodina<sup>3</sup>, A.Yu.Tsivadze<sup>2</sup>, V.N. Romanovsky<sup>1</sup>, D.A.Tkachuk<sup>1</sup>,  
O.A.Filyanin<sup>2</sup>, S.P.Orlov<sup>1</sup>, V.A.Novojilov<sup>1</sup>

<sup>1</sup>Khlopin Radium Institute, <sup>2</sup>Frumkin IPCE RAS, <sup>3</sup>Burnazyan FMBC FMBA Russia; 123182, Moscow,  
Zhyvopisnaya,46; e-mail: gkodina@yandex.ru

One of the most promising radionuclide for nuclear medicine is <sup>188</sup>Re, a daughter of <sup>188</sup>W. A main feature that distinguishes <sup>188</sup>Re from most other therapeutic  $\beta$ -emitters (for example, <sup>90</sup>Sr) is the emission of a soft gamma-ray (15%, 155 keV). This makes it possible to monitor the distribution in tissues and organs and, correspondingly, to calculate very accurately the therapeutic irradiation dose. Research on the RP based on <sup>188</sup>Re, which are already used or under development for therapy of several diseases, is being performed in many leading countries.

**The goals of this work** were to study the use of the centrifugal extractor to isolate medical-grade <sup>188</sup>Re from <sup>188</sup>W. The work included the manufacturing of the two-stage centrifugal extractor, the extraction of Re from W by MEK from alkaline solutions, a determination of chemical impurities in the <sup>188</sup>Re solutions, the construction in a hot cell of equipment for testing the process using actual solutions, a check of the selected extraction conditions, and a determination of the optimal extraction conditions for preparing medical-grade <sup>188</sup>Re.

**Reagents.** The following reagents were used for studying the extraction of Re and W and for analyzing solutions: KOH, WO<sub>3</sub>, and K<sub>2</sub>CO<sub>3</sub> (ultra-high purity); acetone, CHCl<sub>3</sub>, and MEK (chem. pure). MEK was distilled before use as an extractant. <sup>188</sup>W was produced by irradiation of WO<sub>3</sub> in the WWR-M reactor of PNPI (Gatchina). The neutron flux  $1 \cdot 10^{14}$  n·cm<sup>-2</sup>·sec<sup>-1</sup>) is sufficient to prepare 1-2 Ci of <sup>188</sup>W after irradiation of the target during 2-3 months.

**Apparatus and process for preparing <sup>188</sup>Re.** The use of centrifugal extractors is advisable for high-activity solutions because they guarantee the minimal contact time of the high-activity aqueous and organic phases. The apparatus for preparing medical-grade <sup>188</sup>Re with these features was assembled. The shielded box was constructed of steel 100 mm thick. The inner surfaces were lined with stainless steel. Work in the box could be observed through a lead-glass window 150 mm thick. The irradiated WO<sub>3</sub> is dissolved in an alkaline solution containing KOH (2.5 M) and K<sub>2</sub>CO<sub>3</sub> (2.5 M) and fed by pressure into the first stage of the centrifugal contactor. MEK is fed into the first stage of the contactor using a peristaltic pump at 4 ml/min. After passing through the first stage, MEK is scrubbed in the second stage and then is fed into the evaporating apparatus, equipped with a jacket through which hot water (85-95°C) is circulated. After MEK is evaporated the evaporating apparatus is flushed with air for 15-20 min to remove traces of MEK. At this point the evaporating apparatus contains <sup>188</sup>Re. The appropriate aqueous solution is added from an intermediate tank to the evaporating apparatus to dissolve the <sup>188</sup>Re. The solution is bubbled in the apparatus for 3-5 min and fed through a filter into the vial-connector.

**Results and conclusion.** Tests of the equipment using model and actual solutions showed that the Re yield is >85%, the radiochemical purity is >99%, the pH value of the aqueous <sup>188</sup>Re solution is in the range 6.5 to 7.5, the content of radionuclidic impurities is  $<1 \cdot 10^{-7}$ , and the content of stable elements is determined practically by the quality of the aqueous solutions used to dissolve the <sup>188</sup>Re. Such equipment can be a prototype of a regional centralized generator of medical-grade

**Acknowledgement.** The work was partially supported by UNTC contract No. P437.



4.12.

## **<sup>188</sup>W/<sup>188</sup>Re GENERATOR PRODUCTION TECHNOLOGY FOR NUCLEAR MEDICINE**

A.A. Semenova, N.G. Baranov, D.V. Stepchenkov, E.V. Sulim

State Scientific Center of the Russian Federation – Institute for Physics and Power Engineering, Bondarenko sq., 1,  
Obninsk, 249033, Russia

**KEYWORDS:** nuclear medicine, rhenium-188, <sup>188</sup>W/<sup>188</sup>Re generator, adsorbent, elution, static and dynamic sorption, gamma-spectrometry.

### ABSTRACT

The research was done, which aimed at the development of an innovative technology of the production of <sup>188</sup>W/<sup>188</sup>Re chromatographic generator – the first radioisotope generator in Russia for therapeutic application. The generator activity is 100 – 1000 mCi in Rhenium-188.

### INTRODUCTION

Rhenium-188 (<sup>188</sup>Re, T<sub>1/2</sub> = 16.9 h) is considered to be of the perspective radioisotopes for beta-radiation therapy in nuclear medicine. Rhenium-188 is produced via β-decay of tungsten-188 (<sup>188</sup>W, T<sub>1/2</sub> = 69.4 days) in a <sup>188</sup>W/<sup>188</sup>Re generator.

<sup>188</sup>W/<sup>188</sup>Re generator is a promising one for the application in nuclear medicine due to suitability of nuclear and physical characteristics of Re-188 for therapy as well as thanks to the long enough halflife of W-188, which makes it possible to develop generators with a long service life (from 4 to 12 months depending on <sup>188</sup>W initial activity).

*Table 1. Specifications of <sup>188</sup>W/<sup>188</sup>Re generator system*

Daughter radionuclide			Parent radionuclide				Eluent
Isotope T <sub>1/2</sub>	Decay type	Energy and intensity, MeV	Isotope T <sub>1/2</sub>	Decay type	Energy and intensity, MeV	Nuclear reaction	
<sup>188</sup> Re 16.9 h	β <sup>-</sup>	β <sup>-</sup> 2.12 max γ 0.155 (10%)	<sup>188</sup> W 69.4 days	β <sup>-</sup>	□ 0.349 max □ 0.227 (0.22%) □ 0.291 (0,4%)	<sup>186</sup> W(n,γ) <sup>1</sup> <sup>187</sup> W(n,γ) <sup>18</sup> <sup>188</sup> W	0.9% NaCl

The nuclear reaction of dual neutron capture of tungsten-186 by nuclei in a reactor with a high neutron flux ( $2 \cdot 10^{15}$  neutron · cm<sup>-2</sup> · sec<sup>-1</sup>) is used for producing tungsten-188. This radio-nuclide is only produced in RIAR (Dimitrovgrad) in Russia and in Ok-Ridge in the USA.

The advantage of Rhenium-188 as a radionuclide for nuclear medical application is the presence of both beta- and gamma-components (0,155 MeV) of radiation because the first one determines a therapeutic effect, and the other one – imaging in common gamma-chambers that gives information on the bio-distribution of drugs with Re-188. Radiopharmaceuticals based on the generator eluate are synthesized in hospitals for beta-radiation therapy of malignant tumors, bone metastases, rheumatoid arthritis, and other diseases.

## EXPERIMENTAL

“Sodium tungstate ( $\text{Na}_2\text{WO}_4$ ),  $^{188}\text{W}$ ” was used as an initial raw material for carrying out the research. This preparation was produced in RIAR (Dimitrovgrad) by irradiating tungsten trioxide ( $\text{WO}_3$ ) in “SM” high flux reactor with the neutron flux density of  $2 \cdot 10^{15}$  neutron  $\cdot$  cm $^{-2}$   $\cdot$  sec $^{-1}$ . In accordance with the manufacturer’s certificate the specific activity of  $^{188}\text{W}$  was 2–7 Ci/g.

A working solution for sorption was prepared for carrying out the research. The initial “Sodium tungstate ( $\text{Na}_2\text{WO}_4$ ),  $^{188}\text{W}$ ” with pH ~12–13 was conditioned to reach a required pH using the titrated 1.0M and 0.01M hydrochloric acid; it was conditioned to reach a required concentration of tungsten by adding water for injection and 0.001M hydrochloric acid.

The sorption column was filled with an adsorbent – aluminum oxide (pH 4.5) in the quantity of 3.0–6.0 g. The working solution of sodium tungstate,  $^{188}\text{W}$  (pH 2.0–3.0) was passed through the column at the rate of 1.0 ml/min. Then the column was washed with 200ml of sodium chloride isotonic solution. The elution of  $^{188}\text{Re}$  is performed by passing 5–15 ml of isotonic solution of sodium chloride through the column every 3–4 days after  $^{188}\text{W}$  has been adsorbed. Radioactive concentration of technological solution was measured using both dose- calibrator “Atomlab 100 Plus” and a semi-conducting gamma-spectrometer with Ge/Li detector.

## RESULTS AND DISCUSSION

### *The study of $^{188}\text{W}$ adsorption in static and dynamic modes*

The method of radioactive tracers was used during the study of the sorption process for determining a quantitative concentration of W in the experimental process solutions. Sodium tungstate ( $\text{Na}_2\text{WO}_4$ ) solution with  $^{188}\text{W}$  radioactive tracer was used.

The following sorbents were used for studying  $^{188}\text{W}$  adsorption in the static mode:  $\text{ZrO}_2$ ,  $\text{Al}_2\text{O}_3$ ,  $\text{SnO}_2$ . It has been found out that acid alumina in the acidic form is the most effective adsorbent.

### *Static adsorption*

$\text{Al}_2\text{O}_3$  adsorbent (pH 4.5 Fluka) was used. Initial solutions with tungsten concentration of 1.0 mg/ml and different pH values were prepared. Tungsten solution with a radioactive tracer and the weighted portion of aluminum oxide were put into glass vials and, having mixed them thoroughly, 10  $\mu\text{L}$  samples were taken for radiometric measurements in 24 hours. The calculated values of sorption for the taken samples are given in Table 2.

Table 2. The influence of pH of the initial and equilibrium solutions of tungsten sorption

No.	pH of initial solutions	$A_{\text{Vequilibr.}}$ , MBq/ml	Sorption of tungsten, mg/g	pH of the equilibrium solutions
1	2.1	0,23	111,7	2,4
2	3.2	0,29	101,7	4,6
3	4.3	0,40	83,3	5,2
4	4.9	0,59	51,8	5,0
5	6.1	0,74	26,7	8,1
6	6.8	0,88	3,3	8,2

Tungsten sorption was calculated by the formula:

$$Q \text{ (mg/g)} = [(1 - A_{\text{Vequilibr.}}/A_{\text{Vinitial}}) \cdot C_{\text{Winitial}} \cdot V_{\text{Winitial}}] / m \text{ Al}_2\text{O}_3,$$

where:  $A_{\text{Vequilibr.}}$  – concentration activity of the equilibrium solution under study;

$A_{\text{Vinitial}}$  – concentration activity of the initial solution;

$V_{\text{Winitial}}$  – a volume of tungsten solution, ml;

$C_{\text{Winitial}}$  – tungsten concentration in the initial solution, mg/ml.

It follows from the results presented that the adsorption of W should be performed in an acidic medium (pH 2-3).

*Tungsten adsorption on acidic and neutral chromatographic aluminum oxide and calculation of time that is necessary for reaching the sorption equilibrium*

The experiment conditions. The initial solution of sodium tungstate (15 ml) and aluminum oxide in the quantity of 150 mg were put in glass vials. Then samples of 10 μL in volume were taken for performing radiometric measurements each hour during the first three hours and then in 6 hours, 12 hours, and 24 hours.

Tungsten concentrations in the equilibrium solutions were measured by the method of radioactive tracers using gamma-spectrometry. The composition of the initial solution corresponds to the following values: tungsten concentration  $C_w=1.0$  mg/ml, concentration activity  $A_v=1.0$  MBq/ml; pH  $2.7\pm 0.3$ .

Table 3. The results of radiometric measurements and calculation of tungsten sorption on acidic and neutral alumina

Time, hours	$A_{V_{equilibr}}$ , MBq/ml		Static sorption capacity, mg of W/ g of sorbent	
	$Al_2O_3$ , pH 4.5	$Al_2O_3$ , pH 7.0	$Al_2O_3$ , pH 4.5	$Al_2O_3$ , pH 7.0
1	0,65	0,96	35	4
2	0,55	0,90	46	11
3	0,47	0,84	54	17
6	0,23	0,67	78	33
12	0,17	0,63	84	37
24	0,15	0,62	86	39

It follows from the data given in the Table that the sorption of tungsten (85.0 mg/g) at pH 4.5 of the sorbent is twice as much as that at pH 7.0 of the sorbent (38.0 mg/g). Time for reaching the equilibrium state is more than 12 hours.

*The study of  $^{188}W$  in dynamic adsorption*

Dynamic adsorption of  $^{188}W$  was performed directly on the generator's column by passing the working solution through a layer of the adsorbent.

The working solutions were sterilized when they were passed through the sterilizing filter for microfiltration – “Sartorius”. The dimensions of the generator's glass column were as follows:  $\varnothing = 15$  mm,  $L = 85$  mm. Acid  $Al_2O_3$  was used as an adsorbent.

Experiments on W dynamic sorption on acid aluminum oxide (pH 4.5 Fluka), sorbent weight – 1.0g, were done for substantiating and developing  $^{188}W/^{188}Re$  generator loading procedure. The working solution was passed through the chromatographic column using a peristaltic pump at the rate of 1 ml/min. The activities were measured by the gamma-spectrometric method. The results are given in Figure 1 and Table 4.

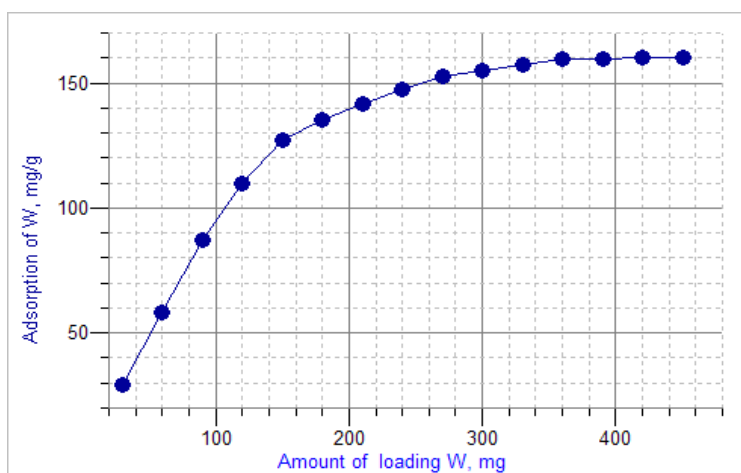


Fig.1. Dynamic sorption capacity as a function of the amount of W passed through the chromatographic column.

The results are given in Figure 1 and Table 4.

Table 4. The amount of W adsorbed on Al<sub>2</sub>O<sub>3</sub> column (1.0 mg) and the amount of W in the tail solution as a function of the amount of W delivered for loading

N os.	Breakthrough of W to the tail, %	W in the tail, mg	Amount of W delivered for loading, mg	W adsorbed on the column, mg	W adsorbed on the column, %
1	3,30	1	30	29,00	96,70
2	3,30	2	60	58,00	96,70
3	3,10	2,8	90	87,20	96,90
4	8,60	10,33	120	109,67	91,40
5	15,20	22,81	150	127,19	84,80
6	24,80	44,6	180	135,40	75,20
7	32,70	68,6	210	141,40	67,30
8	38,60	92,6	240	147,40	61,40
9	43,50	117,6	270	152,40	56,50
10	48,40	145,26	300	154,74	51,60
11	52,30	172,6	330	157,40	47,70
12	55,65	200,3	360	159,68	44,35
13	59,10	230,2	390	159,68	40,90
14	61,90	259,9	420	160,10	38,10
15	64,40	289,9	450	160,10	35,60

It follows from the results given that the maximum *dynamic sorption capacity* of aluminum oxide is 160 mg W/g. The optimal *dynamic sorption capacity* (DSC) of aluminum oxide is 100 mg W/g because the integral sorption is 97% in this case. If a solution continues to be passed through the column, sorption percentage will be lower at a higher value of DSC.

#### Elution curve

Having the generators loaded, an elution curve was plotted for each generator by passing a fixed amount of NaCl isotonic solution by portions of 1.0 ml. The concentration activity of Rhenium-188 was measured in each portion of the eluate. Fig. 2 shows the elution curve of 200 mCi <sup>188</sup>W/<sup>188</sup>Re generator as an example. It follows from Fig.2 that 5ml of the eluate contains more than 80% of Rhenium-188.

#### Optimal parameters of technological procedure

The development of Rhenium-188 generator loading technology was carried out using sorption columns with different quantities of aluminum oxide of “Fluka” or “Merck” trademarks. A shielding lead case was used as radiation shield of the sorption column. Specific activity of tungsten-188 raw material (Technical Specifications 7011-025-20553876-2003) was from 2Ci/g to 7 Ci/g.

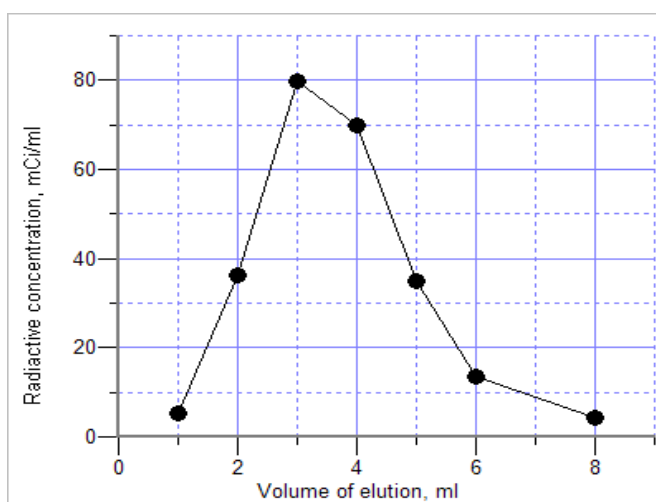


Fig.2. <sup>188</sup>Re elution curve from 200 mCi <sup>188</sup>W/<sup>188</sup>Re generator.

The main optimal parameters of loading of  $^{188}\text{W}/^{188}\text{Re}$  generator with the activity of up to 1Ci have been ascertained on the basis of the results presented and the experiments, which had been done earlier [1-4]:

- adsorbent – acid alumina (for example,  $\text{Al}_2\text{O}_3$ , pH 4.5, Fluka;  $\text{Al}_2\text{O}_3$ , pH 4.0, Merck);
- dynamic sorption capacity 100 mg of W/ g of sorbent;
- loading solution flow rate 1.0 ml/min;
- tungsten concentration 1.0 mg W/ml;
- pH of the loading solution within the range of 2–3;
- volume of the loading solution 0.5–1.0 L;
- loading time 0.5 – 3.0 hours.

#### *Loading of generators of various activities*

It has been found as a result of the studies on loading of Rhenium-188 generators of various activities that the process optimal parameters are as follows (see Table 5):

*Table 5. The optimal parameters of the process of  $^{188}\text{W}/^{188}\text{Re}$  generator loading*

Activity of generator, mCi	Amount of the adsorbent, g	Flow rate of the loading solution, ml/min	Eluent volume, ml
100 - 200	3.0	1.0 – 3.0	5 – 10
300 – 1000	5.0 – 6.0	1.0	10 – 15

#### *Quality control*

The eluates produced from Rhenium-188 generators were subject to quality control. All the parameters regulated by State Pharmacopoeia in relation to radiopharmaceuticals were controlled. The applied methods of the analytical control are listed in Table 6.

*Table 6. Analytical control methods*

Parameter	Analysis method
Radioactive concentration	Gamma-spectrometry (GAMMA 1P)
Tungsten concentration	Spectrophotometry (SF-56)
pH	Potentiometry (“I-130” ion-meter)
Concentration of chloride-ions	Argentometry, titration (“I-130” ion-meter)
Chemical purity	Atom-emission spectroscopy, spectrophotometry
Radiochemical purity	Paper electrophoresis

It has been found out that rhenium-188 yield from  $^{188}\text{W}/^{188}\text{Re}$  generator is not less than 85 %; chemical impurity concentration (Al, Fe) is not more than 5.0  $\mu\text{g}/\text{ml}$ ;  $^{188}\text{W}$  content in the eluate is not more than  $1 \cdot 10^{-3}$  %  $^{188}\text{Re}$  activity; the other radionuclide impurities content is also not more than  $1 \cdot 10^{-3}$  % of  $^{188}\text{Re}$  activity; radiochemical purity of sodium perrhenate,  $^{188}\text{Re}$  is not less than 99.8%.

## **CONCLUSION**

The production technology of a chromatographic 100 – 1000 mCi  $^{188}\text{W}/^{188}\text{Re}$  generator has been developed and mastered.

The quality of  $^{188}\text{W}/^{188}\text{Re}$  generator was competitive with the best foreign analogs: rhenium-188 yield from  $^{188}\text{W}/^{188}\text{Re}$  generator is not less than 85 %; chemical impurity concentration (Al, Fe) is

not more than 5.0 µg/ml; <sup>188</sup>W content in the eluate is not more than 1·10<sup>-3</sup> % <sup>188</sup>Re activity; radiochemical purity is not less than 99.8%.

The SSC RF–IPPE produces tungsten-188 /carrier free rhenium - 188 generators on a routine basis (TS 9452-031-08624390-2006). Registration certificate FS 02032006/5395-06 “Article of medical equipment - Rhenium-188 generator GREN-1”.

About 50 generators in the activity range of 100 – 1000 mCi for Russian and foreign clinical hospitals have been produced since 2004 till the present day.

## REFERENCES

1. Semenova A.A., Stepchenkov D.V., Baranov N.G., Sokolov A.B. *XVII Mendeleev Congress on General and Applied Chemistry*, 2003, Kazan, **2**, 415.
2. Sharkova O.V., Stepchenkov D.V., Semenova A.A., Baranov N.G., Sulim E.V., Petriev V.M., Skvortsov V.G. All-Russian conference “*Modern problems of nuclear medicine and radiopharmaceutics*”, 2002, Obninsk, 15.
3. Baranov N., Stepchenkov D., Nerozin N., Zinchenko M., Semenova A., Minko Yu., Sulim E., Poddubienko V, Petriev V. *European Association of Nuclear Medicine Congress*, 2006, Athens, 417.
4. Stepchenkov D.V., Baranov N.G., Sharkova O.V., Semenova A.A., Sulim E.V., Nerozin N.A., Poddubienko V.P., Minko Yu.V. *The Fifth Russian Conference on Radiochemistry*, 2006, Dubna, 228.



4.13.

## **SUBSTANTIATION OF ENGINEERING PARAMETERS OF RHENIUM-188 STATIONARY GENERATOR INTENDED FOR RADIONUCLIDE THERAPY**

Baranov N.G., Stepchenkov D.V., Nerozin N.A., Sulim E.V., Yu.V.Minko, Semenova A.A.

Federal State Unitary Enterprise “State Scientific Center of the Russian Federation – Institute for Physics and Power Engineering”,  
Bondarenko sq., 1, Obninsk, Kaluga region, 249033, Russia

**Keywords:** nuclear medicine, chromatographic generator, radionuclide therapy, dynamic sorption, yield of Re-188 radionuclide into eluate.

### **Abstract:**

Re-188 generators producing eluates of about 100-500mCi/ml concentration activity are currently in demand in the world nuclear medicine. One of the methods of this problem solving is the development of Re-188 stationary generator. Production technology of 1Ci  $^{188}\text{W}/^{188}\text{Re}$  generator GREN-1 based on  $^{188}\text{W}$  sorption on aluminum oxide in chromatographic column in acid form is the basis of the development. Research results of the choice of effective sorbent, determination of the sorbent optimal granulometric composition, sorbent sorption capacity and rate of initial solution flow through the column, study of the influence of W-188 mother radionuclide specific activity on the eluate concentration activity are presented. Calculation substantiation of shielding material and its size providing the radiation safety during generator operation is presented. It has been established that during the operation of  $^{188}\text{Re}$  generator of up to 5 Ci activity it is possible obtain in fractional elution a sodium perrhenate solution of up to 500 mCi/ml regulated concentration activity.

### **Introduction**

Available separating methods of the mother (W-188) and daughter (Re-188) isotopes can be used in the development of Re-188 generator: distillation, chromatography, extraction. Taking into account the experience of the adsorption-type  $^{99}\text{Mo}/^{99\text{m}}\text{Tc}$  generator operation the research was directed on a study of sorption properties of materials applied in  $^{99}\text{Mo}/^{99\text{m}}\text{Tc}$  generator system. Silica gel, aluminum oxide (in acid, neutral and alkaline forms), zirconium oxide, yttrium oxide, and tin oxide were researched under static conditions. Aluminum oxide in acid form was studied under dynamic conditions. Isotonic solution of sodium chloride only was used for Re-188 radionuclide desorption.

### **Experiment**

Solution of sodium tungstate in sodium hydroxide solution “Sodium tungstate ( $\text{Na}_2\text{WO}_4$ ),  $^{188}\text{W}$ ” of 74-171 GBq/g specific activity in W-188 was used as initial raw radioactive material (Table 1). The product is produced by irradiation of tungsten trioxide  $\text{WO}_3$  in high-flux reactor SM-3 with neutron flux density  $2 \cdot 10^{19} \text{ m}^{-2} \text{ s}^{-1}$  (JSC “SSC RIAR”, Dimitrovgrad).

Table 1. Characteristics of W-188/Re-188 generator system

Daughter radionuclide			Parent radionuclide				Eluent
Isotope, $T_{1/2}$	Decay type	Energy and intensity, MeV	Isotope, $T_{1/2}$	Decay type	Energy and intensity, MeV	Production method	
<sup>188</sup> Re 16.9h	$\beta^-$	$\beta^-$ 2.12 max $e^-$ 0.081, 0.143 $\gamma$ 0.155 (15%)	<sup>188</sup> W 69.4days	$\beta^-$	$\beta^-$ 0.349 max $\gamma$ 0.227 (0.22%); 0.291 (0.4%)	<sup>186</sup> W(n, $\gamma$ ) <sup>187</sup> W(n, $\gamma$ ) <sup>188</sup> W	5, 10, 15 ml 0.9 % NaCl

Semi-conducting spectrometer of gamma-radiation energy “Gamma-1P” and dose-calibrator “Atomlab 100 plus” were used for radiometric control of solutions under investigation. Eluate radiochemical purity was determined by the methods of electrophoresis and ascending chromatography. Hydrogen ion activity in solutions was determined by potentiometric method with the use of ion meter I-130m and pH-tester “Checker”. Sodium chloride concentration in eluate was determined by argentometric method. Chemical element concentration was controlled with the help of spectrometric analysis methods. Sorbent granulometric composition was determined by screen grate “Analysette 3” made by PRO Fritsch. “BINDER GmbH Postfach 102” sterilizer was used.

## Results and discussion

When studying sorption of tungsten compositions in static mode the metal oxides (yttrium, zirconium, tin, aluminum) were used. Seed size was 100-300nm, proportion of sorbent weight and initial solution volume was 1:50, and nanostructured aerogel was Al<sub>2</sub>O<sub>3</sub>·H<sub>2</sub>O. It has been established that aluminum oxide in H<sup>+</sup>-form is the most effective sorbent (Table 2). It follows from the Table 2 that the tungsten sorption by aluminum oxide with pH 4.5 almost twice exceeds the value for sorbent with pH 7.0 within equilibration time 12 hours.

Table 2. Study of <sup>188</sup>W adsorption in static mode

Time, hour	Static sorption capacity, mg W/g of sorbent	
	Al <sub>2</sub> O <sub>3</sub> , pH 4.5	Al <sub>2</sub> O <sub>3</sub> , pH 7.0
1	35	4
2	46	11
3	54	17
6	78	33
12	84	37
24	86	39

Optimal technological parameters of chromatographic generator have been studied in dynamic mode on the columns of different geometrical dimensions with the use of aluminum oxide in H<sup>+</sup> form of definite granulometric composition. Solution of sodium tungstate of 1-10GBq/ml concentration activity and 0.50 – 10 mg of W/ml concentration was used as radioactive solution (Fig.1). It has been established that working solution for tungsten composition sorption should have the optimal concentration 5.5 mg of W/ml. When studying the influence of solution pH on the tungsten sorption properties the initial raw material with pH 12-13 was adjusted to the needed pH value with the help of titrated 1M, 0.01M solutions of hydrochloric acid, to needed tungstate-ion concentration – by addition of water for injections and 0.001 M solution of hydrochloric acid. It has been stated that solution pH in the range of 2.0 –3.0 corresponds to the optimal value (Fig. 2).

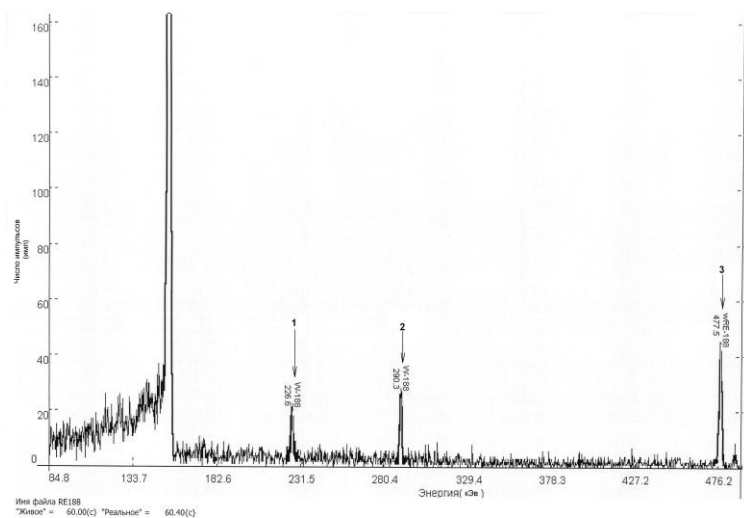


Fig.1. Spectra of solution for loading

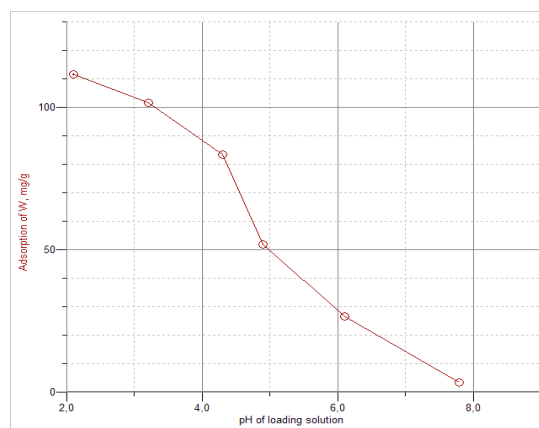


Fig. 2 Influence of solution pH on tungsten sorption properties.

Sorption column was filled with 3.0-19.0 g of pH 4.5 aluminum oxide with seed size in the range of 0.25 – 0.063 mm having uniform granulometric composition. Rate of pH 2.0 – 3.0 solution flow was varied from 0.65 to 4.0 ml/min. The column was washed with 200 ml sodium chloride solution. Elution was performed every 3 – 4 days after the generator loading.

Based on a set of experiments carried out the main optimal parameters of <sup>188</sup>W/<sup>188</sup>Re generator loading of up to 1 Ci activity have been established (Table 3), which are the basis for the development of <sup>188</sup>W/<sup>188</sup>Re generator of 5 Ci activity [1, 2].

Table 3. <sup>188</sup>Re generator loading optimal parameters

Activity of generator, GBq	Sorbent weight, g	Solution flow rate through the column, ml/min	Eluent volume, ml
2.4-7.4	3.0	1	5 – 10
11.1-37.0	5.0 – 6.0	1	15
185	20.0 – 50.0	1 – 3	5 – 50

Experiments on a model facility have been carried out to substantiate 185 GBq <sup>188</sup>Re generator loading technology: sodium tungstate solution concentration activity – 18.5 MBq/ml, tungstate-ion concentration – 5.5 mg/ml in terms of

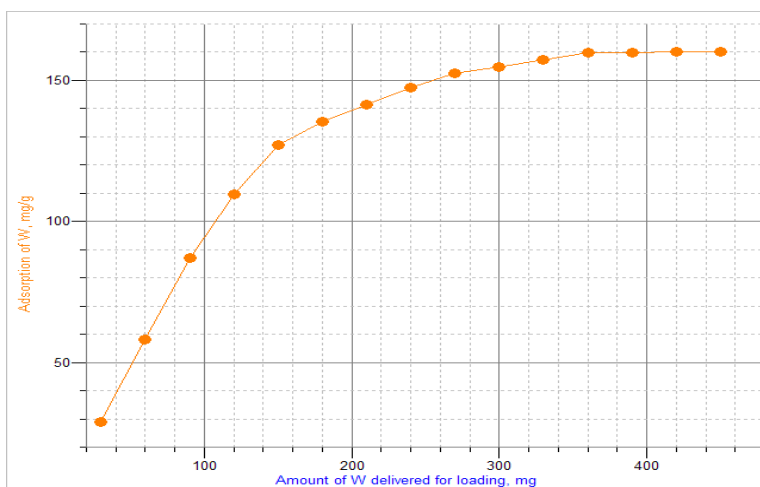


Fig.3. Dynamic sorption capacity (mg W/g) as a function of W amount passed through the chromatographic column.

ungsten, pH of loading solution – 3, the initial solution volume – 1.0 L, elution flow rate – 1.5 ml/min, loading duration – 10 hours, sorbent – aluminum oxide in H<sup>+</sup>-form, sorbent weight – 54.18 g, sorbent seed size – 0.16 – 0.10 mm. It has been stated that the maximal dynamic sorption capacity of this sorbent is 160.1 mg of W/g sorbent, optimal sorption capacity is 100 mg of W/g. In this case the integral sorption is 97 % (fig. 3). When solution further flows through the column at higher DSC value the sorption percentage is less (Table 4). With full elution volume (50ml) the

concentration activity is 0.3 MBq/ml (fig. 4, 5). In this case rhenium yield is 85% of <sup>188</sup>W activity. During successive elution by portions: 30 ml - the concentration activity increases up to 0.5 MBq/ml; 15 ml – the concentration activity increases to 1.3M Gb/ml. Thus, the eluates of different concentration activity up to 11.1 GBq/ml and more can be obtained in fractional elution.

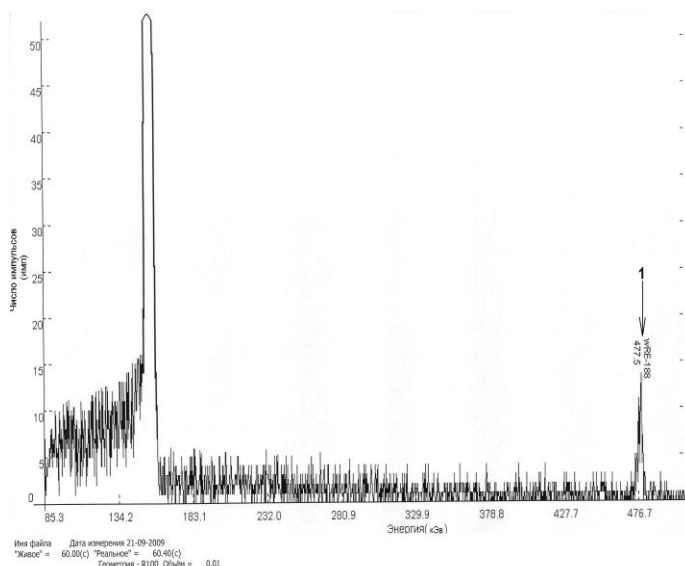


Fig. 4. Spectra of solution of eluate from <sup>188</sup>W/<sup>188</sup>Re generator

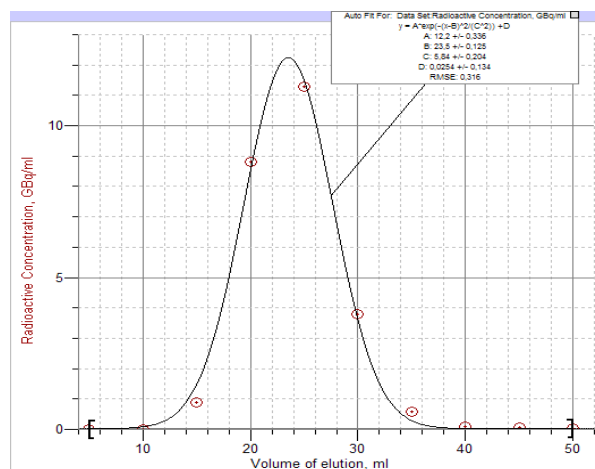


Fig 5. Elution curve of Re-188 radionuclide from stationary <sup>188</sup>W/<sup>188</sup>Re generator.

Table 4. Results of calculation of tungsten weight sorbed on aluminum oxide pH 4.5

#	Weight of tungstate-ion in terms of tungsten, g			Tungsten sorption value, %
	In tail solution	Brought on sorption column	Sorbed on aluminum oxide	
1	1	30	29.00	96.70
2	2	60	58.00	96.70
3	2.8	90	87.20	96.90
4	10.33	120	109.67	91.40
5	22.81	150	127.19	84.80
6	44.6	180	135.40	75.20
7	68.6	210	141.40	67.30
8	92.6	240	147.40	61.40
9	117.6	270	152.40	56.50
10	145.26	300	154.74	51.60
11	172.6	330	157.40	47.70
12	200.3	360	159.68	44.35
13	230.2	390	159.68	40.90
14	259.9	420	160.10	38.10
15	289.9	450	160.10	35.60

Calculation of the maximal and minimal exposure rates on the surface of  $^{188}\text{Re}$  generator shielding container has been carried out in order to estimate the properties of the shield structure designed (radiation source activity was 24 GBq in  $^{188}\text{W}$ ). Calculation has shown that  $^{188}\text{Re}$  radiation gives practically all contribution to the dose rate around the source and insignificant contribution is from  $^{188}\text{W}$ . This is connected with the fact that  $^{188}\text{W}$  emits photons of less than 0.35 MeV energy, for which the optical thickness of the lead shield exceeds 30 free paths, and therefore it is completely shielded. Calculation results obtained are in agreement with the experimental data and present a spatial exposure rate distribution in the neighborhood of  $^{188}\text{Re}$  generator container.

## Conclusion

$^{188}\text{Re}$  stationary generator design and technology have been developed on the basis of the technology of  $^{188}\text{W}/^{188}\text{Re}$  chromatographic generator of 2.4 to 3.7 GBq activity [3, 4]. It has been established that the eluate from  $^{188}\text{W}/^{188}\text{Re}$  generator contains 80 – 90 % of  $^{188}\text{Re}$ , chemical impurity concentration (Al, Fe, W, etc.) is at the level 0.005-5.0mg/ml,  $^{188}\text{W}$  concentration is at the level  $10^{-3}$  %, the other gamma-emitters are totally not more than  $10^{-3}$  % of  $^{188}\text{Re}$  activity, radiochemical purity of sodium perrehenate,  $^{188}\text{Re}$ , is not less than 99.0% [2]. Stationary  $^{188}\text{Re}$  generator of 185 GBq activity allows obtain sodium perrehenate solution of different volume with controlled concentration activity up to 500 mCi/ml. It is a promising way of commercialization of the technology developed. This allows enlarge the range of radiopharmaceuticals synthesized, reduce the cost of patient treatment and increase the efficiency of treatment of socially important diseases.

## References

1. Baranov N.G., Stepchenkov D.V., Petriev V.M., et al. Proceedings of the Annual Congress of European Nuclear Medicine Association EANM06, September 30 – October 4, 2006, Athens, Greece, p.156.
2. Stepchenkov D.V., Baranov N.G., Sharkova O.V., et al. “Radiochemistry-2006”, Dubna, 338.
3. Registration certificate FC 02032006/5395-06.  $^{188}\text{W}/^{188}\text{Re}$  generator for the right of its production as medical equipment.
4. Re-188 generator GREN-1. TS 9452-031-08624390.

4.14.

## MATHEMATICAL MODELS FOR PHARMACOKINETICS AND DOSIMETRY IN EXPERIMENTAL RADIOBIOLOGICAL STUDIES OF BONE-SEEKING RADIOPHARMACEUTICALS $^{188}\text{Re-KHEDP}$

A.N.Klyopov<sup>1</sup>, V.M.Petrev<sup>2</sup>, V.G.Skvortsov<sup>2</sup>, V.A.Sokolov<sup>2</sup>,  
V.V.Kanygin<sup>3</sup>, V.K.Shiryayeva<sup>2</sup>, O.P.Aleksandrova<sup>2</sup>

<sup>1</sup> Obninsk Institute for Nuclear Power Engineering of National Research Nuclear University, Obninsk, Russia

<sup>2</sup> Medical Radiological Research Centre of the Ministry of Health and Social Development of the Russian Federation, Obninsk, Russia

<sup>3</sup> "MEDRADIOPREPAT", Federal Medical and Biological Agency, Moscow, Russia

**Keywords:** radiopharmaceutical  $^{188}\text{Re-KHEDP}$ , pharmacokinetics, dosimetry, mathematical models

### Abstract

The purpose of work was to model pharmacokinetics of radiopharmaceutical  $^{188}\text{Re-KHEDP}$  and calculate the absorbed doses (AD) in critical organs of laboratory animals according to experimental radiobiological studies. Multi-chamber model of  $^{188}\text{Re-KHEDP}$  metabolism in rats was developed. The received results are intended for the further application of data in clinical practice.

### Materials and methods

The study the pharmacokinetics of mono potassium-hydroxyethylidene-1,1-diphosphonic acid (KHEDP) salt was carried out on white rats, females with an average weight of 175 g. Altogether 24 animals. Bone pathology was simulated by fractured right femur. Manipulation of the animals were under ether anesthesia. Over the next 14 days, callus was formed, which served as a model of bone disease. 0.2 ml of  $^{188}\text{Re-KHEDP}$  were injected into the tail vein. In 1, 3, 5, 24, 48 and 72 hours after the injection groups of 4 animals in each time period were decapitated, isolated organs and tissue samples were weighed and measured for radionuclide content by direct radiometry. According to radiometric counting the content throughout the body was estimated in percentage of the injected amount.

With the purpose of definition of the adequate scheme of radiopharmaceutical pharmacokinetics various variants compartment models were involved. As a result space-temporal dependences of radiopharmaceutical accumulation-withdrawal has been realized on the basis of model with 40 chambers. Transport of  $^{188}\text{Re-KHEDP}$  metabolites in extracellular space of organs of a rat was considered. As a whole the model included 62 kinetic parameters (constants of an interchamber exchange) which were defined by a method of numerical identification. Calculation of the absorbed doses was made following the MIRD methodology. Dose factors for organs of rats, including critical bone structures, have been taken from [4, 5].

Mathematical modeling of  $^{188}\text{Re-KHEDP}$  metabolic processes needs to proceed a significant volume of experimental data obtained in animals. Owing to diversity and individual manifestations of interchamber communications initially it was not obvious what pharmacokinetic chamber model can be effective. To determine the principal features of the pharmacokinetics of  $^{188}\text{Re-KHEDP}$  and simplify identification of kinetic parameters it was developed multi-chamber scheme. It was assumed that the main features of the metabolic process will then be truly "caught up" with the next "fractional" multi-chamber models.



Table 1. Distribution of <sup>188</sup>Re-KHEDP in organs and tissues of rats after intravenous administration (% dose/organ)

№	Organ, tissue	Time after administration (%dose/organ)					
		5 min	1 h	3 h	24 h	48 h	72 h
1	Blood	8,60±0,76	3,40±0,37	2,20±0,56	0,43±0,14	0,40±0,07	0,81±0,22
2	Thyroid	0,019±0,003	0,057±0,010	0,085±0,020	0,010±0,003	0,004±0,001	0,016±0,002
3	Lungs	0,17±0,01	0,072±0,02	0,043±0,003	0,011±0,001	0,006±0,002	0,004±0,001
4	Liver	2,40±0,11	1,20±0,05	0,90±0,10	0,41±0,02	0,33±0,02	0,067±0,023
5	Kidneys	2,19±0,12	2,06±0,16	1,71±0,10	0,70±0,02	0,41±0,02	0,26±0,04
6	Heart	0,14±0,02	0,051±0,005	0,024±0,002	0,012±0,001	0,003±0,001	0,009±0,004
7	Spleen	0,13±0,01	0,090±0,010	0,060±0,006	0,034±0,006	0,027±0,005	0,014±0,006
8	Stomach	0,31±0,03	0,17±0,02	0,18±0,02	0,043±0,005	0,028±0,003	0,023±0,008
9	Intestines	1,15±0,15	0,65±0,10	0,60±0,07	0,13±0,02	0,079±0,024	0,24±0,06
10	Muscle	9,25±1,25	2,69±0,62	0,95±0,14	0,87±0,20	0,73±0,04	0,77±0,22
11	Joint	0,94±0,10	1,19±0,06	1,03±0,03	0,71±0,04	0,70±0,06	0,55±0,08
12	Thigh bone	0,52±0,06	0,53±0,04	0,52±0,02	0,39±0,02	0,40±0,04	0,32±0,07
13	Thigh bone with a fracture	1,27±0,22	1,23±0,17	1,07±0,19	0,82±0,11	0,86±0,03	0,52±0,08
14	Shin bone	0,15±0,02	0,16±0,01	0,12±0,01	0,13±0,01	0,11±0,02	0,081±0,019
15	Skull bone	2,55±0,28	2,59±0,12	2,33±0,15	1,76±0,12	1,49±0,126	1,47±0,19
16	Rib Bone	0,63±0,06	0,59±0,084	0,57±0,14	0,41±0,01	0,41±0,04	0,35±0,05
17	Vertebrae bone	6,73±0,82	6,89±0,35	5,97±0,23	3,97±0,31	4,18±0,18	3,12±0,30

We would like to note that using a basic scheme of traditional multi-chamber schemes of chamber models in the form [1] proved to be ineffective. As a result of significant number of tests a reasonable option of the multi-model was offered.

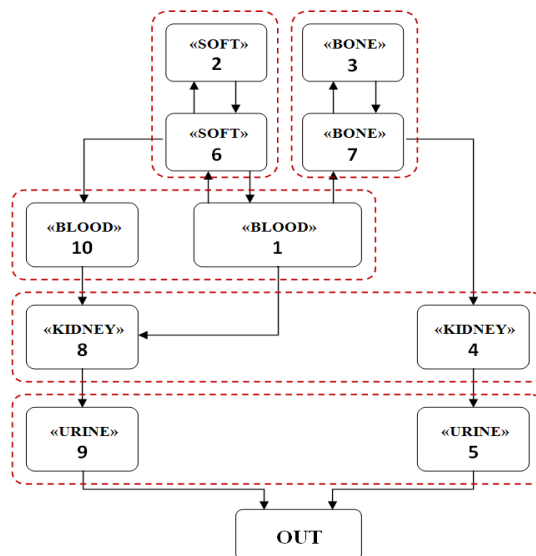


Fig. 1. Compartmental model for <sup>188</sup>Re-KOEDF metabolism.

This option is displayed in the block diagram (Figure 1), and includes a system of equations for kinetics of the corresponding substrates of <sup>188</sup>Re:

blood chamber («BLOOD») – compartments "1" and "10":

$$\frac{dq_1}{dt} = -(a_{61} + a_{81} + a_{71} + \lambda_\delta) \cdot q_1 + a_{16} \cdot q_6; \quad \frac{dq_{10}}{dt} = -(a_{8,10} + \lambda_\delta) \cdot q_{10} + a_{10,6} \cdot q_6 \quad (1),$$

soft tissue chamber («SOFT») – compartments "2" and "6":

$$\frac{dq_6}{dt} = -(a_{26} + a_{16} + \lambda_\delta) \cdot q_6 + a_{61} \cdot q_1 + a_{62} \cdot q_2; \quad \frac{dq_{10}}{dt} = -(a_{62} + \lambda_\delta) \cdot q_2 + a_{26} \cdot q_6 \quad (2),$$

bone tissue chamber («BONE») compartments "3" and "7":

$$\frac{dq_7}{dt} = -(a_{37} + a_{47} + \lambda_\delta) \cdot q_7 + a_{71} \cdot q_1; \quad \frac{dq_3}{dt} = -(a_{37} + \lambda_\delta) \cdot q_3 + a_{37} \cdot q_7 \quad (3),$$

kidney chamber («KIDNEY») – compartments "4" and "8":

$$\frac{dq_8}{dt} = -(a_{98} + \lambda_\delta) \cdot q_8 + a_{8,10} \cdot q_{10} + a_{81} \cdot q_1; \quad \frac{dq_4}{dt} = -(a_{54} + \lambda_\delta) \cdot q_4 + a_{47} \cdot q_7 \quad (4)$$

urine chamber («URINE») – compartments "5" and "9",

where  $\lambda_p$  – the decay constant of  $^{188}\text{Re}$ ,  $a_{ij}$  – coefficients of inter-chamber communications. The initial conditions:  $q_1(0) = 1$ ;  $i_1(0) = 0$ ;  $i_i > 1$ . The "camera" here refers to the combined organs, bodies and tissues, "compartment" – their metabolically different subsystems.

Figures 2-5 show the kinetics of the recovered activity of the  $^{188}\text{Re}$ -KHEDF and its metabolites in chambers «BONE», «BLOOD», «SOFT», «KIDNEY», «URINE», as a fraction of the injected activity and decay of  $^{188}\text{Re}$ .

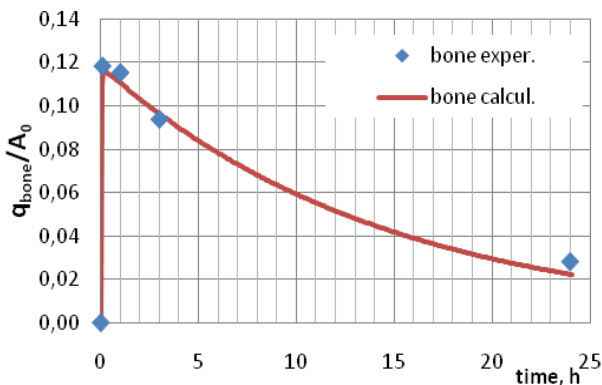


Fig. 2. Kinetics of  $^{188}\text{Re}$  - activity in bone

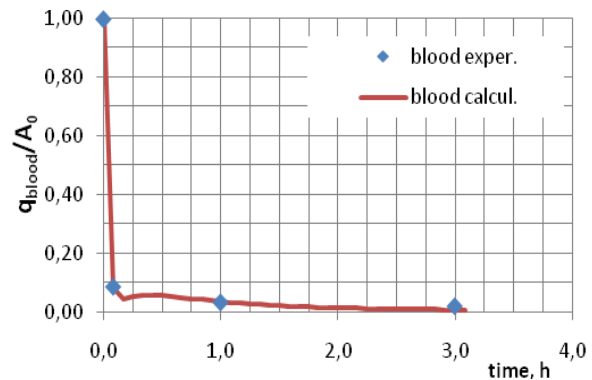


Fig. 3. Kinetics of  $^{188}\text{Re}$  - activity in blood

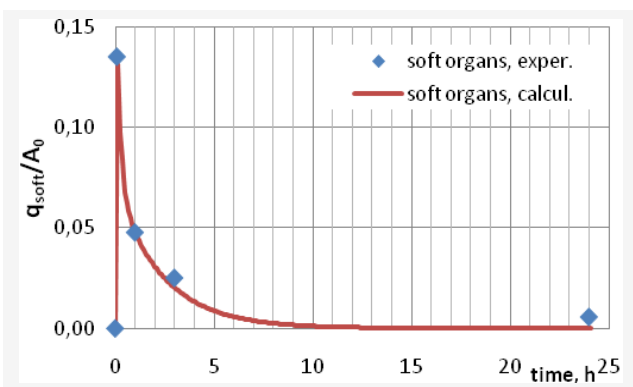


Fig. 4. Kinetics of  $^{188}\text{Re}$  - activity in soft tissues

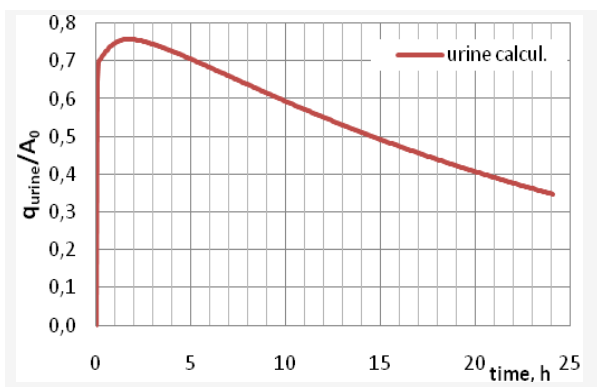


Fig. 5. Kinetics of  $^{188}\text{Re}$  - activity in urine

Absorbed doses (AD) in the critical organs were calculated according to MIRD recommendations [2],

$$D_T = A_0 \cdot \sum_{r=1}^R \tilde{q}_{S,r} \cdot S_r(T \leftarrow S),$$

where  $q_{S,r}$  – the resident time for  $^{188}\text{Re}$  in the source-organ ( $r$ );  $S_r(T \leftarrow S)$  – S-factor [2].

Resident time for the bladder was calculated taking into account its periodic emptying. The cycle time emptying was taken as 0.5 hours. S-factors for the case of  $^{188}\text{Re}$  in relation to a number of critical soft tissues and organs were taken from [3,4]. S-factors for series of energies of monoenergetic electrons and  $\gamma$ -rays have been calculated in [5]. It must be emphasized that in [5] they were obtained for the case of a homogeneous distribution of the nuclides in terms of bone (trabecular and compact). They can be used as lower estimate for "true" values of S-factors, since the volume-distribution of radiopharmaceuticals in the bone are certainly less than S-factors of surface-tropic ones by a larger absorption in the volume of bone. Since the bone structure of rats, especially trabeculae bone, are quite small, the resulting estimates of factors for the absorption of relatively hard  $\beta$ -radiation  $^{188}\text{Re}$ , does not seem to be strongly distorted in comparison with the "true". The results of calculations of the specific AD are listed in Tables 3, 4.

Table 2. The specific partial and total absorbed doses of  $^{188}\text{Re}$ -KHEDP in rats

Contribution in dose: $S \cdot \tilde{A}$ [mGy/Bk]										AD per organ, Gy/Bk
	Bladder	Heart	Kidney	Liver	Lungs	Spleen	Stomach	SI	Skeleton	
Bladder	1,162E-04	9,879E-12	9,489E-10	5,114E-10	7,713E-12	3,586E-11	7,251E-11	6,134E-08	6,657E-08	1,163E-07
Heart	3,504E-10	1,133E-06	2,024E-09	1,007E-07	7,021E-08	8,943E-11	4,368E-10	2,239E-10	9,526E-07	2,259E-09
Kidney	1,243E-09	3,166E-11	4,090E-05	9,653E-08	7,872E-11	3,042E-08	2,893E-08	5,965E-08	1,696E-07	4,129E-08
Liver	9,732E-10	3,239E-09	1,703E-07	6,475E-06	2,058E-08	1,374E-10	4,689E-08	1,727E-08	3,789E-07	7,114E-09
Lungs	3,667E-10	4,885E-08	2,699E-09	4,863E-07	7,846E-07	9,371E-11	4,213E-08	2,540E-10	6,454E-06	7,819E-09
Spleen	1,032E-09	2,587E-11	7,527E-07	1,637E-09	5,904E-11	7,232E-06	9,202E-08	5,400E-08	1,211E-07	8,254E-09
Stomach	9,117E-10	9,282E-11	3,073E-07	2,866E-07	1,125E-08	4,142E-08	3,679E-06	2,747E-08	5,998E-07	4,954E-09
Skeleton	8,426E-09	1,654E-09	1,443E-08	2,278E-08	1,646E-08	5,349E-10	5,970E-09	6,040E-07	3,120E-08	1,449E-09

Table 3. Absorbed  $^{188}\text{Re}$ -KHEDP doses in bone marrow of rats

	Vertebrae bone	Femur bone	Skull bone	Shin bone
Specific absorbed doses, Gy/BkBк	1,83 E-007	4,1 E-008	7,8 E-009	1,4 E-008

## References

1. Savio E., Gaudio J., Robles A.M., Balter H., and et. al. Re-HEDP: pharmacokinetic characterization, clinical and dosimetric evaluation in osseous metastatic patients with two levels of radiopharmaceutical dose. BMC Nuclear Medicine, 2001, 1:2.
2. Bolch W. E., Eckerman K. F., Sgouros G., and Thomas S. R. MIRDO pamphlet No. 21: A generalized schema for radiopharmaceutical dosimetry—Standardization of nomenclature. J. Nucl. Med., 2009, Vol. 50, p. 477-484.
3. Stabin M.G., Peterson T.E., Holburn G.E., and Emmons M.A. Voxel-Based Mouse and Rat Models for Internal Dose Calculations. J. Nucl. Med., 2006; Vol. 47: p. 655–659.

4. Peixoto P.H.R., Vieira J.W., Yoriyaz H. and Lima F.R.A. Photon and electron absorbed fractions calculated from a new tomographic rat model. *Phys. Med. Biol.* 2008, Vol. 53: p. 5343–5355.
5. Xie T., Han D., Liu Y., Sun W., and Liua Q. Skeletal dosimetry in a voxel-based rat phantom for internal exposures to photons and electrons. *Med. Phys.*, 2010, Vol. 37, No. 5: p. 2167-2178.



N. S. Al-Hokbani, N.N. Popova, G. L. Bykov, M.S. Grigoriev

4.P1.

## THE GENERATOR $^{99m}\text{Tc}$ BASED ON INORGANIC SORBENT “TERMOKSID-5”

N.D. Betenekov, E.I. Denisov, L.M. Sharygin\*, M.N. Golubev

UrFU, Ekaterinburg, [ndbetenekov@dpt.ustu.ru](mailto:ndbetenekov@dpt.ustu.ru)

\*Closed joint-stock company RPF TERMOXID, Zarechny, Russia

The eluted activity from a technetium generator will contain small amounts of a variety of impurities. The nature of these impurities and their concentration is important. The following should be considered when preparing  $^{99m}\text{Tc}$  radiopharmaceuticals. This end use places a stringent requirement on the various types of purity of the product. Product purity may be considered to consist of radionuclide impurity, radiochemical purity, chemical purity and biological purity. There are however contaminants that are inherent in the  $^{99}\text{Mo}$  on to the generator column and that may be released from the alumina column during elution. Since these components are frequently present, their allowable concentrations may be defined and quality control tests for their presence and concentration may be applied. The following components contribute to the suitability of the eluted  $^{99m}\text{Tc}$ :  $\text{Al}^{+3}$  ion end activity  $^{99}\text{Mo}$ .

It is impossible to completely eliminate all aluminum ions. Recommended limits for  $\text{Al}^{+3}$  (United States Pharmacopoeia [USP] for example) are 10  $\mu\text{g} / \text{mL}$  when the column is prepared from fission molybdenum and 20  $\mu\text{g} / \text{mL}$  when thermal neutron activation is used to prepare the  $^{99}\text{Mo}$ .

There are varying regulations concerning the allowable levels of  $^{99}\text{Mo}$  in the eluted product or in the radiopharmaceuticals prepared for human administration. A generally accepted requirement (United States Pharmacopoeia) is that the final radiopharmaceutical will not contain more than 0,15 KBq of  $^{99}\text{Mo}$  per MBq of  $^{99m}\text{Tc}$  at the time of administration.

The chemical composition of thermostable inorganic sorbent “Termoksid-5” (T-5) is a mixture of oxides titanium and zirconium. It has high molybdenum selectivity, radiation resistant and chemically stable.

The generator  $^{99m}\text{Tc}$  (based on the brand sorbent T-5) can be produced for bigger activity at smaller sizes of the sorption column. Model experiments of the separation  $^{99}\text{Mo}$  and  $^{99m}\text{Tc}$  showed satisfactory results:  $0,90 \pm 0,05$  technetium and less than  $10^{-5}$  of molybdenum transfer to isotonic solution after multiple elution (more accurate results can be obtained at higher specific activity of the molybdenum).

4.P2.

## INVESTIGATION OF THE SORBENTS ON THE BASIS OF THE NEW PHOSPHORYL-CONTAINING LIGANDS FOR ALLOCATION, CONCENTRATION AND PURIFICATION OF THE MOLYBDENUM FROM THE IRRADIATED URANIUM TARGETS

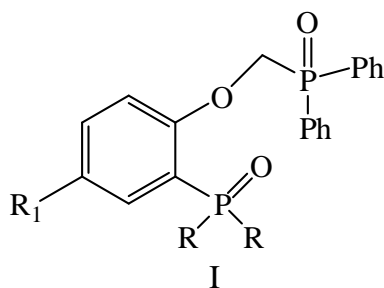
Baulin V.E.<sup>1,3</sup>, Kovalenko O.V.<sup>1</sup>, Usolkin A.N.<sup>2</sup>, Voroshilov Y.A.<sup>2</sup>,  
Yakovlev N.G.<sup>2</sup>, Tsivadze A.Yu.<sup>1</sup>

<sup>1</sup> A.N.Frumkin Institute of physical chemistry and electrochemistry RAS, Moscow, Russia mager1988@gmail.com

<sup>2</sup> Federal State Unitary Enterprise "Production Association" Mayak ",  
Ozersk, Chelyabinsk region,

<sup>3</sup> Institute of Physiologically Active Compounds of the RAS, Chernogolovka, Moscow Region

The <sup>99</sup>Mo is a precursor of <sup>99m</sup>Tc applied for diagnostics in the nuclear medicine. One of the main methods for <sup>99</sup>Mo-<sup>99m</sup>Tc production is the U irradiation in the reactor, <sup>99</sup>Mo being produced due to <sup>235</sup>U fission with the yield of approximately 6%. Preparative chromatography with use of highly effective sorbents (PZC or Thermoxid) is promising separation method of allocation, concentration and purification of <sup>99</sup>Mo from accompanying collateral elements. A new kind of chelating polymeric adsorption materials were developed and synthesized by non-covalent fastening of the new ligands (I) into the pores (40-250 μm) of polymeric (styrene-divinylbenzene) particles to separate effectively of Mo from solutions, obtained by dissolution of the irradiated uranium targets in HNO<sub>3</sub>. The adsorption of some typically simulated elements Mo, Tc, U, Th, Np, Pu towards adsorbent was investigated by examining the influence of the structure of phosphoryl-containing



R=Ph, p-Tol, OEt, OH, R<sub>1</sub>=H, n-Alk

ligands, their percentage contents in an adsorbent, contact time, concentration of HNO<sub>3</sub> and presence of the stripping agents in the solutions. It was found that a number of the investigated materials exhibited excellent selectivity for <sup>99</sup>Mo overall of the tested elements. The optimum conditions for effective adsorption and stripping of these elements have been determined. The dynamic distribution factors were high resulting in quantitative purification of <sup>99</sup>Mo from accompanying collateral elements in demi-industrial pilot scale. The technique for <sup>99</sup>Mo determination in the irradiated uranium targets was proposed. The

obtained data testify the new adsorbents potential for radiochemical manufacturing of <sup>99</sup>Mo-<sup>99m</sup>Tc generators.

The work was supported by RFBR (grant № 11-03-00509-a)



4.P3.

## NOVEL TECHNETIUM AND RHENIUM COMPLEXES WITH THE N-HETEROCYCLIC ALDEHYDE THIOSEMICARBAZONES - POTENTIAL RADIOPHARMACEUTICALS

L. Fuks\*, E. Gniazdowska, P. Kozminski, J. Mieczkowski <sup>1</sup>

Institute of Nuclear Chemistry and Technology, Dorodna 16, 03-195 Warsaw, Poland

<sup>1</sup> Faculty of Chemistry, University of Warsaw, Pasteura 1, 02-093 Warsaw, Poland

\* e-mail: leon.ichtj@gmail.com

**Keywords:** technetium-99m, radiopharmaceuticals, thiosemicarbazones, complexes, radiolabelling

### Abstract

Pyridine- or quinolinecarboxaldehyde thiosemicarbazones and technetium form compounds in which the ligand is bound di- or tridentately. Because the ligand may exist as neutral molecule of the thiourea origin or as the monohydric acid anion coming from the thioenol form, properties of the metal complex strongly depend on the conditions of the synthesis. The aim of presented work is to check, if labelling the N-heterocyclic aldehyde thiosemicarbazones with tricarbonyl [<sup>99m</sup>Tc]-technetium(I) may lead to formation of the complexes suitable for the radiopharmaceutical purposes. Syntheses of the complexes were provided in the conditions analogous to those at present performed in the nuclear medicine laboratories. Main physicochemical properties of the complexes were studied. Semiempirical geometry optimization and energy of the compounds calculation were also performed using the MPW1PW functional or the DPCM (Dielectric Polarizable Continuum Model), respectively, implemented in Gaussian 98.

### Introduction

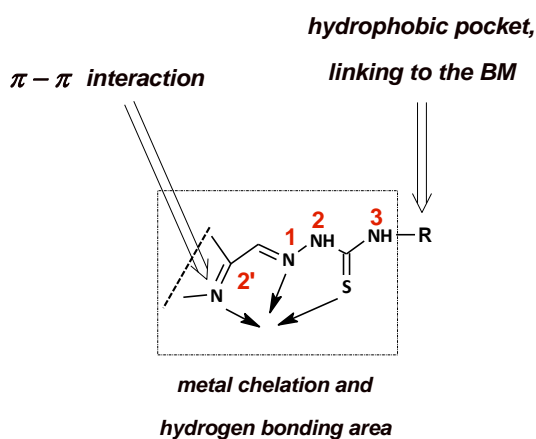


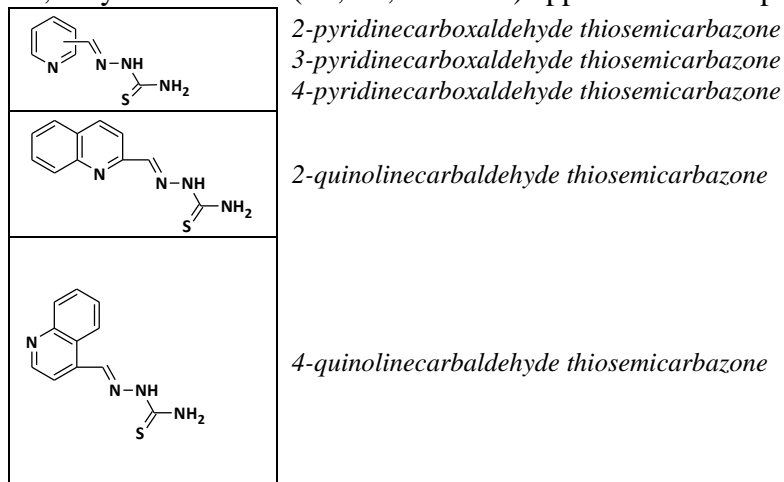
Fig 1. Complexing sites of substituted thiosemicarbazide

In the attempt to develop novel <sup>99m</sup>Tc-complexes - potential radiopharmaceuticals, our interest has been focused on the thiosemicarbazone (TSC) chelators. Inspection of the literature on the TSC complexes with different metals has shown that the compounds may be accounted as prospective pharmaceuticals, because they may bind with a great number of biological targets, e.g. bacteria, fungi and viruses [1], parasites [2], tumorous tissue [3]. They may also serve as the anti-inflammatory agents [4]. TSC ligands are capable of metal coordination in different modes [5] and the complexes are stable enough to be a source of these thiourea derivatives. Conjugated N,N,S donor atoms of the thiosemicarbazide (NH<sub>2</sub>-CS-NH-NH<sub>2</sub>) moiety together with the R<sub>i</sub> substituent (of the parent aldehyde / ketone

origin) form potentially tridentate ligands which alone also exhibit the desired biological activities [6,7].

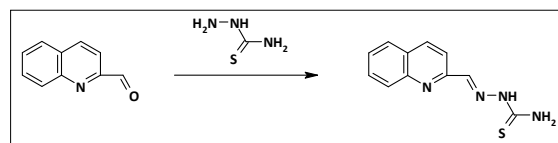
Radiolabeled thiosemicarbazones have been used for treatment of different diseases and/or in medicinal diagnosis for over three decades. Apart from Tc-99m, radionuclides tested up-today were: Cu-62, Cu-64 and Cu-67, Ga-67 and Ga-68, Pd-103 and nonmetallic I-125<sup>1</sup>.

Within our interest on the technetium and rhenium complexes for biomedical applications, we have recently started the synthesis and characterization of their complexes formed with three pyridinecarboxaldehyde and two quinolinecarboxaldehyde thiosemicarbazones. In spite of the fact that both metals in the complexes may exist in one from the nine oxidation states ranging from -1 to +7, only four of them (+7, +5, +3 or +1) appear in the compounds used in the medicinal sciences.



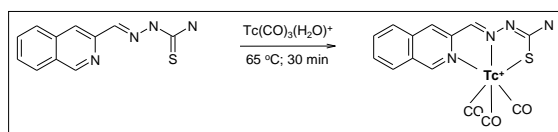
Detailed intent of the presented studies, performed within this more general project devoted to the comparison of the complex formation, stability and basic properties of the aforementioned ligands labeled with Tc/Re in the +5 and +1 oxidation states, is to present results obtained for the tricarbonyl cation  $^{99m}\text{Tc}(\text{CO})_3^+$  complexed with the 2-quinolinecarboxaldehyde thiosemicarbazone (Q2TSC).

## Experimental



**Synthesis of 2-quinolinecarboxaldehyde thiosemicarbazone (Q2TSC):** this ligand was obtained by reaction of 0.1 mol of 2-quinolinecarboxaldehyde (dissolved in 100 mL of an ethanol-water, 1:1, and 5 mL of conc. HCl) with 0.12 mol of the

thiosemicarbazide (in 10 mL of ethanol). After stirring for 2 hrs at RT followed by heating under the reflux for 2 hrs, crude thiosemicarbazide (yellow or orange) in hydrochloride form has been filtered out and recrystallized from ethanol. Thiosemicarbazide hydrochloride dissolved in 200 mL of hot water was slowly neutralized with aq. solution of 10%  $\text{Na}_2\text{CO}_3$ . Crude thiosemicarbazide in neutral form was crystallized from ethanol. Yield: ~ 90 %.



**Synthesis of the  $^{99m}\text{Tc}^{\text{I}}(\text{CO})_3\text{-Q2TSC}$  complex:** For the labeling with Tc-99m, a kit containing 5.5 mg  $\text{NaBH}_4$ , 4 mg  $\text{Na}_2\text{CO}_3$  and 10 mg Na-K tartarate, purged with CO gas prior to addition of  $\text{Na}^{99m}\text{TcO}_4$ , as described elsewhere [8]. Then, 1 mL of an aqueous

mixture of  $[\text{}^{99m}\text{Tc}(\text{OH}_2)_3(\text{CO})_3]^+$  (~ 0.5 GBq/ml) and the TSC ligand ( $6.5 \cdot 10^{-4}$  M) at pH 9.5, reacted at 65 °C for 30 min. The reaction mixture was analyzed by RP HPLC to estimate the yield and the complex was purified by isolating the radioactive peak from the column. The reaction yield was ca 95%.

**Radiochemical purity** of the  $^{99m}\text{Tc}$ -TSC complex was determined by paper chromatography using acetone as the developer.

**All ligands were characterized** by C, H, N and S analyses, IR and  $^1\text{H}$  NMR spectroscopy.

**Analytical HPLC** was run on a SUPELCOSIL C-18 (Supelco) column (particle size: 5  $\mu\text{m}$ , L = 25 cm;  $\phi$  = 10 mm); flow rate of 1mL/min; radiometric and UV detection (254 nm); eluents: A - 0.01 M phosphate buffer (TEAP) pH = 7.4, B - MeOH; method: 0-3 min - 100%A; 3-6 min - 100%A →

<sup>1</sup> See, webpage <http://inisdb.iaea.org/>

75% A; 6-9 min - 75%A → 66% A; 9-20 min - 66% → 0%A; 20-25 min - 0%A; 25-30 min - 0% → 100%A; 30-35 min - 100%A.

**Lipophilicity determination:**  $\log P_{o/w}$  values of the  $^{99m}\text{Tc}$ -complexes were determined by multiple extraction in the *n*-octanol/PBS system (pH 7.40), which mimics the physiological conditions (ambient temperature;  $\gamma$ -radiation counting) [9]. After separation the phases, aqueous solutions were analyzed by the RP-HPLC to check whether the complexes studied had not decomposed during the experiments.

**Paper electrophoresis** experiments were performed in the phosphate buffer (0.1 M, pH 7.40). The analyses were carried out for 60 min at 200 V. After drying the paper strips, distribution of the radioactivity along the strips was determined by the  $\gamma$ -radiation counting.

**Computational details:** As in our previous studies [10], structure optimization (DFT, B3LYP model; 6+311G\*\* basis) and energetic calculations (Dielectric Polarizable Continuum Model, DPCM) were performed using the Gaussian 98 programme.

## Results and Discussion.

The *fac*- $[\text{}^{99m}\text{Tc}(\text{CO})_3]^+$  moiety is nonpolar, has an almost spheric shape, and offers up to 3 sites on an octahedral face for ligand attachment.

All TSCs studied can be effectively radiolabeled with  $^{99m}\text{Tc}(\text{CO})_3^+$  under mild conditions (30 min at 65 °C, pH=9.5, 30 min,  $\sim 5 \cdot 10^{-4}$  M TSC) to form well-defined complexes with a high enough yield. Generally, HPLC analyses of the ligands as well as of the complexes show two / three clearly resolved peaks. Results obtained for the complexes formed by the pyridinecarboxaldehyde ligands (*viz.*, the P2TSC, P3TSC and P4TSC) are published elsewhere [11].

In the presented paper we present results obtained for 2-quinolinecarbaldehyde thiosemicarbazone (Q2TSC). In the ligand, 2-quinoline and thiourea groups can be *syn* (Z) or *anti* (E) with respect the central C2'-C1 and C1=N1 bonds, where C2' stands for carbon atom in the 2-quinoline moiety (for numbering of the atoms, see Scheme in the Introduction). Therefore, rotations around these bonds result in a change of the ligand's conformation. Performed calculation shows, that relative values of the energy of three main isomers - (Z,Z), (E,E) and (Z,E) - are

0, 2.45 and 5.65 kcal/mole, respectively. HPLC retention times for these isomers are 18.2, 18.4 and 19.0 min (assignment of the

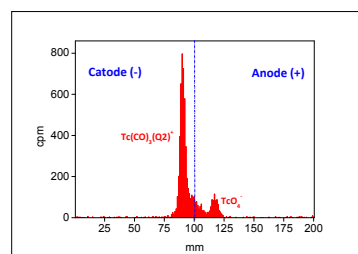


Fig. 4.  
Electrophoregram of  
 $[\text{}^{99m}\text{Tc}(\text{CO})_3\text{L}_{\text{N,N,S}}]^+$

respective isomers has not been done yet) and for the complexes - 21.2, 21.7 and 22.8 min. All complexes were isolated by HPLC their lipophilicity assigned as the  $\log P$  determined in the standard conditions. Respective values are: 1.02, 0.54 and 1.69. These values are significantly greater than these obtained for the pyridinecarboxaldehyde complexes [11].

Charges of the complexes were determined by the paper electrophoresis. Slightly positive values suggest that the tricarbonyl complexes are of the  $[\text{}^{99m}\text{Tc}(\text{CO})_3\text{L}_{\text{N,N,S}}]^+$  composition and are formed by involving three donor atoms of the ligand as shown in the scheme

presented in the Introduction. Thioketo form of the ligand is involved in complex formation.

Separated HPLC fractions of the complex were buffered to pH 7.40 and tested for their stability both in the pure buffer or in the histidine and cysteine challenge experiments. Results obtained show that it is not sufficiently stable to be taken into account as the radiopharmaceuticals' precursor.

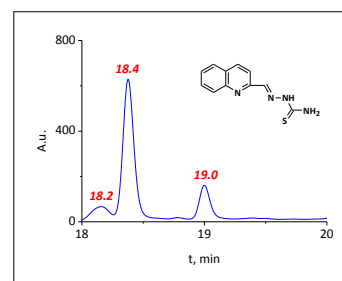


Fig. 2. HPLC  
chromatogram of Q2TSC

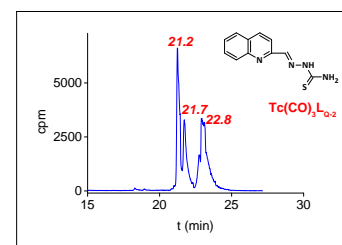


Fig. 3. Radio-HPLC  
chromatogram of  
tricarbonyl complexes  
suggested

The work is in progress.

## Conclusions.

Positively charged complex of [<sup>99m</sup>Tc<sup>I</sup>]-tricarbonyl complex with 2-quinoline carboxaldehyde thiosemicarbazone: (a) exists in the form of three isomers of medium lipophilicity, (b) is not resistant to re-oxidation even for the relatively short time, and (c) shows also small resistance in the standard challenge experiments. As a result, contrary to the pyridinecarboxaldehyde thiosemicarbazone complexes [11], it may not be considered promising candidate for the radiopharmaceutical precursor.

**Acknowledgments:** The work is carried out within the grant of Polish Ministry of Science and Higher Education No N N204 141437. We acknowledge Prof. N. Sadlej-Sosnowska (National Institute of Drugs, Warsaw) for calculations, which were carried out in the Interdisciplinary Centre for Mathematical and Computational Modeling of Warsaw University.

## References.

1. e.g. G. Pelosi, F. Bisceglie, F. Bignami, P. Ronzi, P. Schiavone, M.C. Re, C. Casoli, E. Pilotti, *J. Med. Chem.*, **53**, 8765-8769 (2010).
2. e.g. (a) R. Pingaew, S Prachayasittikul, S Ruchirawat, *Molecules* **15**, 988-996 (2010); (b) C.L. Donnici, M.H. Araújo, H.S. Oliveira, D.R.M. Moreira, V.R.A. Pereira, M. de Assis Souza, M.C.A. Brelaz de Castro, A.C. Lima Leit, *Bioorg. Med. Chem.*, **17**, 5038-5043 (2009); (c) Cerecetto, H.; M. Gonzalez, *Mini Rev. Med. Chem.*, **8**, 1355-1383 (2008).
3. e.g. (a) Z. Afrasiabi, E. Sinn, S. Padhye, S. Dutta, S. Padhye, C. Newton, C.E. Anson, A.K. Powell, *J. Inorg. Biochem.*, **95** 306-314 (2003); (b) L.A. Saryan, E. Ankel, C. Krishnamurti, D.H. Petering, H. Elford, *J. Med. Chem.*, **22** 1218-1221 (1979).
4. e.g. K. Raman, H.K. Singh, S.K. Salzman, S.S. Parmar, *J. Pharm. Sci.*, **82**, 167-169 (1993).
5. T.S. Lobana, R. Sharma, G. Bawa, S. Khanna, *Coord. Chem. Rev.* **253** 977-1055z (2009).
6. X. Du, C. Guo, E. Hansall, *J. Med. Chem.* **45**, 2695-2707 (2002).
7. D.B. Lovejoy, D.R. Richardson, *Blood* **100**, 666-676 (2002).
8. R. Alberto, R. Schibli, A. Egli, P.A. Schubiger, *J. Am. Chem. Soc.* **120**, 7987-7988 (1998).
9. Product Properties Test Guidelines OPPTS 830.7550, *US Environmental Protection Agency*, 1996.
10. (a) L. Fuks, E. Gniazdowska, N. Sadlej-Sosnowska, *Struct. Chem.* **21**, 827-835 (2010); (b) L. Fuks, N. Sadlej-Sosnowska, K. Samochocka, W. Starosta, *J. Mol. Struct.* **740**, 229-235 (2005).
11. L. Fuks, E. Gniazdowska, P. Kozminski, J. Mieczkowski, *J. Radioanal. Nucl. Chem.* DOI 10.1007/s10967-011-1404-4.

4.P4.

## <sup>99m</sup>Tc-LABELLED VASOPRESSIN ANALOGUE d(CH<sub>2</sub>)<sub>5</sub>[D-Tyr(Et<sup>2</sup>),Ile<sup>4</sup>,Eda<sup>9</sup>]AVP AS A POTENTIAL RADIOPHARMACEUTICAL FOR SMALL-CELL LUNG CANCER (SCLC) IMAGING

Ewa Gniazdowska<sup>a,\*</sup>, Przemysław Koźmiński<sup>a</sup>, Krzysztof Bańkowski<sup>b</sup>,

<sup>a</sup>Institute of Nuclear Chemistry and Technology, Warsaw, Poland

<sup>b</sup>Pharmaceutical Research Institute, Warsaw, Poland

\* e-mail: e.gniazdowska@ichtj.waw.pl

**Keywords:** technetium-99m, radiolabelling, radiopharmaceuticals, vasopressin, receptor

### Abstract

The <sup>99m</sup>Tc-labelled conjugate of vasopressin peptide analogue d(CH<sub>2</sub>)<sub>5</sub>[D-Tyr(Et<sup>2</sup>)-Ile<sup>4</sup>-Eda<sup>9</sup>]AVP has been synthesized using the technetium complexes with tetradentate tripodal chelator – the tris(2-mercaptoethyl)-amine, and monodentate isocyanide ligand. The conjugate exhibits high stability in the presence of excess of standard amino acid cysteine or histidine, and satisfactory stability in human serum. The novel vasopressin peptide conjugate can be considered promising diagnostic radiopharmaceutical for patients suffering from small-cell lung cancer (SCLC).

### Introduction

The aim of the work was to synthesize and investigate the conjugate of the d(CH<sub>2</sub>)<sub>5</sub>[D-Tyr(Et<sup>2</sup>),Ile<sup>4</sup>,Eda<sup>9</sup>]AVP peptide, the analogue of vasopressin, with the mixed-ligands “4+1” technetium(III) complex.

Vasopressin (arginine vasopressin, (Arg<sup>8</sup>)-Vasopressin, **AVP**) is a cyclic peptide (disulfide bond between Cys<sup>1</sup> and Cys<sup>6</sup>) containing nine amino acid residue (Cys<sup>1</sup>-Tyr<sup>2</sup>-Phe<sup>3</sup>-Gln<sup>4</sup>-Asn<sup>5</sup>-Cys<sup>6</sup>-Pro<sup>7</sup>-Arg<sup>8</sup>-Gly<sup>9</sup>). AVP is a peptide hormone found in most mammals, including humans. AVP regulates body retention of water, being released when the body is dehydrated (antidiuretic action of AVP, mediated *via* V2 type receptors). In addition to its predominantly antidiuretic and blood pressure activities, vasopressin demonstrates a variety of neurological effects on central nervous system (CNS). It is involved, *via* different receptor subtypes, in higher brain functions, including cognitive abilities and emotionality. In the recent years, interest increased in the role of vasopressin in its participation in such diseases as schizophrenia and autism [1]. The half-life of the vasopressin peptide *in vivo* is about 15-20 min [2]. The overexpression of vasopressin receptor V2 has been found on small-cell lung cancer (SCLC) [3-5]. Physicochemical properties of the <sup>99m</sup>Tc-labelled vasopressin peptide were already studied [6].

The AVP analogue, d(CH<sub>2</sub>)<sub>5</sub>[D-Tyr(Et<sup>2</sup>)-Ile<sup>4</sup>-Eda<sup>9</sup>]AVP, **AVP(an)**, is one of the several effective antagonists (Fig. 1A) of the antidiuretic (V2-receptor) responses to arginine vasopressin [7].

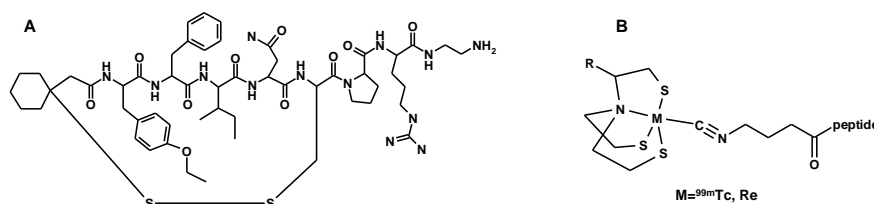


Figure 1.

(A) - d(CH<sub>2</sub>)<sub>5</sub>[D-Tyr(Et<sup>2</sup>)-Ile<sup>4</sup>-Eda<sup>9</sup>]AVP, (**AVP(an)**)  
(B) - <sup>99m</sup>Tc labelled peptides using the “4+1” approach;

(A) - d(CH<sub>2</sub>)<sub>5</sub>[D-



The “4+1” mixed-ligand technetium complex consists of central metal ion Tc(III) coordinated by a tetradentate NS<sub>3</sub> tripodal chelator tris(2-mercaptoethyl)-amine and a monodentate isocyanide ligand previously coupled with the selected biomolecule (Fig. 1B). The identity of the <sup>99m</sup>Tc-labelled AVP(an) was corroborated by investigation of an analogous rhenium compound.

## Experimental

The analogue **d(CH<sub>2</sub>)<sub>5</sub>[D-Tyr(Et<sup>2</sup>)-Ile<sup>4</sup>-Eda<sup>9</sup>]AVP, AVP(an)**, was a gift from Professor Maurice Manning, University of Toledo, Toledo, Ohio, United States.

The compounds: **tetradentate NS<sub>3</sub> ligand** (tris(2-mercaptoethyl)-amine; 2,2',2''-nitrilotriethanethiol, R=H), **aliphatic linker CN-BFCA** (BFCA = Bifunctional Coupling Agent) - monodentate isocyanide ligand (isocyanobutyric succinimidyl ester), **CN-AVP(an)** - the isocyanide linker CN-BFCA coupled with AVP(an) and the “**cold rhenium precursor**” **Re(NS<sub>3</sub>)(PMe<sub>2</sub>Ph)** were synthesized according to the procedures described in Refs. [6,8-11].

MS of CN-AVP(an), (m/z): Calcd: 1231.61, Found: 638.8 [M+H]<sup>+</sup>

Re(NS<sub>3</sub>)(CN-(AVP(an))): MS (m/z): Calcd: 1612.1, Found: 829 [M+H]<sup>+</sup>

The <sup>99m</sup>Tc-labelled AVP(an) conjugate was formed in two-step synthesis, *via* the <sup>99m</sup>Tc-EDTA intermediate complex [6,8,9,11], with the final yield of 95%.

## Results and Discussion.

The HPLC chromatograms of the compounds Re(NS<sub>3</sub>)(CN-AVP(an)), R<sub>T</sub>=15.9 min, and <sup>99m</sup>Tc(NS<sub>3</sub>)(CN-AVP(an)), R<sub>T</sub>=16.3, min are shown in Figure 2.

Figure 2. The HPLC chromatograms of the <sup>99m</sup>Tc/Re complexes prepared in this study (Phenomenex Jupiter Proteo analytical column, 4 μm, 90 Å, 250 × 4,6 mm, under condition: solvent A-water with 0.1 % TFA (v/v), solvent B-acetonitrile with 0.1 % TFA (v/v), gradient elution: 0-20 min: 20 to 80 % solvent B, 10 min-80 % solvent B; 1 ml/min, γ-detection.)

The *log D* value of  $-0.44 \pm 0.03$  for the <sup>99m</sup>Tc-labelled AVP(an) was found (the value may be corrected by introduction a hydrophilic group, R, at the periphery of the NS<sub>3</sub> ligand).

The conjugate <sup>99m</sup>Tc(NS<sub>3</sub>)(CN-AVP(an)) exhibits high stability. Figure 3 shows the percentage of intact conjugate in the challenge experiments with an excess (10 mM) of histidine or cysteine during incubation of the isolated conjugate at 37°C. After 24 h of incubation the obtained HPLC chromatograms have shown the existence of one radioactive species in the solution, of the retention time characteristic for the complex studied.

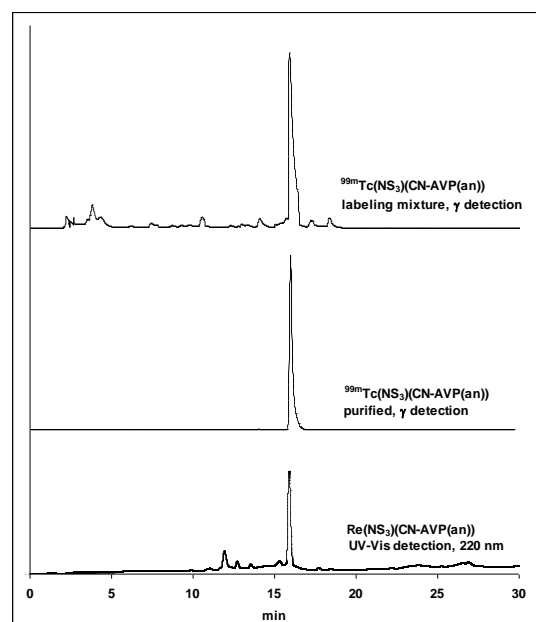


Figure 2. The HPLC chromatograms of the <sup>99m</sup>Tc/Re complexes prepared in this study (Phenomenex Jupiter Proteo analytical column, 4 μm, 90 Å, 250 × 4,6 mm, under condition: solvent A-water with 0.1 % TFA (v/v), solvent B-acetonitrile with 0.1 % TFA (v/v), gradient elution: 0-20 min: 20 to 80 % solvent B, 10 min-80 % solvent B; 1 ml/min, γ-detection.)



The HPLC chromatograms obtained after incubation of  $^{99m}\text{Tc}(\text{NS}_3)(\text{CN-AVP}(\text{an}))$  conjugate in human or rat serum are shown in Figure 4. The conjugate studied is also very stable in human and rat serum, on the contrary to the  $^{99m}\text{Tc}$ -labelled arginine vasopressin peptide. The biomolecule AVP(an), the antagonist of the V2 vasopressin receptor, does not undergo the enzymatic biodegradation *in vivo*, even in rat serum.

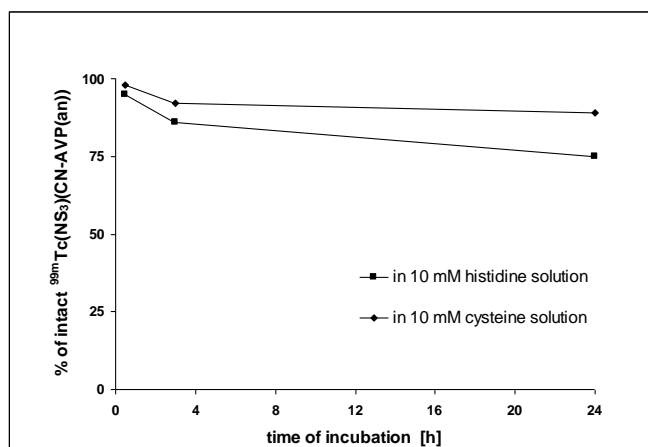


Figure 3. Histidine and cysteine challenge experiments: the percentage of intact  $^{99m}\text{Tc}(\text{NS}_3)(\text{CN-AVP}(\text{an}))$  complex remaining after various incubation times at 37 °C

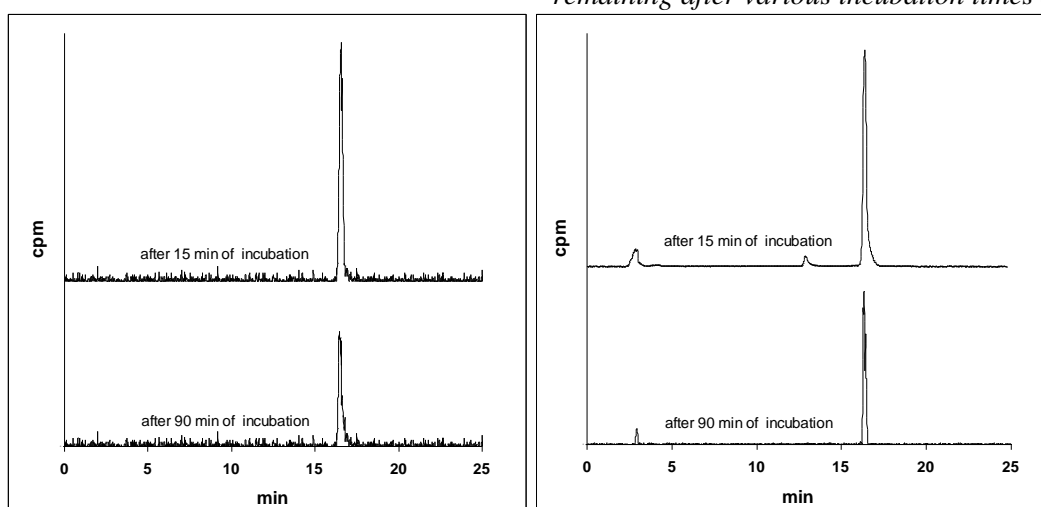


Figure 4. HPLC chromatograms of  $^{99m}\text{Tc}(\text{NS}_3)(\text{CN-AVP}(\text{an}))$  conjugate after incubation at 37 °C in human (left) and rat (right) serum (analyses carried out under the conditions described above)

## Conclusions.

In conclusion, one can say that the novel conjugate of the vasopressin peptide analogue  $\text{d}(\text{CH}_2)_5[\text{D-Tyr}(\text{Et}^2), \text{Ile}^4, \text{Eda}^9]\text{AVP}$  with the “4+1” mixed-ligands technetium(III) complex can be considered promising diagnostic radiopharmaceutical for patients suffering from small-cell lung cancer (SCLC).

## Acknowledgments:

The work was carried out in part as the statutory work of the Institute of Nuclear Chemistry and Technology and within the grant No: N R13 0150 10 (Polish Ministry of Science and Higher Education).

## References.

1. E. Frank and R. Landgraf, *Best Practice & Research Clinical Anaesthesiology*, 22, p. 265-273 (2008).
2. A. C. Guyton and J. E. Hall, *Text Book of Medical Physiology*, 10<sup>th</sup> edition, Saunders W. B., Philadelphia PA., 2000.
3. C. Pequeux, C. Breton, J.-C. Hendrick, M.-T., H. Martens, R. Winkler, J.-J. Legros, *Cancer Research*, 62, 4623–4629, 15 (2002).

4. W. G. North, M. J. Fay, K. A. Longo, Jiniin Du, *Cancer Research*, 58, 1866-1871. I. (1998).
5. C. Pequeux, B. P. Keegan, M.-T. Hagelstein, V. Geenen, J.-J. Legros, W. G. North, *Endocrine-Related Cancer*, 11, 871–885 (2004).
6. E. Gniazdowska, P. Kozminski, K. Bankowski, H.-J. Pietzsch, *Annual Report INCT*, 77-81 (2008).
7. M. Manning, J. Przybylski, Z. Grzonka, E. Nawrocka, B. Lammek, A. Misicka and Ling Ling Cheng, *J. Med. Chem.*, 35, 3895-3904 (1992) and references cited therein
8. S. Seifert, J.-U. Kuentler, E. Schiller, H.-J. Pietzsch, B. Pawelke, R. Bergmann, H. Spies, *Bioconjugate Chem.* 15, 856-863 (2004).
9. J.-U. Kuentler, G. Seidel, R. Bergmann, E. Gniazdowska, M. Walther, E. Schiller, C. Decristoforo, H. Stephan, R. Haubner, J. Steinbach, H.-J. Pietzsch, *J. Med. Chem.*, 45, 3645-3655 (2010).
10. H. Spies, M. Glaser, H.-J. Pietzsch, F. E. Hahn, T. Luegger, *Inorg. Chim. Acta* 240, 465 478 (1995).
11. J.-U. Kuentler, B. Veerenda, S. D. Figueroa, G. L. Sieckman, T. L. Rold, T. J. Hoffman, C. J. Smith, H.-J. Pietzsch, *Bioconjugate Chem.* 18, 1651-1661, (2007).



Ya. Zubavichus, O. Bozhkov, L. Borisova and Ch. Tsvetkova

4.P5.

## COMPLEXES OF TECHNETIUM-99m AND RHENIUM-188 WITH ZOLEDRONIC ACID IN NUCLEAR MEDICINE

A.O. Malysheva, G.E. Kodina, O.E. Klementyeva.

Burnasyan Federal Medical Biophysical Center FMBA Russia (Zhivopisnaya st. 46, Moscow, Russian Federation)

**Keywords:** bone metastases, diagnosis, technetium-99m, therapy, rhenium-188, zoledronic acid

### Abstract:

$^{99m}\text{Tc}$  and  $^{188}\text{Re}$  represent an attractive pair of radionuclides for biomedical use because of their favorable decay properties for diagnosis ( $^{99m}\text{Tc}$ ) and therapy ( $^{188}\text{Re}$ ) and because of their onsite availability, thanks to corresponding generator systems. Furthermore, the elements technetium and rhenium reveal similar chemical properties. This circumstance offers the possibility to simultaneously develop diagnostic and therapeutic tracers with almost identical chemical and pharmacokinetic characteristics. Diphosphonic acid derivatives labeled with  $^{99m}\text{Tc}$  have been widely used as imaging agents for bone diseases. Diphosphonates labeled with  $^{188}\text{Re}$  may be used for treatment of bone metastases. Zoledronic acid (ZA) was chosen as the object for investigation due to its therapeutic effect and accumulation in the bone metastases. The skeletal uptake of  $^{99m}\text{Tc}$ -ZA was about 50 %, the uptake ratio of bone-to-muscle was more than 50 at 1 h after injection. Skeletal uptake of  $^{188}\text{Re}$ -ZA was 20.0 % and 14.2 % after 1 and 3 h post injection respectively.

### Introduction

Bone metastasis is a major complication of several solid cancers: the prostate, breast, lung, kidney, and thyroid are cancers most associated with bone pain (most often, breast and prostate). Although bone metastases are often clinically silent, they can lead to serious sequelae, such as pain, fractures, and hypercalcemia. These complications often reduce performance status and decrease the quality of life. Bone pain due to metastasis is often considered a unique type of pain. It is initially a dull or aching pain, worse at night that improves with physical activity [1]. Skeletal metastases are clinically significant because of associated symptoms, complications such as pathological fracture and their profound significance for staging, treatment and prognosis. Detection of bone metastases is, thus, an important part of treatment planning.

Bisphosphonates are an important class of osteotropic compounds that are effective in treating benign and malignant skeletal diseases characterized by enhanced osteoclast-mediated bone resorption (i.e., osteoporosis, Paget's disease, and tumor-induced osteolysis). The evolution of bisphosphonates has led to compounds with ever-increasing potency. First-generation bisphosphonates, including etidronate and clodronate, contained simple side chains and were relatively weak inhibitors of bone resorption. Second-generation compounds, including pamidronate, alendronate, and ibandronate, have an aliphatic  $\text{R}^2$  side chain containing a single nitrogen atom. These nitrogen-containing bisphosphonates (N-BPs) are up to 100-fold more potent than the first-generation compounds. Zoledronic acid, a novel N-BP with an imidazole substituent, has demonstrated more potent inhibition of osteoclast-mediated bone resorption than all other bisphosphonates in both in vitro and in vivo preclinical models. Recent data suggest that N-BPs inhibit farnesyl diphosphate (FPP) synthase, an enzyme in the mevalonate biosynthetic pathway that is critical for protein prenylation and activation of important signaling molecules. Inhibition of

FPP synthesis also leads to production of triphosphoric acid 1-adenosin-5'yl ester 3-[3-methylbut-3-enyl] ester (ApppI), which induces apoptosis of osteoclasts and tumor cells. Our current knowledge of the pharmacology of N-BPs at the molecular level largely explains their observed effects on bone metabolism and tumor growth in animal models and their clinical activity in the treatment of benign and malignant bone diseases.

$^{99m}\text{Tc}$ -technetium ( $^{99m}\text{Tc}$ ) and  $^{188}\text{Re}$ -rhenium ( $^{188}\text{Re}$ ) represent an attractive pair of radionuclides for biomedical use because of their favorable decay properties for diagnosis ( $^{99m}\text{Tc}$ : 6 h half-life, 140-keV  $\gamma$ -radiation) and therapy ( $^{188}\text{Re}$ : 17 h half-life, 2.12-MeV  $\beta^-$  max-radiation) and because of their onsite availability, thanks to corresponding  $^{99}\text{Mo}/^{99m}\text{Tc}$ - and  $^{188}\text{W}/^{188}\text{Re}$  generator systems.

The aim of this study was to investigate the influence of reaction conditions such as pH, concentration of  $\text{SnCl}_2$ , concentration of the ligand (ZA), adding of carrier (in the case of  $^{188}\text{Re}$ ), time and temperature of reduction and etc. for the synthesis of  $^{99m}\text{Tc}$ -ZA and  $^{188}\text{Re}$ -ZA complexes and describe their biodistribution in experimental animals.

## Experimental

### Radionuclides and chemicals

$\text{Na}^{99m}\text{TcO}_4$  and  $\text{Na}^{188}\text{ReO}_4$  were obtained from the domestic generators (both are produced by the Institute of Physics and Power Engineering, Obninsk, Russia). Zoledronic acid was synthesized in Farm-SynteZ Ltd. Russia; the other chemicals was commercially produced (Merck).

### Preparation of $^{99m}\text{Tc}$ -ZA

5 ml of the  $\text{Na}^{99m}\text{TcO}_4$  solution (5 - 20 MBq) was introduced into the vial with lyophilized mixture of ZA (1.5 mg) and  $\text{SnCl}_2$  (0.3 mg). The radiopharmaceutical is ready to use after incubation at room temperature for 20 min.

### Preparation of $^{188}\text{Re}$ -ZA

1,5 ml of the  $\text{Na}^{188}\text{ReO}_4$  solution (750 – 2250 MBq) was added in the vial with lyophilized mixture of ZA (4.0 mg), gentesic acid (2.3 mg),  $\text{SnCl}_2$  (1.5 mg) and  $\text{Na}^{188}\text{ReO}_4$  (0.045 mg). The vial was heated on the boiling water bath during 30 min and then was cooled to room temperature. The obtained solution was filtered via a Millipore filter 0.22  $\mu$  in the vial with 15 ml of physiological solution.

### Quality control

Radiochemical yields of  $^{99m}\text{Tc}$ -ZA and  $^{188}\text{Re}$ -ZA, free pertechnetate or perrhenate and reduced hydrolyzed technetium or rhenium were determined by silica gel TLC (Merck 5553/acetone) and paper chromatography (Whatman 3MM/0.9 % saline).

### Experimental animals and biodistribution

All animal experiments followed the principles of laboratory animal care. Female white rats about 200 g body weight with and without bone pathology. Experimental animals were housed under conditions of controlled temperature (26 °C), humidity (68%) and daily light cycle (12 h light/12 h dark). The bone pathology was simulated by the closed femur fracture. Biodistribution of both radiopharmaceutical compositions were studied in with bone pathology in 10 days post-fracture model. About 0.2 mCi of  $^{99m}\text{Tc}$ -ZA or  $^{188}\text{Re}$ -ZA was injected intravenously into each of the rats via the tail veins. At the indicated points in time (1 and 3 h) the animals were sacrificed and dissected. The selected tissues were removed and the radioactivity was counted by a  $\gamma$ -counter to determine tissue distribution of the radiotracers. In vivo biodistribution studies were performed in triplicate for each radiotracer and time point. The results were tabulated as percentage of the injected dose per gram of tissue (% ID/g), using reference counts from a definite sample of the initial injected. The radioactivity of the sample and standards was measured by use of a  $\gamma$ -counter (Wizard 2480-0010, PerkinElmer LAS /Wallac).

## Results and Discussion.

Search of the optimal reagent composition «Rezoskan,  $^{99m}\text{Tc}$ » was carried out in the following range: zoledronic acid 0.2 – 0.9 mg/ml,  $\text{SnCl}_2$  0.02 – 0.08 mg/ml. The results of this search are shown on Fig. 1 – 4. It was found that radiopharmaceutical composition of  $^{99m}\text{Tc}$ -ZA with

radiochemical purity > 95 % can be prepared using ligand:SnCl<sub>2</sub> molar ratio from 2.5 to 3.5 at pH 5.0 – 6.5 after incubation for 20 min at room temperature.

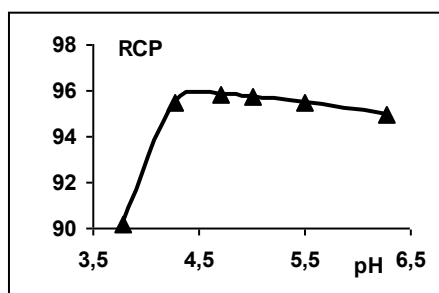


Fig. 1. Dependence of RCP from pH of radiopharmaceutical composition

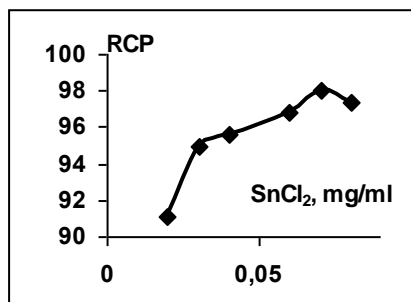


Fig. 2. Dependence of RCP from SnCl<sub>2</sub> concentration

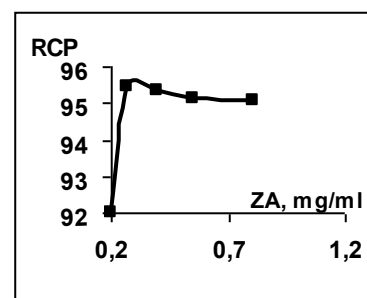


Fig. 3. Dependence of RCP from concentration of zoledronic acid

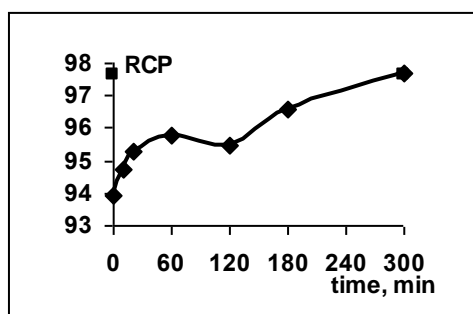


Fig. 4. Dependence of RCP from time incubation of radiopharmaceutical composition at room temperature

Search of the optimal reagent composition “Zoleren, <sup>188</sup>Re” was carried out in the following range: zoledronic acid 1.5 – 2.6 mg/ml; SnCl<sub>2</sub> 0.5 – 2.5 mg/ml; gentic acid 0 – 4.5 mg/ml; NaReO<sub>4</sub> – 0 – 30 μg/ml (or 0 – 20 μg/ml Re). The results of this search are shown on Fig, 5 – 8. The described composition of <sup>188</sup>Re-ZA can be prepared with radiochemical yield > 90 %. The composition was stable during 3 h from the moment of it preparation.

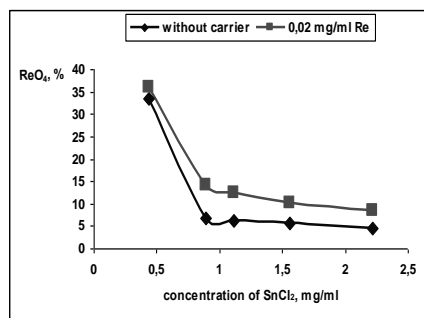


Fig. 1. Dependence of RCP from SnCl<sub>2</sub> concentration

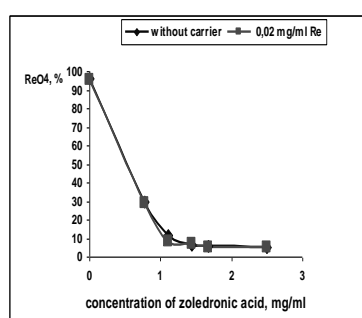


Fig. 2. Dependence of RCP from concentration of zoledronic acid

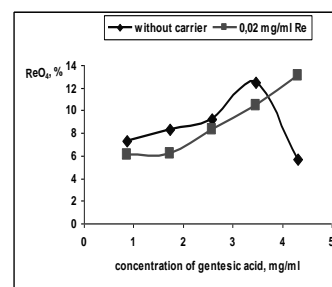


Fig. 3. Dependence of RCP from concentration of gentic acid

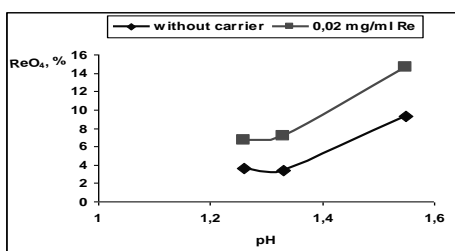


Fig. 4. Dependence of RCP from pH of radiopharmaceutical composition

From our preliminary experiments it was found that pH of the solution on the first step of preparation <sup>188</sup>Re-ZA (during rhenium reduction) should be quite acidic (pH < 1.5). The yield of <sup>188</sup>Re-ZA was decreased to 80 % at pH 2.5 - 3.5. We also observed the influence of adding the carrier on the yield of <sup>188</sup>Re-ZA. Without the carrier the radiochemical yield was also more than 90 %, but the composition was unstable.

### Biodistribution of <sup>99m</sup>Tc-ZA and <sup>188</sup>Re-ZA in vivo

The skeletal uptake of <sup>99m</sup>Tc-ZA was about 50 %, the uptake ratios of bone-to-blood were more than 20 at 1 h and up to 100 at 5 h after injection respectively. Differential coefficient of uptake (CDU) femur-to-femur with pathology was between 1.7 to 2.1. The data of <sup>99m</sup>Tc-ZA biodistribution are shown in Table 1. The pharmacokinetics of <sup>99m</sup>Tc-ZA in the bone pathology



location is characterized by higher uptake and slow release in comparison with a normal bone tissue (Fig 9).

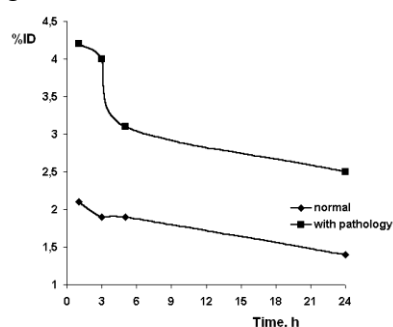


Fig 9. Pharmacokinetics of <sup>99m</sup>Tc-ZA in rat's bones

Table 1 Biodistribution of <sup>99m</sup>Tc-ZA in rats with model of bone pathology

Organ/Tissue	1 h p.i.	3 h p.i.
Blood, %ID/g	2.04 ± 0.81	1.72 ± 0.71
Liver	1.71 ± 0.58	1.13 ± 0.42
Kidneys	1.82 ± 0.83	1.44 ± 0.68
Bladder	35.11 ± 10.53	44.81 ± 3.89
Femur normal	2.13 ± 0.20	1.92 ± 0.42
Femur with bone injury	4.21 ± 1.04	4.03 ± 1.34
Skeleton	57.70 ± 5.54	46.62 ± 7.81
CDU	2.0	2.1

Since the use of <sup>99m</sup>Tc-ZA expected in patients receiving therapeutic dose of zoledronic acid, we studied the effect of this therapy on the quality of SPECT imaging of bone pathology. Experiments were carried out in rats with a bone pathology model, which simulated a fractured right femur. Seven days after fracture the animals were intravenously injected a solution of zoledronic acid in 0.9% saline at the dose of 0.04 mg per rat. The obtained data are shown in Table 2. The data of <sup>188</sup>Re-ZA biodistribution are also shown in Table 2.

Table 2. Biodistribution of <sup>99m</sup>Tc-ZA in animals after preliminary injection of zoledronic acid and <sup>188</sup>Re-ZA (% ID)

Organ/Tissue	<sup>99m</sup> Tc-ZA		<sup>188</sup> Re-ZA		The obtained data suggest that the use
	1 h p.i.	3 h p.i.	1 h p.i.	3 h p.i.	
Blood, %ID/g	0.18 ± 0,06	0.03 ± 0.01	0,43 ± 0,17	0,17 ± 0,07	
Liver	1.71 ± 0,54	0.62 ± 0.04	0,25 ± 0,05	0,14 ± 0,03	
Kidneys	1.55 ± 0,13	1.14 ± 0.34	3,19 ± 1,02	3,85 ± 1,26	
Stomach	0.31 ± 0,02	0.48 ± 0.30	0,18 ± 0,01	0,21 ± 0,11	
Femur normal	2.02 ± 0,20	1.98 ± 0.26	1,16 ± 0,31	1,39 ± 0,68	
Femur with bone injury	3.96 ± 0.60	3.70 ± 0.03	2,57 ± 0,83	2,37 ± 0,48	
Skeleton	55.62 ± 7.70	51.40 ± 6.89	31,96 ± 2,75	38,29 ± 5,47	
CDU	2.0	2.4	2.2	1,7	

of therapeutic drugs based on zoledronic acid does not cause an overflow of the exchange of bone pool and therefore will not have a significant impact on the quality of the SPECT imaging of the skeleton lesions with <sup>99m</sup>Tc. <sup>188</sup>Re-ZA rapidly accumulates and securely fixed in both normal femur bone and in bone pathology.

### Conclusions.

The possibility of simultaneous development of diagnostic and therapeutic radiopharmaceuticals on one chemical base with almost identical chemical and pharmacokinetic characteristics is shown. The optimal conditions for preparation of lyophilized reagent and RPhs “Rezoskan,<sup>99m</sup>Tc” and “Zoleren,<sup>188</sup>Re” were found. Nowadays “Rezoskan,<sup>99m</sup>Tc” is allowed for clinical usage. The preclinical trials of “Zoleren,<sup>188</sup>Re” will be finished in 2011.

**Acknowledgments:** The work was supported by “Farm-Sintez” Ltd., Moscow, Russia.

### References.

A Casciato DA, Chansky HA. Bone and joint complications. In: Casciato DA, Lowitz BB, eds. Manual of Clinical Oncology. 4th ed. Philadelphia, PA: Lippincott Williams Wilkins; 2000: pp. 601–614.



4.P6.

## PRODUCTION OF $^{188}\text{W}$ AND EXTRACTION OF $^{188}\text{RE}$ AT IRT-T

V.G. Merkulov, E.V. Chibisov, V.V. Zukau, Yu.S. Maslennikov,  
G.G. Glukhov

Physical-technical Institute of Tomsk Polytechnic University

Tomsk, 634050, Russia, 30, Lenin Avenue, [lab31radcontrol@rambler.ru](mailto:lab31radcontrol@rambler.ru)

Every year about 480 thousand cases of malignant neoplasmas are diagnosed in Russia. The morbidity has increased by 16% for the past 10 years. Nowadays more than 2.5million patients are registered on the books in oncological medical facilities, it's 1.8% of the country population.

From the view point of effective medical care  $^{188}\text{Re}$  radioisotope is considered the most perspective radionuclide for application of its compounds in beta-rays therapy of malignant neoplasmas, bony metastasis, rheumatoid arthritis and other diseases by open radionuclide sources.

Radioisotope of  $^{188}\text{Re}$  ( $T_{1/2}=16,98$  h) is received as a daughter product at beta decay of  $^{188}\text{W}$  ( $T_{1/2}= 69,4$  days), which in its turn is produced in the reaction ( $n;\gamma$ ) of the second order in nuclear reactors by irradiating tungsten oxide of the natural isotopic composition (28,64 %  $^{186}\text{W}$ ), or by concentrating  $^{186}\text{W}$  isotope more than by 90%. The use of the cheap raw material as a starting target results in further application of concentrating technologies for extraction of daughter radioisotope of  $^{188}\text{Re}$ , the sublimation and extraction technologies are primary ones.

At nuclear reactor IRT-T of Physical-technical Institute of Tomsk Polytechnic University (the maximum flux of thermal neutrons is up to  $1,5 \cdot 10^{14} \text{ H} \cdot \text{c}^{-1} \cdot \text{cm}^{-2}$ ) research works on production of parent  $^{188}\text{W}$  and sublimation extraction of  $^{188}\text{Re}$  from the target of natural isotope compound were carried out. Sublimation extraction of  $^{188}\text{Re}$  from irradiated targets of tungsten oxide (VI) was carried out in the apparatus supplied with a refrigerated condenser, onto which Re precipitated during gaseous phase in the form of  $\text{Re}_2\text{O}_7$ . The research of  $^{188}\text{Re}$  extraction rate was studied in the temperature mode of 600-700<sup>0</sup>C depending on the target mass and heating time. It is shown that the content of  $^{188}\text{W}$  in the fallout does not exceed 0,005% of the daughter isotope activity. The percentage of molybdenum and antimony radio nuclides that are present in initial tungsten oxide (VI) as admixtures is less than the limits of detection. Radiochemical purity of the desired preparation is more than 99%.

Thus, the experiments mentioned above create the preconditions for the development of the regional  $^{188}\text{Re}$  sublimation generator for providing medical facilities with  $^{188}\text{Re}$  based radiopharmaceuticals.

4.P7.

## TC-99M GENERATOR PRODUCTION AND APPLICATION EXPERIENCE

Stepchenkov D.V., Nerozin N.A., Baranov N.G., Sulim E.V., Semenova A.A.

Federal State Unitary Enterprise “State Scientific Center of the Russian Federation –  
Institute for Physics and Power Engineering”,  
Bondarenko sq., 1, Obninsk, Kaluga region, 249033, Russia

**Key words:** nuclear medicine, chromatographic Tc-99m generator, sorbent, eluate, radionuclide purity.

### Abstract:

Results of scientific and production activities at SSC RF – IPPE in the field of manufacturing of Tc-99m generator, one of widely used in the world nuclear medicine are presented in the report. Design and technological features of the short-lived isotope generator are presented. Ways of the product quality improvement are considered.

### Introduction

Improvement of SSC RF – IPPE production activity in the field of medical radioisotope production is a strategic task of promotion of Russian nuclear medicine development. Since 1989 SSC RF – IPPE became one of developers and Russian producers of Tc-99m generators which is widely used in nuclear medicine for diagnostics of different diseases of all essential human organs and systems. The output volume of diagnostic radionuclide products based on eluate from Tc-99m generator occupies the leading position in the world. More than 10000 diagnostic procedures with the use of our  $^{99}\text{Mo}/^{99\text{m}}\text{Tc}$  generators are performed annually at 80 Russian hospitals. Distinguished feature of chromatographic Tc-99m generator produced at SSC RF – IPPE is the use of silica gel modified by manganese dioxide and aluminum dioxide as sorbents. Within the 21-year of production experience the quality parameters of the generator eluates produced have been brought



Fig.1. Tc-99m generator view.

to a level of the best Russian and foreign patterns: daughter radionuclide yield is not less than 80 %; radiochemical purity is not less than 99.8 %; concentration of radionuclide impurities is not more than  $10^{-3}$  % of Tc-99m activity; concentration of stable impurities is not more than 5mg/ml in total. Operation experience and design characteristics of generator have shown evidently their suitability, reliability and safety of their application in clinical practice. Tc-99m generator is designed in the form of compact facility providing radiation safety and automatic elution mode with the use evacuated vials.

However, the most complicated and serious quality problems of the sodium pertechnetate product remain the possibility of its contamination with sorbent material and radioactive impurities of initial material due to radiation chemical processes and accumulation of water radiolysis products.

Work on the improvement of Tc-99m generators directed on the reduction of radionuclide and non-active chemical impurities in eluate, refining of operation parameters, and radiation dose reduction and work place is carried out at SSC RF – IPPE.

## Experiment

Semi-conducting spectrometer of gamma-radiation energy “Gamma-1P” and dose-calibrator “Atomlab 100 plus” were used for radiometric control of solutions under investigation. Eluate radiochemical purity was determined by the methods of electrophoresis and ascending chromatography. Hydrogen ion activity in solutions was determined by potentiometric method with the use of ion meter I-130m and pH-tester “Checker”. Sodium chloride concentration in eluate was determined by argentometric method. Chemical element concentration was controlled with the help of spectrometric analysis methods. Sorbent granulometric composition was determined by screen grate “Analysette 3” made by PRO Fritsch. “BINDER GmbH Postfach 102” sterilizer was used. Brief characteristics of <sup>99</sup>Mo/<sup>99m</sup>Tc generator system are presented in the Table 1.

Table 1. Characteristics of <sup>99</sup>Mo/<sup>99m</sup>Tc generator system

Daughter radionuclide			Parent radionuclide				Eluent
Isotope, T <sub>1/2</sub>	Decay type	Energy and intensity, MeV	Isotope, T <sub>1/2</sub>	Decay type	Energy and intensity, MeV	Production method	
<sup>99m</sup> Tc 6.01h	Isomeric transition	γ 0.140 (91%) β <sup>-</sup> 0.119	<sup>99</sup> Mo 66.02h	β <sup>-</sup>	β <sup>-</sup> 1.23 max γ 0.181 (7%); 0.739 (12%); 0.778 (4%)	<sup>235</sup> U(n,f) ) <sup>99</sup> Mo	5ml 0.9 % NaCl

## Result and Discussion

During investigation of molybdate-ion dynamic sorption it has been stated that the maximal sorption is possible when using sorbents in acid form and initial solutions possessing acid or neutral medium (Table 2).

Table 2. Results of molybdate-ion (<sup>99</sup>Mo) sorption study with 100 mkg Mo/ml initial concentration

Adsorbent, weight 100mg	pH of Mo-99 solution	Adsorption on chromatographic column, %		
		After solution 1 passage (10 ml)	After solution 2 passage (10 ml)	After solution 3 passage (10 ml)
SiO <sub>2</sub> /MnO <sub>2</sub> (neutral)	9.5	9 ± 2	2 ± 1	0
SiO <sub>2</sub> /MnO <sub>2</sub> (neutral.)	6.4	43 ± 5	29 ± 3	17 ± 3
SiO <sub>2</sub> /MnO <sub>2</sub> (neutral.)	2	54 ± 5	35 ± 5	33 ± 5
MnO <sub>2</sub> (кисл.)	6.4	53 ± 5	35 ± 5	27 ± 5
MnO <sub>2</sub> (acid)	2	64 ± 7	53 ± 5	50 ± 5
Al <sub>2</sub> O <sub>3</sub> (alkaline)	9.5	0	0	0
Al <sub>2</sub> O <sub>3</sub> (neutral)	7.7	94.1 ± 2.5	93.2 ± 2.5	78.6 ± 2.5
Al <sub>2</sub> O <sub>3</sub> (neutral)	6.4	93.1 ± 2.5	86.9 ± 2.5	86.3 ± 2.5
Al <sub>2</sub> O <sub>3</sub> (neutral)	2	98.8 ± 0.2	98.3 ± 0.2	98.1 ± 0.2
Al <sub>2</sub> O <sub>3</sub> (acid)	6.4	99.9 ± 0.1	99.9 ± 0.1	99.9 ± 0.1
Al <sub>2</sub> O <sub>3</sub> (acid)	2	99.9 ± 0.1	99.9 ± 0.1	99.9 ± 0.1

To improve the eluate quality a composition of multilayer adsorbent has been suggested, one of the layer of which contains silica gel modified with manganese (IV) dioxide in acid form, and the other layers are chromatographic aluminum oxide in acid, alkaline and neutral forms. Optimal engineering parameters of sorbent preparation have been developed: granulometric composition, control of critical processes and factors, generator loading technology with activity of 0.1 to 4.0Ci

RF patented [1]. Investigations performed allow obtain eluates meeting the requirements of Russian and European Pharmacopoeia.

Russian Tc-99m generator is not worth than the foreign generators, its daughter radionuclide yield is not less than 80% (fig.2). Currently Tc-99m generators are serially produced according to modified technology meeting the requirements of quality assurance system – standards of ISO-9001-2001.

Certified production [2] of Tc-99m generators a system of quality control has been developed and works at all process phases. It includes an inlet control of initial materials and agents, control of products of auxiliary production, control of end product batches within the service life as well as evaluation of application quality of Tc-99m generators delivered to medical institutions [3].

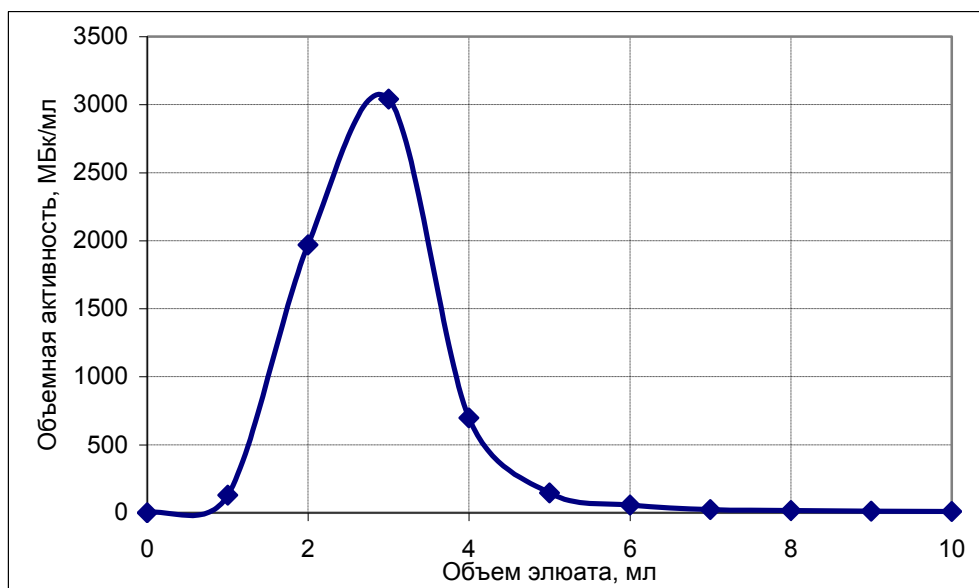


Fig.2. Curve of Tc-99m elution by sodium chloride isotonic solution of  $^{99}\text{Mo}/^{99\text{m}}\text{Tc}$  generator of 11.1GBq activity

### Conclusion

A complex work on reconstruction of the medical production and its quality control is carried out at SSC RF – IPPE in accordance with State Standard P 52249-2009 “Regulations of production and quality control of medicines (GMP)”. Rearrangement of production and quality control system allows provide the competitiveness of Tc-99m-generators at the world level and promote the domestic product to foreign markets.

### References

1. Patent of invention #2153357. Basmanov V.V., Sokolov A.B., Semenova A.A., et al. “Generator for production of sterile radioproduct technetium-99m and method of its preparation”. 2000.
2. License of the federal supervision service in the field of public health and social development #99-03-001619 for the activity on medical equipment production at SSC RF – IPPE, 2009.
3. Registration certificate #FL 2008/03978 of 2008. Tc-99m generator GT-2M according to TS 9452-032-08624390-2008 giving the right to produce, sell and apply it in the territory of the Russian Federation.

4.P8.

## DETERMINATION OF ASCORBIC ACID IN KIT BY HIGH-PERFORMANCE LIQUID CHROMATOGRAPHY

N.B. Epstein<sup>1</sup>, G.M. Khomushku<sup>1</sup>, L.D. Artamonova<sup>1</sup>, V.G. Skvortsov<sup>2</sup>

<sup>1</sup>National Research Nuclear University MEPhI – IATE, Obninsk

<sup>2</sup>Medical Radiological Research Center, Obninsk

[NBepshtejn@mephi.ru](mailto:NBepshtejn@mephi.ru)

Technetium-99m hydroxyethylidene diphosphonate (HEDP) and rhenium-188 hydroxyethylidene diphosphonate were developed at the MRRC for diagnose and treatment of bone metastases, accordingly. The main quality control tests of radiopharmaceuticals are: concentrations of HEDP, Sn(II), ascorbic acid, the percentage of <sup>99m</sup>Tc or <sup>188</sup>Re unbound with preparation (radiochemical impurity or RCI). In the present work, an HPLC method for identification and quantification of AA in non-radioactive kit was developed.

Numerous analytical techniques have been proposed for its determination in different matrices and at different levels. There is no information about AA determination in radiopharmaceutical kits. There are some difficulties in quantifying ascorbic acid in kits due to simultaneous stannous ions presence and AA instability in aqueous solution. AA has limited stability and may be lost from kits during preparation and storage. AA is readily oxidized primarily to dehydroascorbic acid (DHA), which is a reversible reaction. Generally, the total AA is defined as the sum of both AA and its oxidized form DHA. The quantification of DHA is usually performed after its conversion into AA in the presence of reducing agents.

The HPLC system (Shimadzu, SCL-10A), was equipped with UV detector system. The LC-analyses were performed under isocratic mode at a flow rate 1 ml/min with detection at 265 nm. Sample and standard injections of 20 µl were made on a Supelcosil LC-18 column; 5 µm; 4.6\*250 mm; at 25 °C. The separation was performed with a sodium acetate eluent (pH 5.4) containing decylamine as ion pairing agent. Standard solutions (AA and DHA) and samples were prepared daily in volumetric amber glass flasks. Chromatographic peaks were identified by comparing its retention times with external standards. The experimental data were analysed statistically to validate the proposed method.

AA was quantified in standard by means of an external calibration curve in the concentration range 0.005 to 0.5 mg/ml. The HPLC method offers good accuracy and reproducibility, relative short analysis time, unambiguous identification of AA in presence of DHA. To prevent the loss of AA in the standard and the samples solutions, it was necessary to prepare their with deaerated water and protect from light by using amber flasks. The DHA was not quantified in AA standard and in samples. The presence of HEDP and Sn(II) in kit vial had no influence on the results of AA determination by HPLC.

4.P9.

## SYNTHESIS AND CHARACTERISATION COMPLEX OF THE $\{\text{ReO}\}^{3+}$ CORE WITH S/N AND N DONOR LIGANDS LIGANDS AND OF ITS $^{99\text{m}}\text{Tc}$ ANALOG.

Noura Saad Al-Hokbany .

Department of chemistry, College of Science, King Saud University, Riyadh 11451, Kingdom of Saudi Arabia. E-mail:nhokbany@ksu.edu.sa. Tel:+966 1 4772245; Fax: +966 1 4772245

**Keywords:**  $[\text{ReO}]^{3+}$ , DFT, mercaptobenzothiazole ligand, Aminothiazole ligand,  $^{99\text{m}}\text{Tc}$ -gluconate, B3LYP.

### Abbreviations

Mer: mercaptobenzothiazole

Amino: Aminothiazole

ITLC: instant thin- layer chromatography.

SG-TLC: silica gel thin- layer chromatography.

HPLC: High performance liquid chromatography.

DFT: density function theory

### Abstract

A novel mixed ligand  $^{99\text{m}}\text{Tc}$  complex with mercaptobenzothiazole as ligand and Aminothiazole as coligand was prepared and evaluated as potential brain radiopharmaceutical. Preparation at tracer level was accomplished by substitution, using  $^{99\text{m}}\text{Tc}$ -gluconate as precursor and a coligand/ ligand ratio of 5. Under these conditions the labeling yield was over 97% and a major product with radiochemical purity >97% was isolated by HPLC methods and used for biological evaluation.

The reaction of  $[\text{ReO}(\text{Citrate})_2]^-$  with mercaptobenzothiazole and Aminothiazole in hot MeOH yields  $[\text{ReO}(\text{mer})(\text{amino})\text{OH}(\text{H}_2\text{O})_2]$ . The DFT study demonstrated that the complex consists of distorted octahedral  $\text{ReO}(\text{V})$ . The coordination geometry at the rhenium is defined by a terminal oxo-group, the nitrogen and sulfur donors of the chelating mercaptobenzothiazole, the nitrogen of Aminothiazole ligand, is present as deprotonated amido nitrogen.

Biodistribution in mice demonstrated early brain uptake, fast blood clearance and excretion through hepatobiliary system. Although brain/blood ratio increased significantly with time, this novel  $^{99\text{m}}\text{Tc}$  complex did not exhibit ideal properties as brain perfusion radiopharmaceutical since brain uptake was too low.

### 1. Introduction

The  $\gamma$ -emitting technetium-99m is the most widely applied radionuclide in diagnostic imaging. Nevertheless, current research in radiopharmacology involves the exploitation of the coordination chemistry of technetium as well as its congener rhenium to develop new radiotracers [1, 2]. In the past decade, many efforts were focused on brain imaging technetium radiopharmaceuticals that may cross the blood-brain barrier and localize in the brain. Although many of the Tc and Re complexes have been investigated to date, clear structural criteria involved in brain uptake and retention of technetium complexes are not fully documented.

One of the important aspects in Tc radiotracer design is complex lipophilicity [3]. Since distribution and passive transport through membranes are governed by lipophilicity, there is a considerable interest in which way lipophilicity parameters can be controlled by chemical modifications at the



tracer molecule. In this investigation on amine-bearing mixed-ligand rhenium complexes aims toward this goal. These studies are triggered by the fact that the amine-carrying technetium species are able to pass the intact blood-brain barrier and are accumulated in the brain [4, 5]. Keeping in mind that rhenium complexes may serve as nonradioactive surrogates for their technetium analogues due to similar molecular properties, the synthesis of Re (V) complexes requires the presence of metal-containing chemical cores that are, stable enough to exist in aqueous solutions and versatile enough to combine with the selected ligands. An example of such a core is the oxo form  $[\text{Re}^{\text{V}}\text{O}]^{3+}$ , in which the + 5 oxidation state of the metal is stabilized by the oxo-core [5,6]. The literature shows that a search for new radiopharmaceuticals requires studies of new oxorhenium (V) complexes with nitrogen and sulfur donor sets, as well as investigations of the chemical behavior of their  $^{99\text{m}}\text{Tc}$  analogs. In this work, we report the synthesis and characterization of a novel complex of rhenium of the general type  $[\text{ReO}(\text{mer})(\text{amino})\text{OH}(\text{H}_2\text{O})_2]$ . We have also studied the radiochemical properties of the corresponding technetium complex, which was prepared by two methods.

Nowadays, *ab initio* computational techniques are a potent tool for research. Chemistry has changed from a purely empirical science into a discipline in which deductive theory, as represented by first-principles calculations using computers, is increasingly important for interpretation and guidance of experimental work. Recent developments in this area include the field of density functional theory which meets with the requirements of being accurate. Currently density functional theory (DFT) is commonly used for geometric optimization and electronic structure of transition metal complexes. It meets the requirements of being accurate, easy to use and fast enough to allow the study of relatively large molecules of transition metal complexes [7, 8]. Geometric optimization and electronic structure of  $[\text{ReO}(\text{mer})(\text{amino})\text{OH}(\text{H}_2\text{O})_2]$  has been determined on the basis of the density functional theory (DFT) calculations and additional information about binding has been obtained by NBO analysis. The accuracy of the DFT calculations can be tested by comprising the available experimental data against calculation values. In our case study the experimental data available will be the data gathered from spectroscopic measurements such as UV-Vis, FTIR and NMR data.

## 2. Computational details

The GAUSSIAN 03 program [9] (Gaussian 03 program) was used in the calculations. The complex was treated as open shell-system and no symmetry constraints were applied. Geometrical optimization of the investigated complex was carried out with Beck's three parameter exchange functional B3LYP using the Los Alamos LANL2DZ split-valence basis set [10, 11]. A harmonic vibrational analysis was performed following the geometrical optimization of the complex at the same level of theory B3LYP and the same basis set [12]. An additional d function with exponent  $a = 0.3811$  and an f function with exponent  $a = 2.033$  on the rhenium atom were added [13]. Natural bond orbital (NBO) calculations were performed with the NBO code [14] included in GAUSSIAN 03.

## 3. Experimental

### 3.1 Materials and methods

All the reagents used in the synthesis were commercially available and were used without further purification. The  $\text{ReO}(\text{citrate})_2^-$  precursor was prepared according to the literature [15]. IR was recorded on a Perkin Elmer spectrophotometer 1000 in the spectral range  $200\text{--}4000\text{ cm}^{-1}$  with sample in the form of KBr pellets. Elemental analyses were performed on a Perkin-Elmer Analyzer 2400.  $^1\text{H}$ - $^{13}\text{C}$  NMR spectra were obtained in  $\text{DMSO-}d_6$  on JEOL NMR 400 MHz. Electronic spectrum was measured on a UV-Vis Beckman Du-70 spectrophotometer in the range  $190\text{--}700\text{ nm}$  in aqueous medium.

$^{99m}\text{TcO}_4^-$  in saline solution was eluted from a  $^{99}\text{Mo}/^{99m}\text{Tc}$  generator obtained from Cis Bio International Elumatic III, B.p.32. (France). Chemical reactions were monitored by thin-layer chromatography on instant thin layer chromatography (ITLC, SG-TLC) using Whatman No.1 chromatography paper (Whatman International Ltd. UK) and Silica gel-60 F<sub>254</sub> TLC- aluminium sheets (Alltech). HPLC separations were carried out using a normal phase silica column (Econosil 10 $\mu\text{m}$  x 264 mm) using a dual pump (Jasco-pu-2089 plus Quaternary Gradient); methanol/dichloromethane (1:1) was used as the mobile phase with a flow rate of 0.5 ml/min. A JASCO chromatography system equipped with a variable wavelength ultraviolet monitor (JASCO, UV-2075 plus, intelligent UV/Vis detector) was set up in tandem with a Canberra flow through NaI radioactivity detector (TI). Ultraviolet absorption and radiochromatogram was monitored at 254 nm. Chromatography was acquired and analyzed using BORWIN software.

Electrophoresis measurements were carried out in 0.1 M sodium borate buffer (pH 8) using Whatman No.1 chromatography paper. The paper was presoaked in the same buffer for 5 minutes before spotting the radiolabeled sample at the middle of the paper. After a potential of 160 V was applied for 120 min, the chromatography paper was dried, and the distribution of radioactivity was measured in a  $\gamma$ -well counter. The radiochemical purity of the prepared complex was determined by spotting on ITLC-SG strips.

The biodistribution experiments for the  $^{99m}\text{Tc}$  complex were performed in normal female mice to ascertain the *in vivo* distribution profile of the radiotracers according to literature [16]. The animal biodistribution experiments were performed in accordance with institutional, national and international regulations governing the safe and humane use of laboratory animals in research.

Mice (BALB/C, 25–30 g) were injected *via* the tail vein with 0.1 ml of the radiotracer formulated in saline. Each dose contained 20-30  $\mu\text{Ci}$  of radioactivity. Animals were sacrificed at 5, 30 and 60 min post injection and the organs of interest and blood were collected, weighed, and the radioactivity was measured with an automatic gamma counter (Cobra II). The percentage of the injected dose per gram was then calculated for all tissues using a stored sample of the injection solution to estimate the total dose injected per mouse.

### 3.2 Synthesis of $[\text{ReO}(\text{mer})(\text{amino})\text{OH}(\text{H}_2\text{O})_2]$ .

$\text{NaReO}_4$  (1mmol, 0.273 g) was added to a solution of  $\text{SnCl}_2$  (1mmol, 0.256 g) in citric acid (0.5M, 5ml). Amino (1mmol, 0.1004 g) and (mer) (2 mmol, 0.334 g) in ethanol were added dropwise to the mixture. The reaction mixture was stirred at room temperature for 3hr. The pH was adjusted to 9 with NaOH (0.5M), and the precipitate was recrystallized in hot Methanol and acetone according to literature [17]. Attempts to make a single crystal were unsuccessful and the complex was precipitated in micro crystalline form with 98 % yield of the compound: Anal. Calc.(found) for  $\text{C}_{10}\text{H}_{12}\text{N}_3\text{O}_4\text{S}_3\text{Re}$ : C, 23.12(23.46); H, 2.30 (2.05); N, 8.10(8.64); Re,35.8 (36.01)%. IR (KBr,  $\nu/\text{cm}^{-1}$ ): 908 (Re=O), 606(Re-N), 430(Re-O), 561(Re-S).  $^1\text{H}$  NMR (d<sub>6</sub>-DMSO, ppm): 3.4 (s,NH), 7.6(t,Ha), 7.2-7.4(m, Hb, Hc), 7.9(s, Hd) , 7(d, CH=C-N), 6.68(d, CH=C-S).  $^{13}\text{C}$  NMR (d<sub>6</sub>-DMSO, ppm): 122,124,129 (Ph-ring C=C), 107(C-S), 113(mer C=C-C-S), 141(C=C-C-N), 138(CH-C-N), 169(C=N), 190(C=S). UV-Vis ( $\text{H}_2\text{O}$ ;  $\lambda_{\text{max}}[\text{nm}](\epsilon; \text{dm}^3\text{mol}^{-1}\text{cm}^{-1})$ ): 204 nm( 1899), 321 nm(2459), 332 nm(1899). MS (m/z): 520.2[M]<sup>+</sup>.

### 3.3 Synthesis of $[^{99m}\text{TcO}(\text{mer})(\text{amino})\text{OH}(\text{H}_2\text{O})_2]$

Direct method: .A

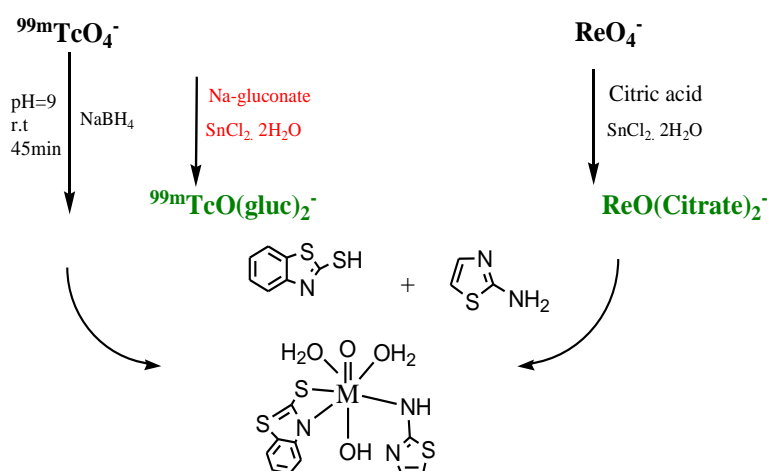
The preparation of the  $^{99m}\text{Tc}$ -complex was achieved by addition of sodium borohydride (0.29 mmol , 11.1 mg) in freshly prepared saline to a mixture containing  $^{99m}\text{TcO}_4^-$  (0.7 ml, 27 mCi) and ligands (mer: 9.0 mg, 0.1 mmol ; Amino: 9.9 mg, 0.10 mmol ) with stirring. The mixture was allowed to stand for 45 min for complete reaction and then extracted with dichloromethane (3x1.5 ml). The combined organic extracts were dried over  $\text{MgSO}_4$ , which was filtered off. The radioactivity content of both the aqueous and organic phase is measured separately. The organic solvent was expelled under a mild stream of nitrogen, and ethanol was added. 30% ethanol final solution was obtained for complex according to literature [16]. The radiolabeling yield was  $88 \pm 3\%$  with >96% radiochemical purity.

ligand exchange method: .B

Preparation of the  $^{99m}\text{Tc}$  complex was accomplished using  $^{99m}\text{Tc}$ -gluconate as the precursor [16]. A vial containing a lyophilized mixture of 200 mg sodium gluconate and 0.2 mg of  $\text{SnCl}_2 \cdot 2\text{H}_2\text{O}$  was reconstituted with 5 ml of water. A volume of 0.5 ml of this solution was mixed with  $[\text{}^{99m}\text{Tc}] \text{NaTcO}_4$  1mmol  $\{(0.5\text{--}1 \text{ ml with an activity of } 5\text{--}50 \text{ mCi (185--1850 MBq)}\}$ . The precursor  $^{99m}\text{Tc}$ -gluconate, (radiochemical purity  $> 95\%$ ) was added to a centrifuge tube containing the mixed ligands. The mixture was stirred in a vortex mixer and left to react at room temperature for 10 min. The complex was extracted with dichloromethane ( $3 \times 1.5 \text{ ml}$ ) and the organic layer was dried with  $\text{MgSO}_4$ , filtered and analyzed by ITLC and HPLC.

## Results and Discussion

The reaction between oxorhenium citrate and the mixed ligands system mercaptobenzothiazole/ Aminothiazole lead to the formation of a  $[\text{ReO}(\text{mer})(\text{Amino}) \text{OH}(\text{H}_2\text{O})_2]$  complex according to Scheme 1.



were  $\text{M}=\text{Re}, ^{99m}\text{Tc}$

Scheme 1.

We found that the labeling yield of the final  $^{99m}\text{Tc}$  complex was higher when the direct reduction method was used compared with the ligand exchange method.

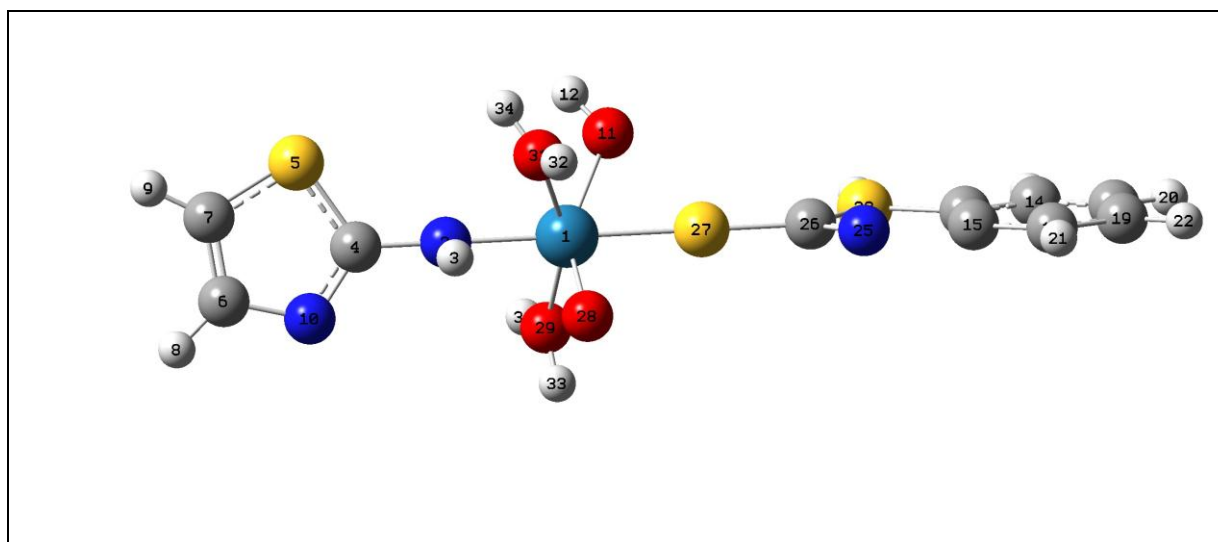
Table 2 presents the atomic charges from the Natural Population Analysis (NPA) for  $[\text{ReO}(\text{mer})(\text{Amino})\text{OH}(\text{H}_2\text{O})_2]$ . The calculated charge on the rhenium atom is considerably lower than the formal charge of +5. This difference is a result of significant charge donation from the Oxo, OH and N-ligand donors. The charge on the Oxo ligand is significantly smaller than (-2) and less negative than the charge on the OH ligand, indicating that there is higher electron density delocalization from the Oxo core to the rhenium [20].

### 4.1 Geometry optimization, charge distribution, electronic structure and NBO analysis:

The geometry of the  $[\text{ReO}(\text{mer})(\text{Amino})\text{OH}(\text{H}_2\text{O})_2]$  complex was optimized in a single state by the DFT method with the B3LYP function as shown in Fig1. The calculated bond lengths and angles for  $\text{Re}=\text{O}$ ,  $\text{Re}-\text{N}$  and  $\text{Re}-\text{O}$  are in quite good agreement with the values reported for other oxorhenium complexes of related structure as listed in Table 1 [18, 19].

Table 1. Some geometrically optimized bond length( $\text{\AA}$ ) and angles( $^\circ$ ) for  $[\text{ReO}(\text{mer})(\text{Amino})\text{OH}(\text{H}_2\text{O})_2]$ .

Bond length ( $\text{\AA}$ )	Bond angle ( $^\circ$ )	B3LYP/LANL2DZ [19]
Re(1)-O(28) 1.7196 (1.7071)	O(28)-Re(1)-O(11)	170.9908 (170.7782)
Re(1)-O(28) 1.9253 (1.8662)	S(27)-Re(1)-N(2)	172.2611 (171.792)
Re(1)-N(2) 2.0531 (1.9322)	N(2)-Re(1)-O(28)	109.4543 (109.260)
Re(1)-S(10) 2.355 (2.233)	N(2)-Re(1)-O(31)	93.4614 (120.723)
Re(1)-O(11) 1.9253 ( 1.862)	N(2)-Re(1)-O(11)	102.2092(102.792)
Re(1)-O(29) 2.1676 (1.9322)	N(2)-Re(1)-O(29)	90.0916 (102.792)
N(2)-C(4) 1.3998(1.398)	O(28)-Re(1)-O(11)	99.2639(100.07)
N(10)-C(4) 1.4066(1.398)	Re(1)-O(31)-H(32)	117.5155 (116.99)

Fig.1. The Optimized structure of  $[\text{ReO}(\text{mer})(\text{Amino})\text{OH}(\text{H}_2\text{O})_2]$ .Table 2. Atomic charges from the natural population analysis (NPA) for  $[\text{ReO}(\text{mer})(\text{Amino})\text{OH}(\text{H}_2\text{O})_2]$ .

Atom	Atomic charge
Re(1)	1.437
N(2)	-0.475
S(27)	-0.562
O(11)	-0.413
O(28)	-0.742

Table 3 presents the occupancy and hybridization of the calculated Re-O bond orbitals (NBOs) for the  $[\text{ReO}(\text{mer})(\text{Amino})\text{OH}(\text{H}_2\text{O})_2]$  complex. Three natural bond orbitals were detected for the core Re-O bond, and one bond orbital was observed for the Re-O bond of the OH ligand. The Re-O bond orbital of  $\sigma$ -character is polarized toward the O atoms, and the s and d-orbitals of the Re participate in the bonding. The Re-O bond orbitals of  $\pi$  character are significantly polarized towards the metal atom and only the d-orbitals of Re are included into the bonding. The complex adopts a distorted octahedral structure in which two water molecule is weakly coordinated to the Re atom, as

seen from the unusual bond length of 2.1676 pm. It is worth mentioning that these calculations are performed in the gas phase. Dissolution of the investigated complex in aqueous medium could result in another H<sub>2</sub>O molecule being coordinated to the rhenium to form a distorted octahedral structure. These results were further confirmed by measuring UV-Vis spectra of the complex in different solvents; shifts in  $\lambda_{\max}$  were recorded by changing the solvent, which indicates coordination of an additional solvent molecule with the Re atom to complete the octahedral geometry typically found for Re=O complexes [20].

Table 3. The occupancies and hybridization of the calculated Re-O natural bond orbitals (NBOs) for [ReO(mer)(Amino)OH(H<sub>2</sub>O)<sub>2</sub>].

BD	Occupancy	Hybridization of NBO
Re(1)≡O(28)	1.95735(0.2786)	0.5196(sd) <sub>Re</sub> + 0.8544(sp) <sub>O</sub>
	1.78553(0.2268)	0.3809(d) <sub>Re</sub> + 0.9246(p) <sub>O</sub>
	1.78648(0.1699)	0.4145(d) <sub>Re</sub> + 0.9101(p) <sub>O</sub>
Re(1)-O(11)	1.89301(0.1667)	0.3359(sd) <sub>Re</sub> + 0.9419(p) <sub>O</sub>
	1.88269(0.1662)	0.2906(d) <sub>Re</sub> + 0.9569(p) <sub>O</sub>
Re(1)-N(2)	1.89452(0.200)	0.4653(d) <sub>Re</sub> + 0.8852(p) <sub>N</sub>

Table 4 compares the calculated and observed vibrational modes of [ReO(mer)(Amino)OH(H<sub>2</sub>O)<sub>2</sub>]. Although one must normally scale the theoretical data by optimal scaling factors, which vary by basis set, the theoretical values are usually higher than the experimental data. Figs 2, 3 show experimentally and theoretically calculated IR spectra of complex. In our case study, however, there was good agreement between the theoretical and experimental data.

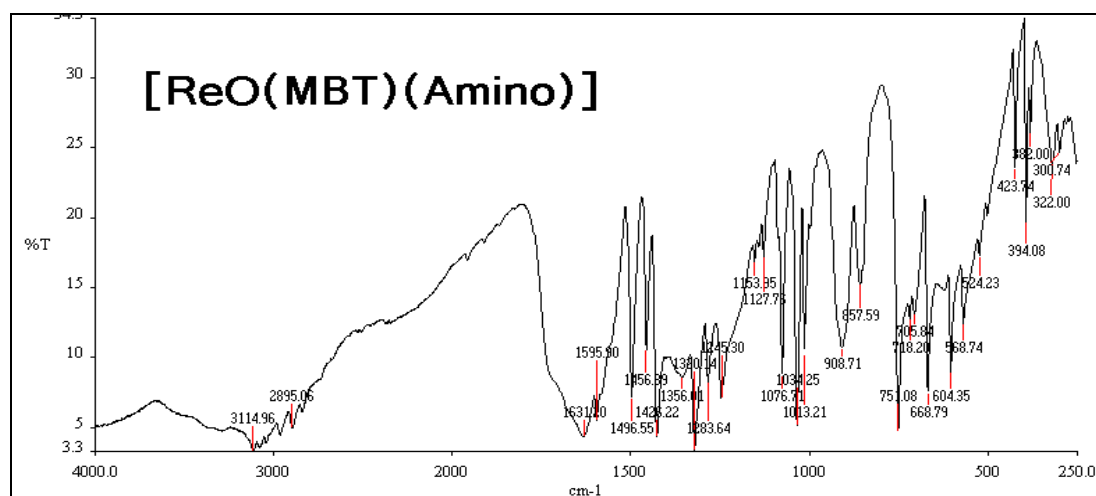


Fig.2 The IR of [ReO(mer)(Amino)OH(H<sub>2</sub>O)<sub>2</sub>] complex.

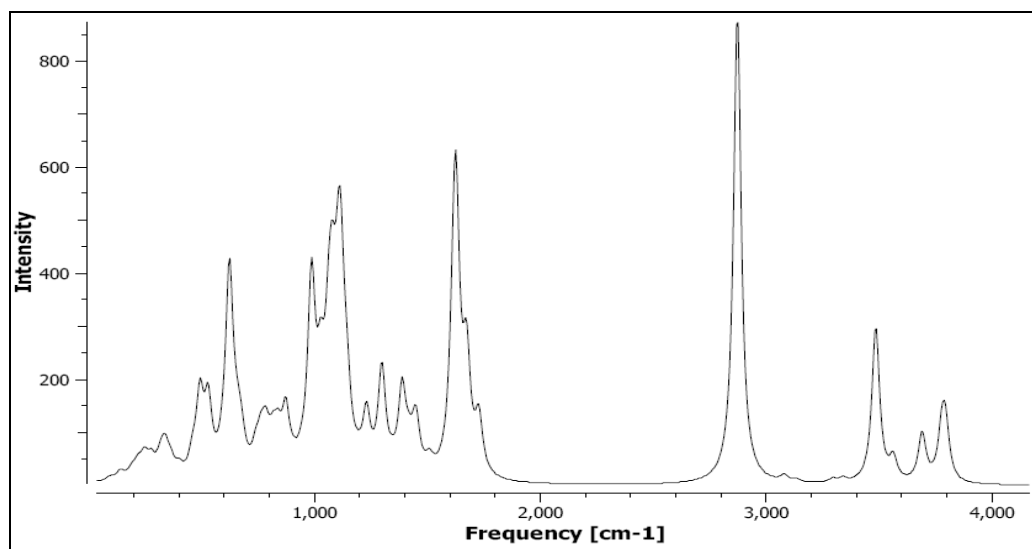


Fig.3 The Theoretical IR of  $[ReO(mer)(Amino)OH (H_2O)_2]$ .

In the IR, (Fig 2) the strong  $\nu(Re=O)$  bond of the  $[ReO(mer)(Amino)OH (H_2O)_2]$  complex was found in the narrow range around  $908\text{ cm}^{-1}$ . This value is in the lower end of the range observed for a  $[ReO]^{3+}$  core, and suggests that the Re-hydroxy bond competes effectively. In many investigated studies concerning the  $M=O_{oxo}$  distances in complexes containing the  $O_{oxo}=M-O_{trans}$  fragment, they found demonstrated that when the *trans* ligand is an alcoholate  $RO^-$  anion, which is a very strong Lewis base, the  $M=O_{oxo}$  distance is long, and the  $M-O_{trans}$  distance is very short. The short bond distance is reflected in a high value of the  $\nu(M=O_{oxo})$  stretching mode, where  $M=Re, Tc$  [18, 20].

Table 4. Comparison of the calculated and observed vibrational modes of  $[ReO(mer)(Amino) OH(H_2O)_2]$ .

Experimental	B3LYP/LAN2DZ	Assignment
524	694	$\nu$ Re-N
568	730	$\nu$ Re-S
908	988	$\nu$ Re=O
524	370	$\nu$ Re-O
1356	1460	$\nu$ $OH_{bend}$
3440	3494	$\nu$ $OH_{str}$
3114	3162	$\nu$ NH

In Electronic spectra (Fig. 4 ) the experimental and calculated electronic spectra for  $[ReO(mer)(Amino)OH (H_2O)_2]$  complex using time-dependent density functional theory TD-DFT of the complex are presented in Table 5. The experimental absorption band at 204 is attributed mainly to intraligand transitions. The band recorded at 321 nm and 323 nm could be attributed to LMCT ligand metal charge transition from  $\pi$ -oxygen-bonding orbital to the *d* orbital of the Rhenium [18, 21].



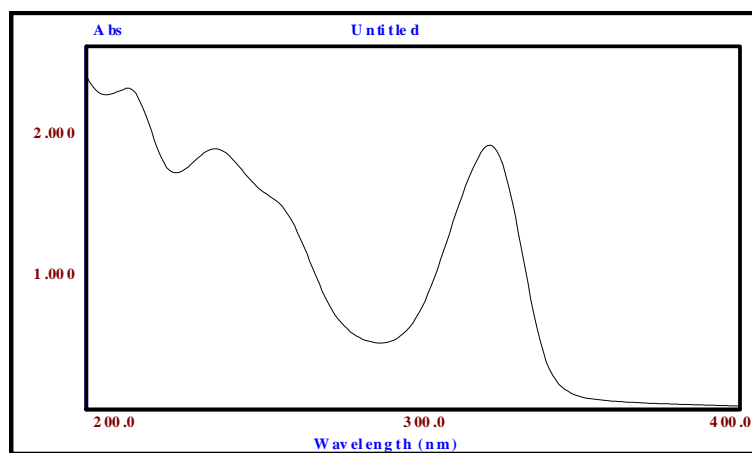


Fig 4. The UV-vis spectra of  $[ReO(mer)(Amino)OH(H_2O)_2]$ .

Table 5. The experimental electronic data.

Character	Experimental data in different solvent $\lambda_{max}$ nm., ( $\epsilon$ ; $dm^3 mol^{-1} cm^{-1}$ )
$\pi \rightarrow \pi^*$	191(2583), 204(2459)
LMCT	321(2459)
LMCT	332(1899)

$\epsilon$ - molar absorption coefficient.

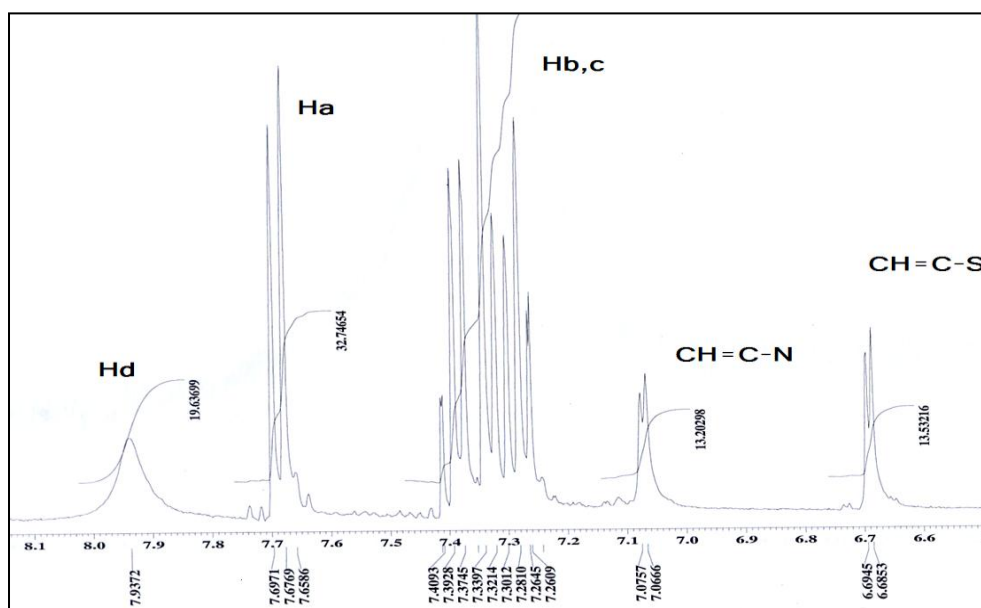


Fig.5. The  $^1H$  NMR of  $[ReO(mer)(Amino)OH(H_2O)_2]$  complex.

The  $^1H$  NMR spectra of a mercapto-ligand show signals assigned to the Ha,b,c,d (the protons of the benzene ring) in different chemical shifts caused by the anisotropic effect, which laminated the protons oriented toward the oxygen that appear deshielded relative to the other protons oriented away from the oxygen (toward or away from the oxo-metal core) [18]. As we see the Ha,d near the Re=O core was assigned to the downfield region of the spectrum at ~7.7-7.6 ppm. The  $NH_2$  proton signals for the amino ligand were absent in the spectrum of the complex and only a signal due to an NH group was recorded at 3.4. The  $^{13}C$  NMR spectra of the complex exhibit two new characteristic peaks for C=S and C-N at lower fields of 189 and 141 ppm compared with the spectra of free ligand mer, indicating that coordination *via* the charged thiolic sulfur and nitrogen atoms occurred. In

Fig.6, the signals at 139 and 107 ppm attributed to the ( $\underline{C}H=C-N$ ) bond and (C-S) bond, respectively. In addition, the spectrum showed signals assignable to the (C=N) bond at 169 ppm of Amino ligand.

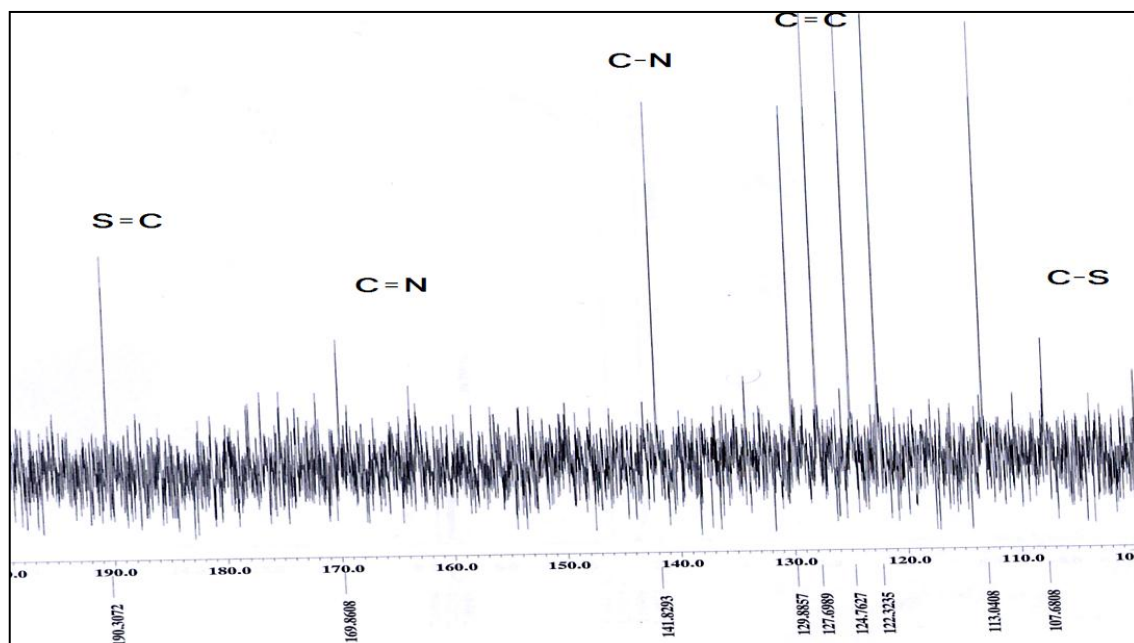


Fig 6. The  $^{13}C$  NMR of  $[ReO(mer)(Amino)OH(H_2O)_2]$ .

#### 4.2 Quality Control of the $^{99m}Tc$ complex.

The  $[^{99m}TcO(mer)(Amino)OH(H_2O)_2]$  complex can be prepared in two-steps. Quality control of the  $[^{99m}TcO(mer)(Amino)OH(H_2O)_2]$  complex was performed by thin-layer chromatography (TLC) and high-performance liquid chromatography (HPLC). The final  $^{99m}Tc$ -oxo hetero complex  $[^{99m}TcO(mer)(Amino)OH(H_2O)_2]$  was obtained in high yield (>97%). TLC and HPLC analyses were used to evaluate the radiochemical purity (RCP) and the stability of the complex. ITLC was performed on instant thin layer chromatography with Whatman No.1 chromatography paper and using acetone and saline as the mobile phase according to literature [16]. The  $R_f$  values for  $[^{99m}TcO(mer)(Amino)OH(H_2O)_2]$  were around 0.78 in acetone; the other values are reported in Table 6.

Table 6. The  $R_f$  values of compounds in acetone.

Compound	$[^{99m}TcO_4]^-$	$[^{99m}TcO(gluco)_2]_{intermediate}$	$[^{99m}TcO-Complex]$
$R_f$	0.9	0.8-1	0.78

The HPLC chromatograms of the  $[^{99m}TcO(gluconate)_2]^-$  intermediate and  $[^{99m}TcO(mer)(Amino)OH(H_2O)_2]$  are shown in (Fig 7). The retention time of the final  $^{99m}Tc$ -oxo complex  $[^{99m}TcO(mer)(Amino)OH(H_2O)_2]$  was found to be about 9.6 min, and that of  $[^{99m}TcO(gluconate)_2]^-$  intermediate was 15.6 min. Their characterization was made using HPLC comparing their retention time ( $\gamma$  detection) with the retention time of the well-defined analogous rhenium complex (UV detection at 254 nm). The paper electrophoresis pattern of showed that the  $[^{99m}TcO(mer)(Amino)OH(H_2O)_2]$  complex, the larger fraction of radioactivity reside at the neutral point with negligible wings toward either sides. (Fig 8).

Corroboration of structure of the  $^{99m}Tc$ -complex was achieved by comparing its HPLC profiles with the corresponding to the Re-complex. Radioactivity and U.V detectors showed identical chromatographic profiles, suggesting that the same chemical structure was formed under both synthesis conditions.

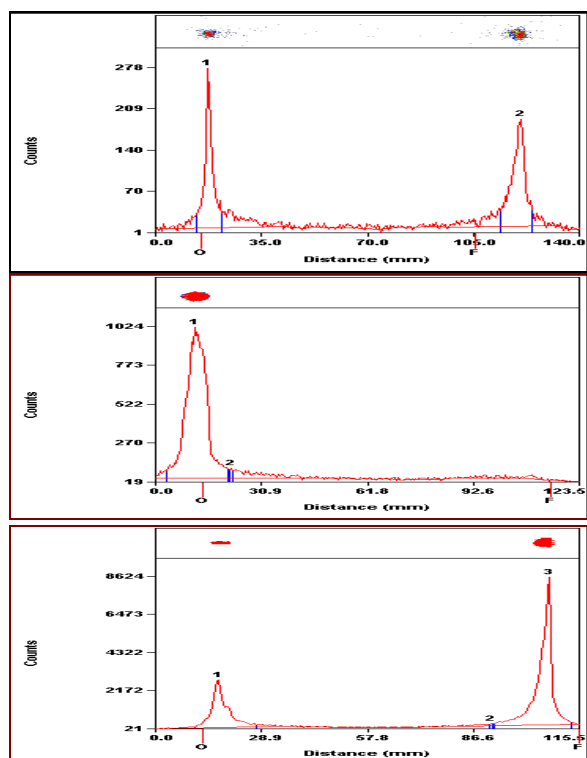


Fig.7. Chromatography ITLC TLC chromatography of mixture(a) reaction in acetone, (b) organic layer in saline, (c) organic layer in acetone .

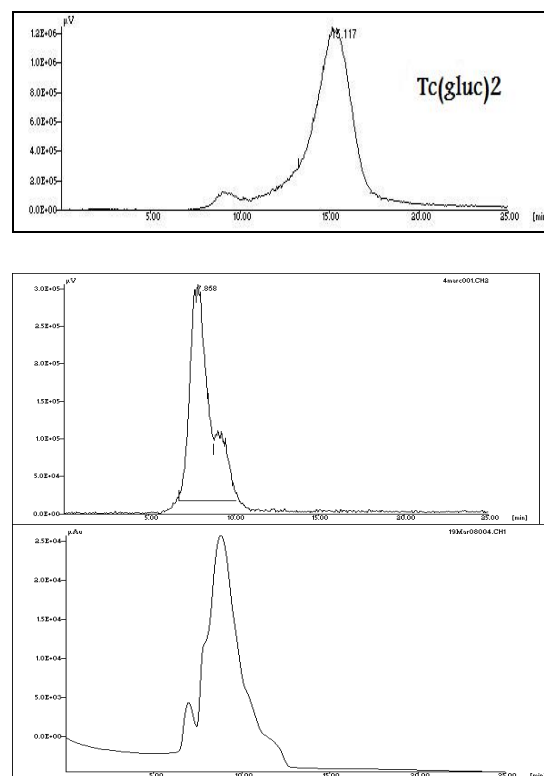


Fig.8. HPLC radio chromatogram for the  $[^{99m}\text{Tc}(\text{mer})(\text{Amino})\text{OH}(\text{H}_2\text{O})_2]$  and  $[\text{ReO}(\text{mer})(\text{Amino})\text{OH}(\text{H}_2\text{O})_2]$ .

*In vitro* stability of the complex was evaluated by measuring the RCP in ITLC at different time points. The RCP was still over 97% after 5 h, which suggested that the complex  $[^{99m}\text{TcO}(\text{mer})(\text{Amino})\text{OH}(\text{H}_2\text{O})_2]$  possessed great stability *in vitro*. Stability studies of the  $^{99m}\text{Tc}$  complex as summarized in Table 7, found that the complex is stable in saline and plasma for at least 5 hours, which is an important parameter to pursue with biological studies. The lipophilicity of the compound was evaluated by determination of the partition coefficient (P) in physiological conditions (n-octanol/ saline). The results obtained, were expressed as  $\log P_{O/W}$  and the data were represented as the mean  $\pm$  0.07 the standard deviation is - 0.153. As expected, the compound has low lipophilicity [22]. As expected, there is increase of the lipophilicity of complexes  $^{99m}\text{TcO}$  [SN] when the benzene ring attached to the mercapto ring the  $\log P$  above 1.5. The  $^{99m}\text{TcO}$  [SN] complex [23], is low lipophilicity it's more hydrophilic than mercapto-ring complexes. It seems that the amino attachment increase the hydrophilic properties to the complex.

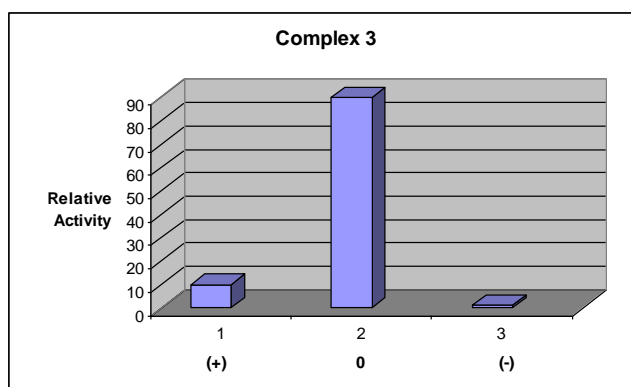
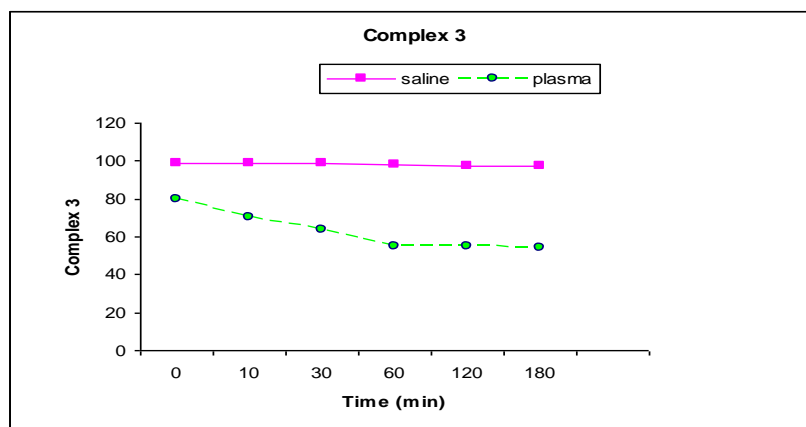


Fig. 9. Electrophoresis histograms of  $[^{99m}\text{Tc}(\text{mer})(\text{Amino})\text{OH}(\text{H}_2\text{O})_2]$ ; (+) Anode; (-) Cathode; (0) neutral.

Table 7. The Stability of compound in Saline/Plasma.

Compound	Log P <sub>O/W</sub>	Saline stability (%)				Plasma stability (%)			
		10 min	30 min	1 h	3h	10 min	30 min	1 h	3h
	- 0.153 ± 0.07	99	99	98	97	70	64	55	54

Fig. 10. Stability of complex of  $[^{99m}\text{Tc}(\text{mer})(\text{Amino})\text{OH}(\text{H}_2\text{O})_2]$  in plasma and in saline.

The animal biodistribution experiments using  $[^{99m}\text{TcO}(\text{mer})(\text{Amino})\text{OH}(\text{H}_2\text{O})_2]$  were performed in accordance with institutional, national and international regulations governing the safe and humane use of laboratory animals in research. In Table 8, the complex is seen to have a significant low brain uptake. The blood uptake was low and its clearance was fast so that the brain/blood ratio was stable, 0.055, 0.062, and 0.057 at 5, 30 and 60 min post-injection, respectively. The complex has exhibited high initial lung and spleen uptake. The liver uptake was significant and remained high at 60 min post-injection, suggesting the hepatobiliary system is the major route of excretion of the administered radioactivity. Hepatobiliary clearance of the complex is inferable from the gradually increasing activity in the intestinal tissue 30 min p.i. It was pertinent to compare the biodistribution parameters with that of  $[^{99m}\text{TcN}(\text{NOEt})_2]$  [24]. The results indicate that a structural modification is required in the design of the ligand. Increasing the polar nature of the final compound could be envisaged as a possibility to reduce the lipophilicity of the complex [25]. This can be achieved by incorporating polar substituents consisting of O, N, CO donor atoms on the ligand backbone, which in turn, will increase the clearance of the complex from the blood [5]. Additionally, it has been documented that suitable modifications such as increase in the number of aliphatic substituents in the molecule enhance its clearance from liver, lungs, etc. [23] due to fast metabolism [24]. A large fraction of the activity (35%) can be seen in the kidneys, which could possibly be due to the small size of the complex [15]. The activity appears to be retained for a long time in the kidney, diminishing a certain extent at 60 min, perhaps owing to the metabolism of the complex within the kidney. One reason could be that the pendent free primary amino group of  $^{99m}\text{Tc}$  complex can be regarded as mimicking the amino group of lysine [25]. Since the pK-value of this amino group is approximately 10.5, a similar value is assumed for the free amino group of complex [24]. At physiological conditions this amino group is protonated and thus positively charged. Re-absorption by the negatively charged membrane of the proximal tubule cells enhances renal accumulation by the attractive effect exhibited by the two opposing charges [25].

Table.8. The distribution data for Complex as %ID/gm in mice at different time intervals.

Organ	5 min	30 min	60 min
Brain	0.58±0.12	0.45±0.09	0.23±0.03
Blood	10.58±5.92	7.30±2.35	4.07±0.72
Liver	18.73±10.31	12.23±9.18	12.92±2.63
Lung	19.2±7.99	16.96±9.77	14.32±7.22
Kidney	14.60±27.25	12.95±7.40	8.55±1.30
Intestine	11.78±0.57	10.78±16.79	10.56±17.36
Heart	3.21±1.12	3.40±2.08	2.46±0.49
Muscle	0.89±0.16	0.75±0.39	0.47±0.09
Spleen	19.5±10.77	14.55±9.75	10.33±7.71

### Conclusion:

The oxorhenium complex was synthesized based on the [S/N] [N], mixed ligand system and fully characterized at the macroscopic level. In this complex, a novel complex [<sup>99m</sup>TcO(mer)(Amino)OH (H<sub>2</sub>O)<sub>2</sub>] was formed using (mer) mercaptobenzothiole ligand and (Amino) Aminothazole ligand and the [ReO]<sup>+3</sup> core. The chemistry was successfully transferred at the tracer level, and the corresponding oxotechnetium-99m complex was prepared using <sup>99m</sup>Tc-gluconate and by direct reduction of pertechnetate in the presence of N/S mixed ligand. Its structure was established by comparative HPLC analysis using the oxorhenium complex as a reference. Tissue distribution studies in normal mice demonstrated.

### The Acknowledgment:

The Author extends the appreciation to the Deanship of Scientific Research at King Saud University for funding the work through the research group project NO. ( RGP-VPP-041)

### References:

1. Jurisson. S. S., Lever. S. Z., Lydon J. D. and Cutler C. S. (2004) New York. Radioactive Metal in Imaging and Therapy Comprehensive Coordination Chemistry II, Chapter 9, Pages 883-911.
2. Schwochau, K. (2000) Technetium Chemistry and Radiopharmaceutical Applications. Wiley-VCH.
3. Papagiannopoulou. D., Pirmettis .I. C., Pelecanou. M., Tsoukalas. Ch., Raptopoulou. C.P., Terzis. A., Chiotellis. E and Papadopoulos. M. (2001) Synthesis and structural characterization of a novel Re[P][NN][S][SO] mixed ligand rhenium (III) complex. *Inorg.Chim.Acta*, **320**, 174-177.
4. Zhang.H., Dai. M., Qi.C., Li. B., Guo. X (2004) Synthesis, biodistribution and quantitative structure-activity relationship studies of new <sup>99m</sup>Tc labeled pseudo-peptide complexes. *Appl. Radiat. Isot*, **60**, 643–651.
5. Dhara. B., Chattopadhyay.P. (2005) New oxorhenium(V) complexes with 2N2S donor sets and radiochemical behavior of their technetium analogs. *Appl.Radiat.Isot*, **62**,729-735.
6. Shan.S., Ellern. A., Espenson. J.H. (2002) Methyloxorhenium(V) complexes with two bidentate ligands. *Inorg. Chem*, **41**, 7136–7142.
7. Gancheff. J., Kremer.C. Kremer. E and Ventura .O (2002) Density functional study of technetium and rhenium compounds. *Theochem*, **580**,107-116.
8. Machura. B., Penczek. R., Kruszynski. R. (2007) Synthesis, crystal, molecular, and electronic structure of [ReOCl<sub>3</sub>(bpzm)] complex. *Polyhedron*, **26**, (12, 23), 2581-2588.
9. Gaussian 98 program ,Gaussian , Inc. pittsburgh. PPA 15106 USA.

10. Becke A. D, Pérez-Jordá.J. (1995) A density-functional study of van der Waals forces: rare gas diatomics. *Chem. Phys. Lett.*, **233**(1-2) 134-137.
11. Parr, R. G., Liu .S. (2000) Homogeneities in density of various LDA energy functional. *J.Mol. Struct: THEOCHEM*, **501-502**, 29-34.
12. Hay. P.J., Chen. S.P., Voter. A.F., Albers. R.C., Boring. A.M. (1989) Theoretical studies of grain boundaries in Ni<sub>3</sub>Al with boron or sulfur. *Scripta Metall*, **23**(2) 217-222.
13. Casida. M.E.,in: J.M.Seminario (Ed); Recent Development and Applications in Modern Density Functional Theory, Theoretical and computational Chemistry, Vol.4, Elsevier Amsterdam, (1996).
14. Glendening. E.D, Reed, A.E,Carpenter .J.E and Weinhold. F, NBO (version 3.1).
15. Pelecanou. M., Pirmettis. I. C., Nock. B. A., Papadopoulos. M., Chiotellis. E., Stassinopoulou C. I. (1998) Interaction of [ReO(SNS) (S)] and [<sup>99m</sup>TcO(SNS) (S)] mixed ligand complexes with glutathione: isolation and characterization of the product. *Inorg.Chim. Acta* **281**, (2),148-152.
16. Rey. A., Papadopoulos. M., Leon. E., Mallo. L., Pirmettis. Y., Manta. E., Raptopoulou.C., Chiotellis. E., Leon. A. (2001) Synthesis, characterization and biological evaluation of a novel “3 + 1” mixed ligand <sup>99m</sup>Tc complex having an aliphatic thiol as coligand. *Appl. Radiat. Isot.*, **54**( 3),429-434.
17. Bouziotis . P., Pirmettis .I., Pelecanou .M., Raptopoulou,. C. P., Terzis. A., Papadopoulos.M., and Chiotellis.E,(2001).Novel Oxorhenium and Oxotechnetium Complexes from an Aminothiols [NS]/Thiols[S] Mixed-Ligand System. *Chem. Eur. J.*, **7**(17).
18. Gardner. J. K., Durig. J. R., Little. T. S., Gounev. T. K., Sullivan. F. (1996) Infrared and Raman spectra, conformational stability, vibrational assignment, and ab initio calculations of chloromethyl isocyanate. *J.Mol. Struct.* **375**(22), 83-94
19. Maresca .K., Femia .F. J., Bonavia .G.H., Babich .J.W. and Zubieta J.(2000) Cationic complexes of the ‘3+1’ oxorhenium–thiolate family *Inorg. Chim. Acta*, **297**, 89-105.
20. Machura, B, Kruszynski, R and Kusz, J (2008). Novel oxorhenium complexes with 2-(20-hydroxyphenyl)-2-benzothiazolinato ligand: X-ray studies, spectroscopic characterization and DFT calculations, *Polyhedron*. **27**, 1679–1689.
21. Machura, B., Kruszynski, R., Jaworska. M and Lodowski,P. (2005) Reactivity of [ReOX<sub>3</sub>(PPh<sub>3</sub>)<sub>2</sub>] complexes towards 1,4-diaminobenzene: X-ray structure and DFT calculations. *Polyhydedron*, **24**, 1454-1460.
22. Giglio. J, Rey. A., Cerecetto. H., Pirmettis. I., Papadopoulos. M., León. E., Monge. A, López de Ceráin. A, Azqueta. A , González. M., Fernández. M., Paolino. A and León. A (2006) Design and evaluation of “3 + 1” mixed ligand oxorhenium and oxotechnetium complexes bearing a nitroaromatic group with potential application in nuclear medicine oncology. *Eur. J. Med. Chem* **41** (10), 1144-1152.
23. Braband. H., Miroslavov. A.E., Lumpov. A.A., Sidorenko. G.V., Levitskaya. E.M., Gorshkov. N.I, Suglobov. D.N., Alberto. R., Gurzhiy. V.V., Krivovichev. S.V and Tananaev I.G. (2008) Complexes of technetium (I) (<sup>99</sup>Tc, <sup>99m</sup>Tc) pentacarbonyl core with π-acceptor ligands (tert-butyl isocyanide and triphenylphosphine). *J.Organometal Chem*, **693**, 4-10.
24. Tsoukalas. Ch., Pirmettis. I., Patsis.G., Papadopoulos. A., Raptopoulou. C. P, Terzis A., Papadopoulos. M., Chiotellis. E. (2001) Ester-modified <sup>99m</sup>TcO[SN(R)S/S] mixed ligand complexes: synthesis and preliminary evaluation. *Nucl. Med. Biol*, **28**, (8), 975-982.
25. Chattopadhyay, P., Chiu, Y.H., Lo, J.M.,Chung, C.S., Lu, T.H. (2000). Synthesis and structural characterization of a Re (V) complex with 2N1S donor and radiochemical behavior of its Tcanalog. *Appl. Radiat. Isot.* **52**, 217–223.



4.P11.

## PREPARATION AND BIOLOGICAL STUDY OF «NANOTECH, <sup>99m</sup>Tc»

N.A. Taratonenkova, A.O. Malysheva, G.E. Kodina, O.E. Klementyeva.

Burnasyan Federal Medical Biophysical Center FMBA Russia (Zhivopisnaya st. 46, Moscow, Russian Federation)

**Keywords:** technetium-99m, rhenium sulfide colloid, nanocolloid, sentinel lymph node, lymphoscintigraphy

### Abstract:

An early radiopharmaceutical used to image the lymphatic system was <sup>198</sup>Au-colloid, having a uniform particle size of 3–5 μm in diameter. However, this agent is not readily available today because of clinical limitations from its isotope being a β-emitter and emitting an unfavorable γ-ray for scintillation camera imaging and because of the difficulties its manufacture. Other widely used technetium-bound radiopharmaceuticals are <sup>99m</sup>Tc-rhenium sulfide colloid and <sup>99m</sup>Tc-nanocolloid. <sup>99m</sup>Tc-nanocolloid is used extensively in Europe, and similar preparations are available (NANOCOLL and ALBU-Res; Nycomed-Amersham Sorin, Milan, Italy). These products result in good lymph uptake and images of flow, but poor retention limits their use in delayed images. The domestic radiopharmaceuticals (RPh) used for this purpose are absent nowadays and the foreign kits does not purchase since 2006. During the investigation we developed a simple technology of kit production and preparation of radiopharmaceutical on its base. All preclinical trials were carried out with this RPh.

### Introduction

The concept of sentinel lymph node imaging is one of the most interesting recent developments on clinical oncology that holds the promise of a major breakthrough in the detection and treatment of early lymphatic metastasis from solid tumors, mainly melanoma and breast cancer. The sentinel node is the first lymph node to receive lymphatic drainage from a tumor site and therefore, it is the most suitable tissue for histological examination. In lymphoscintigraphy, a radiopharmaceutical should move at a rate similar to that of the physiologic flow of lymph and should be sufficiently retained by intervening nodes. Colloids are highly desirable for such studies because their particulate nature allows them to be retained by the lymph nodes by a phagocytic mechanism, yet the rate of colloid transport through the lymphatic channels is directly related to their particle size. Particles smaller than 4–5 nm have been reported to penetrate capillary membranes and therefore may be unavailable to migrate through the lymphatic channel. In contrast, larger particles (~500 nm) clear very slowly from the interstitial space and accumulate poorly in the lymph nodes or are trapped in the first node of a lymphatic chain so that the extent of nodal drainage in contiguous areas cannot always be discerned. After injection, the radiocolloid travels to the sentinel node through afferent subcapsular lymphatics, where they are retained by the sinusoids and phagocytosed by the reticuloendothelial macrophages of the node. Particles smaller than 100 nm show the most rapid disappearance from the interstitial space into the lymphatic channels with good retention in the lymph node. Most larger particles do not move easily beyond the first node site encountered. The permeability of colloids in lymph is maximal for particles smaller than 50 nm. The new procedure of intra-operative lymphatic mapping demands corresponding radiopharmaceuticals with particle size 50 – 100 nm, which now are absent in Russia. The aim of this work was the development of the simple method of sol  $\text{Re}_2\text{S}_7$  preparation and radiopharmaceutical (“Nanotech, <sup>99m</sup>Tc”) on its base, investigation of biodistribution in experimental animals. In this work we compared two methods of sol preparation, using so called “dry” and “wet” technology.

## Experimental

*Synthesis of sol (rhenium sulfide)* was carried out according to two technologies. We called them “wet” (used solutions of chemicals) or “dry” (dry chemicals dissolved in the gelatin solution) technology. Scheme of this synthesis is presented on Fig. 1.

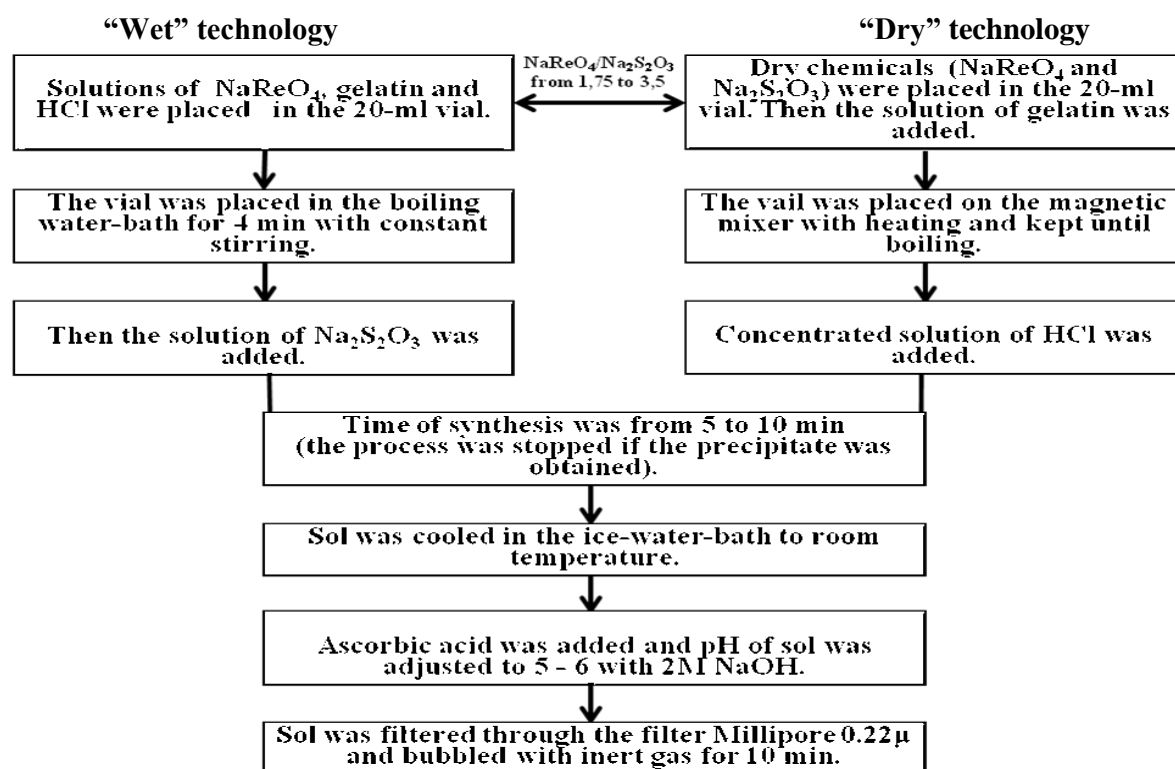


Fig. 1. Scheme of sol synthesis

### Preparation of radiopharmaceutical “Nanotech, <sup>99m</sup>Tc:

The kit of reagents consists of two vials: vial 1 with 1 ml of rhenium sulfide sol and vial 2 with lyophilized mixture of tin dichloride, sodium pyrophosphate and ascorbic acid. 2,0 ml of water for injection was introduced in the vial 2. The vial was shaken to dissolve the lyophilized reagent. Then 0,5 ml from the vial 2 and 2,0 ml of eluate from <sup>99</sup>Mo/<sup>99m</sup>Tc generator were added to the vial 1 with sol Re<sub>2</sub>S<sub>7</sub>. The vial 1 was placed in the boiling water-bath for 30 min. Then the vial was cooled in the ice-water-bath to the room temperature for about 5 min.

### Determination of radiochemical purity (RCP):

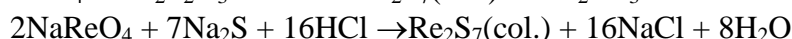
RCP was determined using paper chromatography on Whatman 1 in methyl-ethyl-keton using “MiniScan” (USA). In this system pertechnetate-ions (impurity) migrate with solvent front ( $R_f=1$ ), colloid remains on start of the strip ( $R_f=0$ ).

### Determination of particle size:

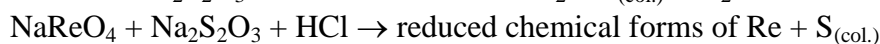
The dynamic diameter of particles was determined using a light-scattering photon correlation spectroscopy on NICOMP<sup>TM</sup> 380ZLS (USA).

## Results and Discussion.

Colloidal form of hentasulfide rhenium can be obtained via the following reactions:



Simultaneously the side reactions take place, so the losses of rhenium during sol preparation are inevitable.



All mentioned above reactions proceed with noticeable rate only during heating.

During sol preparation the influence of the following main reaction conditions were studied:

molar ratio  $\text{Na}_2\text{S}_2\text{O}_3 / \text{NaReO}_4$  was changed from 1,75 to 3,5; time of reaction was changed from 5 to 10 minutes. It was found for all molar ratios if time of the reaction less than 6 min – the obtained product is light coloured, if the time of the reaction more than 6 min the precipitate is obtained. The results of sol preparation is shown in Table 1.

Table 1. The results of sol preparation.

$\text{Na}_2\text{S}_2\text{O}_3 / \text{NaReO}_4$	Time, min	Results
1,75	5 – 6	sol
	10	precipitate
2,2	5 – 6	sol
	10	precipitate
2,7	5 – 6	sol
	10	precipitate
3,5	5 – 6	sol (hardly filtered)
	10	precipitate

The yield of sol was determined by TLC (acetone – silica gel) using  $^{188}\text{Re}$  as label during the synthesis. As shown in Table 2, sol yield was about 30 % and did not depend on technology of its synthesis.

Table 2. Yield of sol  $\text{Re}_2\text{S}_7$

Methods of synthesis	Colloid ( $R_f=0$ )	$\text{ReO}_4^-$ ( $R_f=1$ )
“Wet” technology	24,0 %	69,2 %
“Dry” technology	27,1 %	70,0 %

Colloidal particle size is an important characteristic to consider when choosing a radiopharmaceutical for mapping sentinel nodes in lymphoscintigraphy. The dynamic diameter of particles was determined using a light-scattering photon correlation spectroscopy on NICOMP<sup>TM</sup> 380ZLS. Dynamic diameter of sol particles is shown in Table 3. Dynamic diameter of particles in the ready-to-use radiopharmaceutical was in the range 15 – 50 nm.

Table 3. Dynamic diameter of sol particles

Method of synthesis	D, nm (before sol filtration)	D, nm (after sol filtration)
“Wet” technology	from 25 to 90	from 25 to 80
“Dry” technology	from 20 to 190	from 20 to 70

In Table 4 the results of determination of radiochemical purity in “Nanotech,  $^{99m}\text{Tc}$ ” and pH of RPh are shown. From presented results we can conclude that radiopharmaceuticals with RCP more than 90 % were obtained at molar ratio  $\text{Na}_2\text{S}_2\text{O}_3 / \text{NaReO}_4$  2,2 - 2,7.

Table 4. Determination of radiochemical purity (RCP) of RPh

$\text{Na}_2\text{S}_2\text{O}_3 / \text{NaReO}_4$	Time of synthesis, min	$\text{TcO}_4^-$ , %	RCP, %	pH
1,75	6	7,4	84,4	5,5
2,2	6	4,5	91,3	5,8
2,7	6	4,3	91,9	5,6
3,5	6	12,4	72,6	5,5

The preliminary biological results were shown on Fig.2 and 3. 0,1 ml of RPh «Nanotech, <sup>99m</sup>Tc» was injected into the plantar of the right limb of rats. Dynamic investigations were carried out during 15 min post injection, investigation in static - after 1 and 2 h post injection.

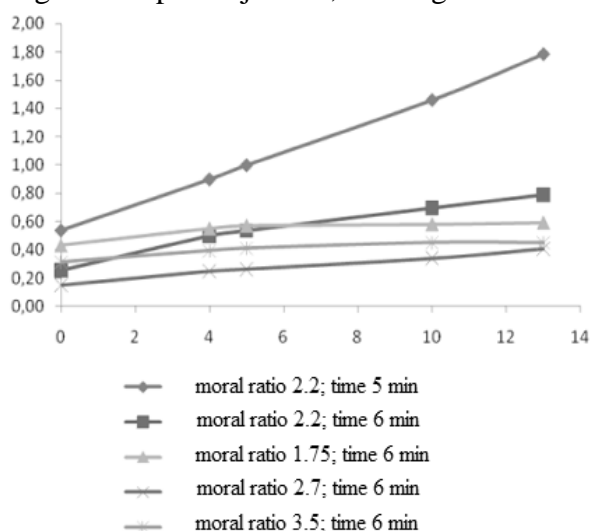


Fig. 2. Accumulation in the inguinal lymph node during 15 min (Y – arbitrary units – ratio of accumulation to the injected dose)

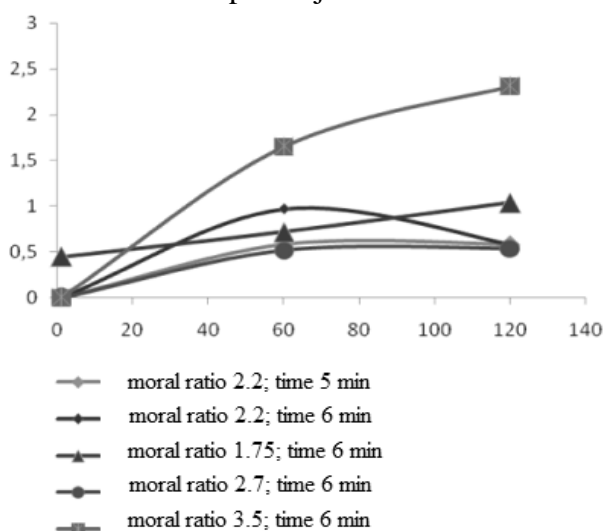


Fig. 3. Accumulation in the inguinal lymph node after 2 h post injection.

### Conclusions.

Two methods of sol  $\text{Re}_2\text{S}_7$  synthesis were compared (“dry” and “wet” technology). It was found: optimal molar ratio  $\text{Na}_2\text{S}_2\text{O}_3 / \text{NaReO}_4$  – 2,2, time of synthesis – 6 min. During the production in commercial scale “Dry” technology allows more easier to increase the volume of sol batch. The yield of sol (using <sup>188</sup>Re as label during synthesis) via “dry” or “wet” technology does not differ and is about 30 %. The mean diameter of sol particles ( $\text{Re}_2\text{S}_7$ ) - 20 - 80 nm. RCP of radiopharmaceutical is more than 90,0 %. According to the results of the biological investigations the maximum uptake in the inguinal lymph node was obtained at molar ratio of  $\text{Na}_2\text{S}_2\text{O}_3 / \text{NaReO}_4 = 2,2$ . Nowadays the preclinical trials with “Nanotech, <sup>99m</sup>Tc” were carried out.

4.P12.

## SORPTION REMOVAL OF Na<sup>99m</sup>TcO<sub>4</sub> FROM EXTRACTS OF EXTRACTION GENERATOR <sup>99</sup>Mo/<sup>99m</sup>Tc

Reshetnik Y.N., Bykov A.N., Kodina G.E., Malysheva A.O.

Burnazyan Federal Medical Biophysical Center, Moscow, [UNReshetnik@runtech.ru](mailto:UNReshetnik@runtech.ru)

Extraction technology of <sup>99m</sup>Tc from irradiated natural Mo or enriched with <sup>98</sup>Mo is well known during more than 30 years [1]. Nevertheless, in the conditions of the ongoing "<sup>99</sup>Mo -crisis", as well as environmental reasons, an alternative in relation to fission <sup>99</sup>Mo and <sup>99m</sup>Tc production methods have received in recent years a new development.

In such method <sup>99m</sup>Tc is extracted from the alkaline solution of irradiated Mo by methyl ethyl ketone (MEK) with the subsequent evaporation to dryness and dissolution of the residue in the saline [2]. This technology more than 20 years is successfully used in Russia as well [3,4]. However, the evaporation of organic solution is the most long-term and insecure operation, in addition, the full automation of process in such performance is difficult to implement.

In the present work we studied <sup>99m</sup>Tc sorption behavior when removing it from MEK without stage of extract evaporation

As a result of experiments it was established that <sup>99m</sup>Tc can be sorbed on alumina (Merck, 0,06-0.20 mm) in both acidic and alkaline forms from MEK solutions pre-cleared out of cations abundance on ion exchange resin (Dowex, 50W-X8, 100-200 mesh). After washing of alumina with water <sup>99m</sup>Tc in the <sup>99m</sup>TcO<sub>4</sub><sup>-</sup> form can easily be desorbed with saline. The table presents the results of determining the <sup>99m</sup>Tc output in sorption stages and process in general.

№	Column 1(Dowex)		Column 2 (alumina)			Yield %
	Sorbtion, %	Eluate, %	Sorbtion, % (% from initial)	Washing , % from initial	Eluate, %	
1	4,3	95,7	99,9 (95,6)	2,1	93,0	86,9
2	7,7	92,3	95,8 (88,4)	0,5	85,3	75,0
3	6,2	93,8	90,0 (84,4)	1,5	89,1	73,8
4	3,2	96,8	89,5 (86,6)	1,5	79,9	74,6
5	2,0	98,0	91,3 (89,4)	2,5	91,7	79,4

The MEK content in the final solution << 0.5 mg/ml (range, regulated domestic and foreign pharmacopoeias). Radiochemical purity (RCP) ≥ 99%. The pH values are 6.5 - 7.4. Thus, we can conclude that the final solution Na<sup>99m</sup>TcO<sub>4</sub> is suitable for medical use.

Other <sup>99m</sup>Tc-radiopharmaceuticals, prepared with the use of the final solution Na<sup>99m</sup>TcO<sub>4</sub> and the domestic <sup>99m</sup>Tc-kits also comply with pharmacopoeia requirements.

1. Boyd R.E. Radiochem. Acta, 1982, 30 N 3, p. 123 - 145.
2. Melichar F., Svoboda K., Prokop J., Budsky F. IAEA-SM-131-50, Vienna, 1986, p.81.
3. Skuridin V., Glukchov G., Chygriaev M. Extraction generator of technetium-99m. USSR Priority1426019; C01G 57//00, 14.04.86, reg. 22.05.88.
4. Zykov M.P., Romanovsky V.N., Kodina G.E. et al. J. Radioanalyt. Nucl. Chem., 1997, 221 N 1 - 2, p. 227 – 230.

## Applications of Tc and Re in technology, including their alloys in Modern Constructing Materials



Chairman of the 5-th Session Boris D. Bryskin with welcome address



5.1.

## **THE FABRICATION DEVELOPMENT OF RHENIUM USED IN HIGH TEMPERATURE ROCKETS AND HIGH TEMPERATURE SPACE POWER REACTOR**

Boris D. Bryskin, Edwin D. Sayre

### **Abstract**

The use of tungsten as the thin liner of high temperature rocket nozzles in solid fuel rockets tended to produce very brittle tungsten carbide with the graphite nozzle structure underneath. It was found that rhenium provided a good bond and it did not react with the graphite and provided a good bond of the tungsten during the entire length of the rocket flow. Rhenium has been found to improve the high temperature jet engine blade service by alloying slight amounts in nickel and cobalt high temperature alloys. In the development of the SP100 Nuclear Space Power System it was found that uranium nitride was the ideal fuel and Nb1%Zr alloy tubing was the best fuel cladding. However it was found that the Nb1%Zr alloy tube reacted with the fuel and fission products at such high operating temperature, (1077<sup>0</sup>C). It was found that rhenium tubing on the inside protected it for the life of the system. No rhenium tubing to meet the requirements had been produced and none was available on the market that could be used for the SP100 Nuclear Space Power System. We in the program had to work with the rhenium sources and develop the rhenium strips needed and develop the tube production process. Rhenium-Molybdenum alloy large tubing was developed for nuclear reactor control. This paper is devoted mainly to the development of the two processes for making the very high quality rhenium tubing. One process produces welded and drawn tubing and the other process produces seamless drawn tubing.

### **Introduction**

Rocket nozzles for less than a minute solid fuel rockets were made with a steel outer container coated with high temperature insulation that was coated with thin carbon graphite layer that had the form of the nozzle for the gas flow control. Then a tungsten layer was finally deposited to protect the carbon and control the flow. Because of the very high operating temperature after less than a minute the carbon would react with the tungsten to make tungsten carbide in the major nozzle inner layers and the brittle layer would crack and flow out with the rocket exhaust and destroy the rocket exhaust control and loose the thrust and cause change in course. The rocket nozzle producers found out from the University of Tennessee that rhenium would be a good barrier layer between the tungsten and the graphite to stop the formation of tungsten carbide.

Aircraft jet engine producers found that rhenium alloyed with turbine blade alloys could increase the operating temperature and the life of the blades<sup>1</sup>

When General Electric ran the NASA SP100 Nuclear Space Power System Program they determined that rhenium was the best barrier between the fissioning fuel and the Nb1%Zr fuel tube. The development of the two processes for making the rhenium tubes is the major part of this paper. One process is to make thin rhenium strips, form them into tubing, weld them, heat treat them and draw them to the final dimensions and properties. The other process is to produce a rhenium powder metallurgy start tube and draw it to the final dimensions and properties.

### **Rhenium Between Carbon and Tungsten in Large, Long Time Solid Fuel Rocket Nozzles**

While developing the long time, large, solid fuel rocket nozzles it was determined that the tungsten nozzle liner on the graphite nozzle was reacting with the carbon and produced brittle tungsten

carbide which continually cracked and ruined the rocket performance after about 30 seconds. While developing the longer (2 minutes plus) nozzle we found out from the University of Tennessee that rhenium would make a good barrier metal coating between the carbon and the tungsten layers in the center flow walls of the rocket nozzles. We produced the outer walls of the nozzle as usual and had the university coat the carbon layer with electroplated rhenium. The rhenium was then finally coated with tungsten in controlled atmosphere system as shown in figure 1. The completed nozzle is shown in figure 2. The nozzle was then tested on a larger space solid fuel rocket for over 2 minutes with a perfect performance.<sup>2</sup> This has become a good usage for rhenium and these nozzles have been used many years in military and space applications.

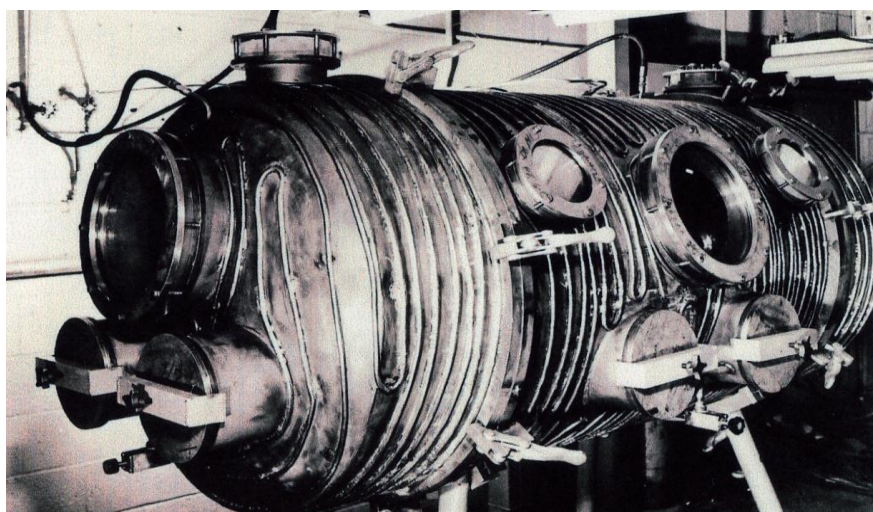


Figure 1. Controlled Atmosphere Plasma Spray Tank

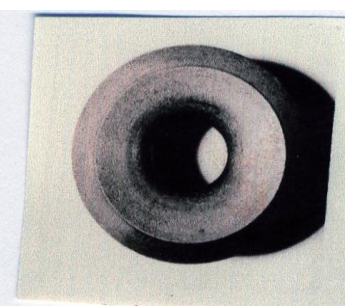


Figure 2. Rhenium Between Carbon and Tungsten Nozzle

### **The Fabrication Development for Rhenium Tubes for Nuclear Space Power Systems**

To get the high efficiency from the nuclear space power system SP100 the reactor operating temperature was established at 1077<sup>o</sup>C. Uranium nitride turns out to be the best fuel for the high temperature operation. The niobium alloy with 1% zirconium and 0,01% carbon was selected for the fuel cladding tubes. It had good properties for the high temperature reactor, but it was decided to use the rhenium bonded to the inside of the fuel tube because it was not nearly as reactive with the fission products and had a much higher strength at 1077<sup>o</sup>C than the niobium alloy. The final thicknesses were (<0.25 mm) rhenium bonded inside layer and (<0.75 mm) PWC-11 outside layer.

#### **Initial Approaches**

Once rhenium was selected for the inner tubes it was determined that no rhenium tubes were available on the market. Three processes were tried to establish the best for the tubing including sintered tube shell, vapor deposited and thin strip formed, welded, heat treated and drawn. Using thin strip, forming it and welding the tube followed by heat treating and drawing turned out to be the fastest developed satisfactory process to get the fuel tube fabrication going. There was very little rhenium thin sheet material to use to make welded fine grained tubes so we worked hard with two producers to get the high quality rhenium strip under production

#### **Producing the Rolled and Welded Thin Walled Rhenium Tubes**

The rhenium strip stock was produced at a thickness of 0.203 mm. Strips for forming the rolled tubes had to be cut very accurately. The strip had to be heat treated to get the minimum hardness for cutting. Several methods were tried for very accurately cutting the final strips for rolling. Mechanical cutting would not be accurately enough because of the very high hardening at the

cutting line. Electrodischarge machining wound up being the successful cutting process. It required chemical cleaning after cutting.

Hydraulic forming was used to form the tubes<sup>3</sup>. The tube forming was very critical because the minimize gap along the weld line is extremely critical. The successful electron beam weld required a maximum gap of less than 0.051 mm and a mismatch of less than 9,938 mm. The weld grains were large and sometimes single ones were from edge to edge as shown in figure 3. These through wall grains tended to rupture during drawing the welded tubes. To solve this problem the welds were shot peened and heat treated to get the grains reduced in size before the drawing of the tubes. The tubes were then drawn and heat treated to wind up as thin walled fine grained rhenium tubes with the same metallurgical characteristics as any drawn tubes. The welded tubes, after the weld is shown on the left in figure 3 and after the first drawing they look like the right side of figure 3. The tubes are then drawn and heat treated several times until they reach the final size.

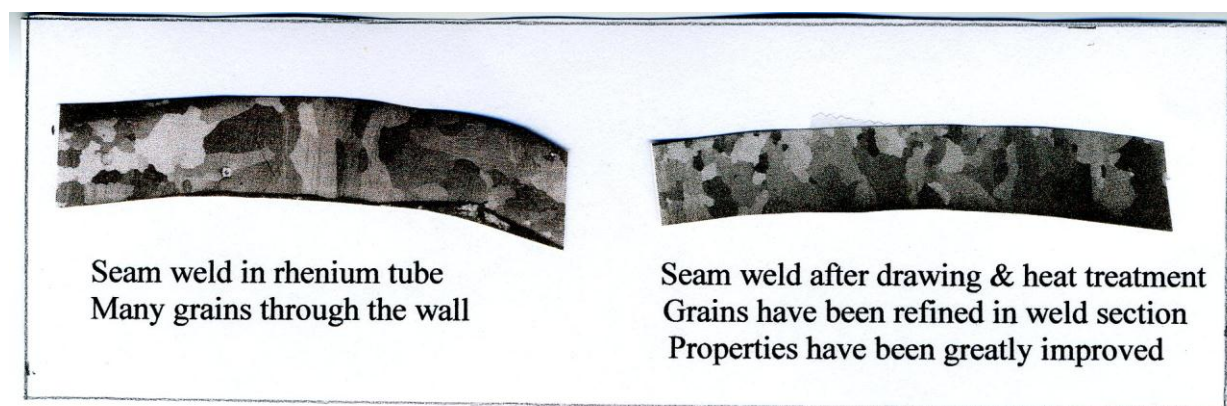


Figure 3. Heat Treatment and Cold Working Effect on Welded Rhenium

After the final draw and heat treatment to final size the rhenium tubes are very soft and this is an important factor in bonding the rhenium tubes inside the niobium alloy tubes<sup>4</sup>. It makes it possible for the tubes to tighten without cracking during the HIPing bonding.

### **Bonding the Rhenium Tubes on the Inside of the Niobium Alloy Fuel Tubes**

When we had both rhenium and PWC-11 tubes meeting all the properties we started the development of the bonding process. Because of the very thin tubes it was decided to use HIPing to provide the heat and pressure to make the bond. In order to HIP bond the two tubes we needed a method to metallurgically bond the two ends with a very good vacuum between the tubes. We found that vanadium was the ideal metal to bond the ends. It has high melting point and bonds well to both metals. The tubes were machined at the ends to provide a gap for inserting the vanadium rings<sup>3</sup>. The tubes were brazed in vacuum with EB welding. The tubes were then HIPed and bonded very well. The brazed ends were cut off HIPing and left solid niobium alloy tubes with well bonded rhenium inside. A micro picture of the bonded tube is shown in figure 4. Several completed tubes are shown in the vacuum heat treatment furnace in figure 5.

### **Making Seamless Rhenium Tube From Rhenium Powder**

The extended development of rhenium seamless tubing by former Sandvik Rhenium Alloys, Inc. with application of Powder Metallurgy was conducted through the following manufacturing steps: pressing, presintering and sintering of rhenium metal powder reduced from ammonium permeate. The sintered tube was cold swaged over a mandrel of molybdenum high speed steel to consolidate structure and decrease diameter and wall thickness. Further deformation by repeating cold drawing on hardening steel mandrel through carbide dies to approximately 0.010 – 0.007” wall with reduction 5.8% per pass was applied. Intermediate annealing of tubes at 1500 – 1800C up to 5-19



min. in hydrogen was introduced. Attempt to deform sintered tube by cold pilfering with reduction 10% was successful and resulted in good surface quality and size precision.

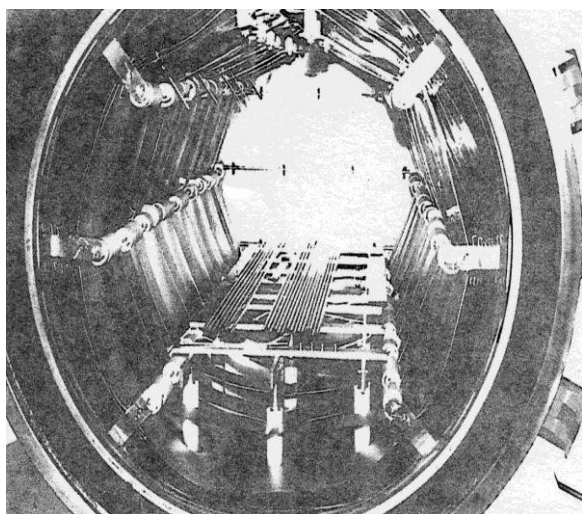


*Figure 4. Micro of Rhenium Inner Tube Bonded to Nb Alloy Outer Tube*

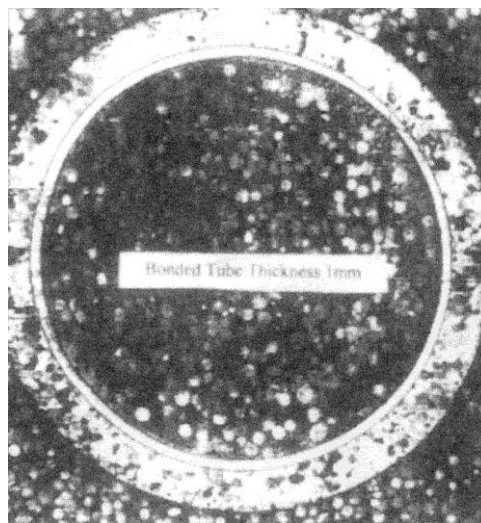


*Figure 5. Several Finished Bonded Tubes in The Vacuum Heat Treatment Furnace*

## References

1. General Electric uses rhenium in the GE 90 jet engine and is recycling the alloy scrap to optimize the use of new rhenium.
2. Edwin D. Sayre, "Application of Rhenium and Rhenium Containing Alloys", Evolution of Refractory/Metals and Alloys", Edited by N. C. Dalder, Toni Grobstein and Charles S. Olsen, RNS Annual Meeting, Denver, Colorado, February 21-25, 1993.
3. Edwin D. Sayre, Thomas J. Ruffo, Donald C. Wadekamper, Mike Kangilaski, "Development of Bonded Rhenium/Niobium-1% Zirconium Tubing For The SP100 Space Reactor", Rhenium & Rhenium Alloys, Edited by Boris Bryskin, Minerals, Metals & Materials Society International Symposium held at the 1997 TMS Meeting in Orlando, Florida February 10-13, 1997.
4. Edwin D. Sayre and Thomas Ruffo, "Manufacturing SP100 Rhenium Tubes", Ninth Symposium on Space Nuclear Power, Albuquerque, New Mexico, 1992, Proceedings Published by American Institute of Physics, New York, 1992, 246.

## 5.2. MAKING AND SHAPING OF RHENIUM AND RHENIUM CONTAINING ALLOYS

Todd Leonhardt<sup>1</sup> and James Ciulik<sup>2</sup>

<sup>1</sup>Rhenium Alloys, Inc. Elyria, Ohio 44256 USA

<sup>2</sup>The University of Texas at Austin, Department of Mechanical Engineering  
Austin, TX 78712-0292 USA

The focus of this paper is to discuss the advancements in the production of rhenium and rhenium containing alloys along with science and understanding of the impact of powder morphology, powder compaction, sintering, and the consolidation methods of hot isostatic pressing and extrusion.

Rhenium is extremely sensitive to processing conditions because of its high work-hardening coefficient. This intrinsic property dominates the processing options available for production. A comparison will be made of the different densification/compaction processes on the microstructures and mechanical properties of powder metallurgy rhenium and rhenium containing alloys of molybdenum and tungsten.

The addition of rhenium in the concentration of 47.5 weight percent rhenium in molybdenum and 25 weight percent rhenium in tungsten has a significant impact on the microstructures and mechanical properties of these alloys.

Several processing methods will be compared and contrasted and the resulting microstructures, morphologies of the fracture surfaces, and mechanical properties obtained from tensile testing at room temperature and up to 1927°C will be discussed.



Corr.-member of RAS A.M. Chekmarev, Prof. M. Ozawa and Prof. I.D. Troshkina

### 5.3.

## HETEROMETALLIC RHENIUM, NICKEL, COBALT-ALKOXIDES AS PRECURSORS FOR FUNCTIONAL MATERIALS SYNTHESIS

I. V. Mazilin, D. V. Drobot

Lomonosov Moscow State Academy of Fine Chemical Technology (Russian Federation, 119571 Moscow, Vernadsky avenue 86)

**Keywords:** Aerospace superalloy, fine powder, soft chemistry, alkoxide precursor.

### Abstract

New technology to obtain Re, Ni, Co hydroxides, simple and complex oxides, fine and nanosized powders of metals and alloys has been developed. Mono- and heterometallic nickel, rhenium and cobalt alkoxides with adjustable metal content were used as precursors to produce final powders. Electrochemical and chemical techniques for synthesis of molecularly mixed precursor compounds were proposed. The said precursors were subjected to hydrolytic and thermal decomposition. By changing precursor composition and/or decomposition parameters, one can obtain powders of different size, chemical and phase composition. Ultrafine ( $D_{50}=501$  nm) nickel-based alloy powder with rhenium and cobalt doping was obtained at as low as 350 °C.

### Introduction

Nickel-based superalloys containing rhenium (6 - 10 %) are known to exhibit excellent mechanical strength and creep resistance at high temperatures, good surface stability, corrosion and oxidation resistance [1]. They are generally applied in fields such as: aerospace, industrial gas turbine and marine turbine industry, e.g. for turbine blades in hot sections of jet engines [1-4]. Some state-of-the-art methods are used to produce these alloys; with all of them including melting of the metals involved. Taking into account huge difference in the melting points of base metal (nickel, 1726 K) and doping metal (rhenium, 3360 K), obtaining of chemically homogeneous alloy becomes an extremely difficult task. Moreover, these processes are energy-consuming because of the necessity to maintain very high temperatures for a long time. It is of common knowledge that chemical uniformity of precursor compound leads to a homogeneous distribution of doping elements in alloys and general chemical composition stability. In the last decades in the context of continuous increase in energy prices, more and more attention is being paid to energy - efficient technologies. Soft chemistry technique has already been applied to refractory materials and alloys synthesis [5-11]. In the present work we have applied alkoxide route for the preparation of nickel-based alloys using trimetallic nickel-rhenium-cobalt methoxocomplexes as a precursors.

### Experimental

It is well - known that some metal alkoxides are water-sensitive and could decompose in the air; therefore, all operations and storage of such compounds are performed in dry inert atmosphere.

The conditions of the syntheses are listed in the table 1. Individual metal methoxocomplexes were obtained electrochemically (Syntheses **I-IV**). To obtain bi- and trimetallic methoxocomplexes both consequent anodic dissolution (Syntheses **V-X**) of metals and chemical reaction between individual methoxocomplexes were applied (Synthesis **XI**).

The former was performed in a glass electrochemical cell with water cooling and a condenser. To prevent the decomposition of the compounds formed the tube with drying agent ( $P_2O_5$ ) was used. We have used water-free methanol (Merck KGaA, purity > 99,5 %, water < 0,1 %) as an electrolyte; a 2 cm<sup>2</sup> platinum plate as a cathode; nickel, cobalt and rhenium plates as an anode. Methanol was dehydrated before it was involved in synthesis by means of boiling with magnesium



shavings followed by distillation. Water-free methanol is known to be an insulating media, for that reason we had to use a background electrolyte – lithium chloride. Lithium chloride was annealed (180 – 200 °C) in vacuum ( $p \sim 1,3$  Pa) for 40 – 60 minutes to dehydrate it. The concentration was chosen to be 0,025 M to provide optimal conductivity and low chlorine concentration. The process was controlled by measuring current, voltage, temperature and anode mass loss. The consequences of dissolution are shown in the column anode of Table 1 (“+” stands for simultaneous dissolution). The latter involves mixing of nickel methoxide and rhenium oxomethoxide in the methanolic media with stirring at room temperature for at least 1 hour.

Once the desired amount of metal was dissolved or the chemical reaction completed, the resulting liquid is transferred into a glass flask and subjected to solvent vacuum evaporation to yield final powder.

Table 1. Syntheses conditions.

#	U, V	I, mA	t, hrs	Anode	#	U, V	I, mA	t, hrs	Anode
<b>I</b>	16	45	21	Ni	<b>VI</b>	7	30	40	Re - Ni
<b>II</b>	16	55	7	Ni	<b>VII</b>	65	60	10	Re - Ni
<b>III</b>	20	65	15	Co	<b>VIII</b>	26	100	20	Ni - Re
<b>IV</b>	31	170	16	Re	<b>IX</b>	31	160	61	Re - Ni
<b>V</b>	9	40	25	Ni + Co	<b>X</b>	20	55	20	Re - Co - Ni
<b>XI</b>	Chemical interaction of 100 ml 0,049 M solution <b>I</b> and 9,25 ml 0,054 M solution <b>IV</b>								

The complexes obtained were analyzed by means of chemical analysis, X-Ray powder diffraction, IR-spectroscopy, SEM and thermal analyses (DTG, TGA, DSC) in air and inert atmosphere.

Nickel was determined using titration with EDTA against murexide [12], cobalt - photometric microdetermination with nitroso-R salt [13], rhenium – gravimetrically as nitron perrhenate  $C_{20}H_{16}N_4 \cdot HReO_4$  [14], carbon and hydrogen – organic microanalysis with CHN–O–RAPID (Heraeus GmbH, Germany). X-ray diffraction patterns were obtained on XDR 6000 powder diffractometer (Shimadzu, Japan) with Cu  $K\alpha$ -radiation; IR-spectra in the range 4000-400  $cm^{-1}$  were taken on EQUINOX 55 spectrometer (BRUKER, Germany) between IR-transparent KRS-5 plates in liquefied petrolatum to prevent decomposition; Thermal analysis in the air was performed on Q–1500 D derivatograph (MOM, Hungary) with heating up to 430°C with 5°C/min rate.

Thermal decomposition of the complexes was accomplished in the air, argon atmosphere and hydrogen atmosphere. The quartz tube with the powders was placed in the pipe furnace. The tube inlet and outlet were equipped with  $H_2SO_4$  vessels to dehydrate argon and hydrogen. Gas flow should be no less than 0.2 LPM. Heating rate was established to be 5°C/min, cooling rate 10-15°C/min. All decomposition products were identified using XRD analysis. Particles size distribution was determined on the Delsa™ Nano PN A54412AA analyzer (BECKMAN COULTER, USA).

## Results and Discussion

At the first stage of the investigation individual nickel, rhenium and cobalt methocomplexes  $Ni(OCH_3)_2$  (I, II)  $Co(OCH_3)_2$  (III) and  $Re_4O_6(OCH_3)_{12}$  (IV) were obtained using anodic dissolution of rhenium, nickel and cobalt in absolute methanol respectively. The said methoxo-derivatives were characterized by XRD, SEM, IR and thermal analysis.

The XRD pattern of I is presented on the Fig. 1 with corresponding literature data for Ni(OCH<sub>3</sub>)<sub>2</sub> [15]. Four wide peaks at the pattern indicate that the said compound has a distorted hexagonal layered Mg(OH)<sub>2</sub> structure with P $\bar{3}$ m1 space group (cell parameters: a = 3,074 Å; c = 7,977 Å). FWHM of first peak (2θ = 10,89 °) was measured to be 3,092 ° and according to the Debye-Shrerrer equation the corresponding grain size is as low as 90 Å. Complexes III, V was found to have the same structure.

The SEM picture of I is presented at Fig. 2. It is easy to see that average particles size is around 1 μm. The difference in calculated and visible sizes of particles can be explained by a strong tendency for nanoparticles to agglomerate.

The IR-spectrum of I contains methoxo-derivatives ν(C-O) intrinsic peak at 1073 cm<sup>-1</sup> and few peaks in the metal-oxygen region: ν(Ni-O(R)-Ni) at 631 cm<sup>-1</sup> and ν(Ni-O(R)) at 454 and 408 cm<sup>-1</sup>, with the former intensity being twice as great. There is also a weak peak at 3294 cm<sup>-1</sup> correlated to ν(O-H) of absorbed methanol. According to the IR spectrum, Ni(OCH<sub>3</sub>)<sub>2</sub> has a continuous structure with Ni-O(R)-Ni bridges. The IR spectra of III are almost alike: ν(C-O) at 1066 cm<sup>-1</sup>; ν(Co-O(R)-Co) at 606 cm<sup>-1</sup>; ν(Co-O(R)) at 450 cm<sup>-1</sup>.

The thermal decomposition mechanism in the air and inert atmosphere was studied by means of DTA/DTG and DSC/DTG techniques respectively. The DTA/DTG curves of I are shown at Fig. 3. At the initial stage of heating in the air (below 100 °C) absorbed methanol evaporation is taking place followed by partial evaporation of ligand (up to 195 °C); the thermal decomposition of I in the air begins at around 235 °C. According to the DTA peak, the final product (NiO) starts to crystallize at 255 °C. The thermal decomposition of III in the air begins at 185 °C with the formation of CoO followed by oxidation to spinel Co<sub>3</sub>O<sub>4</sub> at 235 °C.

The thermal behavior of I in the inert atmosphere deviates slightly. The thermal decomposition begins at 210 °C and ends at 270 °C with the crystallization of NiO; On the contrary, the DSC curve of III contains exo-effect at 307 °C and the final product is CoO (instead of Co<sub>3</sub>O<sub>4</sub> in the air). The XRD pattern, the

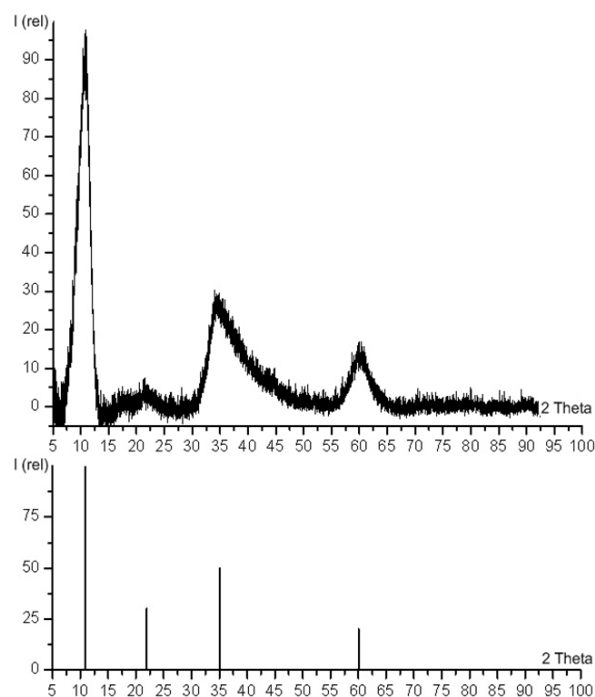


Fig. 1. XRD pattern of I (top) and data for Ni(OCH<sub>3</sub>)<sub>2</sub> [15] (bottom).

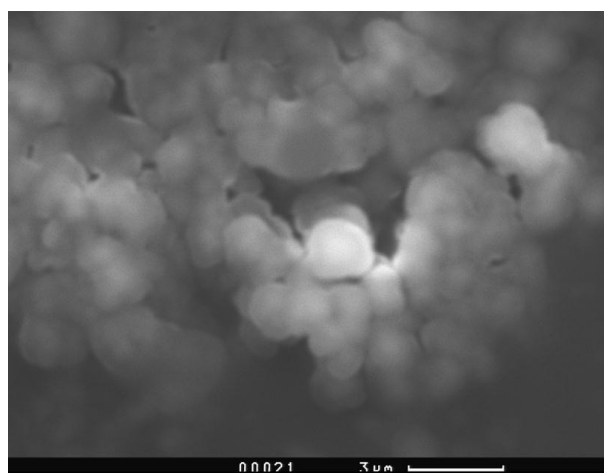


Fig. 2. SEM picture of I.

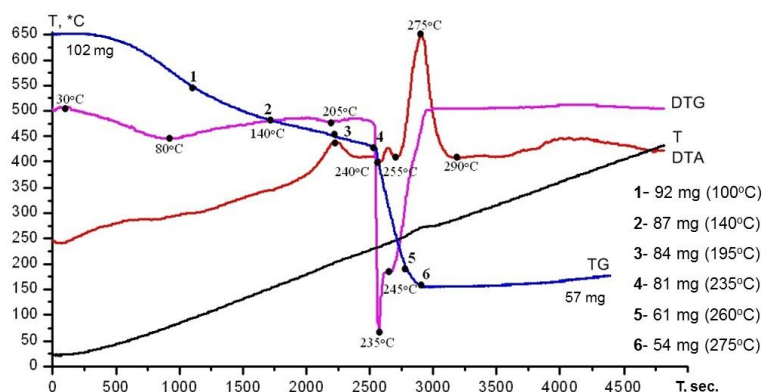


Fig. 3. DTA/DTG curves of I.

crystal structure, the IR spectrum and the thermal analysis of IV were reported by our colleagues [8, 16].

The hydrolytic decomposition of I-III leads to the formation of nickel and cobalt hydroxides with the same structure and a slightly larger grain size determined from Debye-Scherrer equation (140 Å in case of I).

At the second stage of our investigation bi- and trimetallic nickel-rhenium methoxodervatives were obtained and analyzed. The XRD analysis has shown that compounds X, XI with low rhenium have the same structure as I. Bimetallic compounds VI-IX with high rhenium are X-Ray amorphous. The results of the chemical analyses and the IR-spectra peaks positions are shown in Table 2.

Table 2. Chemical compositions and IR-spectra peaks of heterometallic complexes.

#	Ni, wt %	Re, wt %	Formula	Positions of IR peaks, cm <sup>-1</sup>		
				$\nu$ (C-O)	$\nu$ (Ni-O(R))	$\nu$ (Re-O(R))
VI	31,83	19,61	Ni <sub>5.4</sub> Re <sub>1</sub> (OCH <sub>3</sub> ) <sub>8</sub>	1041	640w, 457	909, 550, 418
VII	14,71	37,14	Ni <sub>1.3</sub> Re <sub>1</sub> (OCH <sub>3</sub> ) <sub>5</sub>	1039	639, 458	908, 527, 424
VIII	10,76	51,01	Ni <sub>1</sub> Re <sub>1.5</sub> (OCH <sub>3</sub> ) <sub>4</sub>	1050	652, 465	907, 523, 431
IX	6,80	57,13	Ni <sub>1</sub> Re <sub>2.7</sub> (OCH <sub>3</sub> ) <sub>4</sub>	1058	654, 465	934, 530, 425
X	33,51	14,21	Ni <sub>8</sub> Re <sub>1</sub> Co <sub>0.1</sub> (OCH <sub>3</sub> ) <sub>14</sub>	1045	640w, 456	916, 553, 420
XI	45,41	14,70	Ni <sub>9.8</sub> Re <sub>1</sub> (OCH <sub>3</sub> ) <sub>10</sub>	1049	640w, 455	913, 548, 422

It leads us to a supposition that compounds VI-XI do not have direct nickel-rhenium bond, but these metals are linked by means of oxygen or oxygen-ligand bridges. Having compared the obtained IR-spectra for VI-XI with the ones for I-IV, we determined a shift in the peak positions. This can be used as the evidence of molecularly mixed nickel rhenium precursor compounds formation.

The thermal decomposition mechanism of VI-XI in the air is determined from DTA/DTG curves. The DTA/DTG curves of X are shown at Fig. 4. Gradual evaporation of the absorbed methanol and some part of the ligand gives way to the final decomposition at 210 °C. Even low rhenium content in the bimetallic complex X leads to multistage product crystallization (the main DTA peak at 245 °C is followed by another three). Additional studies are required to determine all the intermediates.

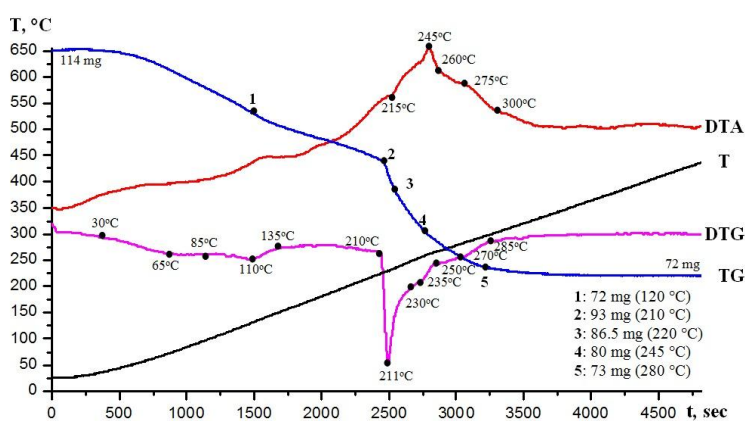


Fig. 4. DTA/DTG curves of X.

All the collected data involving the composition, the structure and the thermal properties of the precursor compounds allowed us to develop a technology to carry out the synthesis of functional materials. Depending on the thermal decomposition conditions we can obtain fine or even nanosized powders of nickel, rhenium and cobalt oxides, hydroxides or alloys with any desirable metals content. This ratio can be set at the precursor synthesis stage and remains almost constant after thermal treatment. All the decomposition products we have obtained are summarized in Table 3.

For instance, let us discuss the case of nickel-rhenium-cobalt alloy powder synthesis with content of metals close to that in aerospace superalloys. The precursor compound X with adjusted content of metals was thermally treated at 350 °C for 2 hours in the hydrogen atmosphere to produce the final powder (its size distribution and the XRD pattern are shown at Fig. 5 and 6) respectively.

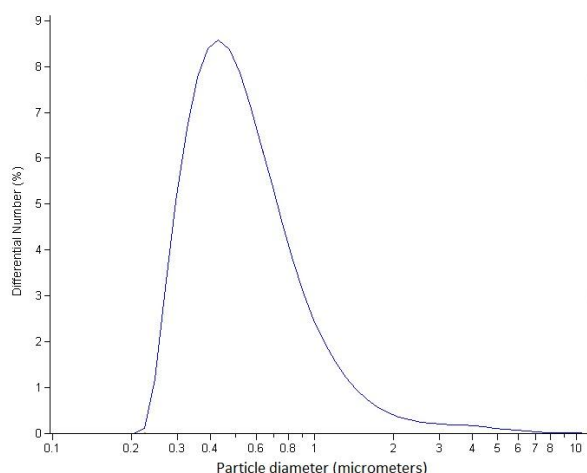


Fig. 5. Particles size distribution of X decomposition product in hydrogen.

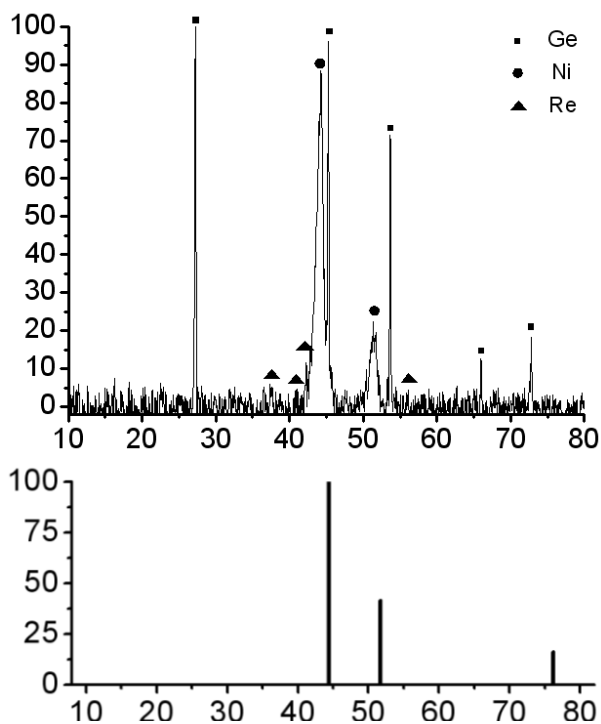


Fig. 6. XRD pattern of X decomposition product in hydrogen (top) and data for Ni ICDD card # 65-0380 (bottom).

The average size of particles is  $D_{50} = 501$  nm and we believe that it can be decreased further by means of changing decomposition conditions. The Ni-based solid solution (sp.gr  $Fm\bar{3}m$ ,  $a = 3,570$  Å) obtained has slightly shifted the XRD peaks indicating the presence of rhenium and cobalt. The rhenium content can be estimated as 14 wt.% according to the cell parameter and the data cited in literature [17].

It is obvious that methoxo-derivatives can be effectively applied as precursors to obtain metals, alloys, ceramic powders and, potentially, coatings by means of the CVD technique.

Table 3. Precursor decomposition products obtained (\*TBD - to be defined).

Precursor compound	Hydrolysis products	Thermal decomposition products		
		In air	In inert gas	In hydrogen
$Ni(OCH_3)_2$	$Ni(OH)_2$	NiO	NiO	Ni
$Co(OCH_3)_2$	$Co(OH)_2$	$Co_3O_4$	CoO	Co
$Re_4O_6(OCH_3)_{12}$	TBD*	$ReO_3, Re_3O_{10}$	$ReO_2$	Re
$Ni_xCo_y(OCH_3)_N$	$x Ni(OH)_2$ $y Co(OH)_2$	$NiCo_2O_4, x NiO,$ $y Co_3O_4$	$xNiO \cdot yCoO$	$x Ni-y Co$ solid solution
$Ni_xRe_y(OCH_3)_N$	TBD*	$NiReO_4, x NiO,$ $y ReO_3$	TBD*	$x Ni-y Re$ solid solution
$Ni_xRe_yCo_z(OCH_3)_N$	TBD*	$NiReO_4, x NiO,$ $y ReO_3, v Co_3O_4$	TBD*	$x Ni-y Re-z Co$ solid solution

## Conclusions

The alkoxo-technology has been proved to be an effective method for the Ni-Re-Co alloy fine powder synthesis with adjustable content of metals (RU 2010132289 Pat. Appl.); Variations in alkoxide decomposition parameters made it possible to obtain simple and complex oxides, hydroxides and alloy powders, fine and nanosized; Thermal properties of nickel and cobalt methoxocomplexes were investigated; The heterometallic Ni-Re and Ni-Re-Co methoxocomplexes were obtained for the first time ever, their properties are being investigated.

**Acknowledgements:** Yuri V. Syrov and Yuri V. Velikodniy – XRD Analyses; Elena E. Nikishina – DTA Analyses; Sergey Savilov – DSC Analyses; Valeri V. Kravchenko – IR Spectra; Tatiana E. Yakovleva – English translation. Work granted by RFBR (projects 06-03-32444 and 09-03-00328).

## References

1. B. Geddes, H. Leon, Xiao Huang; *Superalloys: Alloying and Performance* ASM International, 2010, 176 pp.
2. S. Walson, A. Cetel, R. Mackay, O. Hara, D. Duhl and R. Dreshfield; *Joint Development of a Fourth Generation single Crystal Superalloy*. NASA TM-2004-213062
3. E.N. Kablov, N.V. Petrushin, I.L. Svetlov, I.M. Demonis, *Technology of light alloys*, 2: 6-16 (2007)
4. R. H. Tuffias, R. B. Kaplan, and M. A. Appel. Proc. Int. Symp. Rhenium and Rhenium Alloys Orlando, USA, 10—13 February, TMS, 1997, p.275
5. N. Ya. Turova, E. P. Turevskaya, V. G. Kessler, and M. I. Yanovskaya; *The Chemistry of Metal Alkoxides*, Kluwer Acad. Publ., Boston—Dordrecht—London, 2002, 568 pp.
6. D. Drobot, G. Seisenbaeva, V. Kessler, P. Scheglov, O. Nikonova, S. Michnevich, O. Petrakova, *Journal of cluster science*, 20:23-36 (2009)
7. P. A. Shcheglov, D.V. Drobot, *Russian Chemical Bulletin*, 54: 2247-2258 (2005)
8. P. A. Shcheglov, PhD Thesis, Moscow, 2002, 198 p.
9. P. A. Shcheglov, D. V. Drobot, *Inorg. Mater.*, 40:176 (2004)
10. P. A. Shcheglov, D. V. Drobot, G. A. Seisenbaeva, S. Gohil, and V. G. Kessler, *Chem. Mater.*, 14:2378 (2002)
11. I. V. Mazilin, *Rhenium, nickel and cobalt alkoxides as precursors for functional materials synthesis*, Master's thesis, Moscow, 2009, 113 p.
12. H. Flaschka, G.Schwarzenbach, *Complexometric titrations*, London: Methuen, 1969, p.244-248
13. S. Baybaeva, L. Krylova, *Methods for paint coatings analysis*, Chemistry, Moscow, 1974, 324 pp.
14. V.F. Hillebrad, H.E. Lendel, G.A. Bright, *A Practical Guide to Inorganic Chemical Analysis*, Chemistry, Moscow, 1966, p. 372-381
15. Rogova T.V., Turova N.Ya., Zhadanov B. V., *Coordination chemistry*, 11:784-788 (1985)
16. A. I. Ermakov, V. V. Belousov, D. V. Drobot, P. A. Shcheglov, *Coordination Chemistry*, 32:701–706 (2006)
17. A. Nash, P. Nash, *Bulletin of Alloy Phase Diagram*, 6:348-350 (1985)



5.4.

## METALLOTHERMIC METHOD FOR PRODUCING RHENIUM-BASED ALLOYS

A.P. Parshin<sup>1</sup>, R.N. Manuylov<sup>1</sup>, S.A. Melnikov<sup>1</sup>, G.M. Voldman<sup>2</sup>

<sup>1</sup>. Public corporation «Leading research institute of chemical technology»

33, Kashirskoye shosse, Moscow 115409, Russia, info@vniht.ru

<sup>2</sup>. Lomonosov Moscow State Academy of Fine Chemical Technology

86, prospect Vernadskogo, Moscow 119571, Russia, mitht@mitht.ru

The aim of this work was to design a technology for producing rhenium alloys with low carbon content (<0,05 % of the mass) by metallothermal method.

The initial mixture components such as ReO<sub>2</sub>; CaMoO<sub>4</sub>; NiO and PA – 4 (Aluminium powder) as a reducing agent were used to obtain the master-alloy based on rhenium.

ReO<sub>2</sub> was produced on automated plant VME-8-10,5 by thermal decomposition of ammonium perrhenate in argon atmosphere. Direct metal yield achieve 95,3 %.

Calcium molybdate (technical standards 48-3812-28-87), nickel oxide (GOST (state standard) 609-4125-75), AP – 4 (Aluminium powder) aluminium powder (GOST (state standard) 6058-73) were used in this research. Inert additive of calcium oxide was applied to reduce thermal effect of the reaction.

To study metallothermic processes of obtaining rhenium alloys a variation content of initial mixture components  $m(\text{ReO}_2) : m(\text{CaMoO}_4) : m(\text{NiO})$  in the range from 1 : 0,298 : 0,125 to 0,457:0,197: was conducted, and also the effect of reducing agent excess from 0% to 20% was studied.

The results of the experiments have shown that the optimal compounds mixture was of 1 : 0,38 : 0,155, and percentage of aluminum excess varies from 7 to 10 % of the mass. In this case ingot extraction amounts to 95,3%.

Due to slag processing and extraction of supplementary metallic phase ingot extraction can be increase to 98%.

There was produced an enlarged batch of master-alloy that fully met the requirements of technical standards 1-92-202-2001.

## 5.5.

### **RHENIUM EFFECT IN Mo-Re WELDS**

F. Morito (a), M.I. Danylenko (b) and A.V. Krajinikov (b)

(a) MSF Laboratory, Moriya, Japan

(b) Institute for Problems of Materials Science, Kiev, Ukraine

Rhenium is widely used to alloys VIA group refractory metals. In particular, the strength and plasticity, creep resistance, and low temperature ductility of Mo are all improved with increasing the rhenium content due to the so-called “rhenium effect”. In addition to traditional applications, such as heating elements, electron tube components, etc, Mo-Re alloys are considered as candidate materials for structural applications for chemicals and energy facilities, including elements of fusion or fast breeder reactors. Welds are obligatory elements of practically any complex construction while working conditions are characterized by high temperatures ( $>1000$  K), aggressive medium (liquid metals) and high neutron fluence ( $>10^{21}$  n/cm<sup>2</sup>).

Therefore, good weldability, high radiation performance, thermal stability and corrosion resistance are the key issues for these application fields. Tendency of Mo alloys to embrittle at low temperatures assumes probable degradation of the mechanical properties either during welding or under irradiation. In spite of the fact that significant progress has been achieved in studying the mechanism of rhenium effect, many details of Mo-Re alloy behaviour under extreme operating conditions are not studied yet.

This work analyses several Mo-Re alloys and welds with the Re content 0-50% in as-received state and after electron beam welding and/or radiation treatment. The mechanical properties and microstructure of Mo-Re welds are examined focusing on the effect of Re concentration. Phase stability, microstructural changes and impurity redistribution are studied for better understanding and predicting the long-term performance of Mo-Re alloys at high temperatures and/or high neutron fluences.

In particular, a strategy of welding of Mo-Re alloys is discussed with emphasis on the sensitivity of alloys to pre-weld heatings and on the development of post-weld treatments, such as warm rolling and annealing, to provide optimal phase composition. Grain refinement during directional solidification after welding, ductility improvement and fracture mode change from intergranular to transgranular one are clearly observed with an increase of Re content.

Effect of neutron irradiation on the strength of Mo-Re welds is studied for a wide temperature range. Mo-Re welds exhibit a large radiation-induced strengthening. At room temperature, the strengthening effect is rather limited and unstable because of lack of ductility. The strengthening becomes strongly pronounced at high temperatures. Damaging effect of neutrons at high temperatures is shown to be smaller than that at low temperatures. Intensification of homogeneous nucleation of Re-rich sigma phases in all studied Mo-Re alloys is observed after high temperature neutron irradiation. As a result, all parts of as-irradiated welds display approximately same level of strength.

High-temperature annealings with different heating/cooling rates have been used to simulate thermal conditions in different welding zones. Impurity redistribution in Mo-Re alloys has been studied by surface analysis methods. The role of carbon and oxygen segregation as well as formation of carbides and Re-base phases is discussed to minimise intergranular embrittlement of welds.

5.6.

## USE OF TUNGSTEN AND RHENIUM ALLOYS FOR MANUFACTURING OF HIGH-TEMPERATURE THERMOCOUPLES W5%Re/W20%Re

P.P.Oleynikov, P.A.Zaytsev, A.A.Ulanovskiy<sup>1</sup>, S.N.Nenashev<sup>2</sup>, T.Ju.Goncharuk<sup>3</sup>

Scientific Industrial Association (SIA) "LUCH" (Zhelesnodorozhnaya, 24, Podolsk, Moscow region, Russian Federation)

<sup>1</sup> - Obninsk Thermoelectric Company (OTC), Ltd. (Lenina, 121, Obninsk, Kaluga region, Russian Federation)

<sup>2</sup> - Federal State Institution "ROSTEST-MOSKVA" ("Nahimovskiy pr.", 31, Moscow, Russian Federation)

<sup>3</sup> - Company "Volfram", Ltd. (Bozovaj st., 7, Moscow, Russian Federation)

**Keywords:** tungsten and rhenium alloys, thermocouple, thermoelement, thermoelectric characteristics, electromotive force, EMF, standard specimen, calibration uncertainty, disperse hardening, nanoparticles.

### Abstract

Features of development in Russia and application of thermocouples with thermoelements made of tungsten-rhenium alloys are briefly characterized in the paper. The choice of alloys with the rhenium contents 5 and 20 % is justified [1].

At present time systematic researches of W-Re thermocouples in the range of temperatures 2000 ... 2500 °C are necessary. In this range the following factors are very essential: EMF drift of thermocouples, signal shunting through insulating armature, compatibility of materials at high temperatures. Commonly approved calibration procedure of thermocouples also needs to be developed for this range of temperatures. To increase stability of thermoelectric materials the possibilities of nano-technologies and disperse hardening of alloys should be considered.

### Introduction

Thermoelement materials for W-Re thermocouples are produced by a method of powder metallurgy. Powders of tungsten and ammonium perrhenate (NH<sub>4</sub>ReO<sub>4</sub>) are preliminary mixed, and then the mixture is pressed into cylindrical columns and melted. The columns are forged and drawn into a wire of diameters varied from 0,5 to 0,1 mm. Finished wire is subjected to stabilizing annealing in hydrogen.

The research stage in Russia had been finished by 1977 when technical Specifications on manufacture of thermoelement materials [2] was developed at MELZ (Moscow electric bulbs plant) and the reference table of the thermocouple [3] was standardized. Reference table included in GOST 3044-77 contained three close graduations: A-1, A-2, A-3. Last two graduations lay above and below the basic graduation A-1. Their upper limits had been limited by 1800°C, and the basic - 2500°C.

The temperature range 0...1800°C is inherent for the gages which are widely applied in metallurgy for short-term temperature measurements of liquid metals [4]. The temperatures closed to upper limit were often realized in nuclear and space industries, and also while carrying out of high-temperature scientific researches [5].

According to the national verification scheme (GOST 8.558-93) standard thermoelectric thermometers based on W-Re thermocouples had been developed to transfer temperature unit in the range 900...2500 °C to industrial thermoelectric thermometers. To certificate W-Re wires the Ural's Institute of Metrology (Ekaterinburg, Russia) had developed and introduced into metrological practice standard specimens of thermoelectric materials (SOTM) (wires) for W-Re5 and W-Re20 alloys. They were calibrated with expanded uncertainty about 11 °C at the temperature 2500 °C by a "wire bridge" method [6].

Unfortunately, in 1990-s consumption of W-Re thermoelectric wires was sharply reduced because of falling of industrial production in Russia. Production of tungsten and rhenium wires at MELZ became spasmodic and eventually had been stopped. It took several years for manufacture restoration (at "Rhenium" company, Ltd.). The company could keep invariable both manufacture processing methods, and procedures of certification and selection of alloys for thermocouples.

The present stage of development of high-temperature thermometry is connected with creation of a new generation of installations having limiting parameters. New researches have sharply expanded the nomenclature of high-temperature materials investigated and increased quantity of controllable high-temperature technological processes [7].

The requirements to control high temperature of a technological process have become more severe and they demanded new quality of certification of high-temperature technological and test equipment.

For the decision of the arisen measuring problems high-temperature thermoelectric converters (thermometers) were required with greater number of running cycles while realization of technological control. Also they had to guarantee reliable information on temperature regimes under operation of autonomous installations. The set life-time figures for most of them consist 5 and more years.

By this time manufacturers succeeded to find the ways of essential increase of working resource stability for high-temperature thermometers. Placing their sensitive elements in gas-tight protective tubes filled with neutral gas, working capacity of a measurement device had been provided at the temperatures up to 1800°C both in air and neutral environments during many thousands hours. Such designs with sapphire and molybdenum protective tubes are described in [8,9].

The increased interest to similar developments lead to the decision of international working group N5 of IEC SC65B to include tungsten-rhenium thermocouple of types A (W-Re5% / W-Re20%) (Russia) and C (W-Re5% / W-Re26%) (USA) and their reference tables to a new draft of the standards IEC60584-1 and 2.

As a result of this decision the demand for reproducibility check of thermoelectric characteristics of type A thermocouples produced now in Russia was made. Also it was necessary to check the possible improvements of their metrological stability by modifying of a positive electrode by disperse hardening method. Oxide particles aggregated with alkaline additives entered into initial fusion mixture as it was described in [10].

The similar stabilizing effect was fixed in refractory metals in case of allocation different nano-particles on grain borders of metal. In [11], for example, stabilization of tungsten composite structure was fixed to temperatures 2200-2400°C.

## Experimental

After W-Re thermocouples of types A (W5%Re/W20%Re) and C (W5%Re/W26%Re) including into the new draft of IEC standard 60584-1 and 2 Russian researches had to check reproducibility of thermoelectric characteristics for type A thermocouples manufactured now in Russia. The calibration program and comparison of calibrations results were performed by Russian metrologists (ROSTEST-MOSKVA; VNIIM, OTC, SIA "LUCH") and experts of foreign research laboratories (PTB, Germany; NIST, USA; NIMJ, Japan; NRC, Canada). All participants investigated the thermocouple specimens made of the same pairs of wire coils having diameters 0.5 and 0.35 mm.

The Russian researchers realized calibration of W5%Re/W20%Re thermocouples in the range of

temperatures 600 ... 2500°C by various methods. There were performed "wire-to-wire" comparison of the tested specimens with standard W-Re wires and comparison of W-Re thermocouples with a reference type B thermocouple or a reference pyrometer. In all range of temperatures calibrations data were within 0.7 % limit of permissible EMF deviations from reference table according to Russian standard GOSTR 8.585-2001. New draft of IEC standard installs the limit of permissible deviations  $\pm 1$  %. The results of researches well agreed with the results of foreign participants of the project in the investigated temperature range (600... 1850 °C). New draft of IEC 60584 standard has been fully agreed and in the nearest future it will be transferred for voting to National Committees of the countries - IEC participants [12].

For estimation of prospects of thermal stabilization of a positive thermoelement of type A thermocouple there was manufactured an experimental wire of 0.35mm in diameter, containing 0.1 % (weight) nanoparticles of yttrium oxide with average size 50 nanometers. Nanoparticles were received in scientific research institute of inorganic materials (Moscow) and were added to initial fusion mixture by the way similar to one described in [10].

## Results and Discussion

The following characteristics as thermoelectric uniformity, durability, microhardness (530-540 kg/mm<sup>2</sup>) of the newly received composite practically didn't differ from the values defined for the alloy WAR5 in the work [10]. Microstructures of initial materials were also similar.

Results of electronic microscopy testify that under plastic deformation there is intensive stratification of the material on grain borders and destruction of separate grains in planes of cleavage.

As for the thermoelectric characteristics, the first calibration of an initial alloy against corresponding standard specimen (SOTM) executed before and after 30-minute annealing at 1650°C have revealed negligible difference in behavior between direct and reverse calibration curves in each heating-cooling cycle. But there was essential discrepancy in the results of different cycles (Fig.1). It can be explained by insufficient stabilization of initial alloy structure during unitary annealing of the wire at 1500°C under manufacturing process.

The results received under the subsequent cyclic annealings at 1700°C have confirmed this conclusion. In these experiments the wire cut from regular W-Re20 coil was used as reference thermoelement. Fig.2 shows EMF changes of the thermocouple in three consecutive cycles of heating and cooling after annealing at 1700°C during 4, 5 and 2 hours.

It is obvious that EMF of the thermoelement investigated stabilized only after the second cycle or almost 10 hour annealing. In the last cycle direct and reverse curves have practically coincided taking into consideration the fact that measurements uncertainty in this case, according to [12], was nearly  $\pm 4^\circ\text{C}$ .

It is interesting to trace the EMF variation during high-temperature annealing. As it is shown in Fig.3, during the first hours the working signal of the thermocouple decreased with the rate almost coinciding with earlier observed EMF drift for WAR5 alloy in [13]. After the second cycle the characteristic was restored, practically, to initial level.



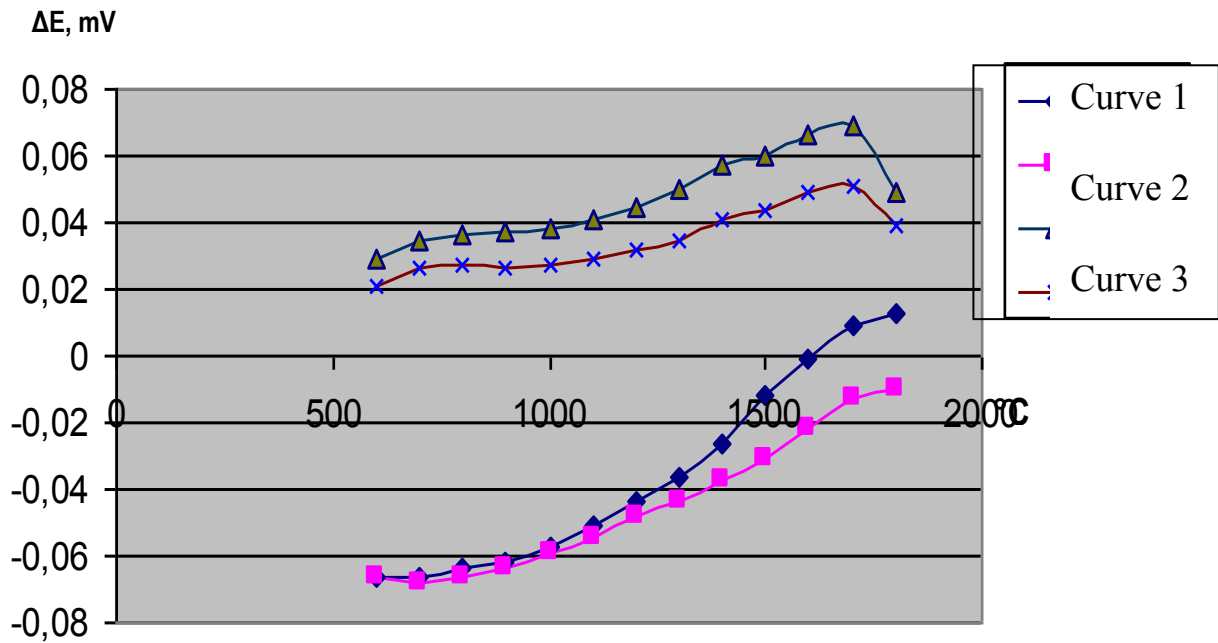


Fig. 1 EMF changes for nanostrengthened thermoelement W-Re5% against SOTM wire while calibrations of initial wire and the wire after 30-minute annealing at 1650°. Curves 1 and 2 – heating and cooling of initial wire, curves 3 and 4 – heating and cooling of the wire after half-hour annealing at 1650°.

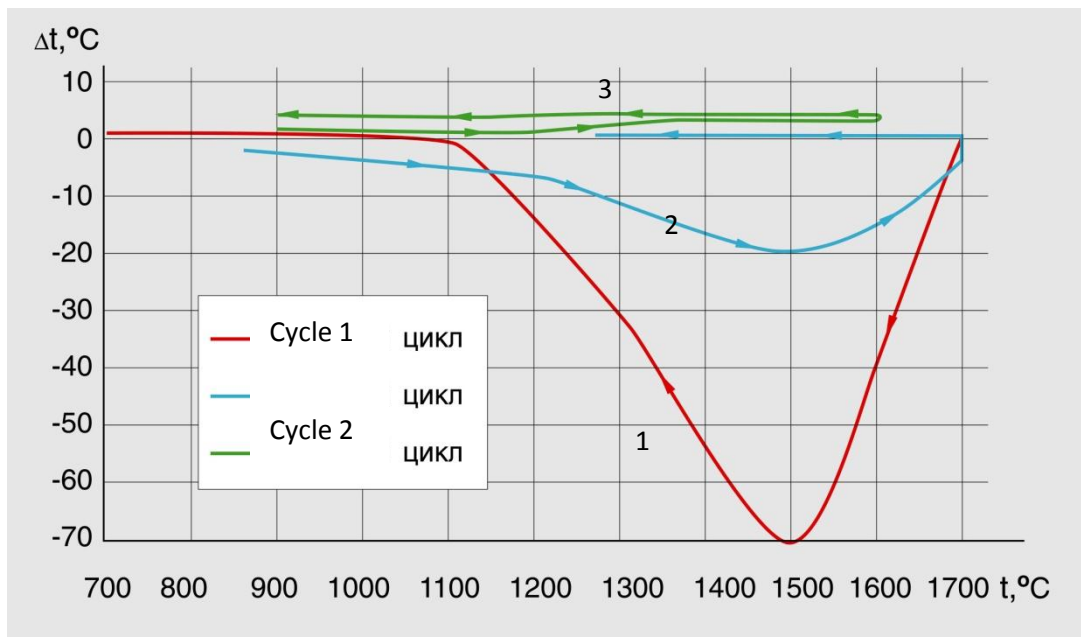


Fig. 2 EMF changes of W-Re5% (0,1% of nanoparticles of yttrium oxide) against W-Re20% (coil 311) thermocouple during three consecutive cycles of heating and cooling.

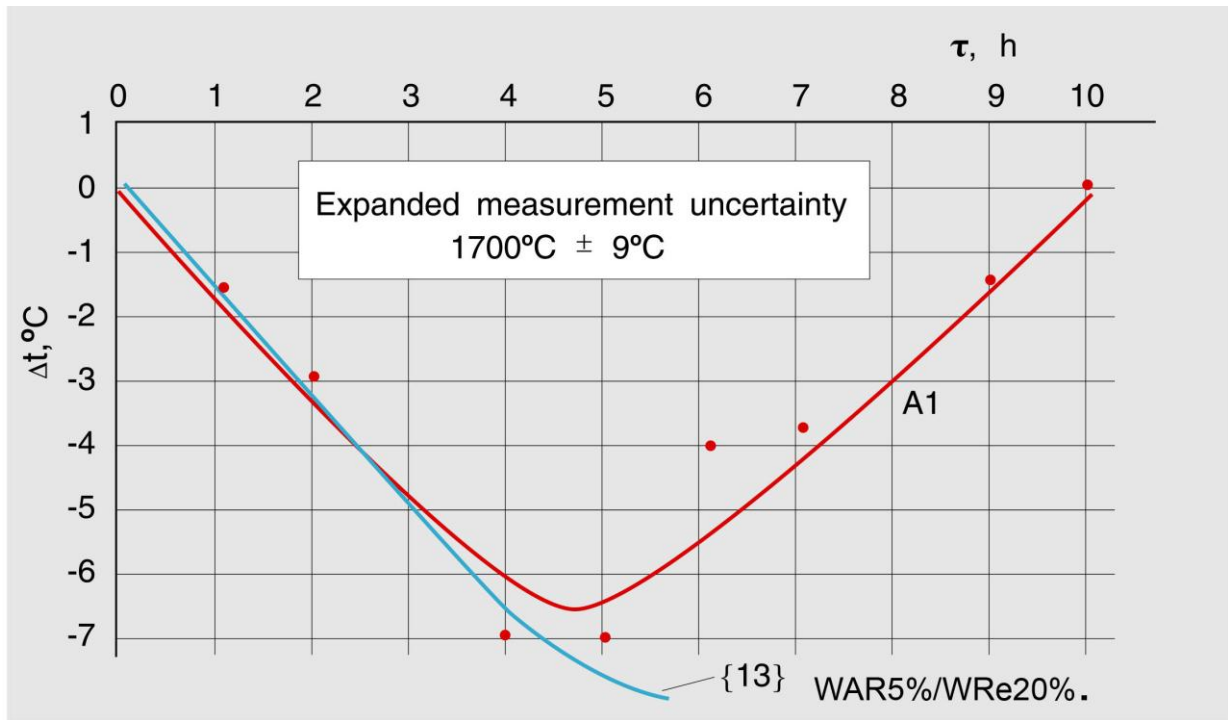


Fig.3 EMF change for W-Re5% (0,1% of nanoparticles of yttrium oxide) against W-Re20% (coil 311) thermocouple relatively initial value observed in the first cycle.

Annealing of experimental thermocouple at 2000°C according to the received results (Fig. 4) led to much faster stabilization of the composite. In this case EMF deviations from nominal values are shown for direct and reverse (after an hour annealing) calibration curves.

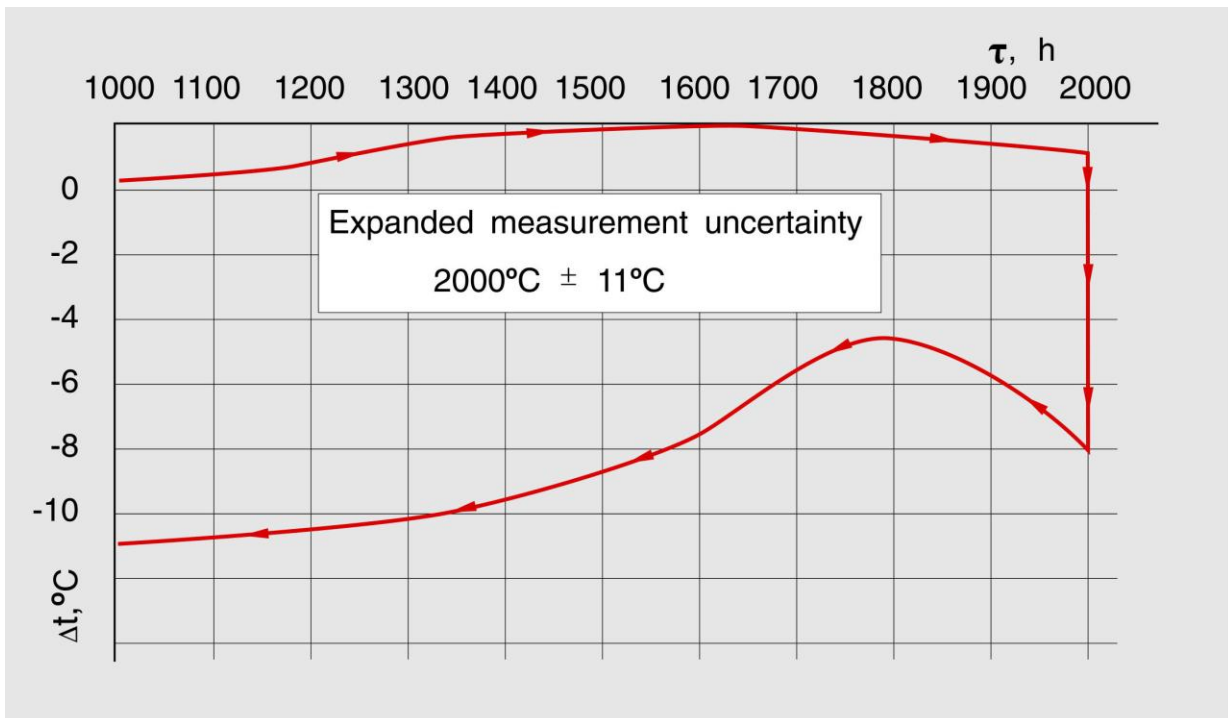


Fig.4 EMF deviation from nominal values for W-Re5% (0,1% of nanoparticles of yttrium oxide) against SOTM wire during heating-cooling cycle with an hour annealing at 2000°C.

## Conclusions

Despite certain convention of such conclusions, essential stabilization of the composite structure is obvious fact that allows optimistic estimations regarding continuation of the researches of thermoelectric properties of nanocomposites. They will allow improving of the next generation of high temperature standard specimens of thermoelectric materials.

## References

1. S.K.Danishevsky, A.N. Gurevich, N.I.Smirnova, E.I.Pavlova. Thermocouples for high temperature measurements having thermoelements on the base of molybdenum or tungsten. AC USSR №108438, *Bulletin of inventions*, **4** (1958).
2. SUO.021.142 TU. The annealed wire made of tungsten and rhenium alloy and graduated for thermoelements of thermocouples. *Specifications* (1976).
3. Thermoelectric converters. Nominal static characteristics of transformation. *SU Standard GOST 3044-77*, Moscow, Standards Publishing House, (1977.)
4. O.A.Gerashenko, A.N.Gordov, V.I.Lah. Temperature measurements. *A guide*. Kiev, Naukova dumka, p.494 (1984).
5. I.I.Fedik, V.P.Deniskin, V.I.Nalivaev, V.S.Konstantinov, The problem of high temperature measurements in fuel assemblies of nuclear propulsion engines. *J. Devices and automation*, **3** (21): 20-27 (2002).
6. *Methodical instructions*. State System of Measurements. Standard specimens of properties of thermoelectric materials made of W-Re5 and W-Re20 alloys (SOTM W-Re5/20). MI 1745-87.
7. P.A.Zaytsev, P.P.Oleynikov, A.A.Ulanovskiy, S.N.Nenashev *Abstracts of 5th International conferences «Power saving up technologies in the industry»*, September 27-30, 2009. Pp.3-17.
8. V.B.Pampura, V.A.Povalyaev, P.P.Oleynikov, A.G.Hotkin, *J.New industrial technologies*, **6**: 61-63 (2007)
9. A.A.Ulanovskiy, B.L.Shmiryov, Y.N.Altuhov, *Devices and automation*, №5(71): 4-13, (2006.)
10. P.P.Oleynikov, V.I.Nalivaev. *Issues of a nuclear science and technics. Nuclear materials technology*. Moscow, VNIINM, **5**, p.97 (1982).
11. S.V.Alekseev, A.A.Pavlov, M.L.Taubin, A.A.Yaskolko. *Abstracts of international conference «Nanotechnology of functional materials»*, S.-Petersburg, Pub. GPU, p.165 (2010).
12. A.A.Ulanovskiy, V.A. Medvedev, S.N.Nenashev, Y.A.Sild, M.S.Matveev, A.I.Pokhodun, P.P. Oleynikov, *Int. J. of Thermophysics*, **31**: 1573-1582 (2010).
13. S.K.Danishevsky, L.D.Oleynikova, S.I.Pavlova, L.I.Trahtenberg, P.P. Oleynikov. *Rhenium in new technics*, Science Pub., Moscow, 190-193 (1970).

5.7.

## MODERN STRUCTURAL MATERIALS BASED ON THE W-Mo-Re SYSTEM

Povarova K.B., Kazanskaya N.K.

Baykov Institute of Metallurgy and Materials Science RAS [povarova@imet.ac.ru](mailto:povarova@imet.ac.ru)

The high-rhenium alloys, based on the bcc Group VI metals of the periodic table (W and Mo) are known. These alloys exhibiting the “Re effect-1” (a simultaneous increase in low-temperature ductility and strength of Group VI metals after the addition of 25-35 at. % Re connected with an additional deformation mechanism by twinning) are lied near the  $\alpha(\text{W},\text{Mo})/\alpha+\sigma$  interphase boundary.

These high-rhenium alloys are as good as W and Mo alloys in high-temperature strength, but, unlike them, are not cold-brittle and do not become embrittled after high-temperature service and thermal cycling.

The binary W-Re, Mo-Re and ternary W-Mo-Re alloys have satisfactory formability and can be produced both as bulk articles and structures and as micron-scale semiproducts (foil, wire), which cannot be produced from Re because Re is expensive metal and demonstrates poor deformability caused by intense strain hardening.

The manufacture of the alloys by vacuum melting (VM) provides a high purity relative to interstitial impurities and a homogeneous Re distribution. This prevents the  $\sigma$  phase formation (deteriorating the plasticity), promotes the deformability, and allows the realization of “Re effect-2” (an abrupt increase in the strain hardening rate of W and Mo alloys due to the Re addition, up to  $\sigma_B = 4500\text{-}6000$  MPa for micron-scale wire).

Such micron-scale wire from alloys of the MRe-47VM type retain the ability to deformation by flattening and to spiral coiling. In the case where high-rhenium alloys are manufactured by the cheaper PM method, none technique of the Re introduction into the initial powder provides a uniform distribution of Re, whose segregates provoke the formation of grain-boundary  $\sigma$ -phase precipitates. Therefore, the Re content in the PM alloys is smaller than in the VM alloys (WRe20PM//WRe27VM and MRe40PM//MRe47VM).

The investigation of the effect of Re on the electronic structure, physical and mechanical properties of W and Mo have revealed the “Re effect-3” (a substantial increase in low-temperature ductility of W and Mo alloys at 2-7 at. % Re).

This allowed the development of low-rhenium high-temperature W-Re alloys for bulk products, including those reinforced by refractory MeC-type carbides and  $\text{Y}_2\text{O}_3$ -type oxides for massive parts of the structures operating at temperatures above 2000°C.

5.8.

## TECHNETIUM - A RARE METAL PRODUCED BY MAN FOR STRUCTURAL AND MEDICAL USE

Edwin D. Sayre

e-mail: [pbmpilot@comcast.net](mailto:pbmpilot@comcast.net)

### Abstract

Technetium-99 is a manmade element made for medical and high temperature structural use. Technetium is too rare in nature for any use so it is made as Tc<sup>99m</sup> with short half life for medical use and Tc99 with long half life and low beta radiation for structural use is provided by the fission products in used nuclear fuel. The needed Tc<sup>99m</sup> for medical use is produced by radiation of molybdenum with nuclear reactors. The Tc<sup>99</sup> metal with very much longer half life and less radiation is separated from the spent nuclear fuel, reduced and purified to pure metal powder and melted to ingots. Technetium has physical properties very similar to Rhenium. Technetium-99 was taken from the waste tanks in Hanford, Washington, purified, reduced to metal powder and melted into an ingot programmed by the author in 1964.(1) The Tc<sup>99</sup> was then used to alloy with tungsten to improve its ductility similar to rhenium. The tungsten alloy with 25% technetium could be cold forged indicating the improved ductility. The current nuclear power plants produce about 800 grams of technetium per metric ton of used nuclear fuel. The commercial value of the technetium produced by a 1000 megawatt reactor in one year is about \$240,000 assuming the value of Tc99 equal to that of rhenium. Almost all of the literature on technetium is about the medical Tc99 since there has been very little removed from used nuclear fuel fission products. The author also had Tc99 inserted to locate cancer cells to be irradiated for destruction. It was successful ten years ago. The value of technetium will help pay for the reprocessing of used nuclear fuel around the world.

### Preface

There are several purposes to write this paper on technetium. Most people have no knowledge whatsoever of technetium99. Most of the public papers are written about the element with the very short half life used for medical purposes. The author wrote a paper on technetium for the International Symposium on Rhenium and Rhenium Alloys on technetium recovered from the fission products in used nuclear fuel. This provided the opportunity to cover both the medical Tc99m and the high temperature structural Tc-99. Both of these applications will be covered in this paper.

### Introduction

Technetium has many properties similar to its sister element rhenium. In 1925 Noddack, Tacke and Berg announced the discovery of the element 43 by X-ray emission spectroscopy on the concentrated sulfates of niobium and platinum. The occurrence of technetium in nature is extremely rare. The first manmade technetium99 was made in 1937 by Perrier and Serge at Berkeley by irradiating molybdenum with neutrons.

As far as is known the first technetium-99 was taken from used nuclear fuel by a program developed by the author and funded by NASA in 1963 at the Hanford Laboratory in Washington state.. The author became interested in technetium in the early 1960s while developing advanced high temperature alloys for jet engines at General Electric. Rhenium was just being introduced and it was found that technetium is a similar element and could also improve high temperature properties of cobalt and nickel alloys for turbine blades.



GENERAL ELECTRIC NEWS FRIDAY, AUGUST 28, 1964



**SAMPLE OF TECHNETIUM 99 is displayed by Ed Sayre, BP&TO, to Paul Holsted, AEC. Ed's interest in technetium 99 began when he was in the Company's Jet Engine Department, was climaxed with a contract with NASA to "prove-out" the value of the Hanford product. Ed was in Washington, D. C. earlier this week discussing progress of the HAPO program with NASA officials.**

Figure 1. Technetium ingot being inspected

The program continued to alloy the technetium with tungsten to see if it improves its ductility like alloys of tungsten with 10% rhenium does. Figure 1 shows a picture of the first small Technetium ingot ever produced being reviewed with the AEC program review manager. The ingot was 1.5 inch in diameter and  $\frac{1}{2}$  to  $\frac{3}{4}$  inch thick. It was then used to be alloyed with tungsten for ductility tests.

The author then found that technetium did not exist. He was then moved to Hanford and found that there was much technetium in the so-called waste tanks. That is when the program was established to remove technetium from the waste, reduce it into metal powder and then arc melt it into an ingot. The program continued to alloy the technetium with tungsten to see if it improved its ductility like rhenium does. Alloys of tungsten with 10%, 15%, 20% and 25% technetium were vacuum arc melted and cast into small test ingots. The test ingots were evaluated and the tungsten 25% technetium was determined to be ductile.

There was a little work just beginning on developing the  $^{99}\text{Tc}$  with the high radiation and short half life from irradiating molybdenum. It is now in very much demand for medical testing to locate and evaluate various cells in the body. The author had it used to locate cancer cells that escaped from his prostate cancer before it was removed. Then high level radiation was used to destroy the cancer cells located by the  $^{99}\text{Tc}$ . It proved to be a very good medical tool to keep the author going into his middle eighties.

### **The Production of Technetium Metal for Structural use From Used Nuclear Fuel**

The only source for production of technetium metal for metallic use is used nuclear fuel. The average production of stable technetium metal for structural use is about 800 grams per metric ton after use for one year. It is one of the useful fission products. If the technetium has the same value as rhenium then the value of the amount per metric ton of used fuel is about \$8,000. The value of the amount of technetium produced each year from a 1,000 megawatt nuclear plant is \$240,000... Right now the amount of used nuclear fuel being stored in the US is about 64,000 metric tons. This contains about 50,000 kilograms of technetium worth about \$51,000,000. In addition to the technetium there are some other very valuable fission product metallic elements.

There is some advantage to storing the used nuclear fuel for about 50 years before separating out the fission products and the actinides. When the used fuel is first taken out of the reactor there are many fission products and actinides that have very short half lives with high level radiation. By leaving these storing for 40 to 60 years they have gone through many half lives. Which means they have only very long half lives and the very low level of radiation left.

Technetium-99 when it is created it has a half life of 6.01 hours and it radiates gamma at 0.14051 and beta at 0.347. After the radiation age change to <sup>99</sup>Tc it has a half life of 2.13 x10<sup>5</sup>a or 213,000 years. It has very low radiation danger unless it is located internally. There is some <sup>97</sup>Tc and <sup>98</sup>Tc in the fission product technetium but there is no certainty of the amount yet. But it is estimated that they are a very small percentage. The different isotopes of technetium are shown in Table 1.

The process to separate the technetium from the fission product solution is to provide an element to get the technetium to precipitate and get separated from the solution. It is then reacted to purify it into ammonium pertechnate. It is then reduced in a hydrogen furnace to pure technetium powder. The powder is pressed into electrodes and vacuum arc melted into ingots. Then the technetium can be alloyed with other metals.

Technetium can be alloyed with tungsten to improve its ductility. Very small additions of technetium to steel tend to improve its corrosion resistance.

Very small additions of technetium in nuclear grade stainless steel may have a significant improvement in radiation assisted stress corrosion cracking.

Technetium may have the same improving effect as rhenium in high temperature jet engine alloys. Because of its characteristics as technetium gets available it will see broad usage.

### Developing the Sources of Technetium

With advanced separation processes for the fission products from the used nuclear fuel there should be adequate technetium available. There are such large quantities of valuable fission products available that their value will make their production very cost effective. The following tables show the amounts and value of most of the usable fission products.

Table 1 Technetium for Commercial Use

Isotopes	Amount gr.	Half life Years	Radioactivity Mev	Commercial Value	
				1 Metric ton of used fuel	Used fuel from 1000 MW Nuc. Plant for 1 Yr.
Tc98	0.006	4.2E6	β 0.40, γ 0.7454		
Tc99	770	2.3E5	β 0.293 γ 0.090		
<b>Total</b>	<b>771</b>			<b>\$7710</b>	<b>\$239,859</b>

Table 2 Natural Elements with Stable Isotopes

Isotopes	Amount Gr.	Half life	Radioactivity Mev	Commercial Value	
				1 Metric ton of used fuel	Used fuel from 203 reactors in the year 2050
Bromine	21.6	stable	none	\$ 22	\$ 50,600
Molybdenum	3,345	stable	none	860	1,978,000
Ruthenium	2,177	stable	none	99,663	229,220,000
Silver	76.2	stable	none	152	349,600
Cadmium	107.8	stable	none	215	494,500
Barium	2,311	stable	none	1,295	2,978,500
Terbium	2.6	stable	none	78	179,400
Dysprosium	1.4	stable	none	7	16,700
Rhodium	467	stable	none	233,500	537,050,000
<b>Total</b>	<b>8,509.6</b>			<b>\$335,792</b>	<b>\$772,320,000</b>

Table 3 Natural Elements with Radioactive Isotopes

Element	Amount gr.	Radioactive Isotope			Radioactive Mev	Commercial 1 Metric ton of used fuel	Value Used fuel from 203 reactors in the year 2050
		Isotope	Percent	Half Life			
Rubidium	365	Rb87	66.8	4.89E10	$\beta$ 0.273, no $\gamma$	\$ 4,300	\$9,890,000
Tellurium	484.58	Te123	0.0017	1.3E13	e?	675	1,552,500
Lanthanum	1215	La138	0.0004	1.05E11	$\beta$ 0.26, $\gamma$ 1.44	2.187	5,030,100
Neodymium	2803.2	Nd144	0.65	2.1E15	$\alpha$ 1.83	6,166	14,177,200
		Nd145	0.24	>6E16	$\alpha$ ?		
Indium	2.6	In115	92	4.4E14	$\beta$ 0.48	26	59,800
Cerium	2,355	Ce142	47.	5E16a	$\alpha$ ~1.5?	662	1,522,600
<b>Total</b>	<b>7,225.38</b>					<b>\$7,850</b>	<b>\$18,055,000</b>

There are several usable fission product metals not listed here. Half the fission products in used fuel that has been aged over 50 years is not radioactive and about half of the other half is so low in radioactivity that it can have good usage. Most of the countries that are reprocessing used nuclear fuel are just storing the fission product solutions with the plan to separate them later.

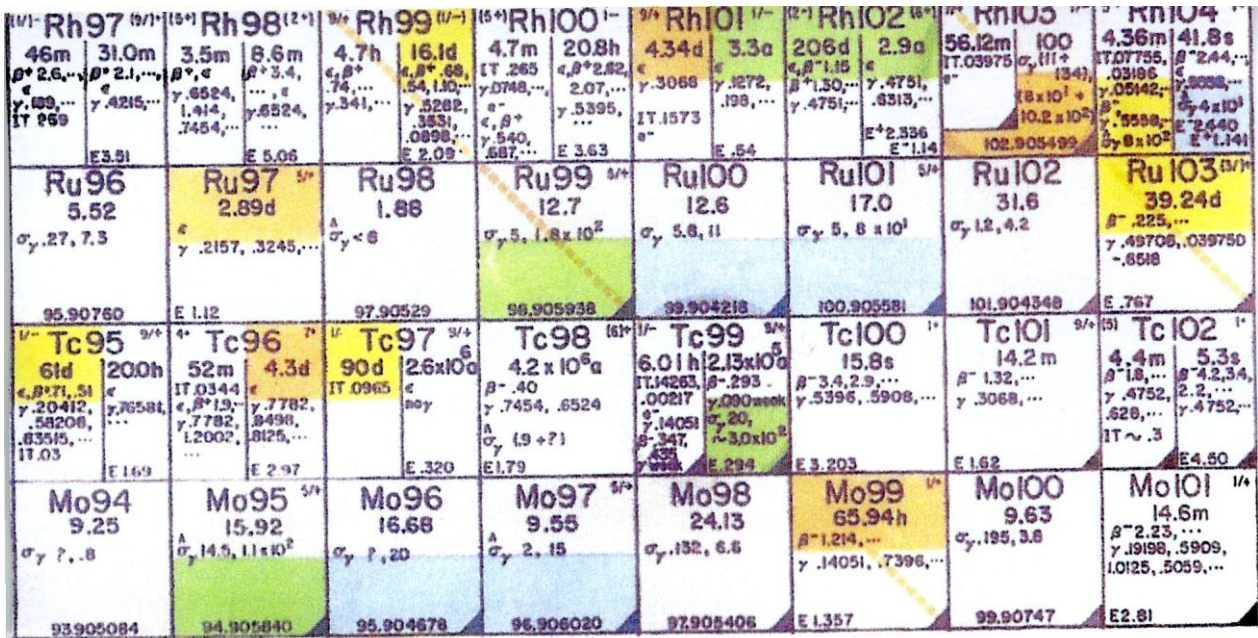


Figure 2 Technetium Isotopes shown in Chart of Nuclides

The cost of producing technetium will be about the same as the cost of producing rhenium so the price of technetium should be about the same as rhenium. It would be a great loss to the world to have technetium and some other fission products buried deep in the ground as is the plan set up by those that have no regard for the value of technetium.

**Producing Technetium99 for Medical Use by Irradiating Molybdenum With Neutrons**

Technetium nuclides are shown in figure 2 which is part of the overall chart of nuclides developed by General Electric.(2) The technetium 99 made by radiating molybdenum with neutrons. The produced technetium-99 is the nuclide shown in the left side of the <sup>99</sup>Tc in the chart in figure 1. Note this nuclide has a very short half life of just 6.01 hours and it has gamma radiation energy level of 0.1405 which makes it a good indication of its location in body cells. This <sup>99</sup>Tc nuclide was injected into the author to locate any cancer cells that left the prostate cancer before it was removed. Several cancer cell locations were discovered and they were taken care of with radiation to destroy them.



Technetium for medical use is quite different from the structural technetium metal, but they both can have a very useful ability and should be continually developed.

Metal wire tubes are put into arteries and veins to keep them open. However for many people the metal becomes coated with the blood contents and blocks the flow. Low level beta radiation stops the deposition of the blood components so it may be a good application of the structural technetium metal for medical use.

### Summary

The nuclear technology period has brought us some very important learnings and there will be millions more worth trillions of dollars to us in the future. Technetium-99m with the short half life for medical use and the  $^{99}\text{Tc}$  with low radiation and long half life are going to see much more use as we learn with time. As we learn to economically take technetium and other useful elements from the used nuclear fuel fission products the so-called waste elements will be a great economic addition to our technical world.

### References

1. Technetium, A Manmade Sister Element And Backup Alloying Element For Rhenium by Edwin D. Sayre, in Rhenium and Rhenium Alloys, Symposium, Edited by B. D. Bryskin, The Minerals, Metals and Materials Society, 1997.
2. The Chart of The Nuclides updated by F. William Walker, Dudley G. Miller and Dr. Frank Feiner, 1983 General Electric Company.



ISTR2011 participants in the Red Hall of Presidium of Russian Academy of Sciences

5.P2.

## INFLUENCE OF OXOCHLORO-THIOPYRINE RHENIUM(V) COMPLEX ON RADIATION RESISTANCE OF CELLULOSE DIACETATE

N.S. Beknazarova, A.A. Aminjonov

Tajik National University. (Rudaki Avenue 17, Dushanbe, Republic Tajikistan). [azimjon51@mail.ru](mailto:azimjon51@mail.ru)

The concentration of the complex which appears to maximum effect as an additive for none owner diacetate cellulose. Based on the analysis of dependencies tensile strength of the radiation dose -radiation has been concluded from the fact that the maxima of these curves can be used to produce cellulose acetate material having improved physical and mechanical properties. Found that tiopirin manifests in relation to cellulose diacetate as light stabilized and antistatic properties.

**Keywords:** polymer,  $\gamma$ - radiation, diacetat cellulose, thiopyrin, rhenium (V) complex.

Products made of polymer materials are widely used in agriculture, aviation, nuclear, electronic and space technology. Based on polymers made household items and medical supplies. In the operation of polymer materials change their transparency, chemical, mechanical and electrical properties. Thanks to modern technology has now developed methods for producing thin films and fibers, which are used as thermal and electrical insulation, and reinforcing materials. During operation and storage of polymers and products based on them are exposed to many physical and chemical factors. Under the influence of these factors is aging of polymers, which is associated with deterioration of their physical, mechanical and other characteristics.

To stabilize the operating characteristics of polymers are used in different ways. One effective way of increasing the polymer stability to the effects of external factors such as light, heat, radiation, and various types of mechanical stress is the introduction into their structure modifying agents. Among the commonly used additives for the stabilization of certain properties of polymer and polymer composite materials occupy special place sulfur-containing compounds. For example, 2-merkaptobenzimidazol used as a stabilizer in rubber and polyolefin's. Thiourea derivatives are effective stabilizers of rubber. 2-mercaptobenzimidazol is an accelerator of rubber and polyolefin stabilizing process. The application of polymeric materials from year to year has greatly expanded.

In [1,2] found that in photo-2-merkaptimidazol and 1-methyl-2-merkaptimidazol show fairly good stabilizing properties in respect of cellulose diacetate (DAC). It is shown that the 1,2,4-triazolitol-3 (5) significantly slows the process of photodecomposition of DAC. The assumption was made that the reason is the screening effect of 1,2,4-triazolitol-3(5). The authors of [3] studied the effect of 2-merkaptobenziazol to the light fastness of DAC. Light stabilized effect this additive has been studied both in terms of photo-aging and in photomechanical destruction. It was shown that the maximum effect of the light stabilizing takes place in photo aging with the introduction of the DAC 0.5% 2-merkaptobenziazol and in photo mechanics 3%. By means of electron spectroscopy and photoluminescence analysis proved that the 2-merkaptobenziazol is a good quencher of electronically excited states of the macromolecules of cellulose diacetate. In [4] experimental data on the effect of different concentrations of N,N-ethylenethiourea light fastness on DAC is presented. It is shown that the introduction of the DAC small amounts of N,N-ethylenethiourea (0.001%) light fastness when exposed to UV DAC - radiation with  $\lambda = 254$  nm at 25-hour exposure increased 3.4-fold.

## Experimental part

We conducted researches on influence the effect thiopyrin for light fastness and irradiation, and to electrifying diacetate cellulose. To obtain polymer films cellulose diacetate solutions in DMF containing different amounts of thiopyrin were prepared and after filtration through the filter of Schott (since 100), evenly placed in a glass cell, and placed on a horizontal surface weight-VLT a specially upgraded for this purpose. After that, the cell was covered with glass and slow evaporation of the solvent took place. The resulting films were dried in a vacuum oven (vacuum 10<sup>-2</sup>) at 500<sup>0</sup>C.

Samples for mechanical testing were produced using the knife of figure that provides the following geometric dimensions: length of the working part of samples  $l = 22\text{mm}$ , width  $d = 2\text{mm}$ . The sample thickness was measured with an accuracy of 20.5  $\mu\text{m}$  and ranged from 40 to 60 microns. As a source of UV light bulb used LUVs - 30, 80% of the radiation which is light with a wavelength of 254 nm ( $J = 0,040 \text{ cal/cm}^2 \text{ min}$ ).

The samples were irradiated with equal doses of UV light, and then were tested in uniaxial tension. Mechanical tests were carried out using discontinuous machines with a constant loading rate 12 mm / min. Breaking removal and tensile strength of the samples was determined by the formula:

$$E_p (\%) = \frac{h_g - h_0}{l_h} \cdot 100\%; \quad \sigma_p \frac{K\Pi}{\text{mm}^2} = \frac{hp}{S} (1 + \varepsilon)$$

$P = K (Hh)$

Where  $n$  - the multiplicity of breaking machines;

$K$ -cruelty springs dynamometer;

$S$  - Cross-sectional area;

$h_g$  - elongation of the samples;

$h_0$  - correction factor;

The radiation intensity of LUVs-30 was measured using a thermoelectric actinometer AT - 50 and recorded the measurements of the emf potentiometer PP - 63. Source - radiation chamber served as RHM-□ - 20, D-0,  $19 \cdot 10^6 \text{ R / h}$ .

## Results and discussion

Table 1 shows the experimental data on the effects of UV - irradiation with  $\lambda = 254 \text{ nm}$  on the tensile strength of the original DAC and DAC containing various concentrations of tiopirina.



Table 1. Effect of UV - irradiation with  $\lambda = 254$  nm on the tensile strength of DAC containing various concentrations of tiopirin

Additive ratio, %	Bursting strength, kg/mm <sup>2</sup>						
	Radiation time, hour						
	0	2	5	10	15	20	25
0	11,2	9,1	6,5	4,4	3,7	2,9	2,6
0,001	10,9	9,9	9,0	7,1	6,2	5,9	5,6
0,05	11,3	9,7	8,9	8,3	7,5	7,1	5,9
0,1	11,4	10,8	9,3	8,9	8,1	7,8	6,2
0,5	11,3	10,9	9,8	9,4	8,8	8,3	6,4
1,0	11,1	11,0	10,1	9,5	9,1	9,0	6,5
2,0	11,6	11,5	10,9	9,8	9,7	9,4	7,1
3,0	11,4	11,2	11,0	10,0	9,8	9,5	7,9
5,0	11,0	10,8	11,0	10,8	10,2	9,1	7,4

The data in Table 1 show that the introduction of the cellulose diacetate thiopyrin concentrations 0,001-5% by weight of the polymer has virtually no effect on its initial tensile strength, but at the same time there is a significant of supplementation light stabilizing effect. Thus, the introduction of 0.001% tiopirina of the DAC within 25 hours of UV - irradiation of the initial tensile strength of the film from DAC decreases from 10.9 to 5.6 kg/mm<sup>2</sup> that is 1.95 times, whereas the irradiation DAC not containing added initial tensile strength decreased from 11.2 to 2.6 kg/mm<sup>2</sup> that is 4.31 times. These data suggest that the introduction of the DAZ 0.001% polymer additive light resistance increases 2.2 times. The data in Table 1 shows that with increasing concentrations of tiopirin resistance to UV - radiation increases. This experimental finding can be interpreted in favor of the screening mechanism of the influence of additives on the light fastness DAC.

Because of the sulfur-containing compounds have a definite effect on the electrified materials based on cellulose acetate, we conducted a study on the effect of different concentrations of tiopirina on electrified DAC. Moreover, electrostatic charges applied by the friction of medical cotton tape. Electrified films from DAC were measured by a vibrating electrode. Registration of the charge decay was performed using a digital voltmeter with an accuracy of 2 mV immediately after application of electrostatic charges.

Table 2 shows the experimental data on the effect of different concentrations of tiopirina on electrified DAC.

Table 2. The dependence of the static charge on the surface of DAC on the time and the percentage of thiopyrine

t, min	The size of the static charge, y.e.				
	Concentration thiopyrina				
	0	0,01%	0,5%	1,0 %	2,0%
0	46,8	32,1	30,2	22,3	14,2
0,5	37,1	30,2	26,4	16,3	12,1
1,0	34,3	28,1	22,2	14,2	11,7
1,5	31,9	26,2	20,1	13,7	11,0
2,0	30,3	22,1	18,4	12,5	10,7
2,5	29,8	20,1	16,8	11,8	9,9
3,0	29,1	19,2	16,0	11,1	9,1
3,5	29,4	19,0	15,1	10,7	8,9
4,0	29,2	18,3	14,8	10,0	8,2
4,5	29,0	18,0	14,2	9,6	8,0
5,0	28,8	17,9	14,1	9,3	7,8
5,5	28,7	17,2	13,8	8,9	7,2
6,0	28,6	17,0	13,7	8,8	7,0
6,5	28,7	16,9	13,5	8,7	6,0
7,0	28,7	16,7	13,3	8,5	6,7
7,5	28,8	16,4	13,1	8,2	6,5
8,0	28,9	16,2	12,9	8,1	6,3
9,0	28,9	16,0	12,7	8,0	6,2
10,0	28,8	15,8	12,1	7,7	6,0

The data in Table 2 shows that the introduction of the 0.01% thiopyrin into the DAC conducts to a reduction in the initial electrified from 46.8 USD to 32.1 cu that is almost 1.5 times. With increasing concentration of antistatic additive activity against DAC increases. Introduction of the DAC additives in a concentration of 2% reduces the electrified polymer in the initial time to 3.3-fold, and for 10 minutes at 4.8 times. In other words, thiopyrin has good antistatic properties in respect of DAC.

Found that thiopyrin manifests in relation to cellulose diacetate as light stabilized and antistatic properties.

We also conducted researches on influences studied the effect of different concentrations of the complex  $[ReOL_2Cl_3] \cdot 3H_2O$ , where L - tiopirin on the electrical characteristics of the ( $v$ ,  $s$ ,  $E_0$ ,  $E_{max}$ ) and the time semi decrease charge ( $\tau_{0,5}$  and 5) from the surface of the film diatseta cellulose (DAC) after charging him corona. The experimental data presented in Table 3.

Table 3. The influence of complex composition  $[ReOL_2Cl_3] \cdot 3H_2O$ , where L- tiopirin on the electrical characteristics of the DAC

Complex concentration, %	$\tau_{0,5}$ , min	$E_0$ , B/cm	$E_{max}$ , B/cm	$\rho_v$ , OM · cm	$\rho_s$ , OM
0	126,4	207	491	$10 \cdot 10^{13}$	$39,2 \cdot 10^{13}$
0,01	76,6	120,3	228,4	$2,9 \cdot 10^{13}$	$9,8 \cdot 10^{13}$
0,05	64,9	90,2	150,3	$2,3 \cdot 10^{13}$	$9,1 \cdot 10^{13}$
0,1	17,4	73,8	139,4	$2,0 \cdot 10^{13}$	$8,9 \cdot 10^{13}$
0,5	4,9	35,8	70,3	$1,9 \cdot 10^{13}$	$8,0 \cdot 10^{13}$
1,0	1,6	20,1	35,9	$1,7 \cdot 10^{13}$	$7,9 \cdot 10^{13}$
2,0	2,7	17,0	30,5	$1,0 \cdot 10^{13}$	$1,5 \cdot 10^{13}$
3,0	2,8	17,3	31,1	$1,8 \cdot 10^{13}$	$2,6 \cdot 10^{13}$

These tables indicate that the introduction of the DAC different concentrations of the complex leads to a significant reduction in time semi decrease charge from the surface of the samples after charging them a corona discharge. At the same time are improving other electrical characteristics ( $E_0$ ,  $E_{max}$ ,  $v$ ,  $s$ ) of the polymer. Semi decrease time charge from the surface of films containing no additive DAC complex appeared to be 2 hours 11 minutes. This figure is the minimum concentration in the management of the complex (0.01%) is reduced to 1 hour and 28 minutes, which is 1.65 times. In the concentration range of complex 0.01 - 1.0% of the value of  $\tau_{0,5}$  is continuously reduced, and a further increase in additive concentration of 2.0 to 3.0% is a small increase in  $\tau_{0,5}$ . The minimum value of  $\tau_{0,5}$  - is observed for films of DAC containing 1.0% of the complex. The value of  $\tau_{0,5}$  - reduced from 126.4 to 1.6, is 79 times. Observed decrease in the values of the electrostatic field of the surface charge technology  $E_0$  (before charging corona). This figure is for samples containing 0.01% of the complex is reduced to 1.72 times, and the introduction of 2.0% additives - a 12.18 time. The minimum value of  $E_{max}$ ,  $v$ ,  $s$  is observed for samples containing 2.0% DAC complex.

Thus, the complex composition  $[ReOL_2Cl_3] \cdot 3H_2O$ , where an L -tiopirin can be used as antistatic agents for effective materials based on diatseta cellulose.

Studies on the effect - radiation on the tensile strength of films diatseta cellulose modify tiopirin and complex rhenium (V) with it set to high none own properties. The experimental data presented in Tables 4 and 5.

Table 4. Dependence of tensile strength on the concentration of DAC thiopyrine time and  $\gamma$ -irradiation (starting dose chamber RHM- $\gamma$  -20,  $D = 0,19 \cdot 10^6$  p / h)

Concentration	Bursting strength, kg/ mm							
	Exposure dose, rent/hr 1 0							
O	8,0	8,4	6,1	5,9	4,8	4,2	3,8	1,6
0,001	7,9	7,6	7,2	6,4	5,7	5,1	4,0	2,0
0,05	8,0	7,8	7,9	6,7	6,0	5,7	4,9	2,2
0,1	8,2	7,9	7,9	7,4	6,9	5,9	5,3	2,0
0,5	8,3	8,0	7,9	7,6	7,4	6,8	5,7	2,1
1,0	8,6	8,2	8,0	7,7	7,6	7,0	6,0	2,2
3,0	8,0	8,3	8,0	7,8	7,7	7,3	6,6	2,1

Table 5. The dependence of the tensile strength of DAC concentration of the complex  $[ReOL_2Cl_3]$ , where L-thiopyrine and  $\gamma$ -irradiation time (Initial dose chamber RHM- $\gamma$  -20,  $D = 0,19 \cdot 10^6$  p / h)

Concentration	Bursting strength, kg/ mm							
	Exposure dose, rent/hr 1 0							
$[ReOL_2Cl_3]$	O	3,2	6,3	9,6	19,0	38,0	95,0	190,0
O	8,1	6,4	6,0	5,0	4,3	4,0	3,3	1,8
0,001	8,3	8,4	8,8	9,4	10,2	9,6	9,0	6,8
0,05	8,6	8,9	9,3	10,2	11,3	11,8	10,2	7,2
0,1	7,9	8,0	9,9	12,3	13,8	12,2	10,0	7,8
0,5	8,2	8,3	10,1	13,4	14,0	14,1	12,4	7,5
1,0	8,5	9,2	10,9	13,6	14,4	14,6	13,7	6,9
3,0	8,4	9,0	11,2	13,8	14,6	15,0	14,2	7,0

It was found that the introduction of the cellulose diacetate uncoordinated thiopyrine its tensile strength under the influence of  $\gamma$ -radiation is much slower than in the original DAC is reduced. Thus, the strength of samples containing 0.1% DAC tiopirin exposed - radiation from X-ray dose of 95 / h compared to samples not containing this additive are 1.4 times greater mechanical strength. With increasing concentration of radiation resistance thiopyrine DAC increases, due to the shielding mechanism of action of this additive. On the curve of the breaking strength of the radiation dose  $\gamma$  - radiation peaks do not appear. A different picture is observed when introducing complex of oxo rhenium (V) with tiopirin. Even with the introduction of low concentrations of oxo rhenium complex (0,001% by weight of polymer) under the action of  $\gamma$ -radiation occur the growing importance of tensile strength. At this concentration, addition of hardening process of cellulose diacetate films from occurs until the effects of radiation dose  $\gamma$ - $19 \cdot 10^4$  Roentgen / hour. At this dose of film hardening factor of 1.3. Further increase in dose lead to a slow decrease in tensile strength values. At a dose of  $190 \cdot 10^{10}$  Roentgen / hour film of unmodified DAC become brittle and to determine their strength becomes very difficult. Samples of the films containing diacetat cellulose 0.001% of the complex of rhenium (V) at the dose of radiation maintain their appearance and plasticity, and their tensile strength by comparison of the modified non-irradiated film decreases from 8.3 to 6.8 kg/mm<sup>2</sup> kg/mm<sup>2</sup> that is 1 2 times. It should be noted that the tensile strength of the polymer containing no additives of the complex under the influence of  $\gamma$ -radiation at a specified dose is reduced from 8.1 to 1.8 kg/mm<sup>2</sup> kg/mm<sup>2</sup>, that is 4.5 times. With increasing concentration of the complex increases its anti-radiation effect. According to the results of

experimental studies defined interval the concentration of the complex which appears to maximum effect as an additive for none owner diacetate cellulose. Based on the analysis of dependencies tensile strength of the radiation dose -radiation has been concluded from the fact that the maxima of these curves can be used to produce cellulose acetate material having improved physical and mechanical properties.

## Reference

1. A.A Aminjanov. Complex compounds of rhenium (V) with amide ligands and tioamidnyimi: avtoref. Dis. ... Dock. Chem. Science. – Ivanovo ( 1992)42p.
2. K.U. Akhmedov, Synthesis and study of complexes of rhenium (V) with tiosemikarbozidom and its derivatives: Author. diss. ... Candidate. Chem. Science - Ivanovo (1986) - 22 p.
3. B.N. Narzullaev, A.A. Aminjanov, K.U. Akhmedov, H.D.Dodomatov, S. Narzullaev .Effect of 2-merkaptobenzthiazola lightfastness on cellulose diacetate, Proceedings of V All-Union Conference on Chemistry and physics of cellulose, Tashkent (1982)
4. E.D.Goziyev N, N'-ethylenethiourea complexes of rhenium (V) and some aspects of their applications Abstract. diss. ... Candidate. Chem. Science Dushanbe, (2007). 22P.



5.P3.

## **PLASTIC DEFORMATION OF RHENIUM AND PLATINUM-GROUP METALS**

I.G.Roberov, N.B.Gorina, G.S.Burkhanov

IMET RAS, Moscow

Plasticity, as well as strength is a complicated function of several terms i.e. the nature of the interatomic bond, macro-and microstructure, various kinds of defects, external factors (temperature, pressure, composition), test conditions (stress state, strain rate, surface condition, scale factor ), etc. Plasticity is not only the property but also the state of matter.

Rhenium and technetium, by their physical and mechanical properties, are close to platinum-group metals. They are distinguished by high degree of strain hardening, which makes the process of obtaining rhenium semi-products very labor-intensive. Rhenium is the only of alloying elements, which increases both ductility and strength of tungsten and molybdenum (rhenium effect), neutralizing the harmful carbon and oxygen effects on physical and mechanical properties.

Of platinum-group metals, only palladium and platinum have high ductility. Rhodium and iridium of technical purity, having the same crystalline structure, are fragile. In the state of technical purity, ruthenium and osmium are practically not deformable.

Deep cleaning of rhenium and platinum-group metals sharply increases their ductility. Investigation of structure and properties of rhenium and platinum-group metals in the pure polycrystalline and single-crystal states has enabled to determine the contribution of impurities to changing their plasticity, the cause of brittleness and deformation mechanisms.

Developed on the basis of studies, the regimes of plastic deformation have enabled to obtain thin foils of iridium, rhodium and rhenium. For the first time, by plastic deformation, it is obtained ruthenium foil by thickness of less than 1 mm.

## 6

### **Tc and Re nanotechnology and applications in the field of nanomaterials**



The chairman of the 6-th section corr.-member RAS B.G. Ershov in the President Hall of RAS

6.1.

## SYNCHROTRON DIAGNOSTICS OF FUNCTIONAL NANOMATERIALS

Ya.V. Zubavichus, A.A. Veligzhanin, A.A. Chernyshov, E.V. Guseva

National Research Centre “Kurchatov Institute” (Kurchatov sq.1, Moscow 123182, Russian Federation)

Synchrotron radiation (SR) offers unique capabilities in structural characterization of complex functional materials. Nowadays, there are about 70 operating SR centers all over the world. Russia hosts two of them located at the Budker Institute of Nuclear Physics (Novosibirsk) and Kurchatov Institute (Moscow).

This lecture surveys current status and future plans of experimental stations installed at the Kurchatov Synchrotron Radiation Source.

The emphasis is placed on the design and recent results obtained with the “Structural Materials Science” end-station. This station is dedicated to structural investigations of non-crystalline and nanostructured materials by a set of mutually complementary methods, viz. small-angle X-ray scattering (SAXS), X-ray powder diffraction (XRD) and X-ray absorption spectroscopy (EXAFS/XANES).

These techniques yield structural information at different distance scales over the range of 0.1-100 nm (interatomic distances, unit cell parameters, size of crystallites/particles/pores, etc.) thus enabling more comprehensive characterization of a material.

### Synchrotron sources in Russia

Siberian Center for Synchrotron Radiation (Budker Institute for Nuclear Physics, Novosibirsk) in operation since mid 1970-ies  
Storage rings VEPP-3 (2 GeV, 120 mA), VEPP-4 (5 GeV, 40 mA) – both 1<sup>st</sup> generation ( $\epsilon$  ~300 nm-rad)  
11 beamlines [ssrc.inp.nsk.su](http://ssrc.inp.nsk.su)

Kurchatov Synchrotron Radiation Source (NRC «Kurchatov Institute», Moscow) in operation since early 2000-ies  
Siberia-1 (booster, 450 MeV) – 3 VUV beamlines  
Siberia-2 – dedicated 2<sup>nd</sup> generation source (2.5 GeV, 300 mA,  $\epsilon$  ~75 nm-rad), 16 beamlines  
[www.kcsr.kiae.ru](http://www.kcsr.kiae.ru)

Zelenograd Synchrotron Radiation Facility (Lukin R&D Institute of Physical Problems),  
<http://www.mifp.ru> – **under construction**

Dubna Electron Synchrotron (JINR) <http://www.jinr.ru/desy> – **project development**

International collaboration:  
Russian-German beamline at BESSY II [http://www.bessy.de/lab\\_profile/04.rglab/RGLab](http://www.bessy.de/lab_profile/04.rglab/RGLab)  
Russian involvement in ESRF consortium (July 2011)  
Russian participation in European XFEL project (scheduled start in 2014 roza, 4<sup>th</sup> generation source)

## Kurchatov Synchrotron Radiation Centre

X-ray stations	
1	Protein Crystallography
2	Precision X-ray Optics
3	X-ray Crystallography and Physicoal Materials Science
4	Medical Imaging
6	Energy-Dispersive EXAFS
7	Structural Materials Science (SMS)
8	X-ray Small Angle Diffraction Cinema (blobbelets)
9	Refraction Optics & X-ray Fluorescence Analysis
10	X-ray Topography & Microradiography
VUV stations	
11	X-ray Photoelectron Spectroscopy
12	Optical spectroscopy for Condensed Matter
13	Luminescence & Optical Investigations
Technological stations	
14	X-ray Standing Waves for Langmuir-Blodgett Films
15	Molecular Beam Epitaxy
16	LIGA



ISTR 2011 Moscow

The station is equipped with a special sample environment chamber to study samples under non-ambient conditions (high/low temperature and a specific gas atmosphere, including vacuum, inert gases, oxidative/reductive gases, etc.). This is especially important for functional materials since a structural study can be performed under conditions similar to those required for their target exploitation.

### Structural Materials Science beamline

- In the user mode since 2004
- Techniques implemented: XANES/EXAFS, XRD, SAXS
- Mission: combined X-ray diagnostics of non-crystalline and nanostructured functional materials



Over the last few years, diverse classes of functional materials have been elucidated, including supported catalysts for petrochemical processes, metal alloys, polymers, functional metal oxides and complexes.

The logic of application of different synchrotron X-ray techniques to solve specific structural problems is discussed. Possibilities and advantages of combined utilization of several techniques are illustrated with a number of examples.

6.2.

## MANUFACTURE OF NANO- AND ULTRADISPERSE POWDERS OF RHENIUM AND REFRACTORY METALS FROM TECHNOGENIC RAW MATERIALS.

A.I. Kostylev, U.G. Pokrovskiy, I.D. Troshkina<sup>1</sup>, N.G. Firsin, A.M. Chekmarev<sup>1</sup>

FSUE «RPA «V.G. Khlopin Radium Institute», (2 Myrinskyi prosp., 28, Saint-Petersburg, Russian Federation)

<sup>1</sup>D. Mendeleev University of Chemical Technology of Russia, (Moscow, Russian Federation)

**Keywords:** powders of rhenium, electrochemical process, rhenium heptoxide, hydrogen reduction, controlled particle size.

### Abstract:

This report contains the results of research concerning the production of powders of rhenium and some refractory metals from industrial wastes. The aim of the work was to develop the best technological solutions and investigate of key stages in pilot industrial scale production: dissolution of raw materials, the separation of multicomponent mixtures of metal compounds and obtaining of high-purity rhenium, tungsten and molybdenum powders of a controlled phase and particle size. Production is focused on getting the final product: nano- and ultrafine powders or microgranules in a form suitable for use in powder metallurgy of superalloys and special refractory alloys.

As a raw material in the process mostly imported waste heat-resistant nickel alloys of GSMX-4 and MK-4 were used. Full technological cycle of processing involves the following stages: electrochemical crushing, sulfuric acid leaching, plasmochemical oxidation, adsorption and ion exchange purification of ammonium perrenate, hydrogen reduction, CVD – process of reception of rhenium.

### Introduction

Consumption of rhenium in the next 10 years is projected at least 70 - 80 tons per year [1 - 3]. For example, in civil and military aviation technology application of the rhenium superalloys according to the plans of leading companies (Cannon Muskegon, Rolls Royce, Pratt & Whitney, General Electric) and estimations of the collaboration of manufacturers of aviation turbine «Engine OEMs Collaborate» will increase at least until 2027 and in the next few years (until 2018) will be at least 60 - 70 tonnes of rhenium per year. That is due to the fact that 40 - 50% of the parts in modern aircraft engines are made from rhenium superalloys. Next important field of the rhenium consumption is production of reforming catalysts and catalysts of natural gas processing in the so-called GLT - process. According to opinion of catalyst leading manufacturers the need of rhenium in this sector over the next 10 years will be about 16 tons per year. Production of primary rhenium in connection with the specifics of the geochemical distribution in this period can be 50 - 60 tons only.

A noticeable increase in the production of rhenium is impossible due to lack of new discovered fields. This deficiency (between the primary production of rhenium and the needs of industry) should be covered by the secondary rhenium obtained by recycling of industrial wastes. Demanded volume of rhenium production from industrial wastes for the next decade is estimated by the world leading producers of rare metals in amount not less than 14 tons per year.

The primary market for recycled rhenium is mainly represented by large pieces and turbine parts made of nickel-based superalloys. Superalloys - complex alloys with heterophase structure whose main elements – disperse (1 - 0.5 micron) particles of  $\gamma'$ -phase on the basis of the ordered intermetallic compound  $Ni_3Al$  and nickel complex- $\gamma$ -solid solution [4]. Practical experience in processing of this raw material was obtained in the operation of pilot production, which was



organized in 2004 in the Federal State Unitary Enterprise " Morozov Plant" in the Leningrad region. Recycling of heat- resistant rhenium alloys (grinding powders) to yield as the main products of rhenium in the form of ammonium perrhenate, powder and sintered rods from it was carried out at this production. As a co-product ultrafine nickel powder and nickel oxalate were manufactured. A large part of produced rhenium in the form of sintered rods (pellets) comes to produce alloys to Stupino Metallurgical Company. Scheme of processing was based on nitric acid leaching followed by separation of rhenium and nickel with the use of crystallization of sparingly soluble salts and ion-exchange treatment. Experience in operating production, mainly using hydrometallurgical techniques, allows to identify the following disadvantages: a large amount of acidic liquid waste, not efficient use of resources: cobalt, tungsten, molybdenum, they are not extracted and remain in solid waste dumps production, poor efficiency, unefficiency of processing of the scrap and scrap waste of heat-resistant nickel alloys. In this regard, parallel works on improving technology in the following areas are carried out: the development of economical method for waste crushing, replacement of nitric acid oxidation to plasma processing of materials to make the process simpler, increase productivity and reduce the amount of liquid waste, integrated processing of raw materials with extraction of valuable components from alloys (nickel, cobalt, tungsten, molybdenum) with modern efficient methods, development and implementation of technology for rhenium production in the form of ultra- and nanopowder.

### Experimental

The unique microstructure of superalloys defines completely unique stability of the material to mechanical stress and chemical agents. The usual dissolution methods of this materials (acidic, alkaline, oxidizing melting, etc.) are not effective [5 – 7]. At the same time, the electrochemical processing of the alloy (in sulfuric acid solution at a potential of the anode  $\approx 1$  and temperature  $t = 20 - 50^\circ \text{C}$ , platinized titanium at potential  $\leq 0,6 \text{ V}$  is used as the cathode) provides quite rapid breakdown of the material. Under these conditions at the anode, electrochemical dissolution reaction of nickel situated in the grain boundaries of the alloy occurs. Except for nickel, as part of the matrix ( $\gamma$ -phase) there are some other components of the alloy: cobalt, iron, chromium and molybdenum. So the electrochemical process of the intergranular fracture of the alloy is accompanied by transition to a solution of these metal ions, cobalt, iron, chromium and molybdenum. Transition to a solution of rhenium as a perrhenate- ion can be observed. In practice, the really attainable level of electricity consumption is about  $1.3 \text{ kW} \cdot \text{h}$  per kg of damaged alloy.



*MK-4 Alloy*



*Product of electrochemical destruction*

*Fig.1. Electrochemical destruction.*

The next stage of the process, sulfuric acid leaching, is carried out in sulfuric acid solution at the temperature of  $85 - 95^\circ \text{C}$  with stirring. The main chemical reactions that occur at this stage are the dissolution reaction of nickel, aluminum, iron, cobalt and chromium. The residue after

dissolution and washing is thin, black powder, containing mainly tungsten, tantalum, niobium, rhenium. Particles of this material have a size of about 5 - 10 microns.

The precipitate is washed to remove the bulk of sulfate and transferred to the oxidation step for rhenium extraction. From the solution after filtration, nickel, cobalt and rhenium presented in solution as an impurity (~ 5% of the total) are recovered. Nickel and cobalt are extracted from the solution by reduction at a controlled pH, and impurity of rhenium is extracted from the mother liquor by adsorption on anionite.

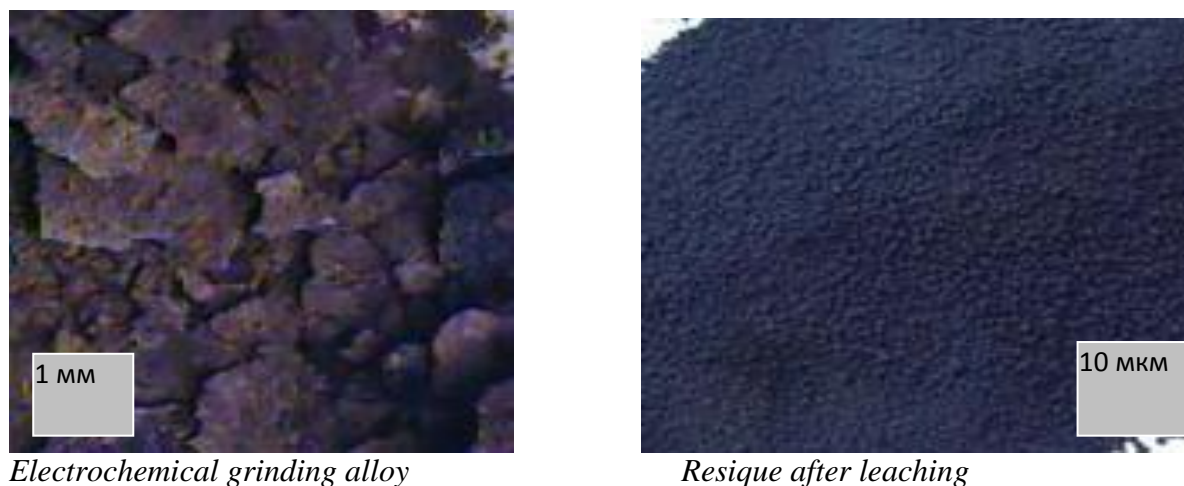


Fig.2. Sulfuric acid leaching

Plasma oxidation is carried out in the installation of air-flame spraying with powder feed processed in the zone of the plasma torch. As an oxidant, air is used. Temperature in the plasma torch is 3000 - 5000 ° C, in the oxidation zone - about 1000 ° C. That provides the oxidation of the powder particles and the diffusion of volatile oxides in the gas phase. The resulting gas mixture is released from the solid cinder in a cyclone and enters into the adsorption column irrigated with aqueous alkali. The cooling of gas stream with an aqueous solution and adsorption of rhenium oxides are carried out in the column. At an arc current of 150 - 200 A and air flow 2 - 3 cubic meters per hour, efficiency is reached up to 5 kg / hour. The degree of rhenium extraction from the material is up to 90%. Additionally molybdenum in the form of ammonia paramolybdate is removed.

Ion exchange purification of ammonium perrhenate produces material with a quality to satisfy to the requirements for "ammonium perrhenate for superalloys." Products have been certified in accordance with the requirements of MMTA (Minor Metals Trade Association). The main amount of rhenium powder so far is obtained by hydrogen reduction. Reduction is carried out in one stage in tube furnaces with a stepped increase in temperature from 250 - 350 ° C to 800-850 ° C. Physical characteristics of the powder are the next: dispersion - 1 μm, bulk density - 2.5 g/cm<sup>3</sup>, color - gray. The resulting powder metal is subjected to further special treatment for compact rhenium obtaining in the form of rods, which are marketable product. To do this, rhenium powder is compressed and then sintered at 1100 - 1200°C in hydrogen atmosphere. Rhenium pellets obtained by this method have purity level of 99.98 - 99.99% and density of 60 - 70% of the theoretical.

To get compact metal from a standard powder produced by hydrogen reduction of ammonium perrhenate procedures of very high sintering (more than 2000 ° C) and subsequent machining operations with intermediate annealing are necessary. That is a disadvantage of obtaining powder method. That is why for organized production, ways to increase the purity of the metal, to reduce the sintering temperature and reduce losses of the metal were suggested.



*Fig.3. Manufacture of pellets of standart from scrap*

This method worked on a laboratory scale is based on the obtaining of powdered rhenium by hydrogen reduction of rhenium heptoxide  $\text{Re}_2\text{O}_7$  in vapor phase. In this case, the quality of the metal can be improved by additional distillation of initial oxide rhenium. Depending on process conditions (ratio of the reactants and the carrier gas, pressure and temperature in the reaction chamber) the rhenium powder with the dispersion at the level of 0.1 - 0.3 microns and a specific surface area of 1 - 2.3  $\text{m}^2 / \text{g}$  can be obtained. The method allows to obtain fine unpyrophoric powders with controlled particle size in the range 100 - 500 nm, purity above 99, 995% and the oxygen content of less than 0.2%. The use of these powders at getting rhenium and its alloys by powder metallurgy methods can reduce the sintering temperature, increase the density of products and improve their physical and mechanical properties.

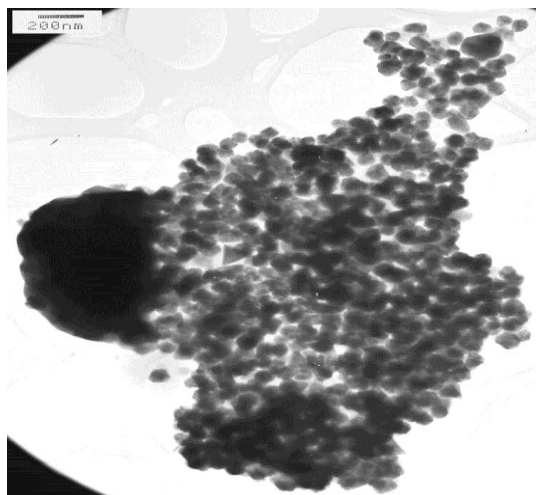


*Fig.4. Nanorhenium powder, ~0,1  $\mu\text{m}$*

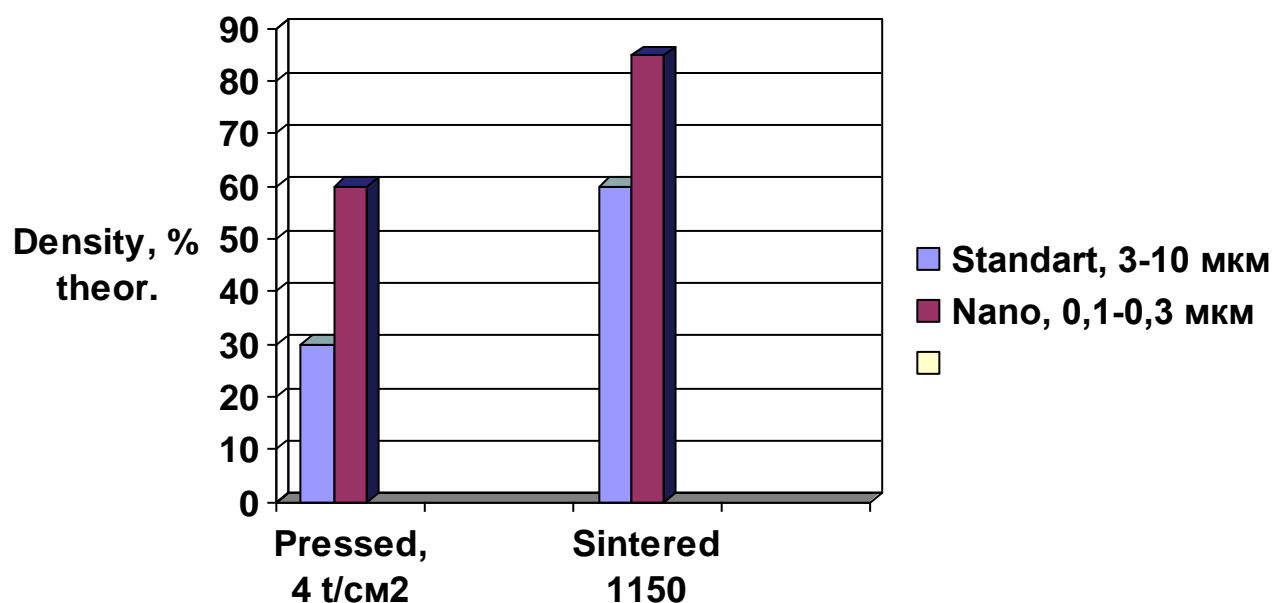


Fig.5. Rhenium powder is compressed under the pressure of 4 tons/cm<sup>2</sup> and then sintered at 1150°C in hydrogen atmosphere.

### Conclusion

Rods, pressed from this powder are the feedstock for obtaining some products of rhenium like wires, foils, rods, etc. They can be rolled, stretched, hammered and put the other mechanically processing. Moreover, with increasing of dispersity, chemical purity and structural perfection of the powders the physical and mechanical properties of final products, such as resistance to plastic deformation and fracture resistance, increase sharply. Creation of material from perfect crystals of nanometer size would allow to achieve almost theoretical strength and ductility. Superalloys, which are currently widely used materials and the main area of rhenium use, are entering into the second era of development. One of the key trends of their development is the use of powder metallurgy methods based on nanopowders.

### Reference

1. Lipmann W., Rhenium 2009 and beyond. The MMTA Int.Minor Metals Conference. Istanbul. Turkey. 2009;
2. The Minor Metals Age. Metals for the Aerospace Industry/Conference, Seattle. October 2009;
3. Magyar M.J., Rhenium. U.S. Geological Survey Minerals Yearbook – 2004;
4. Murakami H., The location of atoms in Re- and V- containing multicomponent nickel-base single-crystal superalloys. *App. Surface Science*, v. 76/77, 1994, 177 – 183;
5. Paul J. Fink et al., Rhenium reduction—alloy design using an economically strategic element. *JOM Journal of the Minerals, Metals and Materials Society*. 2010, Volume 62, Number 1, 55-57;
6. US 2009/0255372 A1 (Publication number). Jun 29, 2007. Recycling of superalloys with the aid of an alkali metal salt bath;
7. A.V. Tarasov, V.M. Paretsky, A.D. Besser and E.I. Gedgagov. Processing of grinding waste of rhenium-containing alloys to manufacture commercial-grade metals. *Symposium General Recycling and Solid Waste Processing: Precious and Rare Metals*. Moscow. 2008.



6.3.

## NON-STOICHIOMETRIC SYNTHESIS OF RHENIUM HEPTASULFIDE HYDROSOL

N.R. Antipkin, G.A. Biljalova, M.A. Bogorodskaya, A.O. Bogorodsky, A.B. Sazonov,  
A.S. Chagovets

D. Mendeleev University of Chemical Technology of Russia  
(Miusskaya sq. 9, Moscow, 125047, Russian Federation)

**Keywords:** nanoparticles of rhenium heptasulfide, rhenium heptasulfide hydrosol, reaction of perrhenate and hyposulfite, colloidal stability of rhenium heptasulfide.

### Abstract

The  $\text{Re}_2\text{S}_7$  nanoparticles were synthesized in the exchange reaction of perrhenate and hyposulfite. Effective hydrodynamic diameter of the nanoparticles is  $55 \pm 15$  nm. The influences of synthesis time, acidity, ratio of reactants, and quantity of the stabilizer on the disperse phase yield were investigated. The kinetic characteristics of this reaction and side reaction of hyposulfite decomposition were obtained. It was found that formation of particles at a temperature of  $100^\circ\text{C}$  finishes in 2 min. The activation energy is 76 kJ/mol and 16 kJ/mol of main and side reaction respectively. The main reaction order was determined to be 1 and 1.35 with respect to perrhenate and hyposulfite respectively. As a result of the work, visually transparent product, stable within a wide range of pH (1-9), not coagulating in saturated solutions of salts (including polyvalent cations) even at long heating up to  $100^\circ\text{C}$  has been synthesized. Hydrosols can be stored in an inert atmosphere for indefinitely long time (years).

### Introduction

Rhenium heptasulfide is an effective and selective catalyst of hydrogenation and reduction. Its stability to catalytic poisons (for example, sulfur or arsenic compounds) is unique. Its catalytic activity is greater than one of palladium or tungsten sulfides and allows getting almost quantitative yield at optimal conditions [1-4]. The major characteristic of a catalyst in heterogeneous catalysis is its specific surface. Therefore, synthesis of the catalyst nanoparticles is interesting from practical point of view.

Hydrosols labeled by radionuclides have found the application in nuclear medicine for diagnostic and therapeutic purposes. The key to success here is not a chemical form of the radiopharmaceutical but the size of its nanoparticles. It's known that optimal contrast substance for lymphoscintigraphy must have radius of its particles in the range of 10-50 nm [5]. Such particles can be removed from tissues with acceptable rate and can not penetrate into the blood. Recently the nanocolloids of technetium –  $^{99\text{m}}\text{Tc}$  have been widely adopted in the technique of intraoperational visualization. This technique allows to reduce a volume of dissection and to perform less traumatic operations in the cases of oncological diseases. Among many studied substances (proteins, antimony sulfides, *etc.*) sulfide of rhenium appeared to be the preferable one. Its X-ray-amorphous irregular shape particles appeared to be the best for radionuclide labeling for diagnostic application. However, the desire of radiopharmaceutists to carry out the synthesis of hydrosol in a solution with isotonic concentrations of substances used to restrict the possibilities of optimization.



The purposes of the present work were the optimization of parameters for synthesis of rhenium heptasulfide nanoparticles, the synthesis of the hydrosol possessing aggregative stability, and the estimation of particle sizes in the dispersoid.

## Experimental

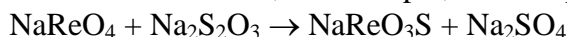
Nanoparticles have been synthesized in the exchange reaction of perrhenate and hyposulfite in acidic medium at elevated temperature and at the presence of a stabilizer [6]:



This reaction is accompanied by a side reaction of hyposulfite decomposition:



and also by formation of intermediate substances, for example, moniotioperhenate  $\text{NaReO}_3\text{S}$ :



During the synthesis rhenium was distributed over different phases as it follows. Primary precipitate of rhenium heptasulfide (RePP) has been codeposited with particles of elemental sulfur. It can be separated from supernatant part by centrifugation. Dispersoid (ReDS) is represented by the

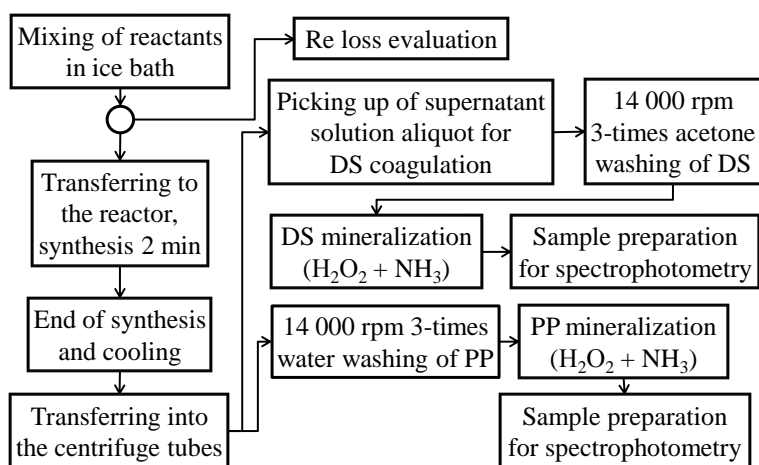


Fig. 1. Experiment layout

nanoparticles of rhenium heptasulfide (probably with incorporated elemental sulfur). The dispersoid can be separated from continuous medium by coagulation after addition of acetone. Continuous medium (ReCM) contains residual perrhenate and intermediate products of the basic reaction. Separation of the phases has been done according to the following chart (Fig. 1).

Hydrosols are not true solutions, and for spectral analysis of dispersoid it must be dissolved in

ammonia solution of hydrogen peroxide or in *aqua regia*. Thus rhenium heptasulfide may be converted into a chemical form of perrhenate or rhenium acid. Coloured compounds are formed after addition of hyposulfite and tin (II) chloride.

Particle size determination was taken at Zeta Potential/ Particle Sizer Nicomp<sup>TM</sup> 380 ZLS (photon-correlation spectroscopy method – PCS), VEGA 3 SB (Scanning Electron Microscope – SEM) and TECNAI-12-3R (transmission electron microscope – TEM). Visual spectra were taken at SP-2000. Separation of the phases has been done with Centrifuge Eppendorf 5415 C.

## Results and Discussion.

Properties of hydrophobic sol depend on many variables: concentrations of reactants, order of their addition, heating, cooling and stirring mode, character of the stabilizer and the moment of its addition.

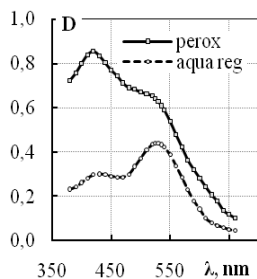


Fig. 2. Reduced rhenium compounds spectra

After rhenium dissolving in peroxide solution, evaporating it, and adding hyposulfite and tin (II) chloride known orange complexes with a maximum of absorption at 410 nm are formed (Fig. 2).

It's not reasonable to evaporate *aqua regia* since rhenium acid is volatile. Absolutely different compounds of violet color were formed at the presence of *aqua regia* residues. Possibly, a nitrosyl-sulfide complex of rhenium with a maximum of absorption at 530 nm was formed in that system. Thus, a new unknown complex of rhenium with molar extinction equal to

$0.82 \cdot 10^4 M^{-1} \text{cm}^{-1}$  has been synthesized. It can be used in spectrophotometric analysis of rhenium as well. However, extinction of a sulphidic compound formed after treatment of rhenium heptasulfide by peroxide is twice above, or  $1.60 \cdot 10^4 M^{-1} \text{cm}^{-1}$ . Therefore, a combination of peroxidic dissolving and hyposulfite treatment should be recommended for analysis.

The first series of experiments has given a chance to estimate influence of acidity on heptasulfide yield as a whole, and its nanoparticles in particular. A total yield of rhenium heptasulfide rises up to 80% when the medium acidity increases (Fig. 3). However, on the curve “dispersoid yield versus acid concentration” the plateau with maximal yield (about 40%) within 0.45-0.65 M concentration range is observed. This can be explained because the acid not only catalyzes formation of rhenium sulfide, but also provokes coagulation of the dispersoid. Therefore, for all further experiments a minimal possible value of hydrochloric acid concentration (0.45 M) has been chosen as the optimal one.

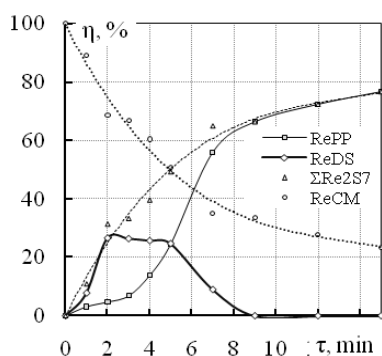


Fig. 4. Finding optimal synthesis time

activation energy of hyposulfite decomposition is equal to 16 kJ/mol, and the temperature factor is 1.2. It is a fast reaction going quickly at room temperature. When temperature rises up from 20 to 100 °C the rate of  $\text{Re}_2\text{S}_7$  formation increases in 800 times, and the rate of hyposulfite decomposition increases only in 4 times. Therefore, to increase the yield of the basic substance and to reduce relative contribution of the hyposulfite decomposition it is necessary to synthesize nanoparticles at the highest possible temperature.

This can be proven by dependence of heptasulfide and elemental sulfur yield on temperature (Fig. 5).

Determination of the basic reaction order with respect to perrhenate was performed at the conditions of a pseudo-zero order with respect to hyposulfite concentration (meaning its excess). Initial reaction rate is directly proportional to the perrhenate concentration; it is a first order reaction.

The dependence of the  $\text{Re}_2\text{S}_7$  formation rate on the hyposulfite concentration is more difficult and that is not a surprise. For determination of a formal order of the basic reaction

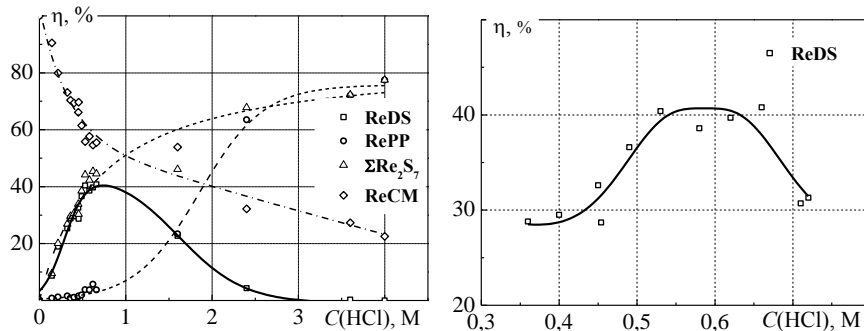


Fig. 3. Influence of acidity on the heptasulfide yield

Time is of great importance for successful synthesis. It is shown that formation of particles at 100 °C comes to the end during 2 minutes (Fig. 4); an increase of the synthesis time doesn't result in increase of the dispersoid yield, but increases a risk of its coagulation.

Since the synthesis of nanoparticles appeared to be unexpectedly quick, it was interesting to determine the activation energies for the basic and side reactions. For this purpose the synthesis temperature has been varied from 40 to 100 °C. The activation energy of the basic reaction is equal to 73 kJ/mol, and the temperature factor is about 2.5. This allows to classify it a reaction going with average rate (at normal conditions its rate is extremely low). The

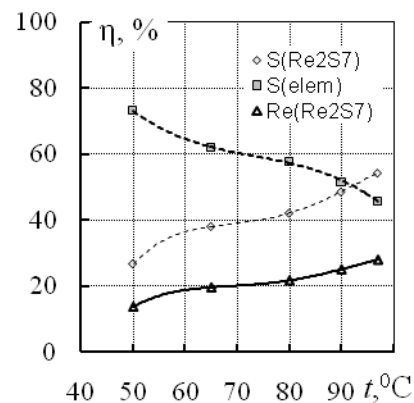
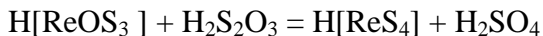
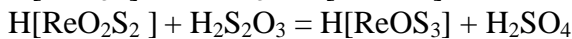
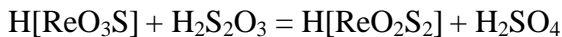
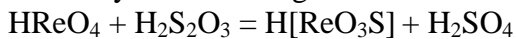


Fig. 5. Temperature dependences of the  $\text{Re}_2\text{S}_7$  and S yields

with respect to hyposulfite the dependence “rate versus concentration” have been drawn in logarithmic coordinates. The formal reaction order is equal to 1.35.

There is a consecutive substitution of oxygen atoms by sulfur atoms in the molecule of rhenium acid formed after perrhenate-ion protonation. So, one of the intermediate products is bright-yellow monotioperrhenate-ion which formation we observed. Stages of the substitution can be described by the following reactions:



The last one is formation of a sulphidic bridge between rhenium atoms.



One can assume that all these reactions go with different rates, and the last one is rate-determining. The formal reaction order is equal to 1.35. Thus, in the synthesis it is reasonable to increase the hyposulfite concentration above a stoichiometric value.

To stabilize hydrophobic soles the amphiphilic polyelectrolytes (for example, gelatin) are used. Thus the surface of nanoparticles becomes hydrophilic and their aggregative stability increases. However, gelatin reduces catalytic activity. Moreover, being used in medicine it may become an allergen as well as any other protein. Therefore it was necessary to determine its minimal possible quantity needed for the synthesis. Shortening of the synthesis time from 7 to 2 minutes allowed expecting possibility of reduction of gelatin concentration. It has been shown that after the increase of gelatin concentration more than 1% the yield of the dispersoid doesn't change. Further synthesis has been performed at the stabilizer concentration equal to 1.2 mass percents (Fig. 6).

Formally the stoichiometric hyposulfite–perrhenate ratio is equal to 3.5. However, because of the side reaction of hyposulfite decomposition, this value can appear insufficient. A total yield of  $\text{Re}_2\text{S}_7$  rises up with an increase of this ratio above the stoichiometric value. However, when the ratio is equal to 5 or 6 the "saturation" of the dispersoid yield is observed (Fig. 7). Further increase of the hyposulfite concentration does not result in an increase of the dispersoid yield.

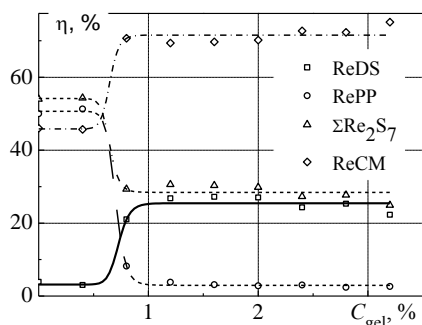


Fig. 6. Finding optimal concentration of gelatin

Though a total yield of heptasulfide increases, the most part of rhenium codeposits with sulfur. It is observed that at a lack of hyposulfite (when the ratio is less than 3.5) visually transparent sols can be produced. Elemental sulfur formed after hyposulfite decomposition is not allocated in a separate phase but incorporated into the structure of  $\text{Re}_2\text{S}_7$  nanoparticles. However, the yield at these conditions is the smallest (less than 20%). Distribution of the particles over their sizes in this case is presented by a curve with a maximum at about 50 nm. Polydispersity is small; 75 mass percents of the particles have hydrodynamic diameters from 35 to 75 nanometers. When the ratio increases, the turbid product with bimodal distribution of particles over their sizes is formed. It may be consequence of different nature of the particles or different mechanisms of their formation. Indeed, the sulfur deposit easily separates during centrifugation and the sol becomes transparent. The maximal yield of rhenium in a disperse phase reaches about 40%. Since the product can be cleared of sulfur easily by centrifugation, without a loss of the dispersoid, the ratio equal to 4.5 has been chosen as the optimum.

Though a total yield of heptasulfide increases, the most part of rhenium codeposits with sulfur. It is observed that at a lack of hyposulfite (when the ratio is less than 3.5) visually transparent sols can be produced. Elemental sulfur formed after hyposulfite decomposition is not allocated in a separate phase but incorporated into the structure of  $\text{Re}_2\text{S}_7$  nanoparticles. However, the yield at these conditions is the smallest (less than 20%). Distribution of the particles over their sizes in this case is presented by a curve with a maximum at about 50 nm. Polydispersity is small; 75 mass percents of the particles have hydrodynamic diameters from 35 to 75 nanometers. When the ratio increases, the turbid product with bimodal distribution of particles over their sizes is formed. It may be consequence of different nature of the particles or different mechanisms of their formation. Indeed, the sulfur deposit easily separates during centrifugation and the sol becomes transparent. The maximal yield of rhenium in a disperse phase reaches about 40%. Since the product can be cleared of sulfur easily by centrifugation, without a loss of the dispersoid, the ratio equal to 4.5 has been chosen as the optimum.

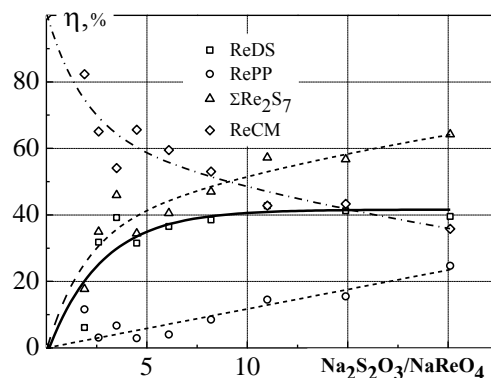


Fig. 7.  $\text{Re}_2\text{S}_7$  yield dependence vs the hyposulfite–perrhenate ratio

For the purified deionized sol an effective hydrodynamic volume-average diameter is equal to 55 nm and a number-average diameter is 35 nm (Fig. 8). Small discrepancy between the two values means that the distribution of particles over their sizes is narrow. Diameter of a dense core determined by a method of transmission electron microscopy turns out to be 10-20 nm (Fig. 9).

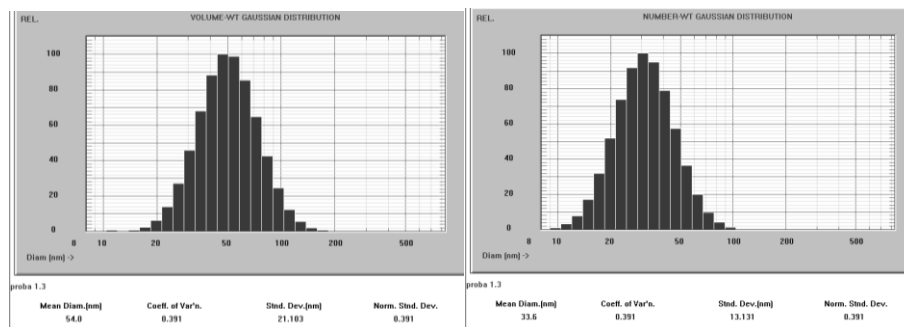


Fig. 8. Particle size distribution (effective hydrodynamic diameter)

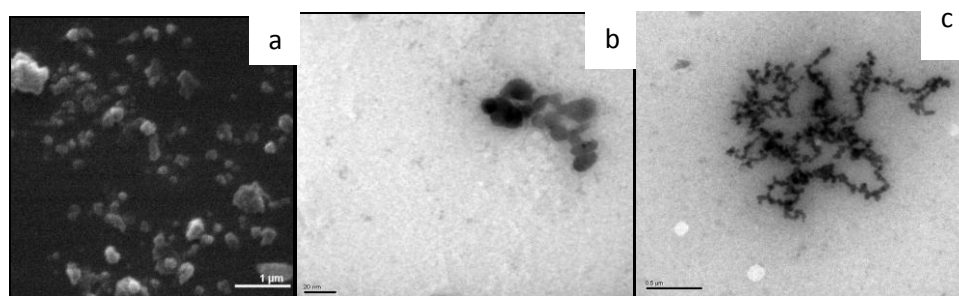


Fig. 9.  $Re_2S_7$  nanoparticles electronic photography: a – SEM, b, c – TEM

Comparison of hydrosols obtained by different methods is given in the Table 1.

Table 1. Characteristics of hydrosols obtained by different methods

Reference	$C_0(Re)$ , g/l	$\frac{Na_2S_2O_3}{NaReO_4}$	$C(HCl)$ , M	$C_{gel}$ , %	Synthesis time, min	Hydrodynamic diameter, nm
[7]	0.36	6.0÷7.0	0.07÷0.11	0.81	3.5	≤ 1000
[8]	0.59	3.0÷7.1	0.125	0.17	6÷10	< 100 (60%) 100÷200 (14%)
[9]	0.48	4.8 ÷7.7	0.20	4.0	3÷5	<50 (20%)
Present work	0.60	4.5	0.40÷0.45	2.2	2	50±20 (100%)

## Conclusions.

As a result of the work, visually transparent non-opalescent hydrosol of  $Re_2S_7$ , stable within a range of pH from 1 to 9, not coagulating in saturated solutions of salts (including polyvalent cations) even at long heating up to 100 °C has been synthesized. An effective hydrodynamic volume-average diameter is equal to 55 nm and a number-average diameter is 35 nm (PCS). An effective hydrodynamic diameter is at least 2 times more than diameter of the dense core.  $Re_2S_7$  nanoparticles are irregularly shaped, X-ray amorphous. Deionized hydrosols can be stored in an inert atmosphere for indefinitely long time (years).

This work may be also helpful in developing synthesis of other hydrosols of metal sulfides (antimony, molybdenum and so on).

## References

1. M.A. Ryashenceva, H.M. Minachev; *Renii i ego soedineniya v geterogennom katalize*, Nauka: Moscow, 1983, p. 248 (in Russian).
2. T.A. Pal'chevskaya, L.V. Boguckaya, V.M. Belousov, *Ukr. Him. J.* №3: 240-243 (1989) (in Russian).
3. V.I. Savel'eva, I.D. Sokolova, B.V. Gromov, M.A. Ryashenceva, *Trudy MHTI im. D.I. Mendeleeva.* **69**: 151-154 (1972) (in Russian).
4. V.I. Savel'eva, B.V. Gromov, M.A. Ryashenceva, *Trudy MHTI im. D.I. Mendeleeva.* 71: 148-151 (1972) (in Russian).
5. N.S. Lyubarskii, A.I. Shevela, M.R. Kolpakov, R.S. Hanaev, V.V. Ilmaev, *Flebolimfografiya.* № 17: 8-14 (2003) (in Russian).
6. G. Remi; *Kurs neorganicheskoi himii.* **2**. Mir: Moscow, 1966. 836 p. (in Russian).
7. Koren. Registracionnoe udostoverenie № 81/1116/3. Vremennaya farmakopeinaya stat'ya 42-1150-81 ot 17 avgusta 1981 g. (in Russian).
8. ISSN: 0315-162X (ISSN print). Patent. Zabel, Pamela Louise; Dunn, Kent. *Colloid for scintigraphy*. Patent Number: US 6706251 Patent Date Granted: March 16, 2004 Patent Country: USA Patent Assignee: London Health Sciences Centre, London, AR, USA Patent Class: 424-129 Official Gazette of the United States Patent and Trademark Office Patents 1280 (3) Mar. 16, 2004.
9. Tsopelas, Chris, *Journal of Nuclear Medicine.* **42**: 460-466 (2001).



6.4.

## CONTROLLED SYNTHESIS OF ULTRA DISPERSED (NANO SIZED) RHENIUM OXIDES (IV) AND (VI): SYNTHESIS OF PRECURSORS AND PROPERTIES OF THE MATERIALS

K.A.Smirnova, D.V.Drobot, A.I.Lvovskiy, O.V.Petrakova

Lomonosov Moscow State University of Fine Chemical Technologies  
(Prosp.Vernadskogo 86, Moscow, Russian Federation)

**Keywords:** rhenium, alkoxides, thermal decomposition, nano sized oxides

### Abstract:

Electrochemical syntheses of complex of rhenium with n-butanol  $\text{ReO}_3(\text{OBu}^n)\cdot m\text{Bu}^n\text{OH}$  (**I**) and heteroligand complex of rhenium with ethanol and isopropanol  $\text{Re}_4\text{O}_x(\text{OEt})_y(\text{OPr}^i)_z$  (**II**) have been elaborated. It was shown that thermal decomposition of (**I**) and (**II**) allowed to produce of nano sized rhenium (IV) and (VI) oxides.

### Introduction

Recently the interest to chemistry of rhenium compounds and a problem of synthesis of new materials on its basis has considerably increased. The interest is caused by unique and important properties of rhenium compounds [1]. In particular, alloys of rhenium with other refractory metals are characterized by a combination of useful mechanical properties (durability, hardness, plasticity) [2]. A significant amount of rhenium compounds are used in manufacturing of catalysts possessing high activity and selectivity in various organic and inorganic reactions [3]. It is known that the application of nano sized particles in catalysis allows to reduce the expense of active components. Therefore ultra and nano sized rhenium oxides arouse the practical interest because of their special physical and chemical properties [4].

The aim of work is development of method of controlled synthesis of functional ultra dispersed (nano sized) materials by using of homo- and heteroligand rhenium alkoxocomplexes as precursors. Electrochemical synthesis was improved to obtain  $\text{ReO}_3(\text{OBu}^n)\cdot m\text{Bu}^n\text{OH}$  (**I**) and  $\text{Re}_4\text{O}_x(\text{OEt})_y(\text{OPr}^i)_z$  (**II**).

### Experimental

The electrochemical method has been used for synthesis of complexes (**I**) and (**II**). The scheme of an electrochemical cell is presented on fig. 1. Conditions of synthesis of complexes (**I**) and (**II**) are presented in Table 1.

**Description:**

- 1 - drying agent ( $P_2O_5$ )
- 2 - reflux condenser
- 3 - water for cooling
- 4 – comparison electrode
- 5 - cathode (Pt)
- 6 - anode (Re)
- 7 - membrane from porous glass
- 8 – thermometer

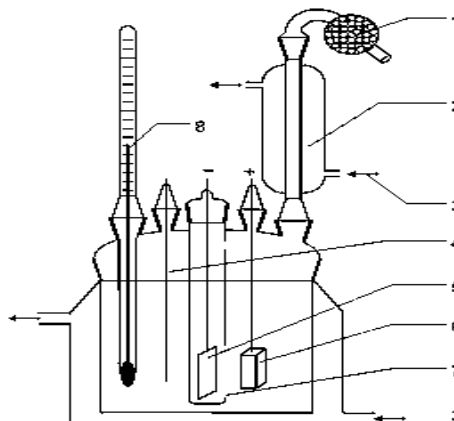


Fig.1. An electrochemical cell for synthesis of alkoxides

Thermal properties of a complex of rhenium  $ReO_3(OBu^n)mBu^nOH$  in the range of temperatures from 22 to 420 °C were investigated. Heating was carried out on air with a speed 5 °C per minute. Differential temperature curve is presented on fig. 2. For studying of thermal decomposition of a complex (I), for determination of structure and investigation of properties of products of decomposition, isothermal annealing has been carried out at five temperatures (180°C, 190°C, 200°C, 300°C, 340°C). The analysis of thermogram allows to state that at  $T=185$  °C the first step of weight loss of the sample comes to the end, therefore the sizes of particles in this area of temperatures (180°C, 190°C, 200°C) have been defined, other two points were chosen so that to come nearer to conditions in which weight loss has ended. The temperature was chosen not above 340 °C as sublimation of  $Re_2O_7$  was possible.

Table 1. Conditions of electrochemical synthesis of rhenium alkoxides

Conditions	I	II
Anode	Re	Re
Cathode	Pt	Pt
Electrolyte	(n-BuOH)	n(i-PrOH) : n(EtOH) = 1:1 mole/mole, membrane
U, B	150-200	200-240
I, mA	30-80	10-50
Duration, h	48,5	112,0
LiCl, mole/l	0,1	0,1
Mass of dissolved Re, g	2,6	1,3

Found for complex (I): C- 40,0; H 5,5; Re 13,5 wt.%. The empirical formula of a complex (I) -  $ReO_3(OBu^n)mBu^nOH$ . IR,  $cm^{-1}$ : 3338 ( $\nu$  O-H), 1072-1114 ( $\nu$  C-O), 2873-2959 ( $\nu$  C-H), 953-1044 ( $\nu$  Re=O), 628 - 904 ( $\nu$  Re - O, the bridge), 516 ( $\nu$  Re - O (R)).

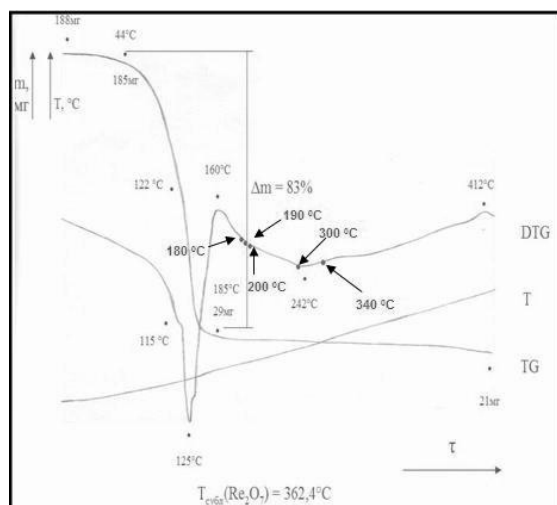


Fig.2. DTG-TGA analysis of complex (I) in air,  $T_{max} = 420$  °C

Found for complex (II): C 9,12; H 1,74 wt.%. The general formula of a complex (II) -  $(Re_4O_x(OEt)_x(OPr^i)_y)_n$ . IR,  $cm^{-1}$ : 1078 ( $\nu$  C-O), 920 ( $\nu$  Re - O - Re), 893 ( $\nu$  C - C), 540 ( $\nu$  Re - O (R)), 464 ( $\nu$  Re - OR (bridge)).

For revealing of dependence of structure of products of decomposition from temperature, isothermal annealing has been carried out in air (Table 2).

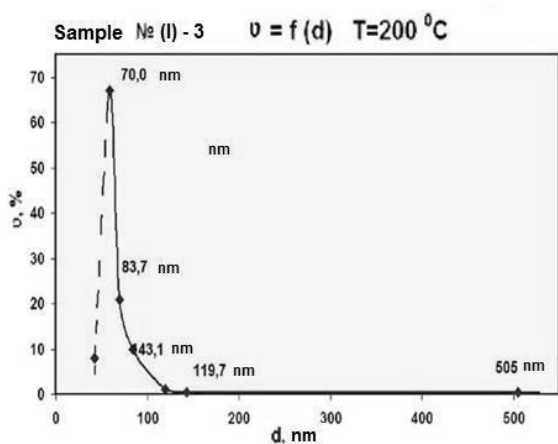
The following stage of work was measurement of the sizes of particles of the samples obtained at isothermal annealing of a complex (I). Measurement of the particles sizes was performed on the Delsa<sup>TM</sup>Nano Submicron Particle Size and Zeta Potential Analyzer PN A54412AA. Also dependences of number of particles ( $\nu$ , %) from diameter ( $d$ , nm) at various

temperatures (Fig. 3 (a)) and number of nano sized particles ( $T, ^\circ\text{C}$ ) (Fig. 3 (b)) were investigated.

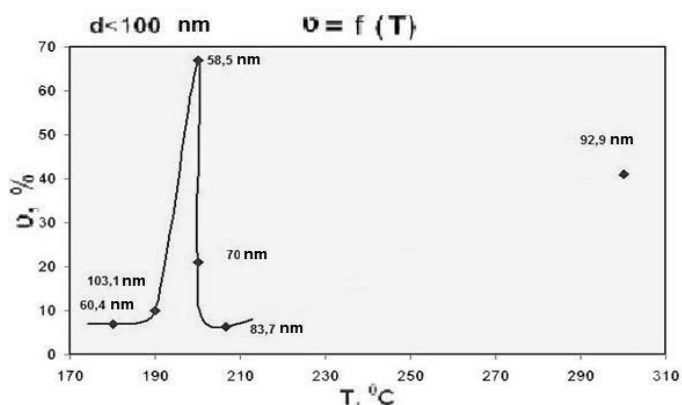
In all dependences there is a maximum which corresponds to the greatest number of ultra dispersed (nano sized) particles formed at the fixed temperature. Such distribution of particles in the sizes is caused by the reason that the complex decomposes not completely; hence, the quantity of nano sized particles is small. The complex decomposes at a rise in temperature and duration of annealing, so the quantity of nano sized particles is increased.

Table 2. Conditions of isothermal annealing of complexes (I) and (II)

Sample	$T, ^\circ\text{C}$	Dur., h	Decomposition product
(I) - 1	180	7	$\text{ReO}_3\text{cub}$
(I) - 2	190	4	-
(I) - 3	200	2	$\text{ReO}_2\text{orth} + \text{ReO}_3\text{cub}$
(I) - 4	300	5	-
(I) - 5	340	6	$\text{ReO}_2\text{orth} + \text{ReO}_3\text{cub}$
(II) -1	245	8	$\text{ReO}_3\text{cub}$
(II) -2	255	34	$\text{ReO}_3\text{cub}$
(II) -3	265	4	$\text{ReO}_2\text{orth} + \text{ReO}_3\text{cub}$



a



b

Fig.3. Dependence of number of particles ( $v, \%$ ) from diameter ( $d, \text{nm}$ ) of the product of thermal decomposing of the complex (I) in air (a) and number of nano sized particles

At the further rise of temperature the agglomeration happens, the number of nano sized particles is decreased. As shown on Fig.3 (b), at temperature  $200^\circ\text{C}$  the maximum quantity of nano sized particles (diameter  $59 \pm 5 \text{ nm}$ ) is formed.

In the Table 3 set granulometric composition of the complex (II) are presented.

Apparently from Table 3, nano sized particles of  $\text{ReO}_3\text{cub}$  with diameter  $24 \pm 5 \text{ nm}$  were obtained at step thermal decomposition of a complex (II) at the maximum temperature ( $255^\circ\text{C}$ ).

Table №3. Distribution of the sizes and number of particles of products of thermal decomposition of the complex (II) depending on temperature of annealing for various ranges of measurement of diameter of particles

Range of measurement of diameter of particles, nm	$T, ^\circ\text{C}$	$v, \%$	$d, \text{nm}$
$d < 100$	255	60	20
		26	24
		14	29
$100 < d < 200$	245	36	119
		29	140
		9	164

## Conclusions

Electrochemical synthesis of complex Re with n-butanol (**I**) was carried out. It is established that at  $T = 200^{\circ}\text{C}$  the complex (**I**) decomposes with formation of a mix of oxides  $\text{ReO}_3$  (cub) and  $\text{ReO}_2$  (orth) in the condensed phase. Electrochemical synthesis of the complex Re with ethanol and isopropanol (1:1 mol/mol, membrane) (**II**) was also carried out. It was shown that at  $255^{\circ}\text{C}$  it decomposes with formation of  $\text{ReO}_3$  (cub).

Methods of obtaining of ultra dispersed (nano sized) oxide Re (VI) with  $d=24\pm 5$  nm and mixes of oxides Re (IV) and Re (VI) with  $d=59\pm 5$  nm were developed.

**Acknowledgments:** This work was supported by Russian Foundation for Fundamental Research (project no. 09-03-00328).

## References

1. Palant A.A., Troshkina I.D., Chekmarev A.M. *Rhenium metallurgy*, 2007. M., «Nauka». p.298
2. Naumov A.V. *Rhenium rhythms (review of world market)*, Nonferrous metallurgy transaction, 2007, V.6, P. 36-41.
3. Ryashenceva M. A., Minachev H. M. *Renii i ego soedineniya v geterogennom katalize*, M.: Nauka, 1983. p.248.
4. J.Bregeault, B. El Ali, J. Martin, C. Martin, F. Derdar, G. Bugli, M. Delamar *Novel rhenium catalysts (chlorides and/or alkoxides dispersed on inorganic supports) for metathesis: a comparison with ammonium perrenate precursors*, J. of Molecular catalysis, 1988, № 46, P. 37-60

6.5.

## VOLATILE TECHNETIUM CARBONYL COMPOUNDS AND PROSPECTS FOR THEIR APPLICATION

G.V. Sidorenko<sup>1</sup>, A.E. Miroslavov<sup>1</sup>, D.N. Suglovov<sup>1</sup>, A.A. Lumpov<sup>1</sup>, and A.N. Yalfimov<sup>2</sup>

<sup>1</sup> Khlopin Radium Institute, Research and Production Association, Federal State Unitary Enterprise, 2-i Murinskii pr. 28, St. Petersburg, 194021 Russia

<sup>2</sup> Russian Research Centre for Radiology and Surgical Technologies, St. Petersburg–Pesochnyi, Russia

The results obtained in synthesis and studies of volatile technetium carbonyl compounds (mainly by the authors) are summarized. The main chemical forms of these complexes are considered:  $Tc_2(CO)_{10}$  and its analogs, Tc(I) carbonyl halides, products of replacement of CO groups and halide ions by other ligands, and technetium carbonyl hydrides. The results of studies of technetium carbonyl complexes in the gas phase by IR spectroscopy and mass spectrometry are analyzed. Vaporization of volatile technetium compounds is characterized by the preparative sublimation conditions and temperature dependences of the saturated vapor pressure. Factors affecting the capability of technetium carbonyl compounds for vaporization are discussed. The thermal stability of technetium carbonyl complexes is analyzed in the aspects of resistance to decarbonylation (for higher carbonyls), loss of  $\sigma$ -donor ligands (for heteroligand complexes containing  $\sigma$ -donor ligands), and deep degradation. Unique properties of  $\beta$ -diketonates as ligands for designing volatile compounds are demonstrated.

The possibility of using technetium carbonyl compounds for chemical vapor deposition of corrosion-resistant technetium coatings is examined. Such coatings can be of interest for protection of certain units operating in seawater from biofouling. Samples of technetium coatings on model supports were prepared from a large series of volatile carbonyl precursors. The chemical and physical compositions of the coatings were determined, and their corrosion resistance in seawater was evaluated. Some samples are not inferior to dense Tc foil in the corrosion resistance.

The volatility of technetium carbonyl compounds opens new prospects for their use in nuclear medicine. First, transfer of the complexes through the gas phase allows preparation of radiopharmaceuticals free of any foreign reagents and of finely dispersed carriers which may exert a side effect on the patient. Second, it becomes possible to perform chemical transformations in nonaqueous media starting from higher technetium carbonyls, i.e., routes to compounds synthetically inaccessible from the standard precursor, tricarbonyl triaqua complex  $[Tc(CO)_3(H_2O)_3]^+$ , are opened. Third, the volatility allows technetium compounds to be directly used for diagnostics of respiratory organs with inhalation administration.

Technetium-99m pentacarbonyl iodide prepared by carbonylation of the eluate from a technetium generator at a high CO pressure in the presence of HI and released into the gas phase in the course of relieving CO pressure demonstrated selective and persistent accumulation in lungs of laboratory animals at intravenous administration. This property, in combination with the volatility of the complex and possibility of its inhalation administration, opens a unique possibility of using the same agent for investigation of both lung perfusion and lung ventilation. The images of lungs of laboratory animals, obtained with intravenous and inhalation administration of  $[^{99m}TcI(CO)_5]$ , are presented. However, additional studies are required to evaluate the selectivity of this agent in revealing possible pathologies.



6.6.

## SYNTHESIS AND CHARACTERIZATION OF Ni-M (M = Pd, Pt) NANOPARTICLE PAIR STRUCTURES

E.V. Abkhalimov, B.G. Ershov

Institution of Russian Academy of Sciences - A.N. Frumkin Institute of Physical Chemistry and Electrochemistry of RAS (Leninsky prosp. 31-4, Moscow, Russian Federation)

The process of interaction of nickel nanoparticles (Ni NPs) with ions of Pd(II) and Pt(II) was studied. Bimetallic nanoparticle pair structures were synthesized.

The process was performed in two steps. The Ni NPs were synthesized through the chemical reduction  $2 \times 10^{-4}$  M Ni<sup>2+</sup> in water in the presence of the  $1 \times 10^{-4}$  M sodium polyacrylate (M. w. = 2100 g/mol) by sodium borohydride.

Nickel ions reduction occurred instantly after adding of NaBH<sub>4</sub>, solution color changed to yellow. In ultraviolet range formation of the specific for Ni NPs absorption band at 215 nm was observed [1]. According to TEM, nickel nanoparticles were of spherical shape and narrow size distribution with mean diameter 5 nm.

Interaction of Ni NPs with Pd(II) и Pt(II) led to formation of palladium and platinum nanoparticles. Reduction of the metal ions took place at surface of the nickel nanoparticles. According to the spectrophotometric data, reduced noble metal layers did not cover the entire surface of Ni NPs. Gradual addition of Pt(II) was accompanied by significant increase of optical density in the whole range of UV-VIS wavelengths. At concentration ratio Ni/Pt  $\leq$  2:1, formation of shoulder at 220 nm in solution spectrum was observed.

Addition of Pd(II) resulted in progressive decrease of light absorption and scattering by the solution. TEM and electron diffraction studies proved that synthesized bimetallic nanoparticles Ni-M (M = Pd, Pt) were of contact pair type.

**Acknowledgments:** The work was supported by Russian Foundation for Basic Research grant 09-03-00432-a.

### References:

1. B.G. Ershov, *Izv. Akad. Nauk, Ser. Khim.*, №10: p. 1733 (2000).

6.7.

## Pd NANOPARTICLES IN AQUEOUS SOLUTIONS: SYNTHESIS AND PROPERTIES

R.D. Solovov<sup>1</sup>, P.A. Morozov<sup>2</sup>, B.G. Ershov<sup>2</sup>

<sup>1</sup> - M.V. Lomonosov Moscow State Academy of Fine Chemical Technology  
(Vernadskogo prosp. 86, Moscow, Russian Federation)

<sup>2</sup> - Institution of Russian Academy of Sciences - A.N. Frumkin Institute of Physical Chemistry and  
Electrochemistry of RAS (Leninsky prosp. 31-4, Moscow, Russian Federation)

Studies on two techniques of palladium nanoparticles (PdNPs) synthesis in aqueous solutions were performed. PdNPs were synthesized through chemical reduction of dissolved of Pd<sup>2+</sup> ions by gaseous hydrogen or photochemical reduction of deaerated Pd<sup>2+</sup> solutions by UV-VIS radiation of xenon high-energy pulsed lamp. Process of photo-induced reduction was enhanced by using of sodium formate as a source of reducing  $\cdot\text{COOH}$  radicals in irradiated samples. Stabilizing agents used were sodium polyphosphate (NaPP) and sodium polyacrylate (NaPA); both polymers were of molecular weight  $\sim 2100$  g/mol.

**H<sub>2</sub>-Process.** Investigation of the effect of stabilizing agent concentration on PdNPs stability proved that sodium polyacrylate was more preferred surfactant: the lowest concentration ratios providing long-term stability of nanoparticles for [Pd<sup>2+</sup>]/[NaPP] and [Pd<sup>2+</sup>]/[NaPA] were 1:20 and 1:2.5 respectively. Studies of chemical reduction of Pd<sup>2+</sup> with concentration up to 0.75 mM showed that the initial concentrations of Pd<sup>2+</sup> allowing to produce sedimentation stable nanoparticles were as high as 0.5 mM; using of higher [Pd<sup>2+</sup>]<sub>0</sub> values led to rapid precipitation of palladium black. Furthermore, the sedimentation of PdNPs stabilized with NaPP was accompanied by particles flocculation, what had not been observed in the similar experiments with NaPA solutions. The atypically significant effect of [Pd<sup>2+</sup>]<sub>0</sub> on sizes of hydrogen-reduced particles was revealed: at [Pd<sup>2+</sup>]<sub>0</sub>=0.35 mM mean diameter of Pd-NPs was 30 nm and at [Pd<sup>2+</sup>]<sub>0</sub>=0.50 mM it was 45 nm. Size distributions and dispersity of PdNPs with both surfactants were found to be quite similar; however polyacrylate-stabilized particles were 2 to 5 times more sedimentation-stable.

**Photochemical process.** The optimal concentration of sodium formate used in irradiation-induced reduction was found to be 10 times as high as Pd<sup>2+</sup> concentration. Obtained PdNPs exhibited narrow size distribution, Pd-NaPP and Pd-NaPA particles diameters were 2–7 nm and 1.5–4 nm respectively (at [Pd<sup>2+</sup>]<sub>0</sub>=0.2 mM). The fact that Pd-NP synthesized photochemically were of lesser size is explained by the difference of nanoparticles formation mechanisms – intensive irradiation of solution results in instant formation of Pd seeds over the entire volume of sample, while the interaction of H<sub>2</sub> with Pd<sup>2+</sup> takes place on the surfaces of a limited number of the most active nucleating centers.

**Acknowledgments:** The work was supported by Russian Foundation for Basic Research grant 09-03-00432a.

6.8.

## WAVELET ANALYSIS OF EXAFS SPECTRA AS APPLIED TO POLYNUCLEAR AND CLUSTER TRANSITION METAL COMPLEXES

V.Yu. Murzin,<sup>1,2</sup> Ya.V. Zubavichus,<sup>1</sup> M.V. Chukalina,<sup>3</sup> A.A. Shiryaev,<sup>4</sup> K.E. German<sup>4</sup>

<sup>1</sup>National Research Centre "Kurchatov Institute", Moscow, Russia

<sup>2</sup>A.V. Topchiev Institute of Petrochemical Synthesis RAS, Moscow, Russia

<sup>3</sup>Institute of Microelectronics Technology RAS, Chernogolovka, Moscow District, Russia

<sup>4</sup>A.N. Frumkin Institute of Physical Chemistry and Electrochemistry RAS, Moscow, Russia

**Keywords:** EXAFS, wavelet transformation, coordination compounds, clusters, nanoparticles, technetium, rhenium, palladium

### Abstract:

An approach to a qualitative analysis of EXAFS spectra based on the Morlet wavelet transformation is extensively tested for a series of Re, Tc, and Pd reference compounds with variable coordination environments of the central atom. A possibility of straightforward differentiation between M-N(O)/M-Cl/M-Br/M-M (M=Pd, Re, or Tc) contributions in the first and second coordination shells based on peak positions in 2D wavelet maps is demonstrated, which is extremely important as an initial stage of EXAFS spectra interpretation prior to model construction and fitting. The potential of this approach in structural studies of complex cluster species and nanoparticles is discussed.

### Introduction

EXAFS spectroscopy is a very common experimental technique capable of retrieving local structure information for functional materials irrespective of their aggregate state and degree of structural ordering therein [1]. Since 1970-s, the Fourier transformation is the most common way for representing EXAFS spectra in a descriptive form [2]. Well separated coordination shells of neighbors around a central atom appear as distinct peaks in the Fourier transform (FT), and thus EXAFS FTs are often referred to as pseudoradial distribution functions in an analogy with atomic pairwise distribution functions (PDF) [3] or radial electron density (RED) [4] obtained from total X-ray scattering.

However, in those cases when a few groups of different atoms are located at similar distances, their contributions in EXAFS overlap producing complex and difficult-to-interpret interference patterns in FTs.

The wavelet transform (WT) represents an alternative and potentially more powerful approach to retrieve useful information from EXAFS spectra, as has been suggested quite recently by M. Chukalina, et al. [5,6]. The WT has been widely used in different fields and applications such as sound and image processing, data compression and digital signal de-noising [7]. When applied to EXAFS data analysis, the WT is capable of providing not only radial distance information, but it resolves data in k space as well giving a quick-glance estimate of the atomic number Z of an element in a specific coordination sphere [8].

## Mathematical background

Fourier transformation  $f_R$  of a one-dimensional signal  $f(k)$  defined over a finite value range is given by:

$$f_R = \frac{1}{2\pi} \int_{-\infty}^{\infty} f(k) \exp(-i\omega k) dk \quad (1)$$

The Fourier spectrum of the signal retains only its coordinate component, whereas the momentum component is lost. The use of windowed Fourier transform [9] partly overcomes this drawback. In the case of windowed Fourier transform, a  $f(k)$  is analyzed only within a limited window  $g_R$ . The Fourier image is then given by:

$$f_R = \int_{-\infty}^{\infty} f(k) g(k) \exp(-i\omega k) dk \quad (2)$$

This implies that the signal is localized within a certain momentum range. Unfortunately, the window has a limited width independently of the specific scale of interest. Furthermore, the width is described by different functions along the coordinate and momentum axes. In contrast, the wavelet transformation automatically gives rise to a window effectively adapted to the signal being processed, i.e., to main distance-frequency contributions present in the spectrum [10].

The wavelet transformation is generally formulated as:

$$f_R = \int_{-\infty}^{\infty} f(k) \psi_{ab}(k) dk \quad (3)$$

where  $\psi_{ab}$  is the so-called mother wavelet function.

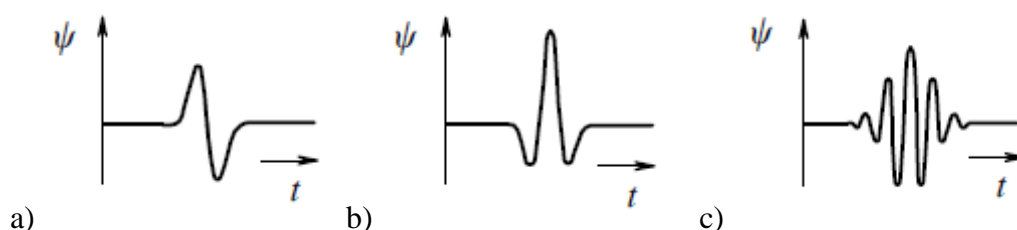


Fig. 1. Examples of mother wavelet functions. a) WAVE, b) MHAT, c) Morlet.

A lot of such functions can be constructed [11] (Fig.1), but the Morlet wavelet is probably one of the most efficient and widespread among them. The Morlet wavelet is given by [12]:

$$\psi_{ab} = \frac{1}{\sqrt{2\pi}\sigma} \left( \exp(i\kappa k) - \exp\left(-\frac{\sigma^2 \kappa^2}{2}\right) \right) \exp\left(-\frac{k^2}{2\sigma^2}\right) \quad (4)$$

Essentially, the Morlet function is an amplitude-modulated sinusoid with a frequency  $\kappa$ , which is evanescent beyond a Gaussian of a specific half-width  $\sigma$ . It is evident that the dependence of the wavelet signal on  $R$  becomes fully analogous to the Fourier transform at large  $\kappa$ . With a decrease in  $\kappa$ , the momentum resolution improves. An increase in  $\sigma$  gives rise to a worse resolution in  $k$  at the costs of a better resolution in  $R$ , which implies that simultaneously high coordinate and momentum resolutions remain elusive.

## Experimental

Experimental EXAFS spectra of a series of rhenium, technetium, and palladium reference compounds have been measured at the Structural Materials Science beamline installed at the Kurchatov Synchrotron Radiation Source [13]. The electron storage ring Siberia-2 operated at an electron energy of 2.5 GeV with an average current stored of 100 mA. A Si(111) channel-cut monochromator was used to monochromatize the incident synchrotron beam. The spectra were measured in the transmission mode using two ionization chambers filled with appropriate Ar-Xe

gas mixtures before and after the sample. Preliminary processing of the raw EXAFS spectra has been performed with Athena program from the IFEFFIT software package [14].

A dedicated software code WAVES (Wavelet Analysis & Visualization for EXAFS Spectroscopy) has been developed to apply the wavelet transformation to normalized oscillating parts of experimental EXAFS spectra. The code is written using the C++ API of the QT programming environment. It reads the experimental background-subtracted unweighted oscillating EXAFS signal as data input along with processing parameters, such as weighting power  $n$ ,  $\kappa$ ,  $\sigma$ , ranges of interest in  $k$  and  $R$  spaces from a dialog window and then performs numerical integration according to the above formulas.

## Results

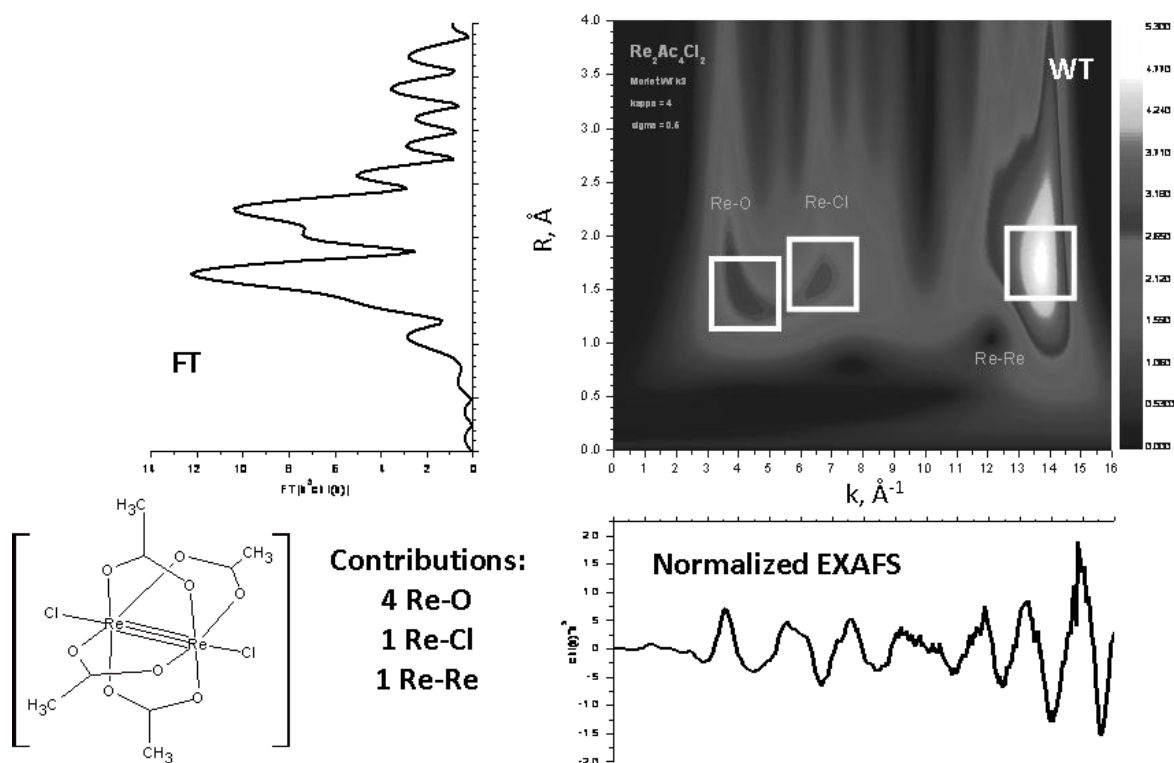


Fig. 2. Comparison of information content in FT and WT representations of Re  $L_3$  EXAFS for rhenium chloroacetate  $\text{Re}_2(\text{Ac})_4\text{Cl}_2$  with very short Re-Re bonds.

An illustrative example comparing traditional FT and the WT-based representations of an EXAFS spectrum is given in Fig. 2, which concerns a dimeric rhenium chloroacetate complex [15]. In this complex, the coordination environment of each rhenium atom includes 4 oxygen atoms, 1 chlorine atom, and 1 rhenium atom at a very short distance of ca. 2.2 Å due to the formally quadruple character of this metal-metal bond as schematically shown in Fig. 2 (lower left panel). The Fourier Transform of the Re  $L_3$ -edge EXAFS spectrum reveals two dominant peaks at around 1.5 and 2.0 Å, neither of which can be reliably attributed to a specific interatomic contact due to a heavy interference between the three contributions. In contrast, all three contributions, viz., Re-O, Re-Cl, and Re-Re, are nicely resolved in the WT map. Furthermore, it becomes evident that both FT peaks are actually dominated by the Re-Re contribution located at (14 Å<sup>-1</sup>; 1.75 Å) but the true maximum of the Re-Re contribution occurs in the FT as an apparent deep between the two maxima due to the interference with the Re-O and Re-Cl signals.



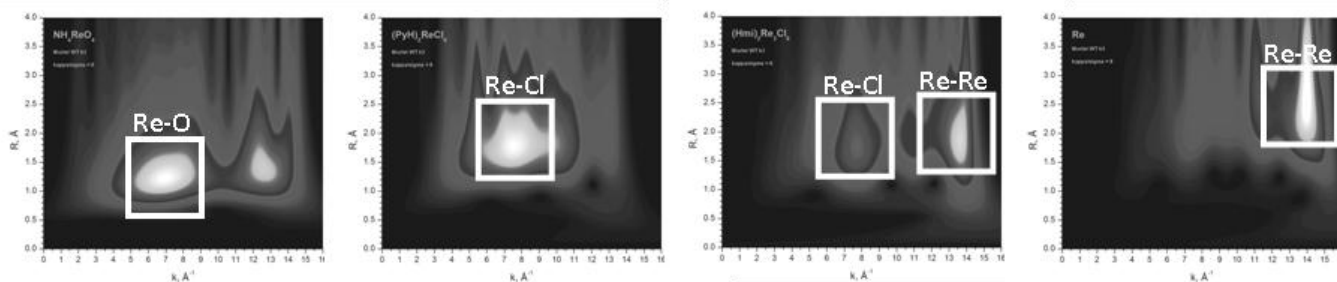


Fig. 3. WT maps of  $Re\ L_3$ -edge EXAFS spectra for reference compounds with different coordination environments of the rhenium atoms. From left to right: ammonium perrhenate  $(NH_4)ReO_4$ , pyridinium hexachlororhenate  $(PyH)ReCl_6$ , hexamethyleneiminium octachlorodirhenate  $(HMI)_2Re_2Cl_8$ , and metallic rhenium.

The high information content of WT maps is further verified in Figs. 3-6, which compare the WT representations of EXAFS spectra for an assortment of rhenium, technetium, and palladium reference compounds. As it can be deduced from the graphs, the peak position corresponding to a specific interatomic contact CA-N (central atom – neighbor) in the WT map is uniquely determined by a combination of parameters  $Z_{CA}$ ,  $Z_N$ ,  $R_{CA-N}$ , and  $\sigma^2_{CA-N}$ . The “rule of thumb” for the interpretation of the positions can be formulated as follows: a WT peak appear at larger  $k$  values for heavier CA-N pairs and for more rigid bonds characterized by narrow distance distributions (which is equivalent to small values of the respective  $\sigma^2_{CA-N}$ ). For instance, the Re-O contributions for chloroacetate and perrhenate along the  $k$  axis occur at ca. 4 and 7  $\text{\AA}^{-1}$ , respectively, which is due to the effect of the Debye-Waller factors: Re-O bonds in perrhenate are more rigid than in acetate, which is additionally characterized by low symmetry. On the other hand, in the series of pure metals, the M-M peak occurs at 8.5, 9.5, and 14  $\text{\AA}^{-1}$  for Tc, Pd, and Re exactly in a series of increasing atomic numbers.

These regularities also apply to the second-coordination-shell neighbors, as demonstrated by the Pd...O (Pd-N-O) peak for tetranitropalladate and Pd...Pd (Pd-O-Pd) peak in palladium oxide.

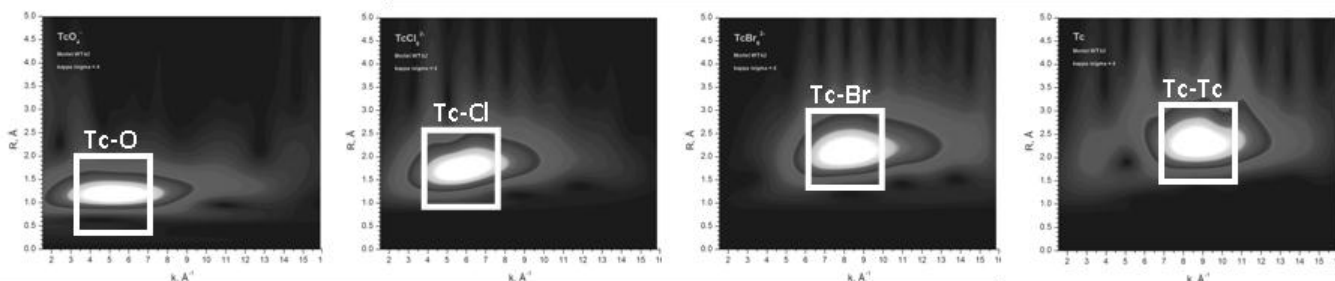


Fig. 4. WT maps of  $Tc\ K$ -edge EXAFS spectra for reference compounds with different coordination environments of the technetium atoms. From left to right: tetraphenylphosphonium pertechnetate  $(TPP)TcO_4$ , tetraethylammonium hexachlorotechnetate  $(TEA)TcCl_6$ , tetramethylammonium hexabromotechnetate  $(TMA)TcBr_6$ , and metallic technetium.

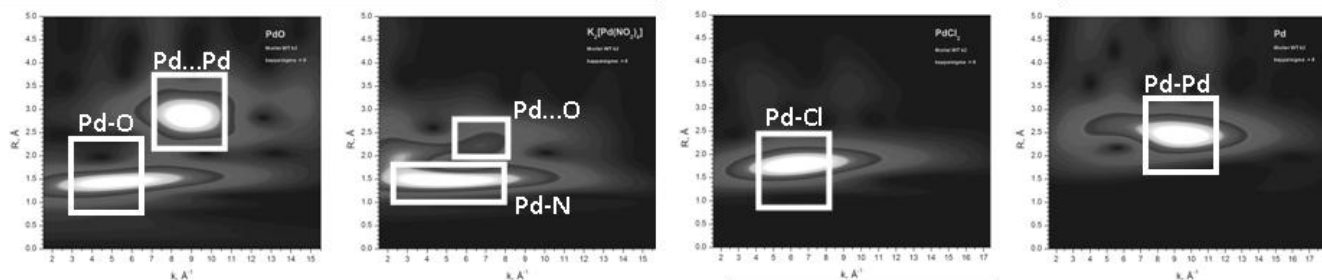


Fig. 5. WT maps of  $Pd\ K$ -edge EXAFS spectra for reference compounds with different coordination environments of the palladium atoms. From left to right: palladium oxide  $PdO$ , potassium tetranitropalladate  $K_2Pd(NO_2)_4$ , palladium chloride  $PdCl_2$ , and metallic palladium.

## Conclusions

The examples shown above clearly demonstrate that the WT is indeed a quite informative and instructive way to represent EXAFS spectra prior to more thorough model-based quantitative analysis. Elements with different atomic numbers  $Z$  (typically, from different rows of the Periodic system) are characterized by clearly distinguishable positions along the  $k$  axis of the wavelet maps. The wavelet representation is especially useful for complex and nanostructured materials with mixed-ligand coordination of metal atoms.

**Acknowledgments:** The work was accomplished using the equipment of the Center for collective use “Kurchatov Center for Synchrotron Radiation and Nanotechnology” supported by Russian federal contract 16.552.11.7003.

## References

1. Y. V. Zubavichus, Yu. L. Slovokhotov. *Russ. Chem. Rev.* **70**, 373-403 (2001).
2. F.W. Lytle, D.E. Sayers, E.A. Stern. *Phys. Rev. B* **11**, 4825–4835 (1975).
3. T. Egami, S.J.L. Billinge (Eds.). *Underneath the Bragg peaks. Structural analysis of complex materials*. Pergamon, Amsterdam, 2003.
4. E.M. Moroz. *Russ. Chem. Rev.* **80**, 315-334 (2011).
5. H. Funke, A.C. Scheinost, M. Chukalina. *Phys. Rev. B* **71**, 094110 (2005).
6. H. Funke, M. Chukalina, A.C. Scheinost. *J. Synchr. Rad.* **14**, 426-432 (2007).
7. Q. Tao, V.I. Mang, X. Yuesheng (Eds.). *Wavelet analysis and applications*. Birkhäuser-Verlag, Basel, 2007.
8. J. Timoshenko, A. Kuzmin. *Comp. Phys. Commun.* **180**, 920–925 (2009).
9. D. Gabor. *J. IEEE* **93**, 429-457 (1946).
10. I.M. Dremin, O.V. Ivanov, V.A. Nechitailo. *Physics-USpekhi* **44** 447–478 (2001).
11. N.M. Astafieva. *Physics-USpekhi* **39** 1085–1108 (1996).
12. P. Goupillaud, A. Grossman, J. Morlet. *Geoexploration* **23**, 85-102 (1984).
13. A.A. Chernyshov, A.A. Veligzhanin, Y.V. Zubavichus. *Nucl. Instr. Meth. Phys. Res. A* **603**, 95-98 (2009).
14. B. Ravel, M. Newville. *J. Synchrotron Rad.* **12**, 537-541 (2005).
15. P.A. Koz'min, M.D. Surazhskaya, T.B. Larina, A.S. Kotel'nikova, T.V. Misailova, *Koord. Khim.* **6**, 1256-1258 (1980) [In Russian].

6.9.

## NANODIAMONDS FOR BIOMEDICAL AND SORPTION APPLICATIONS: STRUCTURE AND DEFECTS

A.A. Shiryaev

Institute of Physical Chemistry and Electrochemistry, RAS, Leninsky pr. 31, Moscow 199991, Russia;  
[shiryaev@phyche.ac.ru](mailto:shiryaev@phyche.ac.ru)

Nanodiamond (ND) particles belong to a broad family of nanocarbon-based materials with a structural diversity that is based on specific synthesis conditions, post-synthesis processes, and modifications. ND particles with sizes up to several tens of nanometers currently find broad application in polishing, structural materials, and lubricants, as well as prospective applications in biotechnology and medicine.

Recently, several important new application areas have been proposed based on the potential of incorporating impurity atoms and point defects into the nanoparticle lattice. Major breakthrough areas where controlled doping of NDs and on-demand production of the nitrogen-vacancy (N-V) centers. The spin state of the negatively charged N-V center can be polarized by optical pumping and can be manipulated using microwaves, permitting implementation of an efficient single photon emitters for quantum information processing or a magnetic sensor with a nanoscale resolution. Optical transitions in the N-V centers in diamond provide bright and stable photoluminescence.

We have recently shown that very small nanodiamond particles (1-2 nm) may also possess bright luminescence from another defect - Silicon –Vacancy complex (Si-V) [1]. Thus, on-demand production of the N-V and Si-V centers in nanodiamond is of paramount importance for quantum information processing and quantum computing, nano-scale imaging magnetometry and photoluminescent probes for bio-research. We will discuss recent advances in understanding defects and structural peculiarities of nanodiamonds, important for various applications.

Another important and yet not fully explored niche for nanodiamonds is their application as sorbents. Various ways of surface modification are invented, thus allowing creation of efficient, durable and reusable nanodiamond-based sorbents. Recent results on radionuclides sorption will be reported.

### References:

1. Shiryaev et al., *Geochim. Cosmochim. Acta.* **75**, 3155-3166 (2011)
2. Vlasov et al., *Small* **6**, 687-694 (2010)

6.10.

## **NANOTECHNOLOGIES IN RADIOCHEMICAL TECHNOLOGY AND RADIOECOLOGY INCLUDING TECHNETIUM SPECIATION AND SEPARATIONS**

Tananaev I.G., K.E. German

Frumkin Institute of physical chemistry and electrochemistry of RAS, 119071, Moscow, Leninsky prospekt, 31/4, geokhi@mail.ru

Modern approaches to sustainable development of Atomic Energy, development and improvement of nuclear fuel cycle in Russia are directly linked to the development of nanoindustry. The following items will be elucidated and discussed herein: major scientific advances in the production of nuclear fuel compositions, search of new technologies for the reprocessing of spent nuclear fuel (SNF) and optimization of existing ones, the solutions of the problem of radioactive waste of different activity levels management, development of radioecology. Information about search results in getting of oxide fuel modified compositions will be presented in the report also. The results on the synthesis and use of heterogeneous catalysts based on noble metal nanoparticles drawn on the carrier surface to improve processing of SNF also will be presented. The advanced technologies of water low-acid and fluid (in liquid CO<sub>2</sub>) dissolution of uranium and plutonium oxides resulting in significant decrease of radioactive waste volume will be also considered.

With respect to nuclear waste treatment we shall discuss the major results for processing both liquid (water/organic) and gaseous wastes using nanocollectors for cleaning of industrial drain productions, pieces of carbon materials (activated and modified coals, nanotubulens), as well as sorbents for fixing of various forms of radioactive iodine based on Ag nanoparticles, respectively key results in producing the above mentioned carbon materials, including development of method of electron-beam conversion of ligno-cellulosic material to obtain nanoporous coals with unique physical and chemical properties will be presented. Also the data on processing of alkali radioactive material handling, methods of improvements of various solid matrixes (cement compounds, glass composition, ceramics materials) by method of nano-additives for immobilization of high-level waste will be proposed.

In the end of the report data on development of methods of radionuclides and especially technetium-99 determination and concentration in environmental media objects using nanostructured high-performance agents – extractans and sorbents will be given. On the basis of the information submitted will provide key conclusions on advisability and development of researches in the field of nanoindustry in radiochemical technology and radioecology.

**Acknowledgments:** The work was partially supported by the Russian Foundation for Basic Research (Projects № 09-03-00017).

6.P1.

## HIGH TEMPERATURE INTERACTION OF RHENIUM, MOLYBDENUM AND TUNGSTEN WITH URANIUM MONONITRIDE

G.S. Bulatov, K.N. Gedgovd, D.Yu. Lyubimov<sup>1</sup>.

Institution of Russian Academy of Sciences – A.N. Frumkin Institute of Physical Chemistry and Electrochemistry of RAS (Leninsky prosp. 31-4, Moscow, Russian Federation)

<sup>1</sup>ENTERPRISE OF “ROSATOM” - FEDERAL STATE UNITARIAN ENTERPRISE “SCIENTIFIC RESEARCH INSTITUTE SCIENTIFIC INDUSTRIAL ASSOCIATION “LUCH” (24, Zheleznodorozhnay st., Podolsk, Moscow region, Russian Federation)

**Keywords:** nuclear fuel, uranium mononitride, rhenium, molybdenum, tungsten, diffusion coefficients

### Abstract:

The interaction between uranium mononitride and refractory metals: rhenium, molybdenum and tungsten at the temperature 1773 were investigated.

Diffusion coefficients of uranium from UN into Re, Mo and W in different structure state (polycrystalline and single crystal metals) have been estimated. The acceleration of uranium diffusion into the depth of the polycrystalline metals was associated with the diffusion at the grain boundaries.

### Introduction

The study was aimed to research the new materials for the utilization in high temperature nuclear devices and to increase their efficiency and safety [1].

### Experimental

The interaction of nitride nuclear fuel  $U(N_{0.90} C_{0.05} O_{0.07})_{1.02}$  with rhenium, molybdenum and tungsten metals acting as cladding materials at  $T=1773$  K was investigated. Uranium in the fuel was enriched in  $^{235}U$  to 90 %. Uranium nitride and metal samples in a form of the disks, possessing 2 -3 mm thickness and 8 – 9 mm diameter were placed in turn into the rhenium, molybdenum and tungsten metal ampoules. The ampoules were welded in vacuum and annealed in the vacuum furnace at 1773 K for 1000 hours. The diffusion coefficients of uranium from UN to Re, Mo and W were determined using layer by layer radiometric analysis, measuring the integral  $\alpha$ -activity of metal samples. The diffusion coefficients values were calculated in terms of diffusion model for the constant source to the semi-infinite body using the equation [2]:

$$I_i / I_0 = \operatorname{erfc} [x_i / 2(Dt)^{1/2}],$$

where:  $I_i$  - integral  $\alpha$ -activity on the depth  $x_i$ ,  $I_0$  - integral  $\alpha$ -activity on the depth  $x_0=0$ ,  
 $D$  - diffusion coefficient,  $t$  – time.

### Results and Discussion

The interaction of uranium mononitride with these metals at 1773 K was accounted for the diffusion of the fuel components to the metal samples (Fig. 1-3). Using autoradiography technique the difference in the diffusion mechanism for single crystals and polycrystalline samples was



established. The acceleration of uranium diffusion into the depth of the polycrystalline metals was associated with the diffusion at the grain boundaries (Fig. 1).

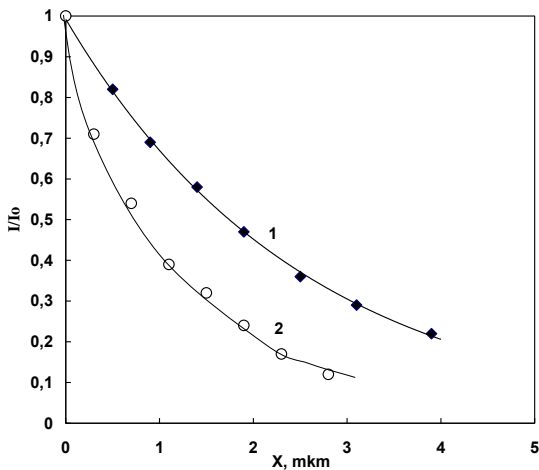


Fig. 1. Radiometric curves for polycrystalline -1 (with a - autoradiography of diffusion  $U \rightarrow Re$ ,  $\times 200$ ,  $X=5 \mu m$ ) and single crystal - 2 rhenium samples

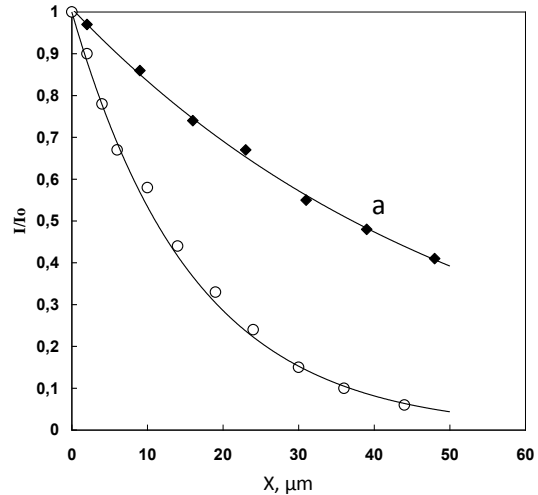


Fig. 2. Radiometric curves for polycrystalline -1 and single crystal -2 molybdenum samples

The corresponding diffusion coefficients values for uranium into polycrystalline ( $D_1$ ) and single crystal samples ( $D_2$ ) were determined as:

$$D_1 (U \rightarrow Re) = 1.2 \times 10^{-18} \text{ m}^2 \times \text{s}^{-1},$$

$$D_1 (U \rightarrow Mo) = 3.7 \times 10^{-16} \text{ m}^2 \times \text{s}^{-1},$$

$$D_1 (U \rightarrow W) = 9.8 \times 10^{-20} \text{ m}^2 \times \text{s}^{-1},$$

$$D_2 (U \rightarrow Re) = 4.0 \times 10^{-19} \text{ m}^2 \times \text{s}^{-1},$$

$$D_2 (U \rightarrow Mo) = 4.9 \times 10^{-17} \text{ m}^2 \times \text{s}^{-1},$$

$$D_2 (U \rightarrow W) = 3.3 \times 10^{-21} \text{ m}^2 \times \text{s}^{-1}.$$

The presented data prove that the diffusion factors for uranium from UN to rhenium metal were lower than corresponding values for molybdenum and higher than for tungsten metals.

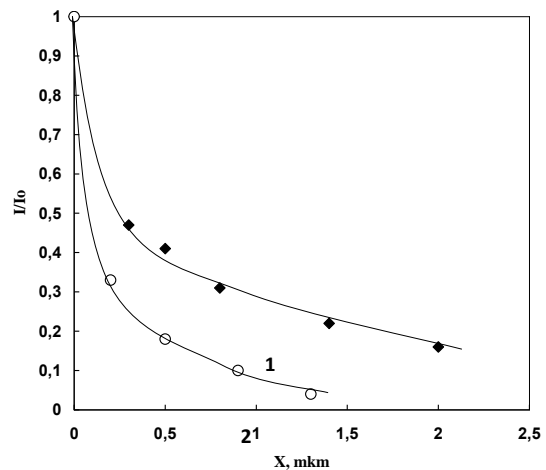


Fig. 3. Radiometric curves for polycrystalline - 1 and single crystal - 2 tungsten samples

### Conclusions.

The presented results may be taken into account in the development of the fuel elements based on uranium mononitride for their utilization in the high temperature reactors for ground and space installations.

### References.

1. V.P. Nikitin, B.G. Ogloblin, E.N. Sokolov. *Atom. Energ.* **88**: 95-108, (2000).
2. Bokshtein B.S. *Diffusion in Metals*, Metallurgiya: Moscow, (1978), 248 p.

6.P2.

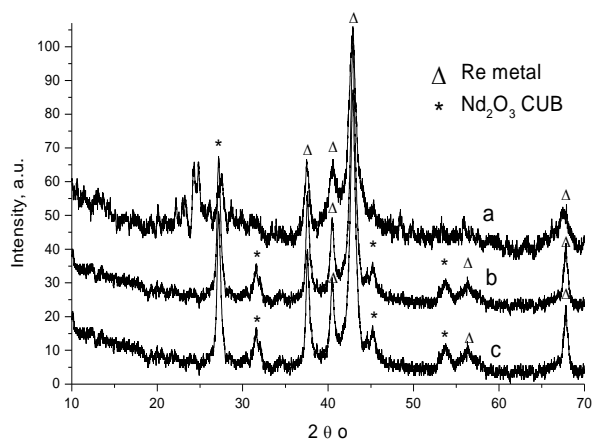
## THERMAL BEHAVIOR OF PERRHENATE COMPLEXES OF NEODYMIUM AND PREPARATION OF NANODIMENSIONAL RHENIUM CERMETES

A.M. Fedosseev, A.A. Bessonov, Ph. Moisy\*

IPCE RAS, Moscow, Leninskii pr.31- 4, 119071 Russia ( e-mail: [fedosseev@ipc.rssi.ru](mailto:fedosseev@ipc.rssi.ru))

\* - CEA – Marcoule, DEN DRCP, BP17171 – 30207, Bagnols sur Ceze, France

Trivalent f-elements perrhenate are proposed as promising precursor agents for cermet composites preparations. Regarding the targets for minor actinides and technetium incineration, the cermet composites are noted as the materials with the best thermal conductivity that can help to reduce the operating temperature. In this work efforts were focused in finding an original approach for their easy production. We propose a method of molecular  $\text{Re}(\text{Tc})\text{-Nd}_2\text{O}_3$  cermet preparation, where the rare earth element may serve as an analogue for americium and rhenium as an analogue for technetium, which transmutation should also be considered. For a complete understanding of the degradation process of the perrhenates under reductive conditions, thermoanalytical diagrams of  $\text{Nd}(\text{ReO}_4)_3 \cdot 4\text{H}_2\text{O}$  and  $\text{Eu}(\text{ReO}_4)_3 \cdot 4\text{H}_2\text{O}$  have been recorded in this work. These compounds originally contain four water molecules and the dehydration mechanism proceeds via similar schemes. Rhenium reduction with 6%  $\text{H}_2/\text{Ar}$  occurs at least in three stages distinctly observed in the TG profile of europium compound. The first reduction step starting at  $430^\circ\text{C}$ , is followed by a step at  $590^\circ\text{C}$  and a last one around  $620^\circ\text{C}$ . This thermodiagram profile leads to the conclusion that perrhenate reduction occurs via  $\text{ReO}_3$  and  $\text{ReO}_2$  intermediates to finally reach the metallic Re. Based on the thermogravimetric data, the temperature for  $\text{Nd}_2\text{O}_3\text{-Re}$  cermet preparation may be established at  $590\text{-}600^\circ\text{C}$ .



*X-ray diffraction patterns of  $\text{Nd}_2\text{O}_3\text{-Re}$  cermet prepared at  $600^\circ\text{C}$ : a: 1 hour, b: 4 hours, c: 10 hours*

X-ray powder diffraction patterns of samples obtained at this temperature show line broadening, obviously due to the low metal crystallinity in the nanodimensional cermet material. Nevertheless, the lines corresponding to rhenium metal as well as to cubic  $\text{Nd}_2\text{O}_3$  may be unambiguously identified. Increasing of the heating time at this temperature leads to very slow nanocrystalline cermet particles recrystallization. SEM, EDX and EDS spectra confirm clearly the high degree of distribution of the primary components in the cermet product.

6.P3.

## TECHNETIUM(VII) SORPTION BY MODIFIED NANODIAMONDS FROM AQUEOUS AND NITRIC ACID SOLUTIONS

Ya.A. Obruchnikova, A.A. Shiryaev, A.M. Safiulina, A.V. Karpukhin<sup>1</sup>  
I.I. Kulakova<sup>1</sup>, K.E. German

Institution of Russian Academy of Sciences - A.N. Frumkin Institute of Physical Chemistry and Electrochemistry of RAS (Leninsky prosp. 31-4, Moscow, Russian Federation)

<sup>1</sup> Lomonossov Moscow State University, (Leninskie gory, 1, Chem. Dept., Moscow, Russian Federation)

Nanodiamonds (ND) produced by detonation of high-energy explosives in oxygen-deficient environment present considerable interest for studies of nanoparticles and are also important for numerous applications in diverse fields ranging from tribology and photonics to biomedicine [1]. Many chemical properties of NDs are determined by surface radicals and currently various types of surface functionalisation are considered [2].

Technetium is a nuclear fission product and its reprocessing is often performed in intense radiation fields, precluding long-term use of many conventional ion-exchangers. High radiation stability of NDs may open new exciting possibilities for their applications in radiochemistry [3]. In our work we have studied Tc sorption on detonation nanodiamonds treated in different ways to modify surface radicals. The sample #1 represents NDs sintered at High Pressures – High Temperature conditions. The sample #3 is commercially available ND powder subjected to primary acid cleaning procedure after detonation. Such samples usually consist of very stable aggregates of ND grains. Whereas the size of the individual ND grains is 4-5 nm, the size of the aggregates lies between several tens to hundreds nanometers. Destruction of these aggregates is notoriously difficult. The sample #7 represents the disaggregated ND sample [4], i.e. it consists of individual 4-5 nm diamond particles. Its surface chemistry was not specially studied, though it is clear that it is dominated by various H- and O- containing radicals. The surfaces of the samples #2, 4-6 was modified by chemical and physical oxidation, see Table 1. The nanodiamond powders were ultrasonicated at ambient conditions.  $10^{-4}$ M Tc in H<sub>2</sub>O and HNO<sub>3</sub> solutions were prepared for sorption tests, the sorption efficiency was determined by  $\beta$ -LSC activity measurements of the solutions. Two samples (#2 – with surface aminogroups and #4 – heated in H<sub>2</sub> atmosphere at 800 °C) showed high efficiency towards Tc(VII) sorption. Their sorption efficiency is comparable to the best anionites. The ionic state of Tc in these solutions is anion pertechnetate TcO<sub>4</sub><sup>-</sup> and the most probable sorption mechanism should be anion exchange at the surficial cationic positions.

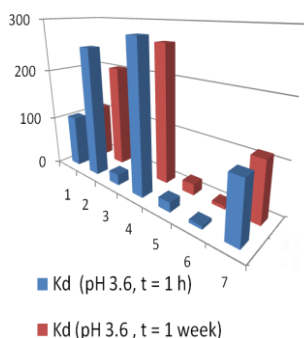


Fig. Distribution coefficients for sorption of Tc(VII) by modified nanodiamonds.

Table 1. Description of samples of detonation nanodiamonds

Sample No	Diamond treatment
1	Sintering at HPHT
2	HPHT sintered and aminated (NH-C <sub>18</sub> H <sub>37</sub> )
3	Standard industrial cleaning by HNO <sub>3</sub>
4	Heated in H <sub>2</sub> , 800 °C, 5 h
5	Oxidized by air at 450 °C
6	Oxidized by HNO <sub>3</sub> +H <sub>2</sub> SO <sub>4</sub>
7	Disaggregated

### References.

1. V.Yu. Dolmatov, *Russ. Chem. Rev.* **76**: 375-397.
2. I.I. Kulakova, *Solid State Physics* **46**: 621-629 (2004).
3. S.I. Chukhaeva, L.A. Cheburina, *Superhard materials (Russ.)* **2**: 43-48 (2000).
4. A. Kruger et al., *Carbon* **43**: 1722-1730 (2005)

6.P4.

## STABILIZATION OF NANO-RHENIUM AND NANO-TECHNETIUM IN AMORPHOUS CARBON MATRIX.

K.E. German<sup>1</sup>, M.S. Grigoriev<sup>1</sup>, A.Ya. Maruk<sup>1,2</sup>, Ya. V. Zubavichus<sup>3</sup>,

V.Yu. Murzin<sup>3</sup>, Ya.A. Obruchnikova<sup>1,4</sup>, A.A. Shiryaev<sup>1</sup>

1 - Institution of Russian Academy of Sciences - A.N. Frumkin Institute of Physical Chemistry and Electrochemistry of RAS (Leninsky prosp. 31-4, Moscow, 119071 RF)

2 - *Burnazyan Federal Medical Biophysical Center of FMBA Russia; 123182, Moscow, Zhyvopisnaya,46; e-mail: amaruk@list.ru*

3 – *National Research Center “Kurchatov Institute” (Kurchatov sq.1, 123182 Moscow, Russian Federation)*

4 - *D. Mendeleev University of Chemical Technology of Russia, Miusskaya Sq. 9, Moscow 125047, Russia.*

**Keywords:** technetium metal nanophase, rhenium metal nanophase, technetium carbide, rhenium carbide, amorphous carbon matrix

### Abstract

Metallic rhenium or technetium nano phases could be generated by thermal decomposition of perrhenates/pertechnetates of organic cations under argon, the parallel carbonization of the cations provides conditions favorable for formation of nano- and microparticles of Re and Tc carbides. For hexamethyleniminium and triphenylguanidinium pertechnetates the conversion proceeds with  $Tc_6C$  formation. In the thermal decomposition of triphenylguanidinium perrhenate only a mixture of Re metal, Re carbide and free carbon is formed. The nanocrystalline phases were X-ray amorphous, while for microcrystalline  $Tc_6C$  phase the cubic lattice with  $a = 3.98 \text{ \AA}$  was deduced. For the annealed sample the determined parameter  $a = 5,095 \text{ \AA}$  and the sp.gr.  $Pm3m$  indicates that the new Re carbide phase is isostructural with a number of Ln carbides.

### Introduction

The noble metals and also Re were considered till recently to have no or very small affinity to carbon [1]. The formation of a carbide  $TcC_{1-x}$  with low content of carbon ( $x = 0.83$ ) was proved [2,3] also indicating low affinity of Tc to carbon. Small amounts of carbon were shown to react readily with Tc metal causing its crystallographic distortion from *HCP* to orthorhombic structure and important enlargement of the specific unit cell volume [3]. This was confirmed by findings of distorted Tc metal and Tc carbide in thermal decomposition product of Tc carbonyls [4]. In this work we employ *in situ* carbonization in course of thermal decomposition of several organic pertechnetates and perrhenates aimed at the preparation of technetium and rhenium carbides.

## Results and discussion

The thermal decomposition of Tc and Re compounds taken as initial salts or supported at the  $\gamma$ -Al<sub>2</sub>O<sub>3</sub> as an inert ceramic carrier was studied in this work. In the first case the metals were micro-particulated and when the initial compounds underwent the fusion before the decomposition, macroagregates of metal or carbide phases were observed.

In the second case the nanophase Tc and Re metals or carbides were prepared depending on the nature of the cation and the macroparameters of thermolyses.

Under the conditions favoring metal Tc formation, the phase was initially X-ray amorphous. But the EXAFS analyses of the sample gave evidence for pure metal phase (Fig.1).

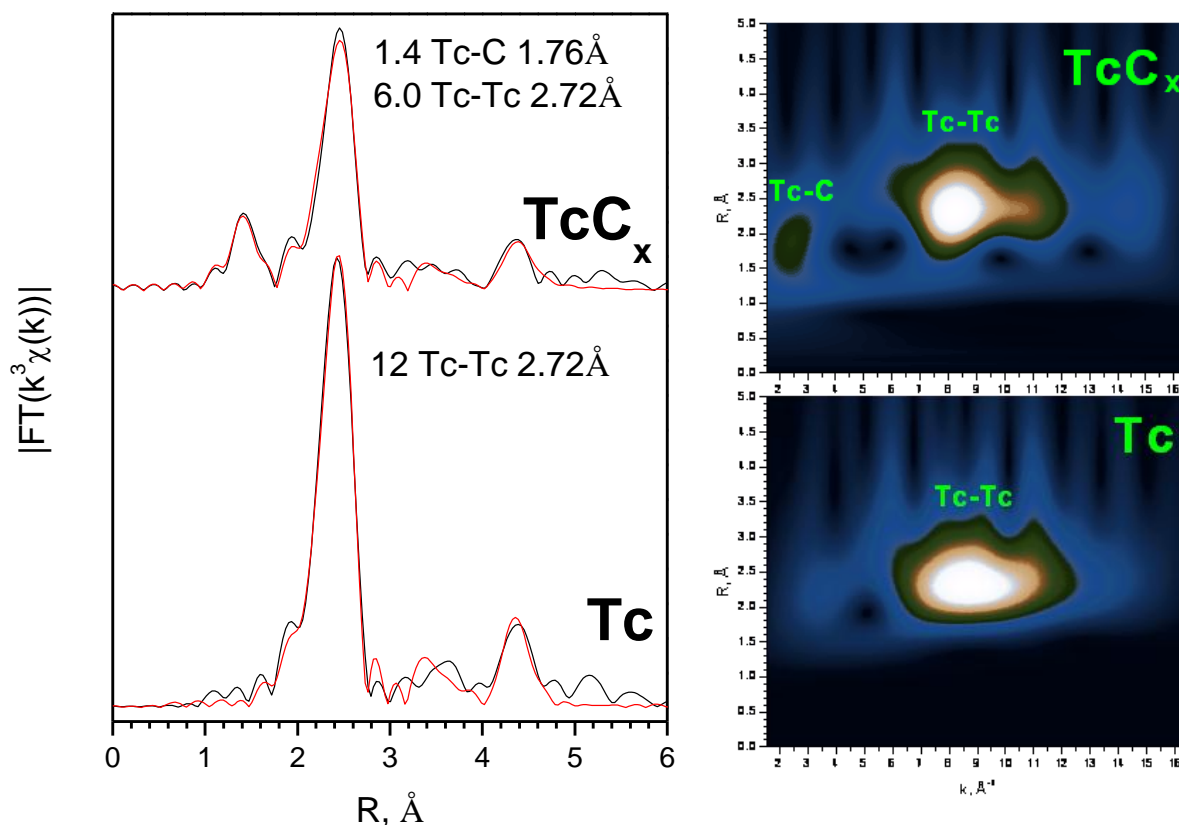


Fig.1. Tc K-edge EXAFS spectra of nanostructured Tc metal and carbide prepared by thermal decomposition of hexametyleniminium pertechnetate represented as Fourier (left) and Wavelet transforms.

Hexametyleniminium pertechnetate and triphenylguanidinium pertechnetate at 600 K in Ar gas undergo conversion to X-ray amorphous technetium carbide that could be stabilized in amorphous carbon matrix. Annealing of this product at 1073-1673 K leads to recrystallization and FCC structure with  $a = 3.98 \text{ \AA}$  forms.

Hexametyleniminium perrhenate and morfolinium perrhenate undergo conversion at 700 K in Ar gas to X-ray amorphous rhenium metal that is recrystallized under the subsequent annealing at 1073-1673 K to form HCP structure. Nanophases supported at the  $\gamma$ -Al<sub>2</sub>O<sub>3</sub> were X-ray amorphous.

In the thermal decomposition of TPGHReO<sub>4</sub> only a mixture of Re metal, Re carbide and free carbon is formed. The product was solid-foam shaped. The principle product was a new phase of rhenium carbide that was not described earlier. This was evidently due to higher concentration of



carbon in the products of organics thermal decomposition. Small-angle X-ray scattering shows that the mean particle diameter was 16 nm. EXAFS pattern of the product reveals a strongly disordered local environment around Re atoms, which can be described by a set on non-equivalent Re-C and Re-Re bonds. (Fig.2).

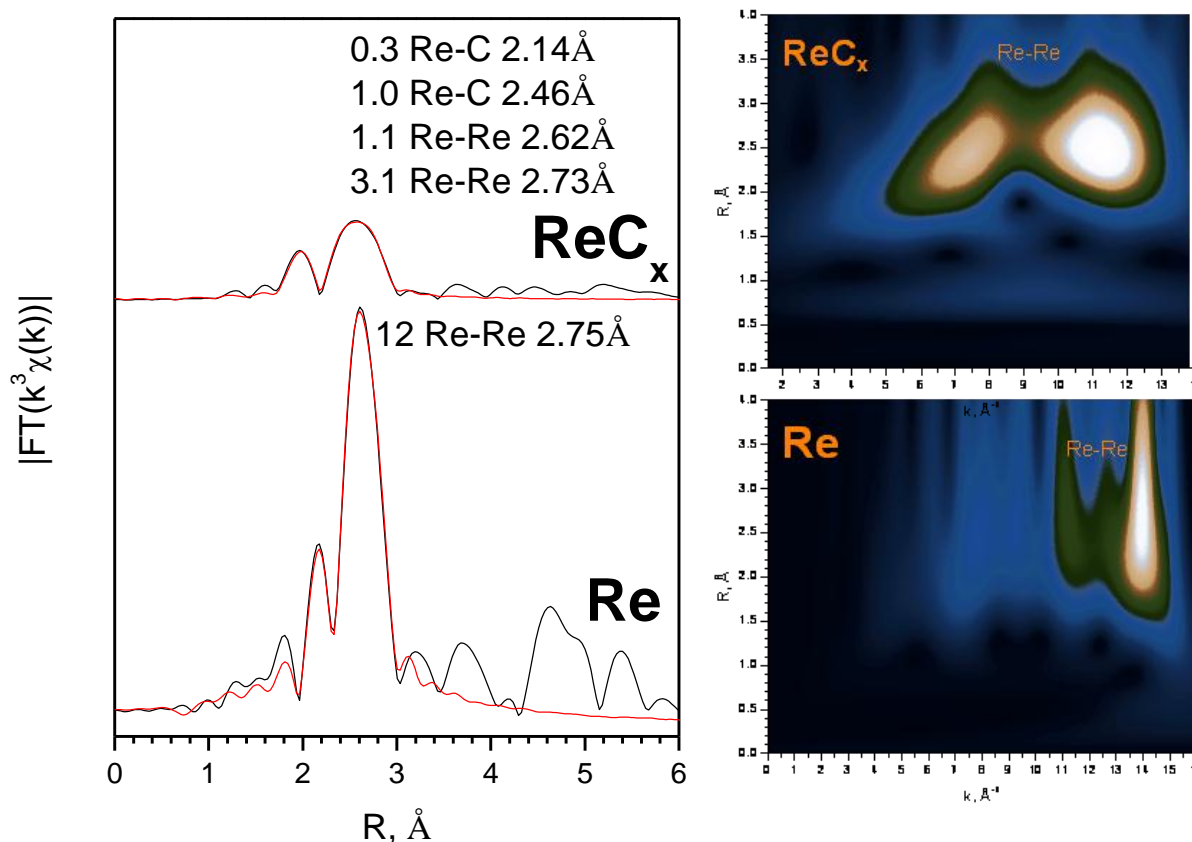


Fig. 2. Re L3-edge EXAFS spectra of nanostructured Re metal and carbide prepared by thermal decomposition of triphenylguanidinium perrhenate represented as Fourier (left) and Wavelet transforms).

Table 1. X-ray diffraction pattern of new Rhenium carbide phase ( $a = 5.095 \text{ \AA}$ ) formed in thermal decomposition of  $\text{TPGHReO}_4$  at 623 K followed by annealing at 1273-1373 K in argon [5].

No	H K L	2Theta (exp.)	2Theta (calc.)	Differ.
1	2 0 2	50.70	50.604	0.096
2	3 1 1	60.30	60.153	0.147
3	4 0 0	74.26	74.374	- 0.114
4	2 3 3	90.20	90.266	- 0.66
5	4 0 4	117.60	117.542	0.070

Indexing of the XRD pattern yielded parameter  $a = 5,095 \text{ \AA}$  with no systematic absences consistent with the sp.gr.  $Pm3m$ , which indicates that the Re carbide phase is probably isostructural to a number of Ln carbides ( $\text{Ho}_3\text{C}$ ,  $\text{Sm}_3\text{C}$ ) [7].

This observation suggests that the usual inactivity of Re towards C is only due to very high melting temperature rather than total absence of affinity. Indeed, when Re metal is generated *in situ* as a nano-phase simultaneously with active carbon formed by organic cations thermolyses, both components are highly reactive and thus able to form Re carbide phase.

Gaseous products of the thermolyses imply the oxidative mechanism of the destruction ( $\text{CO}_2$ ,  $\text{H}_2\text{O}$  and different organic fragments of cations).

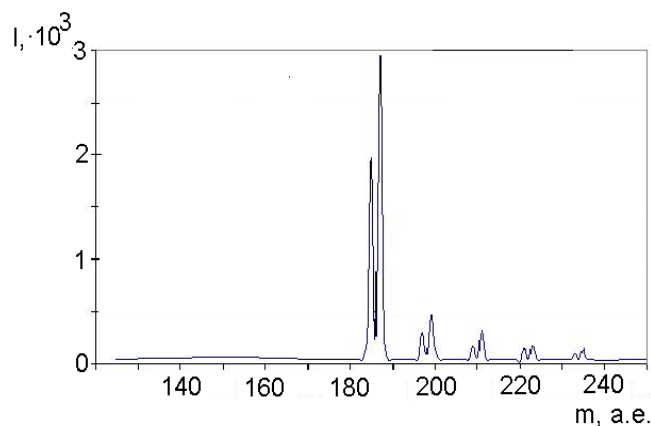


Fig.3. Laser microanalysis mass spectrum registered with the LAMMA-1000 instrument from the product of thermal decomposition of  $\text{TPGHReO}_4$  at 623 K followed by isothermal annealing at 1273-1373 K in Ar gas atmosphere [5].

The laser evaporation of the  $\text{Re-Re}_x\text{C-C}$  composite formed by **5** thermolyses in LAMMA-1000 instrument has given evidence for  $\text{ReC}^+$ ,  $\text{ReC}_2^+$  and  $\text{ReC}_3^+$  ions formation (Fig.3) while the same analyses of non-thermolysed **5** indicated just the first two peaks (185 and 187) presence. This is indicative of considerable affinity of Re to C not only in solid but also in gas phase under such conditions.

## Conclusion.

Metallic rhenium or technetium nanophase could be generated by thermal decomposition of perrhenates/pertechnetates of bulky organic cations under argon, the parallel carbonization of the cation provides conditions favorable for Re and Tc carbide formation as nano and microparticles. For hexamethyleniminium and triphenylguanidinium pertechnetates the conversion possess  $\text{Tc}_6\text{C}$  with a face-centred cubic structure. In the thermal decomposition of triphenylguanidinium perrhenate, just a mixture of Re metal, Re carbide and free carbon is formed. XRD patterns of nano dimension phases were X-ray amorphous, while for micro dimension  $\text{Tc}_6\text{C}$  phase the cubic lattice with  $a = 3.98 \text{ \AA}$  was deduced. For annealed sample the determined parameter  $a = 5.095 \text{ \AA}$  and the sp.gr.  $Pm\bar{3}m$  indicates that the new Re carbide phase is isostructural to a number of Ln carbides.

**Acknowledgments:** The work was supported by RFBR grant 09-03-00017. EXAFS studies were performed using the equipment of the centre for collective use “Kurchatov Centre for Synchrotron Radiation and Nanotechnology” supported via Russian Federal contract 16.552.11.7003

## References.

1. T. Oyama (Ed.), *The Chemistry of Transition Metal Carbides and Nitrides*, Blackie Academic and Professional, London, 1996.
2. H. R. Heines, P. C. Mardok, and P. E. Potter, *Plutonium 1975 and other Actinides, Proc.: 5th Int. Conf. (Baden Baden, 1975)*. Amsterdam, 233-244 (1976).
3. K. E. German, V. F. Peretruchin, K. N. Gedgovd, etc., *Journal of Nuclear and Radiochemical Sciences*, **6**: 211-214 (2005).
4. G.V. Sidorenko, A.E. Miroslavov, D.N. Suglobov. *Radiochemistry*. **51**: 583-584 (2009).
5. K. E. German. *Nuclear Medicine and Biology*, (2010) **37**, Iss. 6, P. 687.

6. K. German. In situ carbonization for rhenium and technetium carbide nano and micro phase preparation. Proceedings of the International Symposium on Technetium and Other Radiometals in Chemistry and Medicine – Forum Brixen – BressanoneCongress Center (Italy) September 8-11, 2010, pp.125 -128.
7. K.A. Schneider and F.W. Calderwood. *Journal of Phase Equilibria*, **7**: 445-446 (1986)..



## 6 th SECTION – NANOTECHNOLOGY OF Tc AND Re

6.P5.

## ION SELECTIVE ELECTRODES BASED ON MONOCRYSTALLINE $\text{KTiOPO}_4$ WITH NANOCAPILLAR CONDUCTIVITY FOR DETERMINATION OF $\text{K}^+$ -IONS.

A.V. Kopytin, Yu. A. Politov, E.G. Ilyin, Yu.I. Urusov, K.E.German.

IGIC RAS, MUCTR, IPCE RAS ( [ionix@igic.ras.ru](mailto:ionix@igic.ras.ru) )

### ABSTRACT

New improved  $\text{K}^+$ -selective electrode based completely on solid single crystal KTP with nano-capillary conductivity is developed. The crystal KTP grown by two different methods had an ordinary orthorhombic structure ( $\text{Pna}2_1$ ) with the chain structure of shared  $\text{TiO}_6$  octahedrons, where the vacantly mobilized  $\text{K}^+$  ions provide the ionic conductivity through nano-dimension capillary. The membranes of 0.8 mm thickness and 6 mm diameter were hermetically sealed without glue materials into a IONIKS 111.080 solid membrane electrode body together with an inner standard Ag/AgCl reference electrode. The electrode presents linear response in the range of  $\text{pK}^+=1 - 5$ , the electrode function slope  $S=58.8\pm 0.4$  at  $25^\circ\text{C}$  and high selectivity coefficients for ions of alkali and earth-alkali elements that permits to use it for practical application in medicine. The electrode had a convenient response time,  $\text{DL}_K$  of  $\text{pK}^+ = 5.2 \pm 0.1$  and the reproducibility of electrode potential  $\pm 0.2$  mV in  $\text{KNO}_3$  solutions during at least 28 months. Investigation of a unique properties a single crystal  $\text{KTiOPO}_4$  (KTP) and the design of new improved  $\text{K}^+$ -selective electrodes based completely on KTP are reported. The studied single crystal KTP were grown by using of two methods: hydrothermal and melting from a solution. They had ordinary orthorhombic structure ( $\text{Pna}2_1$ ) with lattice parameters:  $a=12.814$ ,  $b=6.404$  and  $c=10.616$  Å, and the chain structure made of  $\text{TiO}_6$  octahedrons, where the potassium ions were able to move by vacancy mechanism, providing ionic conductivity.. The membranes of 0.8 mm thickness and 6 mm diameter were hermetically sealed in a IONIKS 111.080 solid membrane electrode body without glue materials. The 0.01 M KCl solution and a standard Ag/AgCl electrode were placed inside of reservoir. The electrode response was linear in the range of  $\text{pK}^+=1 - 5$ , with the electrode function slope equal to  $S=58.8\pm 0.4$  at  $25^\circ\text{C}$ . The high selectivity coefficients for ions of alkali and earth-alkali elements were found. The selectivity of proposed electrode permits to use it for practical application in a medicine. The electrode had a convenient response time,  $\text{DL}_K$  of  $\text{pK}^+ = 5.2 \pm 0.1$  and the reproducibility of electrode potential  $\pm 0.2$  mV in  $\text{KNO}_3$  solutions during at least 28 months.

### Introduction

Ion-selective electrodes for determination of potassium are among the most used in clinical chemistry and agriculture. In this connection the increase of measurement precision by improvement of electrodes parameters remains an important task. This purpose may be achieved in several ways: the improvement of ion-selective electrode construction, the improvement of separate units quality, the optimum selection of membrane composition (with already known components), the search of the new electrodoactive components, as well as the new sensitive elements – membranes (from inorganic materials).

The several kinds of  $\text{K}^+$ -selective electrodes with membranes of a various compositions are at present developed and produced. All of them are assigned to a type of electrodes on the basis of neutral carriers and are described in monographs and reviews [1-2]. The well known and received the wide use is the electrode based on valinomycin [3], which is included in production catalogs of many firms, engaging by production of ionometric equipment. Therefore in our work we compared parameters of new electrode based on monocrystal with valinomycin electrode.



## Theoretical premises

The requirements to membrane materials were formulated yet in the middle of 60's. In spite of it, until now the electrode based on  $\text{LaF}_3$  remained the only electrode with monocrystal membrane. Use of  $\text{LaF}_3$  as a monocrystal is indispensable condition to obtain the electrode with high analytical parameters. The active search of monocrystals with high ionic conductivity (basically 60's–beginning of 70's) as membranes ion-selective electrodes had no positive result.

The first message on an opportunity of application of monocrystal  $\text{KTiOPO}_4$  (KTP) as a membrane  $\text{K}^+$ -selective electrode has appeared in 1994 [4].

For the first time a monocrystal of  $\text{KTiOPO}_4$  (KTP) was identified by French researchers in 1971 [5] and was patented in 1974 for use in electrooptical devices, converting the frequent characteristics of laser radiation [6]. The monocrystal KTP has an orthorhombic structure and concerns to point group  $\text{mm}2$  (space group  $\text{Pna}21$ ). For KTP lattice parameters are:  $a=12.814$ ,  $b=6.404$  and  $c=10.616\text{\AA}$ . Each elementary cell contains 8 formula units. The structure is characterized by chains of  $\text{TiO}_6$  octahedrons, which are connected on two corners and the chains are divided by  $\text{PO}_4$  tetrahedrons. Potassium ions, located in centers of high coordination number, are weakly bound to oxygen atoms, which surround of atoms titanium and phosphorus, and are able to move by vacancy mechanism. For the first time the information about low-temperature ionic conductivity of KTP crystals has appeared at the end of 80's [7]. Data, obtained by various authors have shown, that electrical conduction in KTP in a wide range of temperatures occurs almost exclusively through the movement of potassium ions on channels, which perforate a framework along an  $c$  axis. Electron and anion conductivity are more isotropic and their summary upper limit can be evaluated from resistance of a crystal in perpendicular directions to  $c$  axis. According to work \*197\* this resistance makes about  $10^{12}$   $\text{om}\cdot\text{cm}$  that on 6 - 7 orders of magnitude higher than resistance of a KTP crystal in a direction along the axis  $c$  with under conditions of cation transport. Thus, it is possible to conclude about overwhelming character of cation conductivity KTP. Research of impedance has allowed to establish, that greatest value of ionic conductivity of crystal was  $1.2\cdot 10^6$   $\text{om}\cdot\text{cm}$  [8]. Taking into account availability of low-temperature ionic conductivity and state stability, assumption about a opportunity of use of a KTP crystal (by analogy with  $\text{LaF}_3$ ) as a membrane of  $\text{K}^+$ -selective electrode was made.

## Experimental section

### 1. Equipment and procedure.

All measurements were carried out with use of a ionmeter Orion Research Model-901 (USA). The external reference electrode was a IONIKS-112.024 (Russia) double-junction  $\text{Ag}/\text{AgCl}$  electrode with 1M potassium chloride and 1M lithium sulfate brige electrolyte. Electroanalytical parameters of ion-selective electrode were measured according to IUPAC recommendations [9]. The selectivity coefficients were measured by the method of mixed solutions.

### 2. Synthesis of membrane and the electrode design.

KTP crystals were grown by two methods: hydrothermal and from a solution in melt [10,11]. The conductivity of crystals varied in a range of  $10^7$ — $10^6$   $\text{om}\cdot\text{cm}$ . The membranes of about 0.8 mm thickness and about 6 mm diameter were mounted in a IONIKS 111.080 solid membrane electrode body, in which the hermetic sealing of a membrane was made without glue materials. The 0.01 M  $\text{KCl}$  solution and a standard silver/silver chloride electrode were placed inside of reservoir.

### 3. Reagents.

In this work the standard reagents of the grade “chemically pure” Reakhim (Russia) were used. All standard solutions was prepared using deionized water.

## Results and discussion

A typical electrode characteristic of monocrystal  $\text{K}^+$ -selective electrode is given in fig.1.

The linear response of electrode potential was observed in a wide range of concentration  $1 - 5 \text{ pK}^+$ . The electrode function slope was close to theoretical one and was equal  $S=58.8\pm 0.4$  at  $25^\circ \text{C}$ .

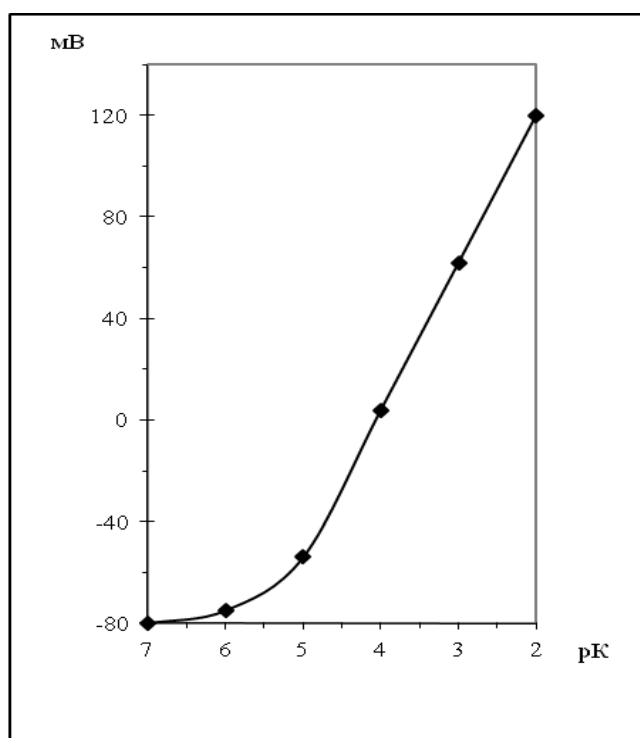


Fig.1 Response of  $\text{K}^+$  - Selective electrodes.

The coefficients of selectivity for ions of alkali and earth-alkali elements are represented in table 1.

Table 1. Coefficients of selectivity of  $\text{K}^+$  -selective electrodes.

Ион	$\text{H}^+$	$\text{Li}^+$	$\text{Na}^+$	$\text{Rb}^+$	$\text{Cs}^+$	$\text{Mg}^{2+}$	$\text{Ca}^{2+}$	$\text{Sr}^{2+}$	$\text{Ba}^{2+}$	$\text{NH}_4^+$
$-\lg K_i$	2.2	2.6	3.4	1.5	3.2	3.3	2.8	1.5	2.1	1.1

A correlation between ionic radius and selectivity coefficient is shown at fig.2.

As follows from this figure, the size of a channel probably plays an essential role in selectivity, in which ionic transport of ions take place. So, when going from potassium to sodium ion selectivity changes almost on three order of magnitude. The figure 3 evidently demonstrates the difference in selectivity between proposed electrode, glass electrode ESL-47-07 (Belarussia) and valinomycin electrode Potencial (Russia).

The measured limit of detection in pure potassium nitrate solutions was  $5.8 \text{ pK}^+$ . Reproducibility of electrode potential in potassium nitrate solutions was not worse than  $0.2 \text{ mV}$ . The changes analytical parameters were not observed for a time of the study (14 months).



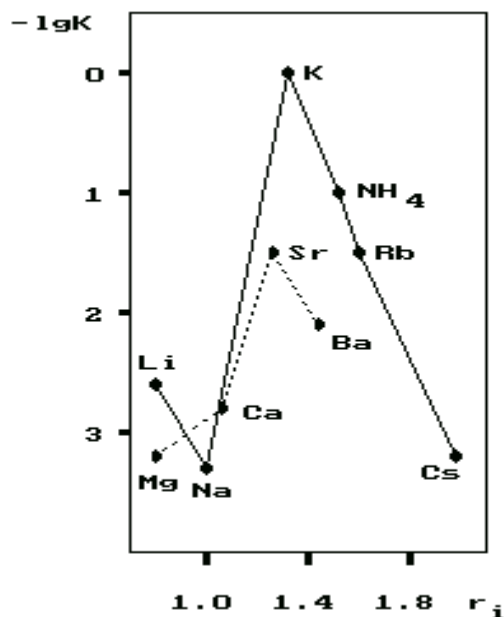


Fig.2 Correlation between ionic radius and selectivity coefficient.

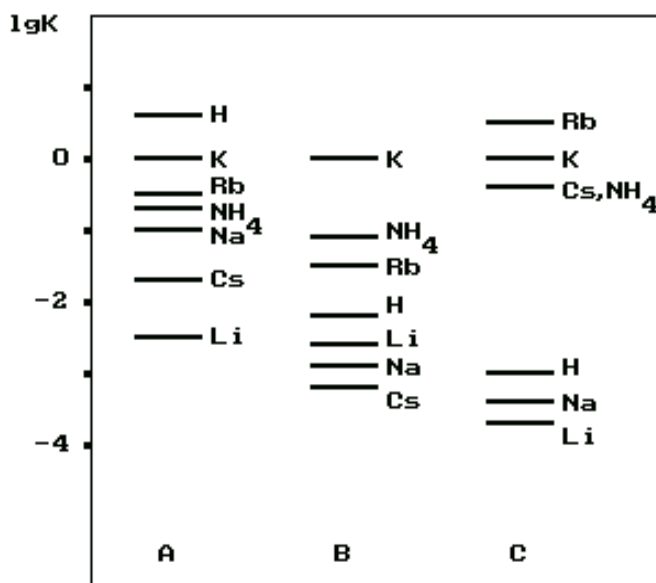


Fig.3.  $Lg K$  (a – glass electrode, b - KTP, c – valinomycin electrode).

Working mechanism of this membrane is not yet investigated, and we hope, that the further study of the electrode characteristics will show that proposed crystal is a unique one as a ion-selective membrane.

### Summary

Inorganic material as a membrane of potassium-selective electrode has been proposed. This material represents a monocrystal of  $KTiOPO_4$ , having an orthorhombic structure. The characteristics of proposed electrode have been investigated. It has been found, that developed electrode have high selectivity in the presence of alkali and earth-alkali ions, comparable with that for electrode based on valinomycin. At the same time high selectivity for potassium in the presence

of rubidium and cesium ions was noticed. Electrode characteristic is linear in a range  $pK^{+1} - 5$  at a theoretical slope.

## References

1. Корыта И., Штулик К. Ионоселективные электроды. М. Мир.: 1989.С.206.
2. Moody G.J., Thomas J.D.R. // Ion-Selective Rev.1979.№1.Р.3
3. Frant M.S., Ross J.W.// Science.1970.№167.Р.987
4. Буслаев Ю.А., Ильин Е.Г., Копытин А.В. и др.//Пат.РФ. №2017146,МКИ G01N27/333. Оpubл.30.07.94.
5. Mase R., Grenier J.C. // Bull. Soc.Franc. Mineral.Cristallogr.1971.V94.,P.437.
6. Bierlein J.D.,Gier T.D.,E.I.Du Pont. //Pat. USA. №3949323.
7. Bierlein J.D., Arweiler C.B. //Appl. Phys.Lett. 1986. V.49, P.917.
8. Маслов В.А., Селяненко В.Н. и др. // Выращивание крупных кристаллов КТР раствор – расплавленным методом. Расшир. Тезисы доклада V11 Всесоюзной конф. по росту кристаллов. 1988. Т.2. с.230.
9. IUPAC Recommendation for Nomenclature of IonSelective Electrodes // Pure. Appl. Chem. 1976. №48. P.127
10. Belt R.F., Gashurov G., Liu Y.S.. КТР as a harmonic generator for Nd:YAG lasers //Laser Focus. 1985. V. 10. P.110-124.
11. Belt R.F., Iradi T.. Hydrothermal growth produces large КТР nonlinear crystals //Technology Guide: Optical materials. 1993. V.11. P. 155-162.



ISTR 2011 International Advisory Committee (G.Kodina, K. German, T. Gerber)

6.P6.

## QUANTUM CHEMICAL STUDY OF SUBNANODIMENSIONAL MIXED CLUSTERS OF TECHNETIUM AND RUTHENIUM

Yu.V.Plekhanov, K.E.German

Institute of Physical Chemistry and Electrochemistry, RAS  
31, Leninskii pr., Moscow, Russia

Previous [1] quantum chemical DV- $X_\alpha$  [2] calculations based on the density functional theory proved adequacy and reliability of cluster models for the metallic technetium electronic structure analysis. We extended these models for mixed  $Tc_xRu_y$  phase appearing due to transmutation of radioactive  $Tc^{99}$  into stable  $Ru^{100}$  [3]. As a bulk phase our simple model clusters used the same electronic density for volume and surface sites. Interatomic distances for mixed models were linearly interpolated by content between pure Tc and Ru metal ones as it's shown in [4]. We took into account all low concentration models of Tc or Ru, but in the middle concentration area we used only statistically averaged data for rather small (~10) random sets of atom positions. Because it is similar character of results for both fragments, only the most informative electronic structure characteristics of 21-atomic model graphic data will be given further. The electronic configurations of pure metallic models  $Tc\ 4d^{5.66}5s^{0.73}5p^{0.60}$  and  $Ru\ 4d^{6.67}5s^{0.71}5p^{0.60}$  for mixed models vary slightly. It is about 10% for 5s5p-states and up to 3% for 4d-states. The most modification of 4d-Tc population is 0.15e for 13-atomic model. 4d-Tc population is monotone weakly logarithmically decreasing while Ru part enlarges. At the same time for effective charges we found approximately linear dependence from Ru content. For all atomic positions and some Ru concentration it was occurred electronic density displacement toward Ru and very similar tendencies.

Fermi level position in our models approximately corresponds to the high occupied cluster orbital. Relative location of this level also linearly drop. Density of states (DOS) at Fermi level dependence has a rather intricate shape. At the low concentration of some metal DOS is relatively less than the same one for the pure metals or for the central part of the graphic. DOS absolute maximum position corresponds to ~70% output of transmutation products. Commonly this parameter has arising tendency during the transmutation process (dashed line). Finally, we estimated models stability by sum of Mulliken bond overlap population indexes over all bonds per one atom of model. It is excellent linear tendency for the bond weakening during transmutation. All this facts also well corresponds with general qualitative theory [5]: new more electronegative atom sublattice results to more strength bonding, correlates with the shift of occupied states in the lower energy area; descends Fermi level from the middle to the end of transition metal row and decreases density of states at Fermi level.

Therefore the same behaviour of electronic structure characteristics for both models arises the probability of these conclusions for the real samples. We can sum up that transmutation causes serious changes in electronic structure of initial metallic Tc, which influences on its chemical activity, physical-chemical and mechanical properties.

**Acknowledgments:** The work was supported by RFBR grant 09-03-00017.

### REFERENCES

- [1] Yu.V.Plekhanov, K.E.German, R.Sekine // Radiochemistry (Russ.), 45(2003) 217.
- [2] H.Adachi, M.Tsukada, C.Satoko // J.Phys.Soc.Jpn. 45(1978) 875
- [3] V.F.Peretrukhin, S.I.Rovnyi, V.V.Ershov et al // Zh. Neorg. Khim.(Russ.), 47(2002), no. 5, 722.
- [4] Y.Shirasu, K. Minato // J. Alloys Comp., 335(2002), nos.1-2, 224.
- [5] R.Hoffmann Solids and Surfaces: A Chemist's View of Bonding, VCH Publisher Inc., 1988.

6.P7.

## DEPOSITION OF TECHNETIUM COATINGS BY THERMOLYSIS OF VOLATILE CARBONYL COMPOUNDS

G.V. Sidorenko, A.E. Miroslavov, and D.N. Suglobov

Khlopin Radium Institute, Research and Production Association, Federal State Unitary Enterprise,  
2-i Murinskii pr. 28, St. Petersburg, 194021 Russia

Technetium carbonyl compounds  $[\text{TcBr}(\text{CO})_5]$ ,  $[\text{TcI}(\text{CO})_5]$ ,  $[\text{TcX}(\text{CO})_3]_4$  ( $X = \text{Cl}, \text{Br}, \text{I}$ ),  $[\text{TcBr}(\text{CO})_3\text{en}]$  ( $\text{en} = \text{ethylenediamine}$ ),  $[\text{Tc}(\text{RCOCHCOR}')(\text{CO})_3(\text{Et}_2\text{NH})]$  [ $\text{R} = \text{CH}_3$  or  $\text{C}(\text{CH}_3)_3$ ,  $\text{R}' = \text{CF}_3$ ],  $\text{Tc}_2(\text{CO})_{10}$  and  $[\text{Tc}(\text{C}_5\text{H}_5)(\text{CO})_3]$  were tested as precursors for chemical vapor deposition of technetium coatings on model supports (external surface of titanium tubes) with the aim to evaluate the possibility of using technetium coatings for biofouling protection of critical units of installations operating in seawater. The deposition conditions and yields were determined. The necessary conditions for ensuring high deposition yield are occurrence of the decomposition in one effective step and, in the case of carbonyl halides, presence of a reductant, internal (ethylenediamine) or specially introduced into the gas phase.

The microstructure of the coatings obtained was examined by electron microscopy. The chemical composition of the coatings (carbon content) was determined. The coatings were studied by X-ray diffraction analysis, and phases of metallic technetium, solid solution of carbon in technetium, technetium carbide, and intermetallic compounds of technetium with titanium (support material) were revealed. Along with the well-known hexagonal phase, a new phase of technetium metal, body-centered cubic with  $a = 0.325$  nm, was revealed; it is usually formed in thin (less than 1  $\mu\text{m}$ ) films. The corrosion resistance of the films in simulated seawater was studied by monitoring the accumulation of technetium in seawater contacting with the coated specimen. The correlation between the precursor composition, conditions of heat treatment of the coatings, chemical and phase composition of the coatings, and their corrosion resistance is discussed. High-temperature vacuum annealing (at no less than 900°C) is the necessary condition for preparing corrosion-resistant coatings. The highest corrosion resistance is attained at low (<2%) and high (>15%) carbon content in the coating. The best samples are not inferior in the corrosion resistance to dense technetium foil.

The most reliable results with respect to the whole set of parameters (deposition yield, adhesion of the coating to the support, corrosion resistance) were obtained with the system  $[\text{TcBr}(\text{CO})_3]_4/\text{ethylene glycol}$ . Ways to further improve the deposition process are outlined. The most important of them is more efficient pumping-off of gaseous reaction products.





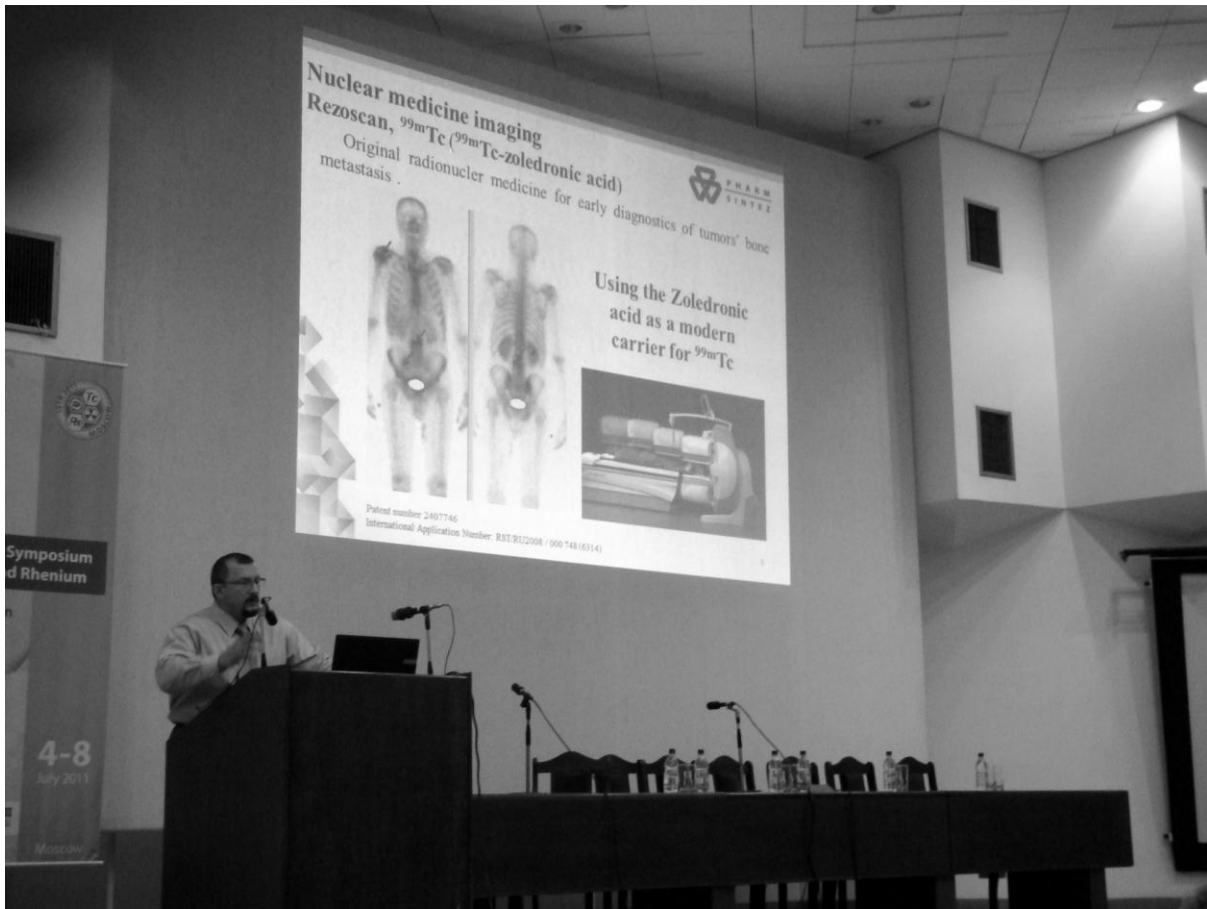
A. Malysheva and A. Maruk



Promising to meet in Chicago (22th floor of Presidium RAS, Moscow)



ROUND TABLE KEY LECTURE

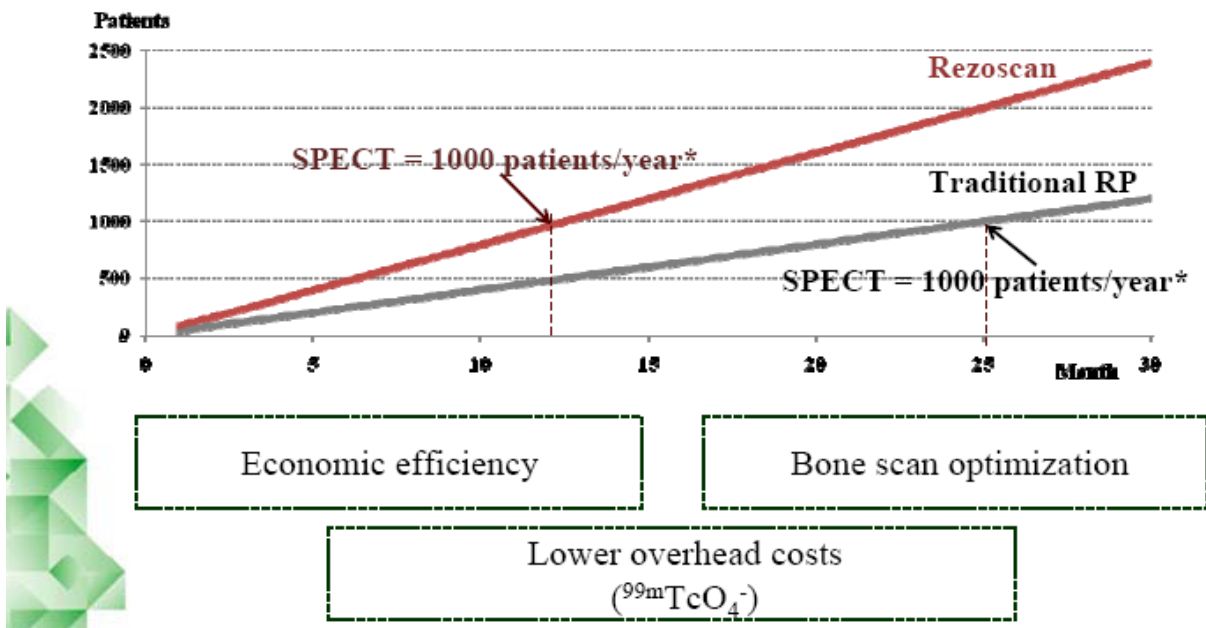


“FARMSINTEZ” CEO Timofei Petrov is giving axial lecture

Rezoscan, <sup>99m</sup>Tc – economic benefits



Scintigraphy 1 hour after the injection of Rezoscan

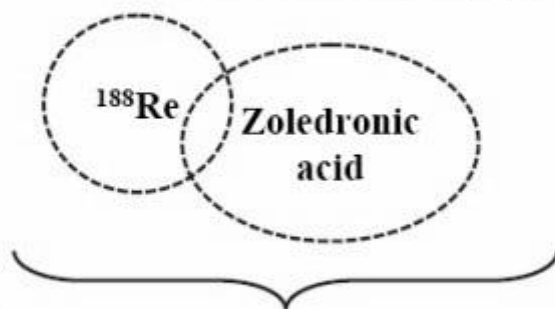


## Nuclear medicine therapy ZoleRen ( $^{188}\text{Re}$ -zoledronic acid)



Innovative therapeutic radionuclear medicine applied for bone metastasis palliative therapy.

**THE FIRST AND ORIGINAL RADIOPHARMACEUTICAL  
METHOD FOR PALLIATIVE THERAPY**



**SYNERGY OF THE  
THERAPEUTIC  
EFFECTS**

The new method allows for:

- outpatient therapy
- high-tech therapy in remote areas
- ease of operation
- the use of  $^{188}\text{W}/^{188}\text{Re}$  generator

Patent number 2407746

International Application Number: RST/RU2008 / 000 748 (6314)



**ISTR2011 Closing ceremony**

## AUTHOR INDEX

Author Name	Page		
Abdrahmanov, T.G.	285	Bruskin, A.B.	307
Abdrahmanova, Z.T.	247	Brylev, K.A.	27, 58, 74
Abdulhatov, M.K.	176	Bryskin, B.D.	375
Abdusalomov, A.A.	281	Bulatov, G.S.	162, 436
Abisheva, Z.S.	208, 235, 241, 247	Burakov, B.E.	190
Abkhalimov, E.V.	427	Burkhanov, G.S.	407
Agapova, L.Ya.	241, 247	Burtsev, M.Yu.	297
Al-Hokbany, N.S.	356	Bychkov, A.V.	10
Al-Jammaz, I.J.	356	Bykov, A.N.	373
Alberto, R.	301	Bykov, G.L.	169
Aleksandrova, O.P.	317, 332		
Aliev, R.A.	150, 192	Chagovets, N.S.	416
Allabergenov, R.D.	272	Chekmarev, A.M.	10, 277-288, 411
Altmaier, M.	31	Chernyadeva, O.A.	277
Alwaer, S.	151	Chernyshov, A.A.	409
Aminjonov, A.A.	65, 73, 86, 91, 102, 400	Chernyshova, O.V.	29, 44
Ananyev, A.V.	121	Chibisov, E.V.	351
Andreev, V.N.	10	Chikova, I.V.	310
Antipkin, N.R.	416	Chiozzzone, R.	53
Anyszkiewicz, K.	148	Chistyakov, A.V.	44
Areshina, N.S.	265	Chmielarz, A.	148
Artamonova, L.D.	355	Chotkowski, M.	137
		Chukalina, M.V.	429
Babain, V.A.	112	Ciulik, J.	379
Balanovskiy, N.V.	277	Cupial, S.	148
Bańkowski, K.	343	Czerwiński, A.	70
Baranov, N.G.	321, 327, 352	Czerwinski, K.R.	10, 28, 55, 57, 99
Bartenev, S.A.	176		
Batuk, O.	193	Danylenko, M.I.	165
Baulin, V.E.	338	Denden, I.	96
Beknazarova, N.S.	400	Denisov, E.I.	337
Belyanin, M.L.	310	Depmeier, W.	135
Benke, G.	148	Didyk, A.Yu.	79
Bessonov, A.A.	438	Dilworth, J.R.	11
Betenekov, N.D.	146	Drobot, D.V.	10, 29, 44, 54, 59, 380, 421
Biljalova, G.A.	416	Dvoeglazov, K.N.	167
Blokhin, A.A.	254, 265		
Bogorodskaya, M.A.	416	Essehli R.	96
Bogorodsky, A.O.	416	Epstein, N.B.	355
Boltoev, Yu.D.	168	Ermolaev, A.V.	74
Bonardi, M.L.	319	Ershov, B.G.	10, 169, 427, 428
Borbat, V.F.	73	Fattahi, M.	96
Borisova, L.V.	138, 144, 223, 262	Fedorov, V.E.	27, 58, 74
Boytsova, T.A.	112	Fedosseev, A.M.	98, 438
Bozhkov, O.	223, 262	Fellhauer, D.	31
Braband, H.	301	Filyanin, A.T.	320
Britvin, S.N.	135	Filyanin, O.A.	320

Firsin, N.G.	176, 411	Kalmykov, S.N.	173, 192, 193
Forester, P.M.	59	Kanygin, V.V.	332
Frolov, K.N.	10	Karpukhin, A.V.	439
Fujii, Y.	107	Kasikov, A.G.	10, 232, 265, 268, 293
Fuks, L.	339	Katayev, E.A.	105
		Kataeva, L.I.	10
Gaona, X.	32	Kazanskaya, N.K.	394
Garbuzov, V.M.	190	Kerlin, W.M.	57
Gayfulin, I.M.	101	Khijniak, T.V.	128, 188
Gedgagov, E.I.	10, 217, 218	Khomushku, G.M.	355
Gedgovd, K.N.	162, 436	Khrustalev, V.N.	54, 105
Gerber, Th.	11, 30	Kilibayeva, S.K.	241
German, K.E.	10, 11, 15, 96, 100, 114, 121, 173-194, 297, 429, 435, 439-450	Kim, E.	59
Gini, L.	319	Kirakosyan, G.A.	99, 105
Glukhov, G.G.	351	Kitamura, N.	27
Gniazdowska, E.	339, 343	Klementyeva, O.E.	347, 369
Goikhman, M.J.	88	Klyopov, A.N.	317, 332
Golovanov, D.	149	Kobayashi, T.	32
Golubev, M.N.	337	Kodina, G.E.	10, 300, 307, 320, 347, 369, 373
Goncharuk, T.Ju.	388	Kolesnikov, G.V.	105
Gorina, N.B.	407	Kolupaev, D.N.	10, 121
Gorshkov, N.I.	311	Konovalov, E.E.	136, 168
Goryunov, E.I.	175	Konovalov I.S.	197
Goryunova, I.B.	175	Kopytin, A.V.	194, 445
Grechnikov, A.A.	144	Kormilitsyn, M.V.	10, 191
Gribanov, A.V.	176	Korneyko, Yu.I.	135, 190
Grigoriev, M.S.	10, 37, 38, 97, 98, 440	Korolev, V.A.	112
Gromov, P.B.	293	Korsunsky, V.N.	308
Groppi, F.	319	Kostylev, A.I.	411
Gurzhij, V.V.	38, 39	Kovalenko, O.V.	338
Gusel'nikov, V.S.	176	Koyama, S.	107
Guseva, E.V.	409	Kozar', A.A.	113, 160
		Kozitsyna, N.Yu.	183
Habashi, F.	104	Kozminski, P.	339, 343
Hartmann, T.	57	Krajnikov, A.V.	387
		Krasikov, V.D.	311
Ilyin, E.G.	445	Kravchenko, N.G.	191
Irtegov, A.I.	56	Kremer, C.	55
Ishizaka, Sh.	27	Krivovichev, S.V.	137
Ismailov, N.P.	281	Krylov, V.V.	317
Ito, A.	27	Kriyzhovets, O.S.	45, 61
Ivanov, I.A.	192	Kudryavtsev, G.E.	10
		Kulakova, I.I.	439
Johnstone, E.	29, 59	Kulikauskas, V.S.	81
Juraev, Sh.	85	Kurachenko, Y.A.	317
		Kurykin, M.A.	56
Kabirov, N.G.	75, 88, 91	Kuznetsov, A.A.	108, 158
Kablov, E.N.	10, 18		
Kadirova, Z.Ch.	85	Lebedev, V.A.	10
Kalantarova, P.E.	253	Leonhardt, T.	379
Kalinnikov, V.T.	293	Leszczynska-Sejda, K.	148

Levchuk, O.M.	271	Nikolaev, A.I.	10
Levin, A.M.	271	Nikonov, B.S.	138
Lapshina, E.	319	Niyazmatov, A.A.	275
Lumpov, A.A.	38, 426	Novikov, J.N.	178
Lvovskiy, A.I.	422	Novojilov, V.A.	320
Lyamina, O.I.	10	Novruzova, F.S.	253
Lyubimov, D.Yu.	162, 436		
		Obruchnikova, Ya.A.	114, 439, 440
Mabatkadamova, K.S.	91	Oleynikov, P.P.	388
Majidzade, V.A.	253	Orlov, S.P.	320
Malakhova, I.I.	311	Oshchepkov, V.N.	308
Maltseva, E.E.	254, 265	Ospanov, E.A.	217
Malysheva, A.O.	347, 369, 373	Ospanov, N.A.	217
Manenti, S.	319	Ozawa, M.	11, 20, 107, 112
Manuylov, R.N.	386		
Maruk, A.Ya.	98, 100, 307, 440	Palant, A.A.	10, 271
Mashkin, A.N.	121, 174	Parpiev, N.A.	87
Maslennikov, A.G.	191	Parshin, A.P.	386
Maslennikov, Yu.S.	351	Peretrukhin, V.F.	10, 11, 113, 114, 160, 181, 187, 191
Matusevich, Eu.S.	317	Petriev, V.M.	321, 332
Mayboroda, A.B.	285	Pet'kov, V.I.	77
Mayer, P.	31	Petrakova, O.V.	45, 61, 422
Mazilin, I.V.	380	Petrova, A.M.	232, 265, 268, 293
Melentev, A.B.	121, 173, 174	Petrov T.	453
Melnikov, S.A.	386	Petrushin, N.V.	18
Merkulov, V.G.	351	Pichuzhkina, E.M.	166
Mescheryakov, N.M.	230	Plekhanov, Yu.V.	454
Mikhaylenko, M.A.	220, 254	Pleshkov, M.A.	254
Minin, V.V.	138	Plevaka, A.V.	288
Minko, Yu.V.	327	Pokhitonov, Yu.A.	112
Minn, A.	288	Poineau, F.	11, 15, 28, 55, 59, 96, 99
Mironov, Yu.V.	28, 60, 76, 101	Pokrovskiy, Yu.G.	411
Miroslavov, A.E.	10, 39, 38, 426	Politov, Yu.A.	448
Misharin, V.A.	121	Ponomareva, E.I.	247
Morito, F.	387	Popova, N.N.	169, 297
Moisy, Ph.	11, 114, 438	Potapova, K.I.	285
Morozov, P.A.	428	Potgieter, K.	31
Murashkin, Ju.V.	254	Povarova, K.B.	10, 58, 394
Murko, A.Yu.	314	Pryamilova, E.N.	30
Murzin, V.Yu.	11, 429, 440		
Myasoedov, B.F.	10, 13, 175	Qeybatova, A.F.	253
Naumov, N.G.	60	Rabinovich, E.Z.	308
Nazarov, E.O.	19, 167	Radchenko, V.M.	191
Nazarova, O.V.	311	Reshetnik Y.N.	373
Nekhoroshev, N.E.	220	Reshetova, O.V.	271
Nenashev, S.N.	391	Roberov, I.G.	407
Nerozin, N.A.	330, 355	Rogov, A.S.	309, 310
Nesterov, E.A.	309, 310	Romanovsky, V.N.	320
Nesterova, J.V.	309, 310	Rotmanov, K.V.	113, 191
Nifantiev, E.E.	177		
Nikishina, E.E.	56		



Ryabukhin, V.A.	146	Tarasov, V.P.	99
Sadkin, V.L.	309, 310	Taratonenkova, N.	369
Sadykanova, S.E.	109	Tkachuk, D.A.	320
Safarmamadov, S.M.	75, 88, 91	Tomilin, S.V.	166
Safiulina, A.M.	175, 297	Troshkina, I.D.	10, 11, 202, 277, 281, 285, 288, 298, 411
Saito, M.	107	Tugarina, O.V.	174
Sakuda, E.	26	Tsivadze, A.Yu.	10, 11, 181, 320, 338
Salahova, E.A.	253	Tsodikov, M.V.	44
Sapukov, I.A.	241	Tumanova, D.N.	114, 181, 288
Sarychev, G.A.	10	Tzvetkova, Ch.	223, 262
Sattelberger, A.	11, 28, 55, 57, 99	Usolkin, A.N.	338
Sayre, E.D.	375, 395	Ulanovskiy, A.A.	388
Sazanov, J.N.	176	Urusov, Yu.I.	194, 445
Sazonov, A.B.	416	Varlamova, N.V.	309
Schibli, R.	311	Vazchenkov, M.V.	298
Scott, B. L.	28, 57	Veligzhanin, A.A.	409
Sekine, T.	11	Vidanov, V.L.	167
Semenova, A.A.	321, 327, 352	Voit, A.V.	288
Sergeeva, L.N.	167	Voldman, G.M.	386
Sharipov, Kh.T.	85, 272	Volk, V.I.	10, 167
Sharipov, R.Kh.	85, 272	Volkov, V.P.	230
Sharygin, L.M.	337	Voroshilov, Yu.A.	338
Shevelkov, A.V.	44, 59	Weck, Ph.	28, 57, 99
Shilov, V.P.	121	Yakovlev, N.G.	338
Shilyaev, A.V.	277, 288	Yalfimov, A.N.	426
Shinohara, A.	26	Yarovoy, S.S.	27
Shiryayev, A.A.	173, 429, 439, 440	Yordanova, T.	55
Shiryayev, S.V.	308	Yoshimura, T.	26
Shiryayeva, V.K.	332	Yudintsev, S.V.	136
Shulepov, S.S.	168	Zagorodnyaya, A.N.	208, 235
Sidorenko, G.V.	37, 38, 426, 451	Zakharova, E.V.	193
Sidorov, V.V.	18	Zakharyan, S.V.	217
Skuridin, V.S.	312, 313	Zaytsev, P.A.	388
Skvortsov, V.G.	332, 355	Zemskova, L.A.	288
Smirnov, N.A.	285	Zhukov, A.F.	194
Smirnova, K.A.	44, 422	Zolotova, Yu.I.	311
Smolentsev, A.I.	74, 101	Zubavichus, Ya.V.	173, 409, 429, 440
Snigirev, Eu.V.	317	Zukau, V.V.	351
Solovov, R.D.	428	Zykov, M.P.	176, 320
Stasiuk, E.S.	312		
Stepchenkov, D.V.	321, 327, 352		
Suglobov, D.N.	37, 38, 426, 451		
Sukhanov, M.V.	75		
Suharev, S.S.	155		
Sulim, E.V.	321, 327, 352		
Suo, Ch.	26		
Suzuki, T.	107, 112		
Tananaev, I.G.	10, 105, 121, 169, 173, 174, 175, 192, 435		
Tarasov, V.A.	113		

### Rezoscan, <sup>99m</sup>Tc (Zoledronic acid)

The novel third-generation bisphosphonate (zoledronate) radiopharmaceutical for bone scintigraphy with radionuclide <sup>99m</sup>Tc.

#### Rezoscan, <sup>99m</sup>Tc indications:

- Detecting, staging, and follow-up of metastatic disease (osteoclastic, osteolytic metastasis);
- Primary and secondary bone neoplasms;
- Infections inflammatory disease (osteomyelitis, tuberculosis of bones & joints);
- Metabolic and endocrine diseases;
- Traumas and vascular bone diseases;
- Osteoarticular disease (arthritis & arthrosis of different etiology).

### Octreotide, <sup>111</sup>In (Pentetreotide)


The drug is designed for radionuclear diagnosis of tumors having high density of somatostatin receptors, as well as for the establishment of receptor status of the tumor for the clinic effects prognosis of treatment with Octreotid.

#### Octreotide, <sup>111</sup>In indications:

- Carcinoid Tumors;
- Islet Cell Tumors (Gastrinoma, Insulinoma, VIPoma, Glucagonoma);
- Small Cell Lung Carcinoma;
- CNS Tumors (Paraganglioma, Pituitary Adenoma, Meningioma);
- Miscellaneous Tumors (Pheochromocytoma, Undifferentiated APUDoma);
- Determination of tumor receptors status in patients receiving therapeutic doses of Octreotid for clinic effects treatment forecast.



CFSC "Pharm-Sintez"  
117312, Moscow, Vavilovastr., 15  
Tel: +7(495) 796 94 33, Fax: +7 (495) 796 94 34  
[www.pharm-sintez.com](http://www.pharm-sintez.com)  
e-mail: [info@pharm-sintez.ru](mailto:info@pharm-sintez.ru)

 **7<sup>th</sup> International Symposium  
on Technetium and Rhenium  
Science and Utilization**



**RESOLUTION**

The International Advisory Committee of ISTR-2011 has resolved that the next *International Symposium on Technetium and Rhenium* will be held in Chicago by Argonne National Laboratory (USA) in 2014

The International Advisory Committee for ISTR-2014 consists of the following scientists:

R. Alberto	(Switzerland)
B. Bryskin	(USA)
K. Czerwinski	(USA)
M. Fattahi	(France)
G.E. Kodina	(Russia)
C. Kremer	(Uruguay)
T.I.A. Gerber	(South Africa)
K.E. German	(Russia)
Ph. Moisy	(France)
M. Ozawa	(Japan)
V.F. Peretrukhin	(Russia)
F. Poineau	(USA)
A. Sattelberger	(USA) – Chairman
T. Sekine	(Japan)
I.D. Troshkina	(Russia)
A.Yu. Tsivadze	(Russia)
T. Yoshimura	(Japan)

We hope that we will all see each other in Chicago.

K.E. German  
Chairman ISTR 2011

F. Poineau

Signed to print on 27.01.2012.  
Format 60x90/16. Edition № 402. Print run 1 000 issues  
Publishing group «Granica»  
123007 Moscow, highway Horoshevskoe, building 38  
Telephone: (495) 941-26-66, fax: (495) 941-36-46  
E-mail: granica\_publish@mail.ru